HIGH PRESSURE WATER JET ASSISTED DRAG TOOL CUTTING OF ROCK MATERIALS

A THESIS Submitted for

The degree of Doctor of Philosophy in Engineering

of the University of Newcastle upon Tyne

by

O. TECEN M.Sc

September 1982

ABSTRACT

Due to limitations of cutting picks in terms of rock strength and abrasivity, the application of present day boom type partial-face tunnelling machines is restricted. It seems that the performances of these machines can be improved considerably by hybridizing cutting picks with high pressure water jets.

There are many questions that needs to be answered before an excavation machine incorporating high pressure water jets and mechanical tools can be used to excavate rock most efficiently. Amongst these questions are; the selection of optimum water jet pressure and nozzle diameter, the influence of nozzle positioning with respect to mechanical tool e.g. side-off, lead-on, stand-off distances, cutting speed and number of passes of the jet.

The research described in this thesis examines the effect of the above variables on the performance of a hybrid cutting system, together with a comparision of mechanical and hybrid cutting systems in terms of tool forces, yield and specific energies recorded for seven rock types. Small scale qualitative finite element stress analysis was also carried out to analize the stress field around the mechanical tool tip to provide an insight into the mechanics of rock failure under high pressure water jet assisted cutting.

CONTENTS

1 INTRODUCTION 1

2 LITERATURE REVIEW ON WATERJETS 6

2.1 Stability of Liquid Jets 6

2.2 Theories on High Pressure Water Jet Cutting of Rock 7

2.2.1 Experimentally Derived Formulas on Jet Cutting 13

2.3 Influence of Hydraulic Variables on Jet Penetration 18

2.3.1 Waterjet Pressure 18

2.3.2 Cutting Speed 21

2.3.3 Nozzle 24

2.3.4 Stand-off Distance 29

2.3.5 Additives 33

2.3.6 Number of Jet Passes 36

2.4 Water Jet Assisted Cutting 37

3 EXPERIMENTAL SET-UP AND APPARATUS 39

3.1 Design of Tool Holders and Tools for Point Attack Cutting . . . 39

3.2 Pumping System 40

3.2.1 Nozzles 41

3.3 Nozzle Carriage Assembly and Jet Positioning 41

3.4 The Rock Cutting Rig 42

3.5 Experimental Variables for High Pressure Waterjet Assisted

Cutting 43

3.6 Parameters to be measured and calculated 47

3.7 Parameter Measurements 49

3.7.1 Triaxial Dynamometer and Data Recording System 49

3.7.2 Calibration of The Dynamometer 50

3.7.3 Measurement of The Volume of Rock Cut by Water Jet 52

3.7.4 The Relationship between Jet Velocity and Pump Gauge Pressure 53

3.7.5 Hydraulic Specific Energy Calculations 56

3.8 Experimental Procedure for Mechanical Cutting 58

3.9 Experimental Procedure for Water Jet Assisted Cutting 59

4 LABORATORY TESTING FOR DETERMINING ROCK PROPERTIES 61

4.1 Mechanical Properties 62

4.1.1 Uniaxial Compressive Strength 62

4.1.2 Indirect Tensile Strength 63

4.1.3 Triaxial Compressive Strength 64

4.1.4 Static Elastic Constants 65

4.2 Hardness Testing 66

4.2.1 Scleroscope Rebound Hardness 66

4.2.2 Plasticity 66

4.2.3 Schmidt Hammer Rebound Hardness 67

4.2.4 NCB Cone Indenter 68

4.3 Physical Properties 70

4.3.1 Bulk Density 70

4.3.2 Grain Density 71

4.3.3 Porosity 72

4.3.4 Apparent Porosity 73

4.3.5 True Porosity 74

4.3.6 Dynamic Modulus (Wave Velocity) 74

5 POINT ATTACK MECHANICAL TOOL CUTTING 76

5.1 Literature Review on Point Attack Cutting 76

5.1.1 German Research 77

5.1.2 Research at University of Newcastle 78

5.1.3 Reseach at M.R.D.E. 80

5.2 The Cutting Action of Point Attack Tools 81

5.3 Experimental Plan 85

5.4 Effect of Depth of Cut 87

5.4.1 On Tool Forces 87

5.4.2 On Yield 87

5.4.3 On Mechanical Specific Energy 88

5.5 Finite Element Stress Analysis 89

5.5.1 Advantages of Finite Element Method 94

5.6 Conclusions 97

6 INITIAL EXPERIMENTS WITH WATER JET ASSISTED DRAG TOOLS 99

6.1 Experimental Design 99

6.1.1 Protodyakonov Method 101

6.2 Analysis of Data - Determination of Empirical Equations 104

6.3 Hybrid Cutting 110

6.3.1 Physical and Mechanical Properties of Springwell Sandstone . .

111

6.3.2 Experimental Plan 113
6.3.3 Effect of Mechanical Depth of Cut 115
6.3.4 Effect of Water Jet Pressure 116
6.3.5 Effect of Side-off Distance 117
6.3.6 Effect of Lead-on Distance 118
6.4 Conclusions 120

7 THE INFLUENCE OF EXPERIMENTAL VARIABLES 122
7.1 Water Jet Pressure 122
7.1.1 Thin Section Analysis 123
7.1.2 Effect of Pressure on Depth of Penetration 126
7.1.3 Effect of Water jet pressure and Mechanical Tool Depth . . 127
7.1.4 Discussion 128
7.1.5 Conclusions 131
7.2 Cutting Speed 133
7.2.1 The Effect of Traverse Speed 135
7.2.2 Discussion 137
7.2.3 Conclusions 139
7.3 Nozzle Diameter 140
7.3.1 The Effect of the Nozzle Diameter 141
7.3.2 Discussion 144
7.3.3 Conclusions 145
7.4 Side-off Distance 146
7.4.1 Effect of Side-off Distance 148
7.4.2 Discussion 150

7.4.3 Conclusions 153
7.5 Lead-on Distance 154
7.5.1 Effect of Lead-on Distance 156
7.5.2 Discussion 158
7.5.3 Conclusions 161
7.6 Stand-off Distance 163
7.6.1 The Effect of Stand-off Distance 164
7.6.2 Discussion 166
7.6.3 Conclusions 168
7.7 Number of Passes 169
7.7.1 The Effect of Number of Passes of the Water jet 170
7.7.2 Discussion 172
7.7.3 Conclusions 173

8 COMPARISION EXPERIMENTS 174
8.1 Experimental Design 175
8.2 Rock Properties 177
8.2.1 Thin Section Analysis 178
8.3 Effect of Depth of Cut 180
8.3.1 On Tool Forces 180
8.3.2 On Yield 181
8.3.3 On Mechanical Specific Energy 181
8.4 Discussion 182
8.5 Limestone C 186
8.5.1 Properties of Limestone 186
8.5.2 Thin Section Analysis: Biosparite (Shelly Limestone) . . . 187

8.5.3 Experimental Plan 187
8.5.4 Effect of Depth of Cut 188
8.5.5 Discussion 189
8.6 Conclusions 190

9 THE INFLUENCE OF ROCK PROPERTIES 193
9.1 The Effect of Rock Properties 195
9.1.1 On Mechanical Cutting 196
9.1.2 On Hybrid Cutting 201
9.2 Discussion 205
9.3 Conclusions 209

10 CONCLUSIONS 212
10.1 Influence of Point Attack Tool Depth of Cut 212
10.2 Influence of Hydraulic Variables 213
10.2.1 Water Jet Pressure 213
10.2.2 Cutting Speed 214
10.2.3 Nozzle Diameter 216
10.2.4 Number of Jet Passes 216
10.2.5 Side-off Distance 217
10.2.6 Lead-on Distance 218
10.2.7 Stand-off Distance 219
10.3 Influence of Rock Properties 219
10.4 Recommendations for Future Work 221

Appendix A : MECHANICAL CUTTING RESULTS 251

Appendix B : INITIAL WATER JET ASSISTED CUTTING RESULTS 253

Appendix C : HYBRID CUTTING RESULTS 265

Appendix D : COMPARISON EXPERIMENTS 288

ACKNOWLEDGEMENTS

The author would like to thank :

Dr.R.J.Fowell, lecturer in Mining Engineering, for providing the opportunity to carry out the research and for his valuable help and supervision,

ETIBANK of TURKEY for supporting him financially during his studies,

Mr.T.Shepherdson,chief technician, and his staff for their assistance and friendship,

Mr.A.Warrender, retired technician, for his enthusiasm and valuable help during the laboratory phase of the project,

Mr.M.Paisley, photographer, for producing excellent photographs at short notice,

Ann and Beryl for typing parts of this thesis.

LIST OF PLATES

PLATE 1 - TOOL HOLDERS AND CUTTING TOOLS

PLATE 2 - WATER JET NOZZLES

PLATE 3 - NOZZLE CARRIAGE ASSEMBLY

PLATE 4 - NOZZLE HOLDER

PLATE 5 - STAND-OFF AND LEAD-ON DISTANCE PIECES

PLATE 6 - THE VIEW OF THE HYBRID CUTTING ROOM

PLATE 7 - CALIBRATION ALONG SIDEWAYS DIRECTION

PLATE 8 - RECORDING INSTRUMENTATION AND STRAIN INDICATOR

PLATE 9 - U.V RECORDING TRACE OF A CUT

PLATE 10 - POINT ATTACK TOOL CUTTING AND ROCK SURFACE AFTER A CUT

PLATE 11 - HYBRID CUTTING

PLATE 12 - SPACING EXPERIMENTS WITH WATER JET AT VARIOUS LOCATIONS

PLATE 13 - MEASUREMENT OF THE VOLUME OF ROCK CUT

PLATE 14 - EFFECT OF HIGH TEMPERATURE ON A TUNGSTEN CARBIDE INSERT

PLATE 15 - DRAG TOOL CUTTERS

1 INTRODUCTION

There is a general increase in the level of mechanical excavation activities taking place underground in both Mining and Civil Engineering Tunnelling fields and the trend shows that these will increase further in the future (69).

The breaking of rock from the rock continuum at the face of the excavation to a size suitable for removal presents the first problem that every excavation system must overcome. Apart from hand mining using pick axes and shovels there are several ways of excavating rock,e.g. drill and blast, tunnelling machines.

The drill and blast method is cyclic in nature and involves individual operations - drilling, blasting, and removing the debris - which cannot be performed simultaneously. It has many advantages e.g. relatively low capital costs for the equipment, adoptable to widely variable rock conditions, and disadvantages, e.g. lack of control on the size and shape of excavation, loosening of the rock surrounding the excavation thus requiring increased support, blasting vibrations (important in urban areas), delays incurred because of the systems inherent cyclic nature. With the introduction of hydraulic drilling machines and smooth wall blasting techniques the method has reached a stage of near ultimate development.

The need to excavate faster and at the same time eliminate the disadvantages of the otherwise highly efficient drill and blast method led to the introduction of continuous tunnelling machines . These can broadly be classified as :

1. machines which excavate the full-face of the tunnel at one time and,

2. machines which excavate only a part of the face at a time.

The common basic functions of all tunnelling machines are : Thrust is applied to drive or hold the rock cutting tools into the the excavation face ,and torque is applied to rotate the cutting tools over the face so that they can continuously break out rock. The speed of head rotation together with torque requirement determines the cutter head power.

The strength of rock and the rate at which it can continuously be excavated is limited by the considerable thrust which must be developed in order to push the cutting elements into the rock face and torque to break it. Most commonly, steel roller disks and tungsten carbide tipped drag tools are used as cutting elements on the cutting heads of tunnelling machines. With the introduction of a new generation of more powerful and heavier tunnelling machines the durability of these tools became the limiting elements in their applicability. Although it may be possible to achieve significant improvements in the tungsten carbide drag pick tool life by optimizing the alloy composition and tip geometry for various rock

types, higher temperatures developed at the tool/rock interface cause increased tool wear due to poor hardness characteristics of tungsten carbide at elevated temperatures and the greater impact loads experienced in hard blocky ground lead to increase in shattered bits.

In an effort to increase the applicability of tunnelling machines to excavate harder ground than is possible at present, and increase the tunnel boring speed, people started to think in terms of developing new methods of breaking rock at a faster rate with less wear to machine parts. Among so called novel excavation techniques which attracted the attention of most investigators was high pressure water jet cutting .

Water has been employed in the extraction of minerals for centuries, and has been used extensively for mineral dressing purposes (145). Much of the early work on high pressure water jets have been done in Russia (106,159). During the last two decades a large number of investigations into the applicability of high pressure water jets to cutting of different materials have been undertaken all around the world (1,2,3,4,5,6,24,60,64,68,82,86,107,148,170). The reasons for this eagerness and enthusiasm were many. If the pressure of the water jet is high enough it could drill through hardest of materials, it will not create dust, does not need sharpening and most important of all could transmit most of the applied power.

The continuous use of high pressure water jets in widely diverging areas as shoe cutting, undersea cleaning, concrete breaking, and drilling

led to the design of new pumps, intensifiers, pipes, seals, and these have been improved so much that their reliability have increased considerably.

The specific energies of water jet devices are high , in the order of 10^4[MJ/m^3] therefore more power is needed to excavate or drill similar diameter holes than is required by the mechanical tools. But exceptionally high specific powers $10^4$to 10^5[MN/m^2] would enable high rates of excavation to be attained. Today it is possible to drill rock many times faster with water jets than mechanical drilling alone (91). Total power requirements would be prohibitively high if the water jets are used to excavate large cross-sectional areas. But if they are used to cut very narrow slots comprising a very small proportion of all the rock broken , the total power requirements may be reduced to practicable values.

The efficiency of mechanical tools can be increased by reducing the forces required for breaking the rock. This would enable lighter, mobile and more versatile universal tunnelling machines to be manufactured which would be applicable to widely varying rock conditions. To achieve this some investigators have proposed to use high pressure water jets together with efficient mechanical cutters. Several research projects have been carried out in Japan, U.S.A , and W.Germany into water jet assisted disk cutting and in S.Africa and U.K into water jet assisted drag tool cutting. Although impressive field performances and hypothetical advantages such as systems ability to cut through very hard materials, dust suppression at source, cooling of tools thus increase their life, reduce frictonal

heating and eliminate the risk of ignition in coal mines have been reported, none of the research up to now have explained the underlying fundamental aspects of hybrid cutting.

The work described in this thesis looks into the principles of rock cutting with high pressure water jet assisted point attack tools with a view to employing them on boom type partial-face roadheaders which are used extensively in U.K

2 LITERATURE REVIEW ON WATERJETS

2.1 STABILITY OF LIQUID JETS

Stability of waterjets is a prime factor in their effect on rock targets. Several theories on the disintegration of liquid jets exist.

For low velocity jets Rayleigh's(122) theory states that a small disturbance causes an oscillation of the jet which is held in balance by surface tension. Helmoltz(70) and Castleman(21) have extended Rayleigh's theory to velocities above Rayleigh's but these velocities are lower than required for rock penetration.

At moderately high velocities several factors are involved in the instability of the jet. Dunne and Cassen(37), Sauer (130) and, Pai(113) had looked into the high velocity jets and their stability. From their findings it appears that

1. Turbulence at both the upstream and downstream sides of the nozzle

2. Air friction

3. Shock waves generated at the jet downstream from the nozzle

in the jet are critical factors in the jet stability. There was no satisfactory theory for water jets approaching and beyond the speed of sound in water.(93)

2.2 THEORIES ON HIGH PRESSURE WATER JET CUTTING OF ROCK

The theories reported in the literature for hydraulic cutting of rock ranges from considering the jet equivalent to a solid body, in the pressure range required for rock cutting, to assuming the jet has the form of a sequnce of clusters due to mixing of air with jet fluid(135). Some of these are briefly described below.

Leach and Walker(82) measured the steady state pressure distribution imposed upon a rigid flat surface by a continuous jet impinging normally at relatively low speed. They also presented an empirical fit to the measurements which Powell and Simpson(118) used as the loading function to calculate the axisymmetric stress field induced in a homogenous linear elastic solid by such a non-penetrating jet. Forman and Secor(47) considered the effect upon the stress field of the diffusion of the impinging jet through a permeable target. Using the Leach and Walker pressure distribution at the surface, they calculated the quasi-static changes in the stress in the rock matrix as the fluid seeps into the rock according to Darcy's law, increasing the pore pressure. They concluded that in the absence of dynamic effects and erosion, the permeability of the rock plays a major role in the process of fracture initiation. The

assumption of water incompressibilty is implicit in all these studies.

Heymann(62) presented a two dimensional approximation for the dynamics of high speed impact between a compressible liquid drop and a solid surface adapted from a closely related analysis of the oblique impact between two solid plates. This is, he claimed, valid only for the initial phase of the impact still remained attached to the target surface, and no lateral outflow took place. The derivations assumed a linear relationship between shock velocity and particle velocity change across the shock front.

Field(45) has found similarities between the type of loading produced by a liquid mass striking a solid surface and that produced by the detonation of small quantities of explosive, since both gave intense pressure peaks of only a few micro-seconds durations. He described and briefly compared the fracture and deformation of glasses, hard polymers, single crystal and ceramic materials by liquid impact at velocities up to 1000 (m/s) with that produced by solid/solid impact and explosive loading.

Crow(30) has developed a steady state erosion theory of hydraulic rock cutting. The theory applies to a continuous jet acting on a rock which feeds under the jet at a constant velocity leaving a slot of uniform depth. The water was assumed incompressible and the rock was presumed to disintegrate as a consequence of the water penetrating under the surface grains thereby reducing the tendency of the surface pressure to hold the grains in place against the tangential drag force at the interface.

$$h = 2\mu_w(dxp)/\tau_0 \int\{\exp[\ w(\theta-\theta_0)\sin\theta d\theta]/[1+(v/c)\sin\theta\} \quad \ldots\ldots\ldots(2.1)$$

Where

d is the jet diameter

p is the initial total pressure of the jet

θ is the instantaneous angle between the direction of the jet stream and the direction of rock motion.

θ_0 incidence angle of the jet, is the initial value of

μ_w represents a coeff. of Coulomb friction between water and rock under cavitational conditions

According to this theory the most important rock property is the permeability.

Hurlburt, Crow and Lade(31) tested Crow's theory of hydraulic rock cutting by conducting experiments on four different rocks. They have realized that, of all the rock properties, permeability has the largest effect on the theoretically predicted depth of cut. The four rocks tested in their program had permeabilities ranging within five orders of magnitude. From their results of experiments on jet-cutting of rock, they have seen that the wide variation in permeability did not produce a correspondingly large variation in slot depth from rock type to rock type as predicted by the theory. In other words, a rock with a high permeability was not cut as easily as the theory predicted, nor was the depth of slot as predicted in a rock with a low permeability. Thus it appears that the mechanism of hydraulic rock cutting proposed by Crow is

inadequate to describe the actual process as applied to the whole range of geologic materials which might be encountered.

Rehbinder(123) derived a theoretical model of cutting rock with a steady high pressure water jet. He performed his tests on eight different rocks, sandstones, granites, diabase and porphyr. The main conclusion he reached was that the erosion resistance of rock is closely connected to its permeability.

Shpitbaum's theory of rock failure under the effect of a high pressure fluid jet considers the jet of non-uniform structure due to mixing of air with the jetted fluid(136). The non-uniformity of the jet amounts to unequal distribution of the volume of the water moving along the jet trajectory. In Shpitbaum's opinion, the jet has the form of sequence of clusters. The variation of force produced by the non-uniformity of the jet, on the rock surface which causes its failure, due to propagation of pre-existing microcracks. The frequency of pressure at the rock surface is given by

$$v_{av} = W/(2\pi) = V/12h \quad \text{.....(2.2)}$$

v_{av} is average frequency of the pressure pulse

The instantaneous velocity in the direction of the jet axis was expressed by the formula

$$v = V + u \quad \ldots\ldots\ldots\ldots\ldots\ldots (2.3)$$

According to Shpitbaum's theory, the depth of cut produced by the jet was maximum when the rock was at a certain distance from the nozzle.

For a very high velocity jet it is not permissible to neglect the compressibility of water. Pulsed jet velocities may be high enough that the impact pressures even cause significant compression in rocks, which are generally much less compressible than water. The compressive stress pulse generated upon impact propagates outward and is reflected at a free surface as a tensile pulse. The resulting spall fracture in the rock is a principal mechanism for rock fragmentation as observed by Cooley(26) in his water cannon impact tests. For impermeable rocks (such as granite) spallation is the dominant failure mode but for more permeable rocks i.e. sandstone, erosion of a deep hole and subsequent hydrofracture are also important fragmentation processes.

Pritchett and Riney(119) developed detailed hydrodynamic computer calculation which characterised the time dependent loading imposed on a rock by normal impact of a cylindrical water jet.

The theories which consider the rock failure due to high pressure water jets equivalent to rock failure by impact of chisels and bit heads on a rock surface is best presented by Ponomarev analysis(116).

Ponomarev has suggested that when a liquid jet impacts upon a rock surface, there were three zones of reaction within the rock. In the first zone rock is ruptured by the jet force. In second zone the applied stresses are reduced by attenuation, diffusion, and divergence of the stress wave front so that the stresses are less than the strength of the rock; however still large enough so that when concentrated on planes of weakness or microcracks, that will cause crack initiation and propagation. In the third zone, the pressure proves insufficient to lead to any overstressing and the elastic waves travel in the same way as sound waves.

Ponomarev defined the first zone as a circle with radius r given by the empirical equation based on his experimental work.

$$r = [4.72\pi f c_w \rho / Ac \,] \quad \ldots\ldots\ldots (2.4)$$

where f is wave frequecy

c_w stress wave velocity

ρ rock density

A cross-sectional area of the nozzle

This equation does not consider the attenuation factor of the rock which Ponomarev finds has a considerable bearing on the radius of the first zone of failure, or the jet pressure or velocity which was proved to have an important bearing on the volume of the rock removal.

2.2.1 Experimentally Derived Formulas on Jet Cutting

Farmer and Attewell(42) after conducting experiments on a selection of relatively low-strength non-igneous rocks, have found that above a transitional velocity, relationship between penetration(s), impact velocity(v) and rate of flow(Q) in the form :

$$S = kd_c[(v/c)^n] \text{ and } s/t = k'Q \quad \ldots\ldots(2.5)$$

where

k,k' are constants

d_c is the crater diameter

c is the longitudinal wave velocity in the rock

n is approximately equal to 2/3

Summers(143) performed regression analysis on the results, based on the 7180 measurement tests of the depth of cut. The rock properties considered in the analysis were Uniaxial Compressive Strength, Young's Modulus, Shore hardness, Schmidt hammer value, Rock Impact Hardness number and Rock Fracture Toughness.

His equations were:

$$\text{DEPTH} = 5.72+24.8\times10^{-4}(\text{VR})+[16\times10^{3}/\text{CS}]+3\times10^{-5}(\text{P}) -7.4\times10^{-2}(\text{SHOR}) \quad \ldots\ldots(2.6)$$

$$\text{S.E.} = -99.4\times10^{3}+8.19\times10^{3}(\text{RIHN})+84.3\times10^{7}/\text{CS}+\text{P}\times1.97 -3.82/\text{SPE} \quad \ldots\ldots(2.7)$$

$$S.E.RATIO = 1228-1.56(VR)+7.4\times10^{7}/YM-0.248(CS)+177(RIHN)$$
$$+6.1\times10^{-4}(YM)-2.0(FT)-42.2\times10^{3}/(SHOR) \quad ..(8)$$

Nikonov(106) and Nikonov and Goldin(107) have shown that Soviet data on the slot depth in coal by continuous jets could be correlated by an equation involving dimensionless parameters.

$$h/d = 0.5(Po/CS - 0.2)[(Vt/Vo)^{0.5}] \quad .....(2.9)$$

where h slot depth

d nozzle diameter

Po jet pressure

CS unconfined compressive strength

Vt nozzle traverse velocity

Vo jet velocity

Nikonov and Goldin established that the optimum jet pressure for slotting coal with minimum energy consumption was about 1.5 to 1.6 times the compressive strength or about 15 to 16 times the Protodyakonov hardness number.

Cooley(25) has attempted to correlate the experimental data on the depth of slots cut in various materials by traversing continuous high pressure liquid jets with nozzle stand-off distances of less than 100 nozzle diameters, approximately by an equation of the form introduced by

Nikonov.

$$h/d = B\,(Po/CS) - 0.2[(Vt/Vo)^{-m}] \quad ..(2.10)$$

where

B constantant for each material

m constant, equal to 0.5 for coal and generally between 0.5 and 1.0 for other materials.

But recommended a further research to seperate the effects of stand-off distance, Reynolds number, nozzle shape and nozzle surface roughness, and the density, permeability, porosity, grain size and initial water content of permeable materials.

Zelenin, Vesselov and Koniashin(170) proposed a formula to determine the slot depth being cut in the rock during the first pass by single water jet stream for the above parameters

$$h=0.5/[f\ w\ (vn^{0.33})]x[Pp-Po(crit)]/[1000-Pp(crit)].....(2.11)$$

where h depth of cut

f coeff. of rock hardness

w area of the working section of the jet stream

vn feed speed jet stream

Pp pressure in the receiver

Pp_{crit} value of critical pressure

Singh and Huck(141) correlated rock properties to damage effected by water jets. They used six rock types and nine properties were determined for each rock variety. They found that

$$\text{crater volume} = 0.16\ [(\text{crater depth})^2] \quad \ldots(2.12)$$

and their regression analysis produced an equation in the form :

$$D = -2.6 + [2.42 \times 10^6 / CS] + 201/SH + 4.37 \times 10^3 (P) \quad \ldots\ldots(2.13)$$

where D crater depth (cm)

CS compressive strength

SH Schmidt hammer value

P maximum stagnation pressure

But they have not noted a minimum in the specific energy consumption although the tests were conducted to specific pressures of 35.

The stagnation pressure is by definition the pressure obtained when the fluid jet is brought to rest isentropically, or the pressure measured along the center line of the jet in a plane at right angles to it(99). Jet velocity is related to the stagnation pressure by Bernoulli's equation

$$Ps - Po = (1/2)\rho v^2 \quad \ldots\ldots(2.14)$$

This expression assumes that the fluid is incompressible and is valid for pressures up to about 700 (MN/m^2). At higher pressures one must consider compressibility and adiabatic expansion effects within the nozzle. A more complicated relationship results

$$v = 2\gamma A/(\gamma-1)\ x(Po/\rho_0)\{[(\rho_s/\rho_0)^{\gamma-1}]-1\} \quad .....(2.15)$$

where ρ_s is the density of the fluid in the reservoir, γ and A are constants.

The mechanics of rock failure due to high pressure fluid jet is highly complicated and poorly understood. This is mainly because the rock is subjected to several separate processes each of which can cause failure. Failure besides mainly results from fluid flow through the rock pores, and pressurizing in the fluid in the pores which start tensile fracturing, it is also results from the effects of dynamic stress waves and erosion action of the fluid loaded with the rock particles.

2.3 INFLUENCE OF HYDRAULIC VARIABLES ON JET PENETRATION

A knowledge of efficiency of a cutting system is important when a selection is to be made between various excavation methods. Specific Energy is a parameter used by most research workers as a measure to evaluate the efficiency (S.E. is inversely proportional to the cutting system efficiency), and is described as the amount of work required to cut unit volume (or mass) of rock. The volume of rock cut - and indirectly the specific energy - is influenced by the water jet pressure, the traversing speed as well as by other factors.

2.3.1 Waterjet Pressure

The change in penetration of target (rock) specimen has been used by most researchers as a measure of the effect of change in water jet pressure. Farmer and Attewell(42) reported that penetration increased with pressure up to a transition jet velocity which for the majority of experimental rocks lay between 250-350 m/sec, at this region the rate of inrease decreased. The penetration above the 300m/sec jet velocity was of the form $S=Kdc[(Vo/C)^{0.66}]$ where S is penetration, K is a constant dependent on the nozzle diameter and profile characteristics, dc is the crater diameter, Vo is the terminal impact velocity and C is the wave velocity. Their experimental results were influenced by the limitation of their experimental apparatus, as they had no control over time. Leach and Walker's(82) results of experiments on five different rocks suggests that

for each rock, there is a certain critical pressure (the threshold pressure) below which significant penetration does not take place. Cooley(26) stated that the threshold pressure was typically 20 to 50 percent of the compressive strength of the rock.

Harris(55) reported that the value of the threshold pressure was not dependent on rock properties only, but must also be a function of the traverse speed and the nozzle size. On the other hand, McClain et al(93) suggested that threshold was independent of nozzle diameter, meaning it was related to the jet velocity, but not to the total momentum or energy of the jet.

Once the pressure is increased toward the compressive strength, penetration increases rapidly with pressure. The trend of data appears to differ from researcher to researcher and is probably due to experimental set-up and variations in the rock properties.

Leach et al, Summers(144), Veenhuizen(158), Ostrovski(110) established that a pressure increase of the water jet will always lead to an increase in depth of penetration and the derived relationship between two parameters tended to be approximately linear. But according to Imanaka(68) as pressure was increased the cutting depth increased with a power of Po>CS>1(1.5 to 2). Furthermore, the results of several experiments have shown that for constant nozzle stand-off distance and exposure time, the relationship was parabolic in nature.

For pressures above 3 times the threshold pressure of rock, the relationship between penetration and jet pressure can be safely represented by a straight line.

Harris and Mellor(55) have shown that for any given value of traverse speed, Specific Energy decreased as the nozzle pressure was increased. With sufficiently high traverse speeds there would be a finite pressure that gives a minimum value of S.E. That is there was no unique value of nozzle pressure that gives maximum efficiency without regard for other variables. Their experimental data was used to make the point, since a plot of S.E. against nozzle pressure for constant penetration (instead of constant traverse speed) showed S.E. decreasing as pressure increases.

Findings of Page(112) showed that if the depth of penetration was restricted to a low figure by decreasing jet residence times as the pressure was increased, then the rate of increase in penetration depth accelerated with increase in jet pressure. If energy requirements for unit destruction were computed these figures would reduce with pressure increase, provided that the jet residence time was decreased and also that these energy requirements did not pass through a minimum. However, according to Cooley(26) Specific Energy decreased from a large value for pressures below threshold pressure to a minimum value for pressures in the range of 2 to 3 times the threshold pressure and then starts to rise again.

2.3.2 Cutting Speed

The other parameter used in specific energy calculation is the time taken by the high pressure waterjet to act over the rock surface which is incorporated in the parameter cutting speed.

For most rocks, at a fixed water jet pressure the penetration varies inversely with the traverse velocity. The nature of the relationship between traverse velocity (time) and penetration varies between the published results of investigators.

Rehbinders(123) results showed that depth of cut grew linearly with time of exposure in the beginning, but became constant later.

Summers and Brook(144) have reported that most of the penetration has been achieved 1/100th of a second. Page's(112) results confirm this by showing that penetration occurred in extremely short times, and the curve of penetration against time rapidly approached to an asymptote and that efficient penetration only took place within specified time of 10 microseconds. Summers(148) further reported that practically no increase in penetration occurred after 30 seconds exposure time.

All these experiments were done to find the effect of time on a static target.

Farmer et al, Leach et al, Summers et al, Sheshtawy all reported that when a certain crater depth is reached, any further increase in the crater depth was prevented by the water cushion formed in the crater, that completely protects the rock mass from destruction. Another reason is as the hole deepens, the impact point recedes from the nozzle and the natural break up of the jet increases with increase in distance from the nozzle.

With traversing targets the effect of time was made more apparent by the change in traverse speed. Nikonov(106) has found that with increasing jet traverse velocity, the area of cut(S.E.) varies reaching its maximum at the optimum jet traverse velocity. He continued by saying that the exact value of S.E. input is related to the volume flow rate and thus to the diameter of the nozzle, the larger the nozzle diameter the greater the S.E. input for a constant jet pressure. Hahs(53) reported that S.E. falls with increase in traverse speed at constant nozzle diameter and pressure, correspondingly estimated pumping and crew cost fell with increase in nozzle traverse velocity. Porkat and Zukal(117) found that area of cut increased steadily with traverse speed.

Crow's(31) theory of hydraulic rock cutting predicts a variation of penetration inversely with the first power of traverse velocity at high values of traverse velocity. Nikonov and Goldin's(107) approximate empirical equation predicts a variation of penetration as the inverse square root instead of the first power of traverse velocity. It appears probable that the shape of each investigators curve of penetration vs traverse velocity is effected by the decrease of jet stagnation pressure

with distance due to turbulent mixing which is a function of several parameters i.e. nozzle shape and roughness, stand-off ratio and Reynold's number.

Cooley(26) suggested that for most rocks, at constant jet pressure, the slot depth varies inversely with the traverse velocity to a power of about 0.17 to 0.47 at low values of traverse velocity, but the variation becomes more rapid at high traverse ratio as predicted by Crow(32). He further adds that for most efficient erosive cutting of rock by steady jets the ratio of jet velocity to nozzle traverse velocity should be less than about 1000.

In Hashish's(58) work the S.E. has been found to have its lowest values above certain traverse velocity when all other parameters are kept constant. Moodie and Artingstall's(100) experiments show that penetration decreases with increasing traversing speed and graphs tend to run parallel to an asymptote after 2 m/s, (Figure 2.1). In contrast, cutting efficiency increases with increase in traverse speed up to a certain point, after that it starts to fall again. Harris(56) concluded that below a traverse speed of approximately 0.7 ft/sec penetration increases rapidly as traverse speed decreases showing high sensitivity at low traverse speeds. Harris and Mellor(55) found that specific energy decreased with increasing traverse speed irrespective of whether pressure was held constant. Their hypothesis concerning minimum S.E. at a certain nozzle pressure implies that within a certain range there must be minimum S.E. with respect to traverse speed for constant nozzle pressure.

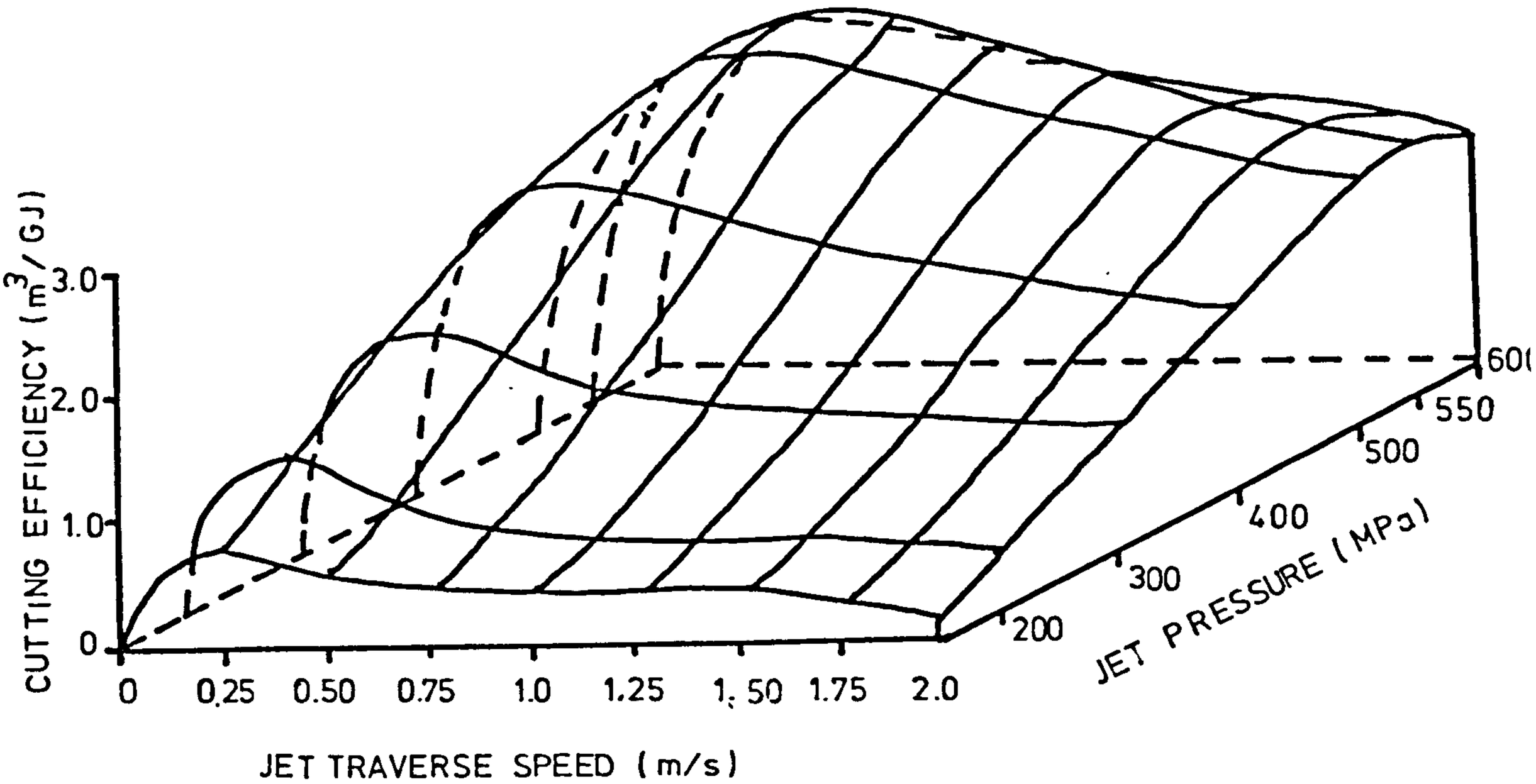

FIG. 2.1 CUTTING DARLEY DALE SANDSTONE: VARIATION OF CUTTING EFFICIENCY WITH JET TRAVERSE SPEED AND WATER PRESSURE .

(after Moodie and Artingstall)

2.3.3 Nozzle

The choice of nozzle shape, size and material is dependent on the kind of high pressure water jet cutting system it is going to be used at. What is desirable for one system is not necessarily so for others. For instance, where hydraulic mining systems are concerned, in which the nozzle is required to operate at large stand-off distances, the nozzle diameter is of the order of several centimeters and the flow rate rather than pressure is more important. Therefore the shape and size of nozzle for this system should be such that disturbances in the flow should be minimized and flow should keep its original shape at large distances.

The selection of best performing nozzle from a class of shapes for particular cutting system requires that a design criteria be available. Several researchers used different methods of performance criteria. The most widely employed one is to measure the pressure exerted by the jet at various stand-off dstances from its exit on a target plate hole. This method evaluates the jet impact pressure, stagnation pressure, which can be made up of continuous core, droplets, etc. The electrical conductivity method is also used at several stand-off distances to evaluate the continuity of the jet.

Nikonov and Shavlovskii(138) developed the best nozzle shape, as the one having a 13 degrees convergence angle followed by a straight section of 2-4 times nozzle diameter, from their investigations of nozzle shapes for hydraulic monitors i.e. low pressure high flow experiments.

The disturbance of the flow in the nozzle is one of the main causes of jet break up. At high pressures concerned turbulence in the jet stream is unavoidable, however well the nozzle is designed. Since it is impracticable to design a nozzle which gives total laminar flow, the aim must be to design a nozzle which will impart the least additional turbulance to the flow.

Farmer and Attewell(42) have deduced that to reduce the turbulance the nozzle should be shorter and consequently its angle of convergence be large, but the angle of convergence must not be too great so as to cause eddies at the base. They suggested that straight sections at the end of the nozzle should be avoided as it is likely to interfere with the jet stream and cause turbulance. Their conclusion was that since under their experimental conditions the nozzle shape had no appreciable effect on the degree of penetration, surface finish of the nozzles was of considerably greater importance than any sophistication in the actual design.

Leach and Walker(82) have compared initially five different nozzle shapes. The best results were given by a shape suggested by Nikonov and Shavlovskii. In order of good performance they were nozzle a,e,c,d,b. Nozzle b is essentially a long straight length of 1 mm diameter pipe, (Fig 2.2.1).They further investigated the effect of rounding off the internal corners, the length of final straight section for a 13 degrees contraction with sharp corners. From their studies they have concluded that the simplest nozzle shape that performs well is a small angle cone (6 to 20 degrees) followed by 2 to 4 nozzle diameters of straight section.

Lohn and Brent(84) have suggested more sophisticated nozzle shapes for borehole mining and hydraulic mining uses. They have used three criteria to judge the quality of the nozzle flow :

1. minimize boundary layer thickness,

2. minimize separation potential,

3. minimize cavitation potential.

Four nozzle shapes were considered. The shapes were generated by a fifth degree polynomial with a varying inflection point (Pentic), two cubic equations with varying match point (bi-cubic), a single cubic equation with a variable exit angle (cubic), and a forth degree polynomial with a straight section of variable angle (quartic-straight), (Fig 2.2.2). The recommended shapes were in order of preference quartic-straight, pentic, cubic and bi-cibic. Lohn et al's conclusions are similar to those of Farmer's, such as the nozzles should have short lenght and large convergence angles, half angles be in the order of 20 to 30 degrees.

Nozzle shapes used for high pressure water jet drilling, cavitation purposes are different from the ones mentioned and fall beyond the scope of this project, therefore they are not treated here. Refs(142) The nozzle diameter is controlled by the power source available and the pressure range desired. Because power requirements increase as the first

NOZZLE SHAPES

Inlet Diameter 4.5mm
Outlet Diameter 1mm
Throughout

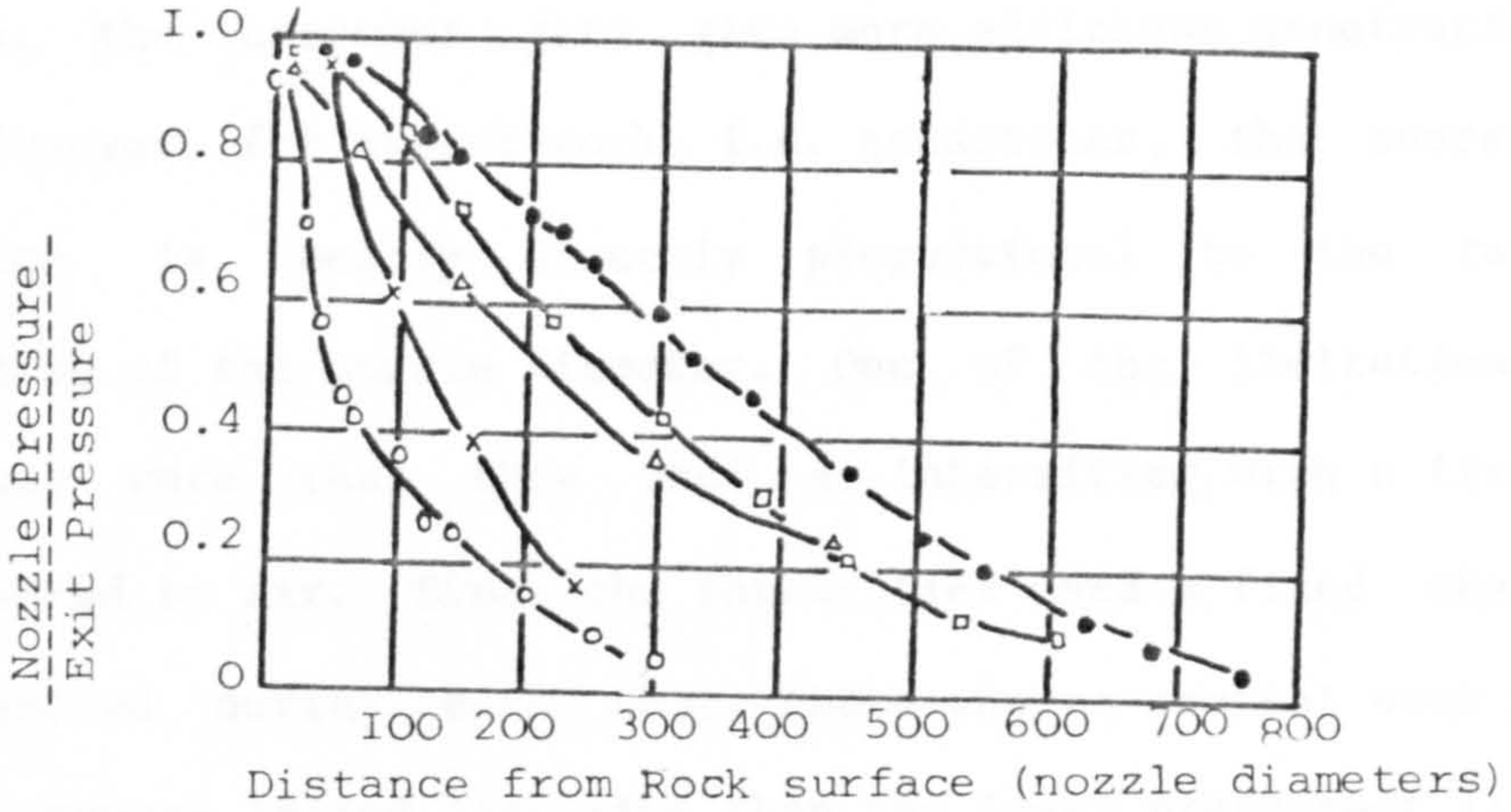

a - Effect of nozzle shape on performance.

(after Leach and Walker)

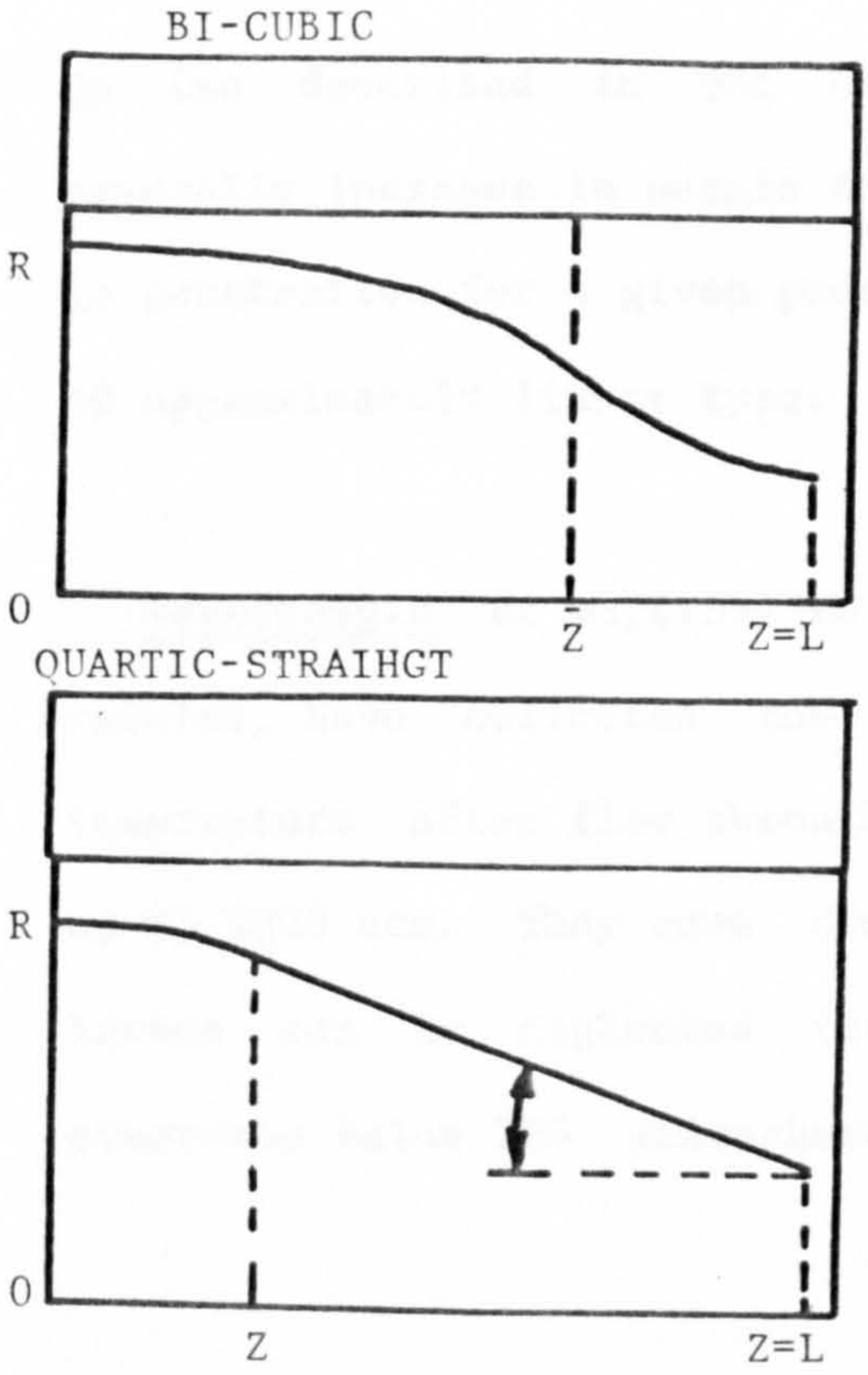

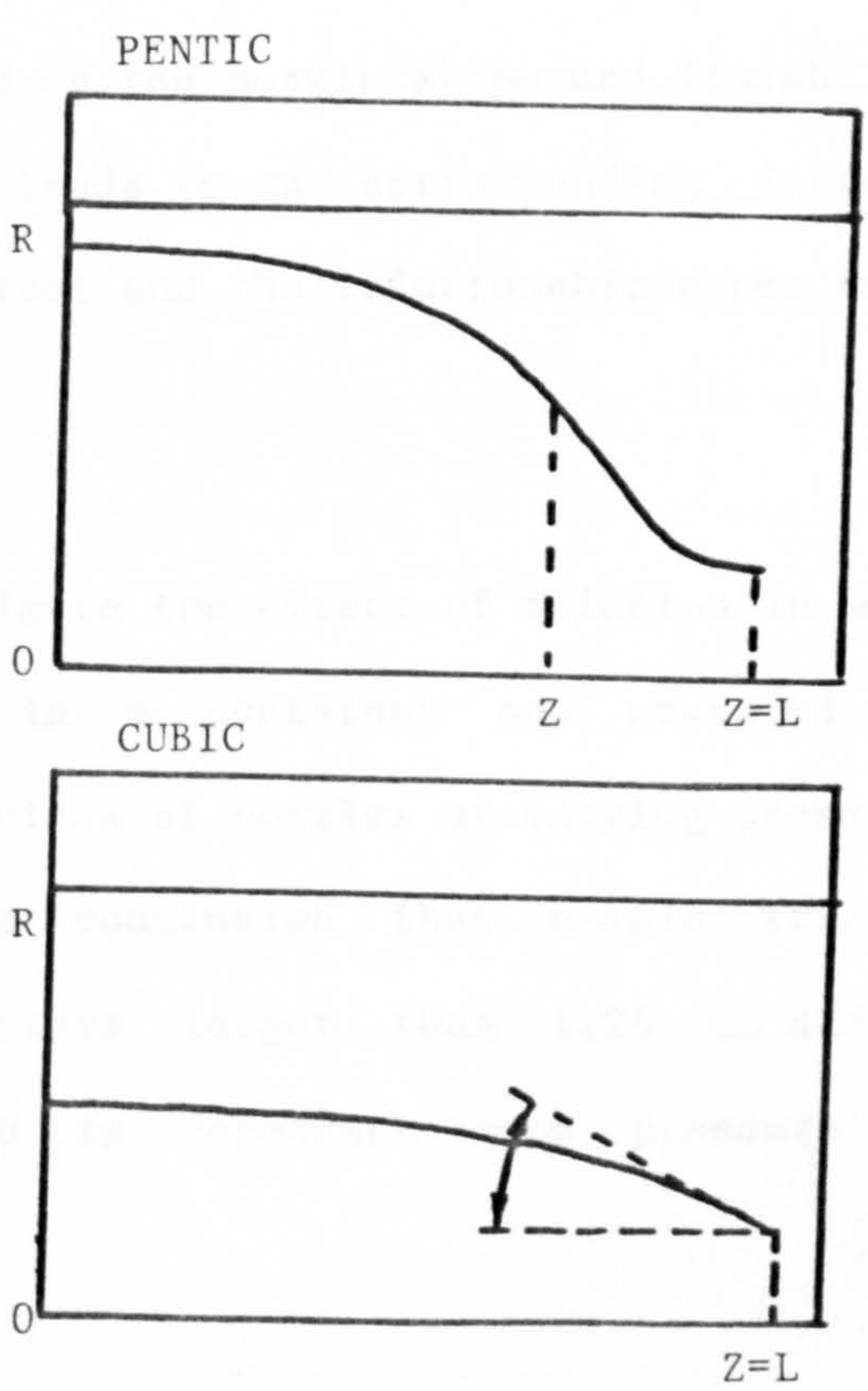

FIG.2.2.b - FOUR CLASSES OF NOZZLE SHAPES

(after Lohn and Brent)

power of pressure and the second power of volume most investigators generally have used smaller diameter nozzles.

Farmer and Attewell's results suggest that at particularly high pressures, the narrower jets give more efficient penetration on harder rocks. However, for softer rocks i.e. sandstones, the average rate of penetration is nearly directly proportional to the rate of flow irrespective of the nozzle diameter. One of the limitations of their experiments were that they used an intensifier with a fixed charge of water powered by air. Since the intensifier used a fixed charge and it was exhausted during each shot, there was no control over time and the higher pressures lasted less time than the lower pressures(112).

The findings of experimenters in some cases seem to contradict one another. This may be due to the different conditions of experimental set up (as described in one case) and on the nozzle shape and finish, but generally increase in nozzle diameter leads to an corresponding increase in penetration for a given pressure level and the relationship seems to be of approximately linear type.

Vereschagin et al,(159) to approximate the effect of friction in small nozzles, have collected the water in a container and measured its temperature after flow through four sizes of nozzles at varying pressures up to 2000 atm. They have drawn the conclusion that nozzle friction losses can be neglected for diameters larger than 1.25 mm and for pressures below 700 atmospheres, and is dependent upon pressure and

diameter. Bresee et al(17) have found minimum specific energy required for rock removal in their experiments where the nozzles have traversed over the samples of rock used. Their nozzles had 2,4,6 mm diameter and varied pressure up to 815 atm on sandstone, limestone and granite. Their results indicate that the values for specific energies did not vary from nozzle size to another.

In general, free jets dissipate by entrainment of air at the water-air interface, thus the ratio of surface to x-sectional area of a jet influences the rate at which a jet will dissipate. Since jet volume increases as the square of nozzle radius, while surface area increases linearly, smaller jets should dissipate in shorter distance than larger jets and decreasing nozzle size produces less penetration due to the reduced power output at the nozzle.

Nozzles have been fabricated from materials such as brass, tungsten carbide, specially treated steels such as hardened chromium-molybdenum alloy steel, maraging steel, 17-4 PH stainless steel with industrial diamond tips and saphire orifice jewels. The main criteria for choosing nozzle material is that it must not be eroded by the jet after long use and be cheap.

2.3.4 Stand-off Distance

The performance of the water jet at various stand-off distances is directly related to the properties of the jet. Russian investigators, Semerchan, Nikonov, Shavlovsky, Lyshevskii, Kuklin (134,86) all agree that a liquid jet of high velocity does not retain its original shape, but breaks up as the stand-off distance increases. They have divided the jet into three sections, namely initial section, basic section and dispersed section by measuring the variation in the magnitude of the axial dynamic pressure with increasing distance from the nozzle. These parts differ from each other not only in the nature of the change in dynamic pressure, but also in structural properties.

Following is taken from Nikonov's(106) paper :

"Immediately following emission from the nozzle and for some distance from it the jet preserves its own central nucleus and continuous with constant velocity. This portion of the jet is referred to as the initial section , and within its limits the axial dynamic pressures of the jet remain unchanged and equal to the emission pressure. Beyond the limits of the initial section of the jet the axial dynamic pressures gradually decrease according to a hyperbolic function. This occurs due to the gradual expansion and disruption of the jet, which initially occurs on the periphery, i.e. the boundary of the water and the surrounding air. The basic section of the jet is considered as the next length from tha nozzle over which there is no break in the flow and the jet remains coherent.

Finally at the greatest distance from the nozzle the dispersed section of the jet occurs, where the flow is a mixture of discrete elements of water and air over the whole section", (Figure 2.3)

The velocity decreases like described by Semerchan et al(134), both along the axis from the nozzle and away from the axis in the cross-section with a corresponding distribution in momentum and energy, (Figure 2.4).

The momentum of the jet is given by :

$$mv=pv^2 \quad \ldots\ldots\ldots(2.16)$$

and

$$v^2=2p/\rho \quad \ldots\ldots\ldots(2.17)$$

where m mass flow rate

v velocity of jet

ρ density of liquid

from the above 2 equations

$$mv=2p\rho \quad \ldots\ldots\ldots(2.18)$$

that is the momentum per unit time is directly proportional to the nozzle pressure.

Above named investigators have related the performance of the jet directly to the length of the initial section. Thus the coefficient of structure they named 'a' is given by a=l/d, where 'l' is the length of initial section and 'd' is nozzle diameter. At low pressures and large

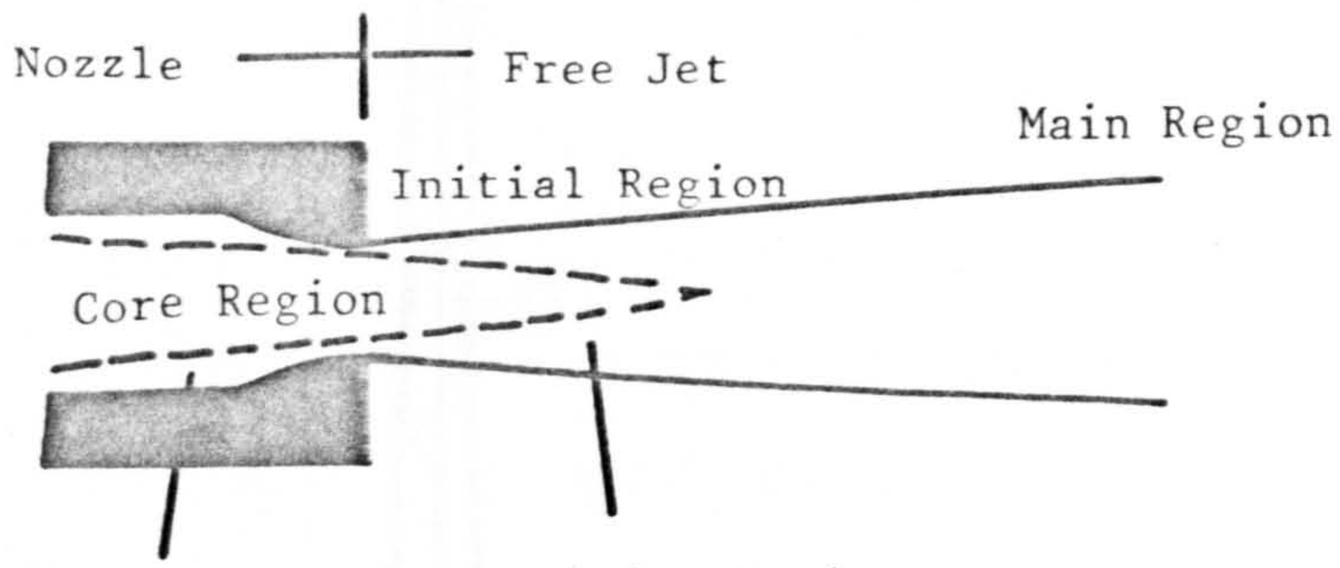

FLOW REGION in NOZZLE JET FLOW
(after Lohn and Brent)

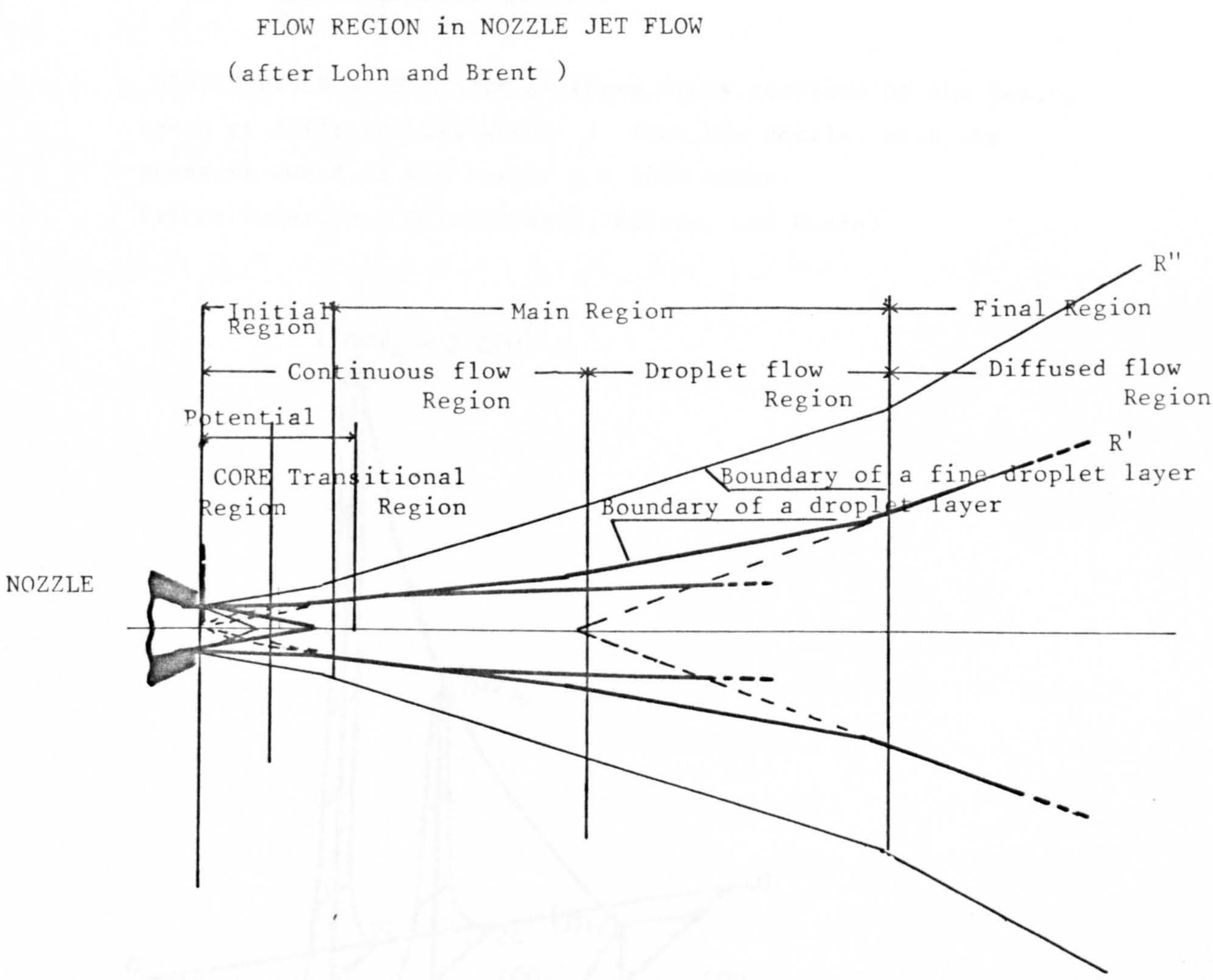

FIG. 2.3 — JET STRUCTURE (after Yanaida and Ohashi)

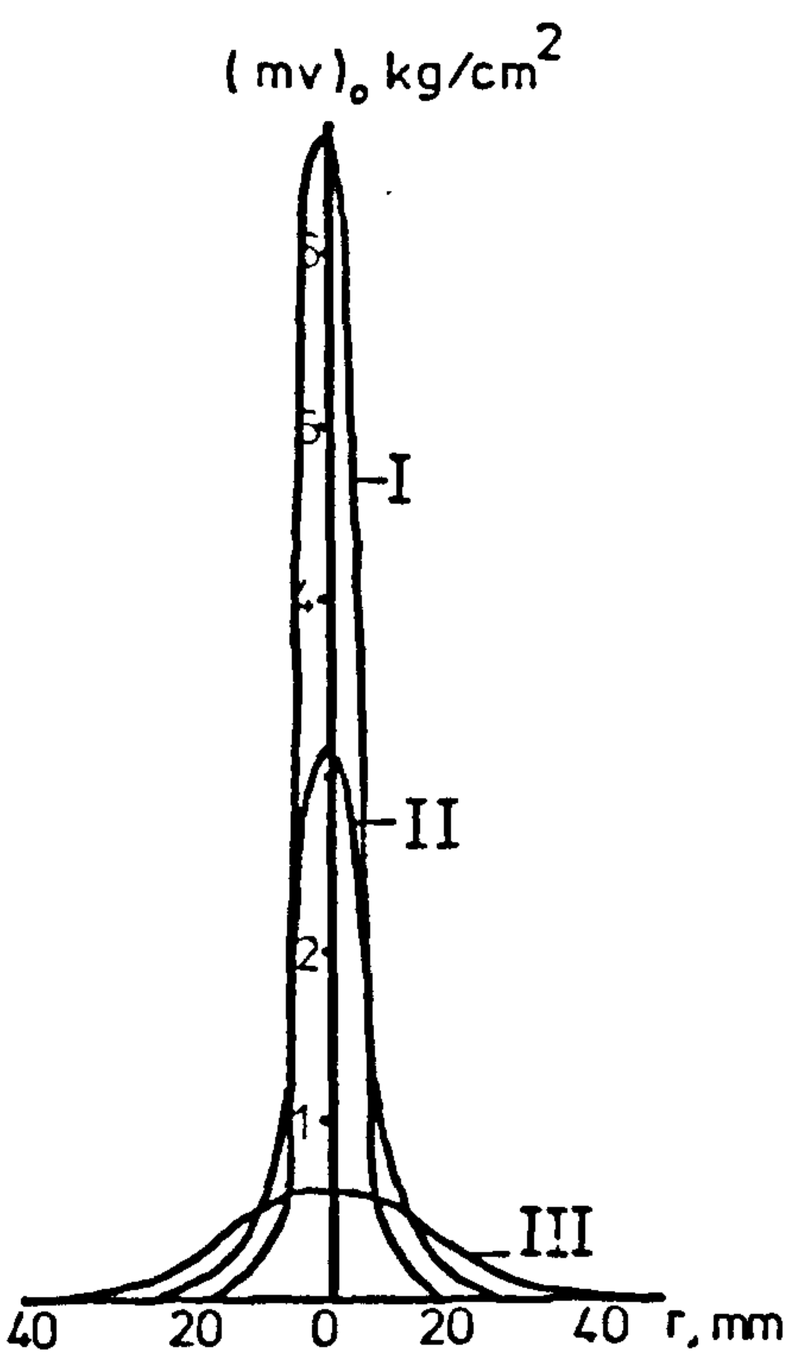

DISTRIBUTION of MOMENTUM at three cross sections of the jet, taken at different distances l from the nozzle, with the pressure ahead of the nozzle p = 1500 atmos.
(after Semerchan, Vereshchagin, Filler, and Kuzin)

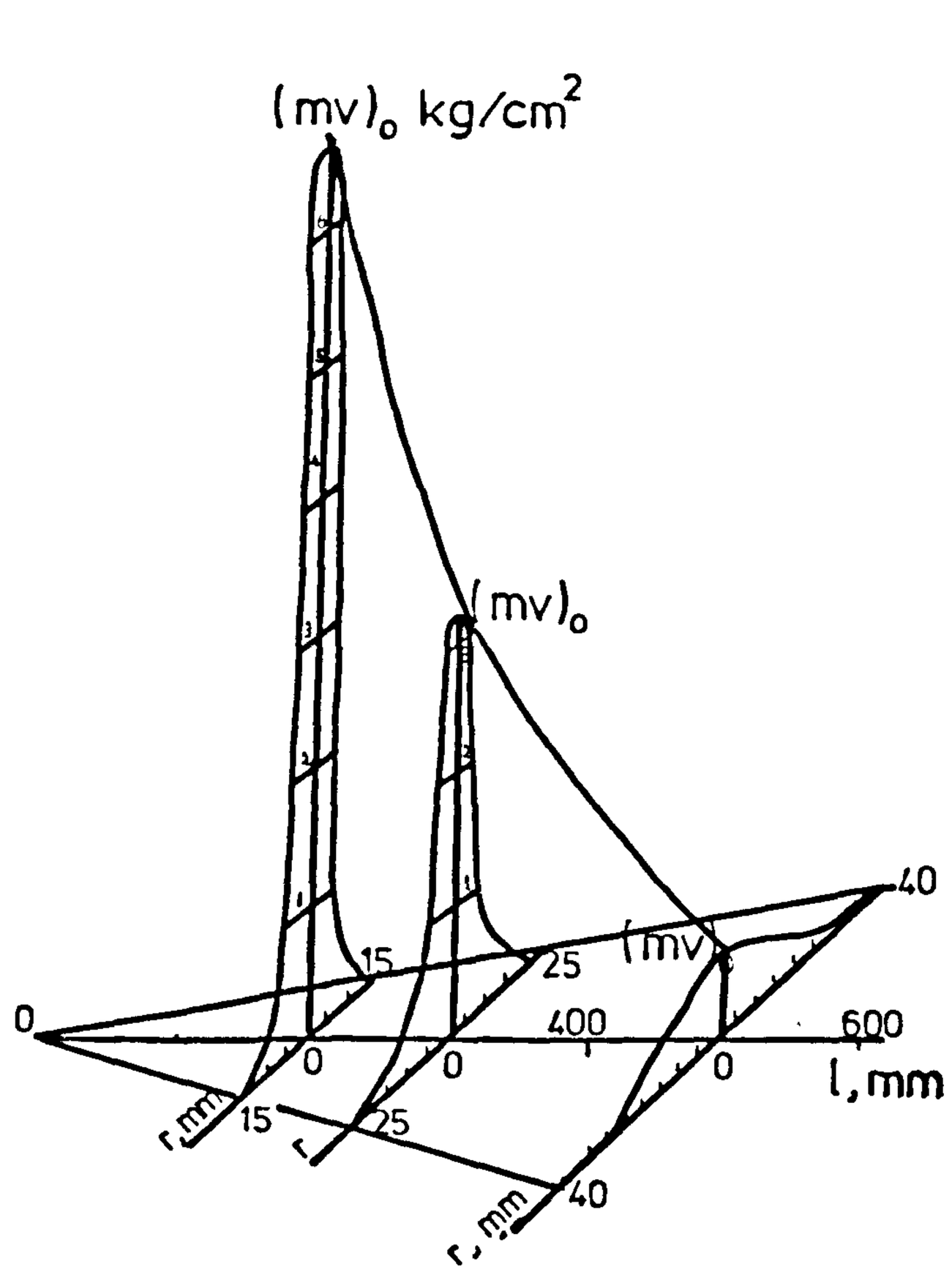

FIG. 2.4

nozzle diameters(50-200mm) Royer found that 'a' is approximately equal to a constant value 20.

Lyshevskii(86) postulated that the effect of the distance between rock and nozzle will show itself differently in each of the sections of the jet. In the initial region, the impact remains practically unchanged and penetration will be independent of stand-off. In the transition sector, the axial pressure of the jet is reduced with increased stand-off distance due to air friction and its expansion, hence the penetration will decrease with an increase in stand-off. But more complete description was given by Erdmann-Jesnitzer et al(38,39), and this will be discussed later.

Zelenin et al(170) states that the relationship between the slot depth and the stand-off distance obtained at pressures of up to 2000 atm show that the maximum slot depth corresponds to the minimum distance of nozzle from rock specimen. Farmer et al, takes this statement further by suggesting that greatest penetration occurs at zero stand-off. Nikonov et al(107), also favours the minimum nozzle-to-face distance.

For water jet cutting purposes it is not practicle to locate the nozzle as near to the face as suggested by above mentioned authors because it will be damaged by rock chippings, plugged with dirt etc. Leach et al, found that the pressure behind the nozzle can be applied to a target 100 nozzle diameters away without great losses (80% over). Matsumato(88) for underwater tests found the penetration decreases exponentially as the stand-off increases and for distances over 70 times nozzle diameter this

decrease is more abrupt. This approximately coincides with the relation given by Leach et al. On the other hand, Ostrovskii(110) in his experiments on a granite target both in air and in water found that the peak penetration is obtained with 55mm stand-off.

The relationship is of linear type between penetration and stand-off distance according to Hoshino's(59,60) data. Similar type of relationship was reported by Harris at al(57), when cutting Berea sandstone, but most of Harris's experimental data were either less than 20mm or more than 50mm with 0.008 in nozzle at 40000 psi pressure. Henneke's(9) graphs show a linear type of relationship with stand-off distance at three experimental levels of 25, 37.5, 50 mm with a nozzle diameter of 0.41 mm. Franz(50) concludes that for gypsum, the optimal stand-off distance for maximum penetration has no apparent relationship with pressure level and hence independent of velocity, but he noted optimum stand-off for ductile metals(Al,Cu). Matsumoto's(88) results suggest a power relationship when $10<s/d<55-100$ usually between 0.2 and 0.4 . Imanake's(68) data shows a variation of 'h' as the inverse square root of s/d. He thought that this effect is associated with the gradual disappearance of the central core of the jet by turbulent mixing. At stand-off ratios about 70 to 300 the jet pressure drops more rapidly with distance and slot depth varies inversely with the stand-off ratio to a power of 0.5 to 0.1 or more. Hence, the general concensus of reports of investigators is that most effective cutting is achieved at small stand-off ratios between 7 and 70.

2.3.5 Additives

The reduced efficiency and effectiveness of high pressure-high velocity waterjets with increased stand-off distance was mentioned in previous section. It becomes a problem to generate coherent, efficient cutting jets with increased velocities. One approach to improve performance is by altering the properties of the working fluid. It has been found that at very high velocities fluid properties such as viscosity, density and surface tension have small effect on jet characteristics(82).

The viscosity effects were examined by Semerchan(134), Leach and Walker(82). As a working fluid Semerchan used water with 10%, 20%, 30% mixtures of glycerin and measured the momentum of jets, which he used as criteria of performance, by displacement of pendulum. He found that there was a smaller decrease in force when liquids of higher viscosities were used and came to the conlusion that the viscosity of the glycerine mixture decreases more rapidly with an increase in stagnation pressure and temperature than with water. This, he said, should increase the permeation rate in permeable materials and enhance erosion more significantly for the glycerine mixture than for water as pressure is increased. Leach et al, used the solution of sodium carboxymethyl cellulose and found it improved performance over long distances from the nozzle. Similar conclusion was reported by Harris who found additional 0.25% sodium carboxymethyl cellulose increased the viscosity of the water from 1.0 to 6.0 centipose, also increased the useful length of the jet by 50%. Leach et al, later used detergent to alter the Weber number of the

fluid and obtained improved performance to distances greater than about 250 nozzle diameters.

Long chain water soluble polymers - such as Polyethylene Oxide(Polyox) can also be used in amounts that yield solutions of substantially greater viscosity at low shear rates than the solvent fluid, i.e. water alone. Detailed analysis on effects of Polyox was done by Sims et al(140). One of the properties of Polyox is that it is a high polymer resin and has long unbranched chain molecules. The significant effect of this property, Sims et al, found was that the addition of the Polyox reduced the drag by up to 40%. Since friction drag is reduced, these polymer solution streams will have an initial velocity greater than that of pure water therefore resulting in higher impact pressures and higher coefficients of discharge he concluded. Summers et al(147), used a concentration of 0.01% Polyox and found that it improved the coefficient of discharge by approximately 6% and also increased the penetration rate of jet by a similar amount. Fourfold increase in the useful length of the jet was reported by Harris with addition of Polyox and Thorne et al(155), states "use of 30 ppm of Polyox erased turbulances and jet assumed the appearance of a smooth glass rod" when investigating for ways of improving the performance of nozzles for fire fighting applications.

Both synthetic and natural long chain molecules have been found effective in improving jet characteristics and performance. Franz(50) recommends the molecular weights between about 10,000 and 7,000,000. Essentially he says, linear molecules, not substantially cross linked to

adjacent molecules are most suitable, although there may be branching within individual chains. Franz found that addition of long chain polymers easily doubles the depth of cut at the optimum stand-off distance observed for plain water on the aluminum samples.

The drawback of Polyox was reported that its effect is reduced by shear which would be induced by the initial mixing, by pumping and any transmission down pipelines(112). Also, the higher the pressure the greater will be the shear so that it is likely that at the very high pressures the effects of Polyox might be greatly reduced.

Baumann et al(9), summed up the advantages of using high molecular liquid polymers "which in low concenrations will substantially increase the viscosity of water. In conjunction with a supplementary lubricating effect brought about by the presence of certain hydrocarbon components beneficial effects expected may include the reduction of the frictional resistance, increase of the flow speed, less wear of the material, less mist formation, improved energy utilization and narrower confinement of the water jet. By using additives in the water jet either the cutting depth was increased up to 70% or pressure reductions up to 40% was obtained".

2.3.6 Number of Jet Passes

The aim of water jet cutting is to make deeper penetrations while minimizing the energy expended per unit area of cut. Deeper penetrations can be achieved by increasing the diameter of the nozzle, as mentioned before, or using several smaller diameter jets in tandem. Since increasing nozzle diameter by, for example, a factor of two to achieve deep penetration causes volumetric flow to increase by a factor of four and the power by similar amount, it may be advantageous to multiply the jets, assuming they do not interfere, rather than to increase the diameter until the advantage is killed off by increased stand-off distance.

Zelenin et al(170), when experimenting on hard rocks found that with repeated passes of the water jet over the same slot, penetration rate decrease gradually. He stated that use of multiple jets is more advantageous for hard rocks i.e. granite than limestone.

Although minimizing energy expended favours the use of small diameter nozzles, because average slot width is about three times the nozzle diameter, the ultimate penetration will be limited because it is dependent on the nozzle diameter. Chermensky(146) reported that after two passes the penetration was about 30% higher than the penetration for an equal energy single pass(i.e. single pass at half the traverse speed) and after three passes the penetration was about 70% higher than the penetration for an equal energy single pass(single pass at one-third the traverse speed). He concluded that high speed multiple passes yield a greater penetration

than a single equal energy low speed traverse.

Summers's(145) results indicate that the jet becomes increasingly inefficient with increasing pass number. Similar conclusion was drawn by Crow that the effects of multiple passes decreases with increasing slot depth and only a limited depth can be achieved for a given cutting conditions.

2.4 WATER JET ASSISTED CUTTING

Several research projects have been carried out in Japan, U.S.A and W.Germany into water jet assisted disk cutting(59,162,9) and in S.Africa and U.K. into water jet assisted drag tool cutting. Hood(63) found out that force acting on a drag bit, when cutting strong rock, can be reduced by directing a high pressure water jet immediately ahead of the bit and reported a two fold increase in depth of cut when the jet position was optimized. Wang et al(162,164) and Henneke et al(9) experimented with water jet assisted disk cutting when mounted on a full-face tunnelling machine with jets positioned at various locations. 2-3 times increase in the penetration rate with water jet assisted cutting was reported by Wang et al (162). Plumpton et al(6) augmented a partial-face roadheader with high pressure water jets and reported 50%, 30% reductions in normal and cutting forces.

Although promising results have been reported by these researchers, none of them has adopted a systematic approach into principles of water jet assisted cutting, therefore could not explain some of their findings and in some cases it was reported that their results were not reproducable.

3 EXPERIMENTAL SET-UP AND APPARATUS

3.1 DESIGN OF TOOL HOLDERS AND TOOLS FOR POINT ATTACK CUTTING

The tool holder used for the normal cutting and high pressure water jet assisted cutting experiments was designed and used by the author previously(152,153).

The tool holder was made of tool steel and its specifications are shown in (Figure 3.1). This had a 6.5 degrees off-set angle and a 45 degrees angle of attack. Previous research has indicated that of the 0, 6.5, 13 degrees off-set angles tested 6.5 degrees gave the best results in terms of tool forces, yield and mechanical specific energy,(Plate 1).

Commercially available cutting tools were used for these experiments though the length of the as supplied tools was reduced to cut down the bending moment experienced by the plate dynamometer,(Plate 1).

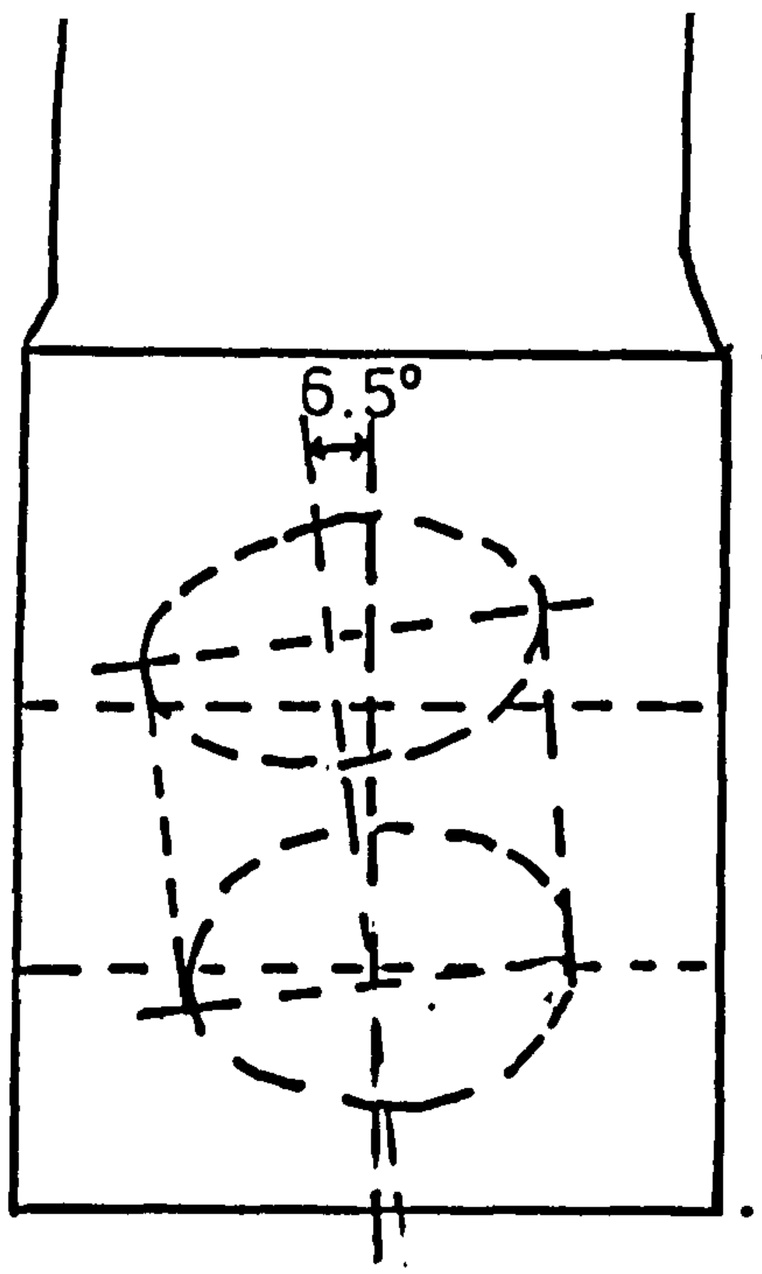

REAR VIEW

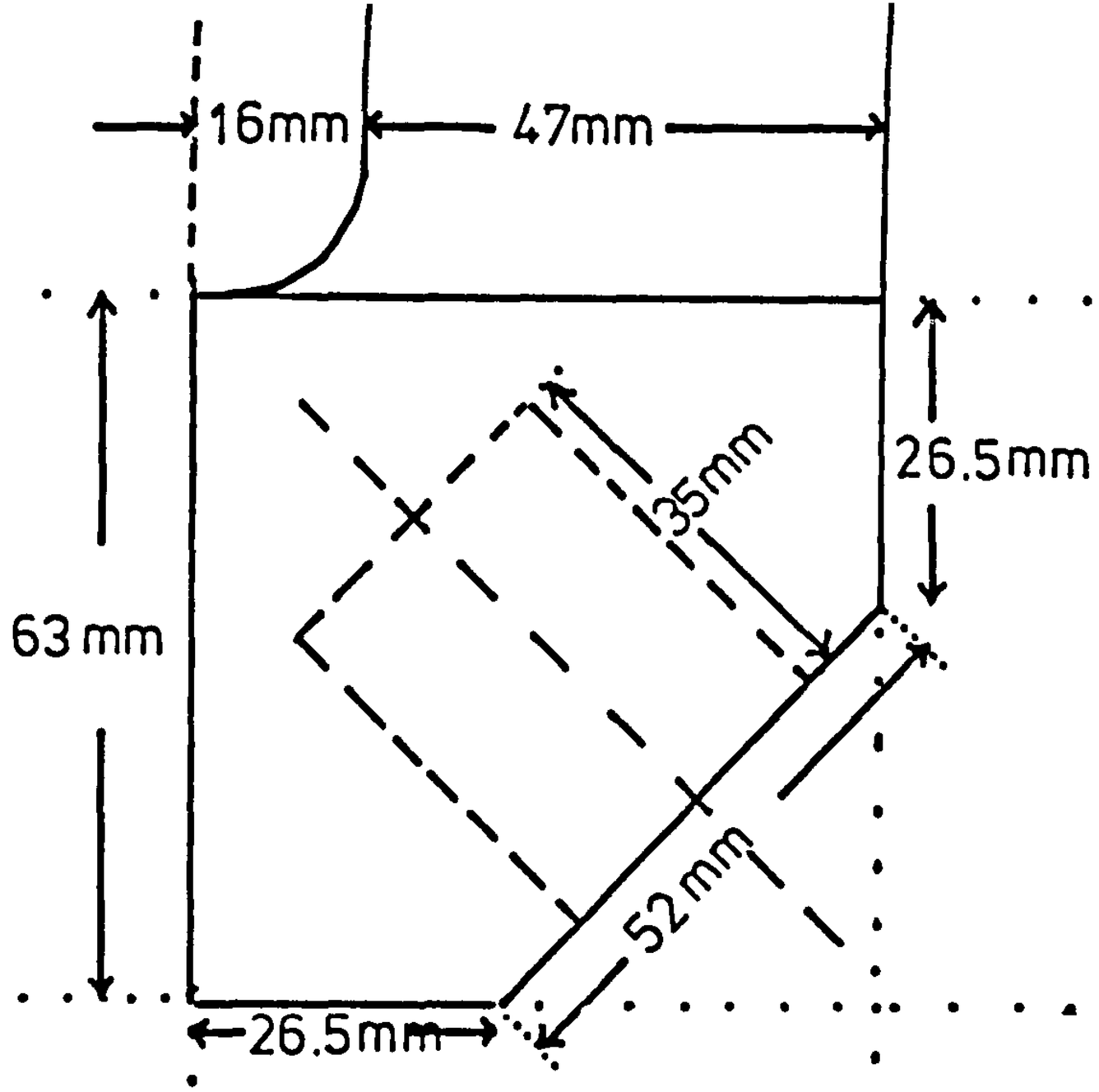

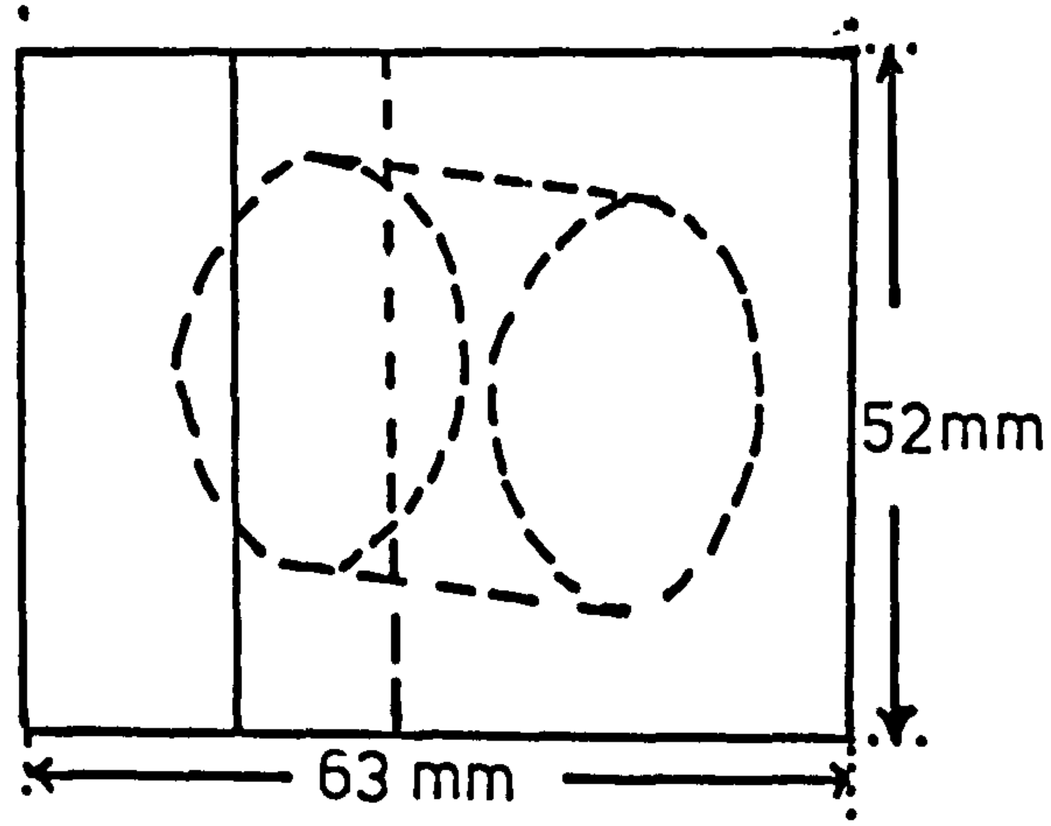

PLAN

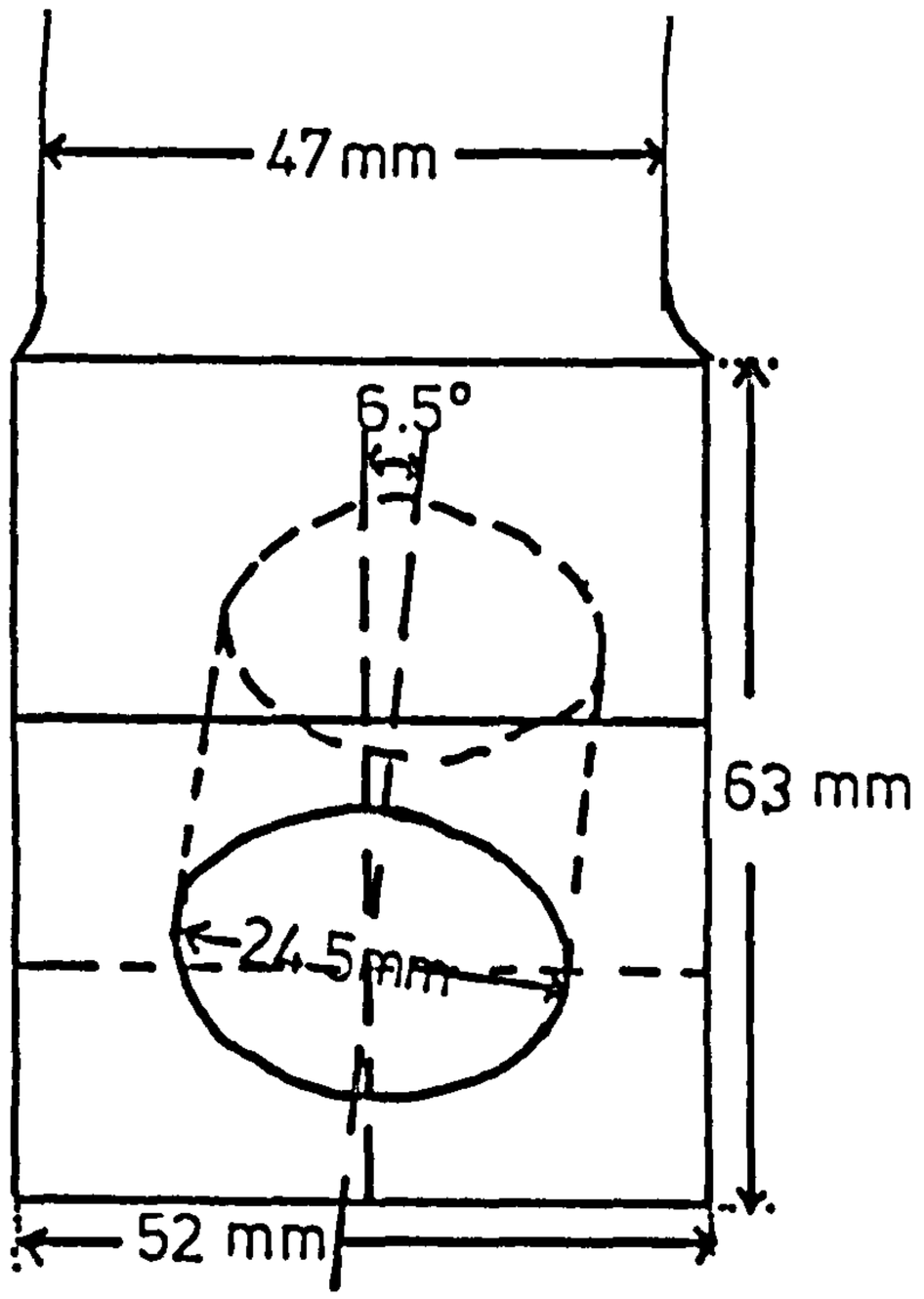

FRONT VIEW

FIG. 3.1 – GEOMETRY OF THE TOOL HOLDER WITH 6.5 OFF-SET ANGLE

DRAWN BY : - ORHAN TECEN

Tool Holders

PLATE 1 - Cutting Tools

3.2 PUMPING SYSTEM

The pump used for the high pressure water jet assisted cutting was a Uraca three piston, positive displacement pump, powered by a continuously rated 30 horsepower electric motor, and delivered 8.62 l/min at a pressure of 48.28 MPa through a nozzle of 0.85 mm exit diameter.

High pressure piping used for water jet cutting can be divided into two classes. Rigid steel piping and flexible piping. Steel high pressure pipe which was mounted on the cutting head of the shaping machine had a 3.175 mm internal diameter and could operate safely at 69 MPa continuous working pressure. The first of the flexible hoses connected the steel pipe to the pump and allowed the movement of the cutting head. This also had a 3.175 mm internal diameter and 69 MPa static working pressure. The second high pressure flexible tubing connected the pump to the water tank and had 9.525 mm internal diameter. This was Synflex super high pressure hose series 3R10 with a static working pressure of 68.97 MPa with a minimum burst pressure of 206.9 MPa. Low pressure steel piping connected the water tank to the pump, (Figure 3.2).

When the pump was put into operation it drew the water from the tank via low pressure piping system. The pump then delivered the water into a manifold in which a 110.35MPa Bourdon Tube type gauge monitored the pressure. The maximum operating pressure of the pump was 68.97 MPa since this was the maximum safe working pressure of the system fitted to the manifold. The pressurised water passed through the manifold and divided

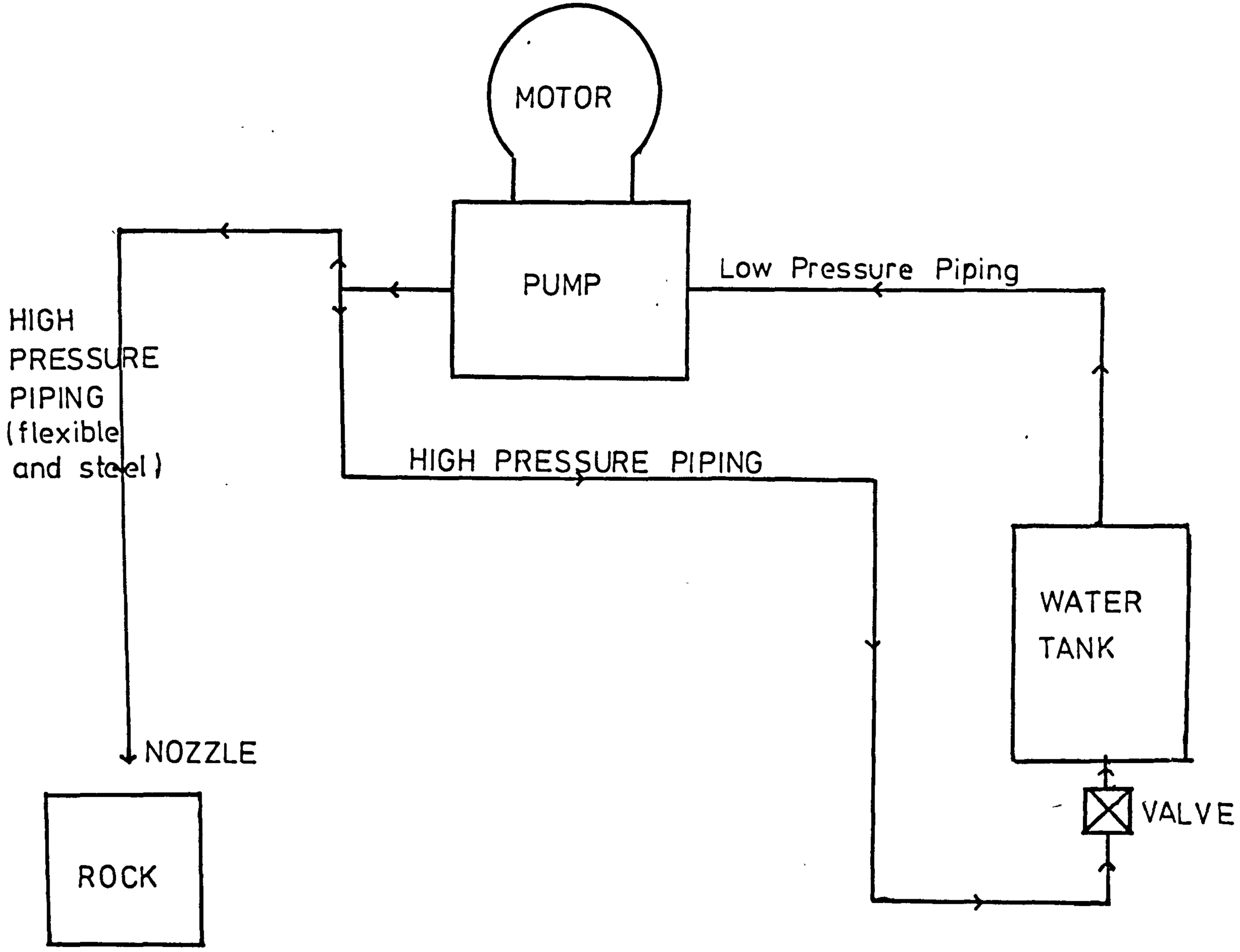
MOTOR
PUMP
Low Pressure Piping
HIGH
PRESSURE
PIPING
(flexible
and steel)
HIGH PRESSURE PIPING
WATER
TANK
VALVE
NOZZLE
ROCK

into two. One section of the water went through the 3.175 mm internal diameter high pressure piping system to the nozzle, and the remainder went through the 9.525 mm internal diameter high pressure piping system back into the water tank. To provide control of the operating pressure a high pressure rated bleed-off valve was incorporated into the system and provided a by-pass back into the supply tank. All the couplings used were high pressure type Ermeto couplings.

3.2.1 Nozzles

Nikonov type nozzles which had 13 degrees contraction angle followed by a nozzle straight section of 3 times the nozzle exit diameter were used for the jet cutting experiments. These were made of silver steel and oil hardened to prevent britleness. Manufacturing of the nozzles were carried out in the Department of Mechanical Engineering in the University of Newcastle upon Tyne on a spark erosion machine,(Plate 2).

3.3 NOZZLE CARRIAGE ASSEMBLY AND JET POSITIONING

A nozzle-carriage assembly was designed to allow the movement of the nozzle up and down with respect to the rock surface, forward and back and sideways with respect to the point attack tool tip.

PLATE 2 - Water Jet Nozzles

Two shafts "Parts A" were attached to the cutting head. "Parts B" could move along these two shafts and by using "Parts C" the lead-on distance could accurately be set. "Part D" which rigidly held the high pressure steel piping tube, at the end of which the nozzle was attached to could move along "Part B",(Plate 3). As can be seen from (Plate 4), the sideways movement of the pipe can be set and then by tightening "Nut 1" it can be rigidly kept in position. The stand-off distance is set by using the distance pieces, (Plate 5). "Part E" is brought down to rest on the "Part B" and 2 Allen screws are tightened so that the pipe did not move up and down while other adjustments were made to the nozzle position. Exploded view of the whole assembly is shown in (Plate 3a), and assembled view in (Plate 3b). Distance pieces and spacers are shown in (Plate 5). The end of the nozzle was shaped like a pipe olive, therefore it did not need additional sealing. The nozzle was kept in place by tightening the "Nut 2" against "Nut 3".

3.4 THE ROCK CUTTING RIG

A modified shaping machine which had a forward stroke of 800 mm was used in the cutting experiments. A maximum in-line thrust force of 5 tonnes could be provided by the machine. A rock specimen of 500mmx500mmx300mm in size could be accommodated on the machine table and lowered and laterally traversed with respect to the cutting tool, (Plate 6).

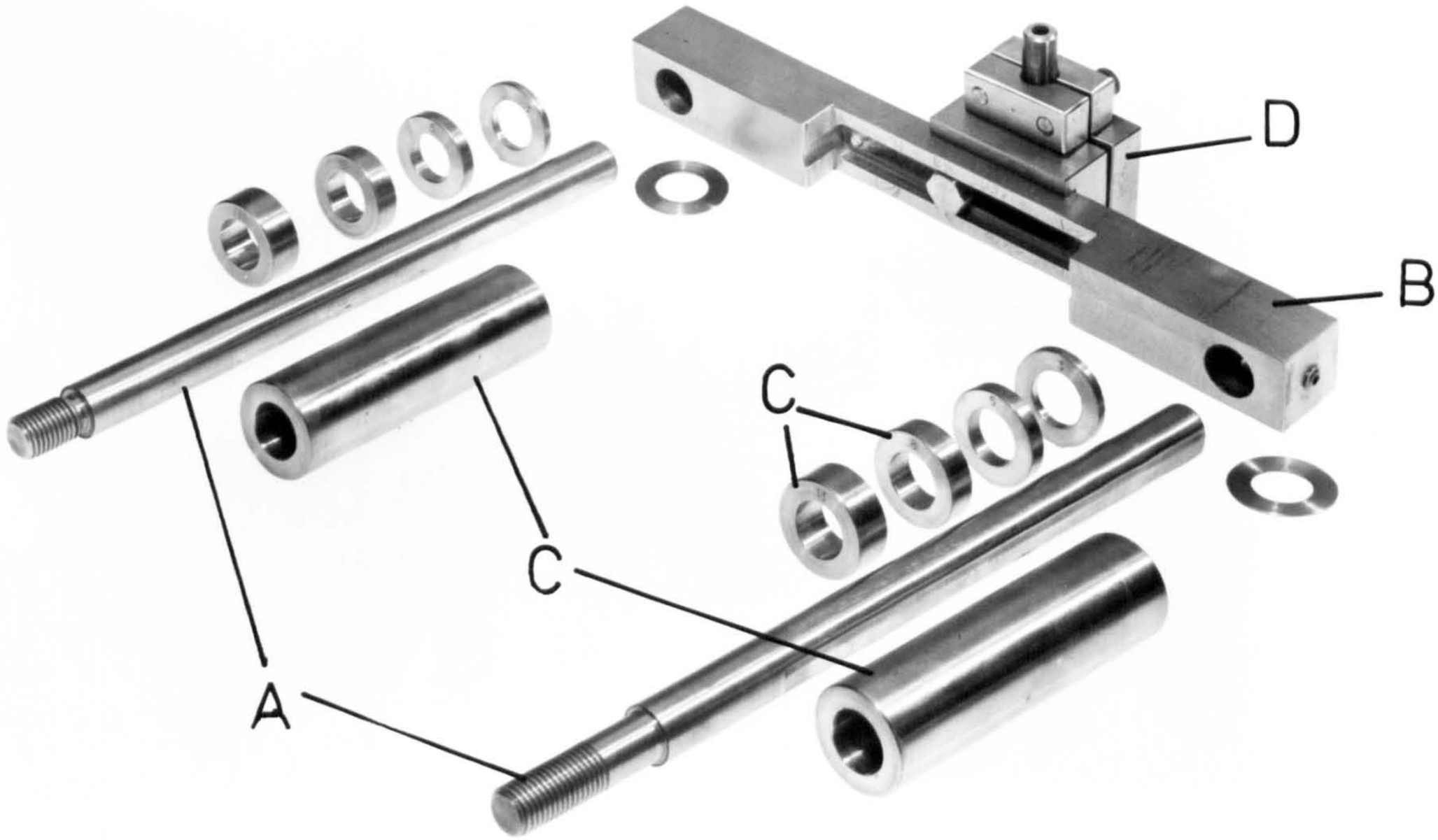

Nozzle Carriage Assembly

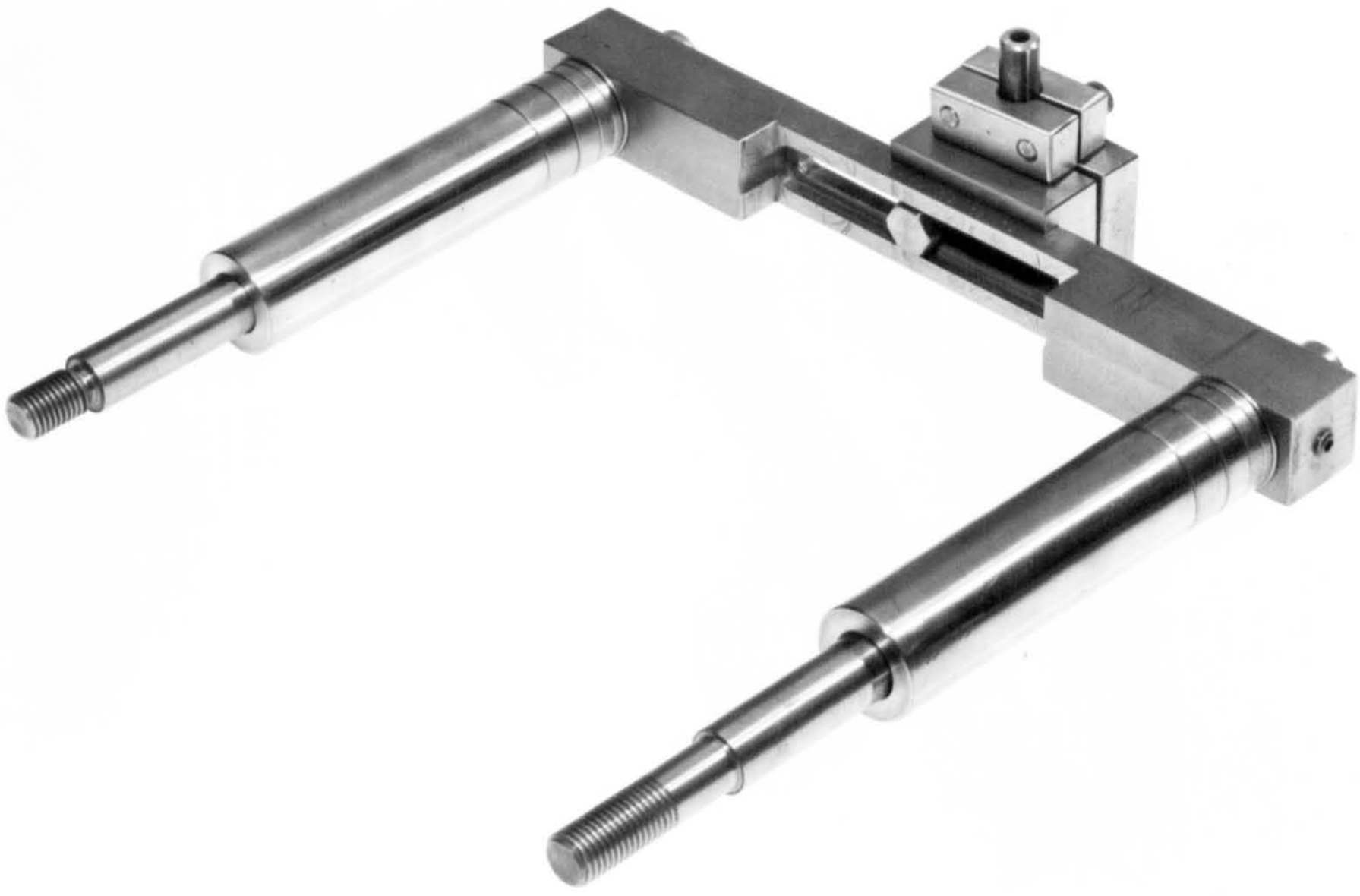

PLATE 3

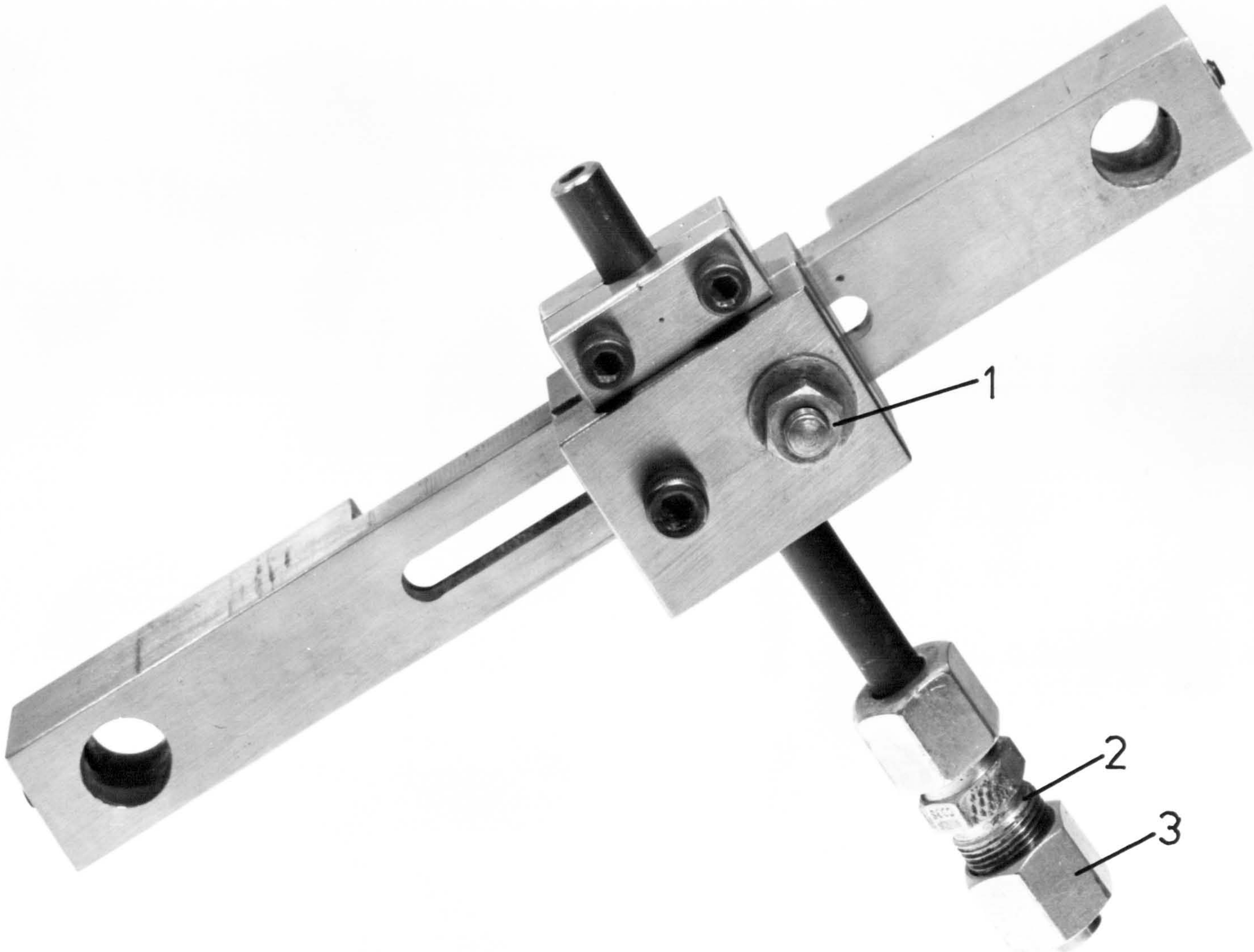

PLATE 4 – Nozzle Holder

PLATE 5 - Lead-on Distance Spacers

PLATE 6 – Hybrid Cutting Room

The rigid piping system travelled over the bridges installed at three locations on the cutting head and was restricted from moving freely by two bars and two collars. Up and down movement was restricted by tightening the two bars, and sideways movement by tightening the Allen screws on the two collars.

3.5 EXPERIMENTAL VARIABLES FOR HIGH PRESSURE WATERJET ASSISTED CUTTING

The number of variables which were considered important when cutting rocks with high pressure water jet assisted point attack tools may be divided into three categories once a choice is made on the type of point attack tool in terms of its tip angle, angle of attack, offset-angle(which is the angle tool makes in its tool holder with respect to cutting direction), and on the nozzle parameters e.g. nozzle internal profile, contraction angle, surface finish.

The choice on the point attack tools were made taking authors past experience in cutting rocks with point attack tools into consideration. The off-set angle chosen was 6.5 degrees, tip angle 87 degrees, angle of attack 45 degrees, (Figure 3.3).

The decision on the nozzle was made after a review of the literature available and the reported experiences of other researchers. This was investigated extensively and has been reviewed in (Chapter 2).

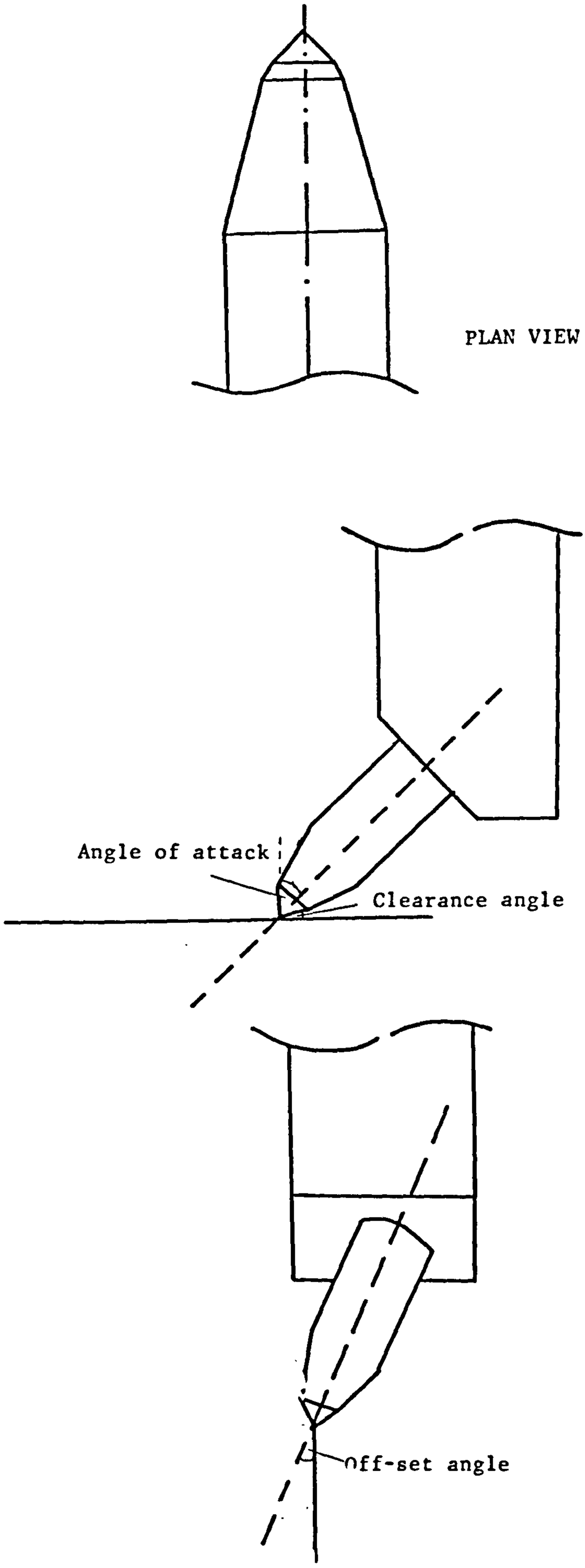

FIG. 3.3

The variables considered were, (Figure 3.4) :

1. Mechanical Tool Variable .....depth of cut

2. Water Jet Variables

   a. Operational variables .....water jet pressure
   .....traverse speed
   .....number of passes

   b. Positional variables .....stand-off distance
   .....lead-on distance
   .....side-off distance

   c. Nozzle variables .....nozzle exit diameter

3. Rock Variables .....physical and mechanical properties(compressive, tensile, triaxial strengths, porosity, hardness, density)

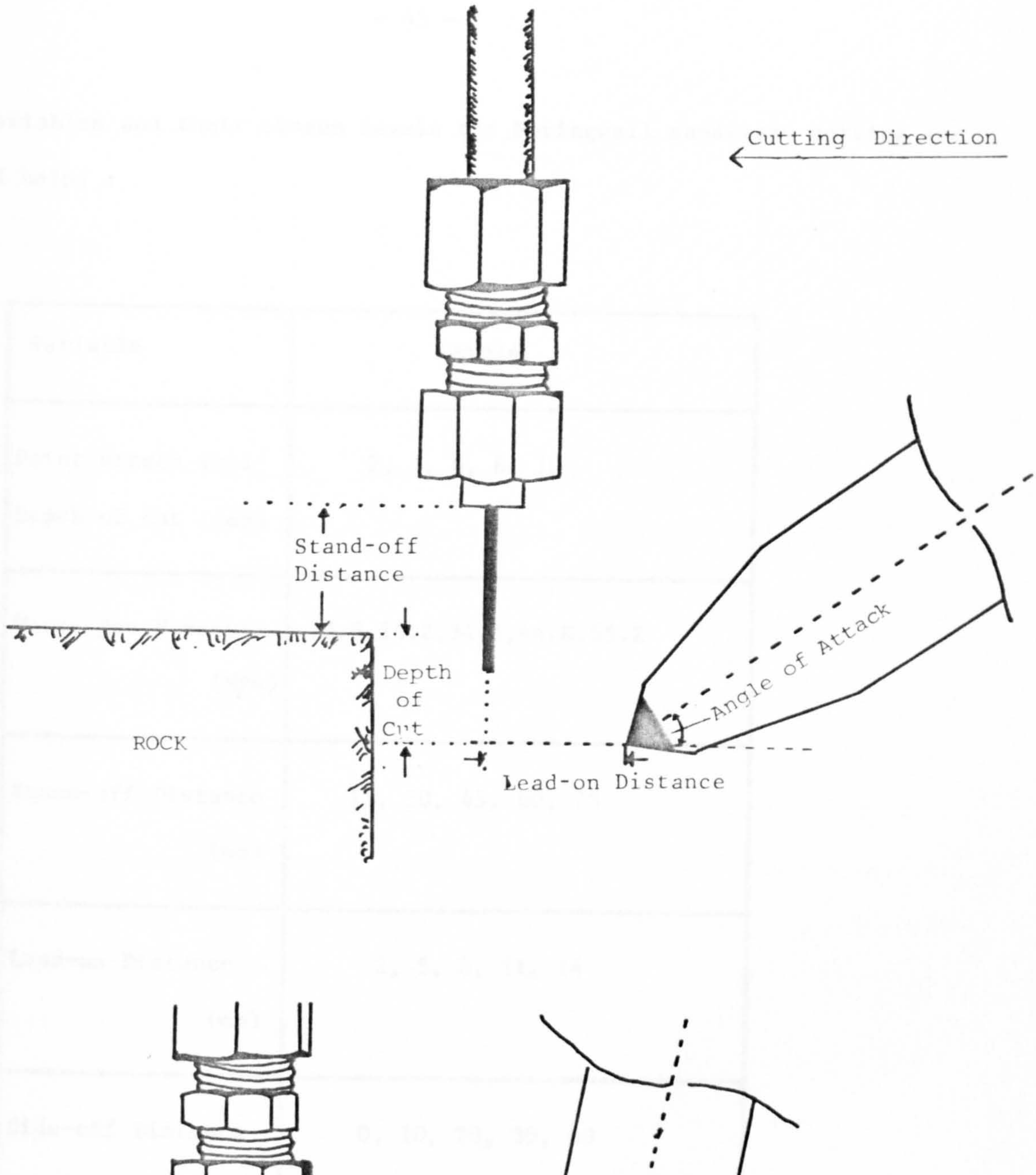
Cutting Direction
Stand-off Distance
Depth of Cut
ROCK
Angle of Attack
Lead-on Distance
Cutting Towards The Viewer
Off-set Angle
Side-off Distance

FIG. 3.4

The variables and their chosen levels for Springwell sandstone cutting are listed below :

Variable	Levels
Point attack tool Depth of cut (mm)	2, 4, 6, 8, 10
Water jet Pressure (MPa)	13.8,24.2,34.5,44.8,55.2
Stand-off Distance (mm)	15, 30, 45, 60, 75
Lead-on Distance (mm)	2, 5, 8, 11, 14
Side-off Distance (mm)	0, 10, 20, 30, 40
Nozzle Diameter (mm)	0.6, 0.85, 1.1
Cutting Speed (m/min)	3.67, 5.97, 7.22, 10.04, 13.0

Number of Jet Passes	1, 2, 3, 4, 5

The first 5 variables were taken and a partial Latin square experimental design was planned to investigate the effects of each change in nozzle positional variables to arrive at an optimal nozzle position.

The effects of other variables were investigated later on but not by partial Latin square design. Because it requires the same number of levels of each variable to be taken into consideration and to find a reasonable empirical formulae they had to have more than 4 levels. Furthermore, they must change in arithmetic progression to simplfy analysis.

3.6 PARAMETERS TO BE MEASURED AND CALCULATED

The measured and calculated parameters obtained for each experimental cut were as follows :

Mean Cutting Force(MCF)

Average force acting on the tool in the direction of cutting. This force multiplied by the distance cut gives the amount of work done.

Mean Peak Cutting Force(MPCF)

The average of the peak forces acting on the tool in the direction of the cutting. This is relevant to the mechanical strength of the tool and its holder.

Mean Normal Force(MNF)

The average forces tending to push the tool out of the rock. This value is the thrust required to maintain the tool at its required depth of cut.

Mean Peak Normal Force(MPNF, PNF)

The average of the peaks and highest peak of the normal forces

Mean Peak Sideways Force(MPSF)

The average of the peak values of the transient force acting horizontally and perpendicular to the direction of cutting.

Yield(Q)

The mass(or volume) of debris produced by a unit length of cut.

Mechanical Specific Energy(S.E)

The work done per unit mass(or volume) of rock cut by the mechanical tool.

Water-Jet Penetration Depth

The depth to which high pressure water jet has penetrated the rock surface.

Hydraulic Specific Energy

The work done per unit mass(or volume) of rock cut by the water jet.

3.7 PARAMETER MEASUREMENTS

3.7.1 Triaxial Dynamometer and Data Recording System

The magnitude and direction of the force acting on the tool during cutting is measured by a specifically designed instrument referred to as the triaxial dynamometer. Electrical signals generated by the dynamometer are amplified and recorded. The dynamometer is attached to the shaping machine cross-head and the tool-holder to which the tool under test is inserted was rigidly fixed to the central plate of the dynamometer.

The dynamometer resolves a generalized dynamic cutting force into its three mutually perpendicular components. These are the cutting force in the direction of cutting, the normal force which acts vertically on the tool and the sideways force (Fig 3.5). The strains induced by these forces are detected by strain gauges arranged in three bridges on beams which support the tool holder. More detailed information on dynamometer design and manufacture had been dealt with in references(33,61,108). The three bridge circuits are supplied with a A.C voltage and the small output from the bridge is amplified and fed continuously to a U.V recorder. The dynamic signals of each bridge are electronically integrated simultaneously and the output from the circuits is also fed to the U.V recorder.

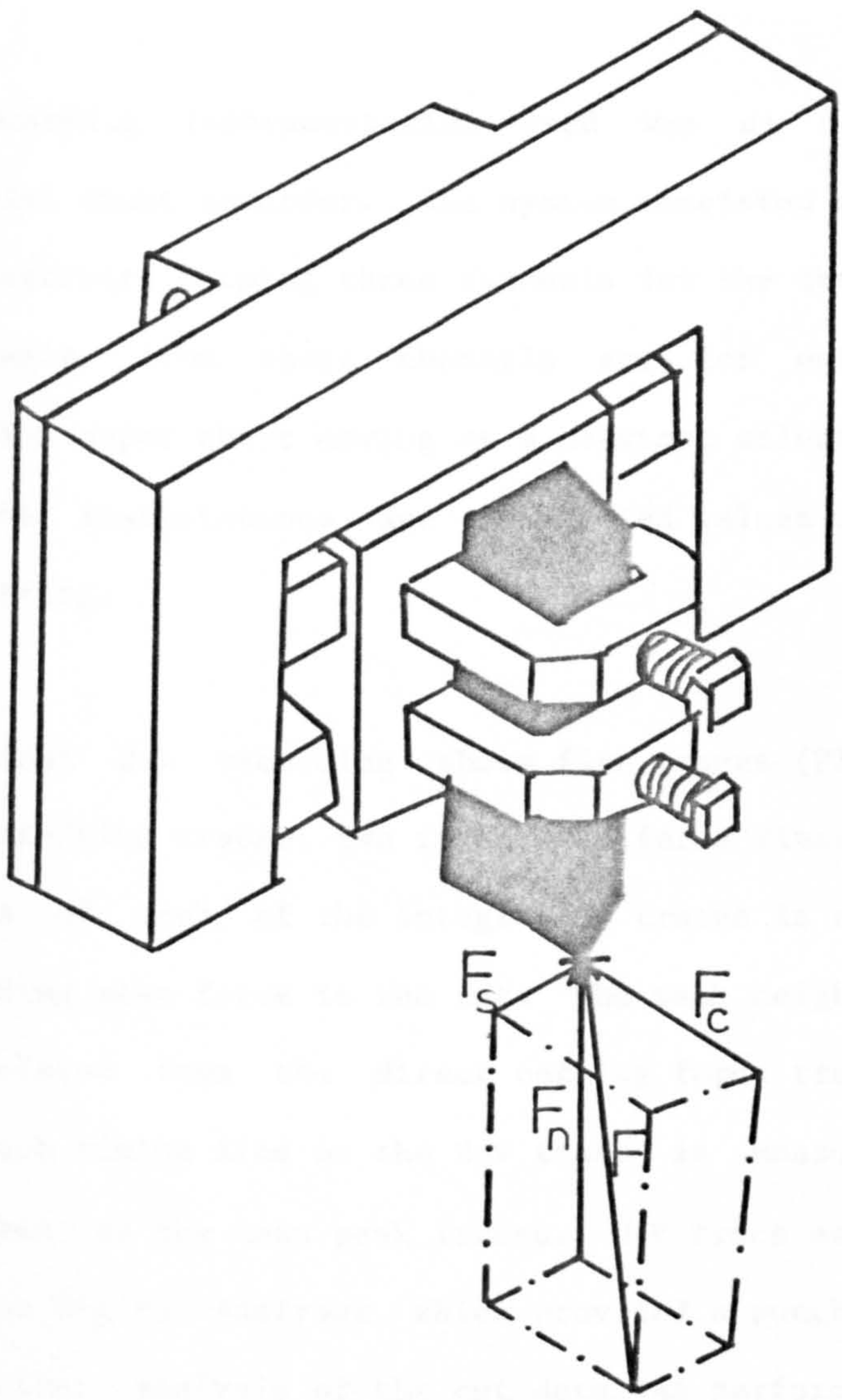

FIG. 3.5 – CUTTING TOOL DYNAMOMETER

Showing Resolution of Force

The recording instrumentation used was an SE4000 system with an Ultra-Violet chart recorder. The system consisted of three amplifiers and three integrators forming three channels for the three respective forces. The signals from these channels are fed onto the U.V sensitive photographic paper chart moving at a constant selected speed. This chart showed the instantaneous and integrated values of the forces generated during cutting.

A typical U.V recording shows five traces (Plate 9). These are two direct force/time traces, two integrated force lines and a reference line. The slope of each of the integration traces is a direct measure of the corresponding mean force in the cut. The peak height and mean peak height are calculated from the direct cutting force traces. The highest peak between each timing line on the U.V trace is measured and the average value taken as the mean peak forces. U.V trace analysis was carried out using D-Mac Digital Analyser, which provided a punched card deck for each cut. Further analysis of the cut data was performed on the University's IBM 360/370 computer system.

3.7.2 Calibration of The Dynamometer

The dynamometer calibration was carried out by analysing the traces obtained during the application of incremental loads of known values by a hydraulic ram, (Plate 7).

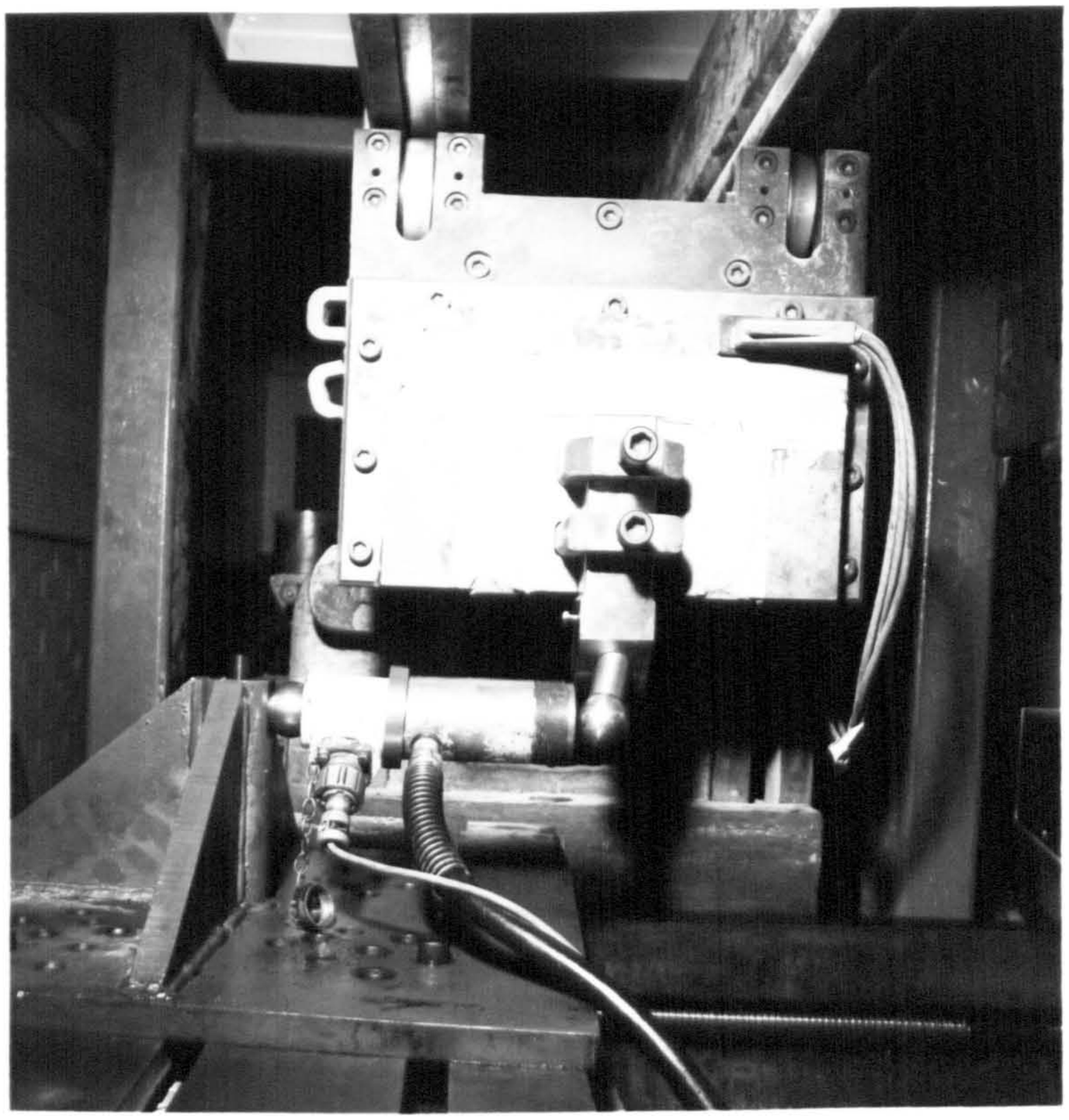

Calibration along Sideways Direction

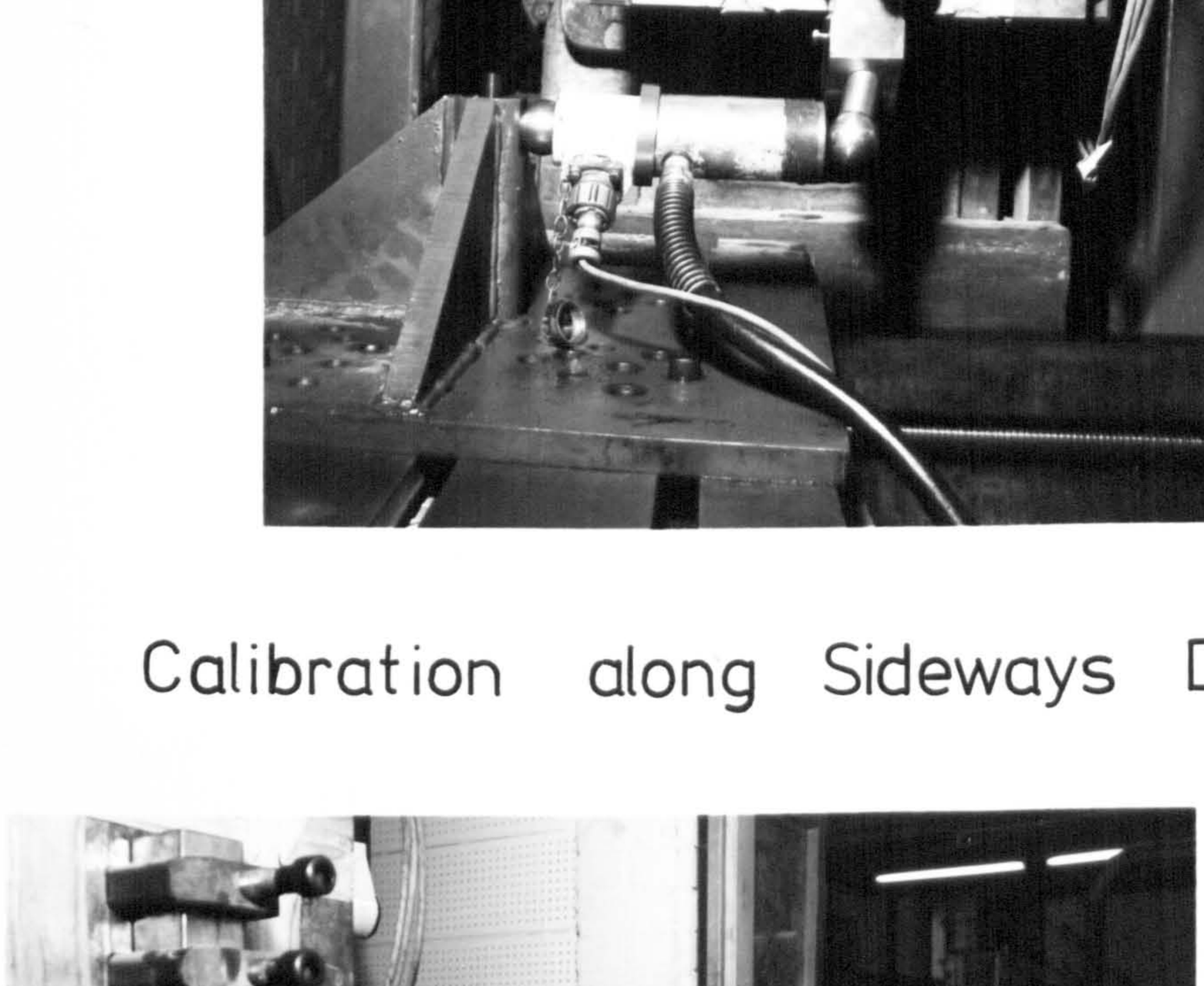

PLATE 7

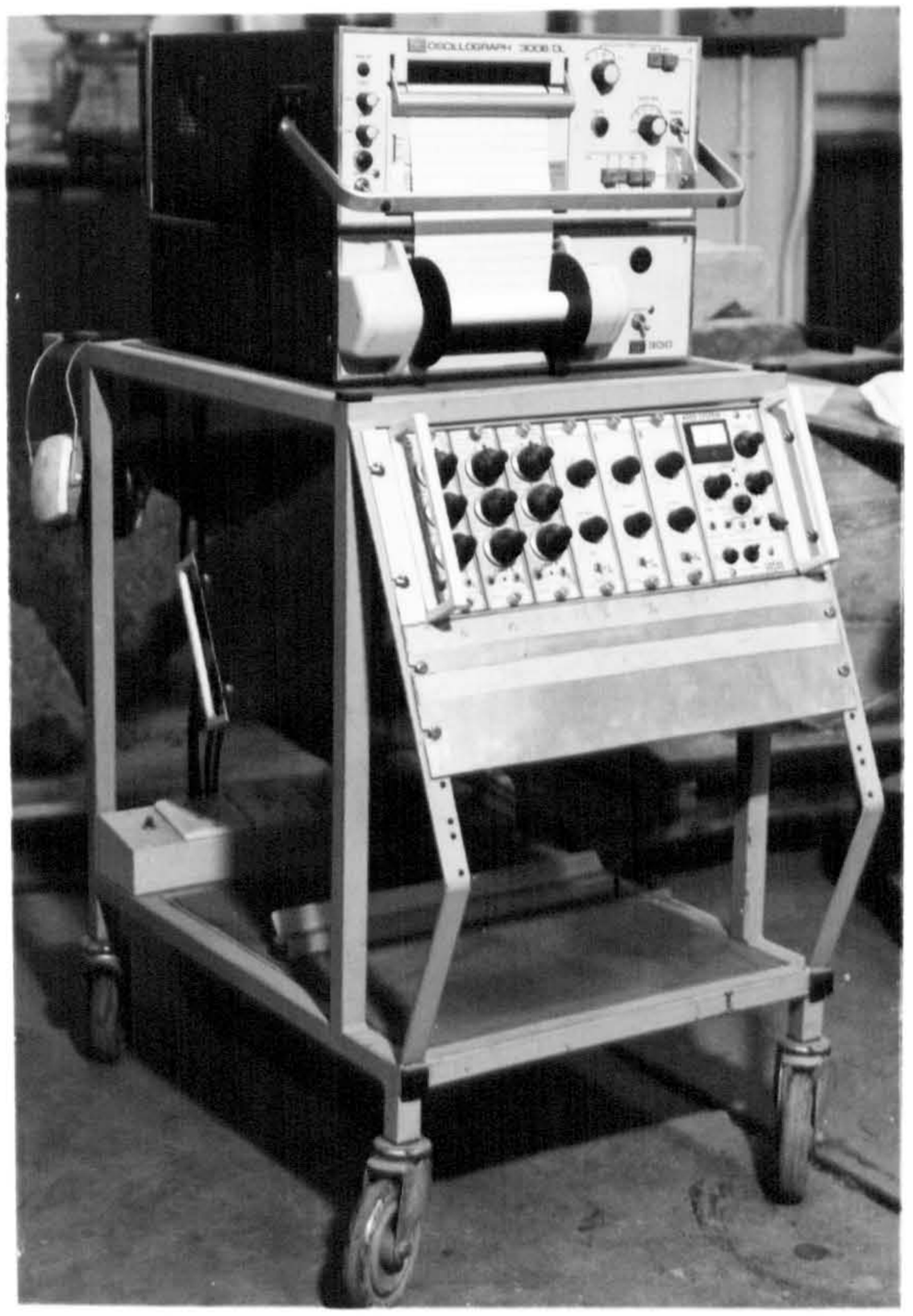

Recording Instrumentation

PLATE 8 - Strain Indicator and Pump

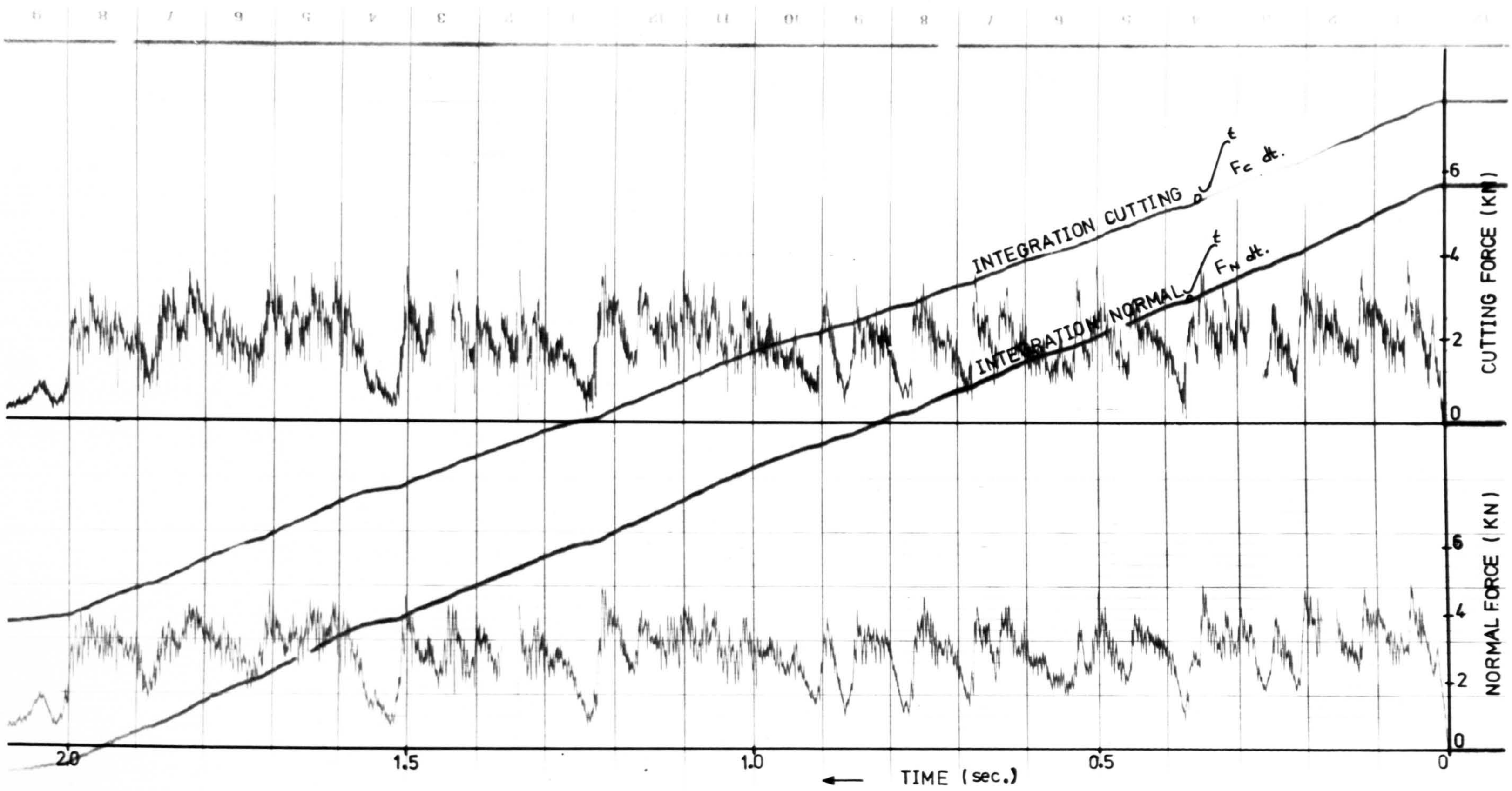

PLATE 9 – U.V. Recorded Trace of a Cut

The dynamometer was calibrated to the maximum loadings likely to be observed during the experiments for cutting, normal and sideways forces for suitable amplification and integration constants.

The hydraulic ram was pushed out via spherical seatings and a load cell which was held in position between two steel balls - one of which was attached to the probe fitted to the tool holder and the other fitted to a pyramidal plate which was bolted to the machine table had indicated the loading level. The hydraulic pressure was applied by a hand pump and a spirit level was used to check the level of the ram since any improper positioning could effect the values of the constants, (Plate 8).

For each of the three forces the traces are recorded using the U.V recorder. A change in load was indicated on the transient trace by a deflection of the trace while the integrated force trace indicated any change in load by a change in slope. From these traces calibration constants and their interactions are evaluated. Multiplying these constants with the results from D-Mac'ing gives the magnitude of the forces acting on the tool.

3.7.3 Measurement of The Volume of Rock Cut by Water Jet

Due to impracticality of weighing the rock before and after each cutting test and because of its size and relative immobility, some other method of measurement had to be found. It was not possible to collect the debris since the high pressure water jet had washed away most of it. Cutting rock with the mechanical tool alone has permitted the collection of the debris.

In searching through the literature on the subject of volume measurement, it was found that several investigators have tackled the problem by using different methods. Among these were that the volume of cut was measured by means of casting a low-shrinkage transparent epoxy resin, or by the amount of water that could be poured onto the cut, or use of mercury poured into the cut or filled with wax or by pouring a fine material into the cut.

Casting of epoxy resin was considered to be expensive and time consuming because the experimental programme required several hundred cuts to be made on the same block of rock. Since the rocks used for the experiments were mainly sandstones therefore porous and permeable, water could not be poured into the cut. For similar reasons the use of other methods were discarded as well.

The chosen method incorporated pouring a finely graded silica sand, the density of which was measured, into the slot which was blocked at both

ends by sticking plasticene, collecting the debris and weighing them. Since the density is known, it is therefore easy to calculate the volume of the sand. By back analysis the volume of the slot and weight of the rock that was removed is found.

12 Volt battery operated PIFCO car vacuum cleaner was used to collect the sand grains from the slot accurately, (Plate 13).

3.7.4 The Relationship between Jet Velocity and Pump Gauge Pressure

It is necessary to know the velocity of the water jet issuing from the nozzle to calculate the power consumption at particular jet pressure. There are several techniques available which can be used to find the velocity of the jet. High speed photographic technique is one of them. But, funds available for the project did not allow the use of sophisticated, expensive equipment for measurement purposes.

The second method, which was used for this project(indirect calculation method), involved the measurement of quantity of water that flowed through the nozzle at different gauge pressures within a known time interval. By back analysis the jet velocity was then calculated.

Measurement of Cut Volume

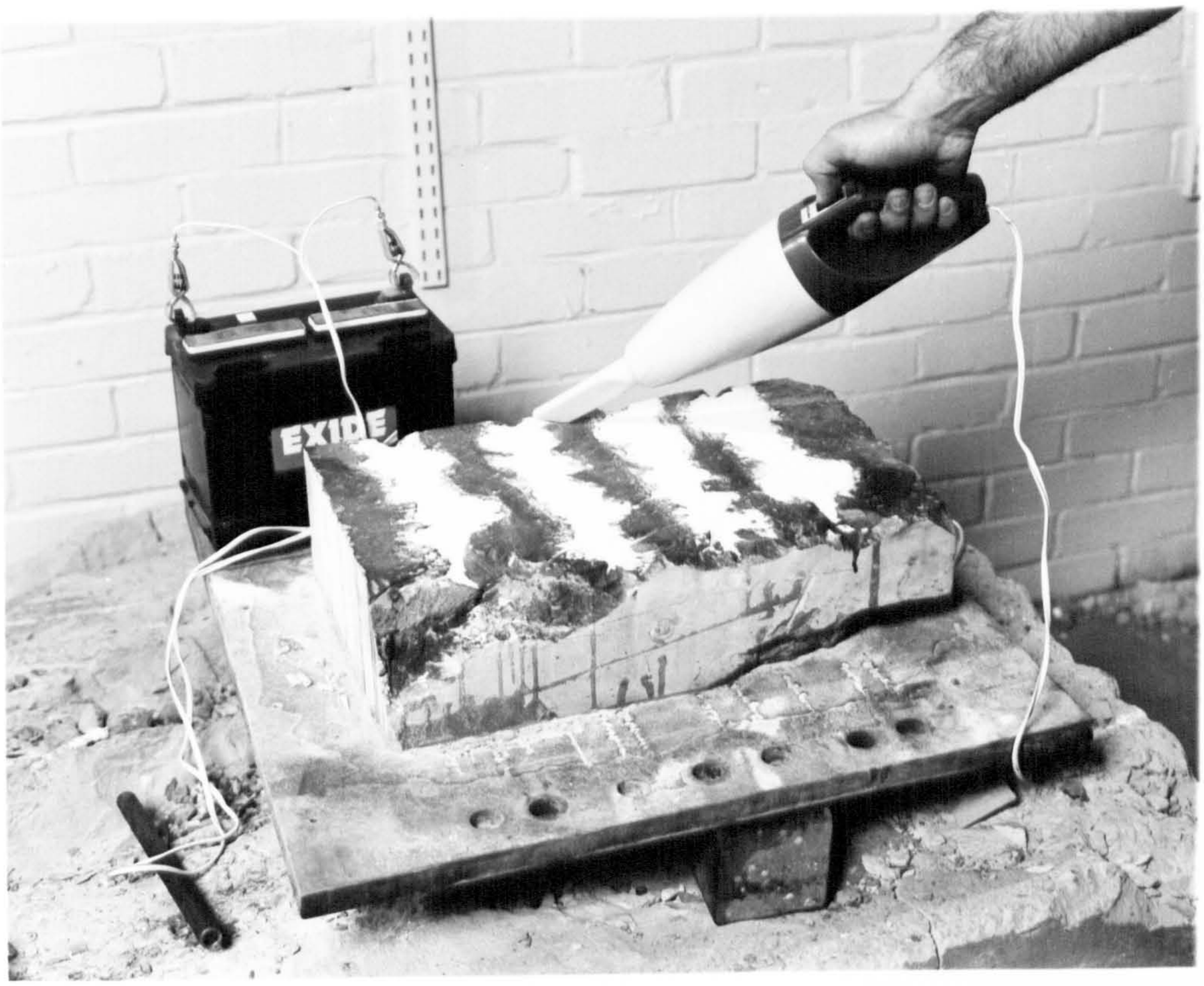

PLATE 13

Timed samples of fluid was collected in a container after a flow through a piping system which was designed for that purpose.

Jet velocity calculations were done as follows :

$$Q = Cc \times A \times Cv \times V \quad \ldots\ldots\ldots\ldots\ldots\ldots (3.1)$$

$$= Cd \times A \times V \quad \text{and} \quad A = \pi d^2/4$$

$$V = [(2gh)^{0.5}] \ldots\ldots (3.2)$$

Where Q = quantity of water (l/min)

A = nozzle exit area (m^2)

V = the jet velocity (m/sec)

d = nozzle diameter (m)

h = pressure head (metres of water)

P = water pressure (atm)

Cd= coefficient of discharge

Cc= coefficient of contraction

Cv= coefficient of velocity

If we assume no contraction of the jet, i.e. Cc=1, then

$$Cd = Q/(AxV) = Q/\{Ax[(2gh)^{0.5}]\} \quad \ldots\ldots\ldots (3.3)$$

$$= Q/\{[\pi d^2/4][(2gh)^{0.5}]\}$$

$$= 4Q/\{[\pi d^2][(2gh)^{0.5}]\} \quad \ldots (3.4)$$

If d=0.85mm and pressure unit is atmospheres, replacing the values of the parameters in the above equation, it becomes :

$$Cd = 2.33xQ/(P^{0.5}) \quad \ldots\ldots\ldots(3.5)$$

where Q = l/min

P = atm.

The values of 'Q' were found from experiments at corresponding gauge pressures 'P'. Replacing these values in equation gave the coefficient of discharge 'Cd'.

P	136.09	204.14	272.18	340.23	408.27	476.32	(atm)
Q	4.58	5.59	6.39	7.28	7.93	8.62	(1/min)
Cd	0.81	0.81	0.80	0.82	0.81	0.82	

Taking the mean value of Cd to be 0.81, the actual water jet velocity can then be calculated using the equation

$$V = Cd[(2gh)^{0.5}]$$

$$= 0.81[(2gh)^{0.5}]$$

If the pressure is in atmospheres, then

$$V = 11.52Po^{0.5} \text{ (m/sec)}$$

Similar calculations ware made with 0.6 mm and 1.1 mm diameter nozzles which gave

$V = 13.65Po^{0.5}$ .....for a 0.6 mm dia nozzle

$V = 12.66Po^{0.5}$ .....for a 1.1 mm dia nozzle

Graphs of volume flow against gauge pressure were drawn for three nozzle diameters (Figure 3.6). As can be seen the relationship between the variables is not of linear form and volume flow is increasing at a decreasing rate with increase in pressure.

3.7.5 Hydraulic Specific Energy Calculations

The efficiency of water jet cutting process is found by calculating the specific energy of that process. Specific Energy, in turn, is calculated, if the jet power and rate of volume removal are known, through series of arithmetic equations.

Power of the jet is given by :

$$W = A \times Vo \times Ps \times Cd \quad \ldots\ldots\ldots\ldots (3.6)$$

and $$A = \pi d^2/4 \quad \ldots\ldots\ldots\ldots\ldots\ldots\ldots (3.6.1)$$

where W = jet power

A = nozzle exit area

d = nozzle exit diameter

Vo= jet velocity

Ps= stagnation pressure

Cd= coefficient of discharge

Assuming a coefficient of unity and placing equation 3.6.1 into equation 3.6 it becomes :

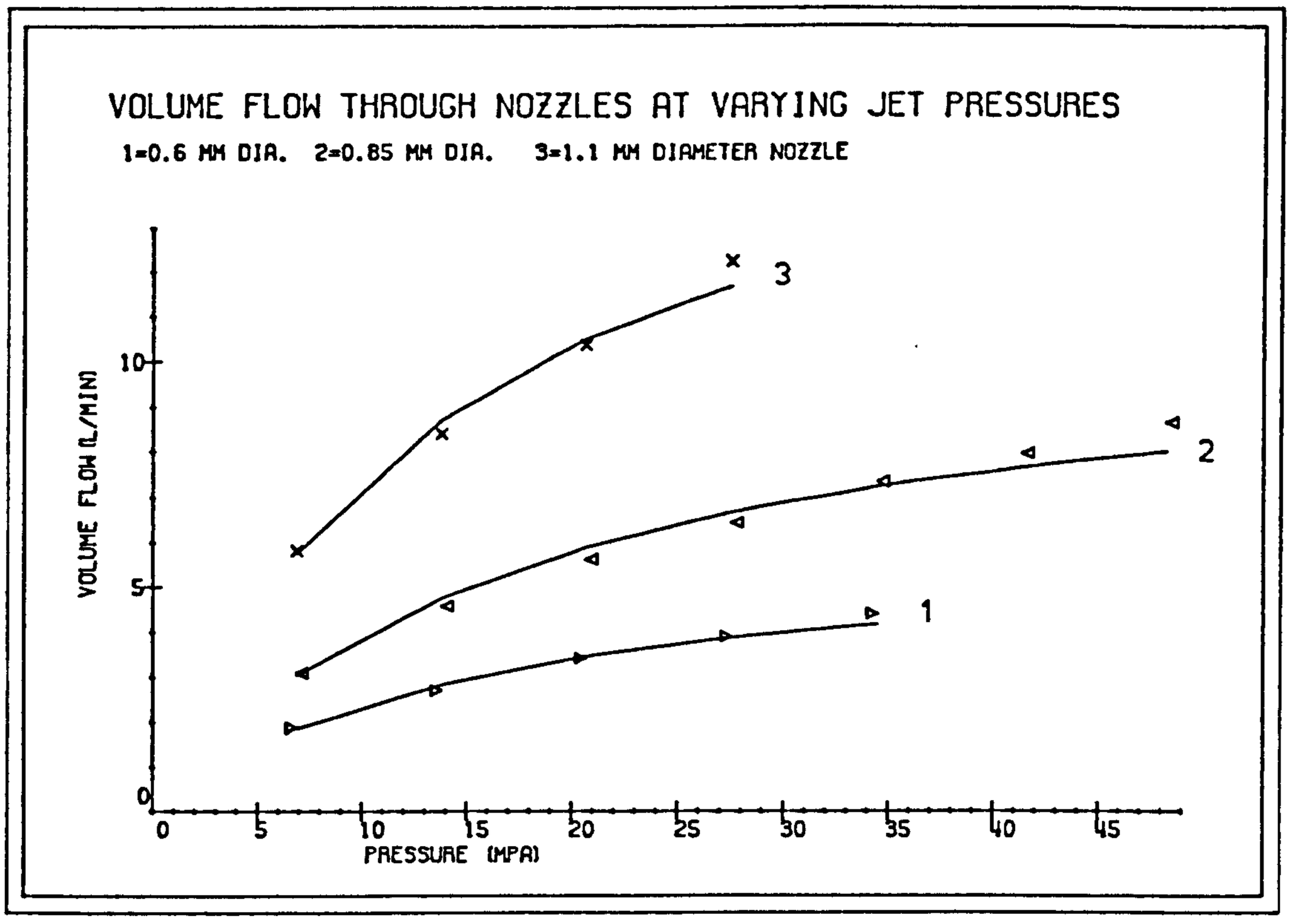
VOLUME FLOW THROUGH NOZZLES AT VARYING JET PRESSURES
1=0.6 MM DIA. 2=0.85 MM DIA. 3=1.1 MM DIAMETER NOZZLE
VOLUME FLOW (L/MIN)
0
5
10
0
5
10
15
20
25
30
35
40
45
PRESSURE (MPA)
1
2
3

FIG. 3.6

$$W = [\pi d^2/4] \times Vo \times Ps \quad \ldots\ldots\ldots\ldots (3.7)$$

Volume removal rate is calculated as

$$V = V/t \quad \ldots\ldots\ldots\ldots\ldots\ldots\ldots\ldots (3.8)$$

where V = volume removal rate

V = volume

t = time to make the cut

$$t = l/ts \quad \ldots\ldots\ldots\ldots\ldots\ldots\ldots\ldots (3.9)$$

where l = cut length

ts= traverse speed

Replacing these in equation 3.7 becomes

$$V = h \times w \times ts \quad \ldots\ldots\ldots\ldots\ldots\ldots (3.10)$$

where h = cut depth

w = cut width

Knowing the above equations, the Specific Energy is given by

$$\text{Hydraulic Specific Energy} = \left\{ \frac{\pi d^2 x Vo x Ps}{4 x h x w x ts} \right\} \ldots\ldots\ldots (3.11)$$

3.8 EXPERIMENTAL PROCEDURE FOR MECHANICAL CUTTING

The block of rock is stuck to a prepared steel plate with Araldite and allowed to cure for at least 24 hours. This is then bolted to the table of the shaping machine and trimmed to a plane surface using a trimming tool. The area surrounding the block is then cleared of all rock chippings.

The U.V recorder is switched on about 20 minutes before cutting, to allow warming up and settling down of any galvonometer drift. It is then necessary to select and position the galvonometer spots appropriately according to which force traces are required. The position of the spots on the trace are altered by adjusting with a non-magnetic screwdriver. The appropriate cutting tool is inserted into the tool holder, which is clamped to the central plate of the dynamometer and the rock is then traversed to the required cutting position. The cutting head is advanced so that the height of the tool could be adjusted to equal height of the cutting surface, in other words, to just touch the rock surface. The cutting head is then withdrawn and the required depth of cut is set by raising the table, measured by a dial gauge accurate to +/- 0.01 mm.

The paper speed of the U.V recorder is set to 125 mm/sec and for every cut : cut number, amplification and integration time levels from U.V recorder, depth of cut, length of cut(measured with a steel tape to the nearest 0.5 mm), and weight of debris were recorded. The block was then repositioned for the next cut and tool is turned in its holder. Depth of

cut is checked at the beginning, in the middle and at the end of cut length using a depth gauge. These values were observed to vary slightly. Therefore, mean of the three readings were taken as depth of cut. The same cut at the same settings was repeated 4 times for statistical purposes, to avoid changes that might occur in rock isotropy from one end of the block to other end.

3.9 EXPERIMENTAL PROCEDURE FOR WATER JET ASSISTED CUTTING

The rock specimen is prepared in the same way as described in previous section. The appropriate cutting tool is inserted into the tool holder which is clamped to the central plate of the dynamometer, and the rock is then traversed to the required cutting position.

The tool is then taken off its holder. Spacers are put onto the nozzle carriage assembly till required lead-on distance is achieved. The cutting head is advanced so that it is over the rock. The required stand-off distance is set by using the appropriate distance pieces. The cutting head is then withdawn. The cutting tool is inserted back into its holder and required side-off distance of the water jet nozzle is set.

The galvonometer spots are balanced. The pump is started and the galvonometers are rebalanced. The required water jet pressure is attained by restricting the amount of water returning back into the tank through by-pass valve. The cutting head is traversed across the rock surface, the

pump is stopped by pressing the remote control knob. The tool is turned in its holder so that it presented a new cutting face. The same cut at same settings are repeated 4 times. The tool is taken off, the nozzle is traversed across the rock surface at the selected pressure level to find the penetration depth of the water jet.

The block is allowed to dry for 24 hours. Grooves made on the rock by the tool were cleaned with a brush and fine silica sand is poured in. This is levelled by scraping the rock surface with a steel ruler. The length of cut is measured using a steel tape accurate to +/- 0.5 mm. The sand is than collected and weighed. The four seperate grooves made by the water jet are divided at 5 cm intervals to measure the penetration depth of the jet. Usually, there were 36 readings and mean value of these is taken to be the penetration depth of the water jet.

Soluble oil was added to the water in 50 to 1 proportion to prevent rusting to any part of the pump and the shaping machine. The same proportion was maintained throughout the water jet cutting experiments and its density was measured. Finally, the position of the nozzle in its holder was noted and the same position was used throughout the experimental programme.

4 LABORATORY TESTING FOR DETERMINING ROCK PROPERTIES

An important part of laboratory testing is Specimen Preparation . Utmost care must be taken in obtaining good rock samples as structual discontinuities that may be present in rock, e.g. cracks, bedding, joints, cause inconsistent poor results.

Differences in the behaviour of rock are observed at varying strain rates. Most rocks being stronger at high strain rates and weaker and more ductile at low strain rates. A constant loading rate of 0.69 MN/(M 2) per second was used for laboratory testing.

Properties of rocks may broadly be classified as:

1. Mechanical e.g. compressive, tensile, shear strengths

2. Physical e.g. bulk density, porosity, dynamic modulus

3. Petrographic e.g. thin section analysis

Strength testing was done mainly to classify rocks for both strength and deformation properties to obtain a rough index of cuttability.

Samples were taken from the rock samples after the cutting experiments were completed on the same rock block. There are several factors that

effect the results of strength testing done in the laboratory. Amongst these are; the ratio of length to diameter L/D , moisture content and end conditions of the specimen, i.e. effect of slight deviations of the sample from being parallel. It was ensured that the ends were ground parallel, and all specimens were air dried.

4.1 MECHANICAL PROPERTIES

4.1.1 Uniaxial Compressive Strength

A right cylinder of rock, which had 2:1 length to diameter ratio was loaded uniaxially between steel platens of the testing machine to failure. The dimensions of specimens were d=41mm ,l=82mm , where d is the diameter and l is the length.

The true mode of fracture is obscured by several factors. Although specimen is under compression, it fails either in shear or if a material of low modulus is used as end pieces to eliminate the frictional effects, specimen fails in tension, splitting longitudinally.

If F is the failure load and A the cross-sectional area of the specimen, then the compressive strength is given by :

$$CS=F/A \quad \ldots\ldots\ldots\ldots\ldots\ldots\ldots\ldots\ldots\ldots(4.1)$$

Tests were repeated minimum of six times for each rock type and mean value is taken to be the strength.

4.1.2 Indirect Tensile Strength

This parameter is important in connection with theories of failure. Rocks tensile strength is considerably less than their compressive strength and, the tensile strength of rock is more variable and more influenced by specimen size than any other mechanical property of rock.

Indirect tensile tests are more commonly used and Brazilian disc test is one of them.

A cylindrical specimen of 2:1 diameter to thickness ratio was placed between platens and loaded to failure under compression.

If F is the failure load and, D the specimen diameter and, T its thickness then tensile strength is given by :

$$TS=2F/\pi DT \quad \ldots\ldots\ldots\ldots\ldots\ldots\ldots\ldots\ldots\ldots(4.2)$$

4.1.3 Triaxial Compressive Strength

Most rocks exist under a certain degree of confinement. The effects of confining pressures on the compressive strength are studied using a triaxial cell.

A specimen of 2:1 length to diameter ratio was placed inside a tightly fitted impervious jacket of the special triaxial cell. Hydraulic confining pressure was applied to the curved surfaces of the specimen through the jacket and at the same time specimen was loaded axially in compression to failure. Same test was repeated at increasing confining pressures. The strength of rock increases with increasing confinement.

From obtained results Mohr stress circles and Mohr failure envelopes were drawn and angle of fracture plane with respect to major principal stress was determined.

If F is the axial load at failure, the principal stresses in the specimen at failure are :

$$\sigma_1 = F/A \ , \ \sigma_2 = \sigma_3 = p \quad \ldots\ldots\ldots\ldots\ldots\ldots (4.3)$$

where F = failure load

p= hyd. confining pressure

A = cross-sectional area

4.1.4 Static Elastic Constants

The most commonly used elastic constants are Young's Modulus (modulus of elasticity,E) and Poisson's ratio(ν).

A right cylindrical specimen of 2:1 length to diameter ratio was strain gauged at the mid-point. Two sets of gauges (one in horizontal and the other in vertical direction) were mounted at diametrically opposite points to compensate for possible asymmetrical loading.

The specimen under compression was loaded incrementally up to two thirds of its uniaxial compressive strength and unloaded at same increments. Changes in strain parallel and normal to the direction of loading were noted. Same loading-unloading cycle was repeated three times and graph of load against strain is drawn. From these curves, tangent and secant modulus of elastic constants are determined at fifty per cent of the uniaxial compressive strength value.

Poisson's ratio is also found by :

ν=lateral strain/longitudinal strain .....(4.4)

4.2 HARDNESS TESTING

4.2.1 Scleroscope Rebound Hardness

Principle of operation of portable scleroscope is that a small, round nosed tungsten carbide tip falls onto and rebounds freely from the surface of a rock specimen and the rebound height is noted and taken to be the rebound hardness.

The hardness of the test specimen controls the rebound height of the tip and is effected by the mineralogical content of the rock tested and its grain size.

The specimen surface was specially prepared (ground parallel) and divided into a grid of 1 cm square sections and average of the rebound values for each rock type was found from 100 readings.

4.2.2 Plasticity

This is an additional use of the sclerescope. It involved conducting a series of rebound tests with the sclerescope held in one position on the surface of the test specimen.

The principle of operation is that the area under the tip compacts with increasing rebound number and the rebound value varies with the degree of compaction, reaching a constant value as the rock changes to a compacted powder.

The change in rebound value due to compaction or plasticity is defined as :

$$K=[(Rf - Ri)/Rf]x\ 100\ \% \quad \ldots\ldots\ldots\ldots\ldots\ldots(4.5)$$

Where K = coefficient of plasticity

Ri= initial rebound reading

Rf= final rebound reading

With softer rocks the rebound value increases noticeably, with harder rocks the rise is not so pronounced and for brittle rocks the final reading may be lower than the initial one.

4.2.3 Schmidt Hammer Rebound Hardness

Originally designed and developed for concrete testing, this portable instrument is normally used to test rock in-situ and requires relatively large specimens for testing.

The principle of operation of Schmidt hammer is similar to that of Sclerescope. The instrument is held perpendicular to the rock surface and by pushing the rod against the surface a steel mass inside the hammer is spring loaded and released, the steel mass travels a constant distance as a result of sudden pressure release and rebounds from the target surface. The rebound height is recorded on a chart scale of 1 to 100 and, a histogram is produced.

Schmidt hammer gives particularly good results for medium strength rocks and values obtained are related to the compressive strength of the rock by[172]:

$$\text{Log}_{10}(CS) = 2.128 + 1.422\,\text{Log}_{10}Sh \quad \ldots\ldots\ldots(4.6)$$

where CS= compressive strength

Sh= mean schmidt hammer

4.2.4 NCB Cone Indenter

NCB Cone Indenter was developed by Mining Research and Development Establishment (MRDE). It is a portable instrument designed to determine the hardness of rock by measuring its resistance to indentation by a hardened tungsten carbide cone.

The instrument and its method of application and calculation of hardness values are reported in detail elsewhere (8,105)

The cone indenter has been found suitable for all rocks with a grain size of less than 0.05 mm , the limit at which grains just becomes visible to the naked eye. The indenter may be used to test coarse-grained rocks, but the indentation should be between grains rather than on them (105).

The values obtained using the cone indenter show a strong correlation with the uniaxial compressive strength of similar rocks (105).

A minimum of ten readings were taken and mean value of these was used for hardness calculation.

4.3 PHYSICAL PROPERTIES

4.3.1 Bulk Density

Commonly referred to as density, it is defined as the mass of a unit volume of a rock (79) and depends upon the mineralogical composition, porosity and amount of water present in the pores.

Cylindrically shaped specimens were weighed, their physical dimensions i.e. diameter and length measured. The volume is then calculated.

The bulk density is given by :

$$\rho = M/V \quad \ldots\ldots\ldots\ldots\ldots\ldots\ldots\ldots\ldots\ldots (4.7)$$

where ρ= bulk density

M= bulk mass

V= bulk volume

Usually the dry density of rock is determined and quoted as one of the rock parameters. For this thesis both dry and saturated densities of rock were found and stated at appropriate sections.

4.3.2 Grain Density

Grain density ρ_g is the mass of a unit volume of the grains of a rock (79).

It is calculated by following relationship :

$$\rho_g = Mg/Vg \quad \ldots\ldots\ldots\ldots\ldots\ldots\ldots\ldots (4.8)$$

where Mg = mass of grains

Vg = volume of grains

The grain density is commonly determined by either of the two methods : Pyconometric method and Buoyancy method.

The rock was powdered and sieved through between 120 and 30 mesh sieves. A density bottle was taken and weighed to an accuracy of 0.0001 grams. Approximately 20 grams of sieved powder was put into the bottle and weight of (bottle+sample) was found. The density bottle was half filled with distilled water and stirred to get rid off some of the air bubbles. Then it was put into a vacuum jar and at 27 units mercury pressure stayed until no air bubbles were left in the bottle. The bottle was topped up with distilled water and weight of (bottle+sample+water) was recorded. The bottle was then filled with distilled water only and (bottle+water) weight was noted.

The specific gravity was then calculated as follows :

$$S.G. = (W2-W1)/[(W3+W2)-(W4+W1)] \quad \ldots\ldots\ldots\ldots\ldots(4.9)$$

where W1 = bottle weight

W2 = bottle+sample

W3 = bottle+water

W4 = bottle+sample+water

4.3.3 Porosity

The porosity of a rock is defined as the ratio of the volume of internal open spaces (pores, interstices or voids) to the bulk volume of the rock (79).

$$\text{Porosity, } n = \text{Pore Volume/Bulk Volume} \quad \ldots\ldots\ldots(4.10)$$

The porosity can also be expressed in terms of grain density ρ_g and dry density of rock ρ_d as follows :

$$n = (\rho_g - \rho_d)/\rho_g \quad \ldots\ldots\ldots\ldots\ldots\ldots(4.11)$$

The porosity of a rock depends upon its mode of formation. There are open pores (pores inter-connected with each other and linked to the external surface) and closed pores (pores that are locked up in the rock

having no connection with the external surface or open pores) in a rock. Therefore, porosity is expressed as either total(true) or apparent porosity. When all the pores are taken into account, the porosity value is called true porosity and when open pores only are considered, then it is called apparent porosity.

4.3.4 Apparent Porosity

Cylindrical rock specimens were oven dried for 24 hours at 105 centigrade degrees to determine the mass of grains mg. They were then saturated with water (completely immersed in water) under vacuum, surface dried with moist cloth and their mass mw sat. determined.

The pore volume Vp is calculated as :

$$Vp = (mwsat-mg)/\rho_w w \quad \ldots\ldots\ldots\ldots\ldots\ldots (4.12)$$

where ρ_w = density of water

The volume obtained by this method is only that of the open pores connected to the surface.

4.3.5 True Porosity

If ρ is the bulk density, S.G. the specific gravity of the grains and e the void ratio of the samples, then porosity (n) is calculated as follows:

$$(1+e) = S.G./\rho \quad \ldots\ldots\ldots\ldots\ldots\ldots (4.13)$$

$$n = e/(1+e) \quad \ldots\ldots\ldots\ldots\ldots\ldots (4.14)$$

4.3.6 Dynamic Modulus (Wave Velocity)

This is related to physical rock properties and to microfracturing in the rock (96). The Pundit Velocity Tester was used to determine the 'wave velocity'.

Cylindrical specimen of appropriate length (82 mm) (selected as described in the users manual) was taken, pulse generator and receiver were attached to either end using grease as coupling. Pulse generator caused vibrations along the specimen when switched on and the travel time of the fastest wave through the specimen to the receiver was measured.

If L is the length of the specimen, the wave velocity is calculated in metres/second. Dynamic modulus is given by :

$$DEM = v^2 \rho(x10^{-6}) \quad \ldots\ldots\ldots\ldots\ldots\ldots (4.15)$$

where DEM = dynamic elastic modulus [MN/m^2]

V = wave velocity(m/s)

ρ = bulk density of rock (kg/m^3)

In general, the velocity of a pulse of ultrasonic vibrations travelling longitudinally in an elastic solid is given by :

$$V = \{ (DEM/\rho)x[(1-\nu)/(1+\nu)(1-2\nu)] \} \quad \ldots\ldots\ldots\ldots\ldots (4.16)$$

where ρ = density

ν = poisson's ratio

5 POINT ATTACK MECHANICAL TOOL CUTTING

There are a wide number of cutting elements varying in shape, make and size available to the excavation industry today e.g. drag tools, disk cutters, button, steel tooth etc. Economical applicability of these tools depend mainly on the cutting conditions. If the conditions are such that little wear or breakage of the tools is occurring the type of cutting tool used will be different from if the machine is cutting in an abrasive and or hard rock environment.

5.1 LITERATURE REVIEW ON POINT ATTACK CUTTING

Much research has been done on disk cutters and drag tools of varying shapes. These are described in detail elsewhere (8,14,61). Most of the machine driven roadways in British Coal Mines are excavated by boom type tunnelling machines which increasingly use point attack tools as the cutting elements. Point attack tool cutting experiments were carried out in this department back in 1978(152). M.R.D.E. conducted further research into point attack tools later in 1979 (65,66). Similar research previously had been conducted in Germany (152). These are described briefly in chronological order in which they were carried out.

5.1.1 German Research

The cutting performances of four types of tools as installed on a shearer drum were compared in addition to the wedge-shaped drag tools used on coal ploughs.

The tools compared were as follows:

Type 1 - Pyramidal-shaped tip (four faces) with wedge angle 75 degrees or 55 degrees, 15 degrees rake angle and 0 degrees back clearance angle.

Type 2 - Welded on conical tip with 43 degrees tip angle, 28 degrees rake angle 17 degrees back clearance angle.

Type 3 - Flat, trapeze-shaped cutting face; edge angle 250 degrees, back clearance face rounded with r = 5mm with 70 degrees wedge angle, 20 degrees rake angle and 0 degrees back clearance angle.

Type 4 - Conical, hard metal insert, with large cone angle, 80 degrees tip angle, 10 degrees rake angle and 0 degrees back clearance angle.

Type 5 - Drag tool with braised-on hard metal plate, tool width 20mm with 50 degrees wedge angle, 30 degrees rake angle and 10 degrees back clearance angle.

The results of experiments showed that the wedge angle or cone angle has great influence on the cutting action and the group with the conical tools, including the pyramid-shaped tool, require relatively high forces and produce low breakout. The tools with a flat rake face were found to be most advantageous.

5.1.2 Research at University of Newcastle

This was carried out to determine the cutting characteristics of Dumfries Sandstone with point attack tools. Experimental variables that were investigated included :

Variable		Level
Depth of cut (mm)	:	3, 6, 9, 12, 15
Tool spacing (mm)	:	10, 20, 30, 40, 50, 60, 70, 80
Tool tip angle (degrees)	:	80, 87, 110
Off-set angle (degrees)	:	0, 6.5, 13
Angle of attack (degrees)	:	45

The reason for changing off-set angles was that according to some manufacturers, at certain off-set angle the tool was supposed to turn in its holder, and thus self-sharpening occurred while the rock was cut. But, during cutting experiments, no such self-sharpening occurred. This

was thought to have been due to the friction between the cutting tool and the tool holder. If it had been possible to vibrate the tool holder during cutting, as it occurs in practice, it may then have been possible for the tool to turn in its holder. Industrial grease was introduced between two steel surfaces to reduce friction but during rock cutting dust particles entered in and eliminated any useful effects that the grease might have produced.

All the forces (cutting and normal, mean and mean peak) exhibited linear relationship with increase in depth of cut.

Yield increased markedly with increasing depth of cut, showing a power law relationship, which was very near to a square. Coarseness Index increased but the rate of increase decreased and Specific Energy decreased with depth. The relationship was hyperbolic in nature.

Spacing experiments were conducted at 8mm depth of cut. Tool spacing increase resulted in an increase of tool forces, the increase being sharper during the first levels of spacing. Towards the end increase had levelled off to a constant value. Coarseness Index and Yield followed similar patterns, increasing rapidly, then at certain depths of spacing cut (28-35mm) it reached a maximum value, before dropping to a stable value. Specific Energy decreased with increased spacing, reaching a minimum value between spacing/depth raios of 4.35 to 5 then increased again before levelling out to an asymptote.

Forces decreased with increasing off-set angle (from 0 degrees to 6.5 degrees). A further increase caused increase in tool forces. Statistical analyses have shown that the 'critical conclusion difference' between 0 degrees off-set angle and 6.5 degrees off-set angle, and 0 degrees and 13 degrees off-set angle were significant. However, the 'critical conclusion difference' between 6.5 degrees and 13 degrees was not significant. The best (low) results were given by 6.5 degrees off-set angle.

5.1.3 Reseach at M.R.D.E.

The M.R.D.E. did some tests to compare a point attack tool and two types of conventional wedge tools, a round nose chisel and a v-face, in both sharp and blunt conditions.

When sharp, the v-face tool had the smallest tool force components and the point attack the largest, while the round nose chisel in general have exhibited intermediate force values. Blunting had a much greater effect on the two wedge tools, so that after 600m of cutting, the point attack had the lowest tool forces at all depths of cut. In addition, they have noted that the point attack tool had the largest dust make, both when sharp and blunt. Due to its shape - the steel body behind the tungsten carbide tip is wider than the tip itself and comes into contact with uncut rock - frictional sparking was produced in sandstone and this is a hazard in coal mines since methane ignition can occur.

These experiments revealed that up to 30 degrees, off-set angle had no great effect on the measured cutting forces, although there was some indication of a minimum Mean Cutting Force at a value of about 15 degrees. This value differs from the findings at Newcastle where a 6.5 degree angle was found to yield better results. The experiments at Newcastle were done at 3 angle levels, whereas the M.R.D.E's were done at 6 angle levels.

MRDE noted that in some cutting conditions the tool did rotate in its holder, but reported that this idea did not result in self sharpening, as the tool tip wears in a symmetrical pattern to approximately twice the angle of attack imposed on it, (Figure 5.1).

Experiments on effects of angle of attack have shown that increasing the angle of attack has the effect of increasing the back clearance angle and reducing the rake angle. A rise in cutting forces with reducing rake angle was noted but only for angles of attack greater than 50 degrees. At values less than this, they implied, cutting forces increased rapidly and a back clearance angle of at least 12 degrees is necessary for efficient cutting with the point attack tool, (Figure 5.2).

5.2 THE CUTTING ACTION OF POINT ATTACK TOOLS

Cutting action of a point attack tool may be examined in two stages. Initially, when a point attack tool penetrates a brittle rock, stresses are set up in the vicinity of tool/rock interface. While the tool is

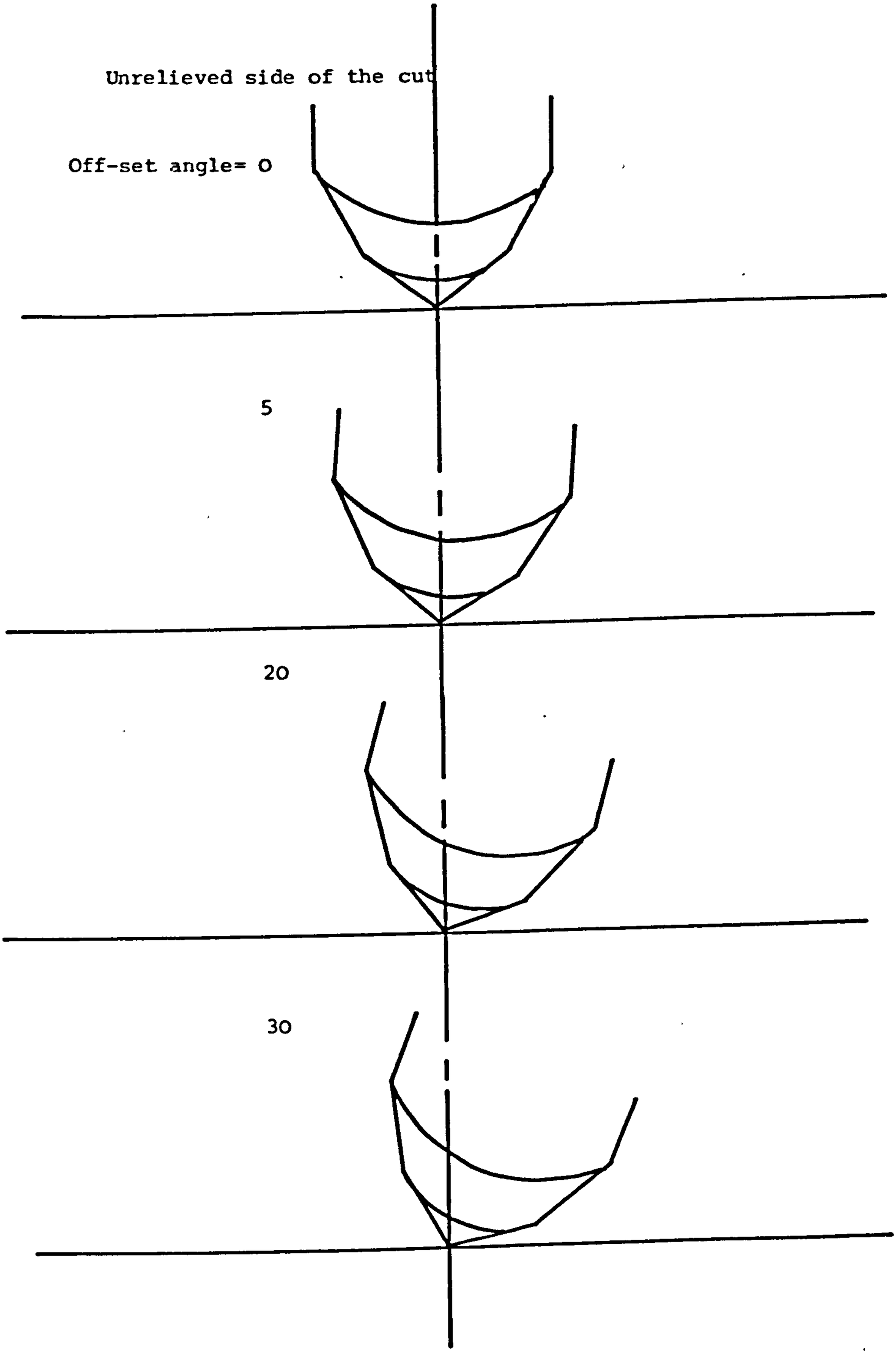

FIG.5.1 - Profiles of the Tool tips at various Off-set Angles

(after Hurt and Jones)

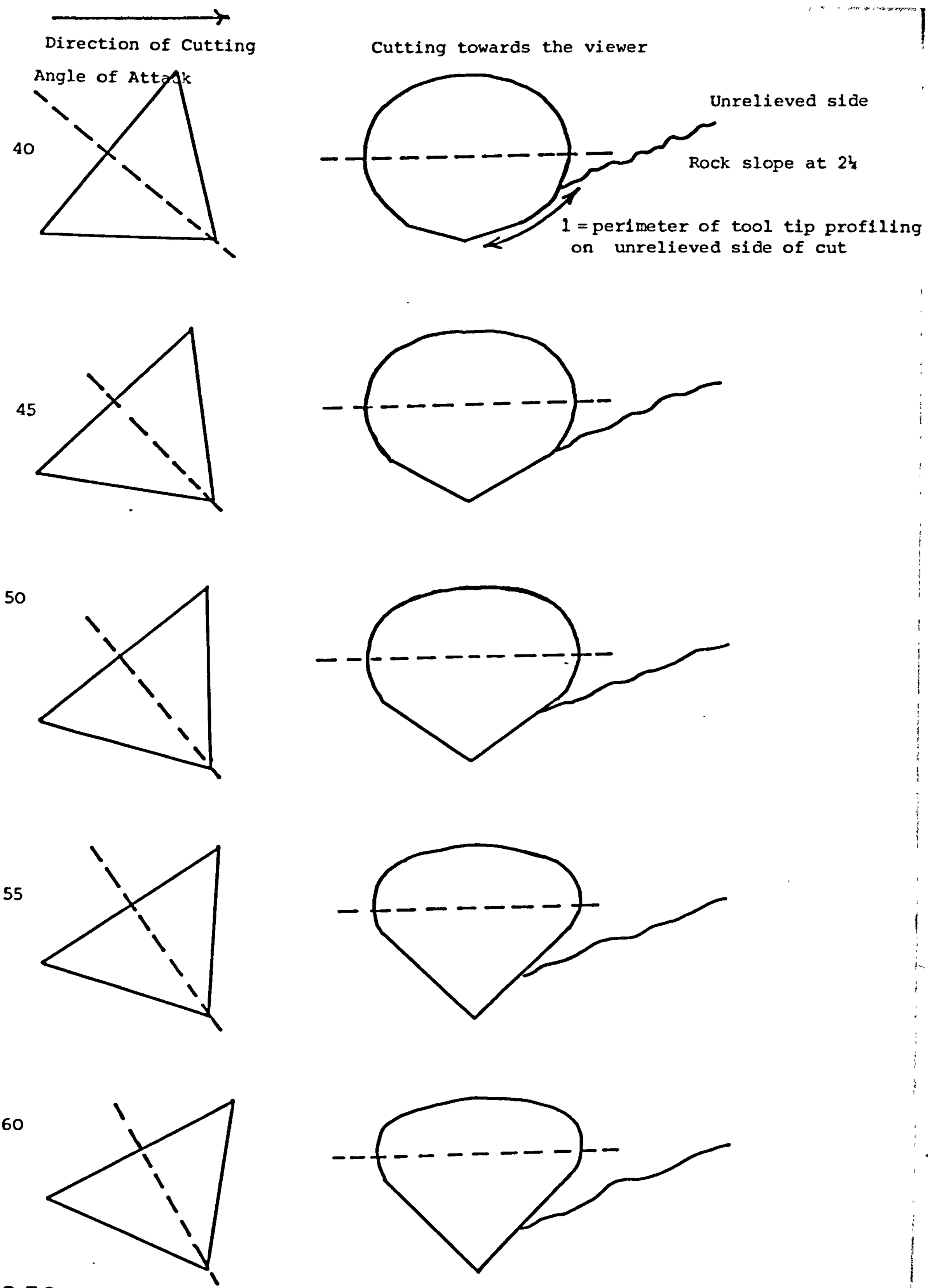

FIG.5.2- Profiles of the Tool tips at various angles of attack
(after Hurt and Jones)

pushed through, at some critical force level(which varies with rock type), its tip initiates tensile fracture and with the assistance of sides of the tip causes final breakage of rock ahead of the tool. The rock face is left with V-shaped sloping surfaces after the initial action of the tip, (Figure 5.3.1).With further penetration, due to its shape, the tip makes a rubbing contact with the sides of the cut and causes failure in the remaining rock material, which leads to higher forces. The second action of the tip is therefore, to shear through the rock along the cut length and leave behind a secondary groove, (Figure 5.3.1). As the cutting progresses, crushed and pulverized powder is reconstituted as flakes, (Plate 10), (Figure 5.3.2), due to the rubbing action of the sides of the point attack tool.

Due to complicated three-dimensional action of the point attack tool, there is no comprehensive theory available, at present, applicable to it. However, at M.R.D.E. they have tried, with some success, to predict the geometry of the groove produced by the tool in unrelieved cuts. On examination of debris it was reported to have an half angle of 68 degrees for sandstone and limestone cutting. By taking into consideration a simple conical point tool attacking a buttock of rock, they have reasoned that 'radial compressive stresses are produced in the rock, accompanied by tensile hoop stresses. Tensile cracks will open up at the interface between tool and rock when the stress equals the tensile strength of the rock. The cracks will propagate to the unstressed surface of the rock if the conditions are favourable, (Figure 5.4).

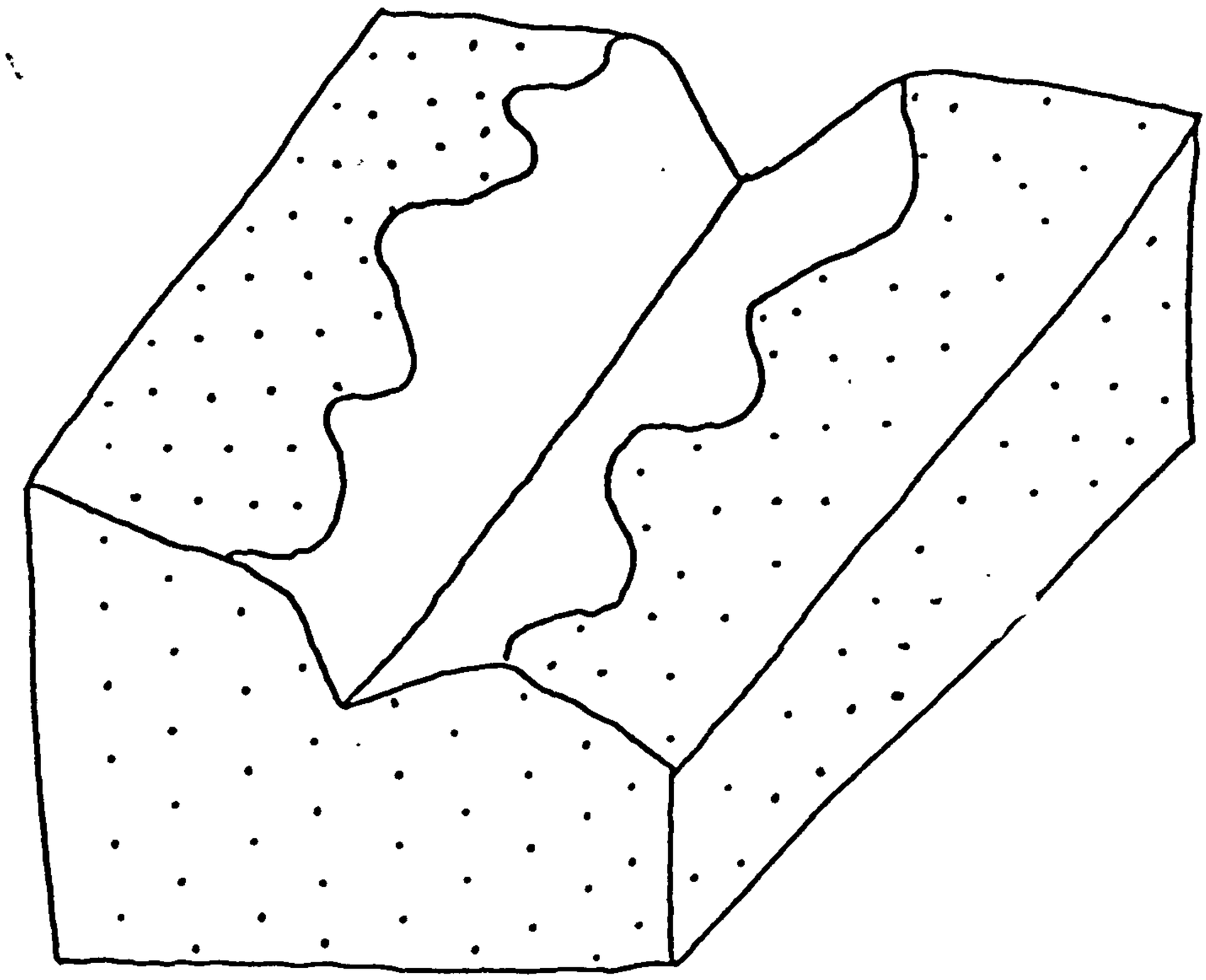

a - Rock Surface after the Initial Action of the Tool Tip

(Idealized view)

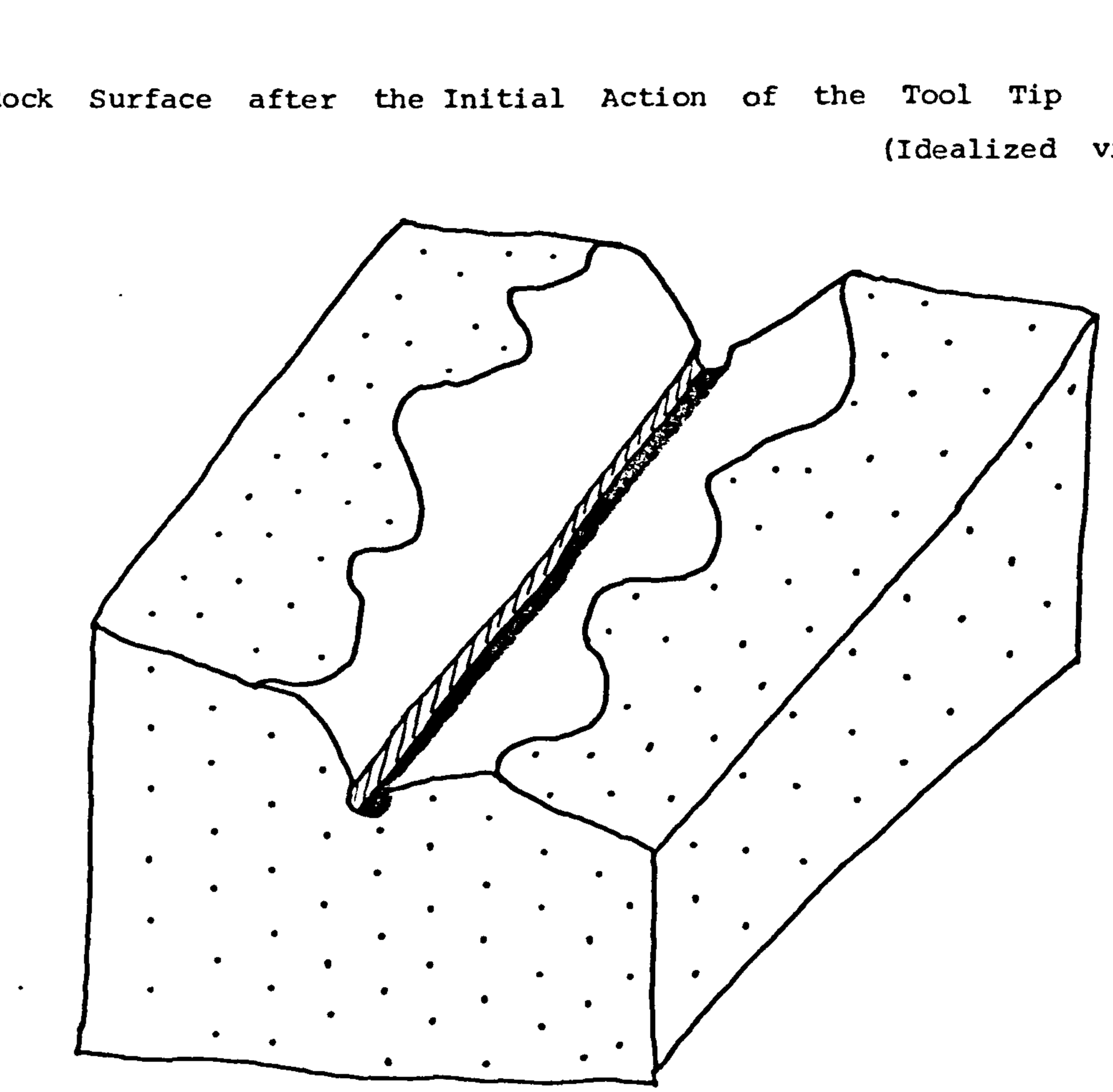

FIG. 5.3.b - Rock Surface after the Shearing Action of the Tool Tip

(Actual)

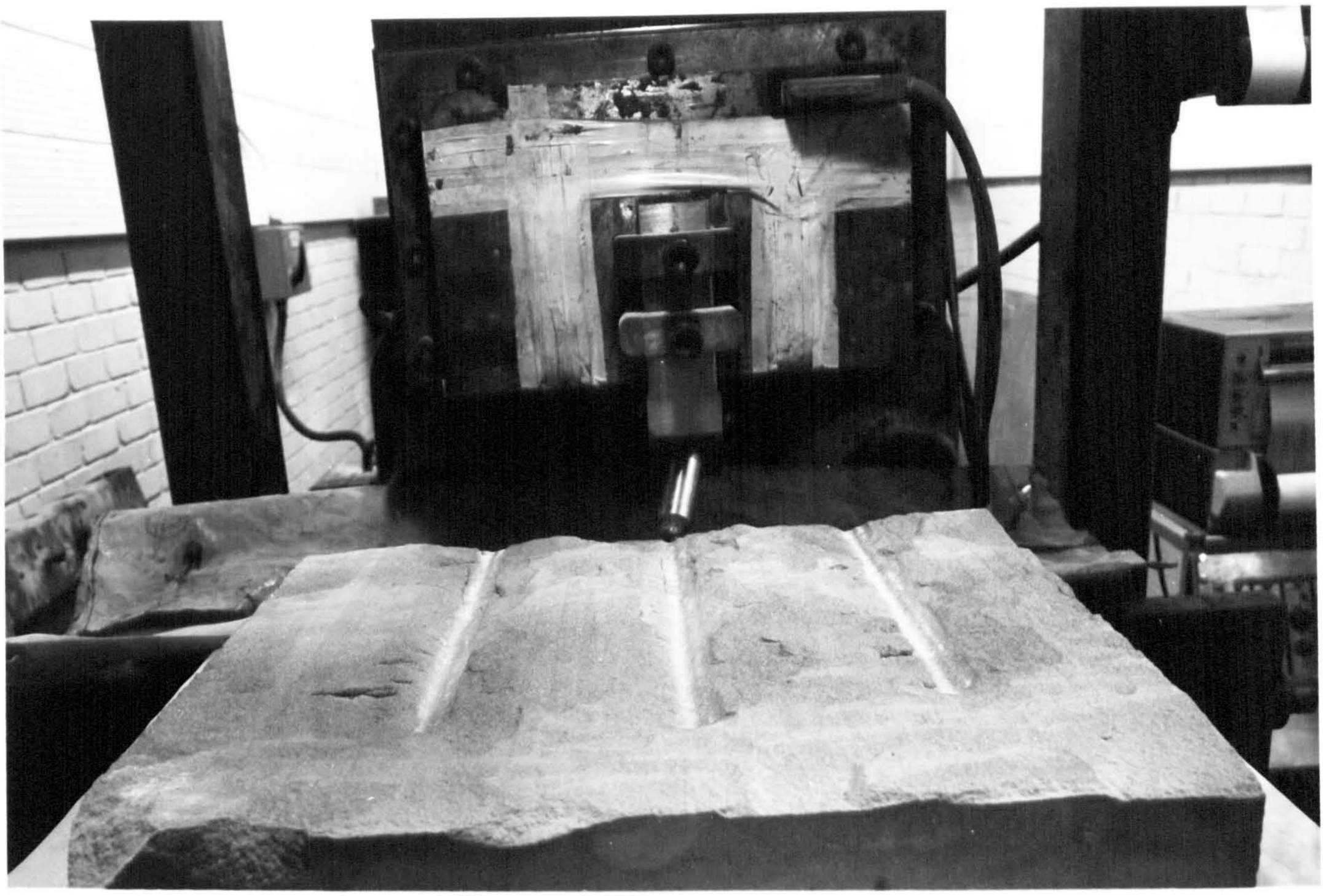

Point Attack Tool Cutting

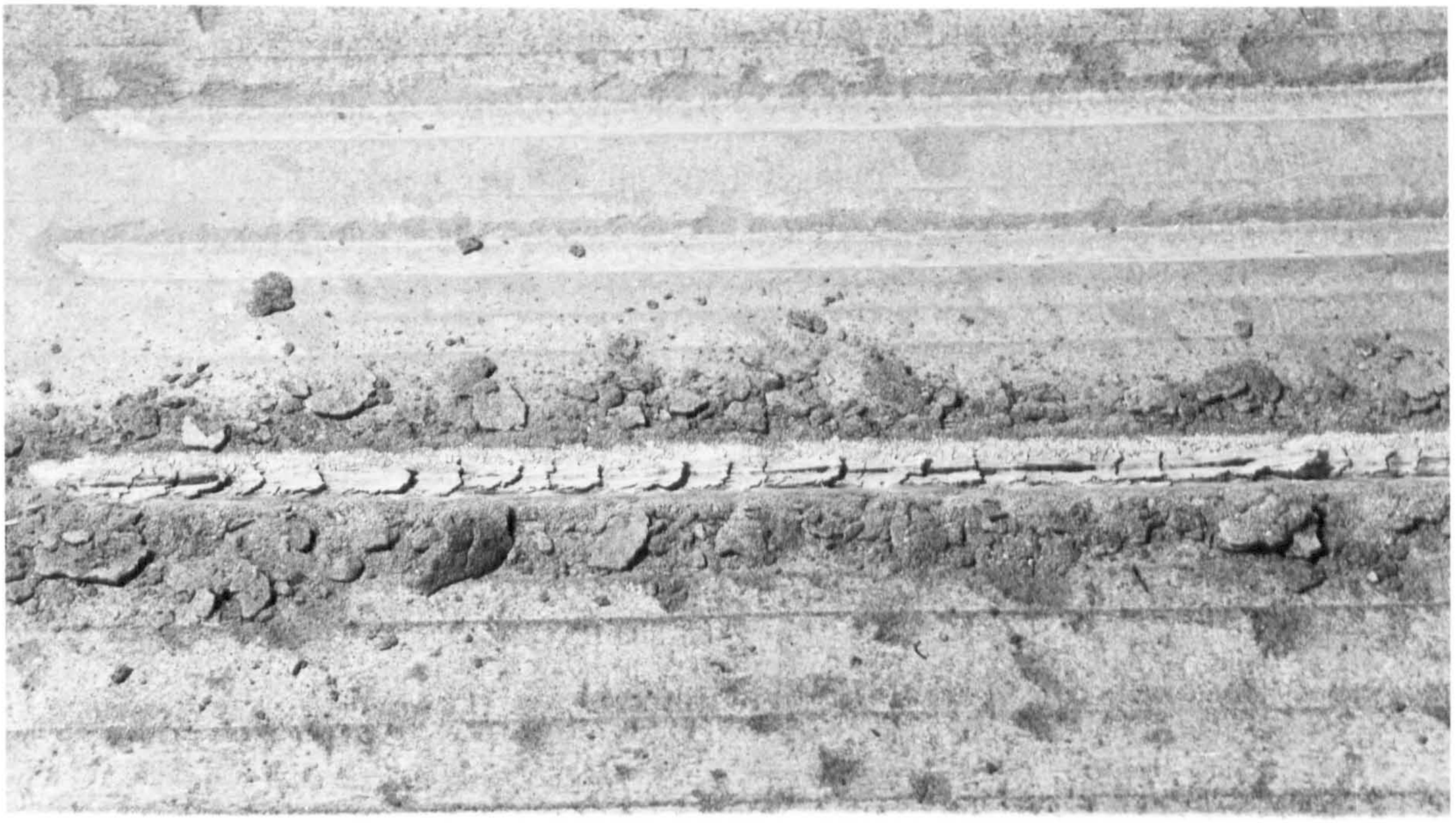

PLATE 10 – Rock Surface after a Cut

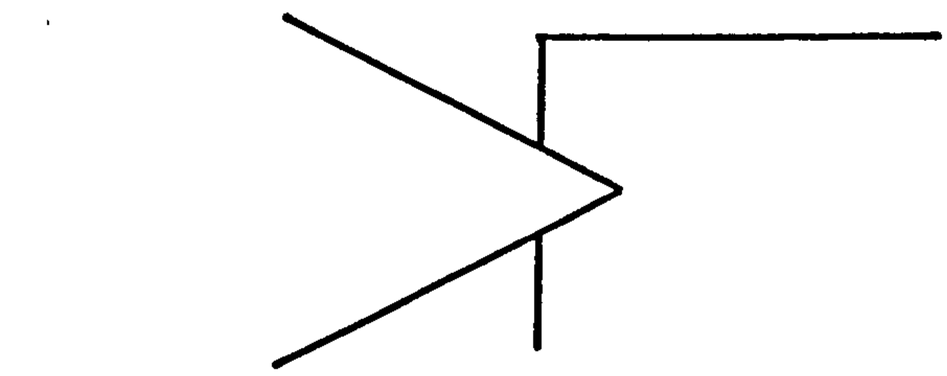

Pencil Point Attacking a Buttock of Rock

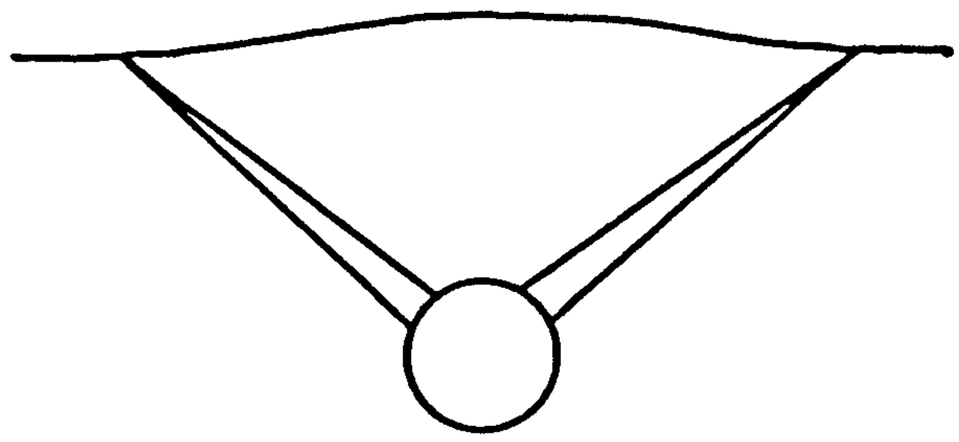

Pattern of Breakout

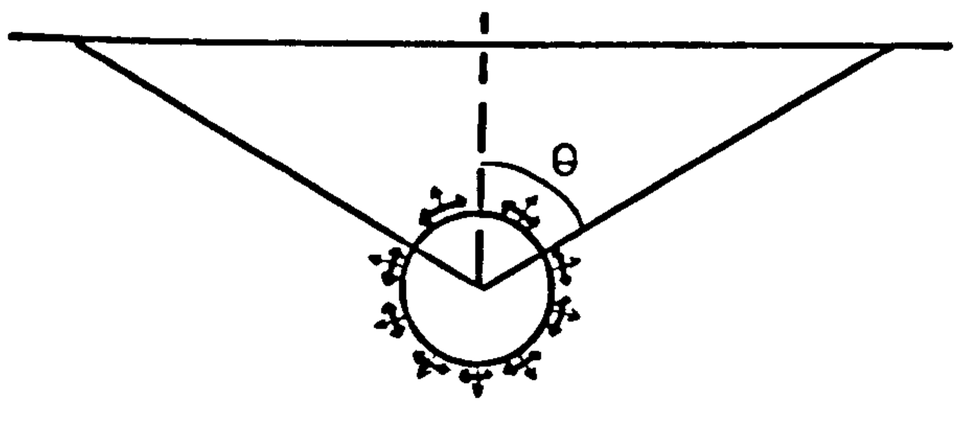

View along Direction of Cut

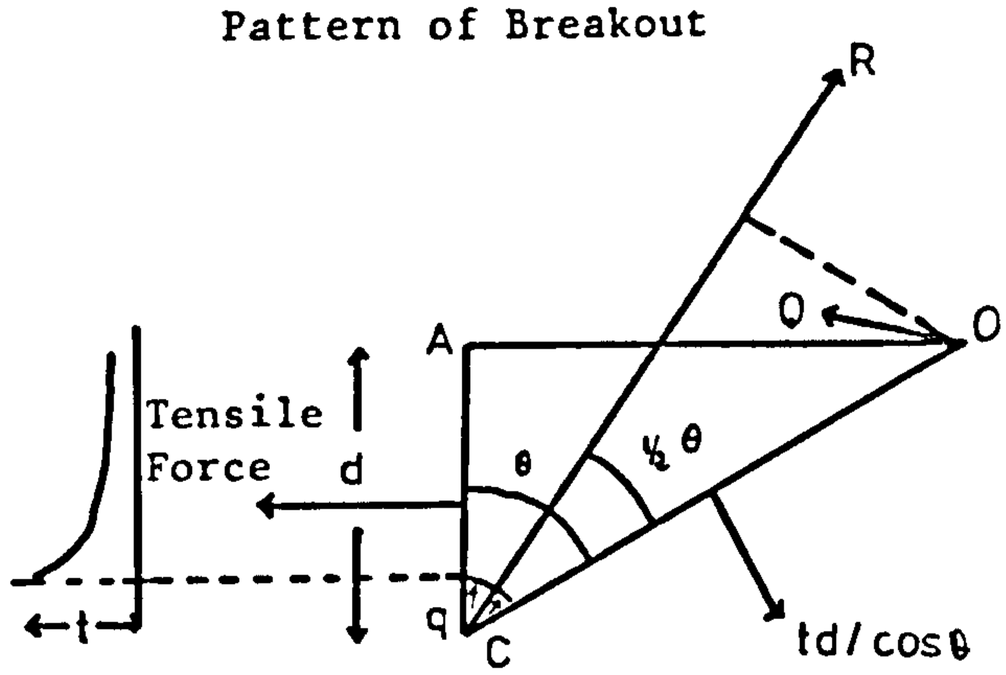

Stress on Half-Segment

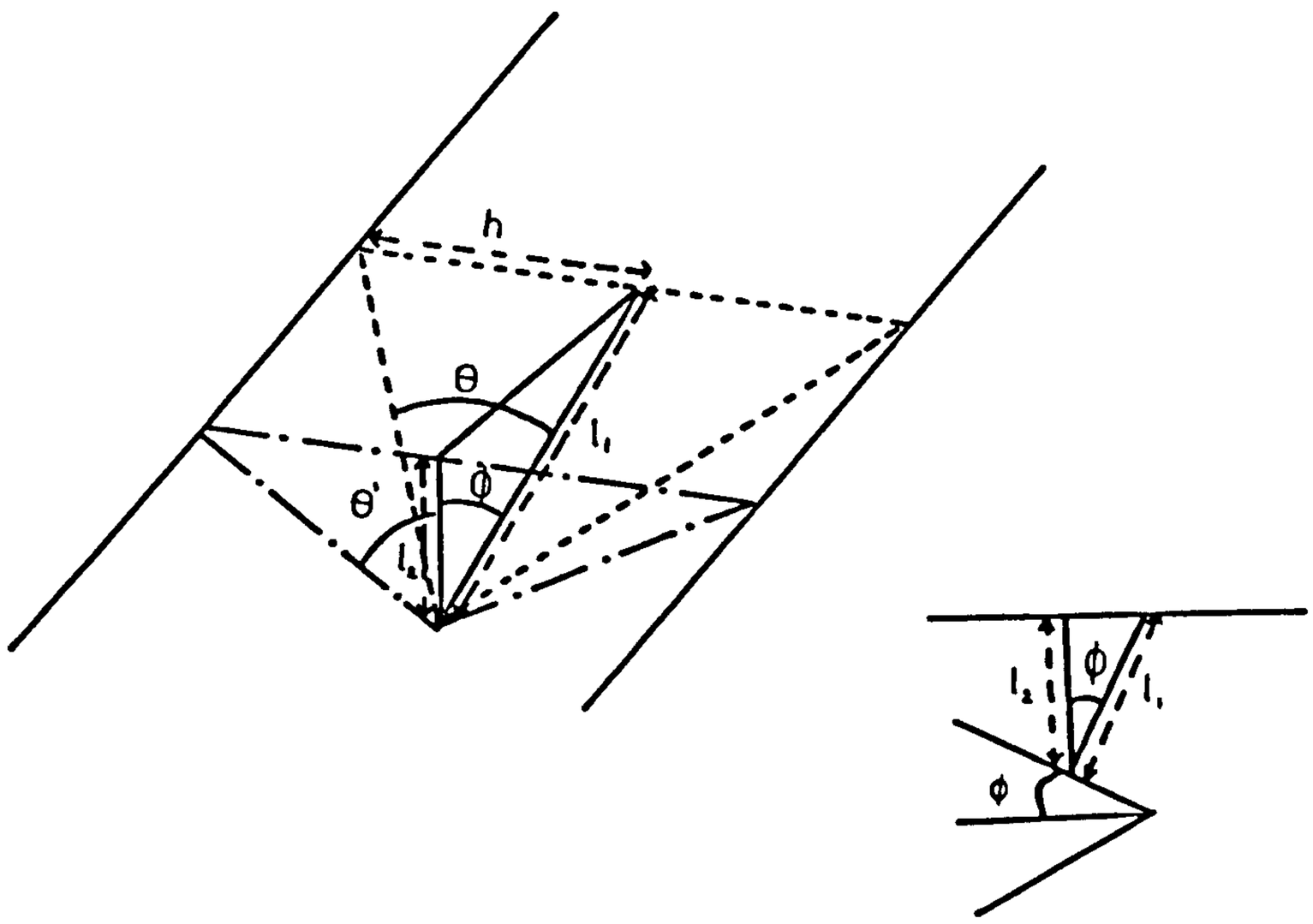

FIG.5.4 - Relation Between V-Angles at Various Inclinations

(After Hurt and Evans)

Forces acting on the half-segment are:

- Tensile force along OC = $t.d/\cos\theta = t.d\sec\theta$

- Radial compressive bursting force $R = qa\theta$

- A tensile force acting across the vertical radius $\sigma_{hoop} = t(a^2/r^2)$

- A force Q required to lever off the broken rock

To eliminate the effect of Q. take moments about P.

$$R(d/\cos\theta)\sin(\theta/2)+ta^2\int_a^d(1/r^2)(d-r)dr=(td/\cos\theta)(1/2)(d/\cos\theta)$$

.....(1)

Assume d/a is large

$$ta^2\int_a^d(1/r^2(d-r)dr=ta^2[(d/a)-\log(d/a)] = tad$$

equation (1) becomes

$$[qad\theta\sin(\theta/2)]/\cos\theta = td[(1/2)(d/\cos\theta)-a]$$

$$=(1/2)t(d/\cos\theta)$$

$$q = (1/2)t(d/a)[1/\theta\cos\theta\sin(\theta/2)] \quad .....(2)$$

Correction for θ (=60.9 degrees found by interpolation)

$$\tan\theta' = \tan\theta/\cos\phi$$

where ϕ is the half angle of the conical point

θ = 60.9 degrees

ϕ = 37.5 degrees

θ'= 66 degrees which compares with measured angle of 68 degrees.

Springwell sandstone and Darney Sandstone were chosen, because of differences in their rock properties, as the two main experimental rocks for extensive analysis.

A further five rock types, including three limestones of varying rock properties and two more sandstones were used to compare the performances of mechanical and hybrid cutting tools.

In this section, results of the point attack tool cutting tests performed on Springwell and Darney sandstone are given. Cutting results for other experimental rocks will be given in (Chapter 8) where comparisons between the tools are made.

5.3 EXPERIMENTAL PLAN

There are many variables that should be taken into consideration if a point attack tool is to be used for cutting tests. These can be divided into three distinct categories:

1. Point attack tool variables - tip angle
   tool shape (length, diameter)
2. Tool holder variables - angle of attack
   off-set angle
3. Operational variables - depth of cut
   tool spacing
   cutting speed

Previous research done both at Newcastle and the M.R.D.E have highlighted the effects of some of these variables in terms of tool forces and energy consumption. Therefore, some point attack tool variables were kept constant to keep the experiment size to a manageable level. The 87 degree tip angle with constant tool shape was used throughout the experiments on all rocks. The tool shape and its dimensions are given in (Figure 3.3).

Angle of attack of 45 degrees with 6.5 degrees off-set angle tool holder is chosen as the tool holder, specifications of which are given in (Figure 3.1) (Chapter 3).

Cutting experiments were carried out with tools cutting in isolation and as reports from several investigators had shown that cutting speed did not have significant influence on tool forces within the range that could be achieved with the shaping machine cutting head used. A constant cutting speed was adopted, although at high speeds the wear of the tool tip would increase with distance rapidly resulting in higher forces. Depth of cut was changed in arithmetic progression, as the only operational variable and five depth levels were chosen to give reasonable relationships in terms of depth of cut.

Variable	Level
Tip angle (degrees)	87
Angle of attack (degrees)	45
Off-set angle (degrees)	6.5
Tool spacing	cutting in isolation
Cutting speed (mm/sec)	165
Depth of cut (mm)	2, 4, 6, 8, 10 for S'well sandstone
	3, 5, 7, 9, 11 for Darney sandstone

Least squares method curve fitting analysis is done for experimental results and index of determination values and regression equations are given in appendix for the functions chosen.

5.4 EFFECT OF DEPTH OF CUT

5.4.1 On Tool Forces

Cutting and normal forces have increased with increasing depth of cut, with force values for Darney sandstone obtaining higher values than Springwell sandstone, (Figures 5.5 and 5.6).

If the compressive strengths of the rocks under test are examined, it would show that Darney sandstone had the highest compressive and tensile forces and Springwell sandstone having the lowest.

5.4.2 On Yield

Rock yield increased with increasing depth of cut, exhibiting a power law relationship, (Figure 5.7.1).

The volume of rock excavated remained approximately constant at shallow depths of cuts. However, more yield was produced when cutting higher strength rocks at deeper cuts.

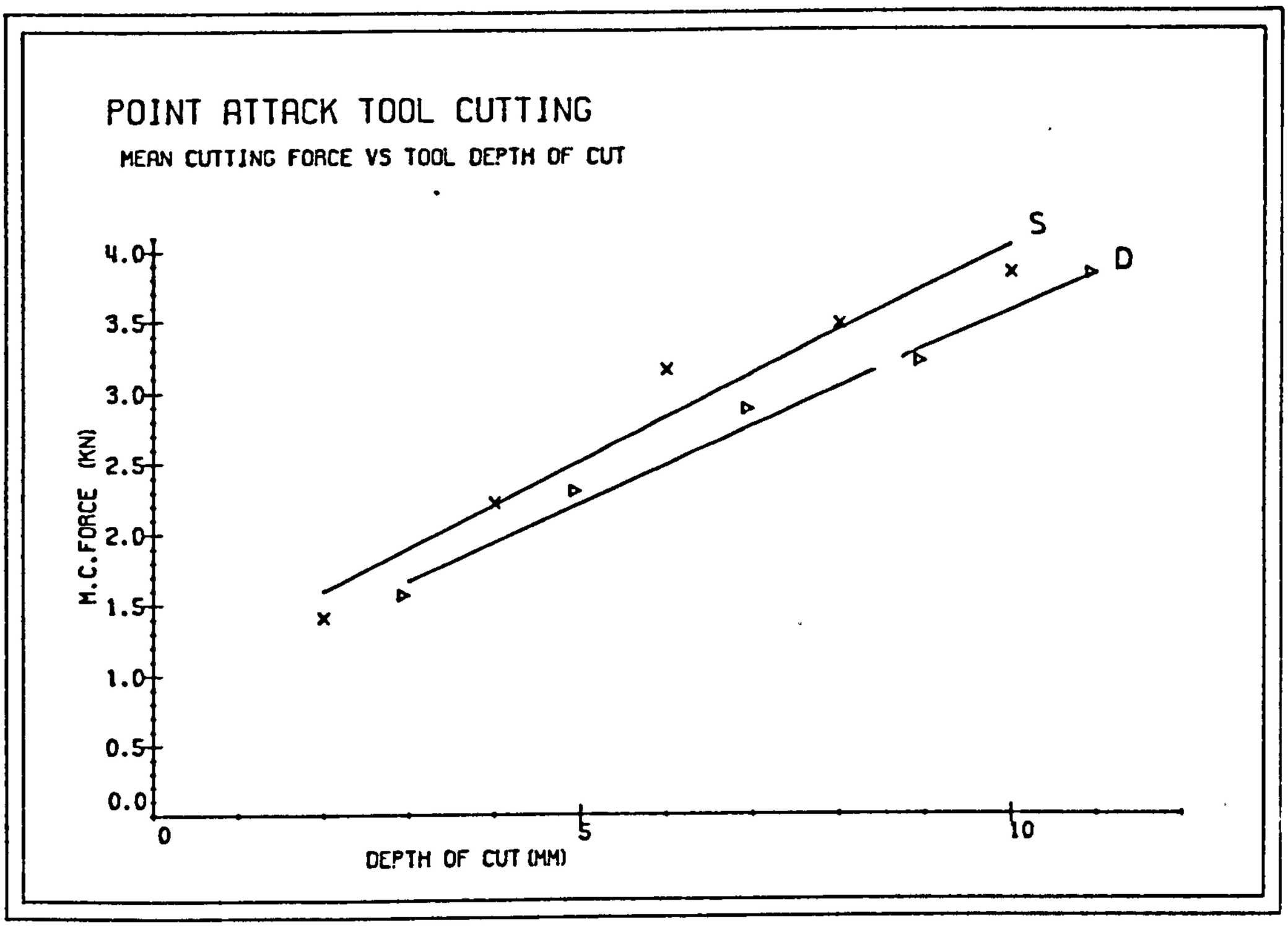
POINT ATTACK TOOL CUTTING
MEAN CUTTING FORCE VS TOOL DEPTH OF CUT
M.C.FORCE (KN)
4.0
3.5
3.0
2.5
2.0
1.5
1.0
0.5
0.0
0
5
10
DEPTH OF CUT (MM)
S
D

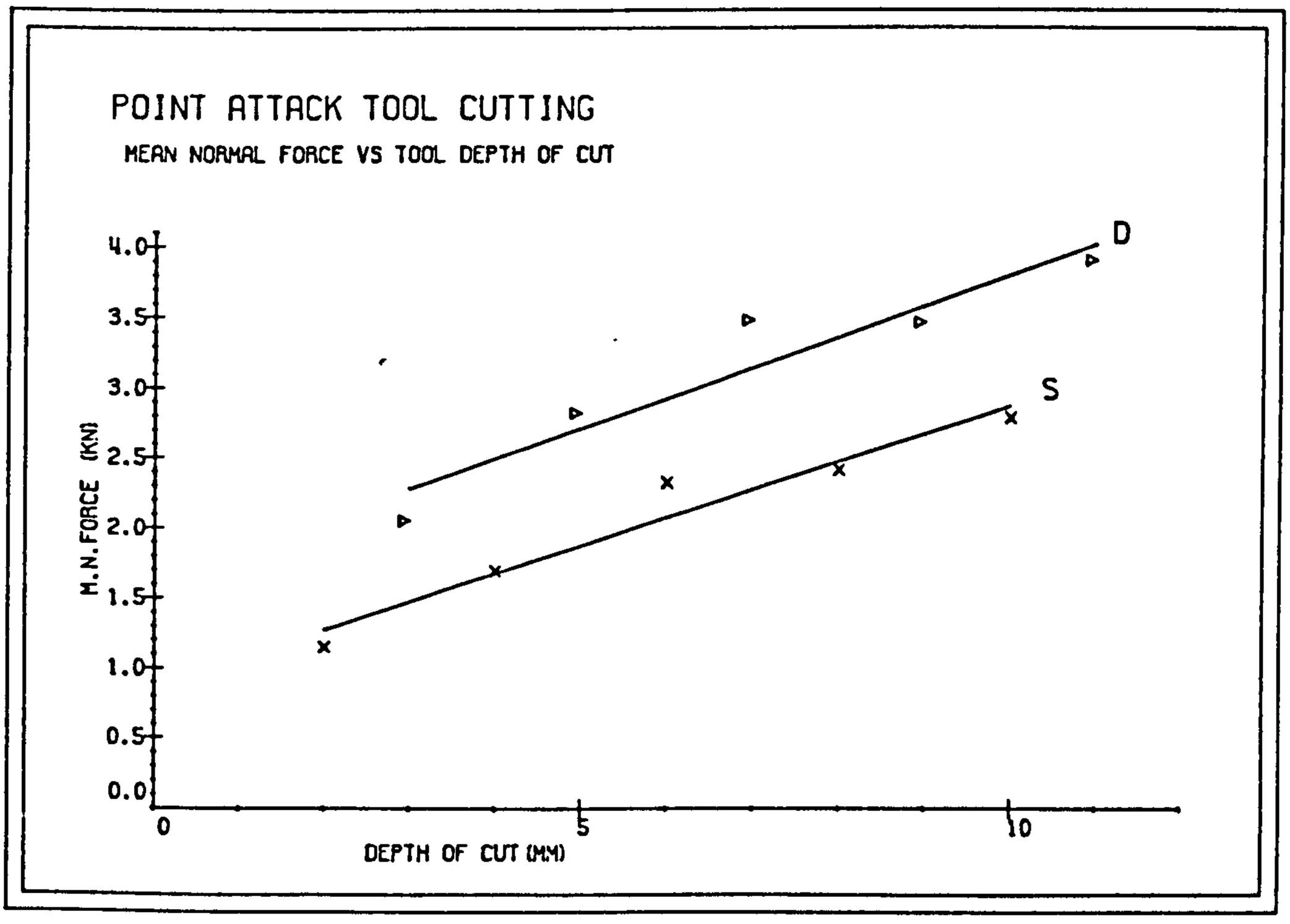
POINT ATTACK TOOL CUTTING
MEAN NORMAL FORCE VS TOOL DEPTH OF CUT
M.N.FORCE (KN)
4.0
3.5
3.0
2.5
2.0
1.5
1.0
0.5
0.0
0
5
10
DEPTH OF CUT (MM)
D
S

FIG. 5.5

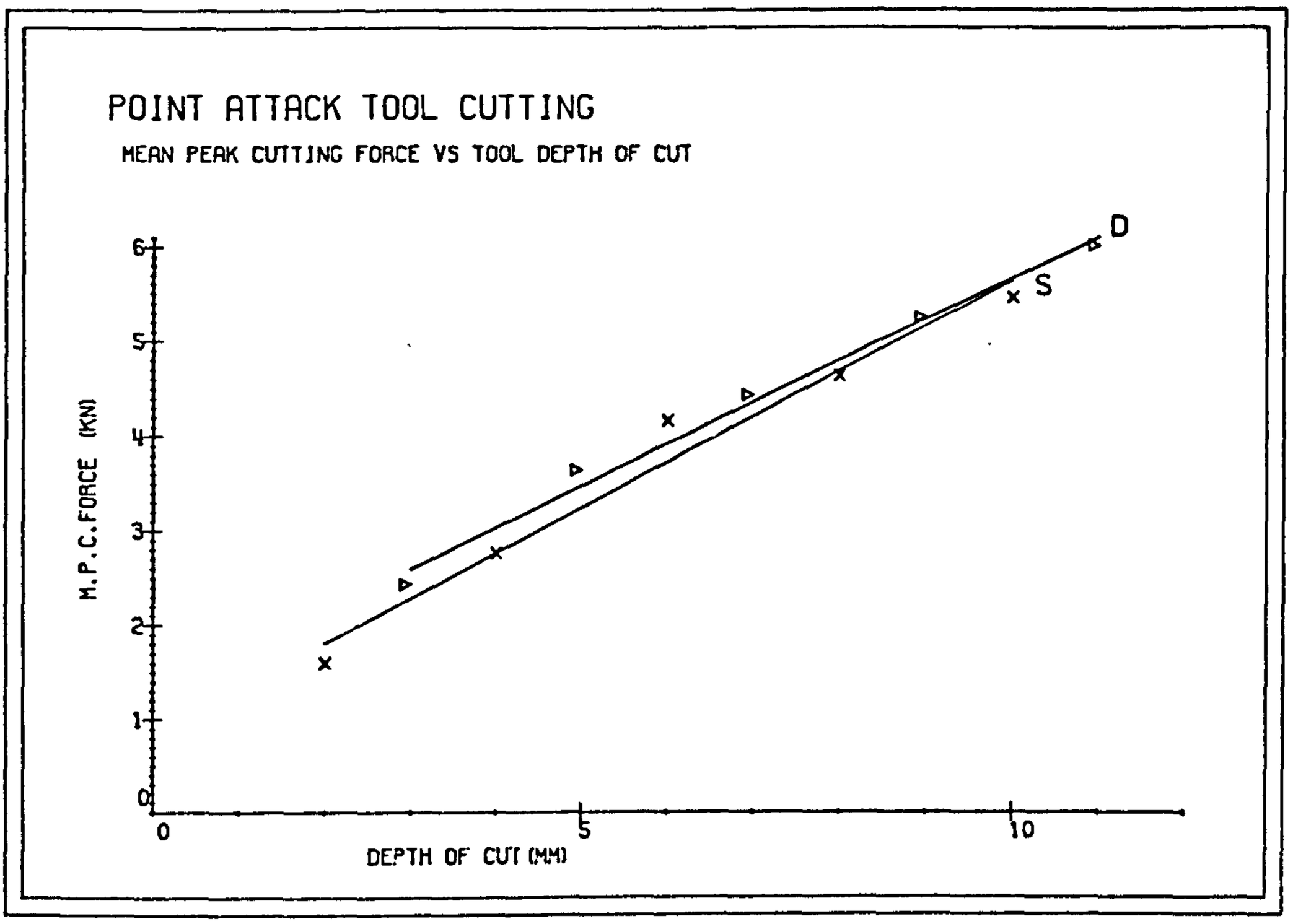
POINT ATTACK TOOL CUTTING
MEAN PEAK CUTTING FORCE VS TOOL DEPTH OF CUT
M.P.C.FORCE (KN)
0
1
2
3
4
5
6
D
S
0
5
10
DEPTH OF CUT (MM)

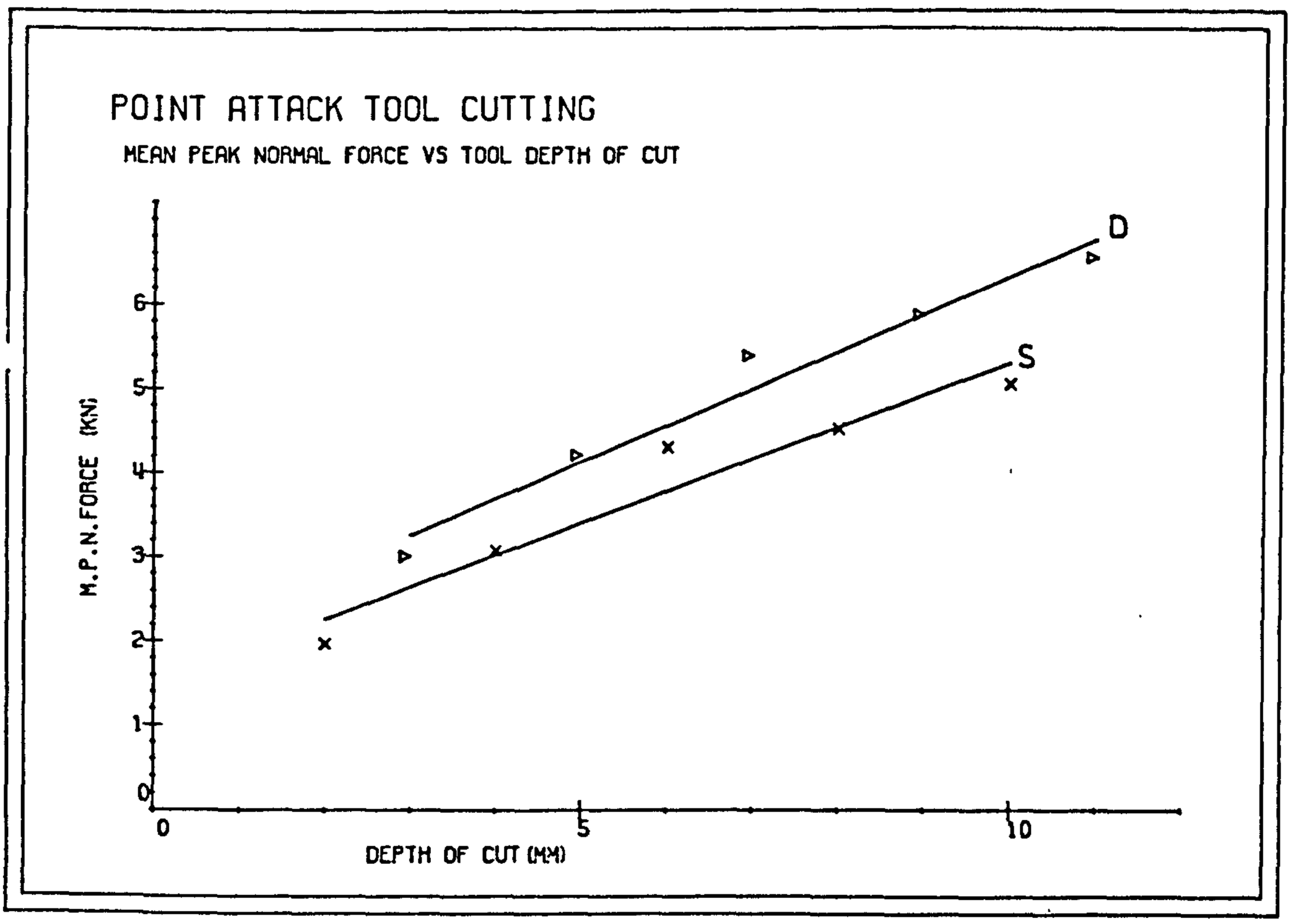
POINT ATTACK TOOL CUTTING
MEAN PEAK NORMAL FORCE VS TOOL DEPTH OF CUT
M.P.N.FORCE (KN)
0
1
2
3
4
5
6
D
S
0
5
10
DEPTH OF CUT (MM)

FIG. 5.6

5.4.3 On Mechanical Specific Energy

Mechanical Specific Energy decreased hyperbolically with increasing depth of cut, hence cutting efficiency has increased, (Figure 5.7.2).

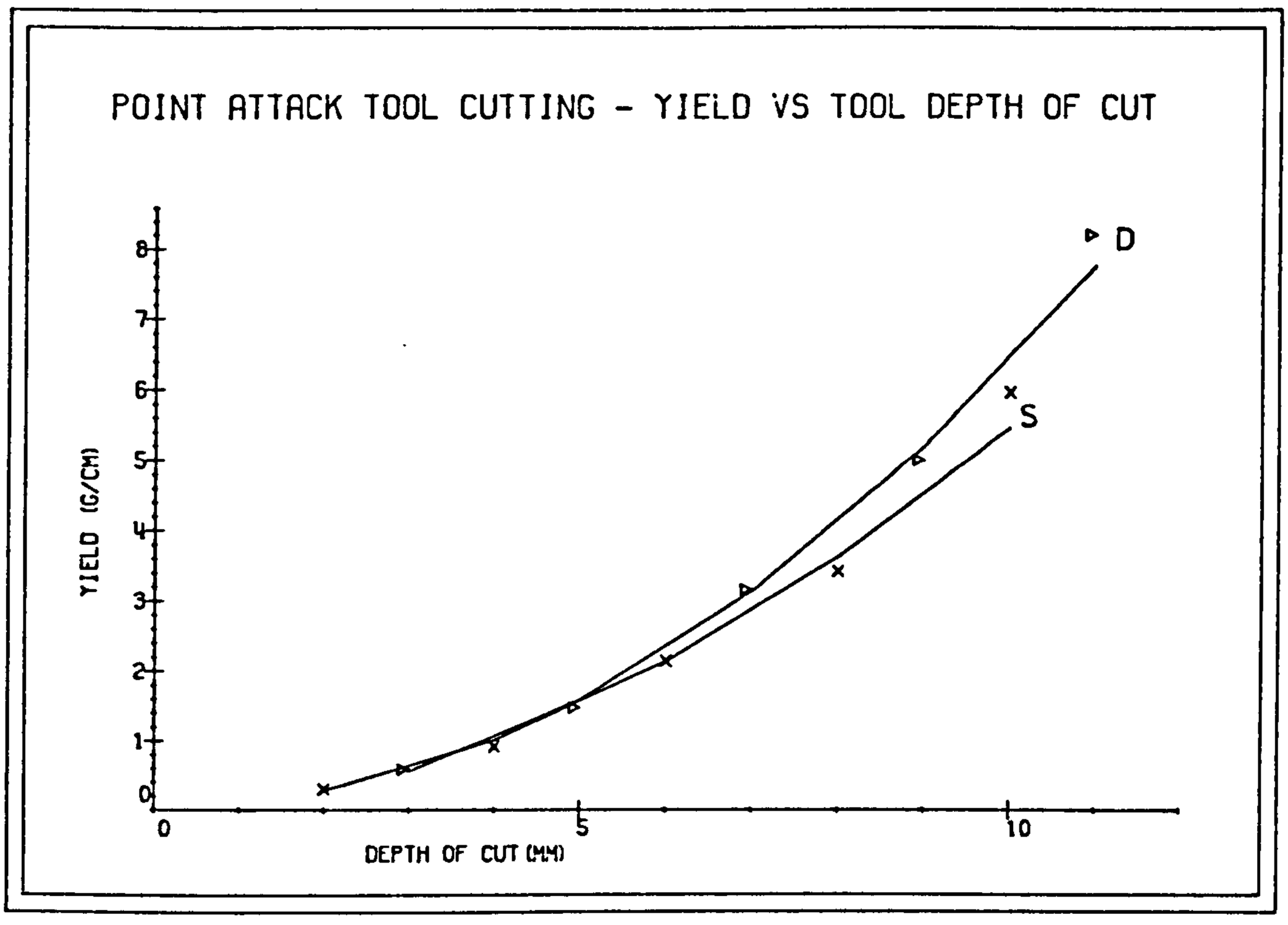
POINT ATTACK TOOL CUTTING - YIELD VS TOOL DEPTH OF CUT
YIELD (G/CM)
0
1
2
3
4
5
6
7
8
0
5
10
DEPTH OF CUT (MM)
D
S

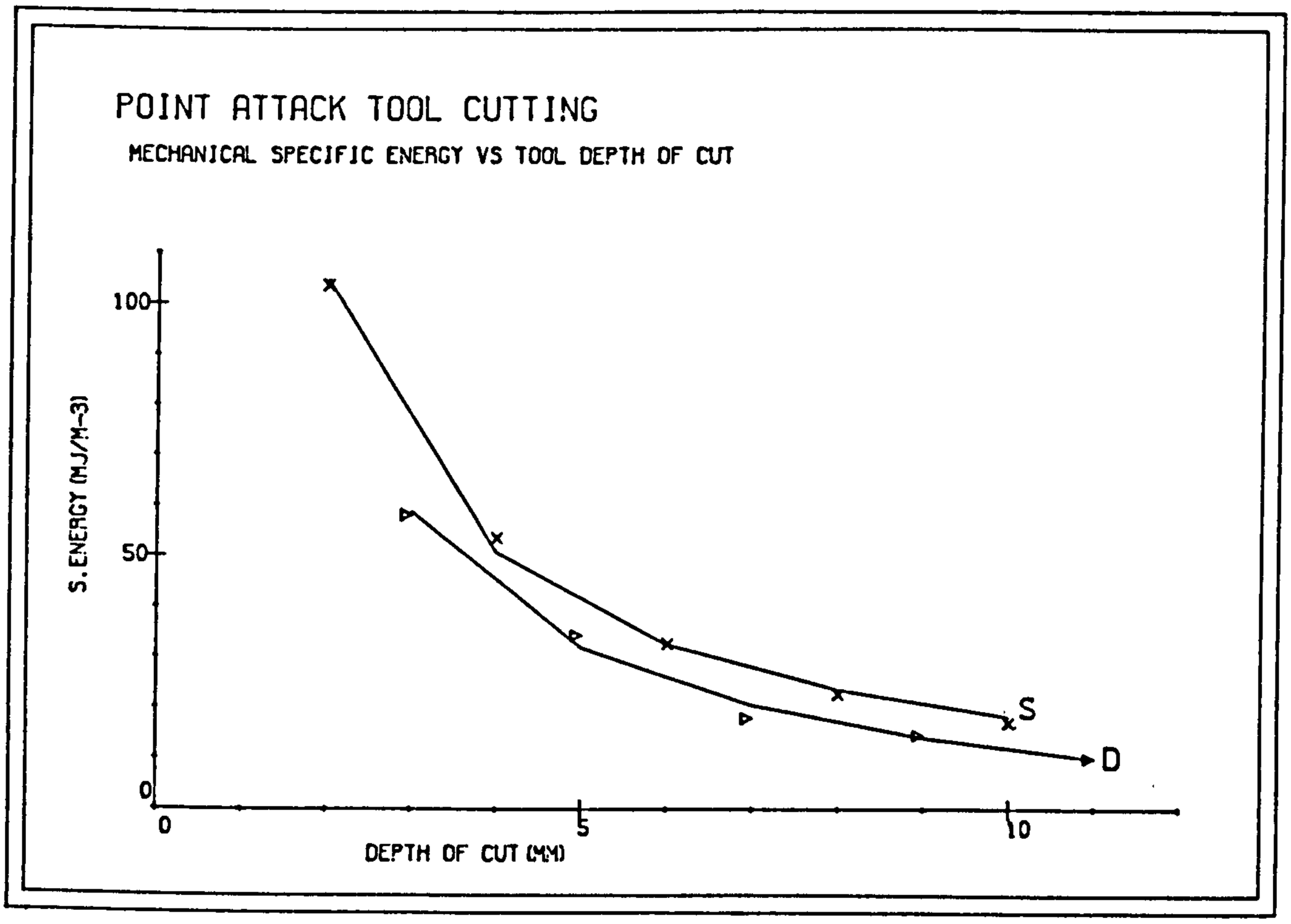
POINT ATTACK TOOL CUTTING
MECHANICAL SPECIFIC ENERGY VS TOOL DEPTH OF CUT
S.ENERGY (MJ/M-3)
0
50
100
0
5
10
DEPTH OF CUT (MM)
S
D

FIG. 5.7

5.5 FINITE ELEMENT STRESS ANALYSIS

It is necessary to know the action of the tool during cutting, in terms of stresses induced at the tool tip or in the rock at the vicinity of the tool tip, before an improvement can be made in its performance.

There are number of techniques available for stress analysis, e.g. 2-D and 3-D photoelasticity method, electrical analogue methods, grid and moire methods and numerical methods. Numerical stress analysis methods are better suited to rock cutting purposes than the other mentioned methods.

There are number of numerical procedures available and the Finite Element Method is one such method. It has a number of distinctive features which make it superior to most other methods, i.e. Finite Differences (104)

Basic concepts of Finite Element method will be mentioned briefly in following sections. There are numerous books available on the subject and references (104,126,171) give more basic information related to Finite Element method.

Finite Element Method

When an external force is applied to a structure it causes internal forces and deformations. For this cause-effect relationships in structures to be evaluated three basic conditions must be observed (126). These are:

- the equlibrium of forces
- the compatibility of displacements; and
- the laws of material behaviour.

The first condition requires that the internal forces balance the external applied loads. Compatibility requires that the deformed structure fits together and before this condition can be used it is necessary to know the relationship between load and deformation for each component of the structure. This relationship is the third condition, which in problems of linear elasticity reduces to the use of Hooke's Law.

The use of these three conditions is a fundamental requirement of any method of structural analysis.(126)

The basic concept of the Finite Element method, and of matrix structural analysis in general, is that every structure may be considered

to be an assemblage of individual structural components or elements (171). The structure must consist of a finite number of such elements interconnected at a finite number of joints or nodal points. The nodes may be thought of as nut-and-bolt devices, which secure adjacent finite elements through their ends or corners and hold them together (104). It is the finite character of the structural connectivity which makes possible the analysis by means of simultaneous algebraic (or matrix) equations, and which distinguishes a structural system from problems of continuum mechanics. (171)

The matrix methods of structural analysis may be formulated in three different ways:(126)

- Stiffness (displacement) method
- Flexibility (force) method
- Mixed method

The stiffness and flexibility methods differ in the order in which the two basic conditions of nodal equilibrium and compatibility are treated. In the stiffness method, the displacement compatibility conditions are satisfied and the equations of equilibrium set up and solved to yield the unknown nodal displacements. In the flexibility method the conditions of joint (nodal) equilibrium are first satisfied and the equations arising

from the need for compatibility of nodal displacements solved to yield the unknown forces in the members. In addition to these two basic approaches, in recent years a mixed formulation involving both approaches has also been used.

If the Stiffness method is considered; after the initial stage in which the body (structure) is replaced by a system of finite elements and nodes connecting them, the next step in this method of analysis is to determine the element stiffness matrix of the individual elements representing the body (104). These will then be assembled to form the overall stiffness matrix for the entire discretized body by requiring that the continuity of displacements and equilibrium of forces prevail at all nodes, in the finite element model of the body. This will led to the matrix equation

$$[K]\ (r) = (R) \quad \ldots\ldots\ldots\ldots\ldots\ldots (5.1)$$

in which [K] denotes the overall stiffness matrix of the body. (R) is the applied nodal forces and (r) is the resulting nodal displacements. [K] represents the force required to produce unit displacement of the body. Therefore, if we think of the finite element model of the body as an equivalent spring, then [K] will be a spring-constant representing its stiffness. Thus, the finite element method is essentially one in which the analysis of the body is carried out from the point of view of its stiffness.

For a given set of prescribed boundary conditions and external forces acting on the body, eqn. 1 can be solved uniquely for the nodal displacements (r), from which the stresses and strains within the body can subsequently be computed.

To summarise, the basic operations of a displacement method analysis of any structure consists in:

1. Sub-division of the body into a system of finite elements, expressed in any convenient local (element) co-ordinate system.

2. Evaluation of the stiffness and other properties of the individual structural elements and transformation of the element stiffness matrix from the local co-ordinate expression to a form relating to the global co-ordinate system of the complete structural assemblage.

3. Solution of equation 1 with prescribed conditions to determine (r) and

4. Calculation of strains and stresses within the elements from the computed nodal displacements (r).

5.5.1 Advantages of Finite Element Method

1. Owing to the flexibility of their sizes and shapes, finite elements are able to represent a given body, however complex its shape may be more faithfully.

2. Bodies with one or more holes in them or those with corners can be dealt with no difficulty.

3. Problems involving variable material properties and/or variable geometry, do not present any additional difficulty. Geometrical and material non-linearities, even time-dependent material properties can be dealt with relatively easily.

4. Problems of cause-effect relationship are formulated in terms of generalized forces and displacements which are related through the overall stiffness matrix. This aspect of the finite element method facilitates and simplifies the understanding of the problem and its solution.

5. Boundary conditions are easily dealt with.

6. The versatility and flexibility of the finite element method can be used very effectively to evaluate the cause-effect relationship in complex structural, continuum, field and other problems.

Finite difference treatment of 1, 3, 5 and particularly 2 is usually beset with considerable difficulties(104).

Finite element method of stress analysis forms only a small portion of the thesis and is done mainly for qualitative and not for quantitative purposes to give some idea with regards to stress fields generated, and the extent to which these fields spread in the rock so that if an improvement is to be made to tool performance, additional assistance could be directed towards this region thus stressing the rock further and ensuring fracture initiation and propagation at a lower mechanical tool force level. The PAFEC 75 finite element computer program is available at Newcastle University and was used for rock cutting stress analysis.

PAFEC stands for Program for Automatic Finite Element Calculations. The PAFEC 75 scheme is a version of PAFEC which has been designed so that users may input in a very straightforward manner (111)

PAFEC 75 data is input in a modular form. Each module begins with a header or 'module card'. After this there is a card giving the headings for the columns which form the remainder of the module. This card is called the contents card. For each type of module there is a standard layout for the columns which is taken if the contents card is omitted. The data is input as described in ref.(111). Within each of these Phases certain intructions may be given whereby the user requests that the standard actions taken within a Phase be modified.

The stresses are examined at 5 depths of cut levels (2, 4, 6, 8, 10mm) and Springwell sandstone is taken as the test medium. Normal and Cutting force values that were obtained with Springwell sandstone cutting tests were used for stress analysis, (Figure 5.8). Cutting and Normal forces were applied to the body simultaneously, so that actually it is their resultant components which was acting on the tool. The stress contours were drawn and these are shown in (Figures 5.8-5.11) for different depth of cuts.

As can be seen from (Figure 5.8), maximum tensile stresses occur immediately below the cutting tool tip. This was observed at all depths of cut. Compressive stresses however, have exhibited a different relationship. Minimum compressive stresses occurred further away from the tool for all depth of cut cases. For a 2mm depth of cut it was 8mm away from the edge of the rock, for a 4mm depth it was 9.5mm, for 6mm depth of cut it was 10.5mm, for 8mm depth of cut it lay 11mm away and finally for 10mm depth of cut it lay 11.5mm away from the edge of the rock at the point that the cutting tool was applied to the rock. Maximum compressive stresses occur nearest to the tool tip, for a 10mm depth of cut it being approximately 0.5mm away from the tool tip.

The results of finite element analysis suggested that, stresses which are both compressive and tensile occur immediately around the tool tip in the rock. If an improvement is to be made to the performance of the cutting tool, additional assistance must be provided and directed towards the stressed region, where maximum stresses occur. If any assistance is

TITLE -POINT ATTACK CUTTING AT 2MM DEPTH OF CUT

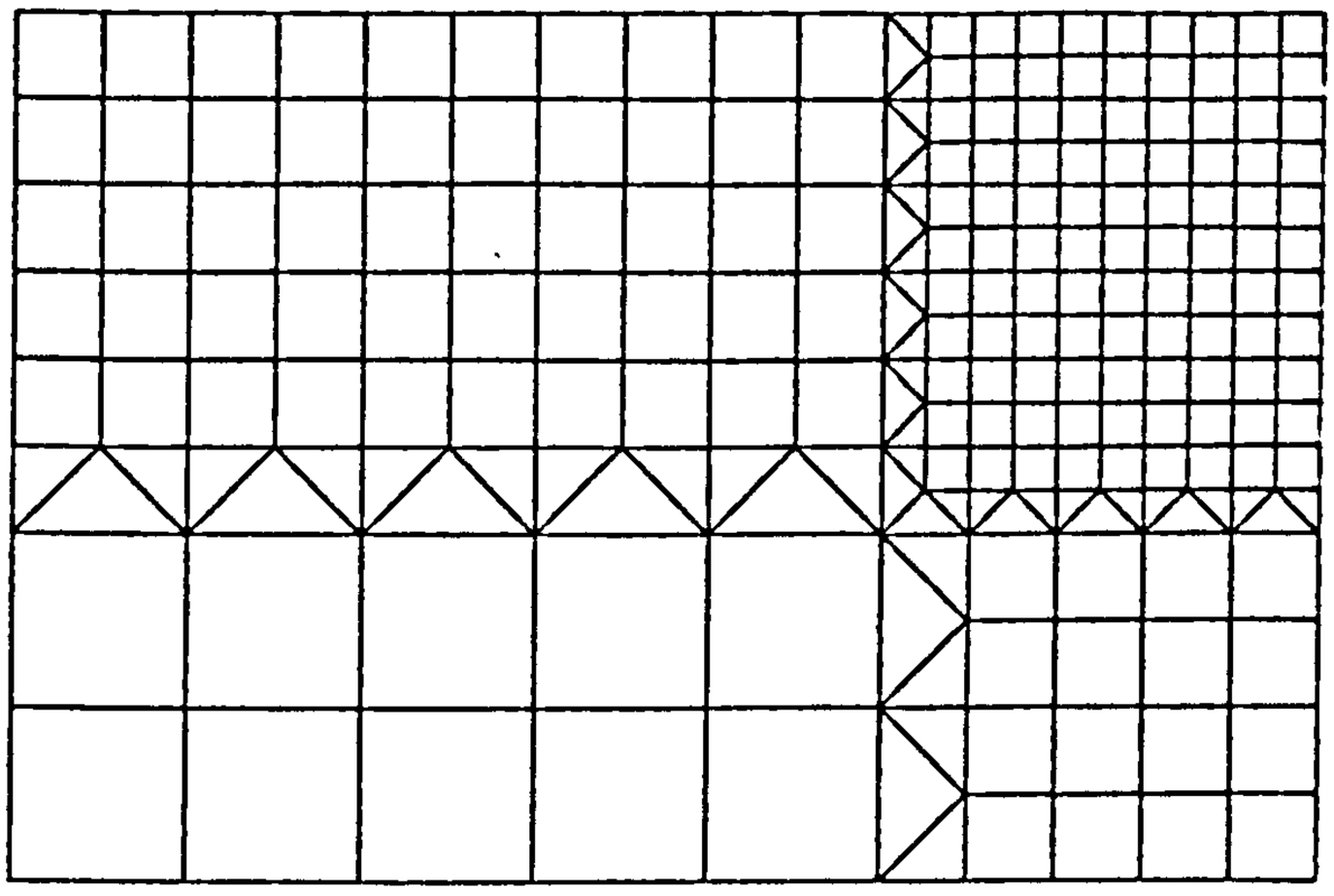

PAFEC 75

VIEW FROM X = 0.00
Y = 0.00
Z = 1.00

Y
X

Z TOWARDS VIEWER

WHOLE STRUCTURE DRAWN

MM.
STRUCTURAL UNITS

0 1 2 3 4 5

MULTIPLY BY 10^0

DRAWING NO.3
SCALE 6.67 :1

TITLE -POINT ATTACK CUTTING AT 2MM DEPTH OF CUT

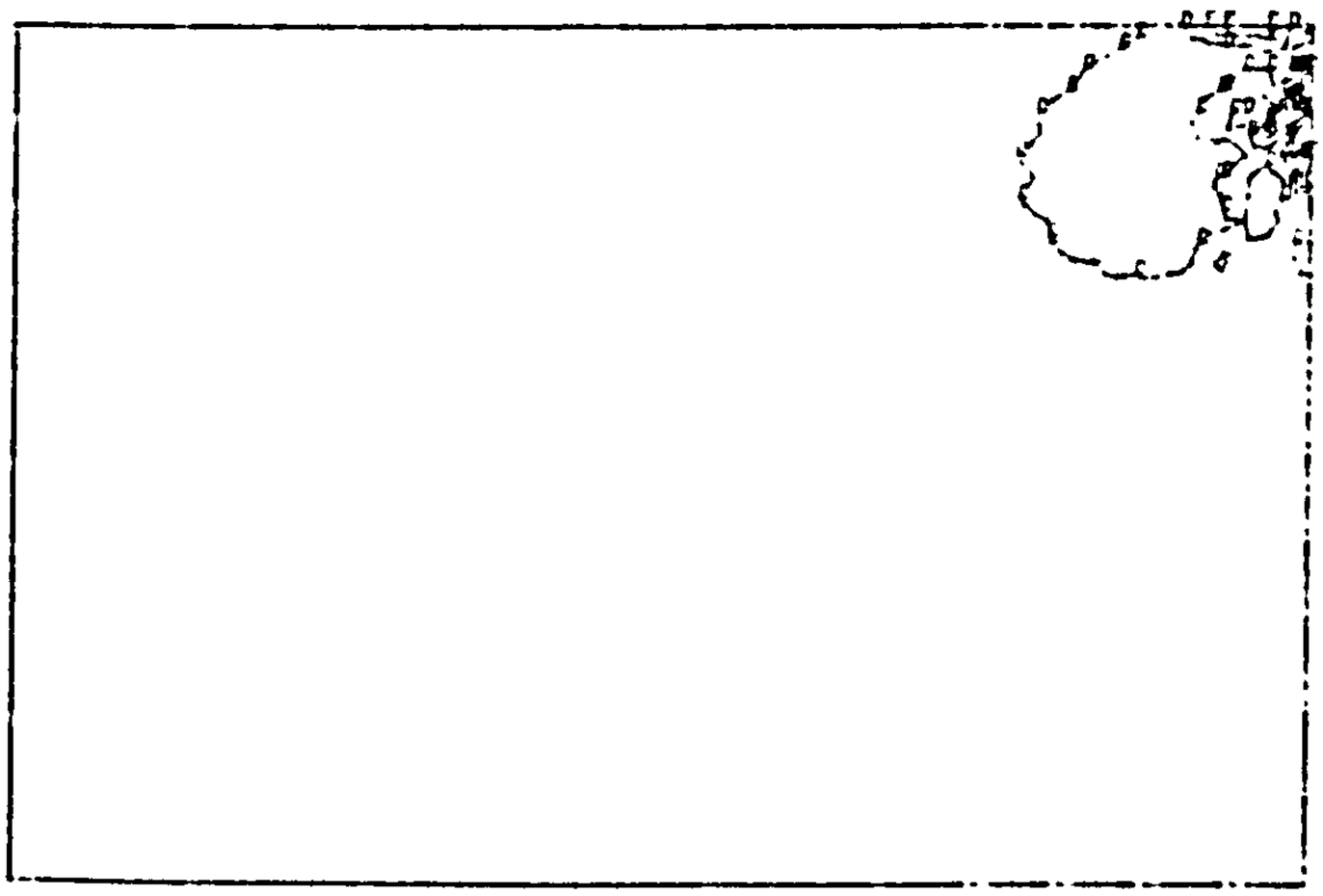

PAFEC 75

VIEW FROM X = 0.00
Y = 0.00
Z = 1.00

Y
X

Z TOWARDS VIEWER

MAXIMUM PRINCIPAL (MOST POSITIVE) STRESS
MULTIPLY BY 10^8

-0.15
-0.07
0.01
0.09
0.17
0.25
0.33
0.41
0.49
0.57

LOAD CASE #1

WHOLE STRUCTURE DRAWN
AS DEFINED IN FROM.DAT

MM.
STRUCTURAL UNITS

0 1 2 3 4 5

MULTIPLY BY 10^0

DRAWING NO.4
SCALE 6.67 :1

FIG. 5.8

TITLE -POINT ATTACK CUTTING AT 2MM DEPTH OF CUT

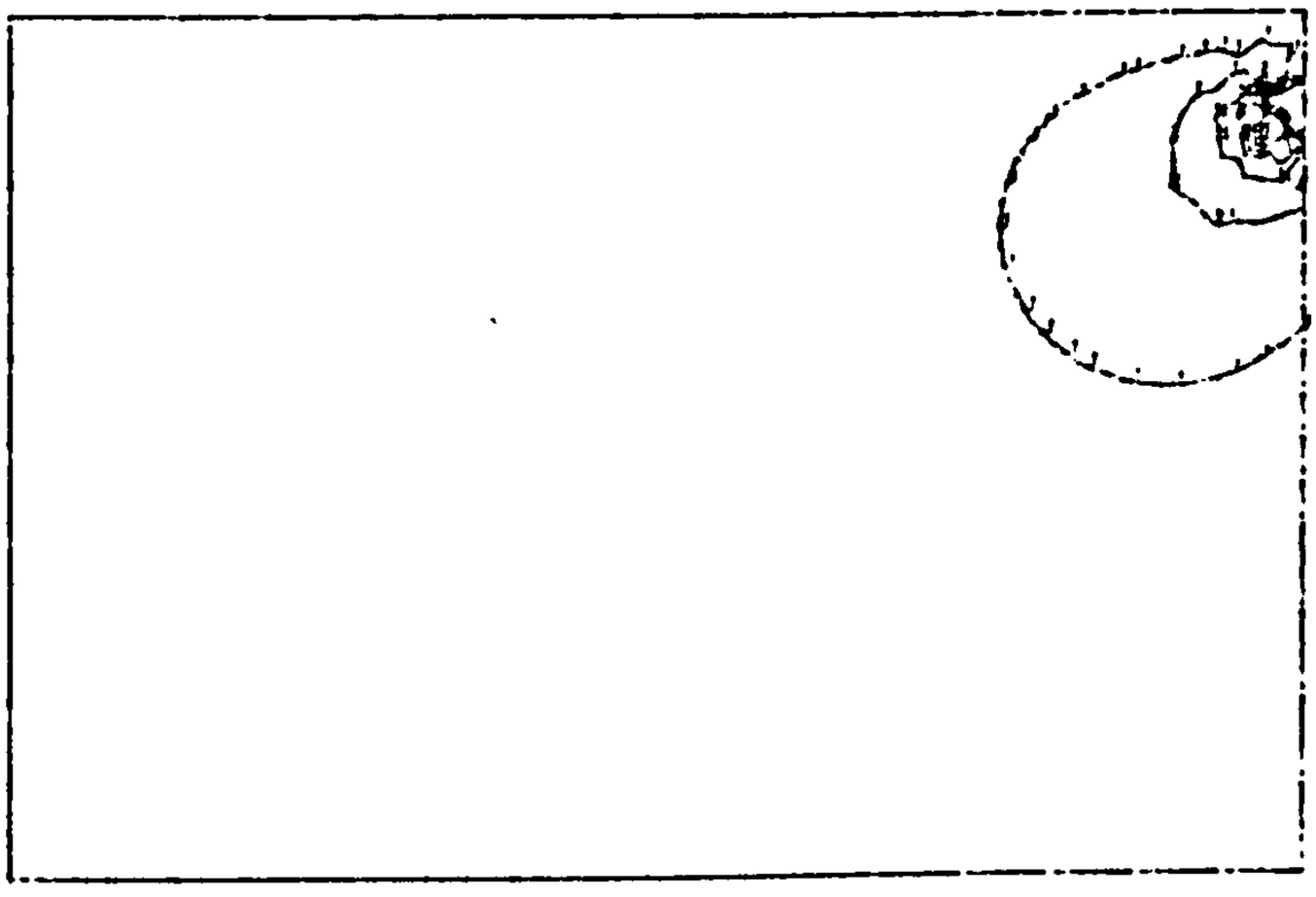

PAFEC 75

VIEW FROM X = 0.00
Y = 0.00
Z = 1.00

Y
X

Z TOWARDS VIEWER

MINIMUM PRINCIPAL (MOST NEGATIVE) STRESS MULTIPLY BY 10^6

-2.00
-1.79
-1.59
-1.39
-1.18
-0.98
-0.78
-0.57
-0.37
-0.16

LOAD CASE =1

WHOLE STRUCTURE DRAWN
AS DEFINED IN FRONT.ORDER

MM.
STRUCTURAL UNITS

1 0 2 0 3 0 4 0 5 0
MULTIPLY BY 10^{-3}

DRAWING NO.5
SCALE 6.67 :1

TITLE -POINT ATTACK CUTTING AT 4MM DEPTH OF CUT

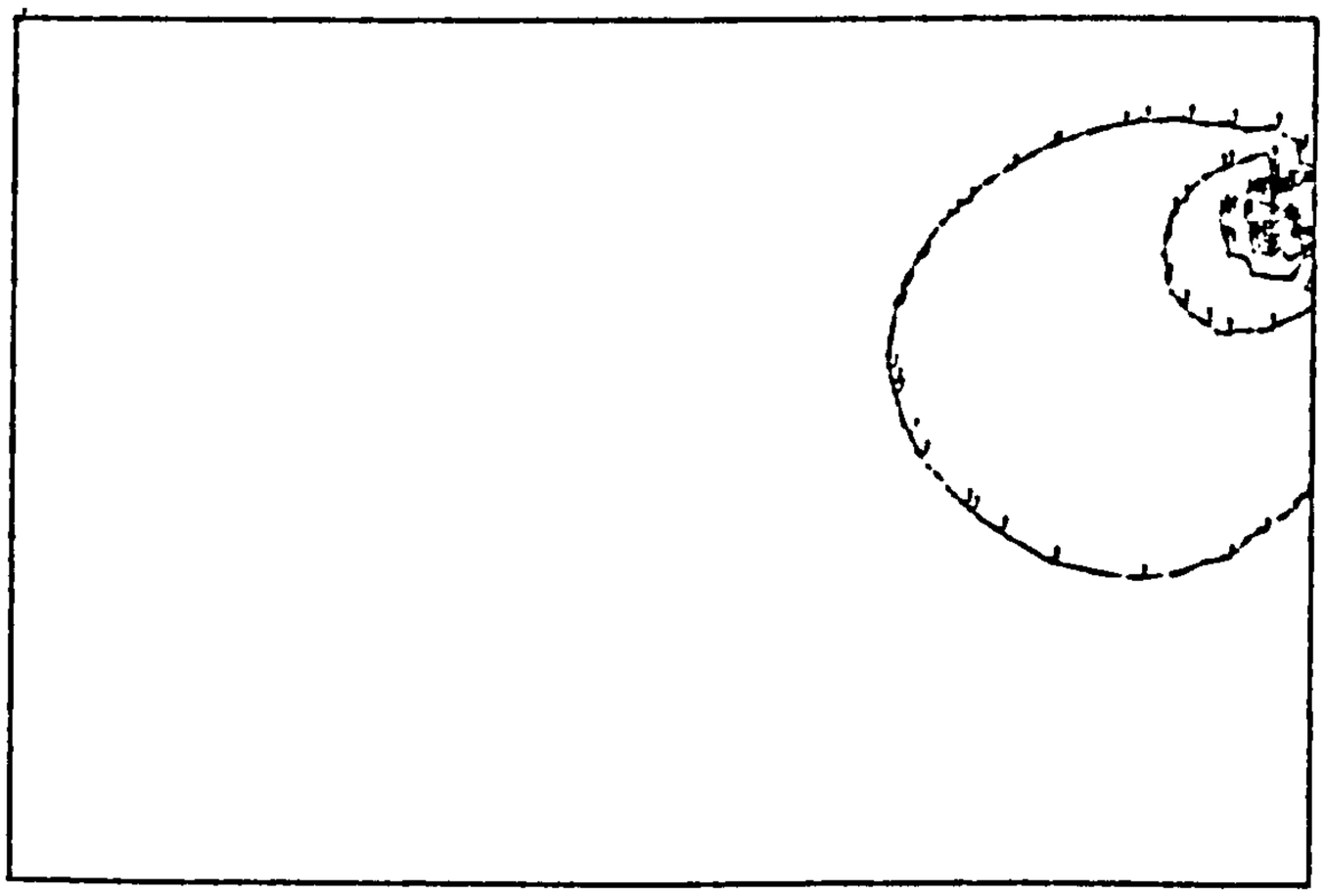

PAFEC 75

VIEW FROM X = 0.00
Y = 0.00
Z = 1.00

Y
X

Z TOWARDS VIEWER

MINIMUM PRINCIPAL (MOST NEGATIVE) STRESS MULTIPLY BY 10^6

-3.05
-2.73
-2.41
-2.09
-1.77
-1.45
-1.13
-0.82
-0.50
-0.18

LOAD CASE =1

WHOLE STRUCTURE DRAWN
AS DEFINED IN FRONT.ORDER

MM.
STRUCTURAL UNITS

1 0 2 0 3 0 4 0 5 0
MULTIPLY BY 10^{-3}

DRAWING NO.5
SCALE 6.67 :1

FIG.5.9

TITLE -POINT ATTACK CUTTING AT 6MM DEPTH OF CUT

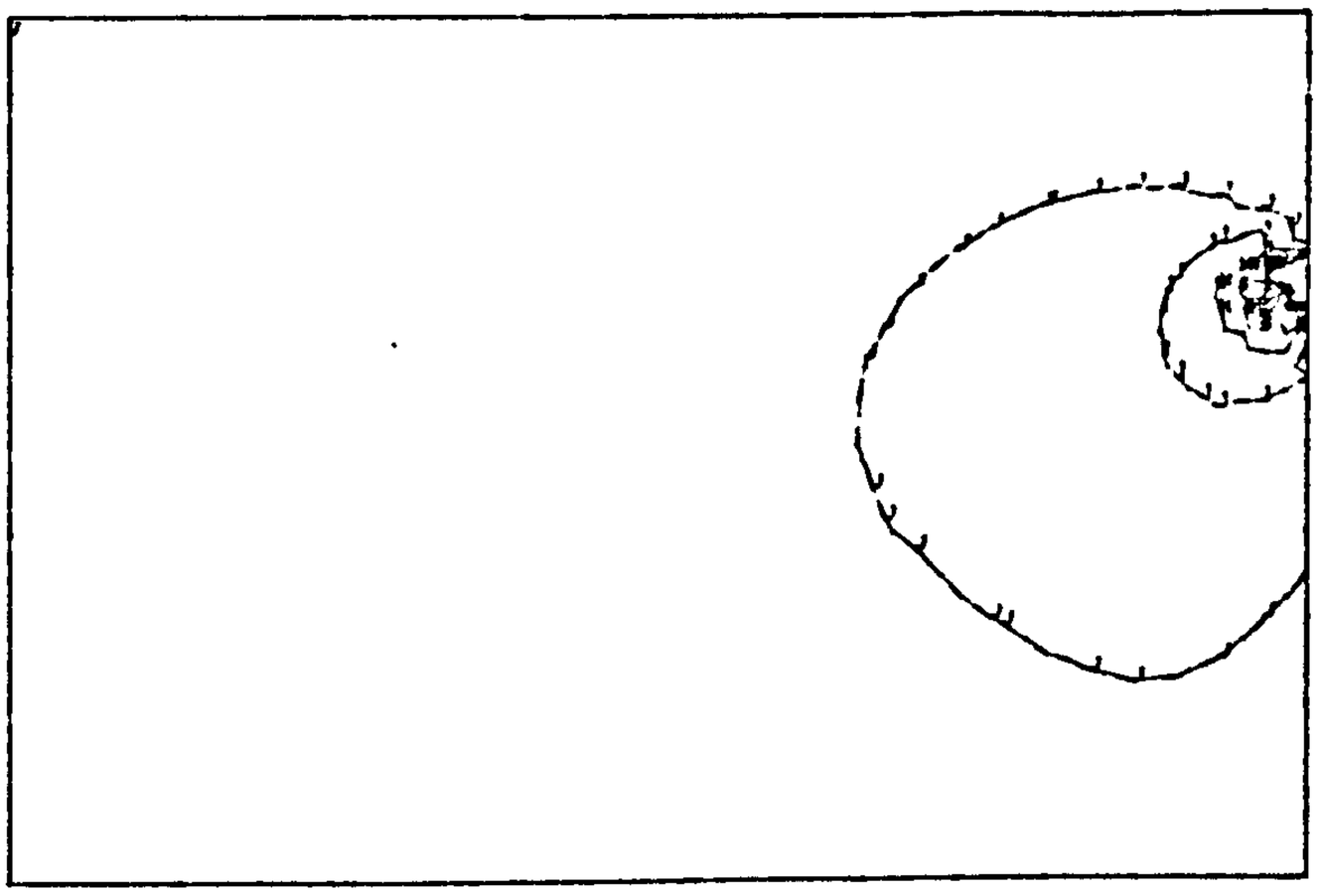

PAFEC 75

VIEW FROM X = 0.00
Y = 0.00
Z = 1.00

Y
X

Z TOWARDS VIEWER

MINIMUM PRINCIPAL (MOST NEGATIVE) STRESS MULTIPLY BY 10^6

-4.28
-3.63
-3.38
-2.94
-2.49
-2.04
-1.59
-1.14
-0.70
-0.25

LOAD CASE 1

WHOLE STRUCTURE DRAWN
AS DEFINED IN FRONT ORDER

MM.

STRUCTURAL UNITS

1 0 2 0 3 0 4 0 5 0

MULTIPLY BY 10^3

DRAWING NO.5
SCALE 6.67 :1

TITLE -POINT ATTACK CUTTING AT 8MM DEPTH OF CUT

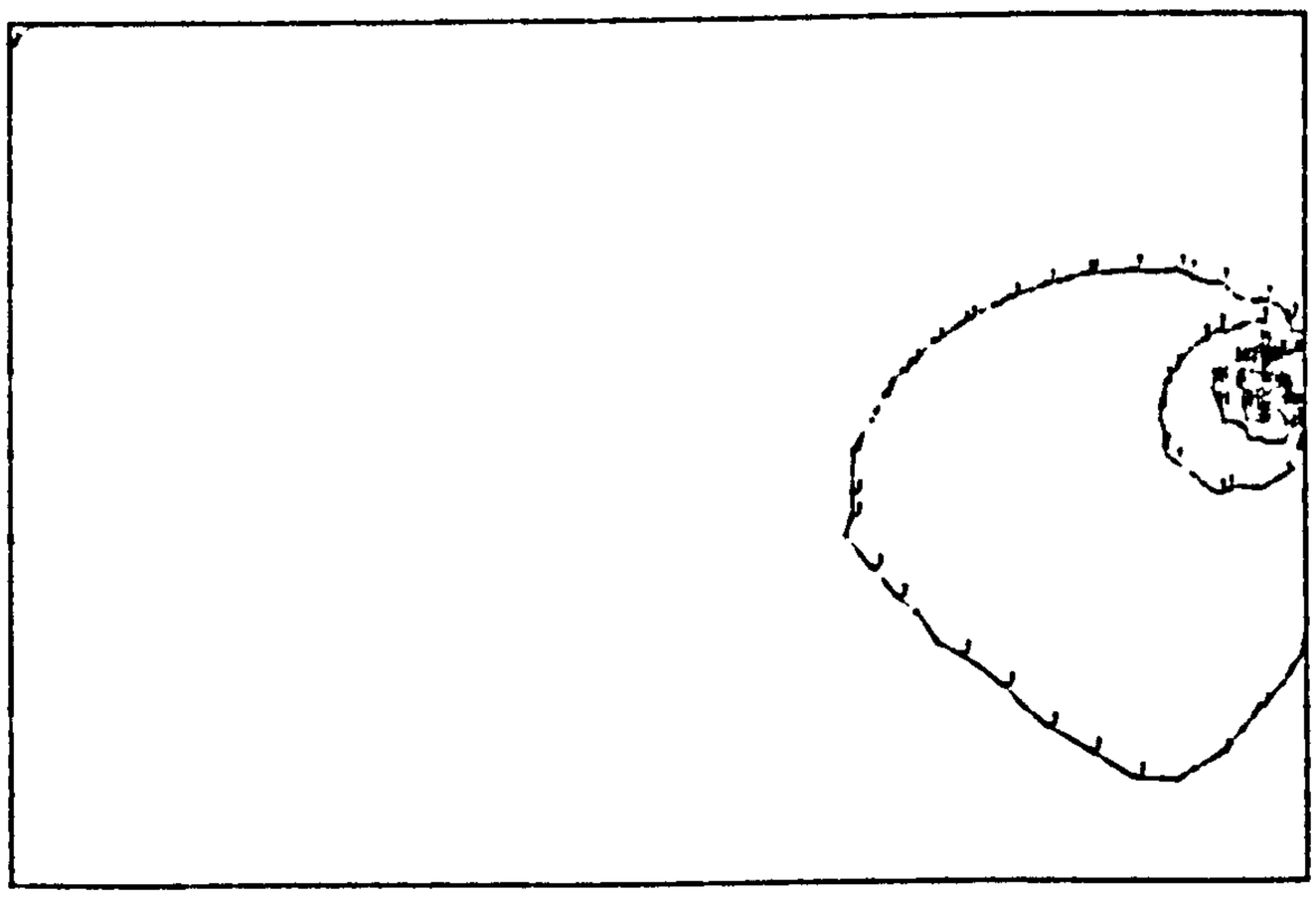

PAFEC 75

VIEW FROM X = 0.00
Y = 0.00
Z = 1.00

Y
X

Z TOWARDS VIEWER

MINIMUM PRINCIPAL (MOST NEGATIVE) STRESS MULTIPLY BY 10^6

-4.67
-4.18
-3.69
-3.20
-2.71
-2.22
-1.73
-1.24
-0.76
-0.27

LOAD CASE 1

WHOLE STRUCTURE DRAWN
AS DEFINED IN FRONT ORDER

MM.

STRUCTURAL UNITS

1 0 2 0 3 0 4 0 5 0

MULTIPLY BY 10^3

DRAWING NO.5
SCALE 6.67 :1

FIG. 5.10

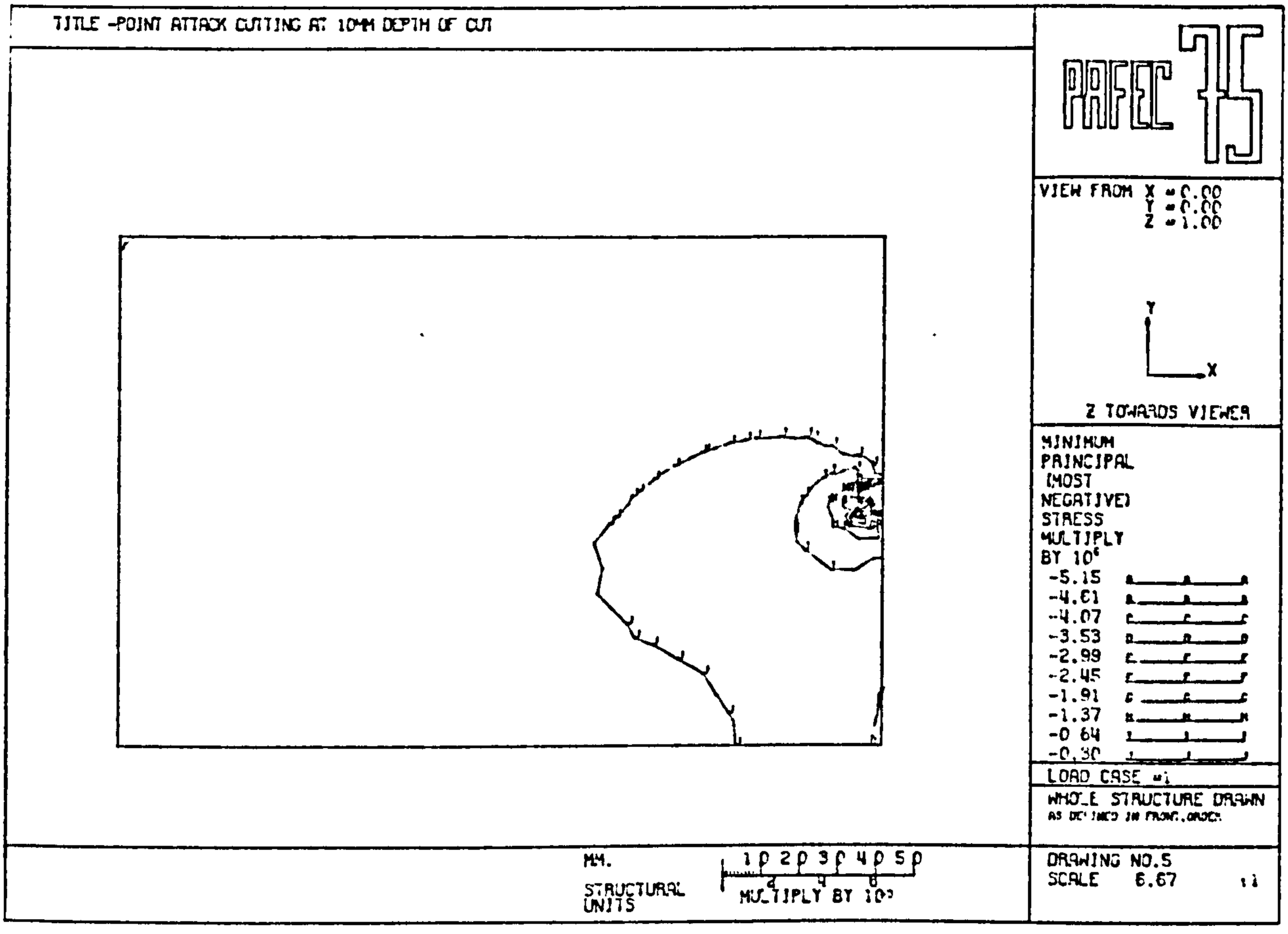
TITLE -POINT ATTACK CUTTING AT 10MM DEPTH OF CUT
PAFEC 75
VIEW FROM X = 0.00
Y = 0.00
Z = 1.00
Y
X
Z TOWARDS VIEWER
MINIMUM PRINCIPAL (MOST NEGATIVE) STRESS MULTIPLY BY 10^6
-5.15
-4.61
-4.07
-3.53
-2.99
-2.45
-1.91
-1.37
-0.84
-0.30
LOAD CASE 1
WHOLE STRUCTURE DRAWN
MM.
STRUCTURAL UNITS
1.0 2.0 3.0 4.0 5.0
MULTIPLY BY 10^3
DRAWING NO.5
SCALE 6.67

FIG. 5.11

to be provided, it must be as near to the tool tip as possible.

5.6 CONCLUSIONS

The influence of mechanical tool variables when cutting a particular rock with point attack tools have been found at different research institutes. These show that forces and mechanical specific energy values decrease and then start to rise again with increasing off-set angle with minimum values being obtained at 6.5 degrees. Increasing the angle of attack means reducing the rake angle and increasing back clearance angle. For an angle of attack greater than 50 degrees, a rise in cutting forces was noted and a back clearance angle of at least 12 degrees is necessary for efficient cutting with the point attack tools (66).

Compressive and Tensile stresses are produced in the rock when a simple conical point tool attacks a buttock of rock. When the stress applied by the tool equals the tensile strength of the rock, tensile cracks will open up at the tool-rock interface, and if the conditions are favourable these cracks will propagate to the surface of the rock.

Increasing the depth of cut caused corresponding increases in tool forces (cutting and normal) with forces obtaining higher values when Darney sandstone -which had the highest compressive and tensile strength in comparison to Springwell sandstone- is cut. The volume of rock (Yield) produced increased with depth of cut, exhibiting a power law relationship.

Mechanical Specific Energy decreased hyperbolically with increasing depth of cut. The lowest values were obtained at deeper depths of cut.

Although, two sandstone results are discussed here, there seems to be some sort of correlation between rock properties and forces experienced when cutting rocks with point attack tools. These will be discussed in (Chapter 9).

It is necessary to know the nature of the stresses induced in the rock during cutting before an improvement can be made to the performance of a point attack tool. Small scale finite element stress analysis was undertaken to reveal qualitatively these stress fields and their extent of spreading in the rock. Cutting and normal forces were applied simultaneously and stress analysis was carried out at five different depth of cut levels. The results showed that the highest compressive stresses occur immediately beneath the tool-rock interface and the minimum compressive stress values occur at 11.5mm distance away from the tool tip at 10mm depth of cut. These suggest that if an additional cutting method i.e. high pressure water jet is to be used to assist the point attack tool, it must be directed towards the high stress region surrounding the tip and as near to the tool tip as possible.

When the intensity of stress field in the rock is increased by applying a high pressure water jet to this region, the rock is broken at a lower mechanical tool force level. This should also increase the tool life.

6 INITIAL EXPERIMENTS WITH WATER JET ASSISTED DRAG TOOLS

6.1 EXPERIMENTAL DESIGN

The aim of any experimental design is to relate the measured parameters or quantities to the experimental variables. The way in which the experiments are designed will determine how much information can be derived on the effects of individual variables and their interaction.

Experiments can be designed either in the form of full factorial or partial factorial experiments. In full factorial design, it is required to test all possible combinations of the levels of each variable, to yield an empirical relationship between a parameter and the experimental variables. The number of tests involved is n^m, where m is the number of variables, and n is the number of different levels of each variables. So for a 5 variable, 5 level experimentation it is required to do $5^5 = 3125$ experiments and it has been statistically found that each experiment has to be repeated at least 4 times to yield a good approximated result. Therefore, all together, 12,500 experiments needed to be done if full factorial experimental design was used. Since it would require many years to complete, the only solution to the problem is the planning of partial experiments.

In partial factorial experiments the number of tests is reduced by selecting only certain combinations. There are four ways used for partial factorial experimentation :

1. By reducing the number of levels of each variable. Even though this would determine the effects of the variables, it would not be possible to obtain empirical relationships.

2. Studying the effect of each variable at constant levels of other variables. But it is not possible to find the interaction, if there is any, between variables.

3. Joint variation of each pair of variables with the other variables at constant levels. With this method it is not possible to find the effects of each variable separately.

4. The random balancing method proposed by Protodyakonov (Sr) studies the effect of each variable in a random combination of the levels of the other variables. Thus, as the experimental data is grouped according to each variable, the effects of other variables are neutralised. Protodyakonov (Sr) recognised the limitations of random selection as being only appropriate to very large experiments.

Protodyakonov (Jr) and Teder have further developed the random balancing method by using a systematic selection of level combinations

instead of a random selection. It is an essential feature of the method that each level of a variable appears in only one combination with each level of the other variable (61).

6.1.1 Protodyakonov Method

Partial factorial experiments based on the Protodyakonov method require the selection of combinations of levels so that each of these combinations occurs only once. The selection can either be done graphically, or by using numerical matrices. The graphical method is manageable for experiments involving up to four variables.

In addition to the graphical or positional method we can use numerical methods. The experimental plans for this method can be constructed on the basis of orthogonal Latin squares. Two squares are said to be orthogonal with respect to each other, if on superimposition, all the paired combinations of figures occur only once. It is required that the number of levels chosen must be always odd. For reasons relating to symmetry, on even number of levels cannot be used.

To find an experimental plan for a certain number of variables, a system of mutually orthogonal squares have to be generated. The number of squares is determined by the number of levels. The orthogonal squares are generated from an ordered square by displacement of the columns and circular rotation of the numbers. As shown in (Figure 6.1), the second

FIG.6.1 - GENERATION OF LATIN SQUARES

①

1	1	1	1	1
2	2	2	2	2
3	3	3	3	3
4	4	4	4	4
5	5	5	5	5

→

②

1	2	3	4	5
2	3	4	5	1
3	4	5	1	2
4	5	1	2	3
5	1	2	3	4

→

③

1	3	5	2	4
2	4	1	3	5
3	5	2	4	1
4	1	3	5	2
5	2	4	1	3

→

④

1	4	2	5	3
2	5	3	1	4
3	1	4	2	5
4	2	5	3	1
5	3	1	4	2

⑤

1	5	4	3	2
2	1	5	4	3
3	2	1	5	4
4	3	2	1	5
5	4	3	2	1

→

1	1	1	1	1
2	2	2	2	2
3	3	3	3	3
4	4	4	4	4
5	5	5	5	5

→

⑥

1	2	3	4	5
1	2	3	4	5
1	2	3	4	5
1	2	3	4	5
1	2	3	4	5

111111	123452	135243	143524	154325
222221	234512	241353	253144	215435
333331	345122	352413	314254	321545
444441	451232	413523	425314	432155
555551	512342	524133	531424	543215

FIG. 6.2 - SUPERIMPOSITION OF ORTHOGONAL LATIN SQUARES OF A SIX VARIABLE EXPERIMENT.

square results from a vertical displacement of adjacent columns by 1 row, notice the first column is not changed, together with renumbering of the columns. Thus, we obtain the next system of mutually orthogonal squares, in which the initial square is an ordered one, while the rest are Latin squares. This procedure is followed until the first square is reproduced. So far there are five mutually orthogonal squares. A sixth square can be produced by turning the ordered square through 90 degrees. A superimposition of these six squares gives an experimental plan for six variables, each at five levels, where each square contains a combination of levels for one test out of a total of 25, (Figure 6.3).

The number of mutually orthogonal squares in one system is thus equal to (n+1), where n is the number of rows (levels). The number of tests in an experiment designed in this form is, therefore, reduced by a factor of $[n^{m-2}]$ from the full factorial matrix. Notice however, that the number of variables that can be studied is dependent upon the number of mutually orthogonal squares. For a four variable, five level experiment it is only necessary to combine four orthogonal squares out of a possible number of six. This plan was used to construct the first set of experiments to be performed on Springwell sandstone.

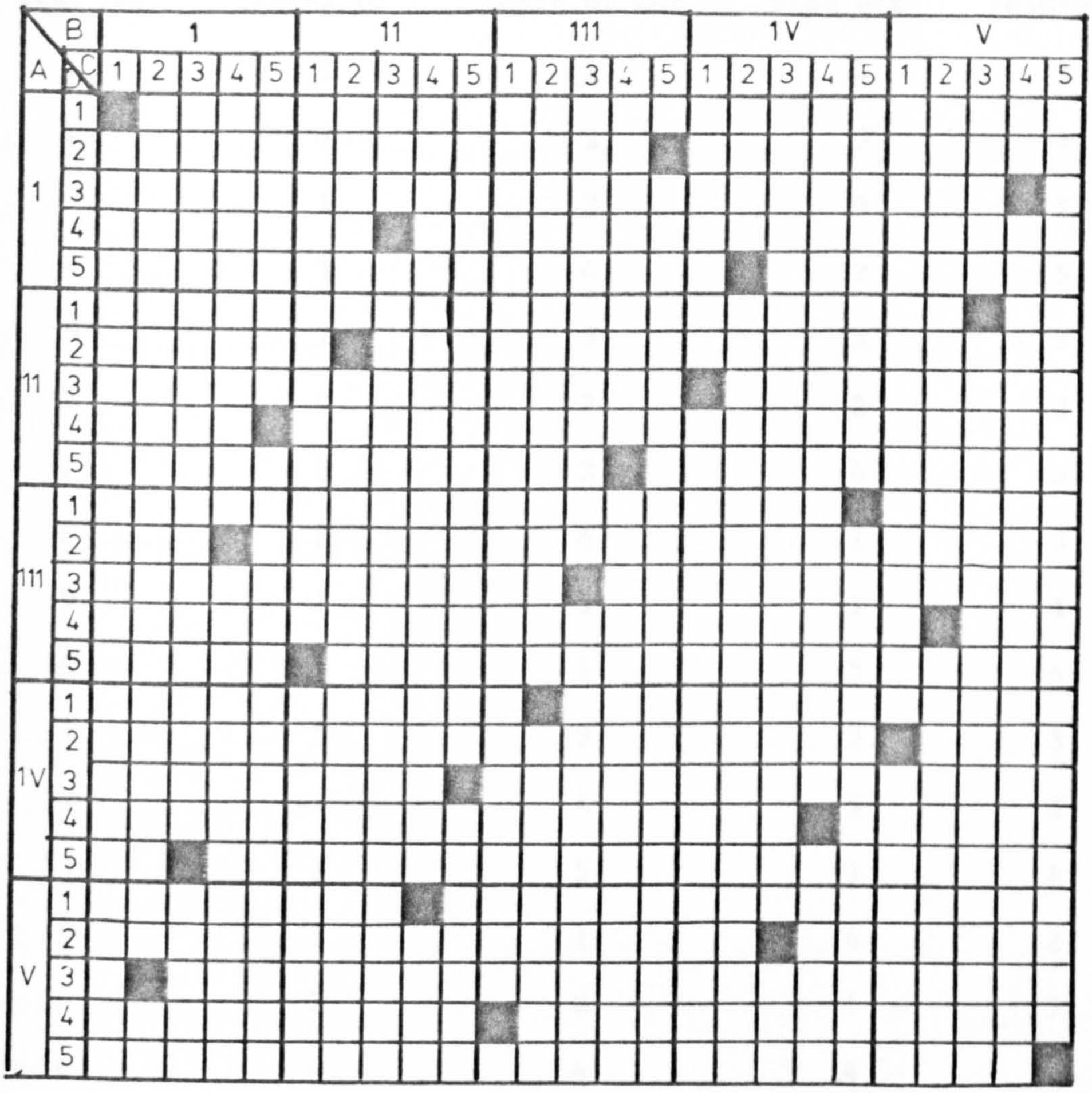

FIG. 6.3 – GRAPHICAL PRESENTATION OF EXPFRIMENTAL PLAN FOR A FOUR VARIABLE EXPERIMENT

Experimental Plan for four variables each having five levels

Test No.	Levels of Pressure	Depth of Cut	Side off	Lead-on
1	1	1	1	1
2	1	2	3	4
3	1	3	5	2
4	1	4	2	5
5	1	5	4	3
6	2	2	2	2
7	2	3	4	5
8	2	4	1	3
9	2	5	3	1
10	2	1	5	4
11	3	3	3	3
12	3	4	5	1
13	3	5	2	4
14	3	1	4	2
15	3	2	1	5
16	4	4	4	4
17	4	5	1	2
18	4	1	3	5
19	4	2	5	3
20	4	3	2	1
21	5	5	5	5
22	5	1	2	3

23	5	2	4	1
24	5	3	1	4
25	5	4	3	2

Besides the Latin squares, the experiments can be planned according to the system of mutually orthogonal Latin cubes. A Latin cube is formed from (n) layers of Latin squares, arranged in such a manner, that any one section parallel to the facets of the cube forms a Latin square.

6.2 ANALYSIS OF DATA - DETERMINATION OF EMPIRICAL EQUATIONS

It is the feature of the partial factorial program that if data is grouped according to the levels of one of the variables, each group will contain data at all the levels of all the other variables(152).

For example, grouping the data according to Lead-on distance gives five groups of test numbers: 1-5, 6-10, 11-15, 16-20, 21-25. If these grouped results are meaned, the effects of the other variables are averaged to their experimental level (D) depth of cut = 3, (S) side-off distance = 3, (P) pressure = 3, (SD) stand-off distance = 3. This procedure can be used for any of the variables SD, S, D, P. Thus, by changing the order of averaging, it is possible to obtain the effecs of all the variables using the data from 25 tests.

The effects of each variable are obtained by grouping and averaging the data as described above. From these partial functions the next stage is the development of the complete empirical equation, describing the combined effect of all the variables.

Determination of Empirical Equation will be explained with an example to illustrate the steps needed. Take the case of finding equations for the YIELD. By looking at the graphs it was decided that stand-off distance and lead-on distance had no effect on the yield,but the other three variables have exhibited some sort of relationship. The exact combinations of the functions are found by the method of successive approximation. First, the initial data is grouped according to each variable and a partial function is determined for the most effective variable. All the data is then rescaled using the value of this function for each combination of levels. Thus, the effect of the first variable will be eliminated and the scatter in the data will be reduced, so that the effect of the second variable will be more apparent. The data is grouped according to the second variable from which a partial function of that variable is defined. A further rescaling is then carried out, using the second partial function, to eliminate the effect of the second variable. This process is repeated for the remaining variables.

Rescaling of the data can be done be either subtraction or division of the values of each partial function. The effects of a particular variable can only be eliminated if the method of rescaling is in accordance with the manner in which the variable combines with the other variables.

If a wrong method of rescaling is used, it would show itself simply by effecting the rescaling of the other variables. Instead of eliminating the scatter in the data for other variables, it will increase it.

First of all the mean value of Q (Yield) is calculated for each group of variables. For the case of level 1 for depth of cut it is 0.418, for the pressure it is 1.695, for side-off distance 1.47, etc.

Then, from these meaned data a table is drawn

	Depth of Cut (mm)	Pressure (MPa)	Side-off Distance(mm)	Lead-on Distance(mm)
Level 1	0.418	1.695	1.47	1.785
Level 2	0.872	1.680	1.77	1.25
Level 3	1.574	1.680	1.785	1.77
Level 4	2.442	1.785	1.88	1.755
Level 5	3.432	1.995	1.92	1.88

Then the graphs of these variables against the levels are drawn. Notice that for instance, in the case of depth of cut the relationship between yield and depth of cut is at mean values of other variables.

The next step is to find the relationships, by looking at the graphs. Two of these are curves, the others are linear. From the graphs, notice

that there is no change in the values of yield as the lead-on distance is increased. So, we can say it does not effect it. The relationship for the other variables can be represented by equations in the form:

$$Q = Ad^2 + B \qquad \text{(Power)} \quad \ldots\ldots \quad (6.1)$$

$$Q = (S + C)/(S+D) \qquad \text{(Hyperbolic)} \ldots\ldots \quad (6.2)$$

$$Q = EP + F \qquad \text{(Linear)} \quad \ldots\ldots \quad (6.3)$$

The letters A, B, C, D, E and F are constants. One should remember that these are only partial equations and constants cannot, therefore, be single valued.

Now, assume that these partial equations combine as a product of each other:

$$\text{i.e.} \quad Q = f1(D) \times f2(S) \times f3(P) \ldots\ldots \quad (6.4)$$

where f1, f2, f3 are the equations 1, 2 and 3.

The next step is to find the values of the constants in the equations. For this, take the most influential variable slope of which is the steepest, e.g. depth of cut, Eqn (6.1) first. To be able to determine the effects of other variables to the overall equation, the major influence of equation (6.1) has to be neutralised.

Equation (6.1) has the form:

$$f1(D) = Ad^2 + B = 3.13 \times 10^{-2}d^2 + 0.37$$

we can write the equation as

$$f1(D) = [d^2 + B/A]xA = d^2 + 11.833$$

If now we divide the original data by $[d^2 + B/A]$ we eliminate the effect of depth of cut from the data set.

We now have 25 different new values instead of our original data. These 25 values are then grouped and meaned at the appropriate levels of the second most important variable, i.e. in this case side-off distance.

Levels of	Side-off Distance(mm)	Mean Yield 'Q' x (10^{-2})
	0	2.483
	10	3.27
	20	3.09
	30	3.25
	40	3.263

Now, it is possible to calculate the general constants associated with side-off distance. by regressing these calculated values against side-off

distance gives a partial equation:

$$f2(S) = (S+0.641)/(S+1)$$

In order to find the effects of pressure it is necessary to eliminate the effect of side-off distance from data set. $\{Q/[d^2 + B/A]\}$ values are divided by $[(S+C)/(S+D)]$ to give a new data set. This is then averaged according to the levels of P and new mean values of $Q/[d^2+ B/A][(S+C)/(S+D)]$ are regressed against P.

Levels of Pressure (MPa)	Mean 'Q' ($x10^{-2}$)
13.79	2.93
24.14	3.34
34.48	3.19
44.83	3.58
55.17	3.94

This gives the final constants to give the general equation:

$$E = 2.18 \times 10^{-4}$$

$$F = 2.644 \times 10^{-2}$$

$$F3(P) = 2.18 \times 10^{-4} P + 2.644 \times 10.2$$

So the final equation is:

$$Q = [d^2+11.833][(S+0.641/(S+1)] \ (2.18 \times 10^{-4}P + 2.644 \times 10^{-2})$$

The validity of this equation can easily be checked by comparing the predicted values with the measured ones. This can be represented in a graphic form. When the actual and predicted values are regressed, it showed a linear relationship with equation

$$\text{Actual} = 0.97 \text{ Predicted} + 8.05\text{x}10^{-2}$$

which gave a correlation coefficient of 0.985.

Similar analysis was performed on experimental results to yield empirical equations for Mean Cutting Force, Mean Peak Cutting Force, Mean Normal Force, Mean Peak Normal Force, Mean Peak Sideways Force and, finally, Mechanical Specific Energy.

6.3 HYBRID CUTTING

The effect of positioning of the water jet with respect to the mechanical tool is investigated before the effects of other variables. Positional variables that can have an effect on cutting results are categorised as follows:

1. Stand-off distance

2. Lead-on distance

3. Side-off distance

Springwell sandstone is a medium grained, low medium strength sandstone which was used extensively as an ideal experimental rock for cutting tests previously in the laboratory and is chosen for hybrid cutting tests.

6.3.1 Physical and Mechanical Properties of Springwell Sandstone

Description and Mineralogy

Springwell sandstone is composed predominantly of medium grained quartz fragments. Poor rounding suggests an alluvial origin in which the grains have have not yet been subjected to high energy conditions. The cement often shows iron staining(8).

Sphericity	:	poor to moderate
Rounding	:	poor
Mineralogical content	:	(500 No. of points counted)
		%

Quartz	63
Rock fragments	17
Ferromagnesion	3
Feldspar	1
Iron oxide	2
Matrix	14

Grain size distribution of the quartz grains:

Between 0.5mm and 0.75mm	7%
Between 0.25mm and 0.50mm	83%
Between 0.10mm and 0.25mm	10%

Mean Quartz grain size = 0.32mm

Uniaxial Compressive Strength (MPa) : 43.21 ∓ 1.51

Indirect Tensile Strength (Disc) (Mpa): 2.99 ∓ 0.22

Triaxial Strength

Confining Pressure (MPa)	Failure Stress (MPa)
0.00	43.21
3.45	63.62
6.20	81.05
10.34	95.44
13.79	113.23
17.24	127.25
20.69	132.55
24.14	144.67
27.58	157.17

Static Elastic Moduli (GPa) Etan : 15.4

Esec	: 13.8
Dynamic Elastic Modulus (GPa)	: 17.9
Poisson's ratio	: 0.26
Bulk density (gm/cm^3	: 2.21
Apparent Porosity (%)	: 16.36
Coefficient of friction ( )	: 0.448∓0.014
Shore Rebound Hardness	: 36.70 ∓ 6.29
Plasticity (%)	: 42.24
Schmidt Hammer Rebound Number	: 52.03 ∓ 1.07
I.S.I.	: 61.53 ∓ 1.32
Cone Indenter Hardness	: 1.98 ∓ 0.41
Machineability (mm^3	: 6.52
Machineability Index	: 10.83
Abrasivity (10^{-4}mm 2)	: 7.31

Partial Factorial Experimental Design was adopted for the study of the experimental values.

6.3.2 Experimental Plan

Water jetting nozzles have to operate at some distance from the rock surface when they are located on an excavation machine cutting head, and this distance must be such that any detrimental effect that can result from rock chippings and dirt is minimised.

The two other positional variables have a differing influence on the cutting mode of the excavation system. Small scale finite element stress analysis was undertaken and results were shown in Chapter (5). The effects of Lead-on distance and side-off distance are examined at five experimental levels.

Variable Levels for Experimental Programme

Variable	Level				
	1	2	3	4	5
Mechanical Depth of cut (mm)	2	4	6	8	10
Water Jet Pressure (MPa)	13.79	24.14	34.48	44.83	55.17
Lead-on Distance (mm)	2	5	8	11	14
Side-off Distance (mm)	0	10	20	30	40
Stand-off Distance (mm)	15	30	45	60	75

The cutting speed was kept constant and a nozzle of 0.85 mm. diameter was used. Experimental procedure and parameter measurements and calculations were described in (Chapter 3).

Each cut was repeated four times and the diameter of the point attack tool was measured to note any changes. The position of the nozzle in its holder was noted and the same position was maintained throughout the

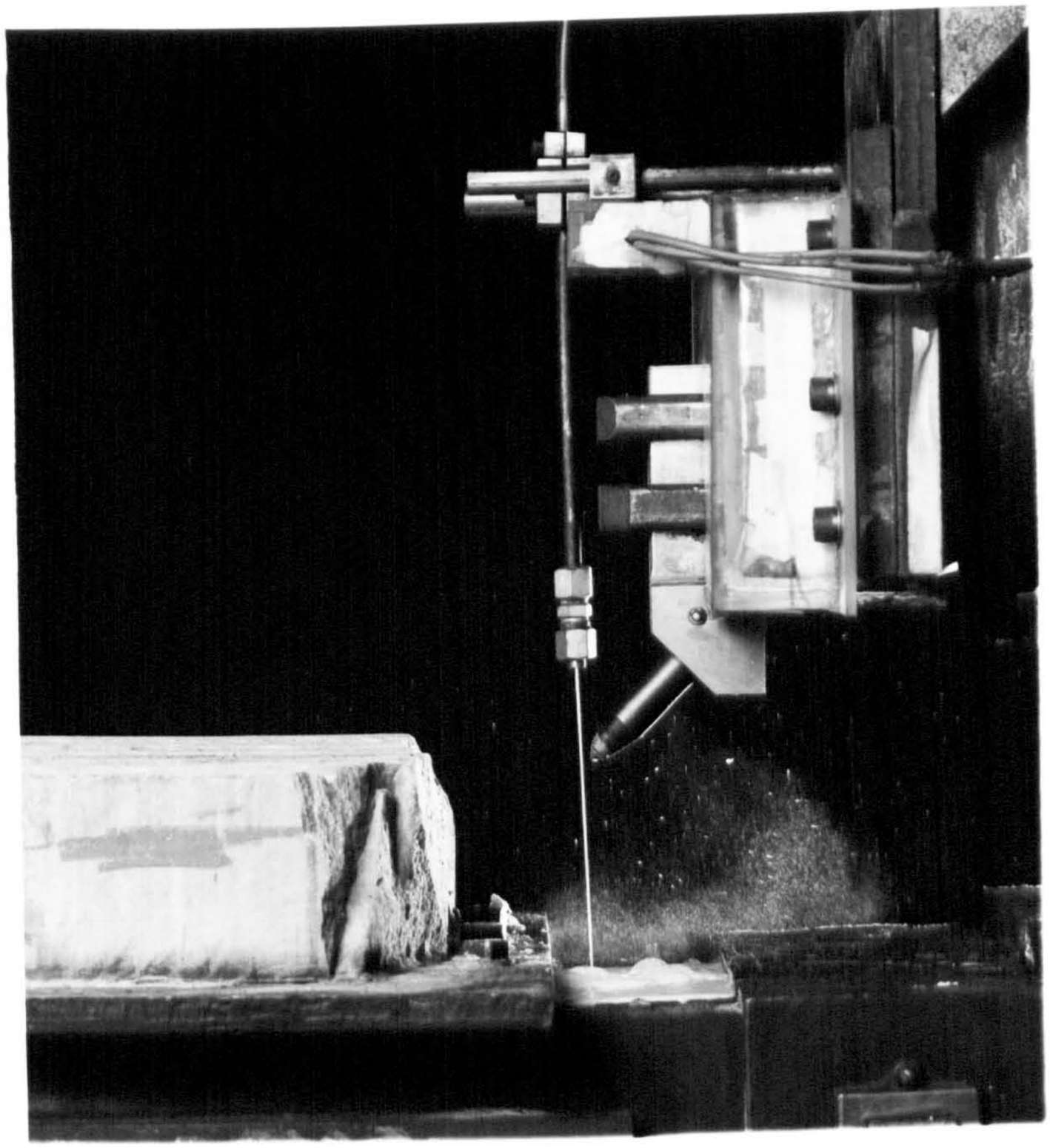

Before

During

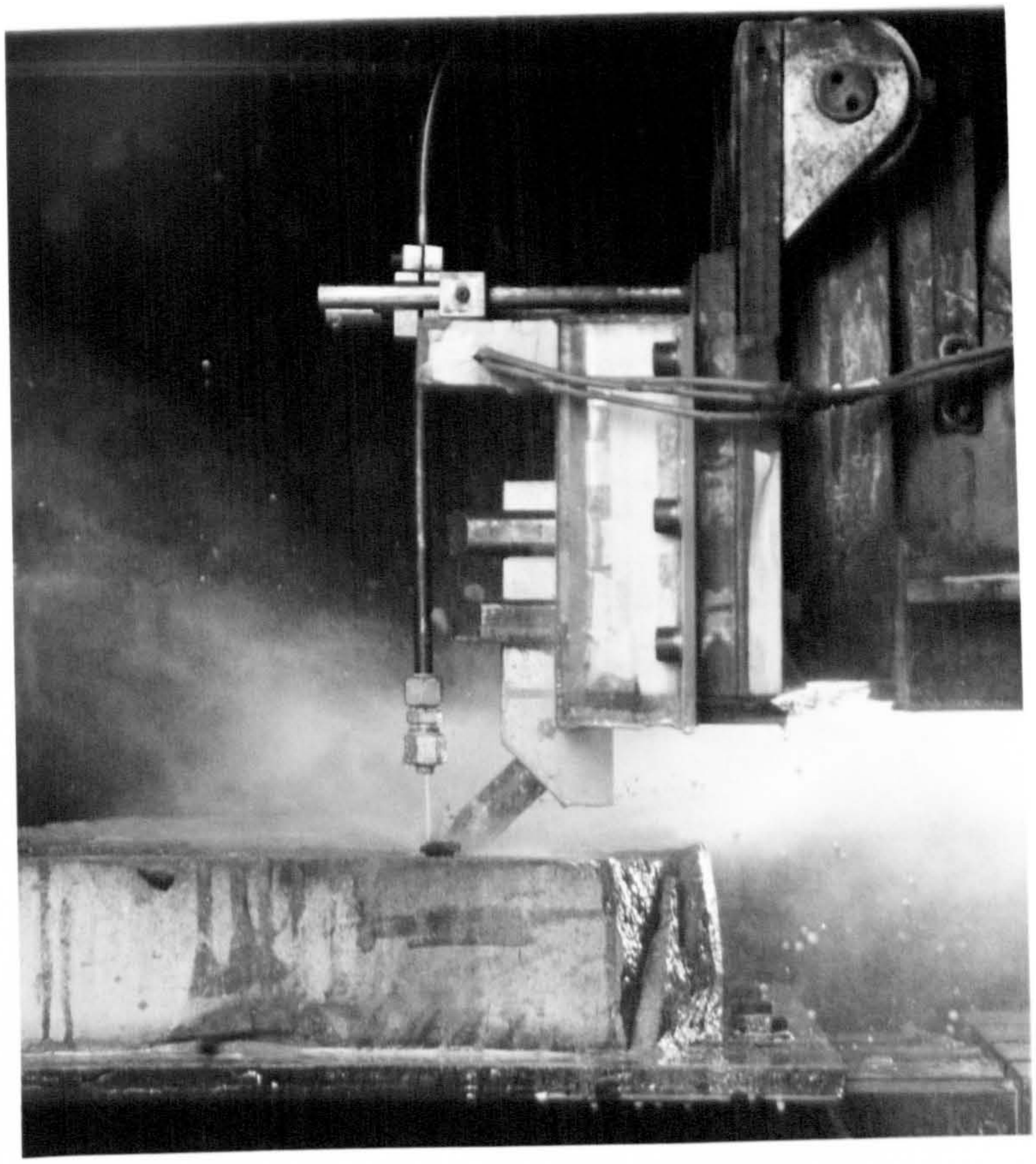

PLATE 11 – Hybrid Cutting

experimental programme, (Plate 11).

6.3.3 Effect of Mechanical Depth of Cut

On Forces

Mean, Mean Peak and Peak Cutting and Normal forces all increased rapidly with increase in depth of cut. The nature of the relationship between tool forces and depth of cut was of linear form within the experimental range, (Figures 6.4,6.5).

On Yield and Mechanical Specific Energy

Yield has shown a power relationship with depth of cut (Fig 6.6). As the depth of cut was increased, yield increased quickly at an accelerating rate, indicating the advantages of taking a deeper depth of cut.

Mechanical Specific Energy(S.E) has decreased at a decreasing rate with increase in depth of cut with S.E. displaying higher sensitivity (rapid drop) between the first two experimental levels and the curve had shown a tendency to level out at deep depth of cuts. Efficiency of cutting process is inversely proportional to the specific energy, hence it can be said that deeper the cut is more efficient the cutting becomes.

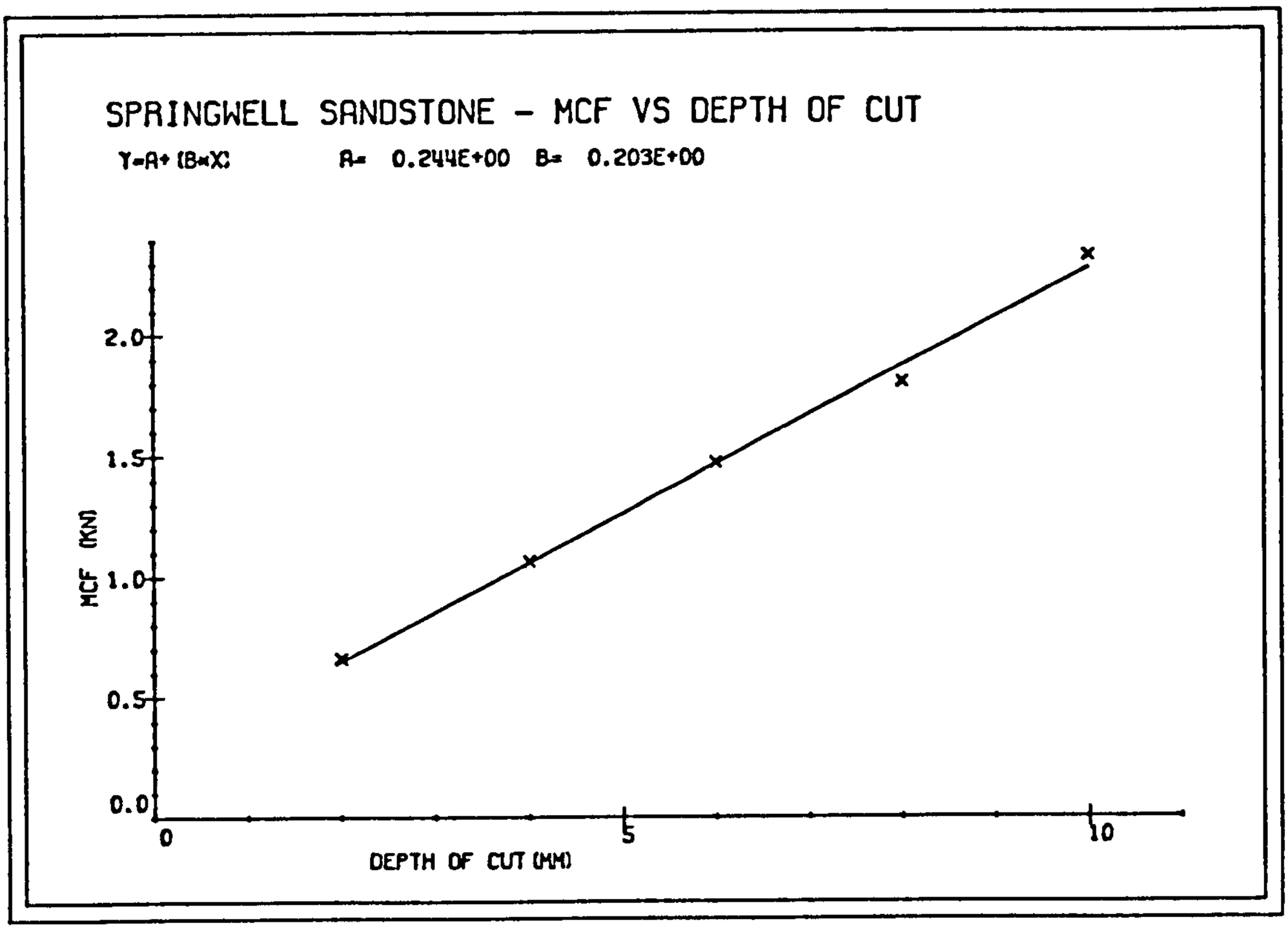
SPRINGWELL SANDSTONE - MCF VS DEPTH OF CUT
Y=A+(B*X)
A= 0.244E+00 B= 0.203E+00
2.0
1.5
1.0
0.5
0.0
MCF (KN)
0
5
10
DEPTH OF CUT (MM)

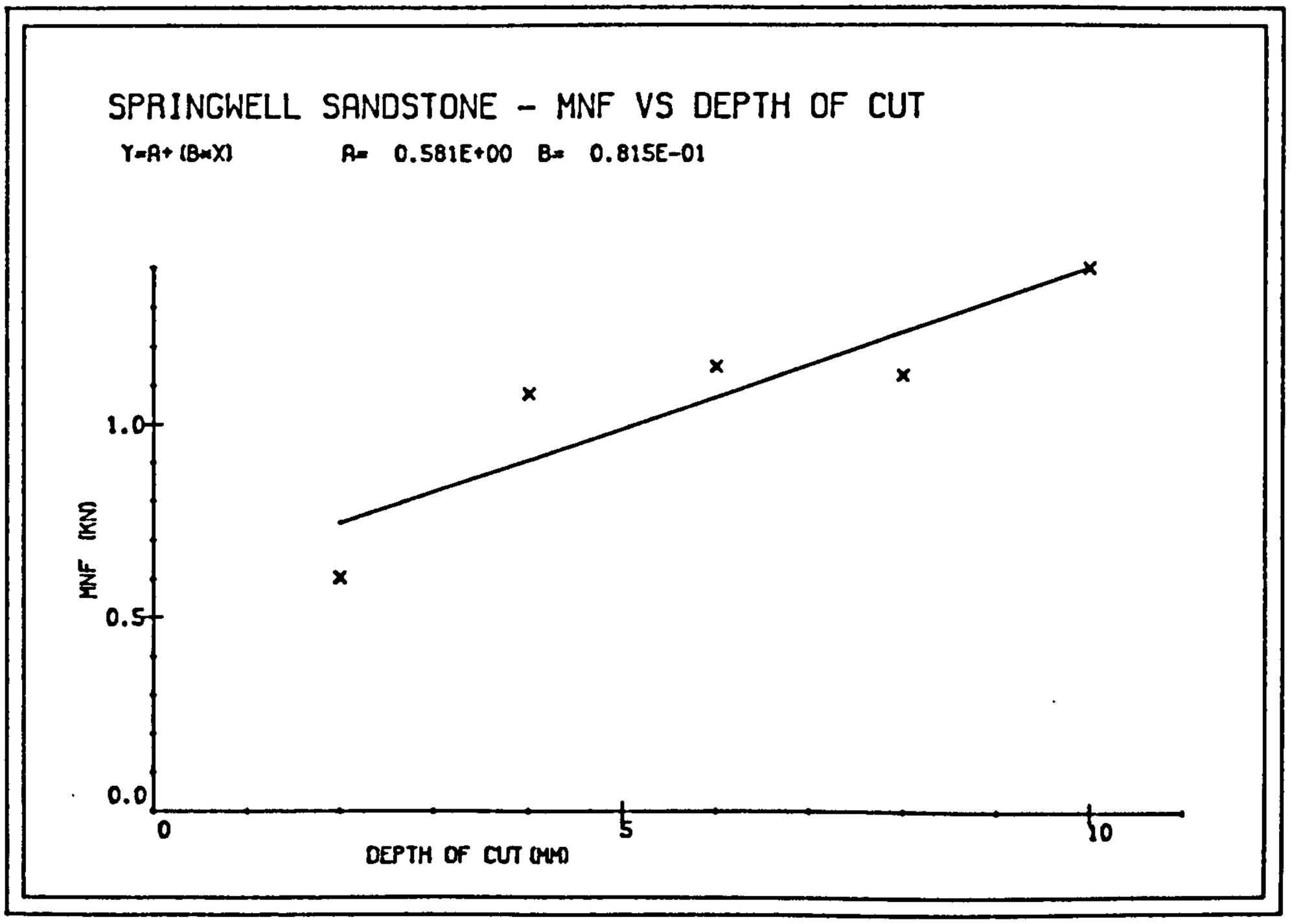
SPRINGWELL SANDSTONE - MNF VS DEPTH OF CUT
Y=A+(B*X)
A= 0.581E+00 B= 0.815E-01
1.0
0.5
0.0
MNF (KN)
0
5
10
DEPTH OF CUT (MM)

FIG. 6.4

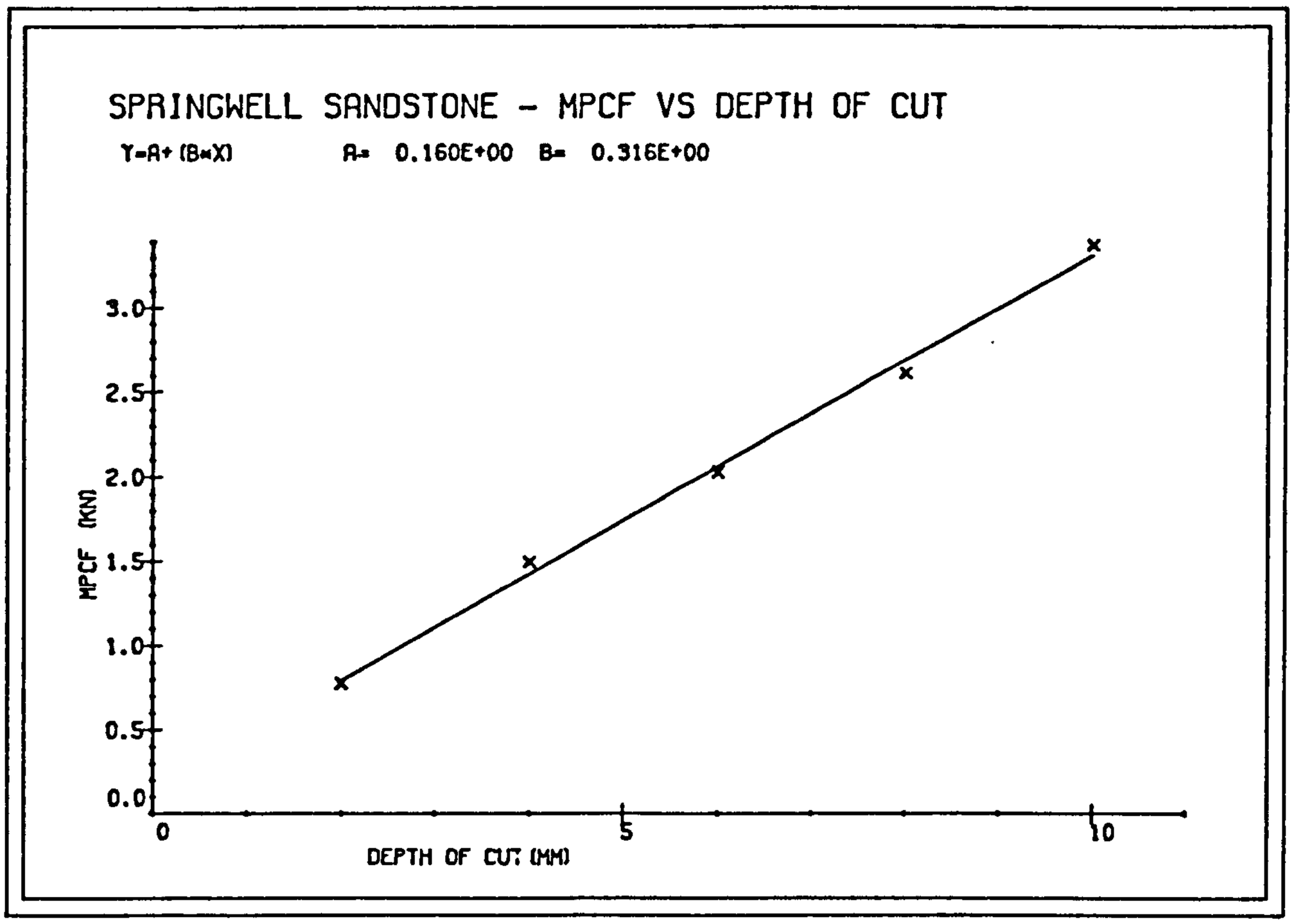
SPRINGWELL SANDSTONE - MPCF VS DEPTH OF CUT
Y=A+(B*X)
A= 0.160E+00 B= 0.316E+00
3.0
2.5
2.0
1.5
1.0
0.5
0.0
MPCF (KN)
0
5
10
DEPTH OF CUT (MM)

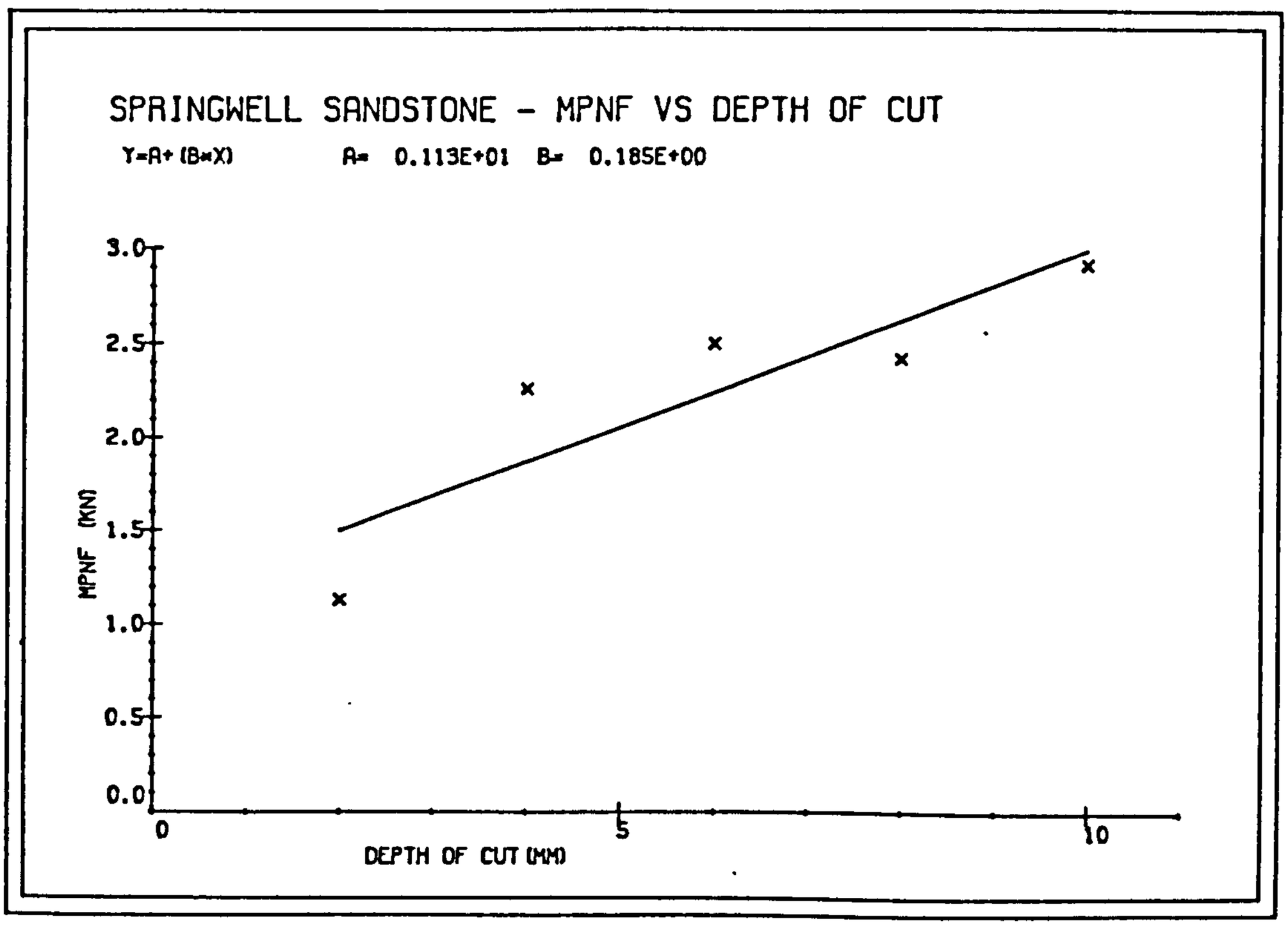
SPRINGWELL SANDSTONE - MPNF VS DEPTH OF CUT
Y=A+(B*X)
A= 0.113E+01 B= 0.185E+00
3.0
2.5
2.0
1.5
1.0
0.5
0.0
MPNF (KN)
0
5
10
DEPTH OF CUT (MM)

FIG. 6.5

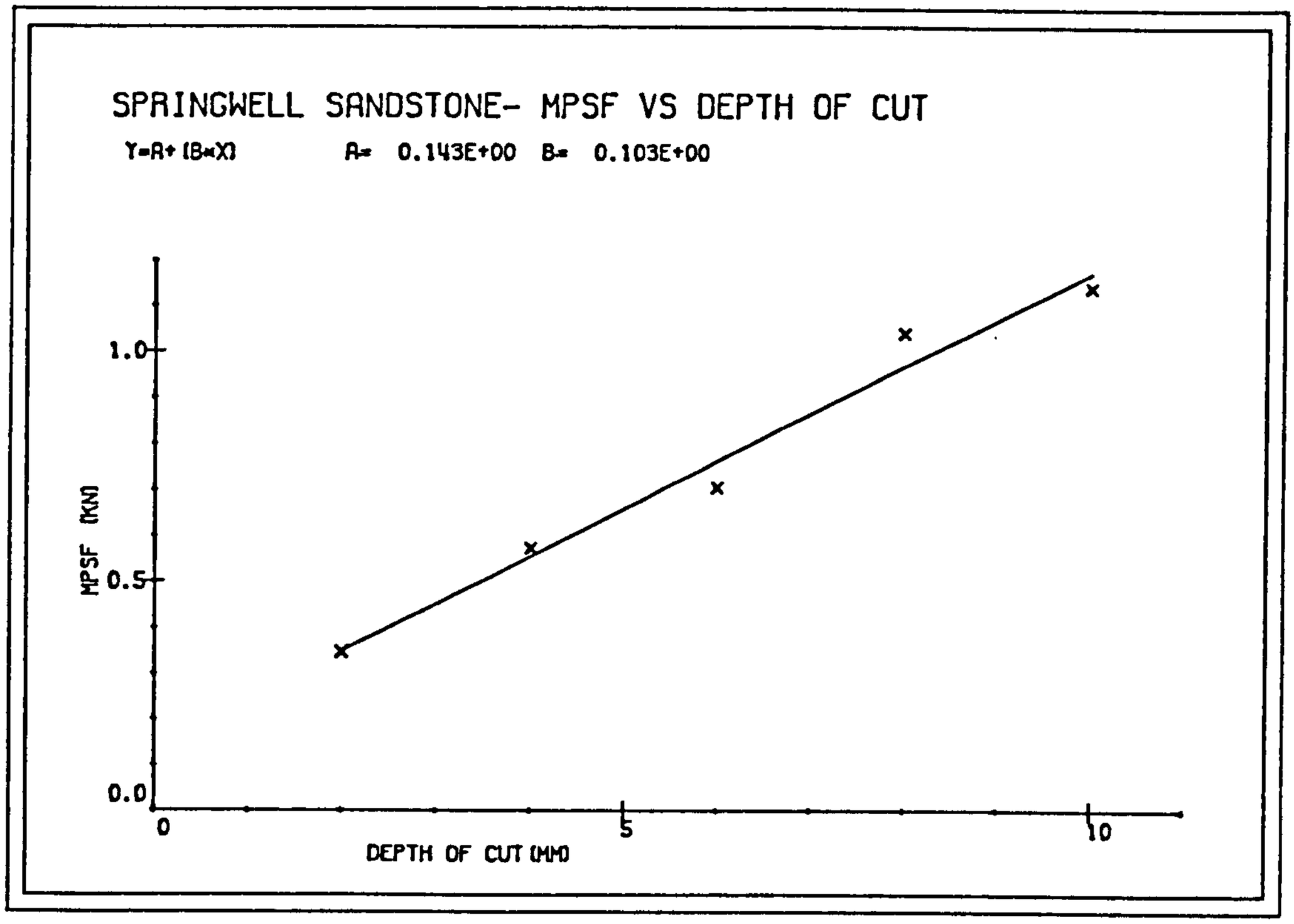
SPRINGWELL SANDSTONE- MPSF VS DEPTH OF CUT
Y=A+(B*X)
A= 0.143E+00
B= 0.103E+00
1.0
0.5
0.0
MPSF (KN)
0
5
10
DEPTH OF CUT (MM)

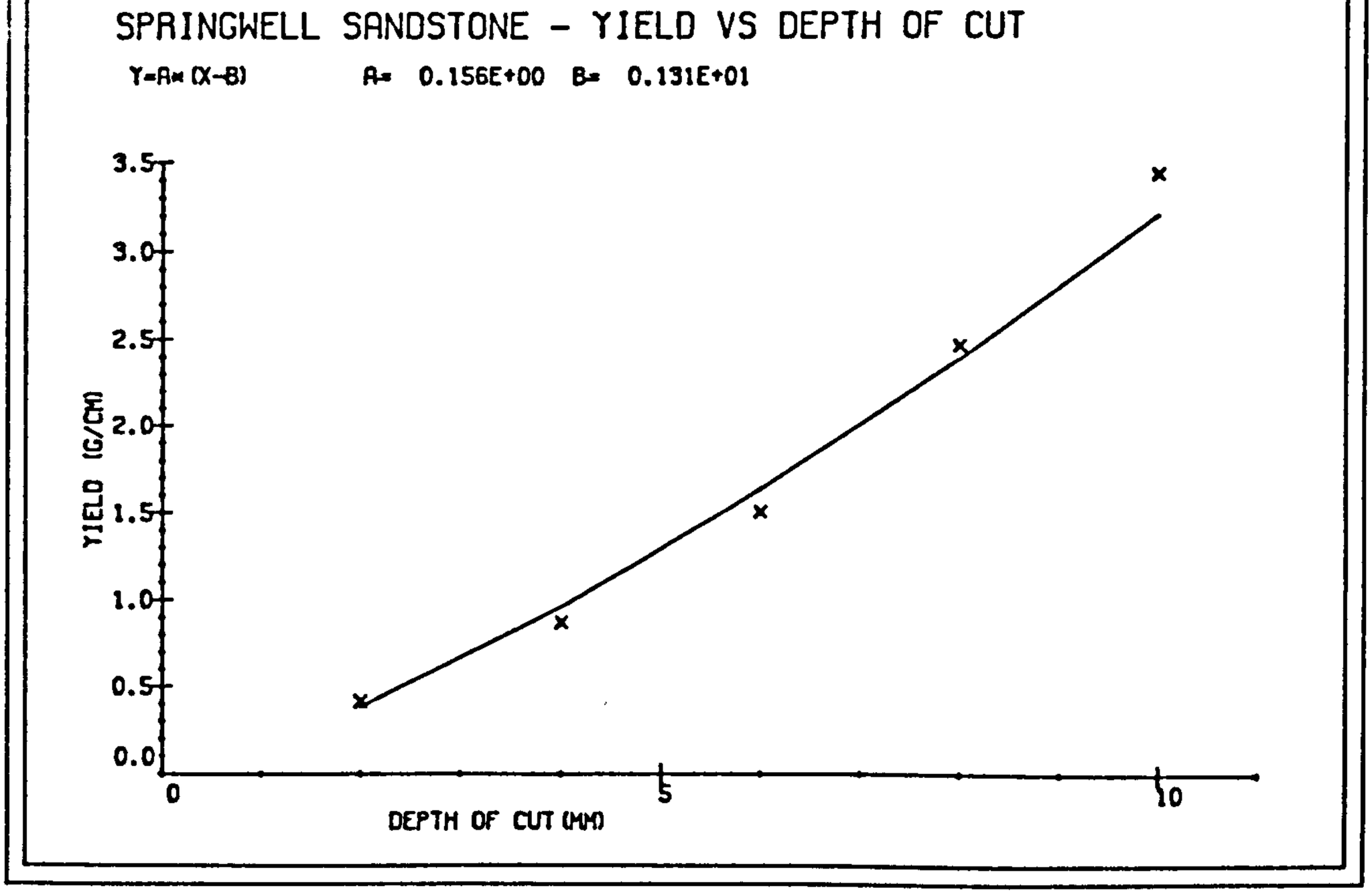
SPRINGWELL SANDSTONE - YIELD VS DEPTH OF CUT
Y=A*(X-B)
A= 0.156E+00
B= 0.131E+01
3.5
3.0
2.5
2.0
1.5
1.0
0.5
0.0
YIELD (G/CM)
0
5
10
DEPTH OF CUT (MM)

FIG. 6.6

6.3.4 Effect of Water Jet Pressure

On Jet Penetration

The effect of change in water jet pressure was measured directly by the change in the penetration depth it produced on the rock sample. Penetration has increased linearly with increase in jet pressure within experimental range. When the curve was extrapolated, it cut the pressure axis at 6.25 MPa pressure level which is the threshold pressure required to initiate cutting (Figure 6.7).

On Tool Forces

All forces (cutting, normal and sideways) have decreased at a decreasing rate with increase in water jet pressure (Figures 6.8,6.9). Normal forces seemed to show a higher sensitivity to change in pressure than cutting forces with an exponential type relationship.

It must be remembered that, because the partial factorial experimental design was used for the tests, when the influence of one variable is investigated the levels of other variables assume their mean values, i.e. for this case; a depth of cut = 6mm, Lead-on distance = 8mm, side-off distance = 20mm and stand-off distance = 45mm. Comparison of group means is a direct comparison of the relative effect between the two levels of the variable under consideration, provided that interactions are insignificant.

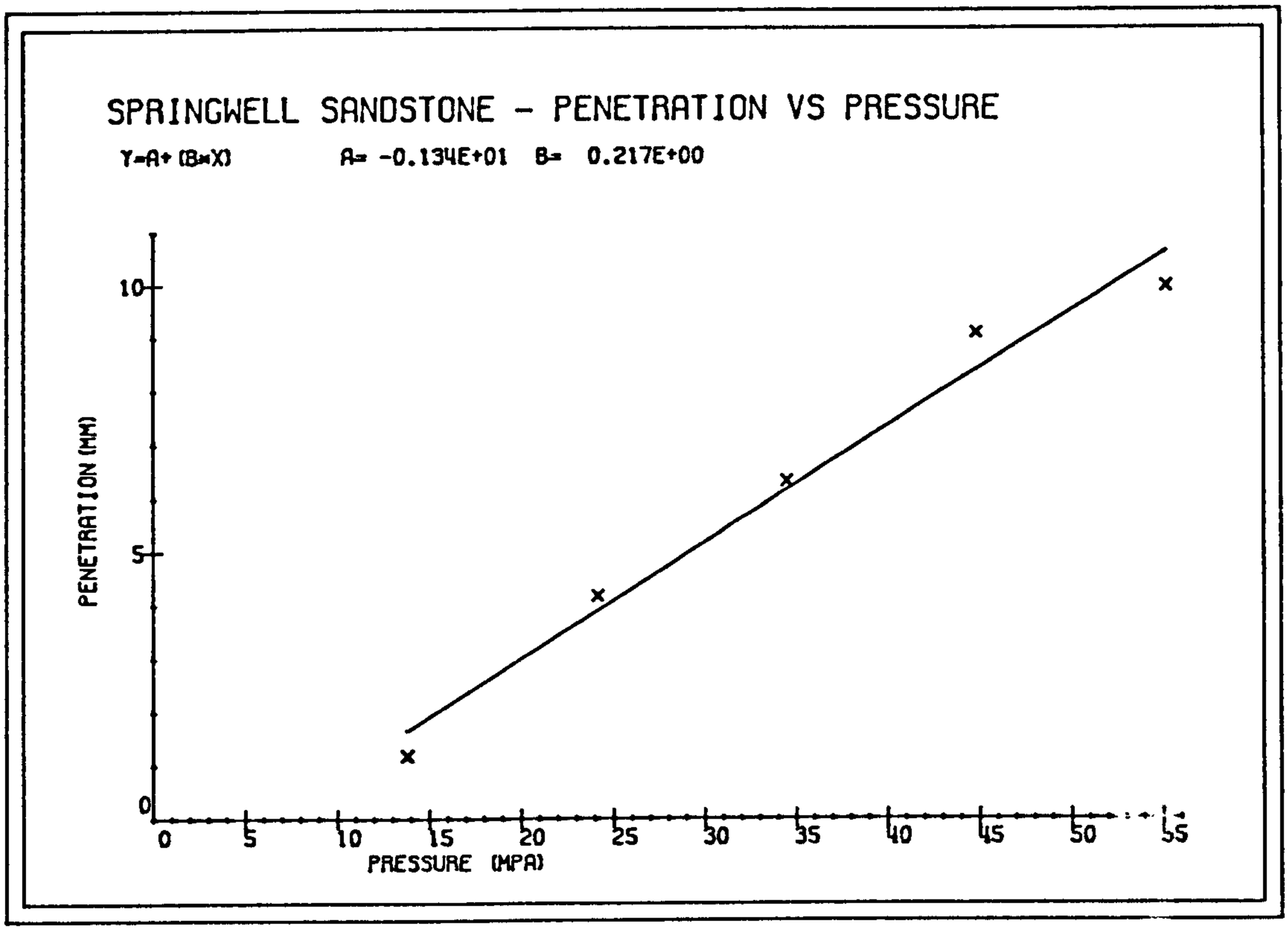
SPRINGWELL SANDSTONE - PENETRATION VS PRESSURE
Y=A+(B*X)
A= -0.134E+01 B= 0.217E+00
PENETRATION (MM)
10
5
0
0
5
10
15
20
25
30
35
40
45
50
55
PRESSURE (MPA)

FIG. 6.7

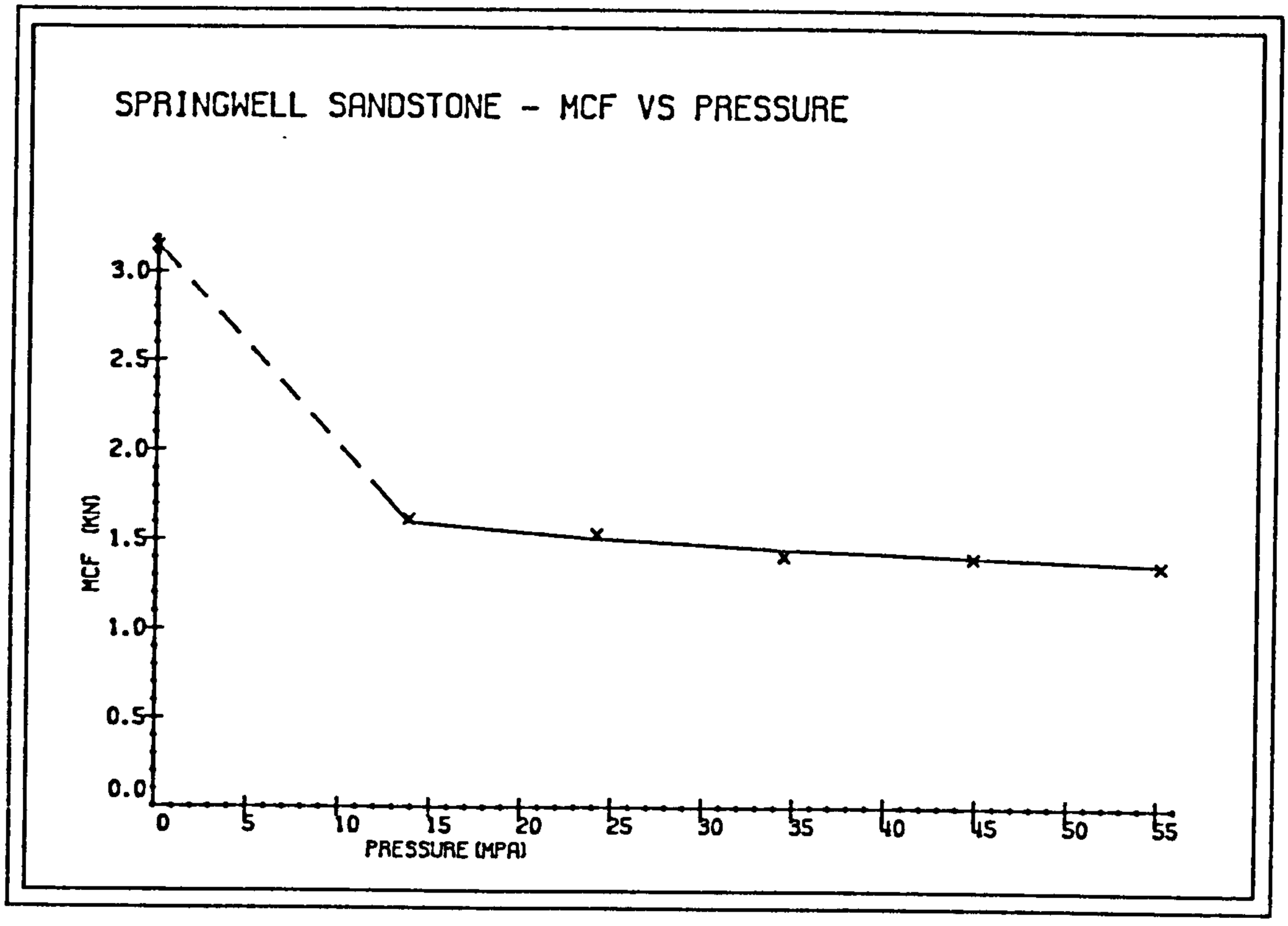
SPRINGWELL SANDSTONE - MCF VS PRESSURE
MCF (KN)
3.0
2.5
2.0
1.5
1.0
0.5
0.0
0
5
10
15
20
25
30
35
40
45
50
55
PRESSURE (MPA)

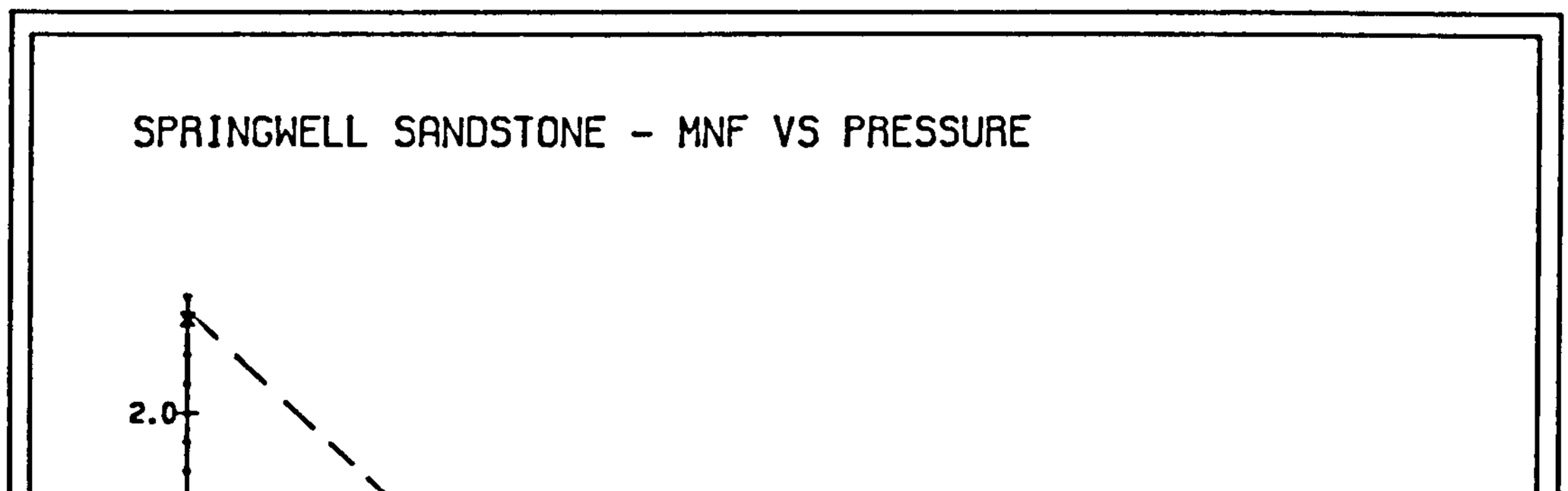
SPRINGWELL SANDSTONE - MNF VS PRESSURE
MNF (KN)
2.0
1.5
1.0
0.5
0.0
0
5
10
15
20
25
30
35
40
45
50
55
PRESSURE (MPA)

FIG. 6.8

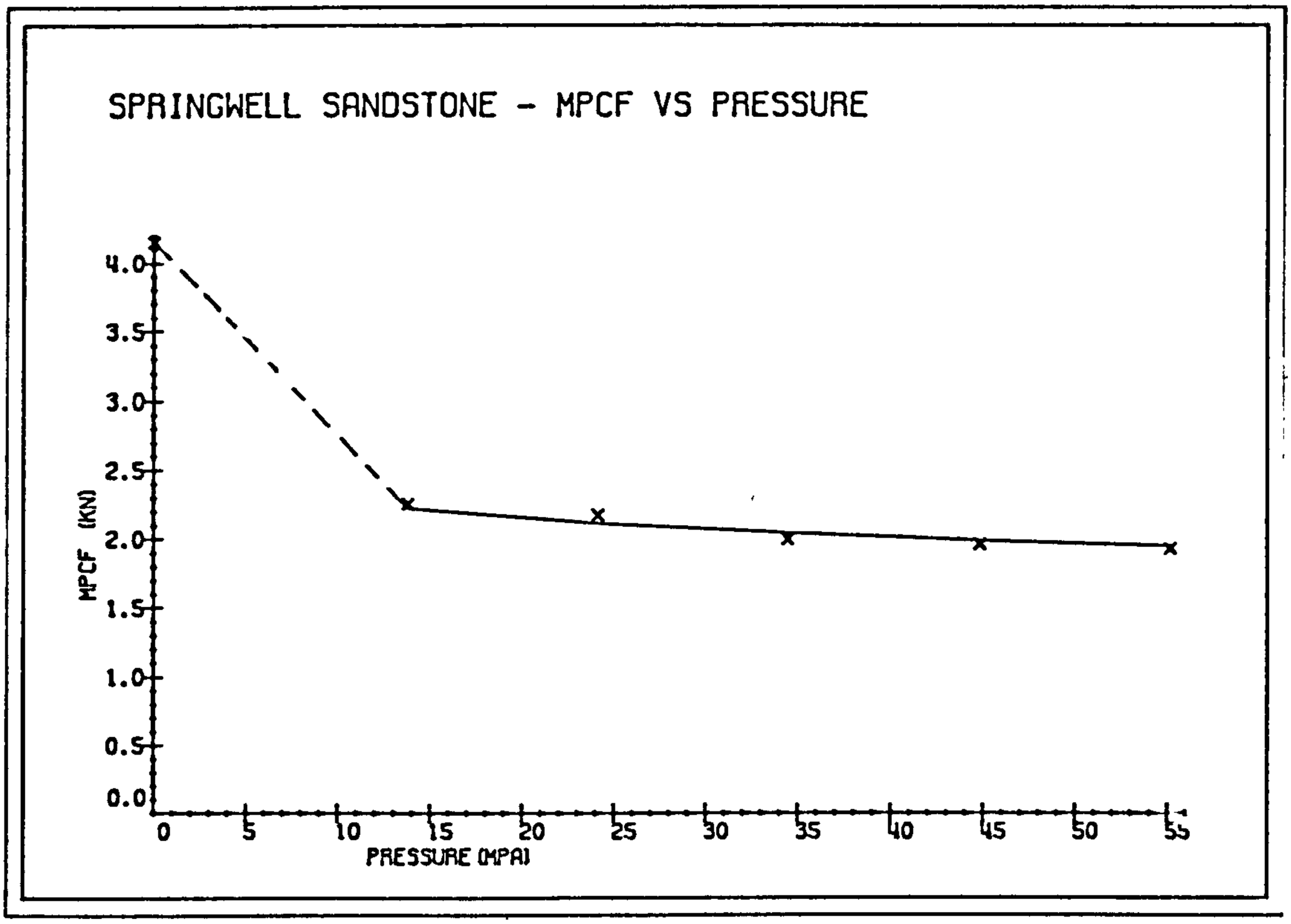
SPRINGWELL SANDSTONE - MPCF VS PRESSURE
MPCF (KN)
4.0
3.5
3.0
2.5
2.0
1.5
1.0
0.5
0.0
0
5
10
15
20
25
30
35
40
45
50
55
PRESSURE (MPA)

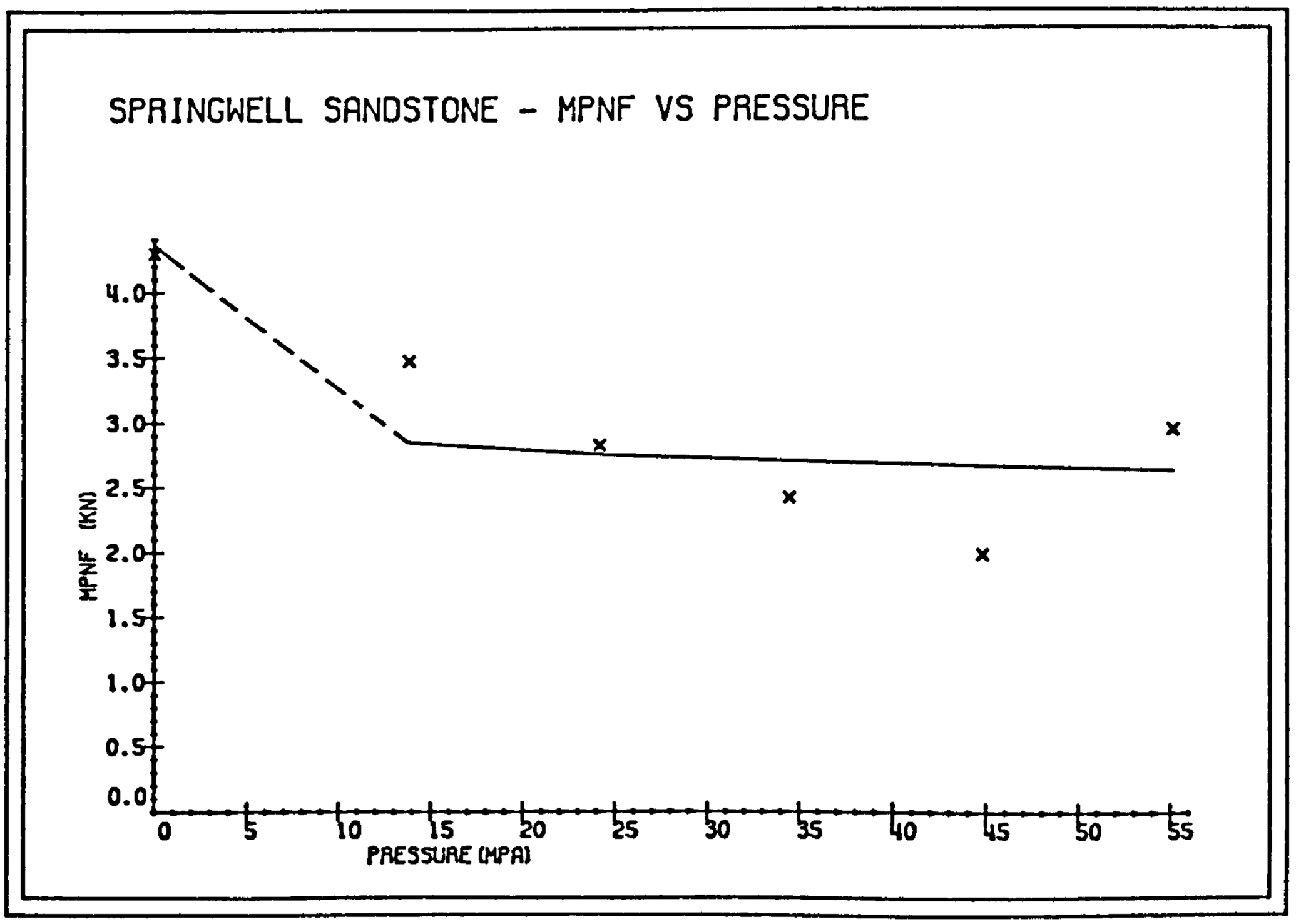
SPRINGWELL SANDSTONE - MPNF VS PRESSURE
MPNF (KN)
4.0
3.5
3.0
2.5
2.0
1.5
1.0
0.5
0.0
0
5
10
15
20
25
30
35
40
45
50
55
PRESSURE (MPA)

FIG. 6.9

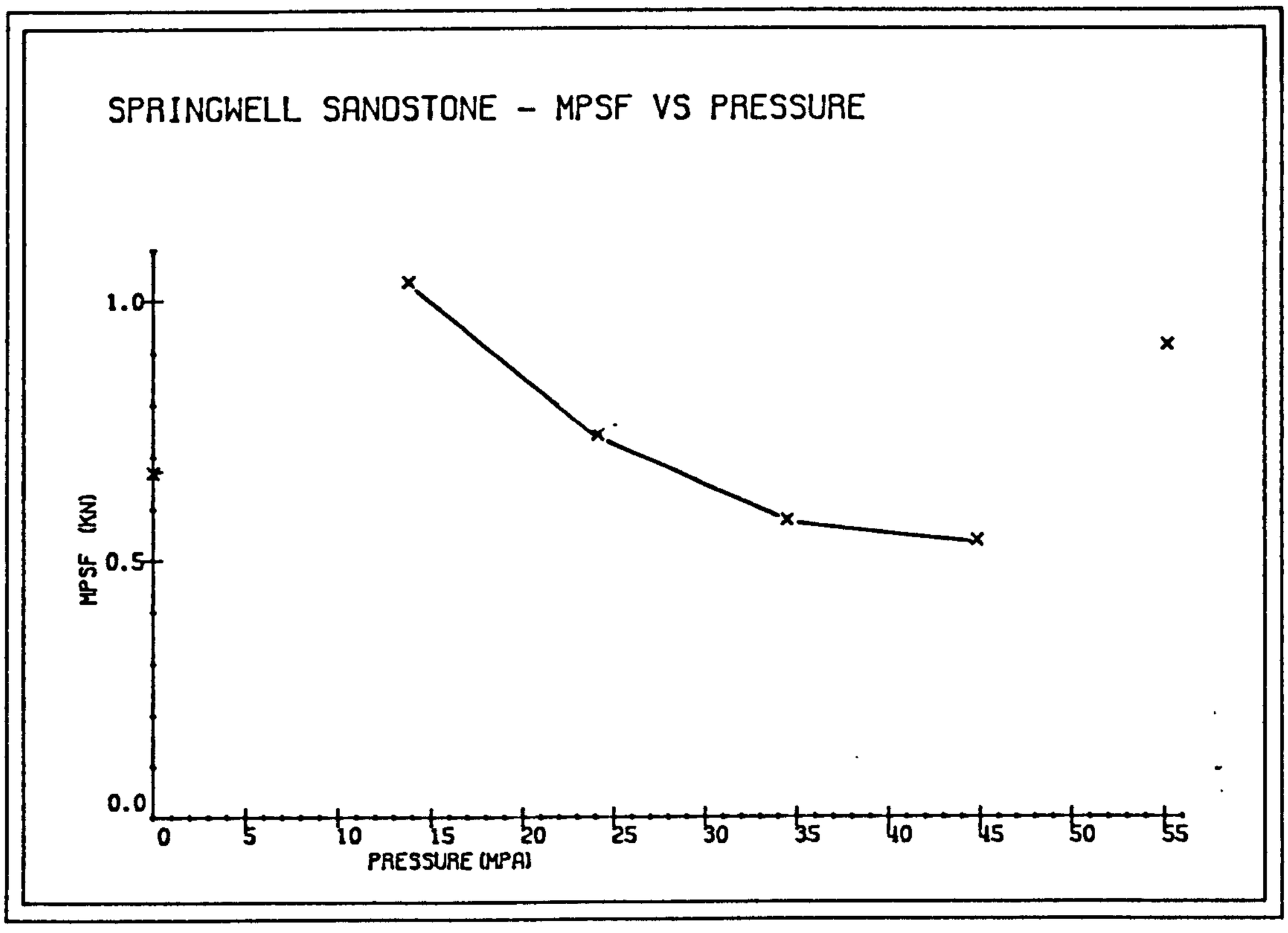
SPRINGWELL SANDSTONE - MPSF VS PRESSURE
MPSF (KN)
1.0
0.5
0.0
0
5
10
15
20
25
30
35
40
45
50
55
PRESSURE (MPA)

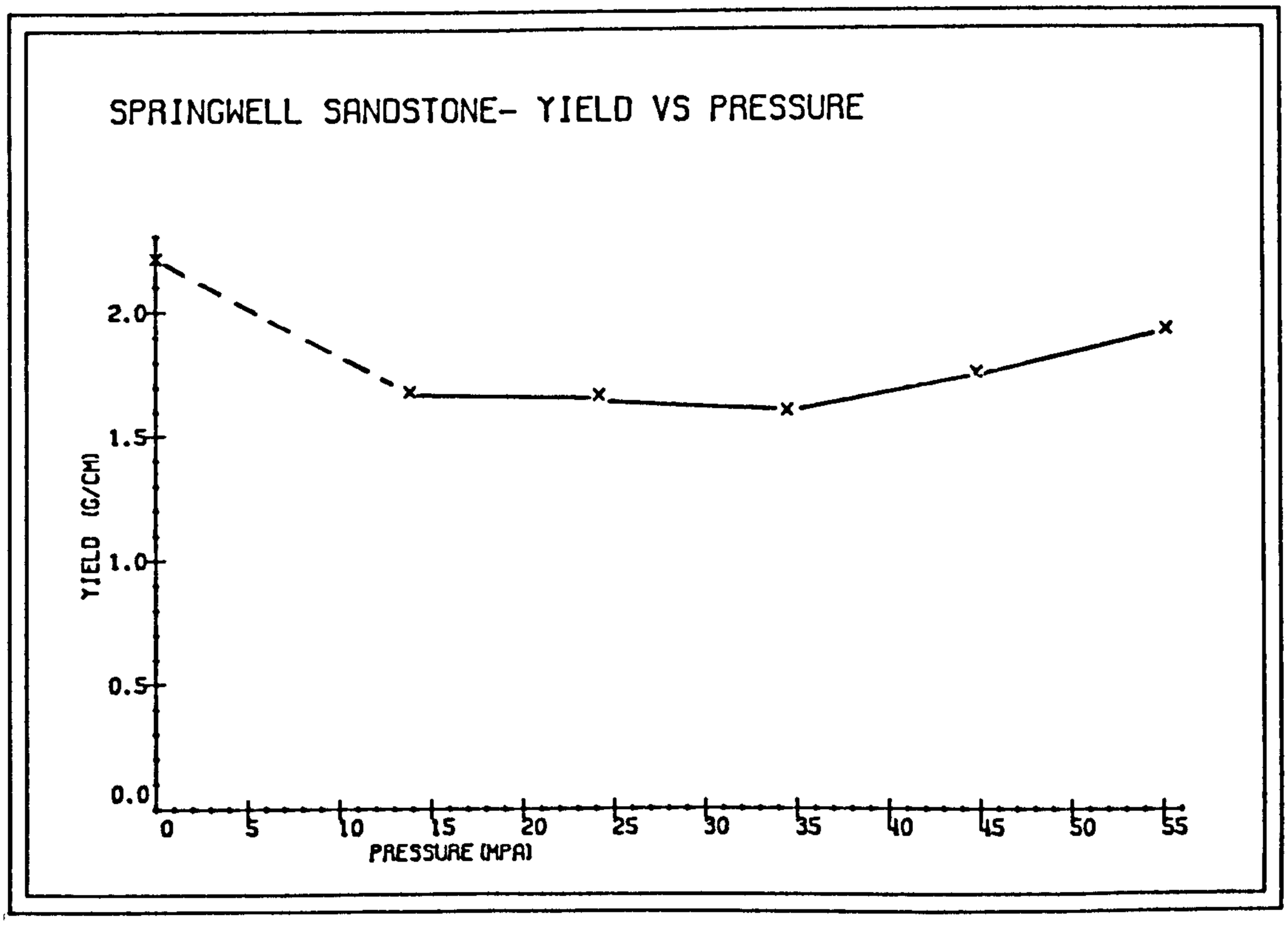
SPRINGWELL SANDSTONE- YIELD VS PRESSURE
YIELD (G/CM)
2.0
1.5
1.0
0.5
0.0
0
5
10
15
20
25
30
35
40
45
50
55
PRESSURE (MPA)

FIG. 6.10

On Yield and Mechanical Specific Energy

Yield has increased with increase in water jet pressure but the magnitude of the increase was small, (Figure 6.10). Mechanical specific energy has decreased with the increase in water jet pressure (Figure 6.11).

6.3.5 Effect of Side-off Distance

On Tool Forces

Mean and Mean Peak Cutting Forces have increased with increase in side-off distance, but the magnitude of this increase was small (Figure 6.12).

Mean and Mean Peak Normal and Mean Peak Sideways forces had shown more sensitivity to changes in the side-off distance. With increasing side-off distance the curves display a tendency to run parallel to an asymptote, (to horizontal) (Fig 6.13).

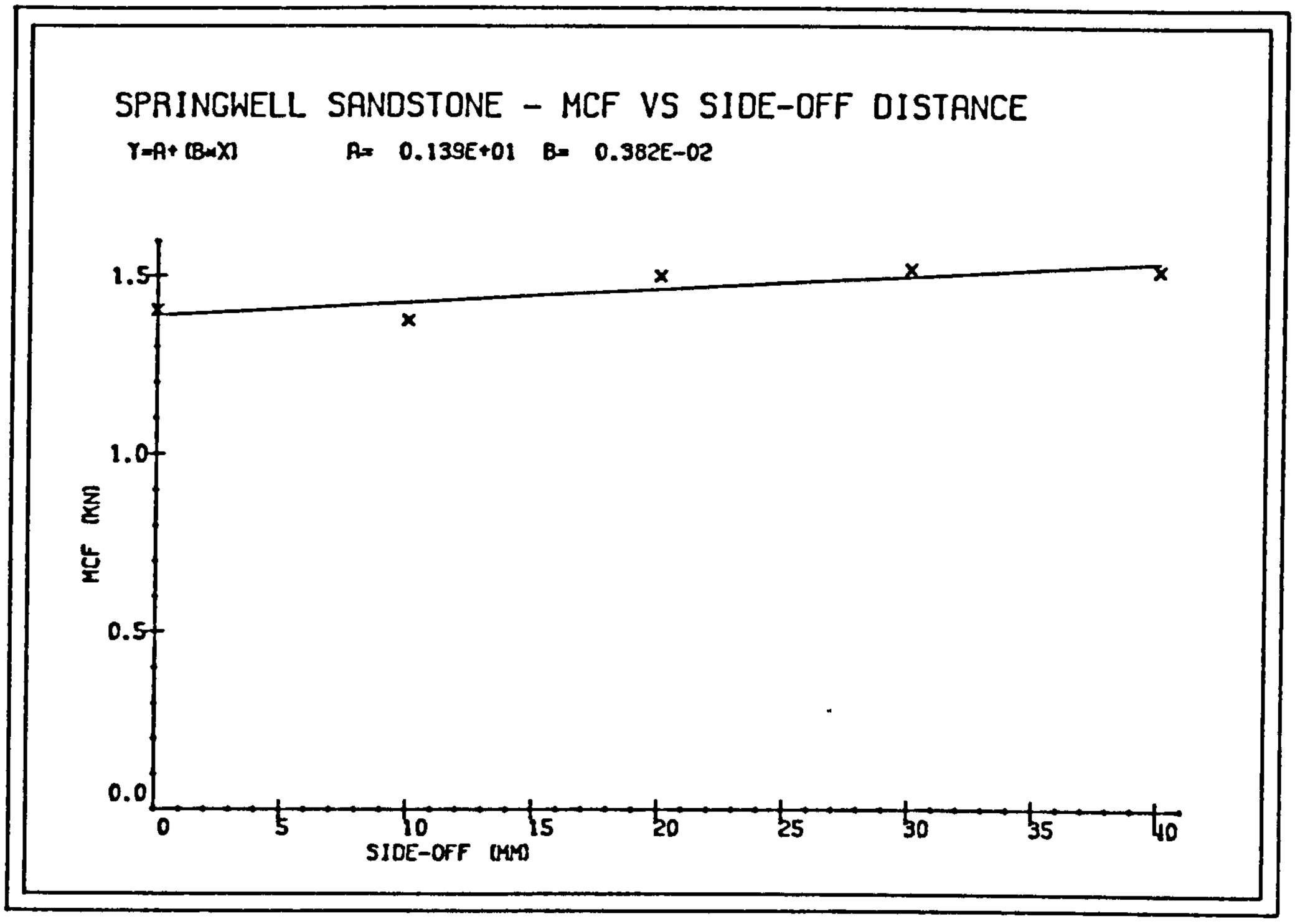
SPRINGWELL SANDSTONE - MCF VS SIDE-OFF DISTANCE
Y=A+(B*X)
A= 0.139E+01
B= 0.382E-02
1.5
1.0
0.5
0.0
MCF (KN)
0
5
10
15
20
25
30
35
40
SIDE-OFF (MM)

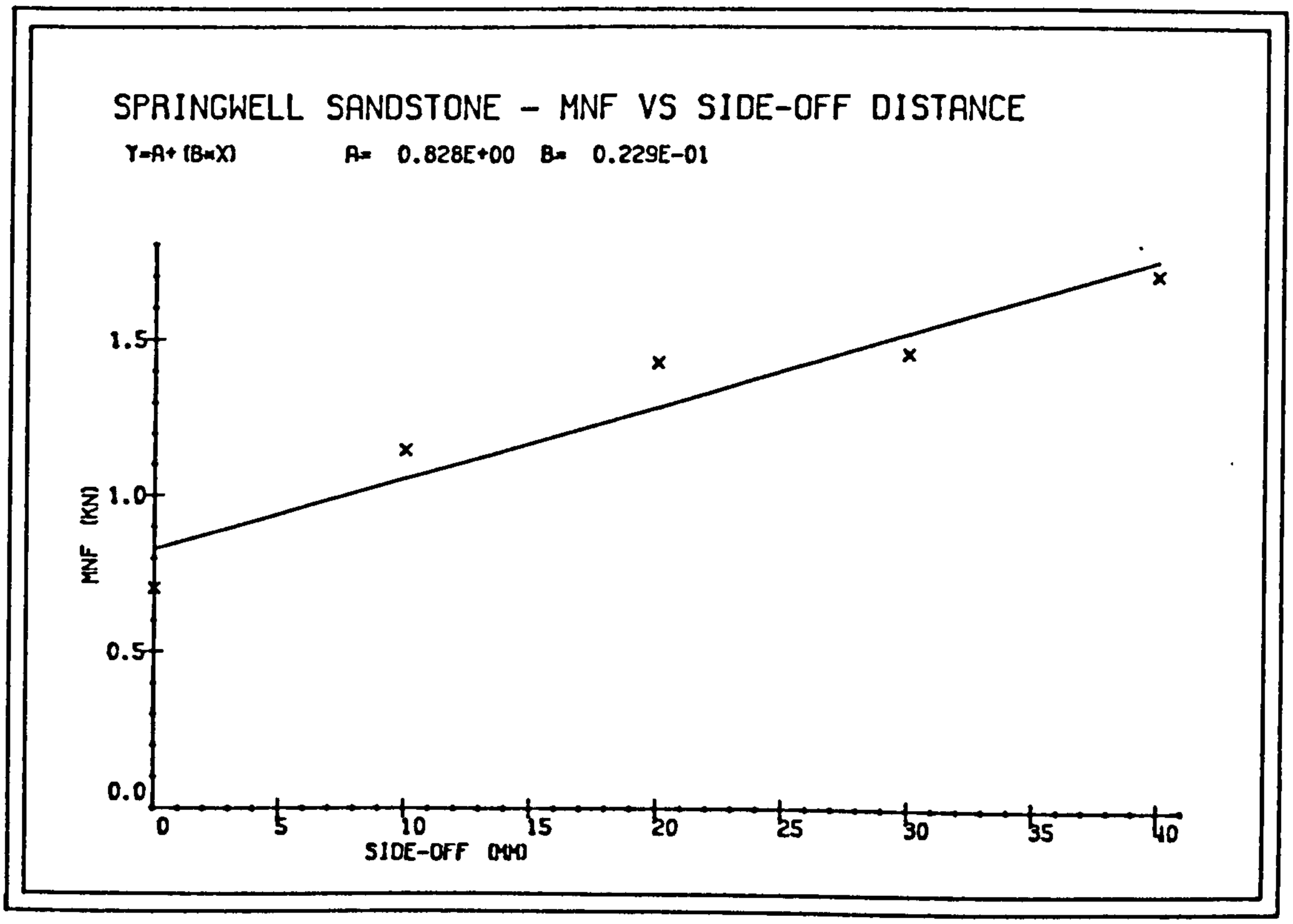
SPRINGWELL SANDSTONE - MNF VS SIDE-OFF DISTANCE
Y=A+(B*X)
A= 0.828E+00
B= 0.229E-01
1.5
1.0
0.5
0.0
MNF (KN)
0
5
10
15
20
25
30
35
40
SIDE-OFF (MM)

FIG. 6.12

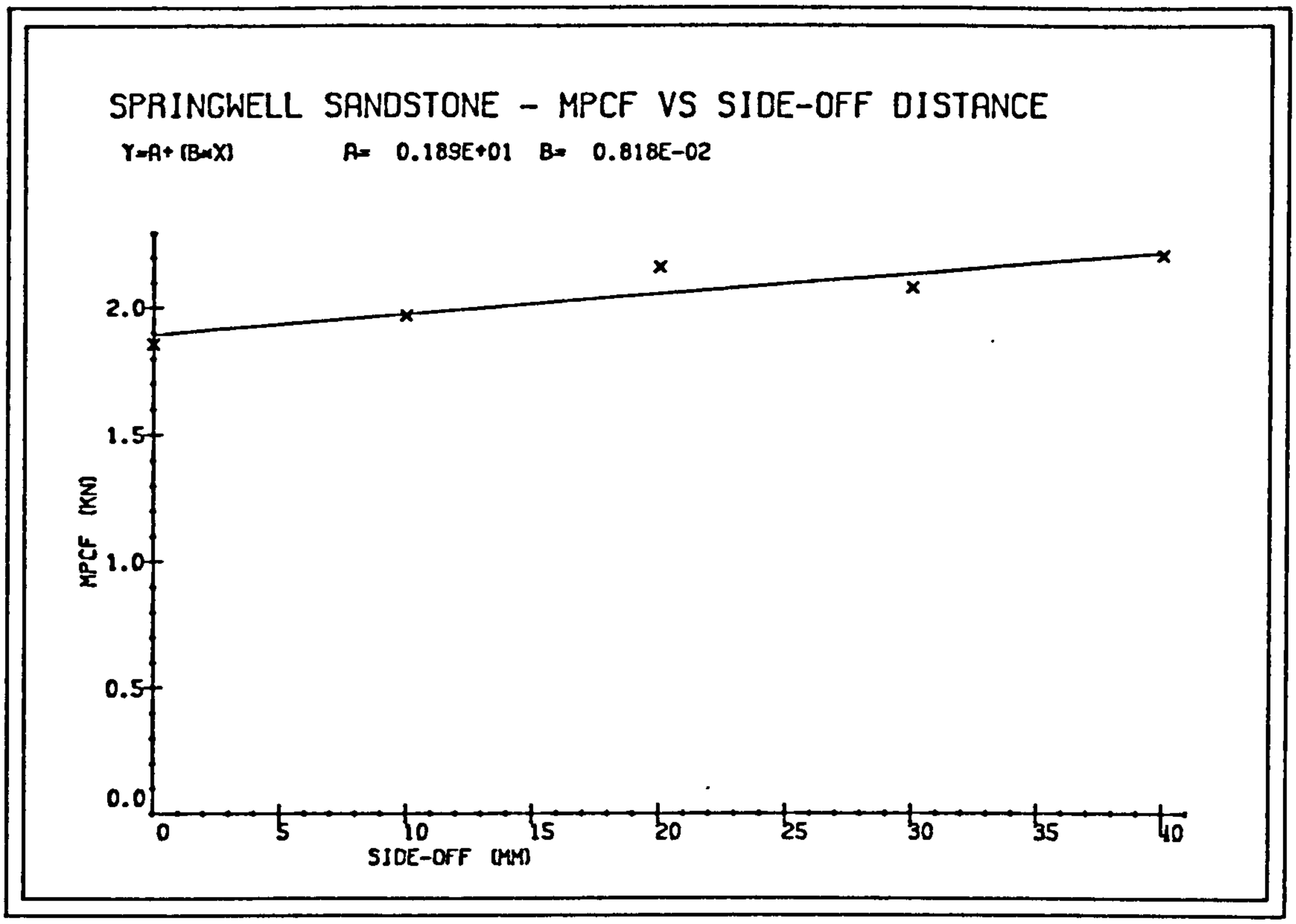
SPRINGWELL SANDSTONE - MPCF VS SIDE-OFF DISTANCE
Y=A+(B*X)
A= 0.189E+01
B= 0.818E-02
MPCF (KN)
2.0
1.5
1.0
0.5
0.0
0
5
10
15
20
25
30
35
40
SIDE-OFF (MM)

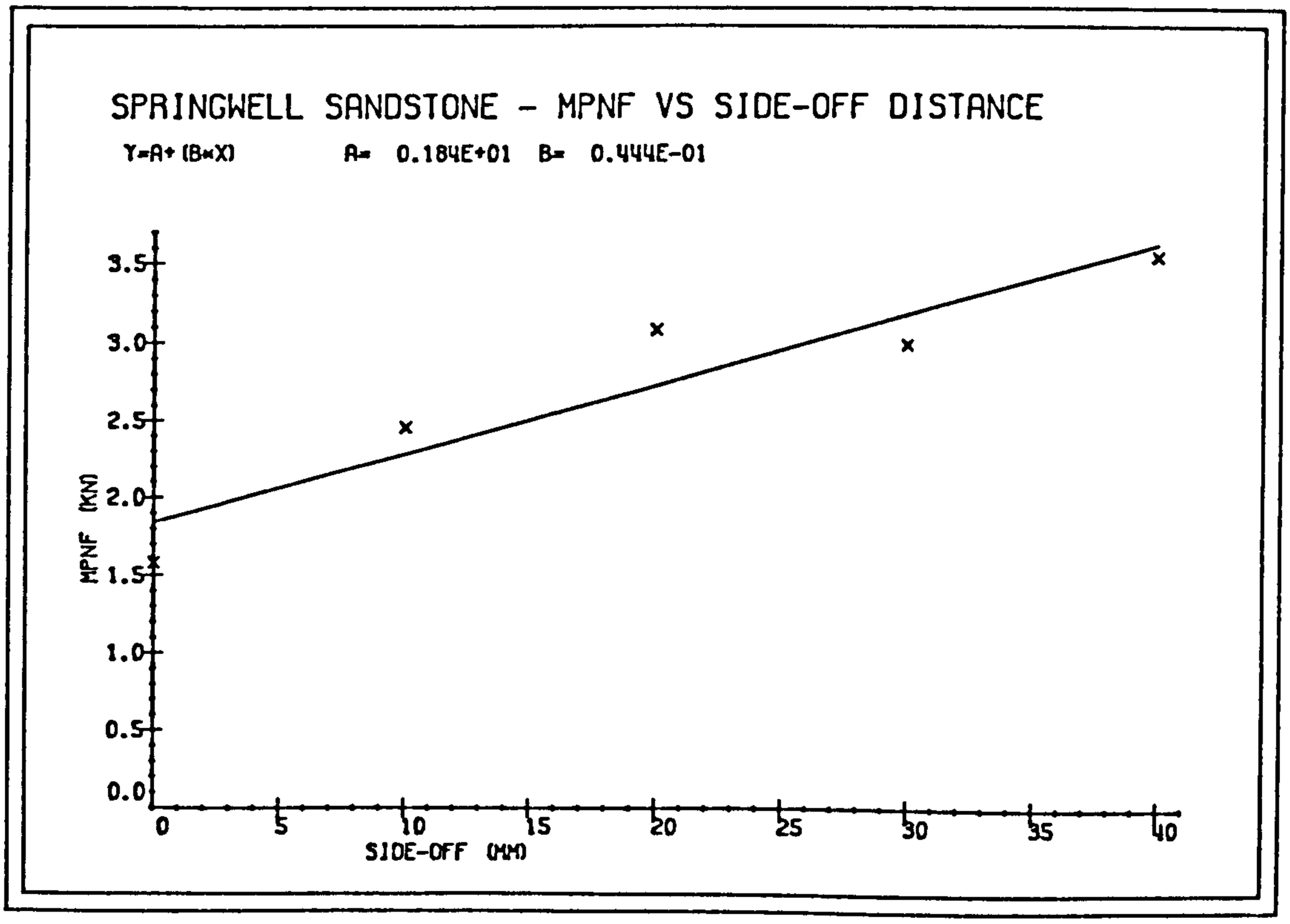
SPRINGWELL SANDSTONE - MPNF VS SIDE-OFF DISTANCE
Y=A+(B*X)
A= 0.184E+01
B= 0.444E-01
MPNF (KN)
3.5
3.0
2.5
2.0
1.5
1.0
0.5
0.0
0
5
10
15
20
25
30
35
40
SIDE-OFF (MM)

FIG. 6.13

On Yield and Mechanical Specific Energy

Yield increased rapidly between 0mm and 10mm side-off distance. Further increases in side-off distance did not result in more yield, (Fig 6.14).

Mechanical specific energy has decreased then started to increase again before it levelled off to a constant value with increasing side-off distance. Optimum side-off distance was the distance at which mechanical specific energy was at its minimum and this corresponded to a side-off/depth of cut ratio of 3.33. A further increase in side-off distance means each cutting system is cutting in isolation with no interaction occurring between the two.

6.3.6 Effect of Lead-on Distance

Results had shown by how much the water jet nozzle has to lead the mechanical tool if it is located between the mechanical cutters.

On Tool Forces

Cutting and Normal forces decreased exponentially with an increase in Lead-on distance. The slope of the lines were very small in magnitude, (Figures 6.15,6.16).

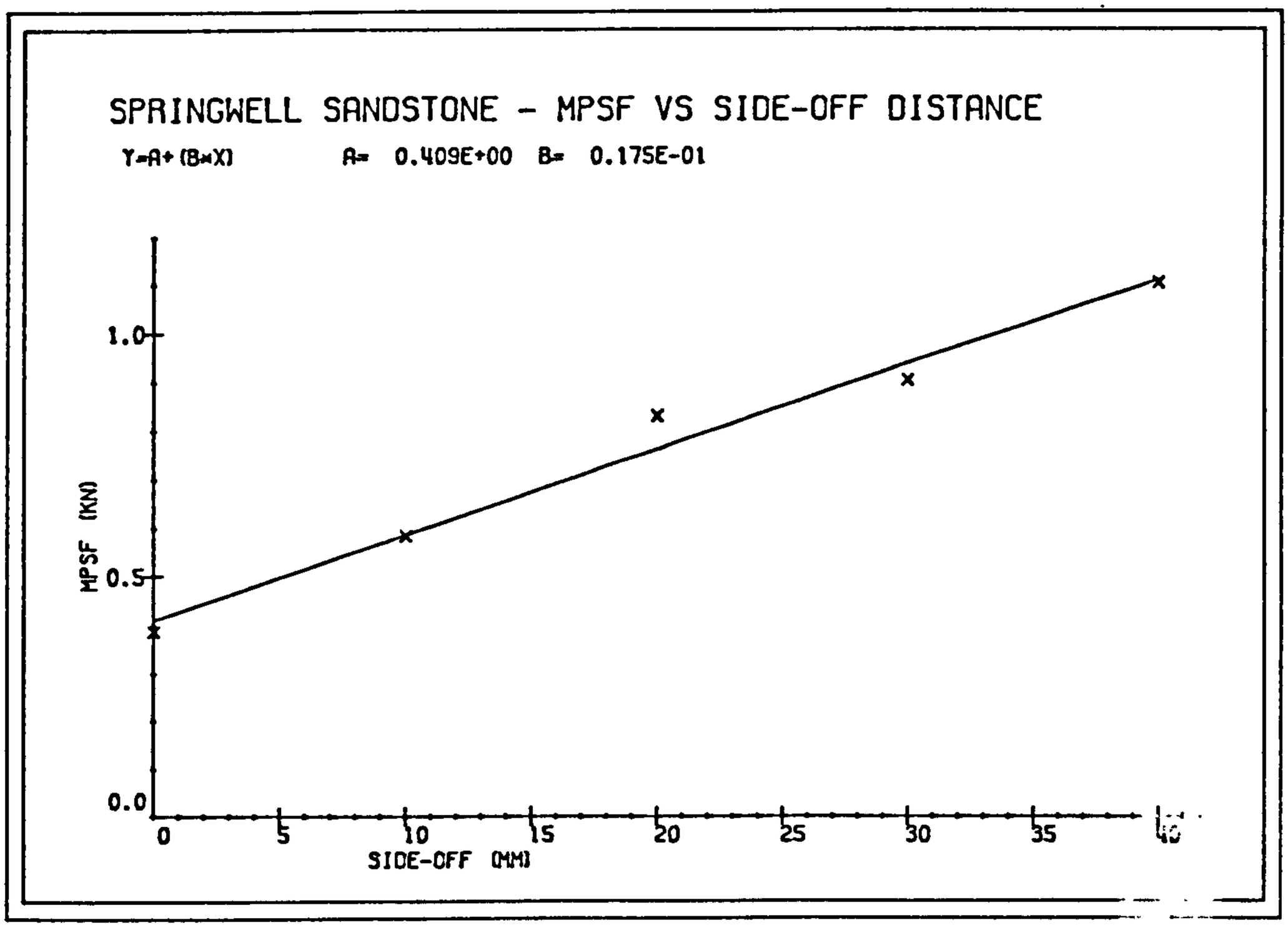
SPRINGWELL SANDSTONE - MPSF VS SIDE-OFF DISTANCE
Y=A+(B*X)
A= 0.409E+00
B= 0.175E-01
MPSF (KN)
1.0
0.5
0.0
0
5
10
15
20
25
30
35
40
SIDE-OFF (MM)

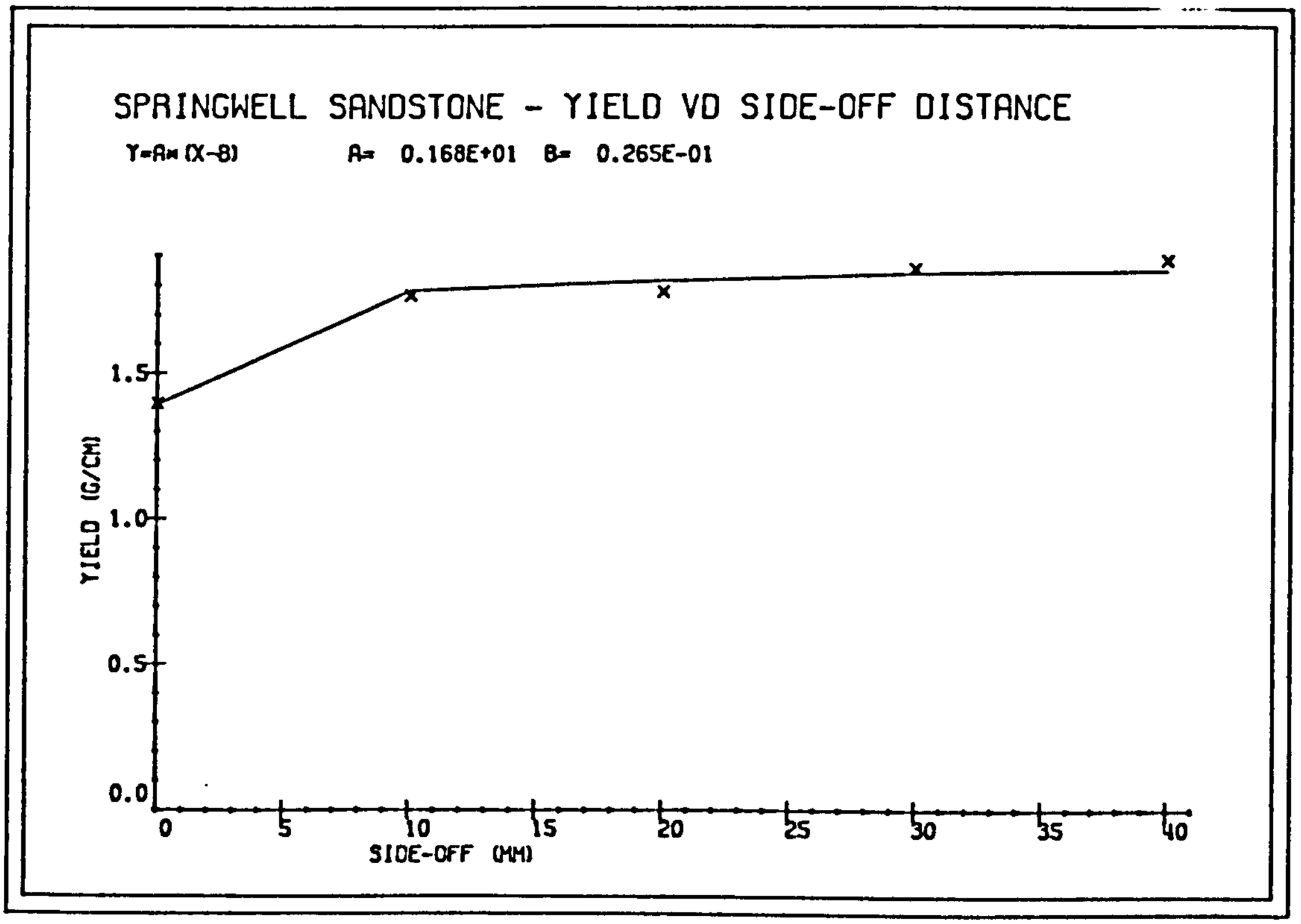
SPRINGWELL SANDSTONE - YIELD VD SIDE-OFF DISTANCE
Y=A*(X-B)
A= 0.168E+01
B= 0.265E-01
YIELD (G/CM)
1.5
1.0
0.5
0.0
0
5
10
15
20
25
30
35
40
SIDE-OFF (MM)

FIG. 6.14

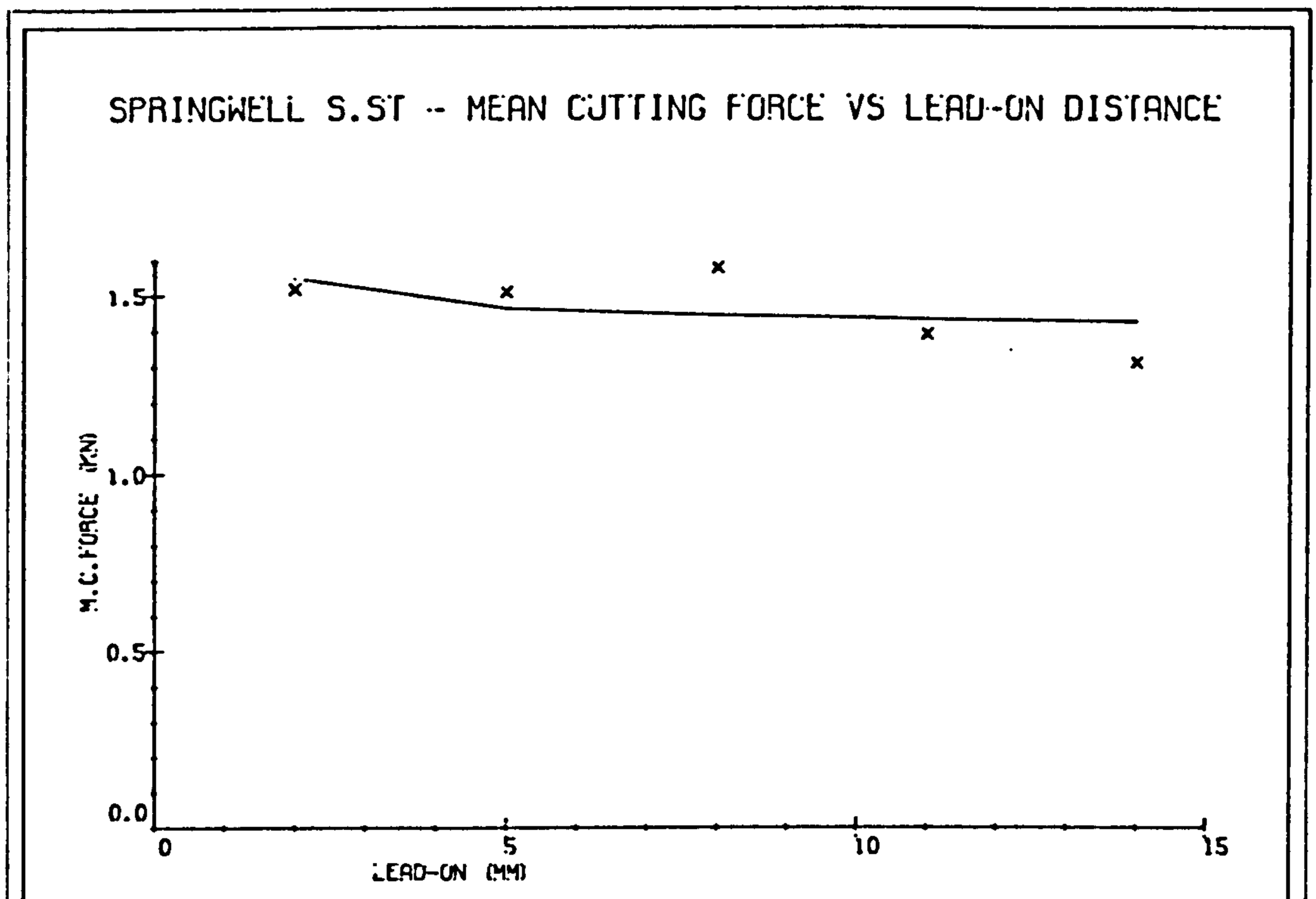
SPRINGWELL S.ST -- MEAN CUTTING FORCE VS LEAD-ON DISTANCE
1.5
1.0
0.5
0.0
M.C.FORCE (KN)
0
5
10
15
LEAD-ON (MM)

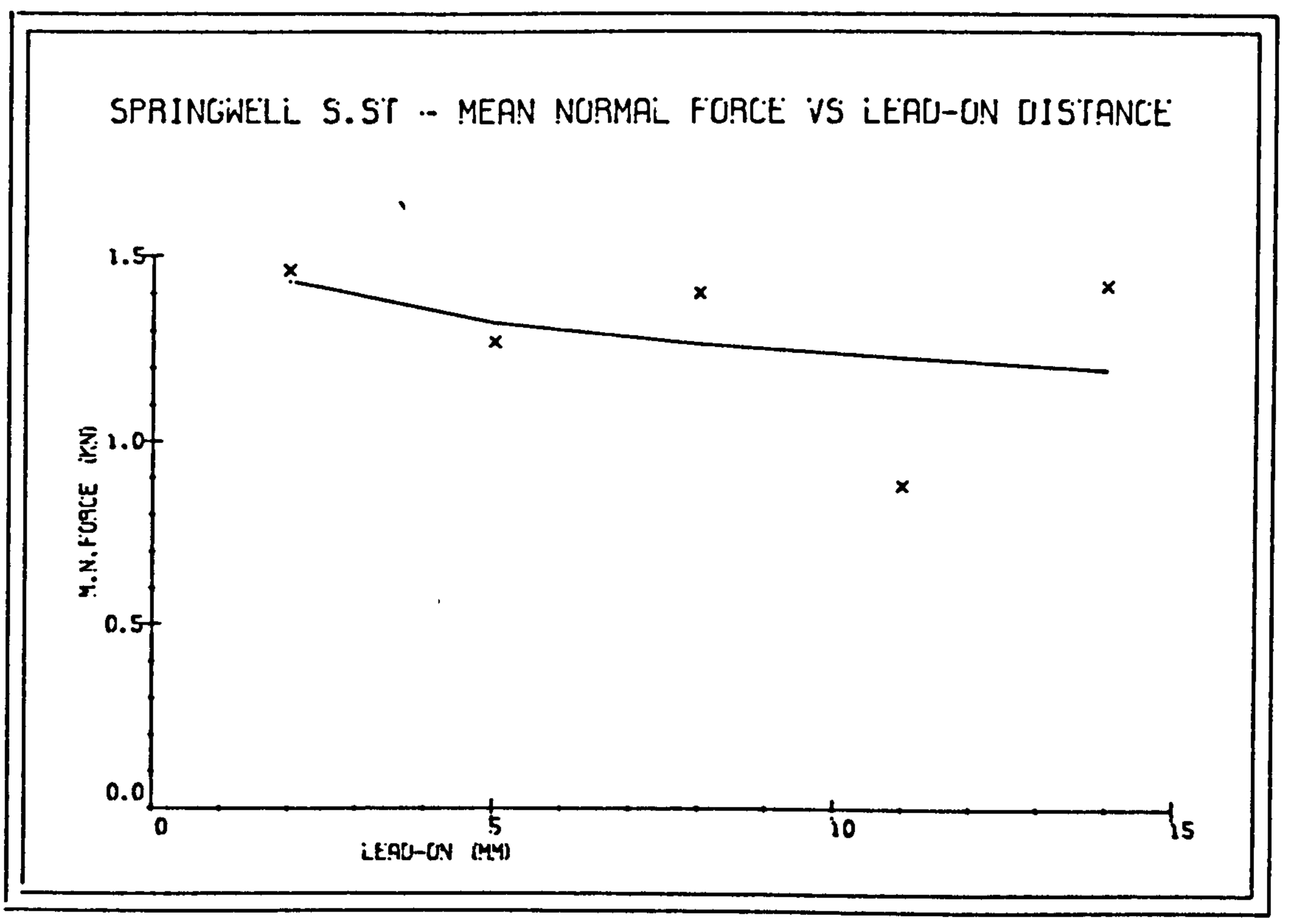
SPRINGWELL S.ST -- MEAN NORMAL FORCE VS LEAD-ON DISTANCE
1.5
1.0
0.5
0.0
M.N.FORCE (KN)
0
5
10
15
LEAD-ON (MM)

FIG. 6.15

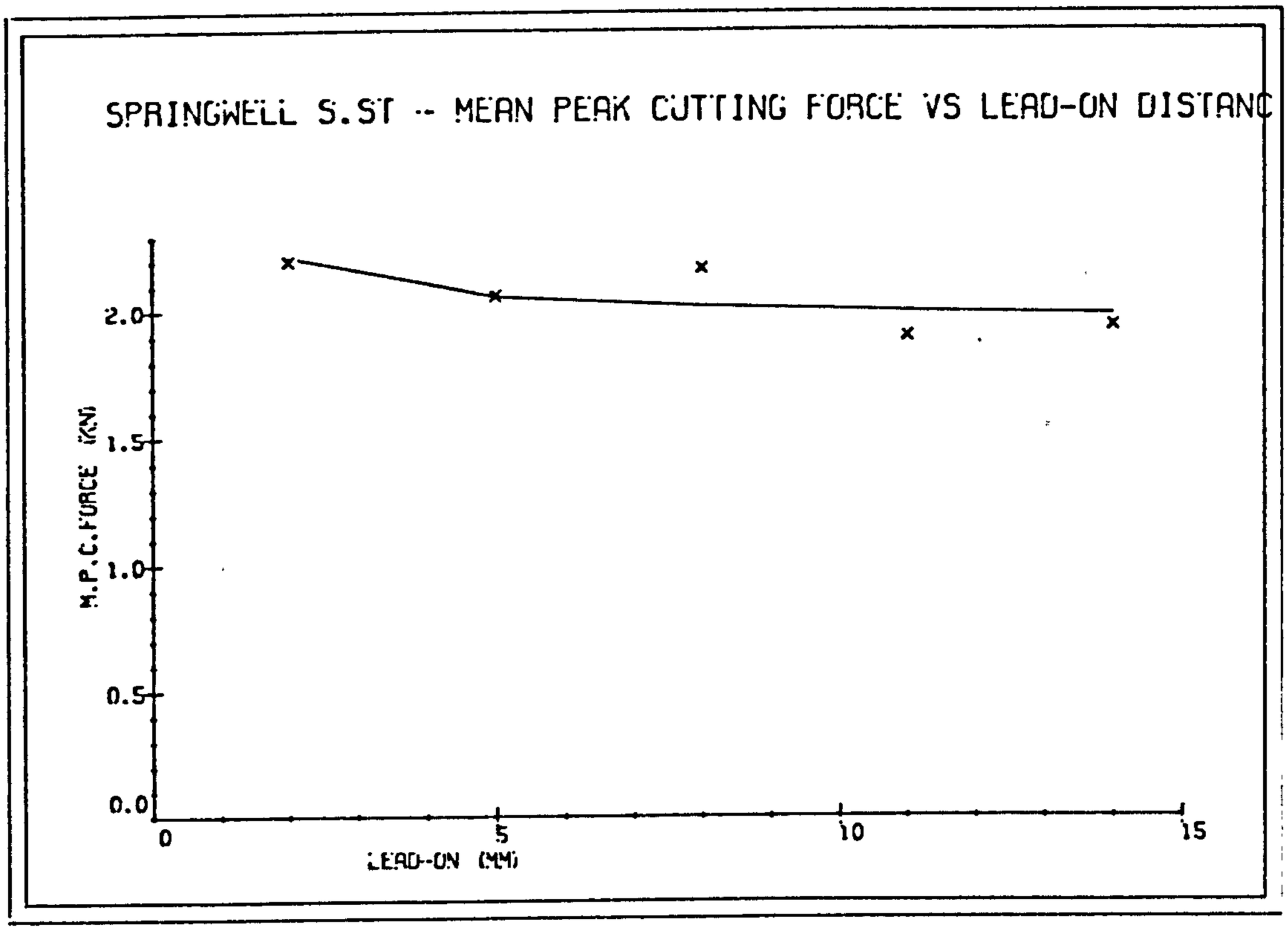
SPRINGWELL S.ST -- MEAN PEAK CUTTING FORCE VS LEAD-ON DISTANC
M.P.C.FORCE (KN)
2.0
1.5
1.0
0.5
0.0
0
5
10
15
LEAD-ON (MM)

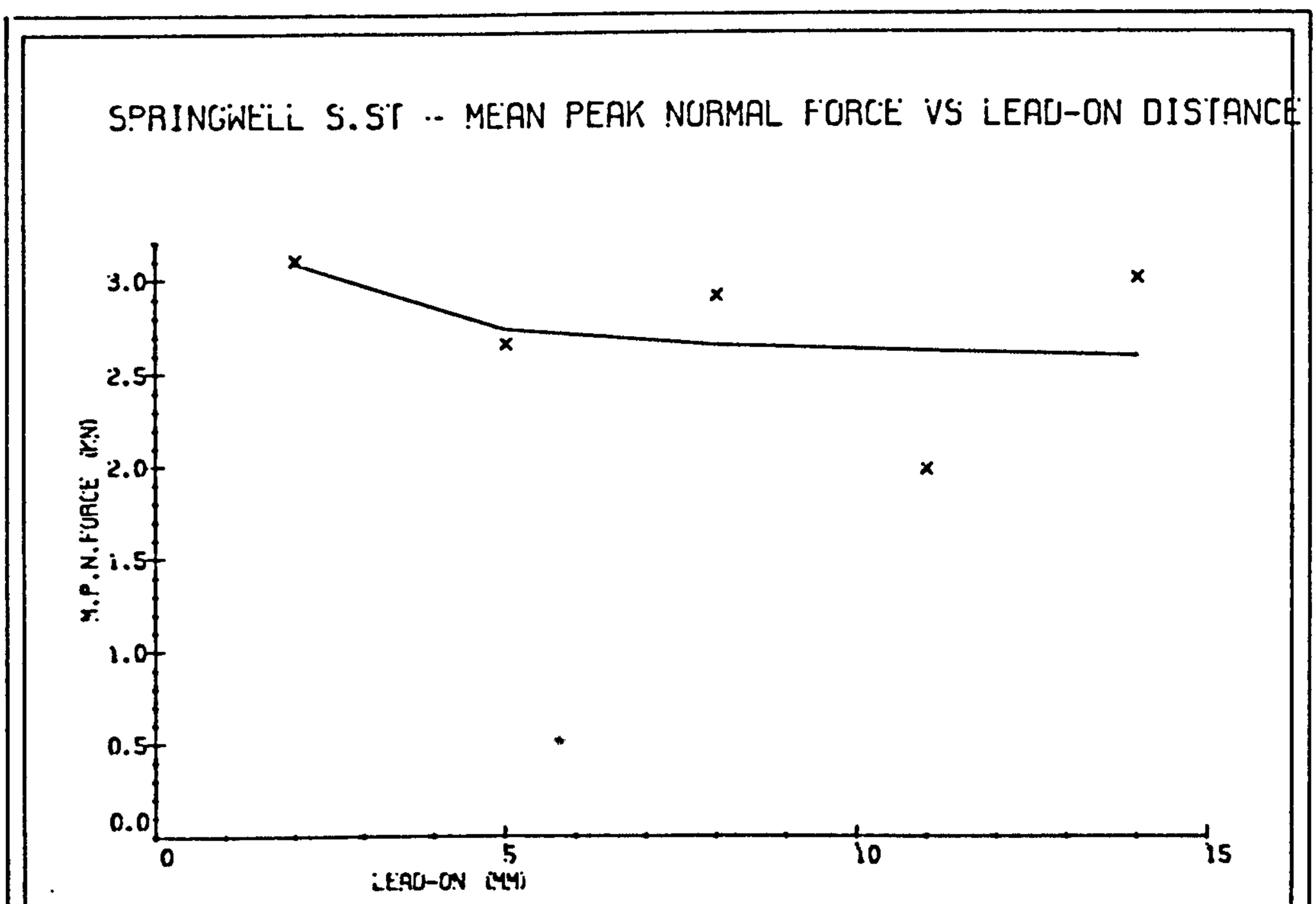
SPRINGWELL S.ST -- MEAN PEAK NORMAL FORCE VS LEAD-ON DISTANCE
M.P.N.FORCE (KN)
3.0
2.5
2.0
1.5
1.0
0.5
0.0
0
5
10
15
LEAD-ON (MM)

FIG. 6.16

On Yield and Mechanical Specific Energy

Yield showed a very small increase to the increase in Lead-on distance. The increase was in such a magnitude that it may be considered negligible, (Fig 6.17). Mechanical Specific Energy decreased with increasing Lead-on distance, and displayed a tendency to level out after the last experimental level. The most efficient cutting occurred when the jet was leading the mechanical tool by lead-on distance/depth of cut ratios greater than 2.5.

Empirically derived equations from cutting experiments are as follows :

$$MCF = (D+1.20)(S+255.0132)[e(-4.27\times10^{-3}P-7.07)][e(-9.06\times10^{-3}L+0.734)-0.94]$$

$$MPCF = (D+0.51)(S+199.82)[e(6.99\times10^{-6}P+5.48\times10^{-2})-0.045][e(-431\times10^{-3}L+1.41)-2.95]$$

$$MNF = (D+2.09)(S+37.09)[e(-2.02\times10^{-5}P-5.08\times10^{-2})-0.947]$$

$$MPNF = (D+1.41)(S+43.48)[e(-1.89\times10^{-5}P+0.692)-1.99) \quad -3.98]\times10^{-2}$$

$$MPSF = (D+1.38)(e(3.72\times10^{-4}S+1.79)[e(-1.87\times10^{-4}P+3.26)-24.95][37\times10^{-2}L+1.19]$$

$$Yield = (D^{2}+11.833)[(S+0.641)/(S+1)](2.18\times10^{-4}P+2.644\times10^{-2})$$

6.4 CONCLUSIONS

Tool forces (cutting, normal and sideways) all have increased linearly with increasing mechanical tool depth of cut. Yield increased exhibiting a power relationship and Mechanical Specific Energy decreased at a decreasing rate with depth of cut. Therefore, cutting becomes more efficient at deeper cuts. Forces acting on the tool are reduced with increase in jet pressure. Reduction in cutting forces was small after 13.69 MPa pressure. but Normal forces have shown continuous improvement indicating the improved efficiency which resulted from water jet assistance.

Placing of the nozzles between the mechanical tools which during cutting would cut the rock before the mechanical tool and thus create a free surface to which a mechanical cutter breaks the rock into, had considerable effect on cutting performance. All the tool forces increased at an decreasing rate with increase in side-off distance with curves displaying tendency to level off after the fourth experimental level to force values equivalent to the unrelieved cutting values. The advantage of water jet creating a free surface was lost at a distance at which both cutting components incorporating the hybrid cutting system were operating in isolation. The rock yield produced increased rapidly during the initial stages, then increased linearly at a very small rate with side-off distance and Mechanical Specific Energy results had shown that the optimum cutting position occurred at side-off distance/depth of cut(s/d) ratio of 3.33.

Lead-on distance results had shown that the water jet nozzle has to lead the tool at least a lead-on distance/depth of cut(l/d) ratio of 2.5. Mechanical Specific Energy decreased then levelled off with lead-on distance increase. The ideal operating position for a hybrid cutting system when the nozzle is between the mechanical tools and the pressure of the water-jet is high enough to penetrate the rock to a distance equalling the mechanical tool depth of cut was at an s/d ratio of 3.33 and l/d ratio of 2.5 for Springwell sandstone cutting.

Further experiments were planned and carried out to investigate the effects of stand-off distance, nozzle diameter, traverse speed, and number of passes of the jet on the measured and calculated parameters using Springwell sandstone as the test medium. The results of these tests, together with experimental designs, are given in appropriate sections of the next chapter in which more extensive analysis was carried out on Darney sandstone.

7 THE INFLUENCE OF EXPERIMENTAL VARIABLES

7.1 WATER JET PRESSURE

The effect of high pressure water jet on a rock surface is measured in terms of its depth of penetration and this depth varies with changes in the hydraulic parameters i.e. pressure, traverse speed, nozzle size, number of passes, stand-off distance.

Numerous researchers have investigated the influence of jet pressure on rock penetration depth. Their works have revealed that for most rocks, there is a threshold pressure below which no measured penetration takes place and the depth of this penetration increases directly with increase in pressure.

Experiments were designed for cutting Springwell and Darney sandstones with a hybrid system to investigate the influence of water jet pressure -when it was increased from the threshold pressure of the rock to the pressure approaching the rock's compressive strength- on the tool forces, yield and mechanical specific energy.

The Springwell sandstone results were given in the previous chapter. The Darney sandstone experimental plan and analysis is dealt with in this chapter.

7.1.1 Thin Section Analysis

Darney sandstone is a medium strength sandstone ,and is composed predominantly of medium and fine grained quartz fragments.

Mineralogical Content

	%
Quartz	75
Clay/Chlorite	18
Calcite	2
Fe	Trace
Voids	5

Grain Size (mm)		Grain %	Volume %
Medium	(1/2 - 1/4)	46	54
Fine	(1/4 - 1/8)	51	45
V. Fine	(1/8- 1/16)	3	1

Angularity	%
Sub Angular	46
Sub Rounded	48
Rounded	6

Cement	%
Quartz	30
Clay/Chlorite	53
Calcite	4
Voids	13

Darney sandstone is poorly cemented with clay forming a mantle round the quartz grains.

Uniaxial Compressive Strength (MPa) : 64.53 +/- 3.55

Indirect Tensile Strength (MPa) : 4.34 +/- 0.42

Triaxial Strength :

Confining Pressure (MPa)	Failure Stress (MPa)
6.90	119.82
13.79	157.35
20.69	177.56
27.59	217.26
34.48	241.80
41.38	270.69
48.28	283.66

Angle of friction (degrees) : 41

Unconfined Shear Strength (MPa) : 10.00

Bulk Density (g/cm^3 Dry : 2.18

Saturated : 2.36

Grain Density : 2.65

Poisson's Ratio : 0.28

Static Young's Modulus	Etan	: 22.50
(GPa)	Esec	: 13.50
Dynamic Elastic Modulus (GPa)		: 9.97
Apparent Porosity (%)		: 8.5
True Porosity (%)		: 22.4
Shore Sclerescope (Rebound Hardness)		: 35.3
Plasticity (%)		: 30.57
Schmidt Hammer (Rebound Hardness)		: 43.38
N.C.B. Cone Indenter Hardness		: 2.53

Nozzle diameter, cutting speed, stand-off distance, lead-on distance, side-off distance were kept constant at their respective mean levels to isolate the effect of water jet pressure.

It was thought beforehand that the influence of pressure might vary with mechanical tool depth of cut. Therefore, the experimental programme incorporated the investigation of effects and interactions of two main variables namely pressure and the mechanical tool depth.

Experimental variables and their levels are tabulated as follows:

Exp. Variable	Level
Nozzle diameter (mm)	0.85
Traverse Speed (mm/sec)	165
Stand-off Distance (mm)	45
Side-off Distance (mm)	0

Lead-on Distance (mm)	5
Water jet Pressure (MPa)	13.79, 24.14, 34.48, 44.83, 55.17
Mechanical depth of cut (mm)	3, 5, 7, 9, 11

Total of 5 x 5 = 25 tests were planned and each cutting test was repeated four times, to counteract any changes that might occur in the rock properties and operating conditions. The same rock surface was cut with water jet alone to determine the depth of penetration and width of cut at each pressure. Experiments were carried out in random order.

A Least Squares curve-fitting computer analysis of experimental results was undertaken. Whenever it gave several good fitting curves through data points with equal correlation coefficients, linear function was chosen. The experimental results and the functions fitted to curves are tabulated in (Appendix C).

7.1.2 Effect of Pressure on Depth of Penetration

An increase in water jet pressure lead to a corresponding increase in depth of penetration. The relationship between the variables, within the experimental cutting range, was of linear form. The threshold pressure for Darney Sandstone was found by extrapolation to be 9.12 MPa (Figure 7.1).

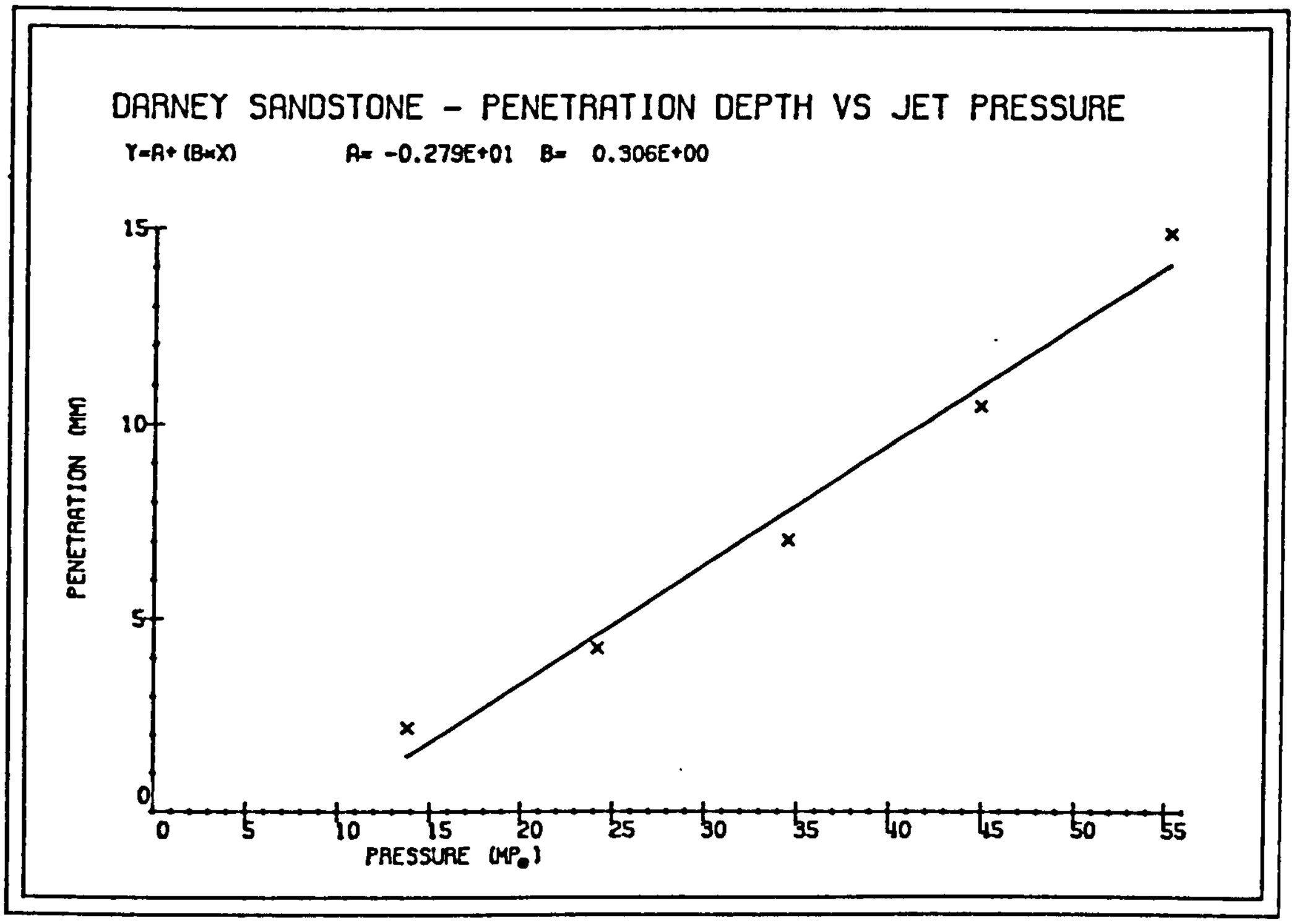
DARNEY SANDSTONE - PENETRATION DEPTH VS JET PRESSURE
Y=A+(B*X)
A= -0.279E+01
B= 0.306E+00
PENETRATION (MM)
15
10
5
0
0
5
10
15
20
25
30
35
40
45
50
55
PRESSURE (MPa)

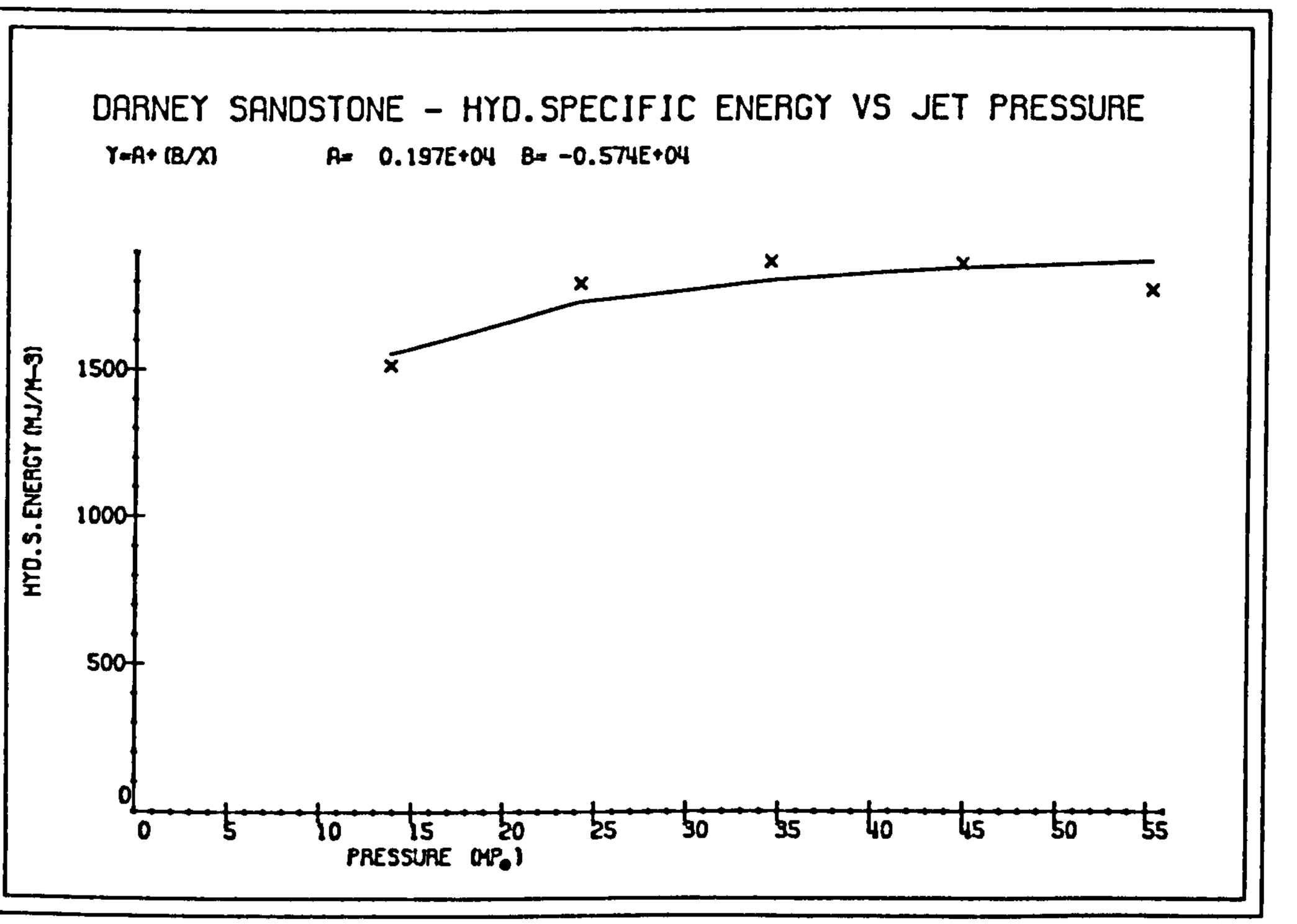
DARNEY SANDSTONE - HYD.SPECIFIC ENERGY VS JET PRESSURE
Y=A+(B/X)
A= 0.197E+04
B= -0.574E+04
HYD.S.ENERGY (MJ/M-3)
1500
1000
500
0
0
5
10
15
20
25
30
35
40
45
50
55
PRESSURE (MPa)

FIG. 7.1

Hydraulic Specific Energy requirements at each pressure was calculated and these showed that it decreased with increasing pressure and did not pass through a minimum (Figure 7.1), contradicting Harris and Mellors (55) and supporting Page'(112) findings.

7.1.3 Effect of Water jet pressure and Mechanical Tool Depth

On Tool Forces

Cutting and normal forces have increased approximately linearly with the depth of cut, when the water jet pressure was held constant and the mechanical tool depth of cut was increased from 3mm to 11mm in steps of 2mm, (Fig 7.2). The curves for each pressure run nearly parallel to one another, and after 44.83 MPa pressure a further increase in pressure did not cause a significant change in tool forces (Figure 7.3)

The forces have decreased with increasing water jet pressure, displaying a hyperbolic type relationship, when the depth of cut was held constant. Curves have shown tendency to become asymptotic at high pressures to x-axis (Figures 7.4-. ,7.5). Normal forces seemed to show more sensitivity to change in pressure than cutting forces. The most of the reduction in forces has occurred by 24.14 MPa pressure level.

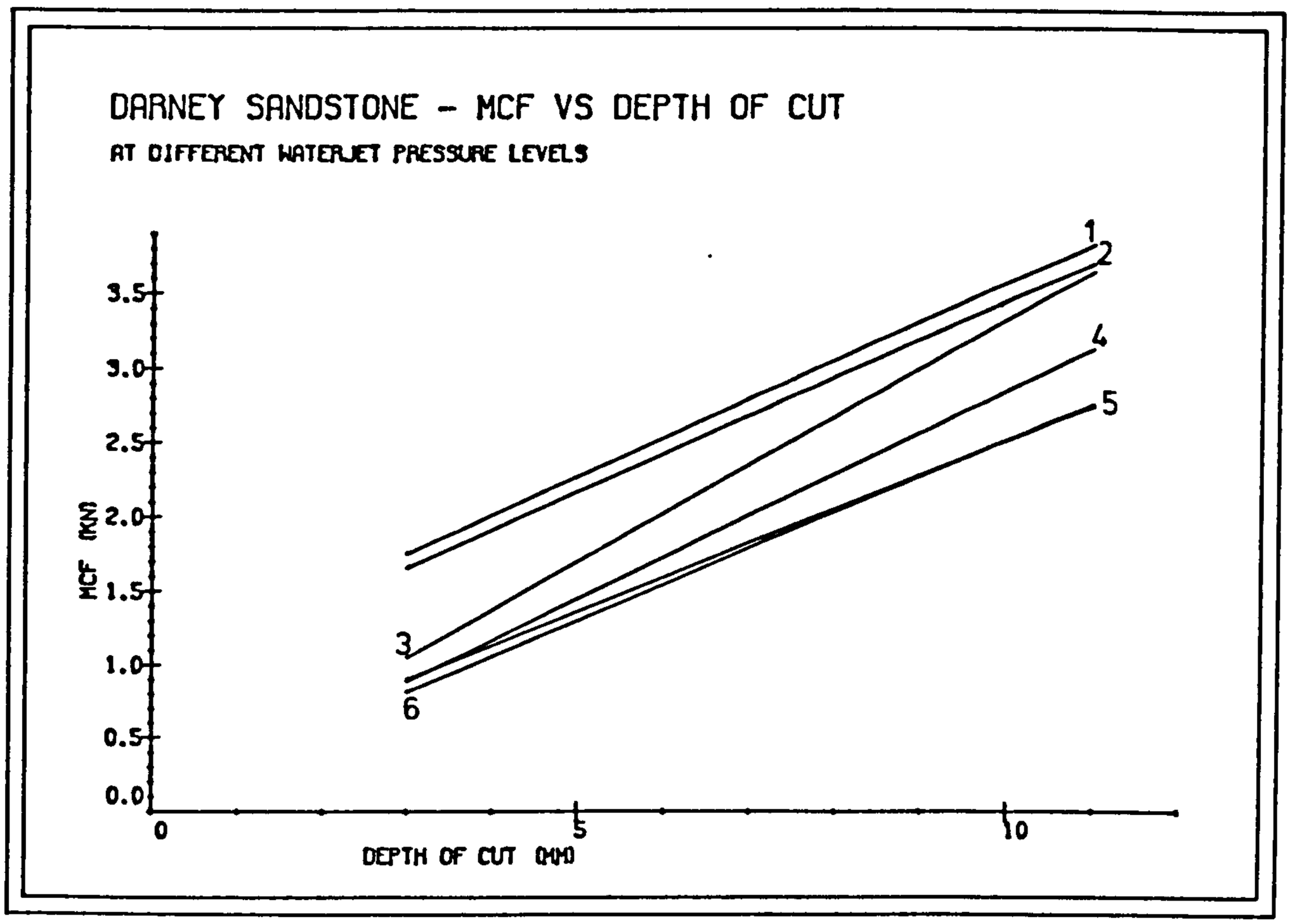
DARNEY SANDSTONE - MCF VS DEPTH OF CUT
AT DIFFERENT WATERJET PRESSURE LEVELS
MCF (KN)
3.5
3.0
2.5
2.0
1.5
1.0
0.5
0.0
0
5
10
DEPTH OF CUT (MM)
1
2
3
4
5
6

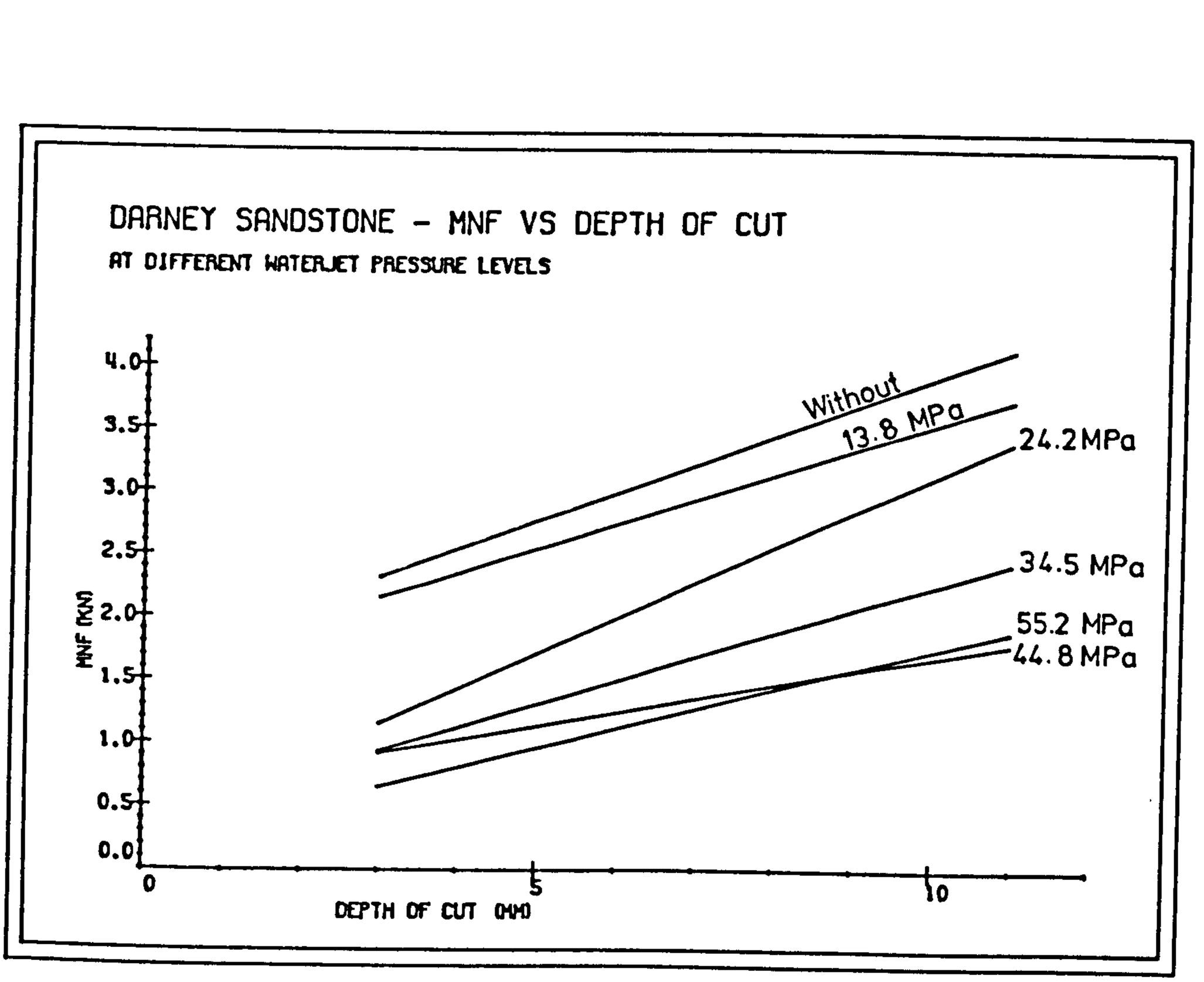
DARNEY SANDSTONE - MNF VS DEPTH OF CUT
AT DIFFERENT WATERJET PRESSURE LEVELS
MNF (KN)
4.0
3.5
3.0
2.5
2.0
1.5
1.0
0.5
0.0
0
5
10
DEPTH OF CUT (MM)
Without
13.8 MPa
24.2MPa
34.5 MPa
55.2 MPa
44.8 MPa

FIG. 7.2

DARNEY SANDSTONE - MPCF VS DEPTH OF CUT

AT DIFFERENT WATERJET LEVELS

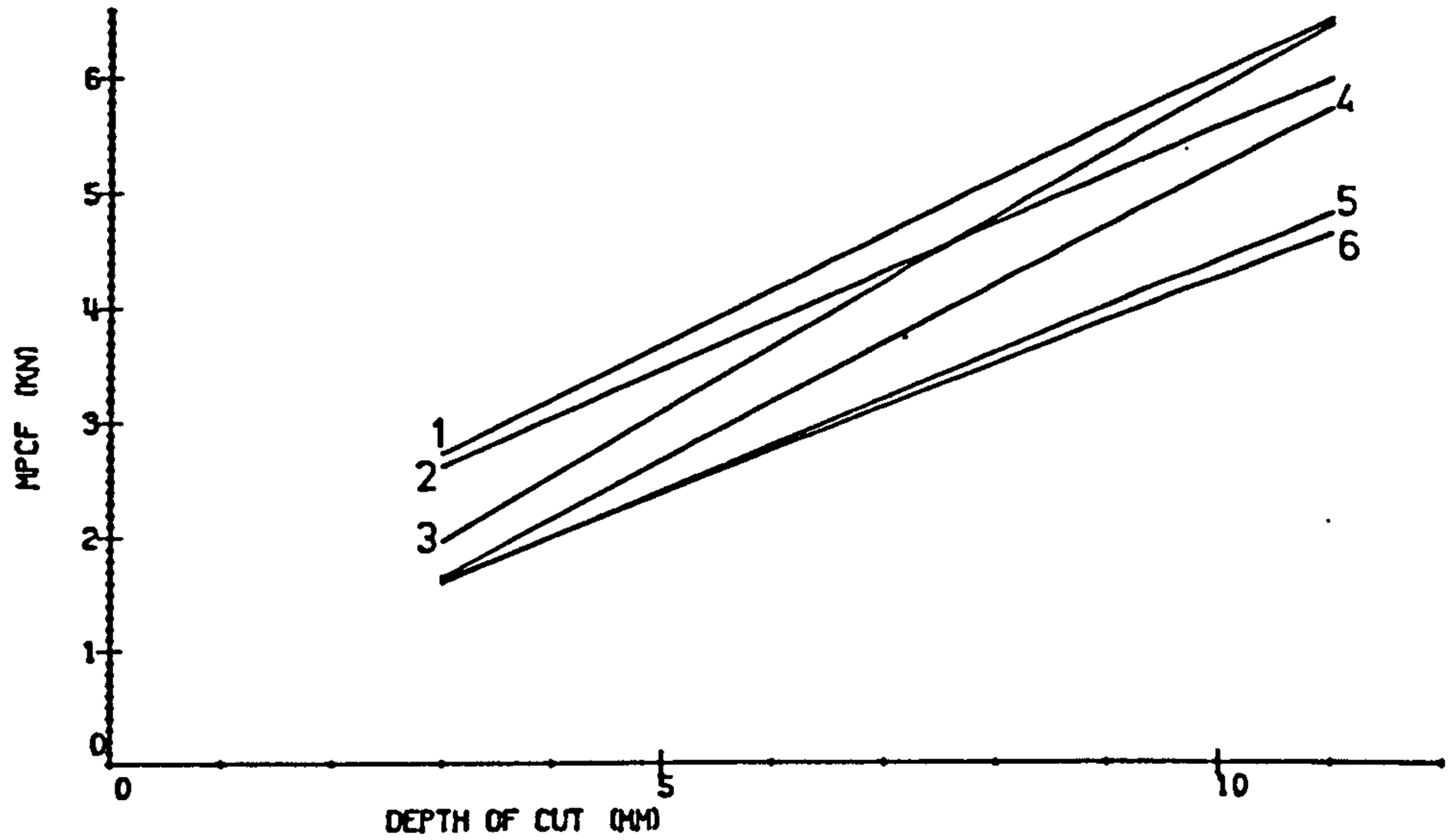

DARNEY SANDSTONE - MPNF VS DEPTH OF CUT

AT DIFFERENT WATERJET PRESSURE LEVELS

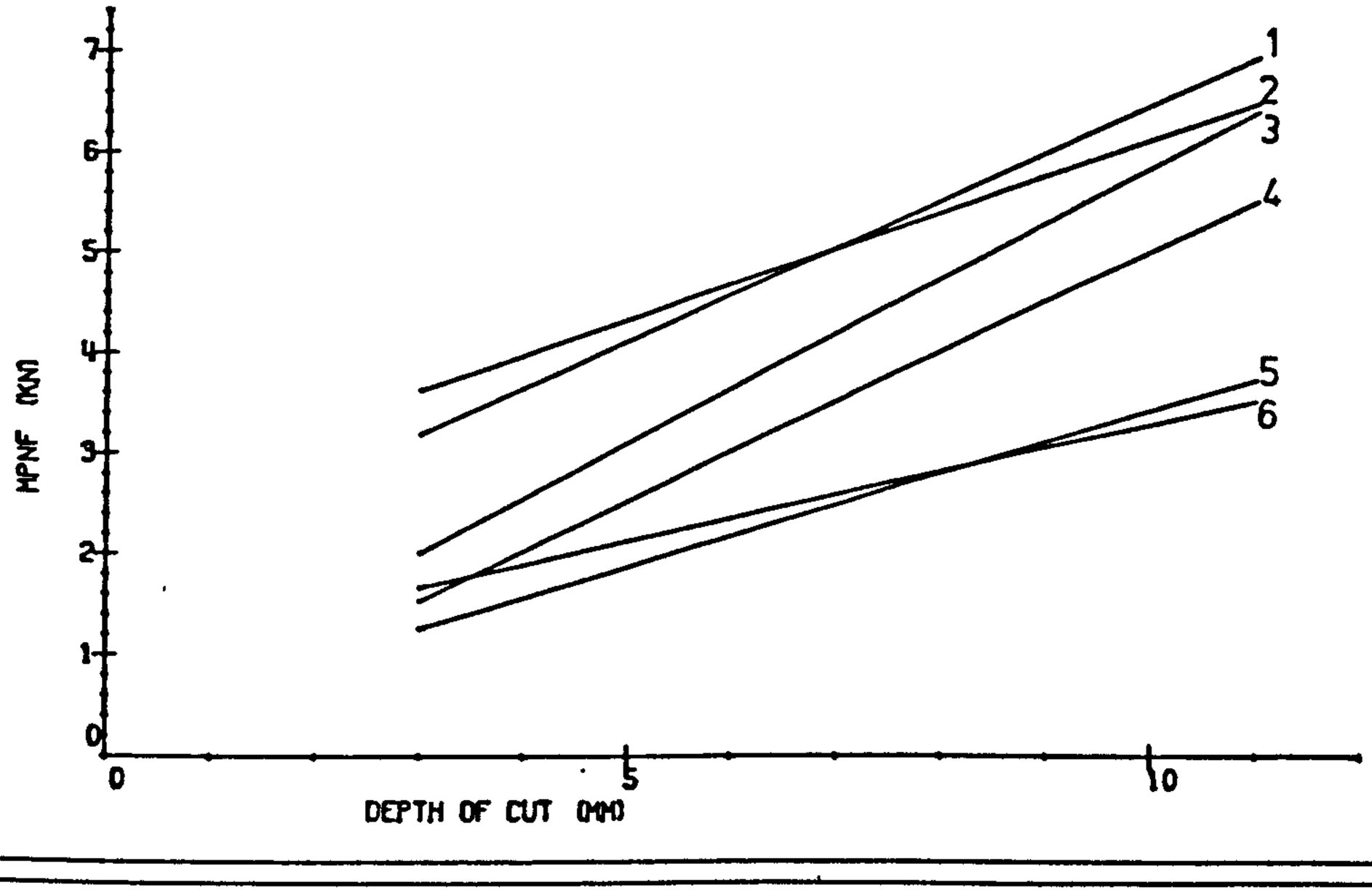

FIG. 7.3

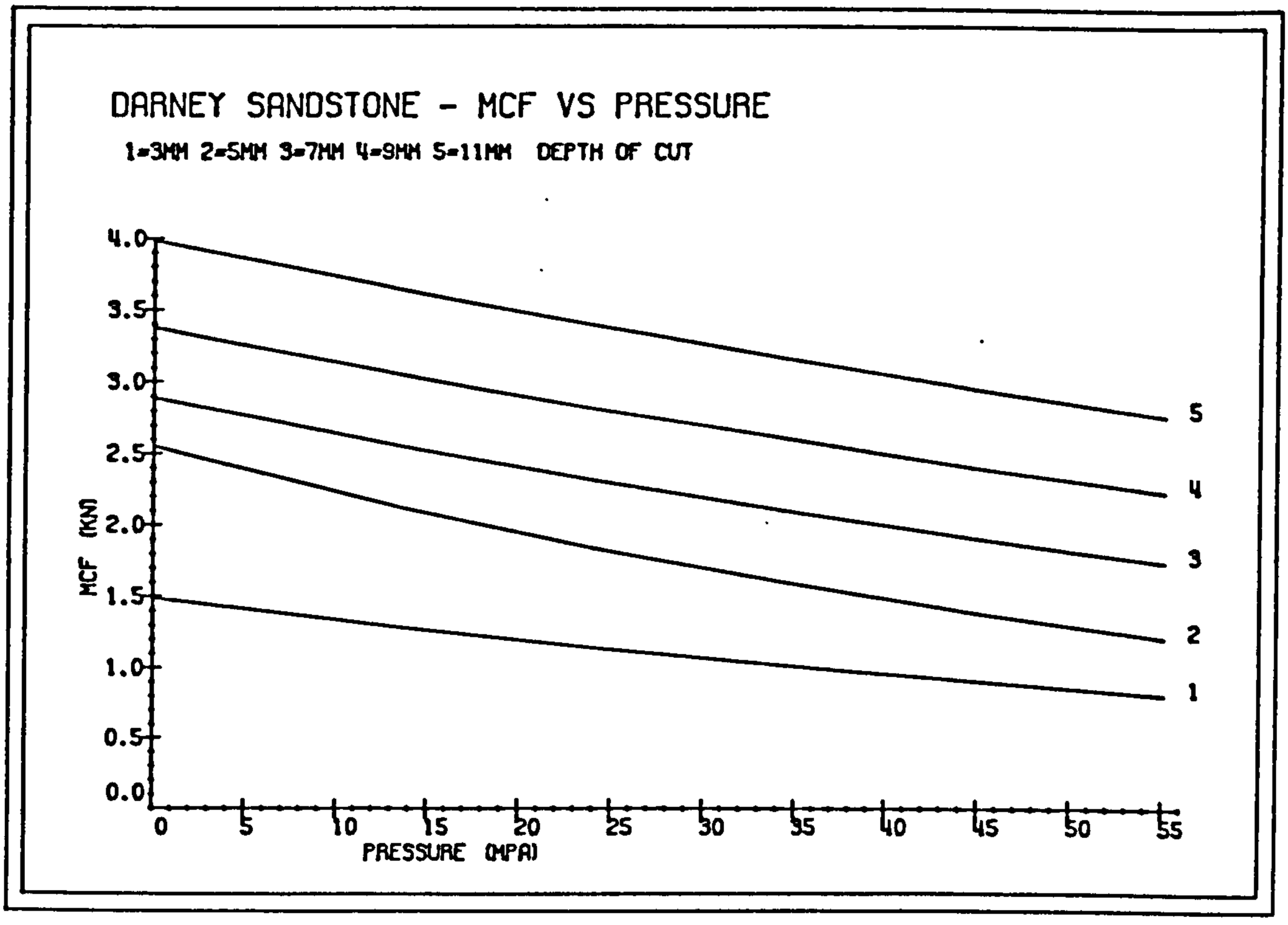
DARNEY SANDSTONE - MCF VS PRESSURE
1=3MM 2=5MM 3=7MM 4=9MM 5=11MM DEPTH OF CUT
MCF (KN)
4.0
3.5
3.0
2.5
2.0
1.5
1.0
0.5
0.0
0
5
10
15
20
25
30
35
40
45
50
55
PRESSURE (MPA)
5
4
3
2
1

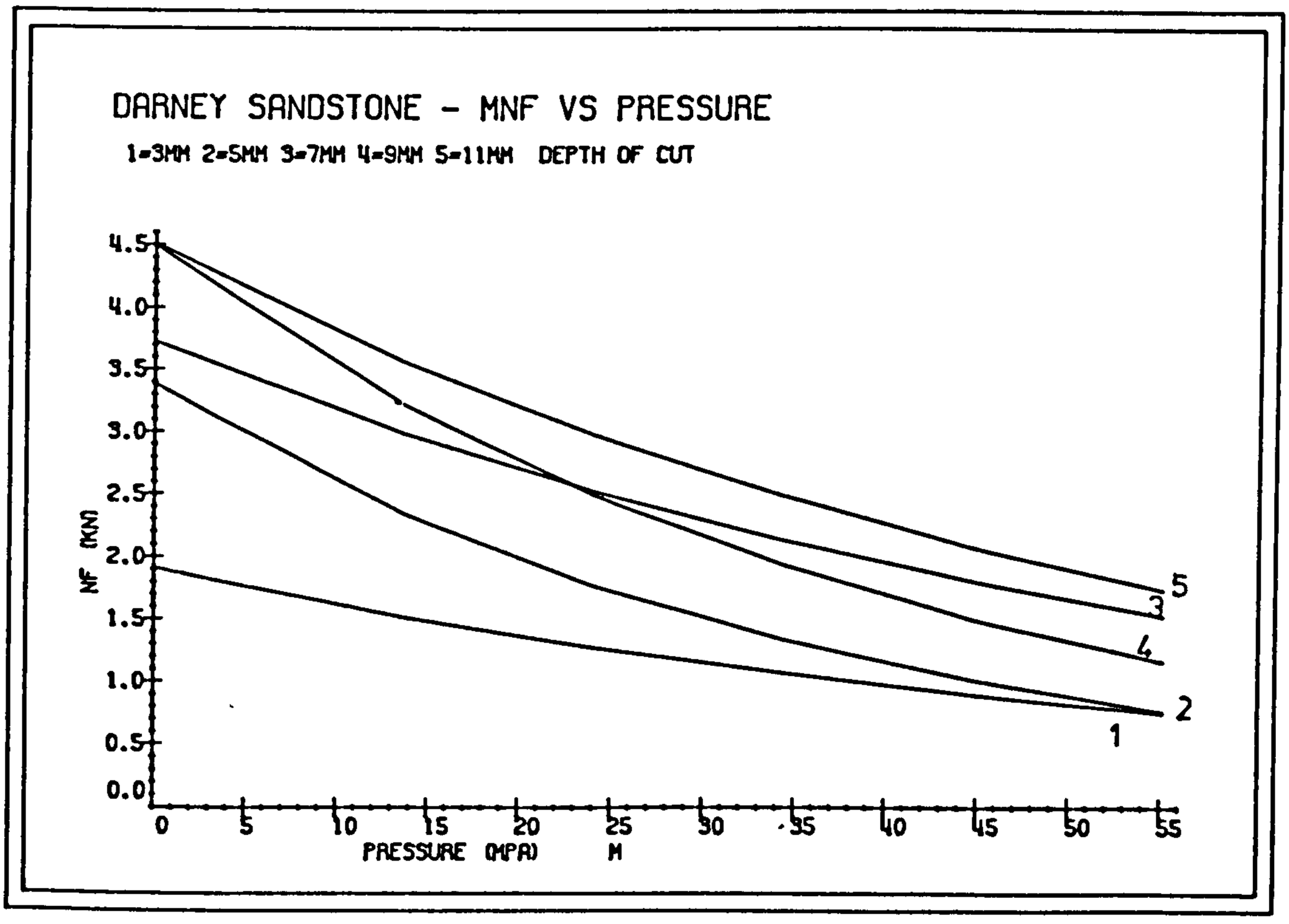
DARNEY SANDSTONE - MNF VS PRESSURE
1=3MM 2=5MM 3=7MM 4=9MM 5=11MM DEPTH OF CUT
MF (KN)
4.5
4.0
3.5
3.0
2.5
2.0
1.5
1.0
0.5
0.0
0
5
10
15
20
25
30
35
40
45
50
55
PRESSURE (MPA)
5
3
4
2
1

FIG. 7.4

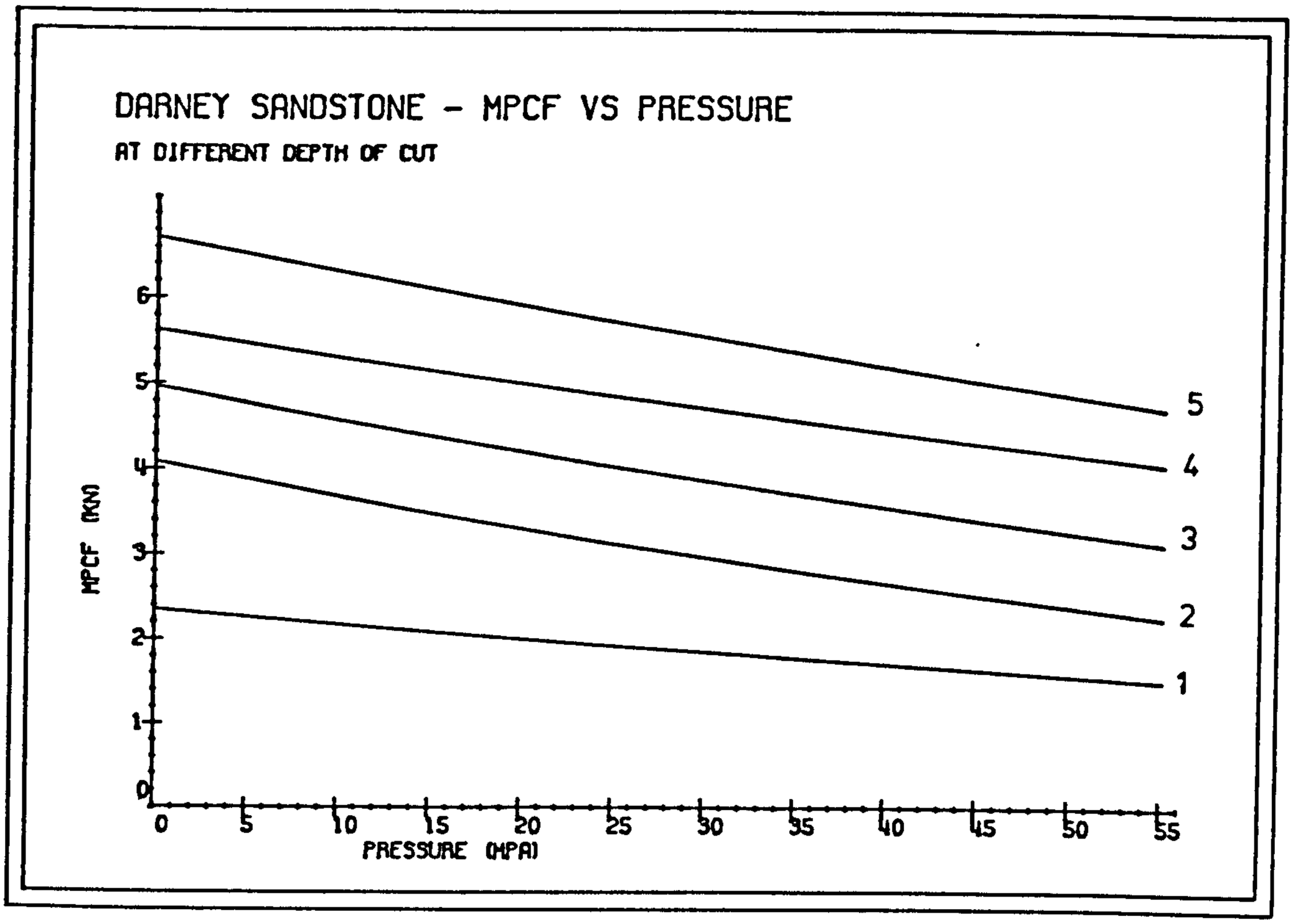
DARNEY SANDSTONE - MPCF VS PRESSURE
AT DIFFERENT DEPTH OF CUT
MPCF (KN)
0
1
2
3
4
5
6
0
5
10
15
20
25
30
35
40
45
50
55
PRESSURE (MPA)
5
4
3
2
1

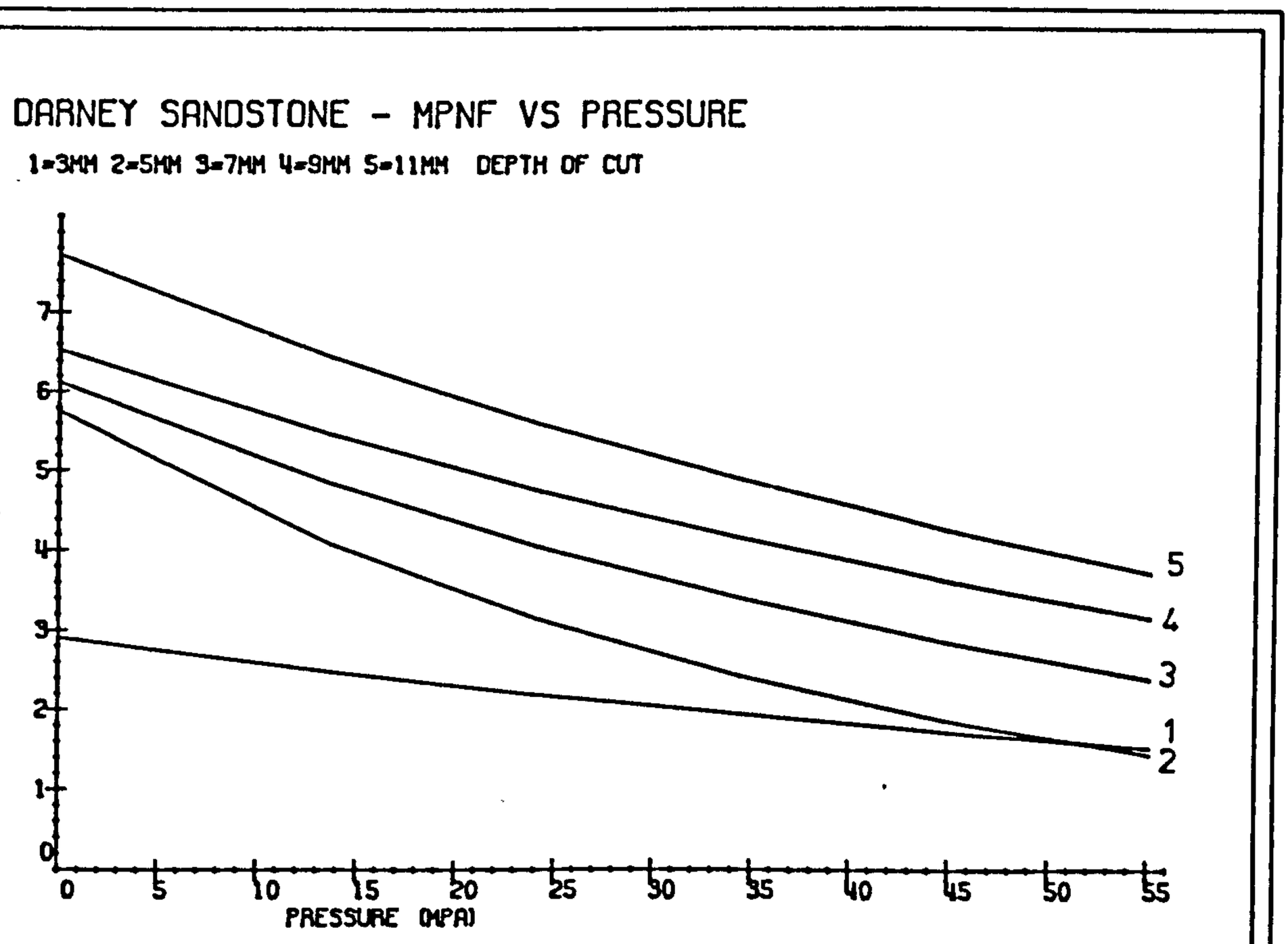
DARNEY SANDSTONE - MPNF VS PRESSURE
1=3MM 2=5MM 3=7MM 4=9MM 5=11MM DEPTH OF CUT
MPNF (KN)
0
1
2
3
4
5
6
7
0
5
10
15
20
25
30
35
40
45
50
55
PRESSURE (MPA)
5
4
3
1
2

FIG. 7.5

On Yield

The graphs of yield against depth of cut at increasing water jet pressures all seemed to display a power relationship, although the value of the power remained, within limits, approximately constant when the pressure was greater than and or equal to 24.14 MPa. Mechanical tool cutting has produced more yield than hybrid cutting (Figures 7.6,7.7).

On Mechanical Specific Energy

Mechanical Specific Energy decreased with increase in the mechanical tool depth of cut at constant water jet pressure levels (Figure 7.6). All the curves seemed to level off after 11mm depth of cut.

The effect of increasing water jet pressure can be more clearly seen when graphs of mechanical specific energy are drawn at constant depth of cut (Fig 7.7). These have demonstrated that Mechanical specific energy had decreased(cutting became more efficient).

7.1.4 Discussion

Experimental results have indicated that the penetration depth of the water jet consequently its pressure has a strong influence on the efficiency of the hybrid cutting system. The penetration depth varied

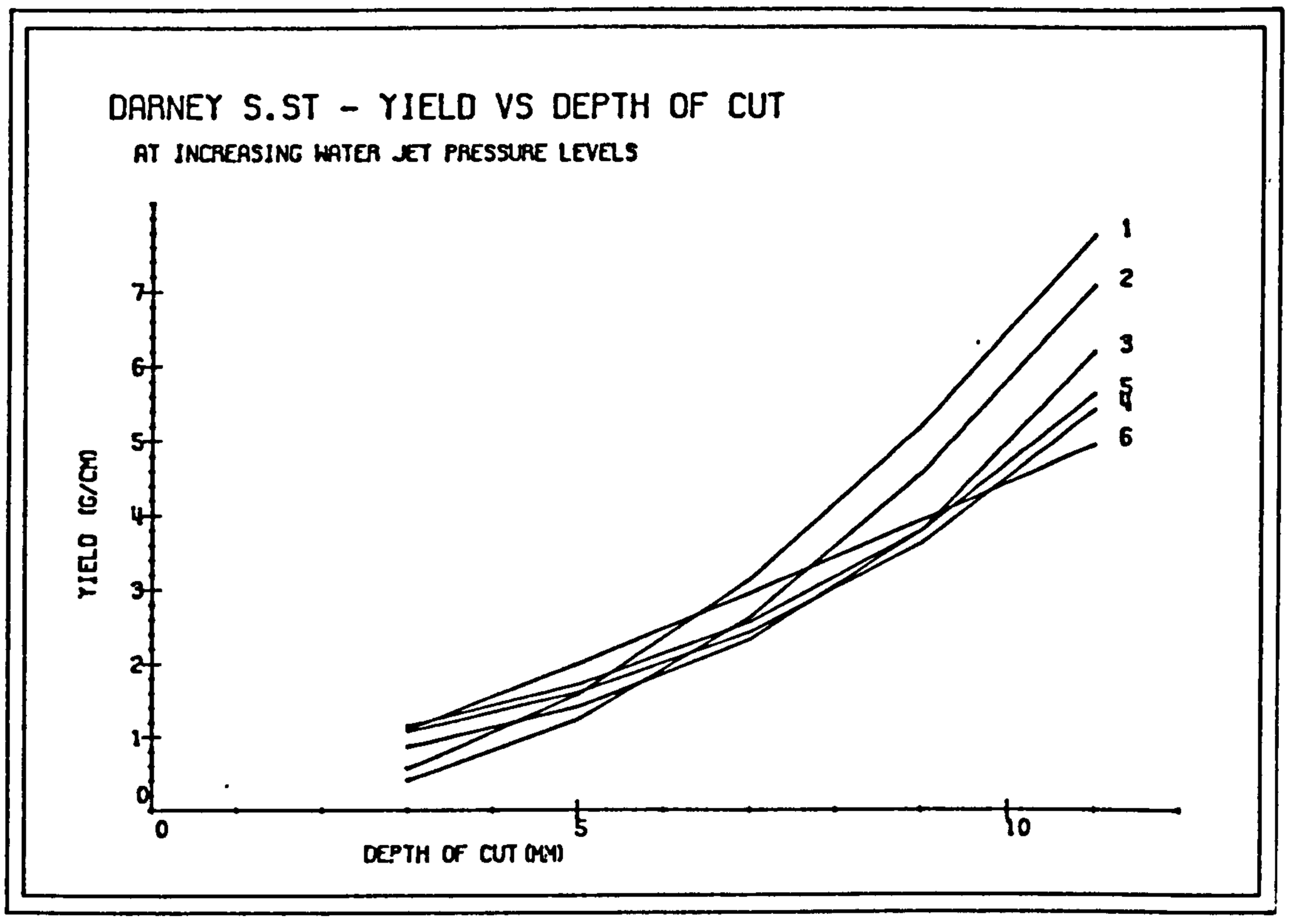
DARNEY S.ST - YIELD VS DEPTH OF CUT
AT INCREASING WATER JET PRESSURE LEVELS
YIELD (G/CM)
0
1
2
3
4
5
6
7
0
5
10
DEPTH OF CUT (MM)
1
2
3
4
5
6

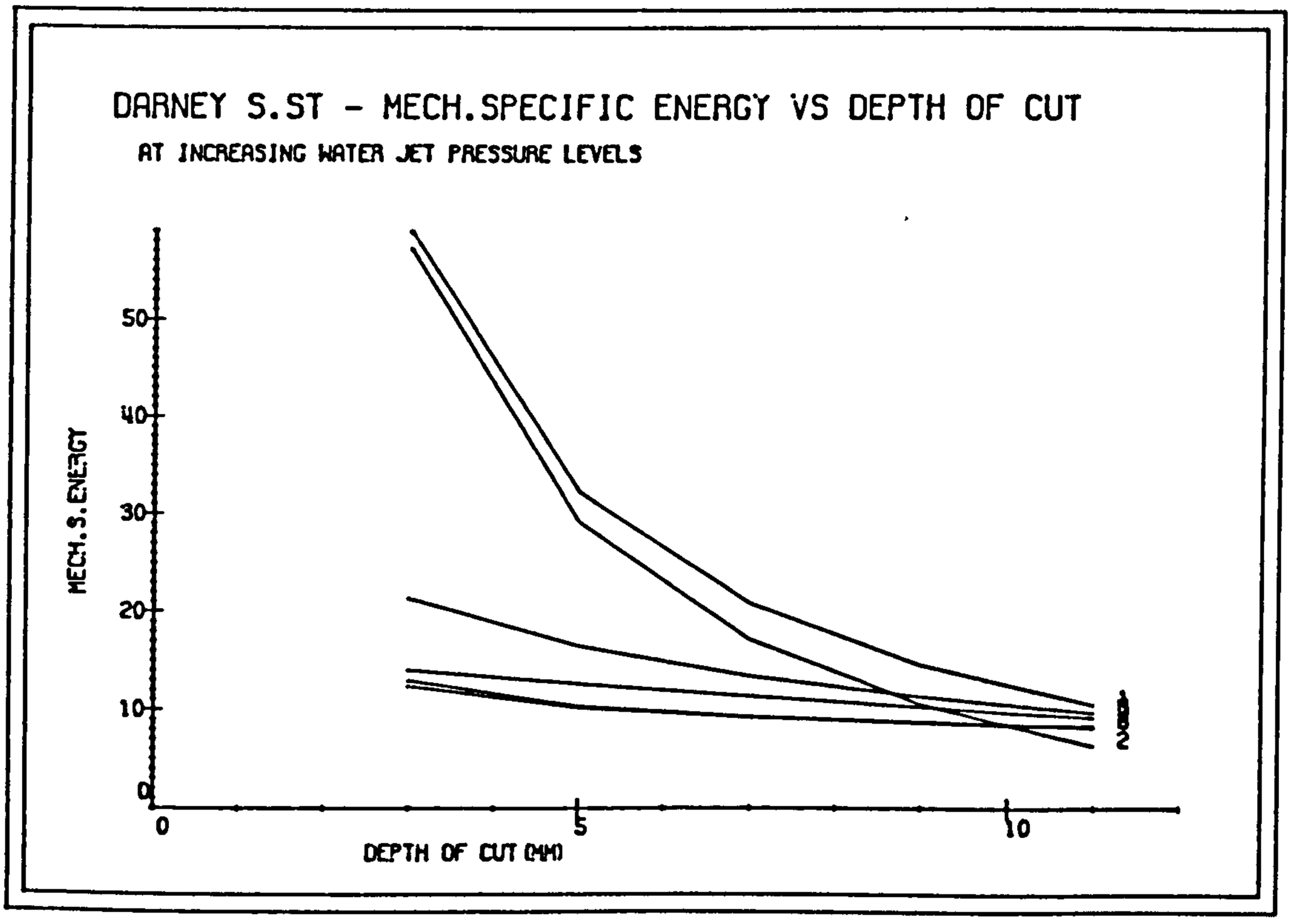
DARNEY S.ST - MECH.SPECIFIC ENERGY VS DEPTH OF CUT
AT INCREASING WATER JET PRESSURE LEVELS
MECH.S.ENERGY
0
10
20
30
40
50
0
5
10
DEPTH OF CUT (MM)

FIG. 7.6

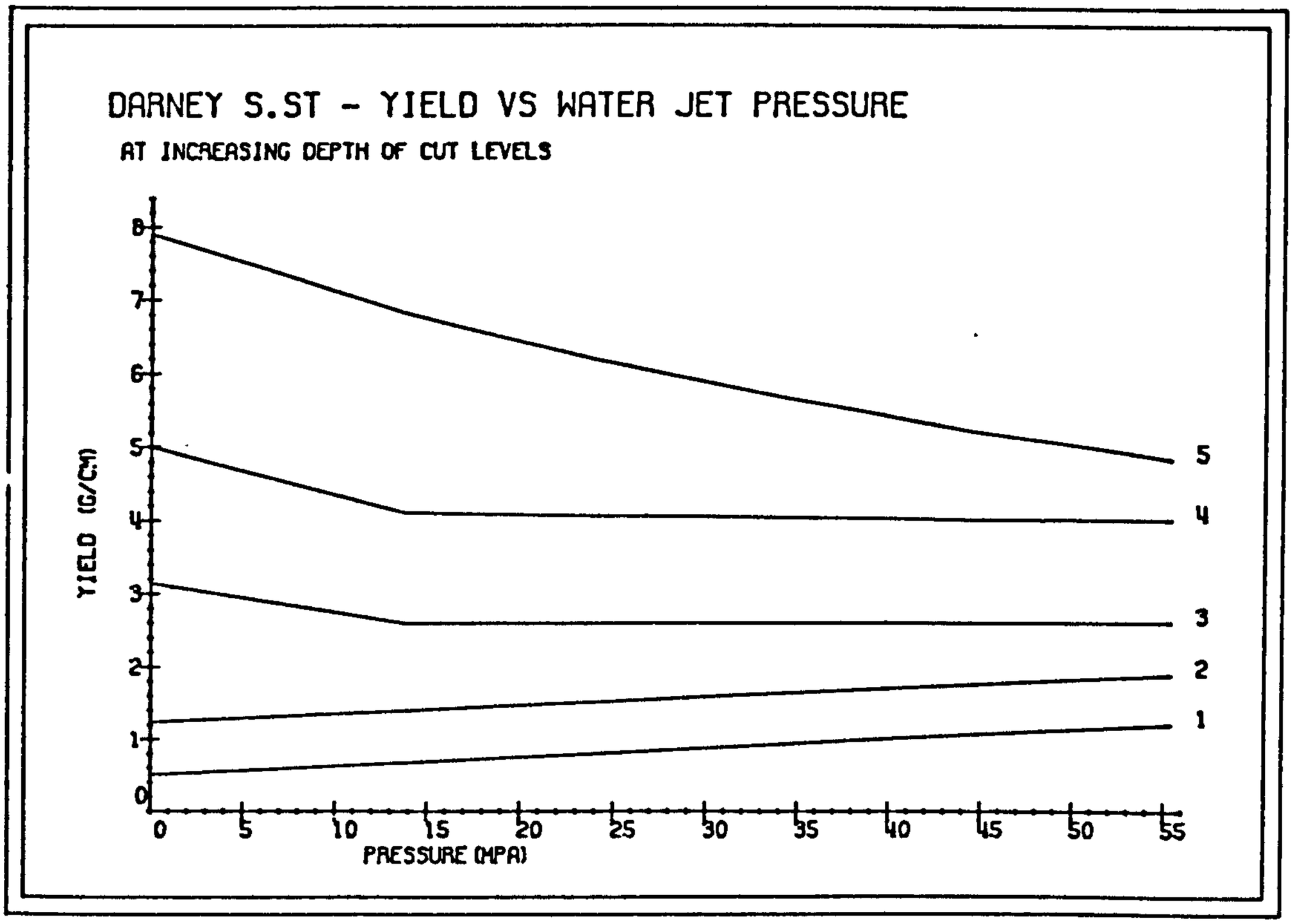
DARNEY S.ST - YIELD VS WATER JET PRESSURE
AT INCREASING DEPTH OF CUT LEVELS
YIELD (G/CM)
0
1
2
3
4
5
6
7
8
0
5
10
15
20
25
30
35
40
45
50
55
PRESSURE (MPA)
5
4
3
2
1

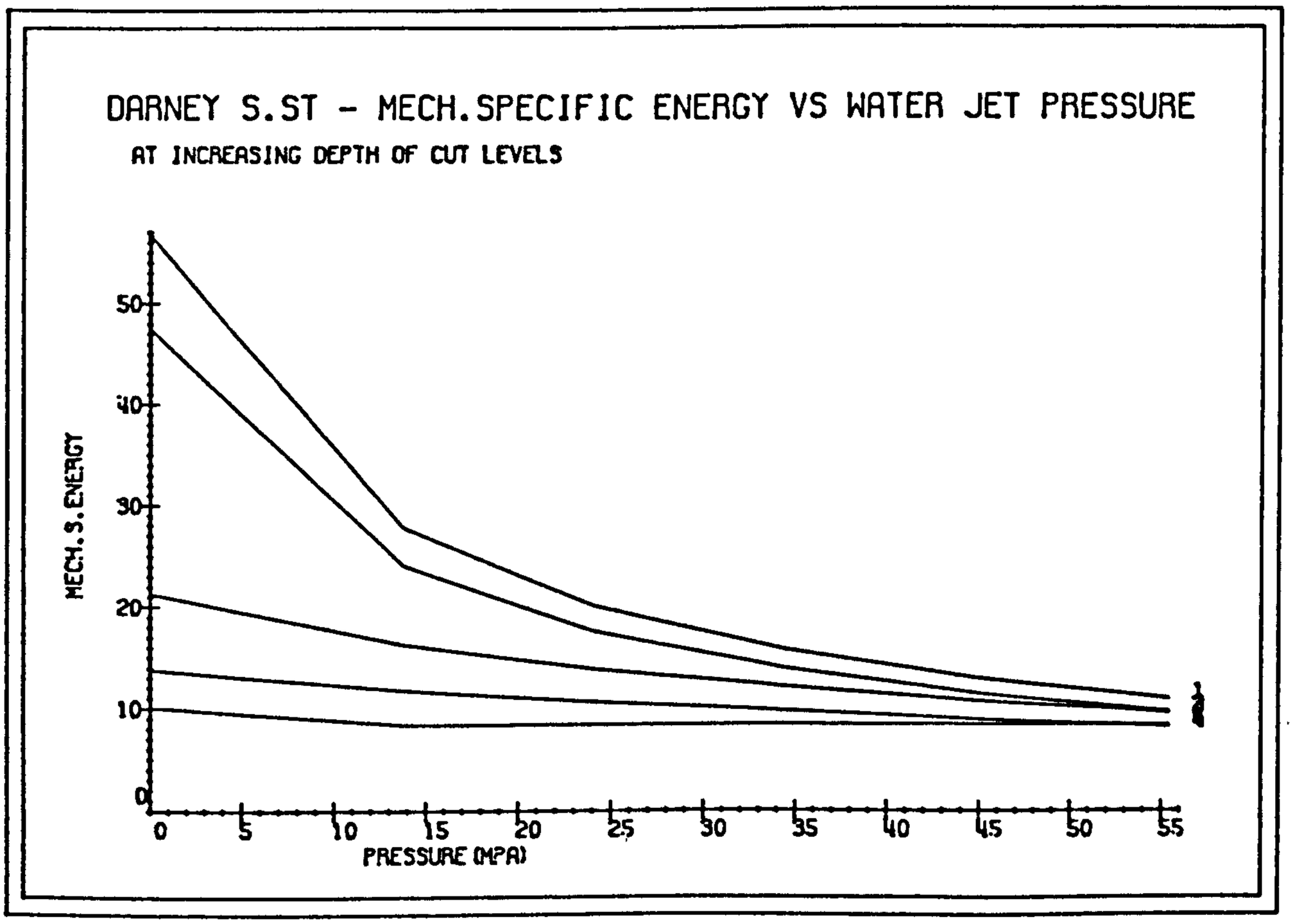
DARNEY S.ST - MECH.SPECIFIC ENERGY VS WATER JET PRESSURE
AT INCREASING DEPTH OF CUT LEVELS
MECH.S.ENERGY
0
10
20
30
40
50
0
5
10
15
20
25
30
35
40
45
50
55
PRESSURE (MPA)
1

FIG. 7.7

directly with jet pressure as reported by Brook (144), showing a linear relationship within the experimental range. The threshold pressures required to initiate penetration for Springwell Sandstone and Darney Sandstone were found by extrapolation. The values were 9.12 MPa for Darney and 6.25 MPa for Springwell sandstone. Cooley has reported that 'threshold pressure was typically 20 to 50 per cent of the rock's compressive strength'. The results obtained from the cutting of two sandstones contradicted this suggestion as threshold pressure for Darney sandstone was 14.13% and for Springwell sandstone 14.5%. It must be remembered that experiments were conducted at a constant traverse speed of 165 mm/sec. This speed is slow in comparison to the speeds attained by cutting heads of excavation machines. If the suggestion of Harris, who reported that the value of threshold pressure was dependent on traverse speed, is accepted this may explain the difference. If a power relationship between pressure and penetration was chosen, as suggested by Imanaka, it would have yielded power values of 1.55 for Springwell sandstone and 1.38 for Darney sandstone.

Increase in water jet pressure results in increased energy input available for rock cutting which leads to a deeper jet penetration. Hydraulic specific energy was decreased but did not pass through a minimum. Again, this may be due to low cutting speed.

If a high pressure water jet is to be used to assist mechanical tool for cutting, its pressure must be such that it should not penetrate the rock more than the mechanical tool depth of cut. Taking the example of

11mm mechanical tool depth of cut; as can be seen from the graphs, when pressure was increased above 44.83 MPa, no significant reduction in cutting and normal forces had taken place. This may be due to the fact that at this pressure, the water jet penetrated the rock to a distance equal with mechanical tool depth. When the pressure was increased further it resulted in deeper jet penetration. But since the mechanical tool depth was less than this, no useful gain was made by the increase in pressure. In fact it had a harmful effect in terms of energy costs as the power requirements for achieving pressures increase with increase in pressure.

Increasing both the depth of cut of the mechanical tool and pressure of the water jet have caused reductions in mechanical specific energy. But, when both hydraulic specific energy and mechanical specific energy were taken into account, the total specific energy for water jet assisted cutting was very much higher than when cutting with the mechanical tool at the same depth of cut.

The increase in depth of cut lead to a production of more yield at a constant water jet pressure. Curves showed a power relationship between variables indicating the advantages of taking a deeper depth of cut. However, at a fixed depth of cut an increase in water jet pressure resulted in differing yield values that is, the yield did not increase with pressure after a certain depth of cut. For Darney sandstone up to and equal to 5mm depth of cut, yield increased linearly with pressure, but at higher depth values yield has decreased. An increase in yield with an

increase in pressure at shallow depth of cuts may be explained by the fact that, at these levels the water jet has produced more yield than the mechanical tool. The cutting action of the mechanical tool was changed at deeper depths of cuts by the assistance of the water jet. Instead of the tool tip initiating and causing fracture, it was the sides of the mechanical tool that was doing the work. As a result, less yield was produced.

7.1.5 Conclusions

The depth of penetration of the water jet varies directly with pressure, exhibiting approximately a linear type relationship within the experimental range. The threshold pressures for Springwell sandstone an Darney sandstones were 6.25 MPa and 9.12 MPa respectively. These values in turn correspond to 14.5 per cent and 14.13 per cent of the rocks' compressive strengths. The penetration depth was very low at the threshold pressure, but increased rapidly with increase in jet pressure.

'At a fixed water jet pressure, Cutting and Normal forces have increased linearly with the increase in mechanical tool depth of cut when the experimental rocks were cut with the 'hybrid system'. The jet was leading the mechanical tool at a zero side-off distance. Yield has increased exhibiting a power law relationship and the mechanical specific energy has decreased at an decreasing rate with the increase in tool depth of cut.

At constant mechanical depth of cuts, increasing the pressure leads to a decrease in tool forces. Up to 5 mm depth of cut yield has increased with pressure. But,when the depth of cut was increased further, yield has decreased. The decrease was more pronounced at the first three pressures.

Cutting experiments on Darney and Springwell sandstones have indicated that the highest pressure of the water jet should be such that the jet should not penetrate the rock surface more than the mechanical tool depth of cut to keep the power requirements to a minimum.

The optimum pressure is not necessarily the highest pressure for hybrid cutting. It depends on the rock type and shows a relationship to threshold pressure. As can be seen from graphs of Mechanical Specific Energy against pressure, the optimum pressure for Darney Sandstone lies somewhere between 24.14 and 34.48 MPa pressure levels, which is approximately three times the threshold pressure.

7.2 CUTTING SPEED

Cutting speed is an important variable which has a strong controlling influence on the excavation rate. Previously, mechanical tool i.e. disk and drag tool cutting experiments have been conducted on various rock types by several researchers at this Department(8,14,54). They have reported that, within the speed ranges that can be attained by the cutting head of the shaping machine (which was going to be used for the hybrid cutting tests) in the absence of wear the effect of the traverse speed on the parameters was negligible. Therefore, by changing the speed of the cutting head one can find the influence of the water jet in terms of changes that takes place in its penetration depth. The slowest speed that the shaping machine cutting head was capable of achieving was 40 mm/sec and the maximum speed 220 mm/sec. These values are low compared to speeds attained by picks on the cutting heads of present day boring machines. However, experimental results of 'traverse speed influence tests' would yield data which might be used for extrapolation purposes if necessary.

Two sets of experiments were planned for the two main sandstones (Springwell and Darney). Other hydraulic parameters were kept constant to isolate the effect of traverse speed. Experimental variables and their levels were as follows:

Variable		Level	
		Springwell S.st	Darney S.st
Depth of Cut	(mm)	8	7
Water jet pressure	(MPa)	44.83	27.58
Nozzle diameter	(mm)	0.85	0.85
Stand-off distance	(mm)	45	45
Lead-on distance	(mm)	2	5
Side-off distance	(mm)	0	0
Traverse speed	(mm/sec)	61,100,120,167,216	56, 121, 145, 168, 189, 205.

The water jet pressure for each rock was chosen such that at the slowest speed it penetrated the surface to a depth approximately equal to that of the mechanical cutter. The reasoning behind this was that because the influence of the water jet is measured in terms of its penetration depth, increasing traverse speeds will cause the jet to penetrate less each time.

Each cutting test was repeated four times and the order at which they were carried was out randomised to counteract the influence of any change in rock properties.

Overall, 5 x 4 = 20 cutting tests were performed on the Springwell sandstone and 6 x 4 = 24 cutting tests on the Darney sandstone.

Computer curve-fit analysis was carried out on the experimental results and the best-fit functions chosen for parameters together with correlation coefficients are listed in (Appendix C).

7.2.1 The Effect of Traverse Speed

On Water jet Penetration Depth

The graphs of water jet penetration depth against the traverse speed were drawn, (Figures 7.8,7.9). For both rock types, increase in the traverse speed led to a decrease in penetration depth. The rate of decrease however was not uniform. The curves showed a tendency to level off after certain traverse speeds. The relationship between the variables was of inverse power type. Power values were: -0.495 for Springwell and -0.453 for Darney sandstones.

The hydraulic specific energy versus traverse speed graphs showed that the faster the traverse speed was more efficient the cutting became. After 144 mm/sec speed, hydraulic specific energy curve started to level off (Fig 7.8,7.9). These findings support the conclusions of Summers (145) and Page (112) that most of the water jet penetration does occur in extremely short times (e.g. 10 ms).

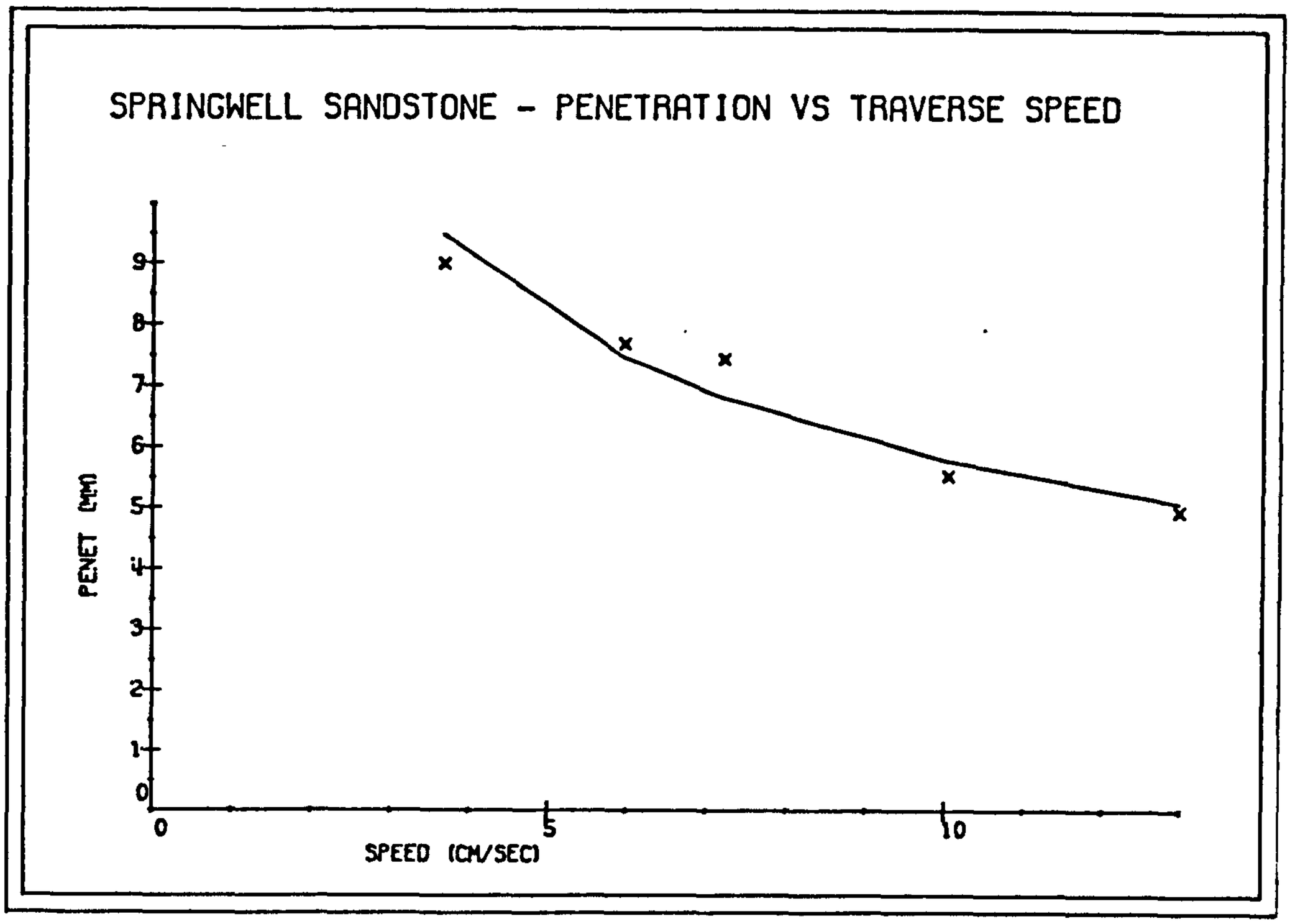
SPRINGWELL SANDSTONE - PENETRATION VS TRAVERSE SPEED
PENET (MM)
9
8
7
6
5
4
3
2
1
0
0
5
10
SPEED (CM/SEC)

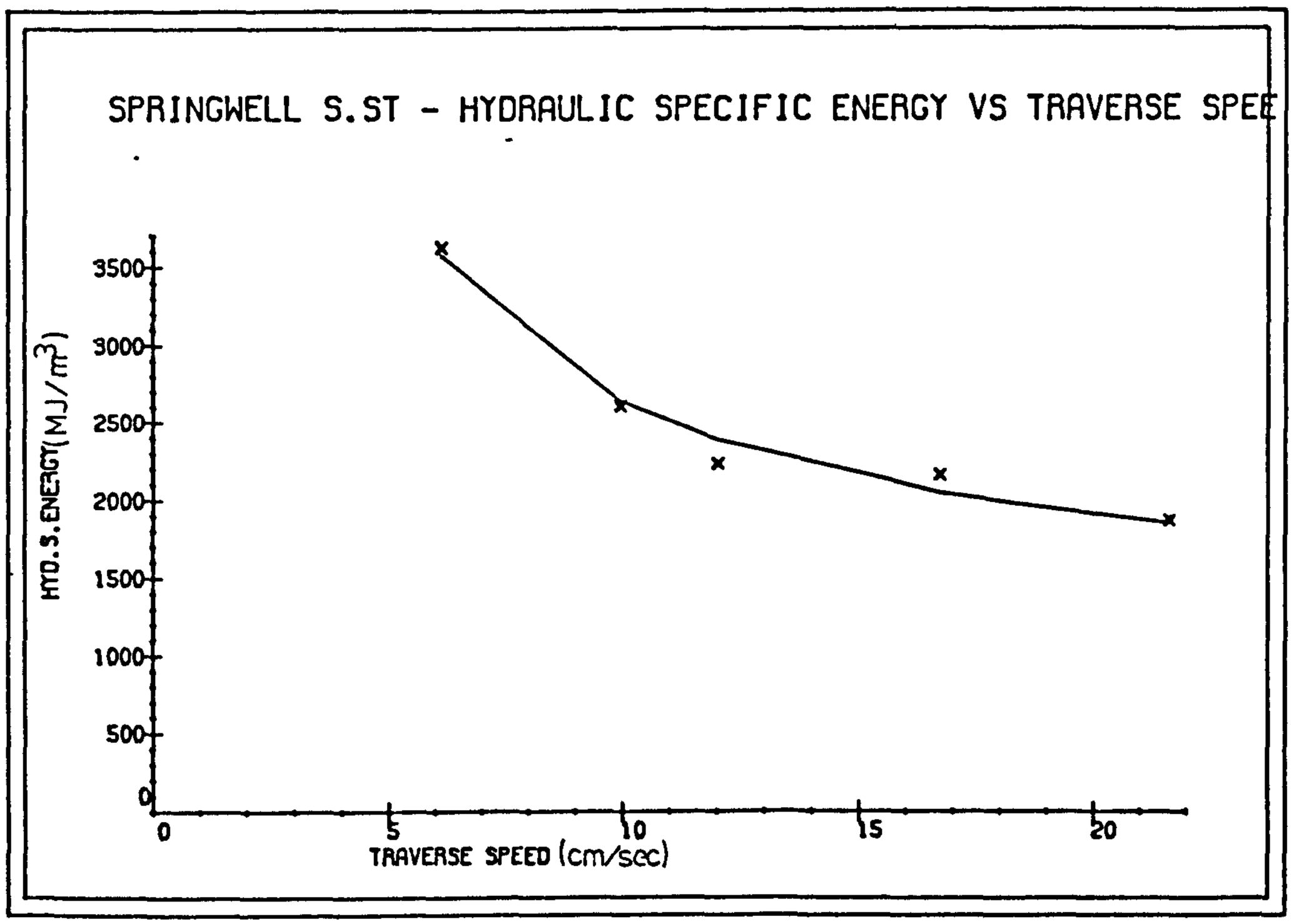
SPRINGWELL S.ST - HYDRAULIC SPECIFIC ENERGY VS TRAVERSE SPEE
HYD.S.ENERGY(MJ/m3)
3500
3000
2500
2000
1500
1000
500
0
0
5
10
15
20
TRAVERSE SPEED (cm/sec)

FIG. 7.8

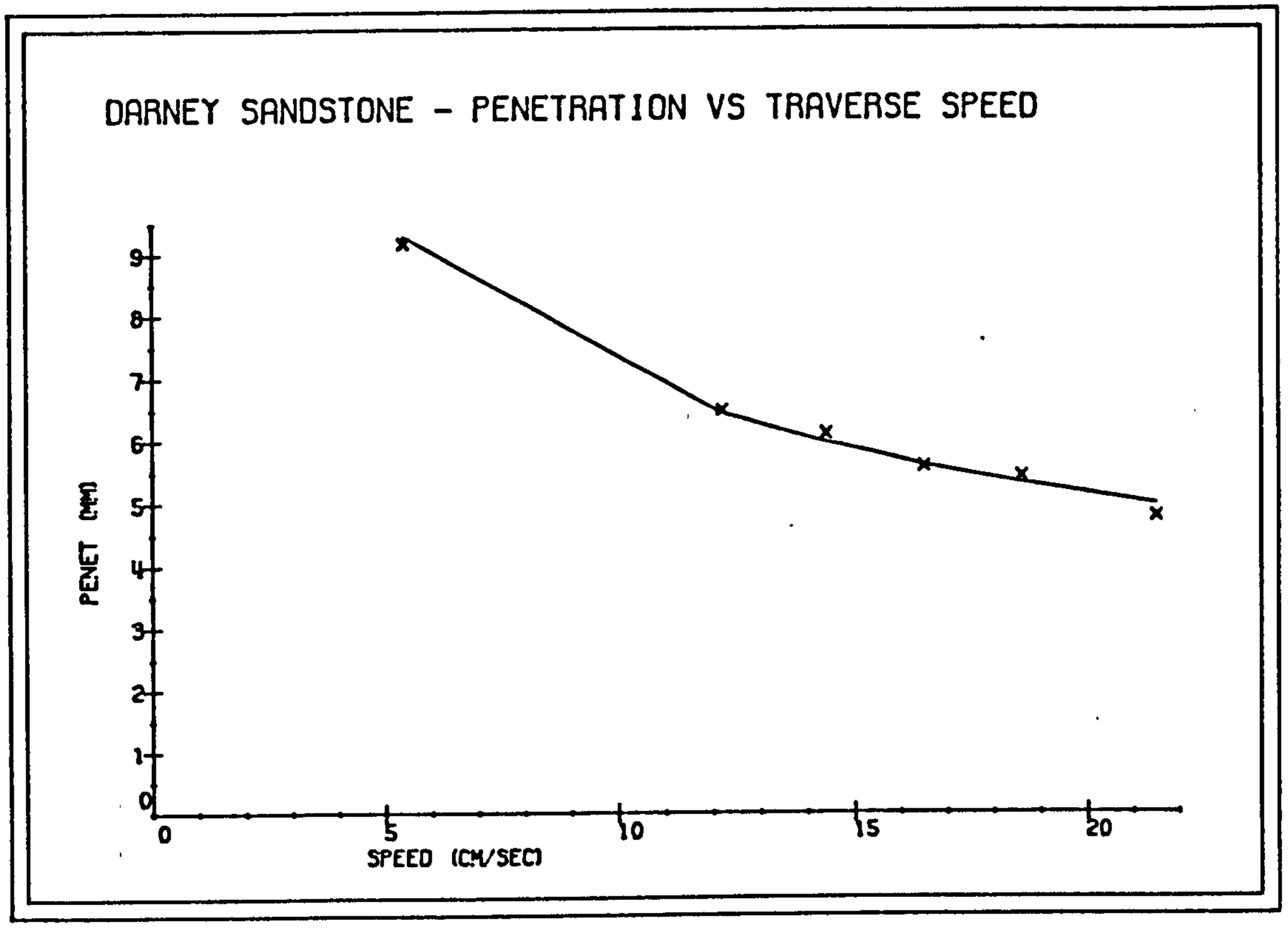
DARNEY SANDSTONE - PENETRATION VS TRAVERSE SPEED
PENET (MM)
0
1
2
3
4
5
6
7
8
9
0
5
10
15
20
SPEED (CM/SEC)

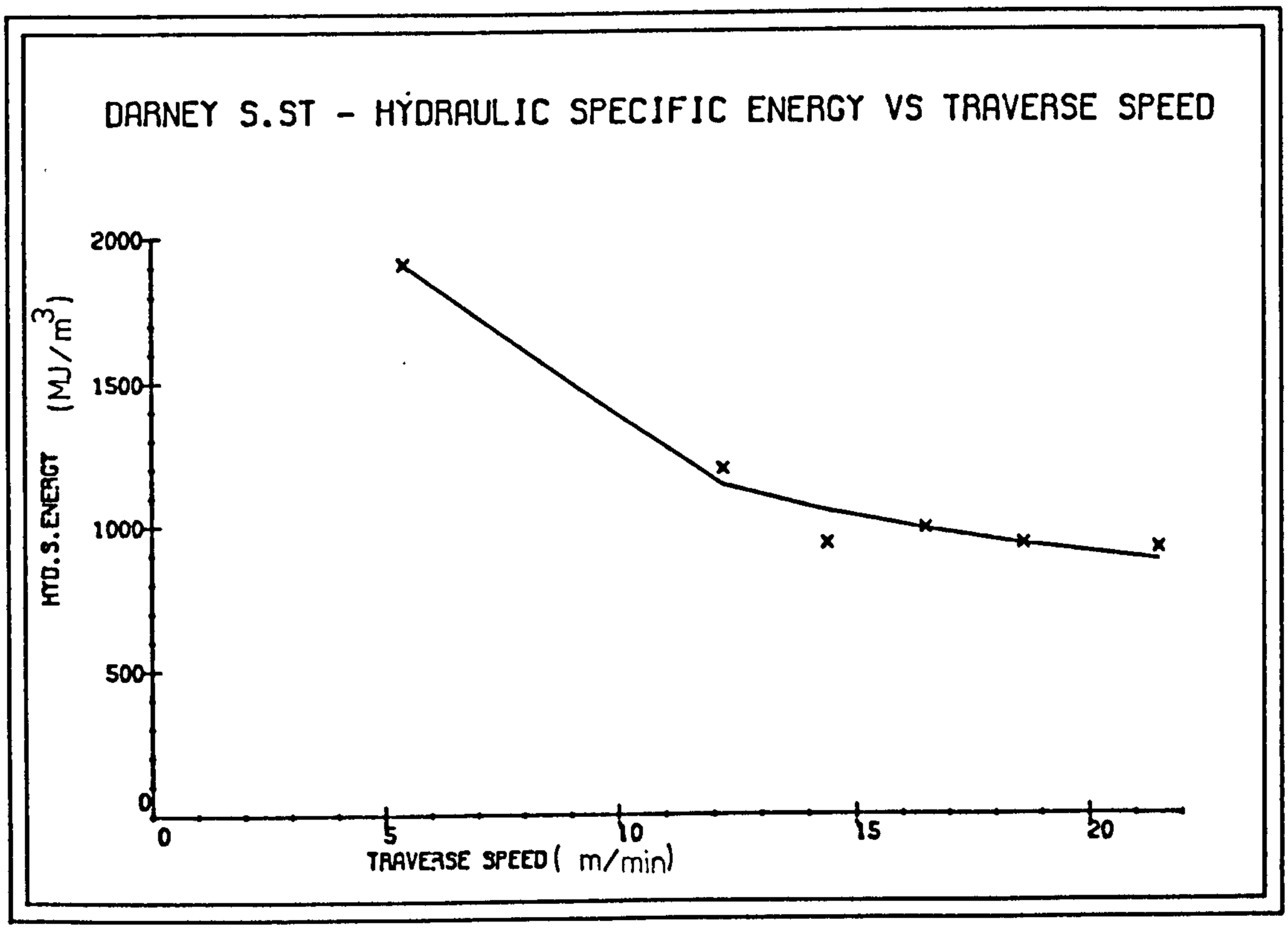
DARNEY S.ST - HYDRAULIC SPECIFIC ENERGY VS TRAVERSE SPEED
HYD.S.ENERGY (MJ/m3)
0
500
1000
1500
2000
0
5
10
15
20
TRAVERSE SPEED (m/min)

FIG. 7.9

On the Tool Forces

Cutting and Normal forces have increased at a decreasing rate with increase in traverse speed (Figures 7.10-7.15). The slopes of the curves suggest that at high speeds they may reach a constant value and run parallel to the x-axis.

On Yield

Traverse speed increase have caused a corresponding decrease in rock yield (Figures 7.16,7.17), but the decrease soon levelled off after 150 mm/sec. The Nature of the relationship between the variables was of hyperbolic form.

On Mechanical Specific Energy

Mechanical Specific Energy has exhibited a hyperbolic relationship, increasing at a decreasing rate, with increase in traverse speed, (Figures 7.16,7.17). It is evident from the graphs that, results are more sensitive to change at slow traverse speeds, especially between 50 mm/sec and 100 mm/sec.

Whilst the Hydraulic Specific Energy was decreased with increase in cutting speed, Mechanical Specific Energy has increased.

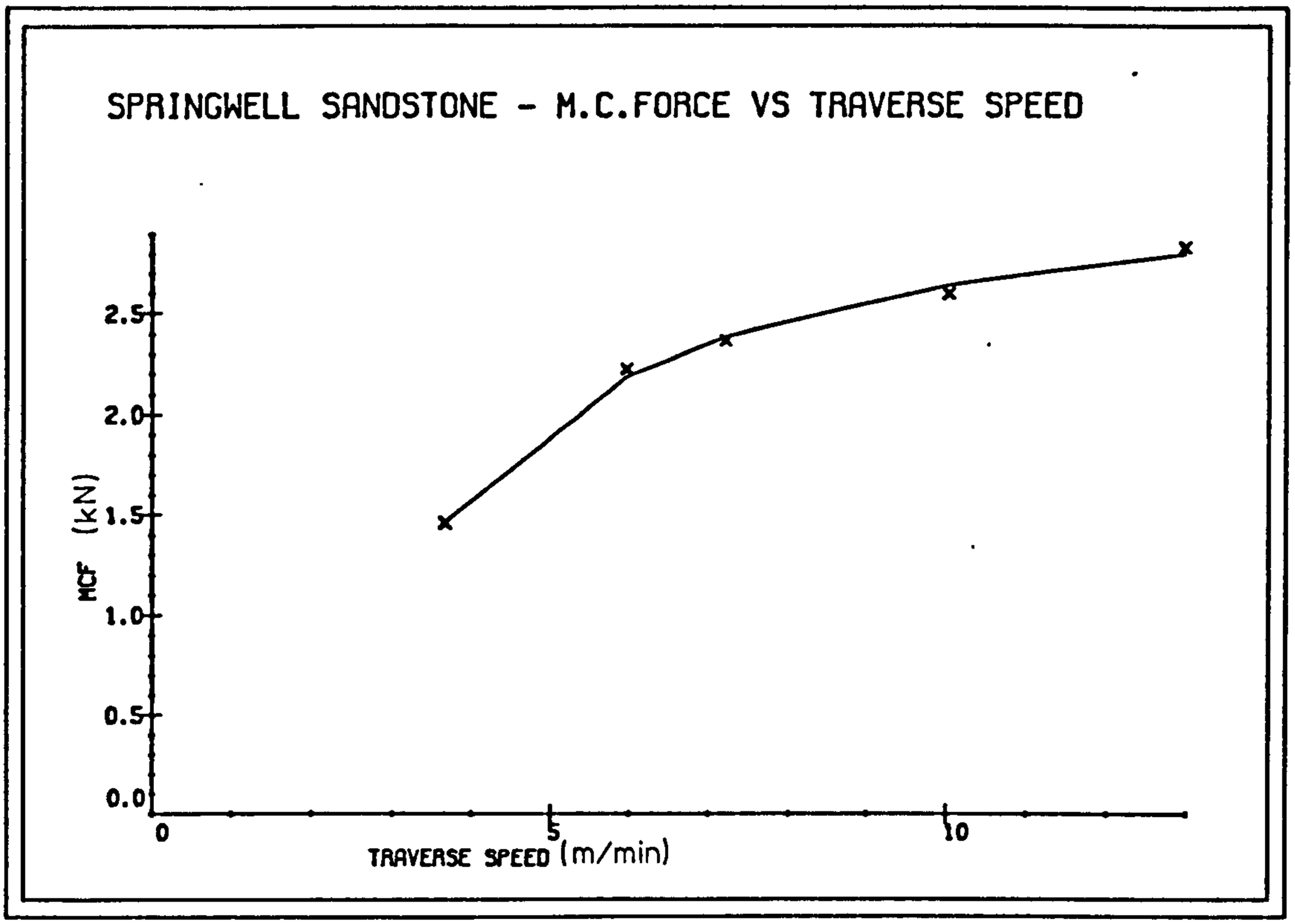
SPRINGWELL SANDSTONE - M.C.FORCE VS TRAVERSE SPEED
MCF (kN)
2.5
2.0
1.5
1.0
0.5
0.0
0
5
10
TRAVERSE SPEED (m/min)

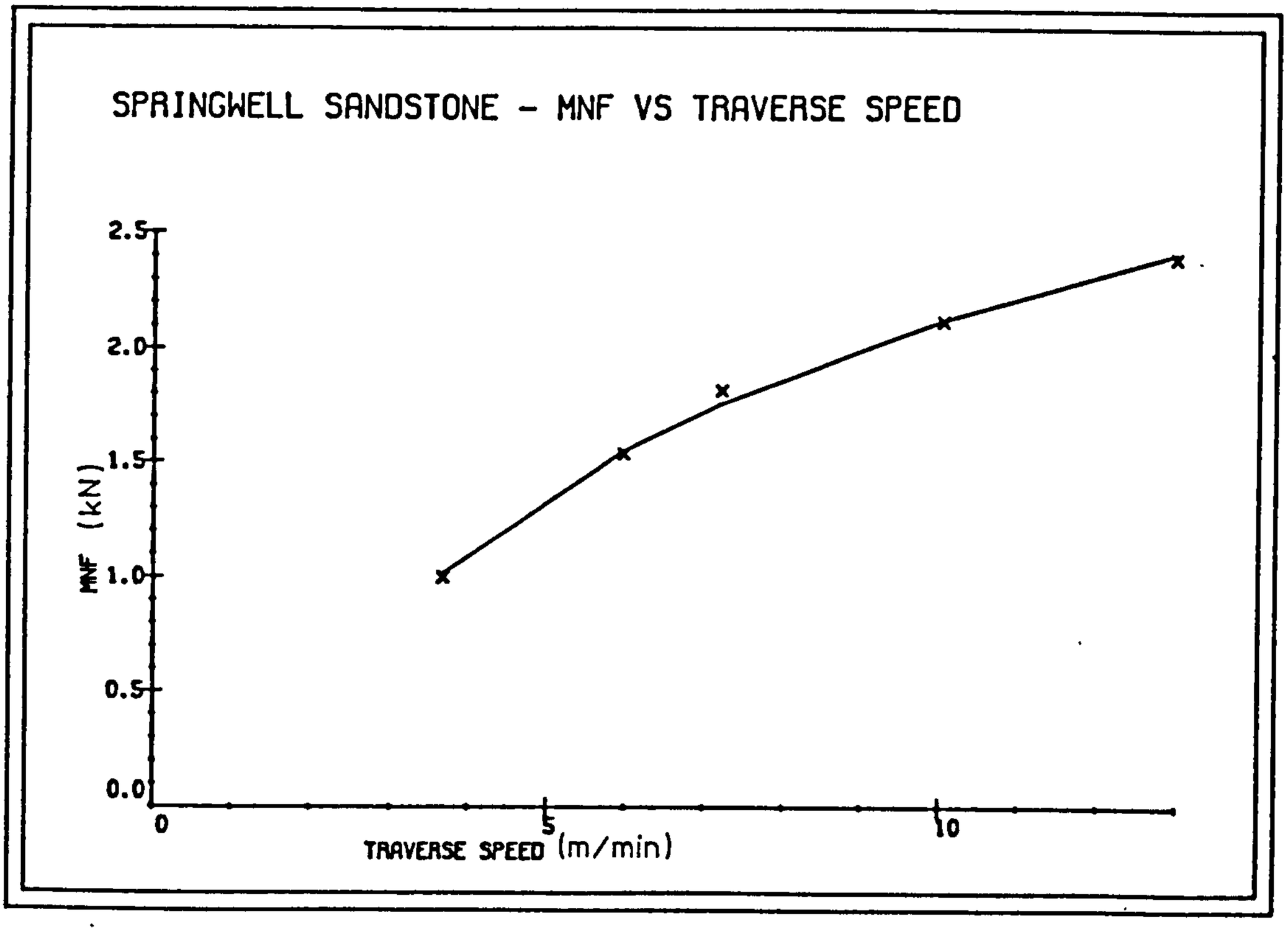
SPRINGWELL SANDSTONE - MNF VS TRAVERSE SPEED
MNF (kN)
2.5
2.0
1.5
1.0
0.5
0.0
0
5
10
TRAVERSE SPEED (m/min)

FIG. 7.10

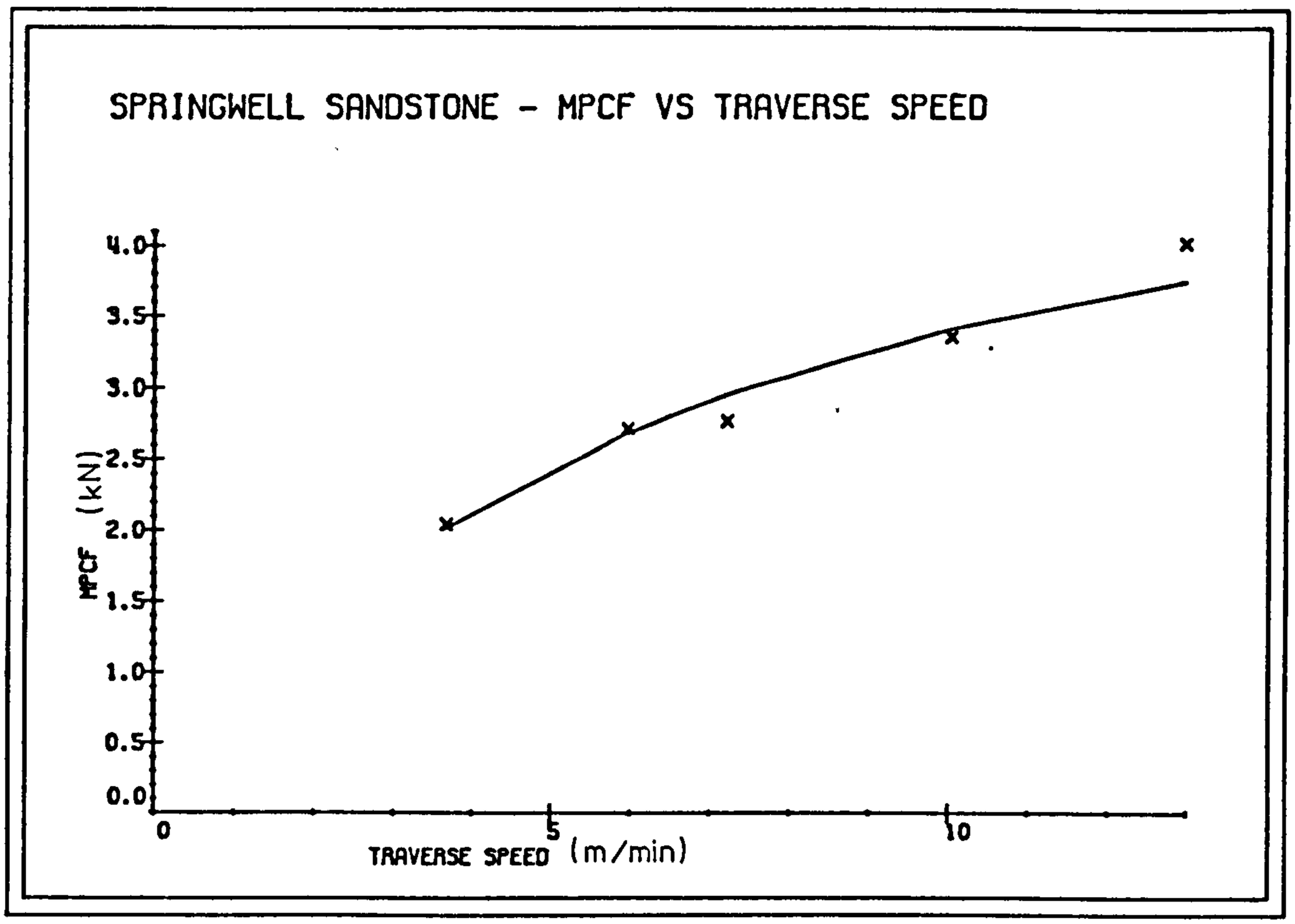
SPRINGWELL SANDSTONE - MPCF VS TRAVERSE SPEED
4.0
3.5
3.0
2.5
2.0
1.5
1.0
0.5
0.0
MPCF (kN)
0
5
10
TRAVERSE SPEED (m/min)

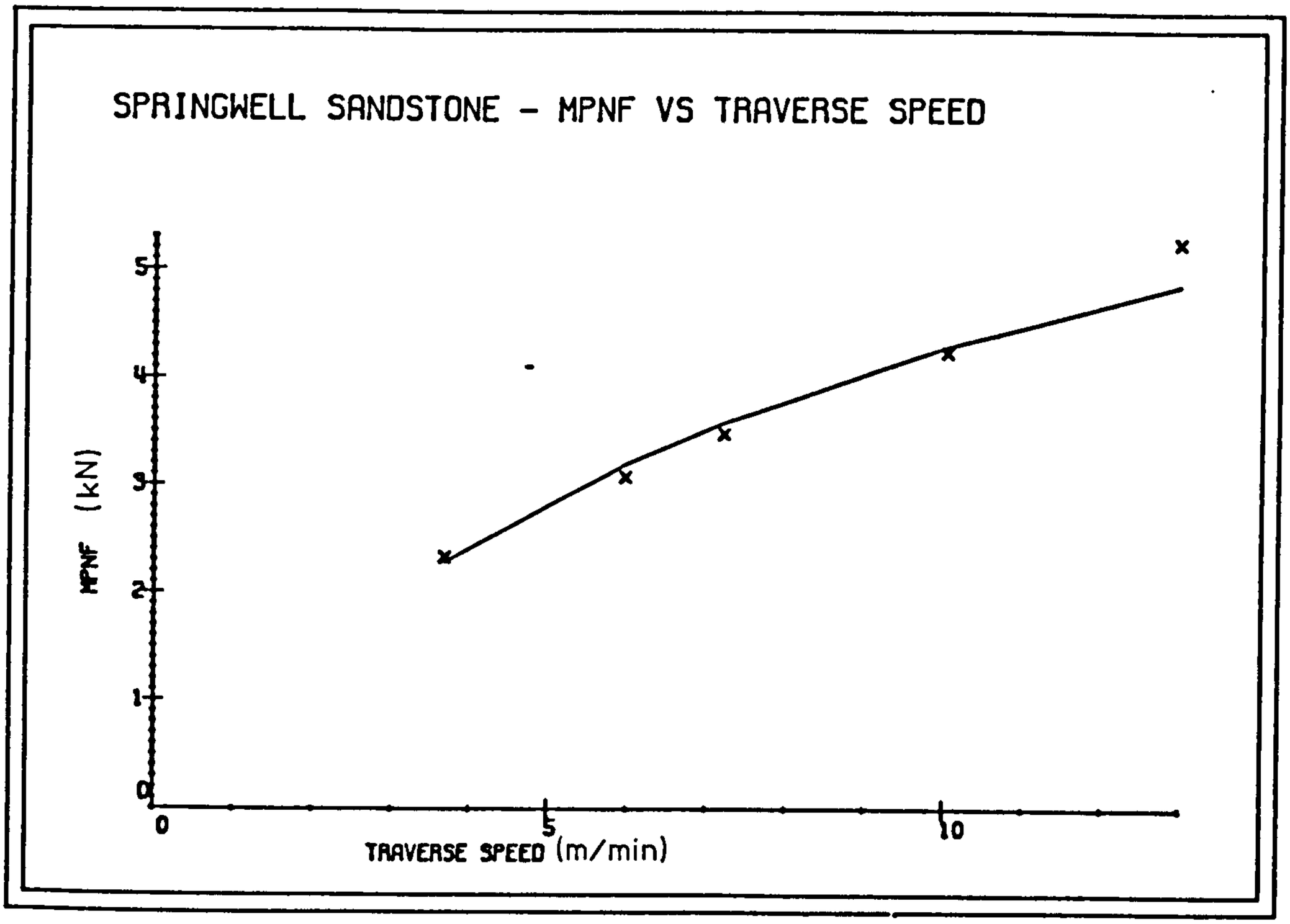
SPRINGWELL SANDSTONE - MPNF VS TRAVERSE SPEED
5
4
3
2
1
0
MPNF (kN)
0
5
10
TRAVERSE SPEED (m/min)

FIG. 7.11

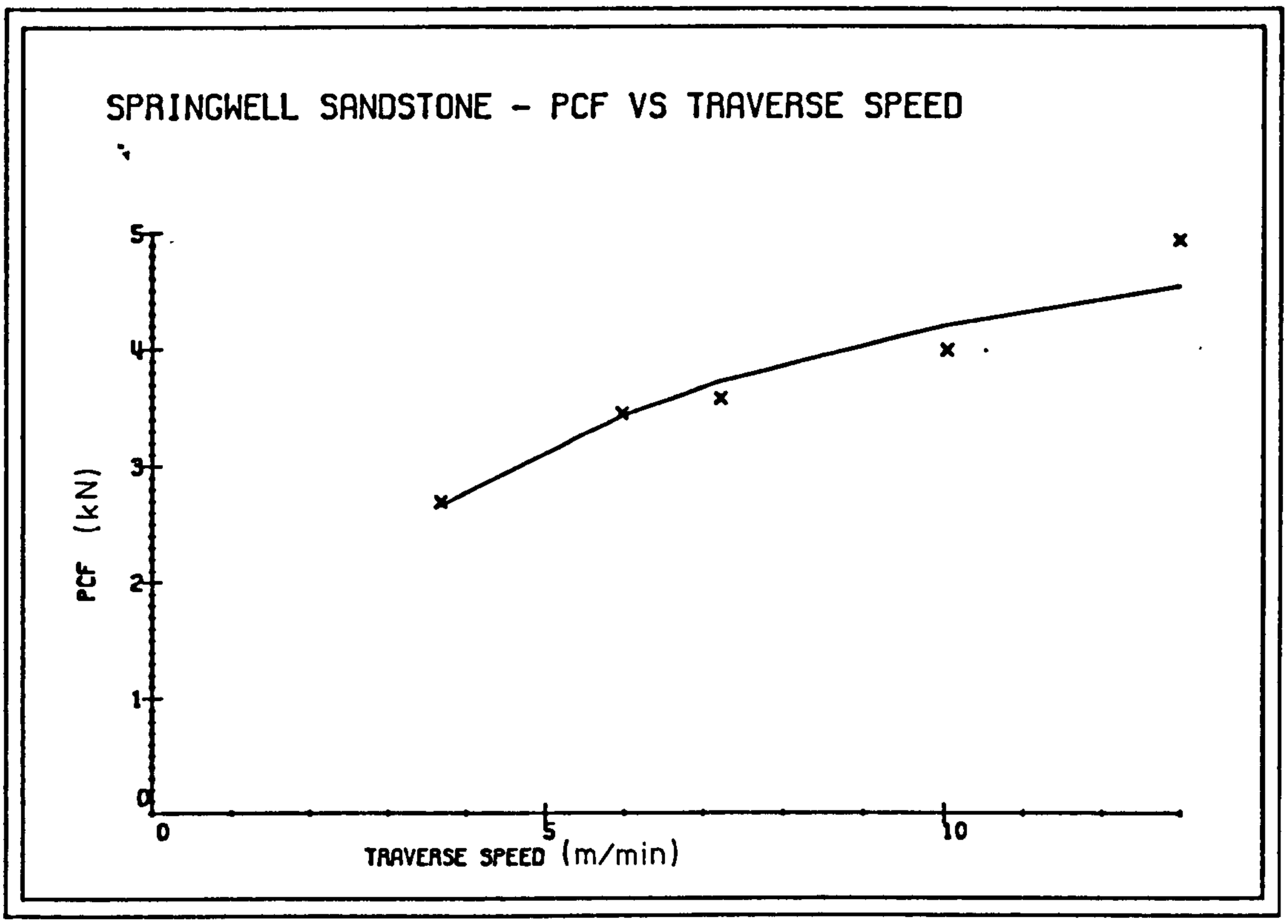
SPRINGWELL SANDSTONE - PCF VS TRAVERSE SPEED
PCF (kN)
0
1
2
3
4
5
0
5
10
TRAVERSE SPEED (m/min)

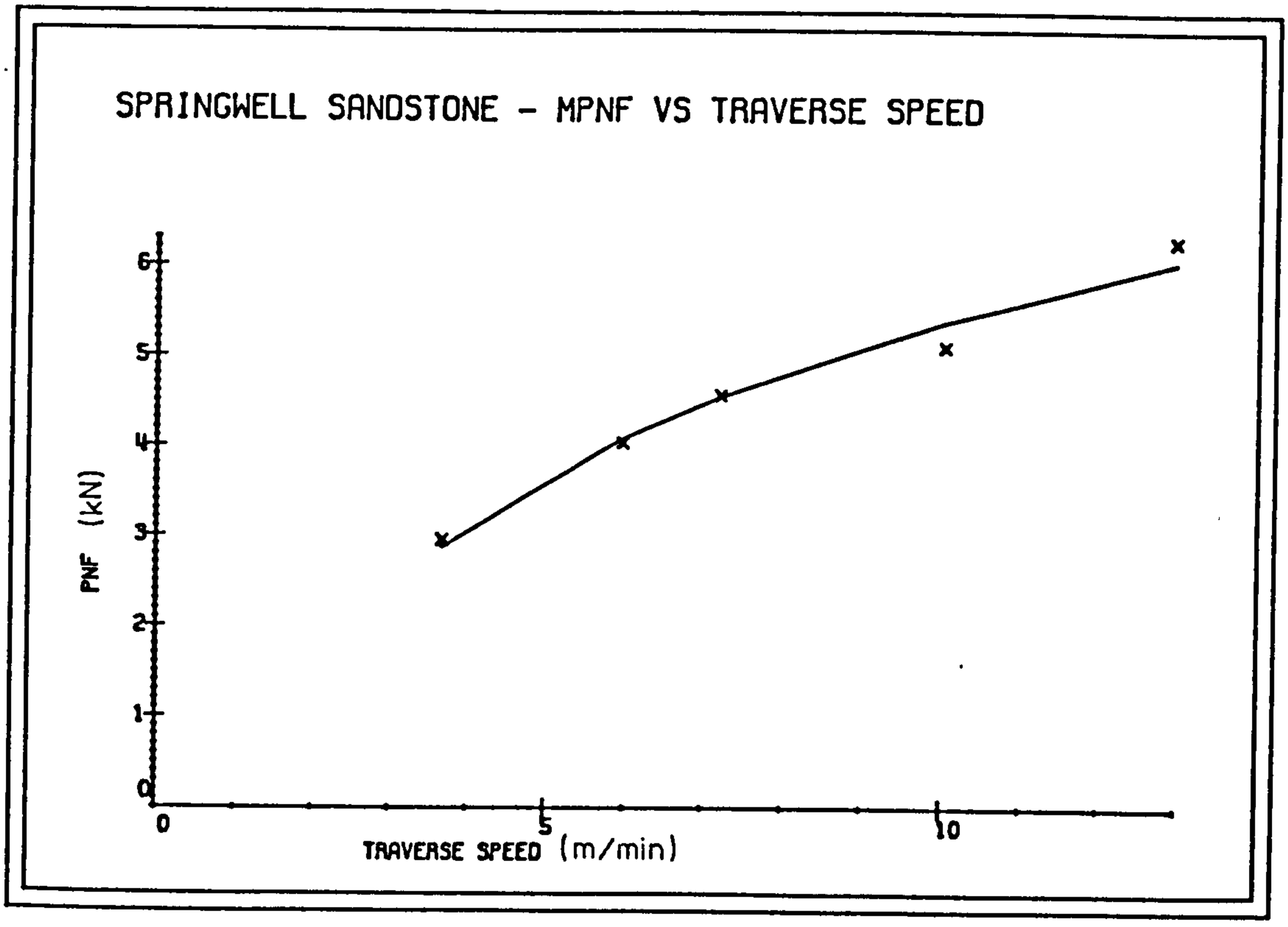
SPRINGWELL SANDSTONE - MPNF VS TRAVERSE SPEED
PNF (kN)
0
1
2
3
4
5
6
0
5
10
TRAVERSE SPEED (m/min)

FIG. 7.12

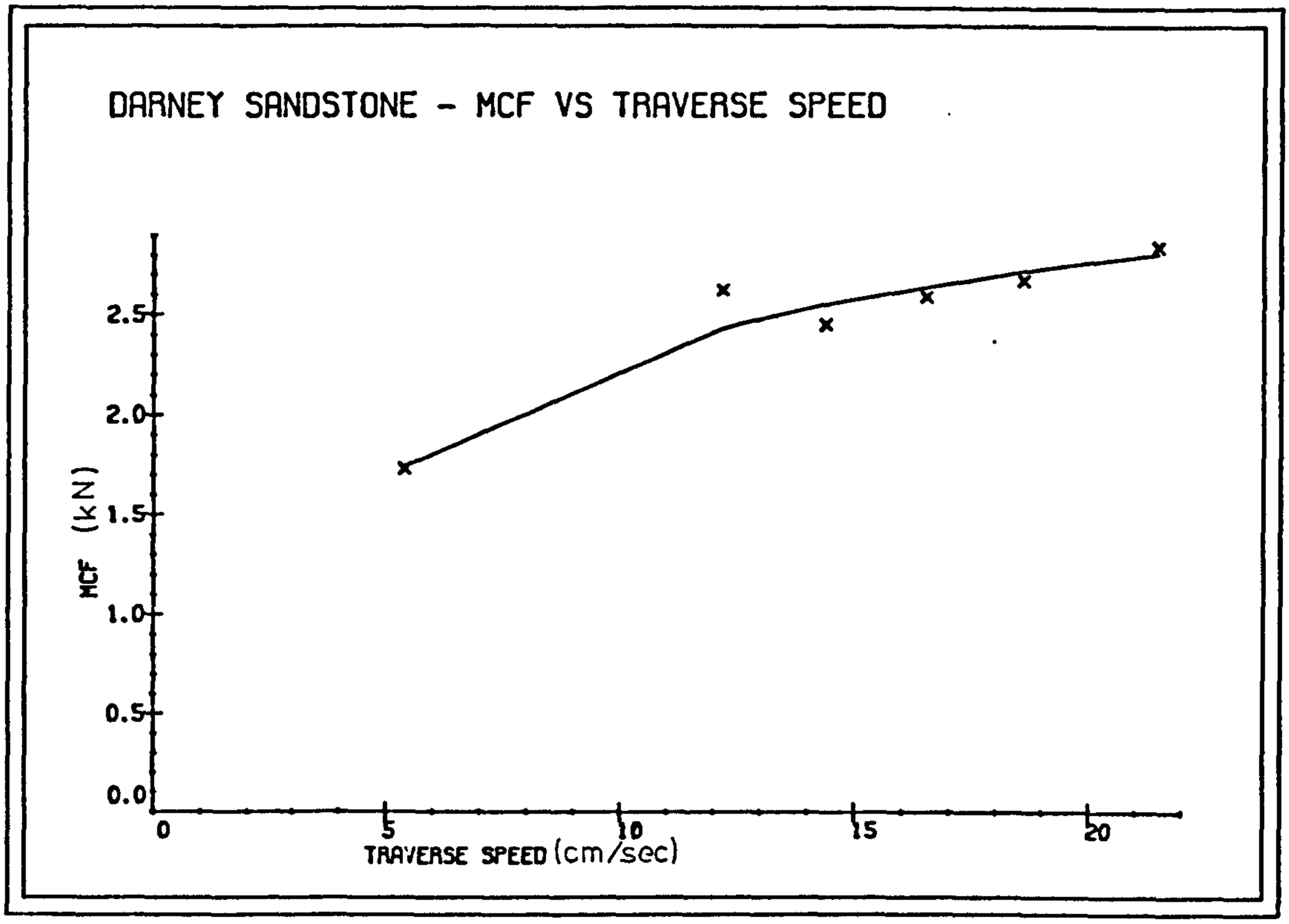
DARNEY SANDSTONE - MCF VS TRAVERSE SPEED
MCF (kN)
2.5
2.0
1.5
1.0
0.5
0.0
0
5
10
15
20
TRAVERSE SPEED (cm/sec)

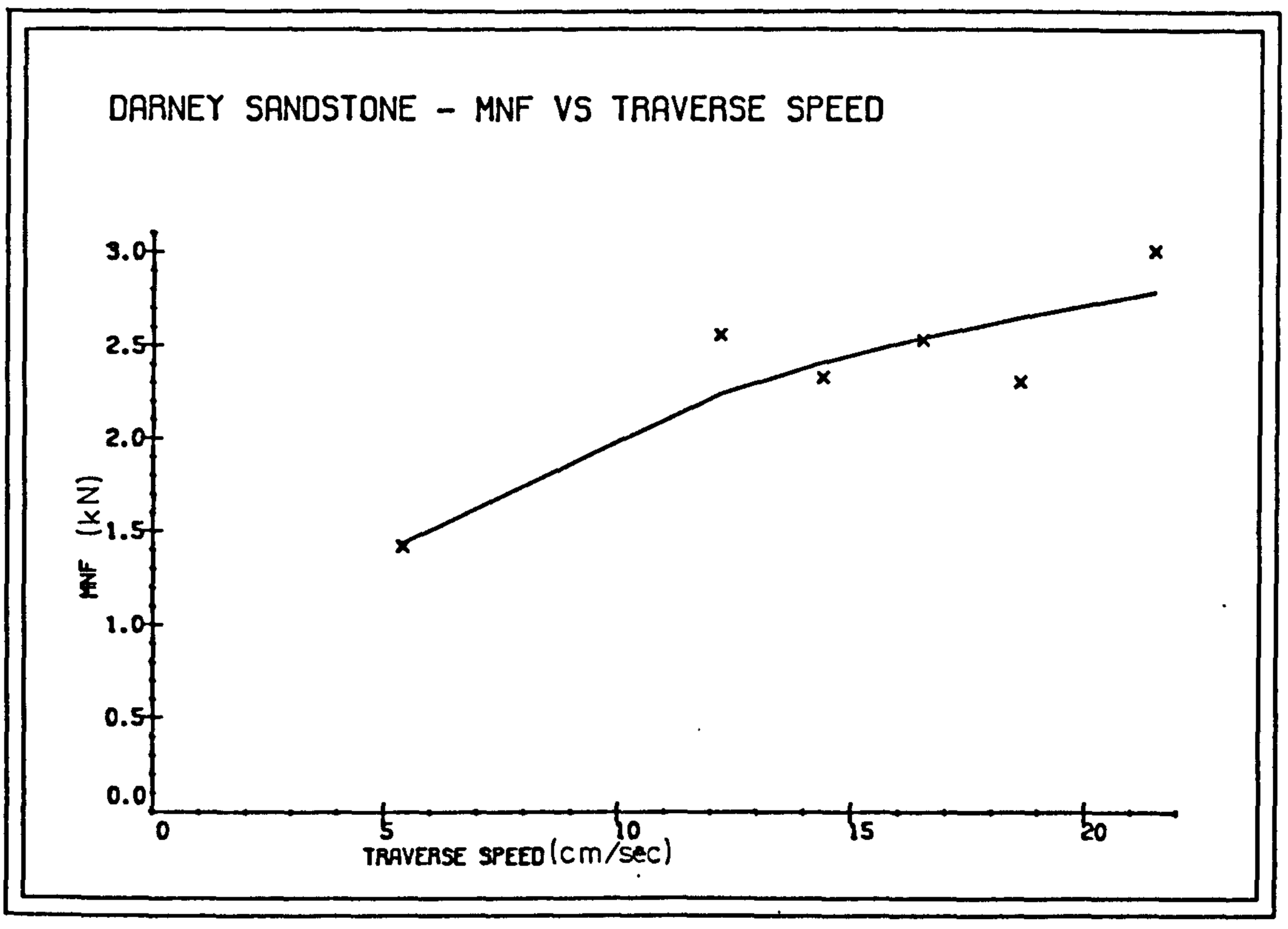
DARNEY SANDSTONE - MNF VS TRAVERSE SPEED
MNF (kN)
3.0
2.5
2.0
1.5
1.0
0.5
0.0
0
5
10
15
20
TRAVERSE SPEED (cm/sec)

FIG. 7.13

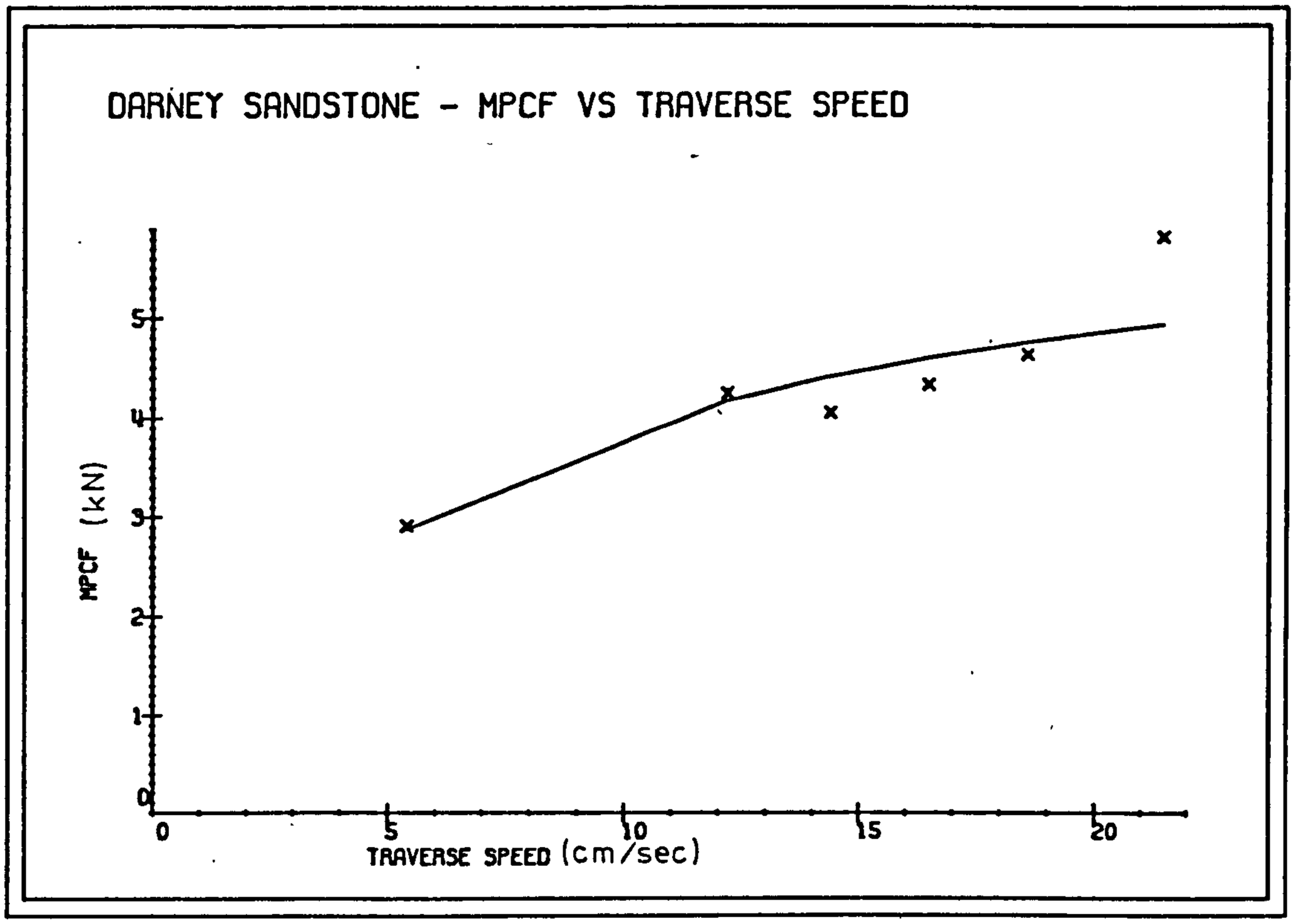
DARNEY SANDSTONE - MPCF VS TRAVERSE SPEED
MPCF (kN)
0
1
2
3
4
5
0
5
10
15
20
TRAVERSE SPEED (cm/sec)

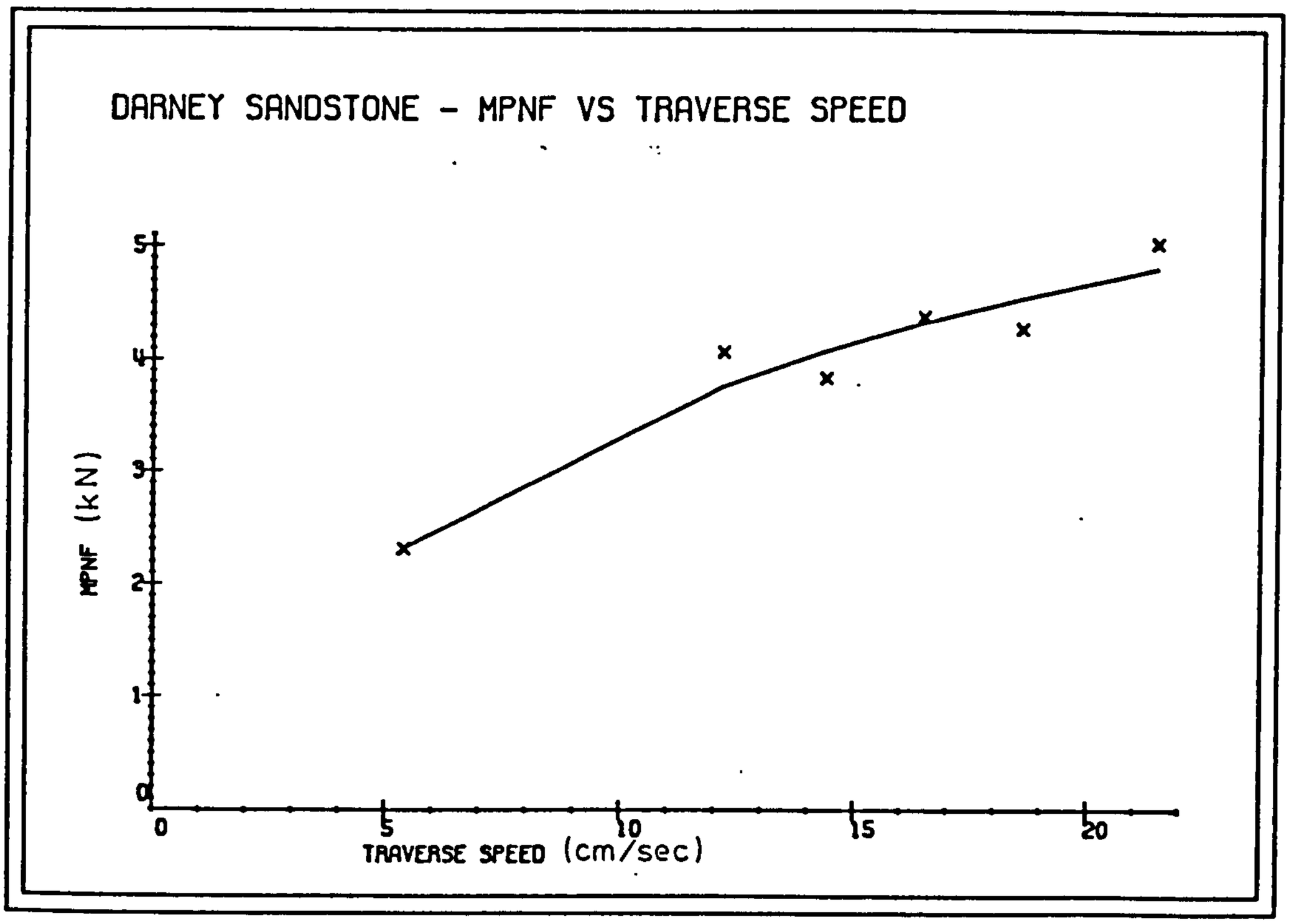
DARNEY SANDSTONE - MPNF VS TRAVERSE SPEED
MPNF (kN)
0
1
2
3
4
5
0
5
10
15
20
TRAVERSE SPEED (cm/sec)

FIG. 7.14

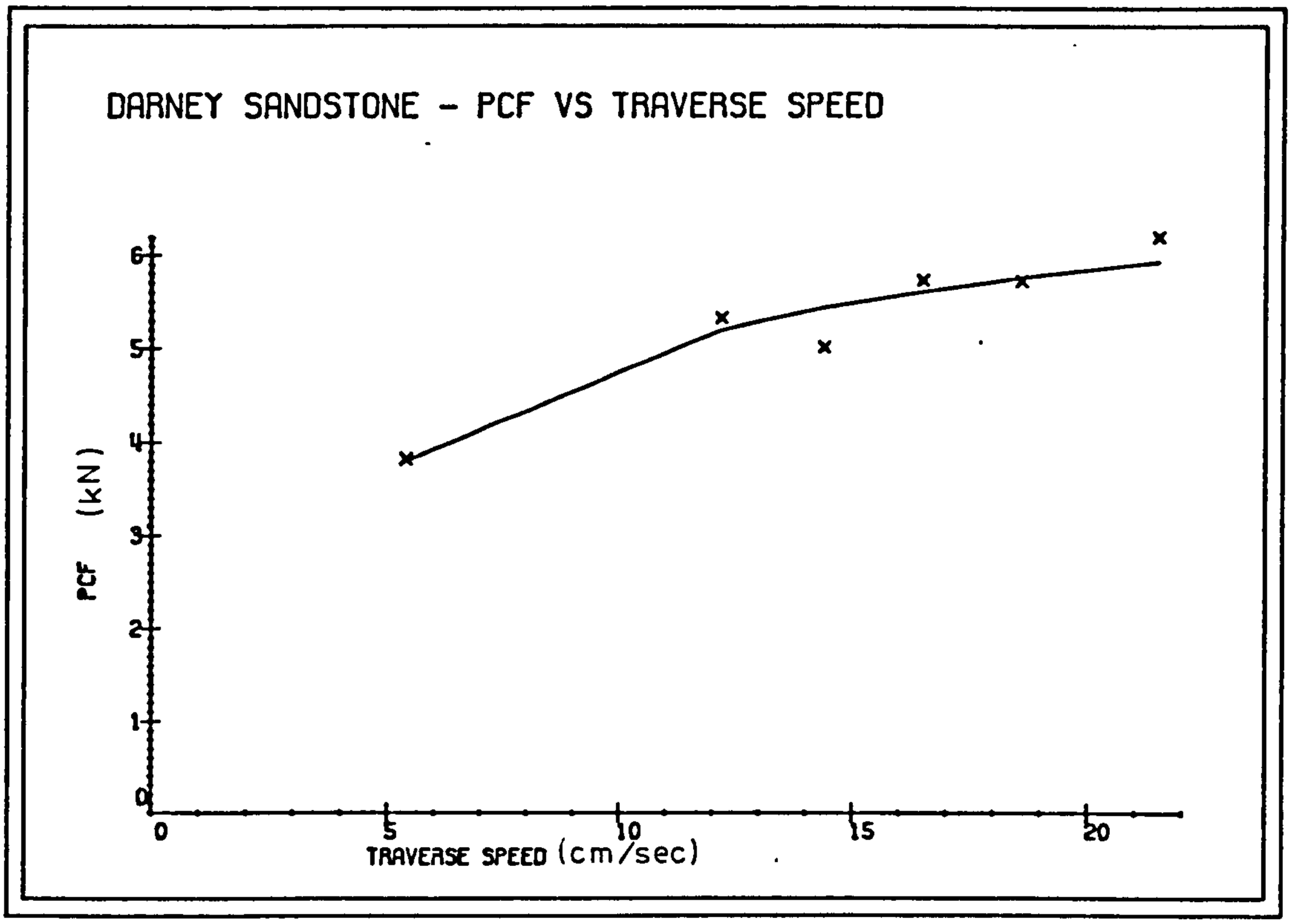
DARNEY SANDSTONE - PCF VS TRAVERSE SPEED
PCF (kN)
0
1
2
3
4
5
6
0
5
10
15
20
TRAVERSE SPEED (cm/sec)

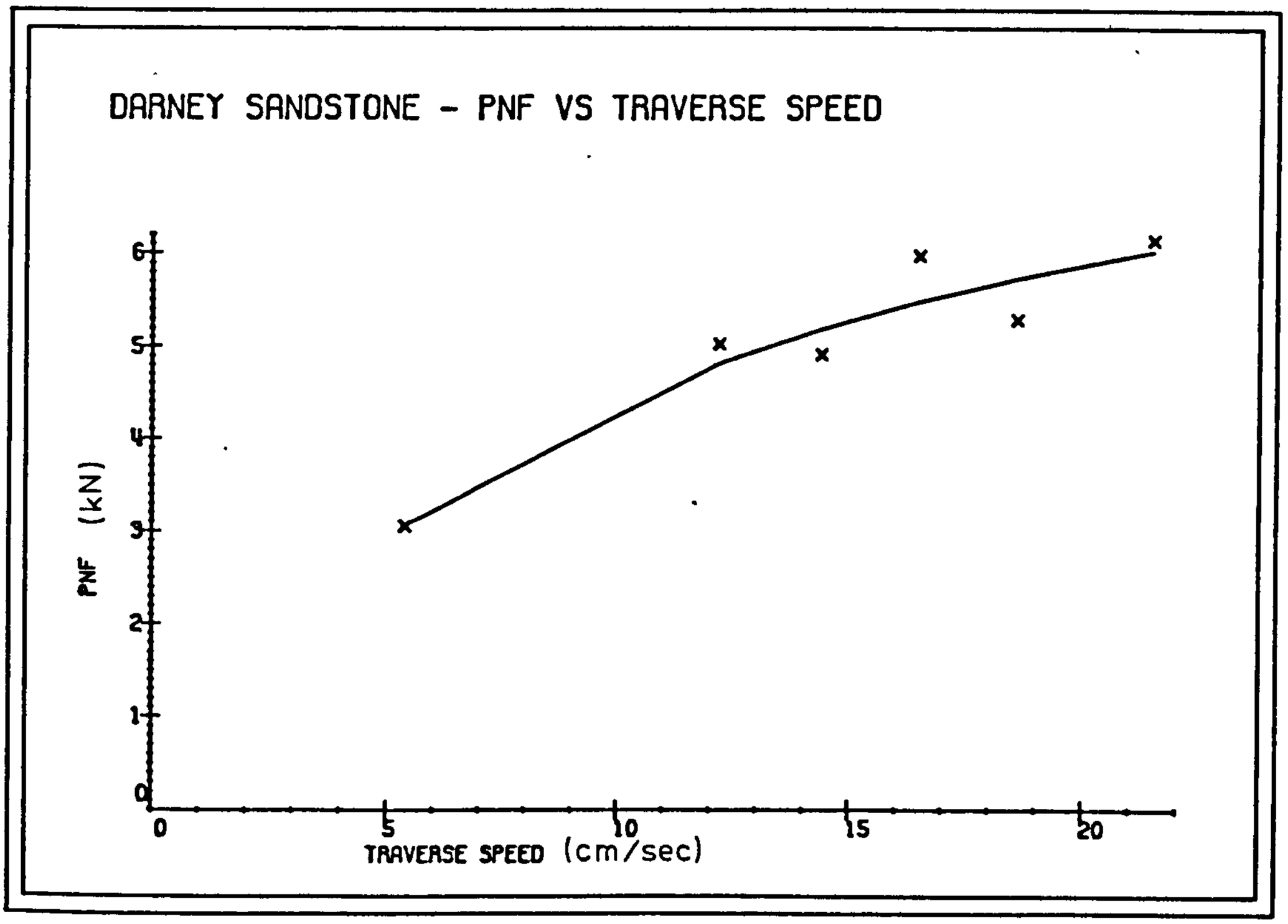
DARNEY SANDSTONE - PNF VS TRAVERSE SPEED
PNF (kN)
0
1
2
3
4
5
6
0
5
10
15
20
TRAVERSE SPEED (cm/sec)

FIG. 7.15

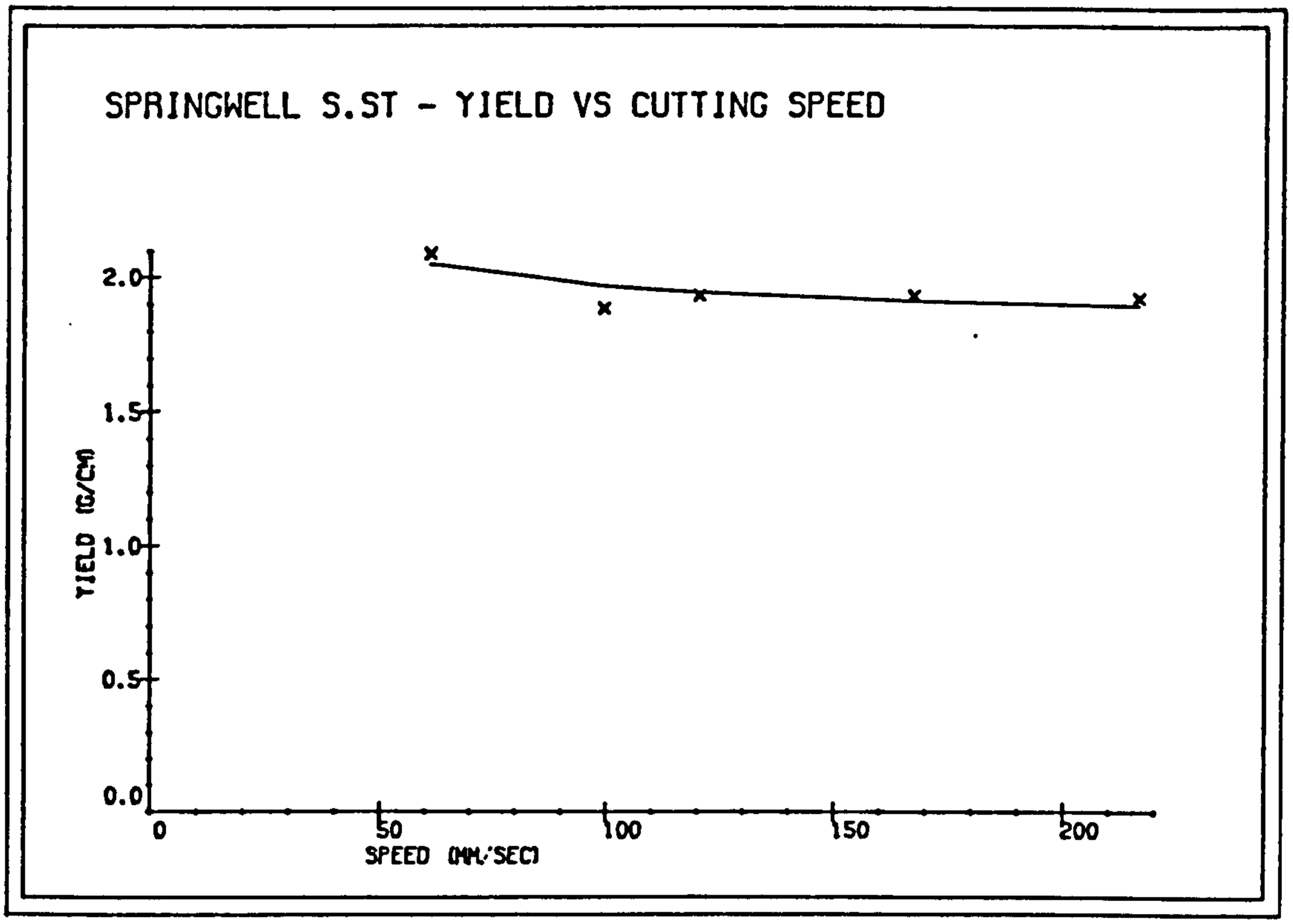
SPRINGWELL S.ST - YIELD VS CUTTING SPEED
2.0
1.5
1.0
0.5
0.0
YIELD (G/CM)
0
50
100
150
200
SPEED (MM/SEC)

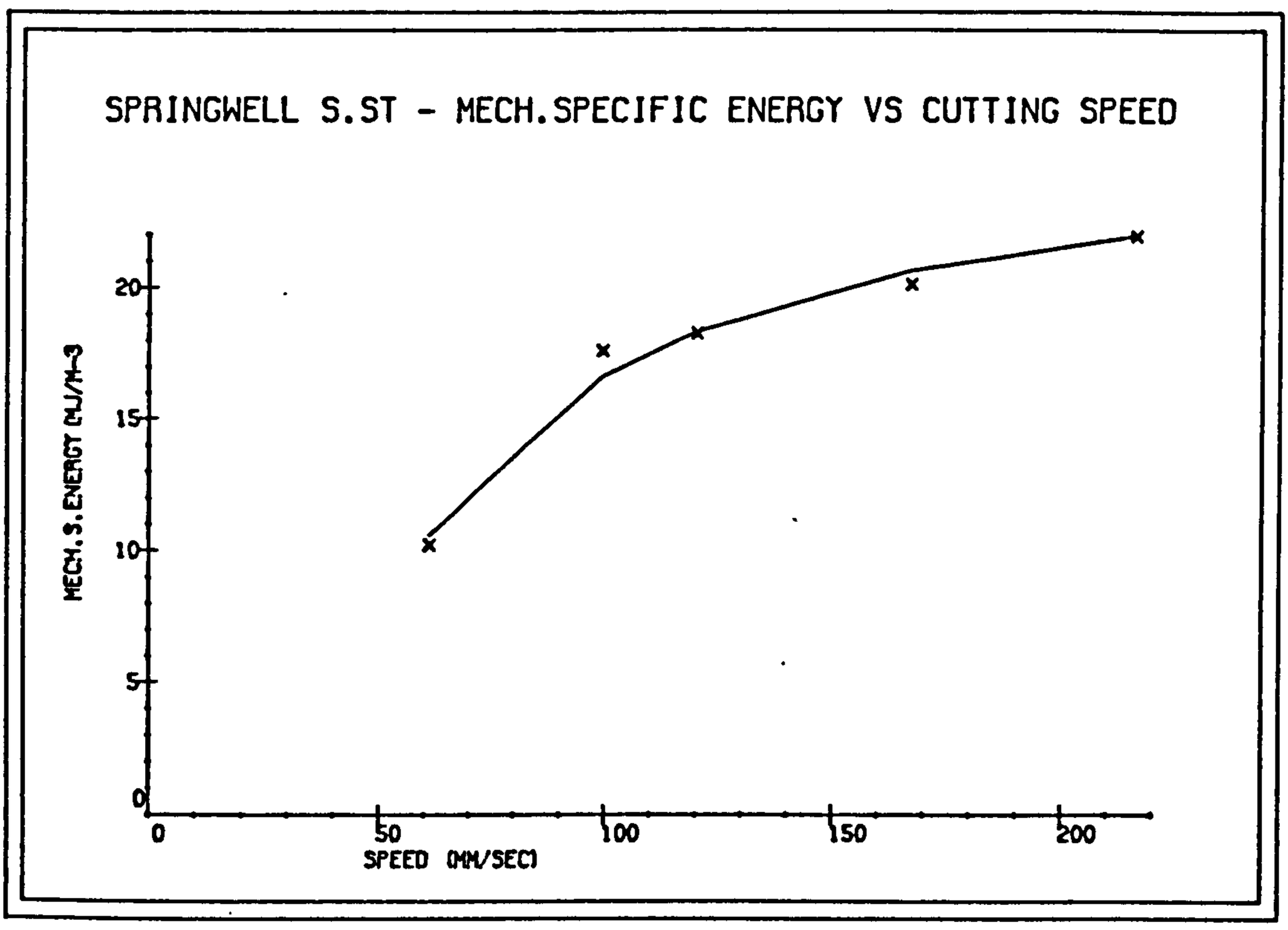
SPRINGWELL S.ST - MECH.SPECIFIC ENERGY VS CUTTING SPEED
20
15
10
5
0
MECH.S.ENERGY (MJ/M-3
0
50
100
150
200
SPEED (MM/SEC)

FIG. 7.16

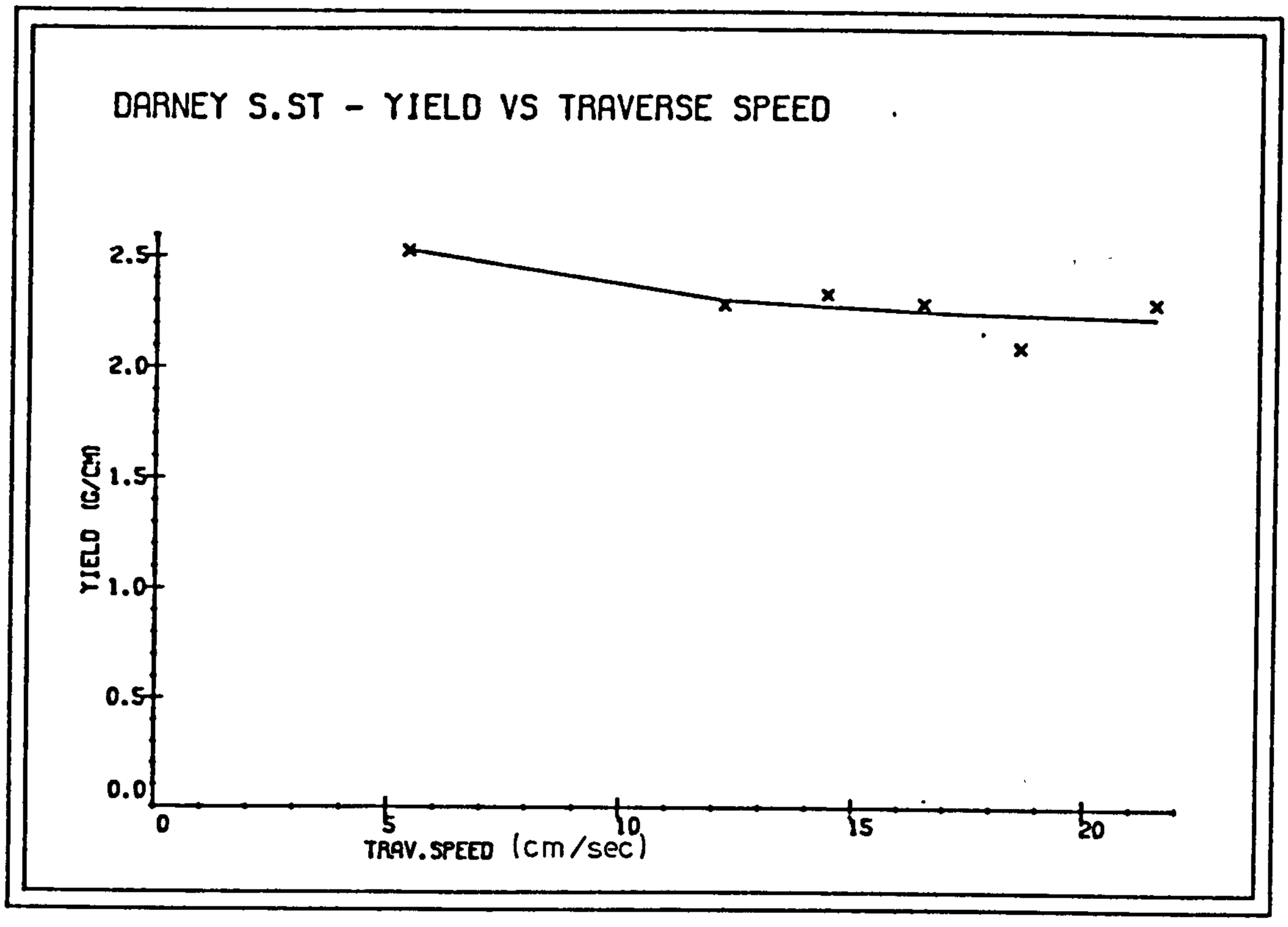
DARNEY S.ST - YIELD VS TRAVERSE SPEED
2.5
2.0
1.5
1.0
0.5
0.0
YIELD (G/CM)
0
5
10
15
20
TRAV.SPEED (cm/sec)

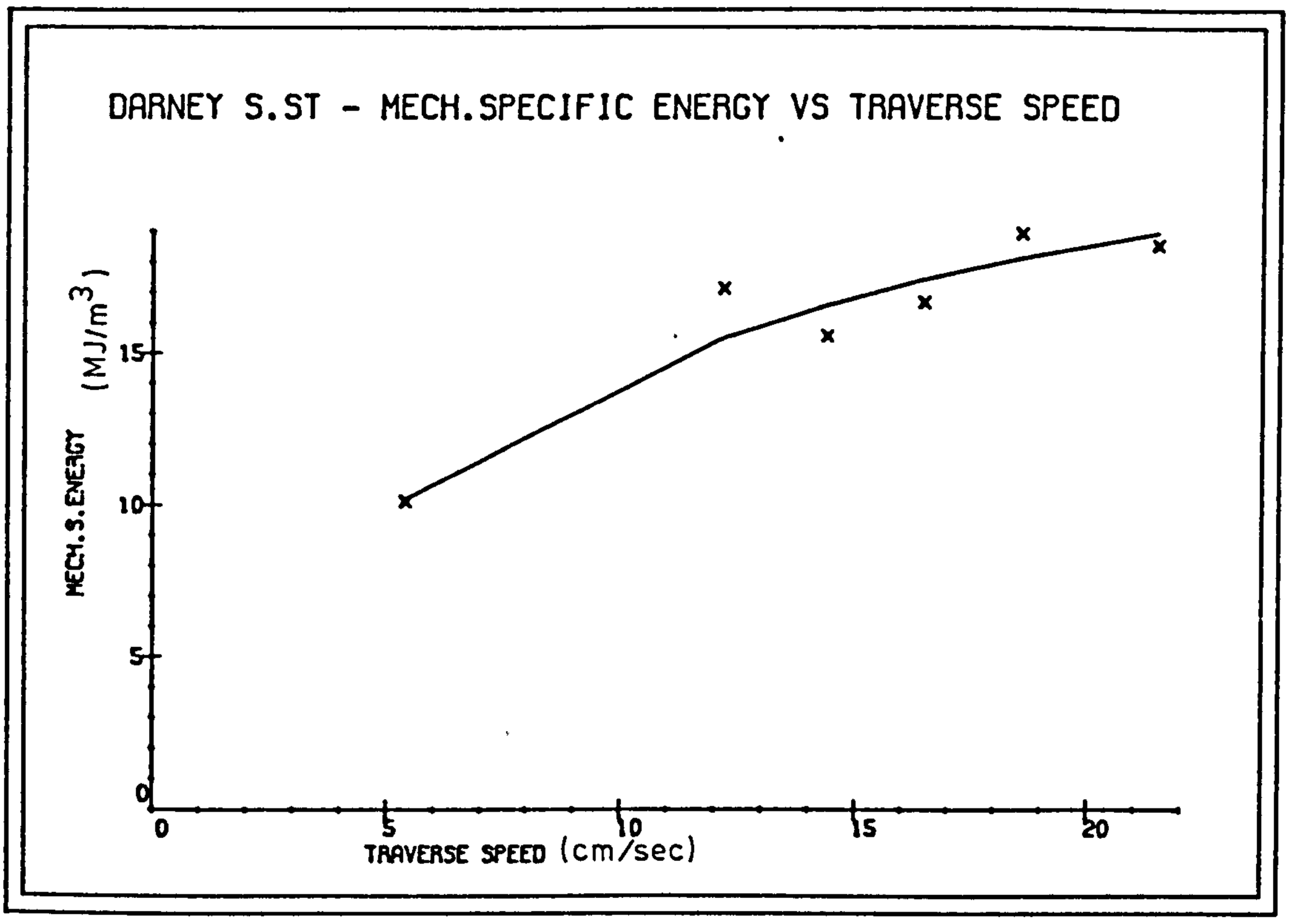
DARNEY S.ST - MECH.SPECIFIC ENERGY VS TRAVERSE SPEED
MECH.S.ENERGY (MJ/m3)
15
10
5
0
0
5
10
15
20
TRAVERSE SPEED (cm/sec)

FIG. 7.17

7.2.2 Discussion

The influence of cutting speed has to be examined separately on the mechanical and hydraulic components of the hybrid cutting system.

Mechanical Component: Effect of speed becomes more apparent with the increase in length of cut and the condition of the tool determines the degree of influence of cutting speed. At the beginning, when the distance cut is comparably small, the cutting tools are in sharp condition and tool forces and mechanical specific energy are not significantly effected by the variations in cutting speed. As the distance cut increases, due to accummulation of heat and rise of temperature at tool/rock interface, wear of the cutting tools progresses . Once a critical speed is reached, depending on the critical temperature of hardmetal, wear increases dramatically. Altinoluk(8) has found that factors such as the shape of the tool, properties of rock and cutting conditions also modify the temperature attained by a worn tool. The hardness of tungsten carbide decreases considerably and in some instances fall below the hardness of quartz at very high temperatures which lead to wear. The increase in tool wear causes a corresponding increases in tool forces and mechanical specific energy. Therefore, it may be assumed that, in the absence of wear, cutting speed has a negligible influence on the mechanical part of hybrid cutting system.

Hydraulic Component : The effect of time on water jet penetration depth is made apparent by the change in cutting speed.

There is a limit to the amount of penetration depth that can be attained by a slow traversing jet. At the slowest traverse speed -when the exposure time over a point on the rock is in excess of a minute- no more increase in penetration depth takes place after 30 seconds (142). This is due to the fact that when a certain crater depth is reached any further increase in depth is prevented by the water cushion formed in the crater. Most of the penetration takes place in very short times (1/100th of a second).

The penetration depth varies inversely with the traverse speed at a constant water jet pressure. Although increasing the traverse speed causes a reduction in jet penetration depth, actual area of cut increases.

Between the lowest and maximum ends of the speed spectrum, there is an optimum jet traverse speed -which according to Harris changes with water jet pressure- at which hydraulic specific energy reaches its minimum (most efficient) value. Springwell and Darney sandstone cutting tests have revealed that, within the experimental speed range, penetration depth varied inversely with the traverse speed to a power of -0.495 and -0.453 respectively. Consequently, mechanical cutting and normal tool forces were increased at a decreasing rate with increasing cutting speed. For most efficient cutting therefore, as demonstrated by the experimental results, the water jet pressure should be such that it would penetrate the rock to a depth equal to that of mechanical tools at a given traverse speed.

7.2.3 Conclusions

The longer the target surface is exposed to a high pressure water jet, the deeper will be the its penetration depth, assuming the water jet pressure exceeds the threshold pressure of the rock. The time taken by the water jet to act over the rock surface is incorporated in the traverse speed and this is one of the important parameters used in specific energy calculations.

Springwell and Darney sandstone experimental results have shown that the penetration depth varied inversely with the traverse speed, showing a power relationship. The power values for Springwell sandstone was found to be -0.495 and -0.453 for Darney sandstone. The results had shown more sensitivity to change at slow traverse speeds, especially between 50-100 mm/sec. Cutting and Normal tool forces had increased as a result of a decrease in jet penetration depth. Curves tend to reach a constant value and run parallel to the x-axis with further increases in speed. Mechanical Specific Energy increased at a decreasing rate with an increase in traverse speed, exhibiting a hyperbolic relationship. Traverse speed has different effects on the components of the hybrid system. Increasing cutting speed leads to a decrease in the hydraulic specific energy and to an increase in mechanical specific energy. Therfore a comprimise has to be found for each cutting condition. For most efficient hybrid system cutting, the water jet pressure should be high enough to cause a penetration depth equal to mechanical tools at a selected cutting speed.

7.3 NOZZLE DIAMETER

Nikonov and Shovlovskii's and of Leach and Walker's experimental results had shown that, the best nozzle shape for water jet cutting was the one having a small cone angle, followed by 2 to 4 times the nozzle diameters length of straight section. Farmer and Attewell have concluded that the surface finish of the nozzles was of greater importance than any sophistication in the actual design. Above mentioned authors findings have formed the basis of nozzle design used for experiments.

Two sets of experiments were planned and conducted on Springwell and Darney sandstones to investigate the influence of the nozzle diameter on the measured and calculated parameters. The water jet pressure was changed as well to see its effect on optimal nozzle performance for each nozzle. Experimental variables and their levels were as follows:

Variable	Level	
	Darney	Springwell
Depth of cut (mm)	7	8
Traverse speed (mm/sec)	165	165
Stand-off dist. (mm)	45	45
Lead-on dist. (mm)	5	5
Side-off dist. (mm)	0	0
Water-jet pressure (MPa)	13.79, 27.58	13.79, 34.48
Nozzle diameter (mm)	0.6, 0.85, 1.10	0.6, 0.85, 1.10

Each cutting test was repeated four times and the cutting order was randomised. Overall, 2x3x4 = 24 tests were conducted on each sandstone. The positioning of the nozzles in the nozzle holder were noted and the same positions were maintained throughout the nozzle experiments.

Many curves of different types could pass through three points. Therefore no curve-fit analysis was attempted on the experimental results.

It was thought, before the experiments were carried out, that the influence of the nozzle diameter would be negligible if it was placed between the mechanical cutters, but would be significant if the jet was leading the tool. Therefore, experiments were planned accordingly.

7.3.1 The Effect of the Nozzle Diameter

On Water jet Penetration Depth

The penetration depth increased approximately linearly with increasing nozzle diameter at a constant stand-off distance and cutting speed, (Figures 7.18,7.19). The gradients of the curves were steeper for the higher pressure jet than for the lower pressure jet. This indicated that the effect of the nozzle diameter would be more pronounced at high water jet pressures.

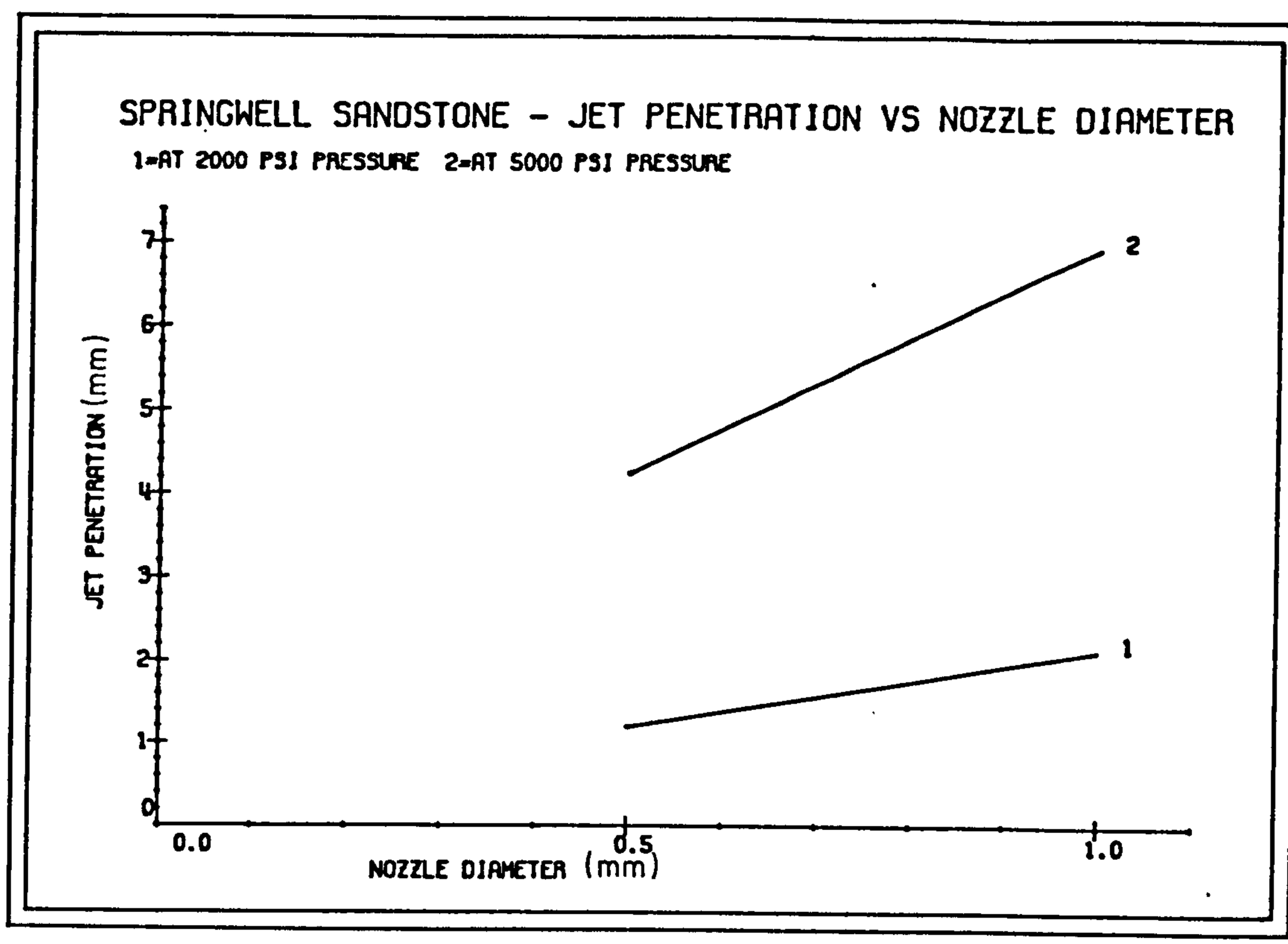
SPRINGWELL SANDSTONE - JET PENETRATION VS NOZZLE DIAMETER
1=AT 2000 PSI PRESSURE 2=AT 5000 PSI PRESSURE
JET PENETRATION (mm)
0
1
2
3
4
5
6
7
2
1
0.0
0.5
1.0
NOZZLE DIAMETER (mm)

FIG. 7.18

The graph of Hydraulic Specific Energy drawn against nozzle diameter showed that the cutting operation became less efficient with increasing nozzle diameter, (Figure 7.19).

On Tool Forces

Lower pressure (13.79 MPa) experiments were conducted at a constant stand-off distance/nozzle diameter ratio on Springwell sandstone. It was observed that, (Figures 7.20-7.22) no significant improvement was gained by increasing nozzle diameter. The 34.48 MPa pressure jet experiments on Springwell sandstone were conducted at a fixed stand-off distance, and results indicated that cutting forces were reduced with increasing nozzle diameter up to 0.85mm. Forces remained approximately constant with further nozzle diameter increase. The normal forces however showed continuous improvement (reduction).

Experimental results obtained from Darney sandstone cutting tests revealed that for both water jet pressures, increasing nozzle diameter caused a decrease in cutting forces, like those observed with Springwell sandstone. The reduction was more rapid between 0.6-0.85mm than 0.85-1.10mm. Normal forces responded more to diameter change and were reduced more in magnitude than cutting forces, (Figures 7.23-7.25).

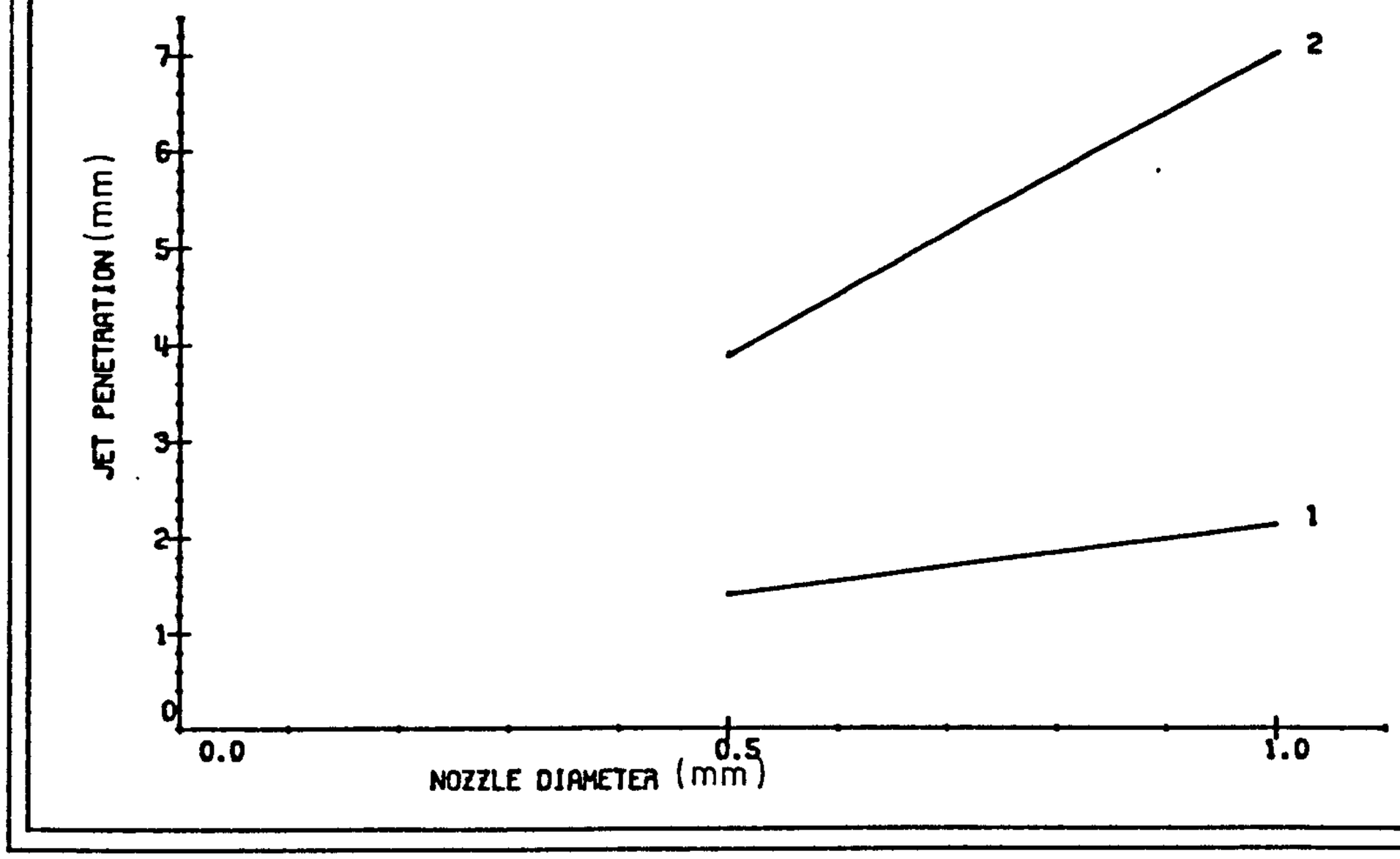
DARNEY SANDSTONE - JET PENETRATION VS NOZZLE DIAMETER
1=AT 2000 PSI 2=AT 4000 PSI
JET PENETRATION (mm)
0
1
2
3
4
5
6
7
0.0
0.5
1.0
NOZZLE DIAMETER (mm)
1
2

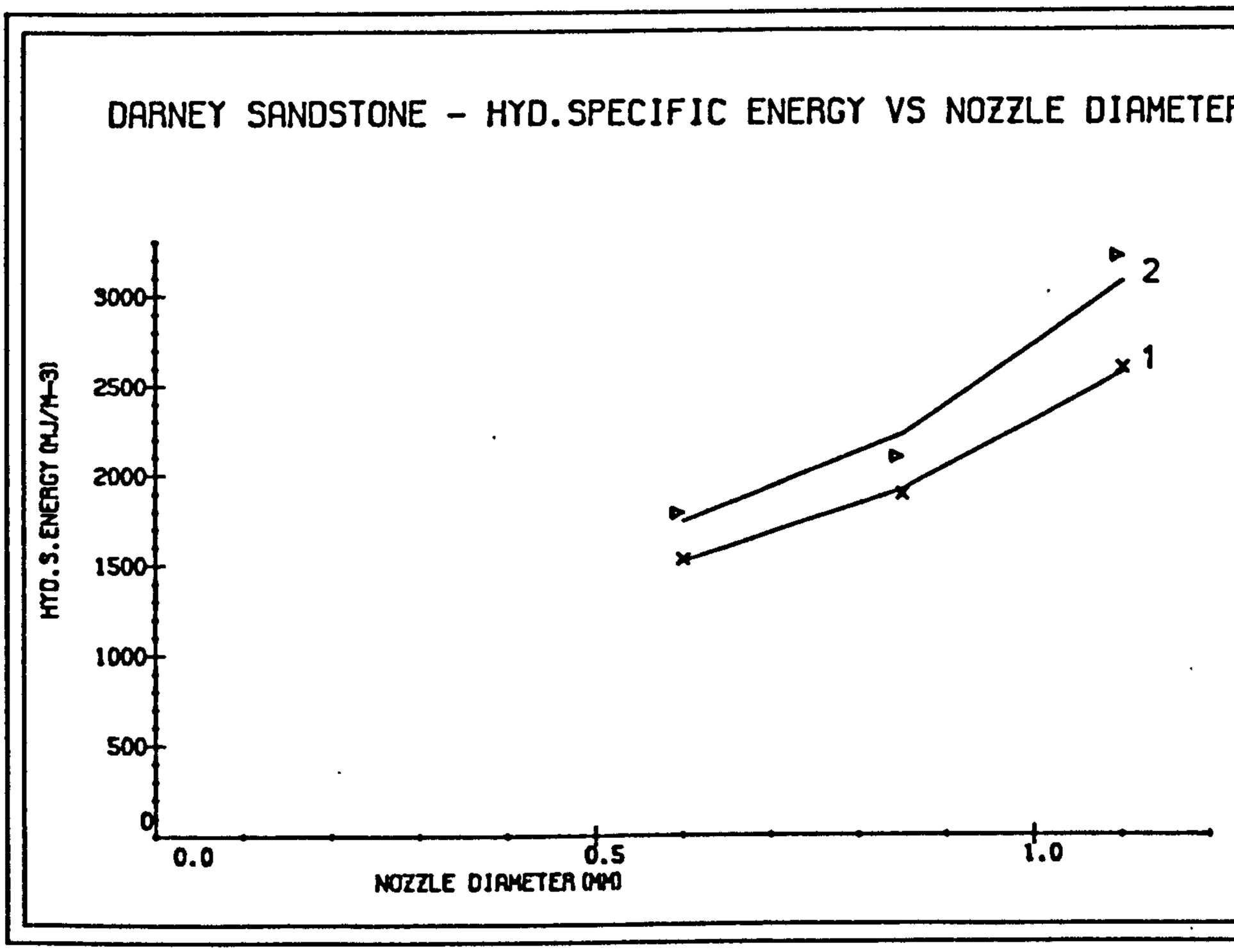
DARNEY SANDSTONE - HYD.SPECIFIC ENERGY VS NOZZLE DIAMETER
HYD.S.ENERGY (MJ/M-3)
0
500
1000
1500
2000
2500
3000
0.0
0.5
1.0
NOZZLE DIAMETER (mm)
1
2

FIG. 7.19

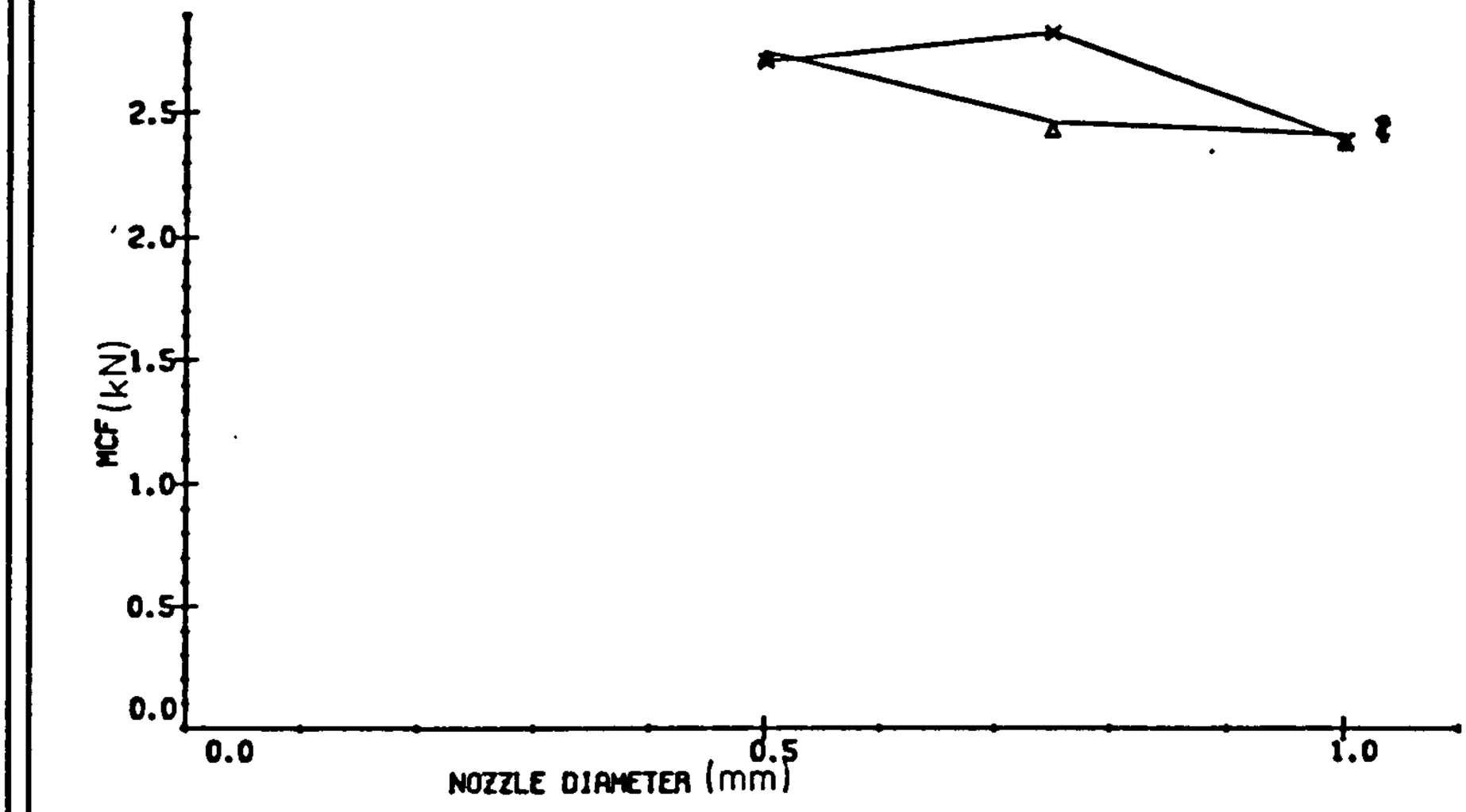
SPRINGWELL SANDSTONE - MCF VS NOZZLE DIAMETER
1=AT 2000 PSI 2=AT 5000 PSI
2.5
2.0
1.5
1.0
0.5
0.0
MCF (kN)
0.0
0.5
1.0
NOZZLE DIAMETER (mm)
1
2

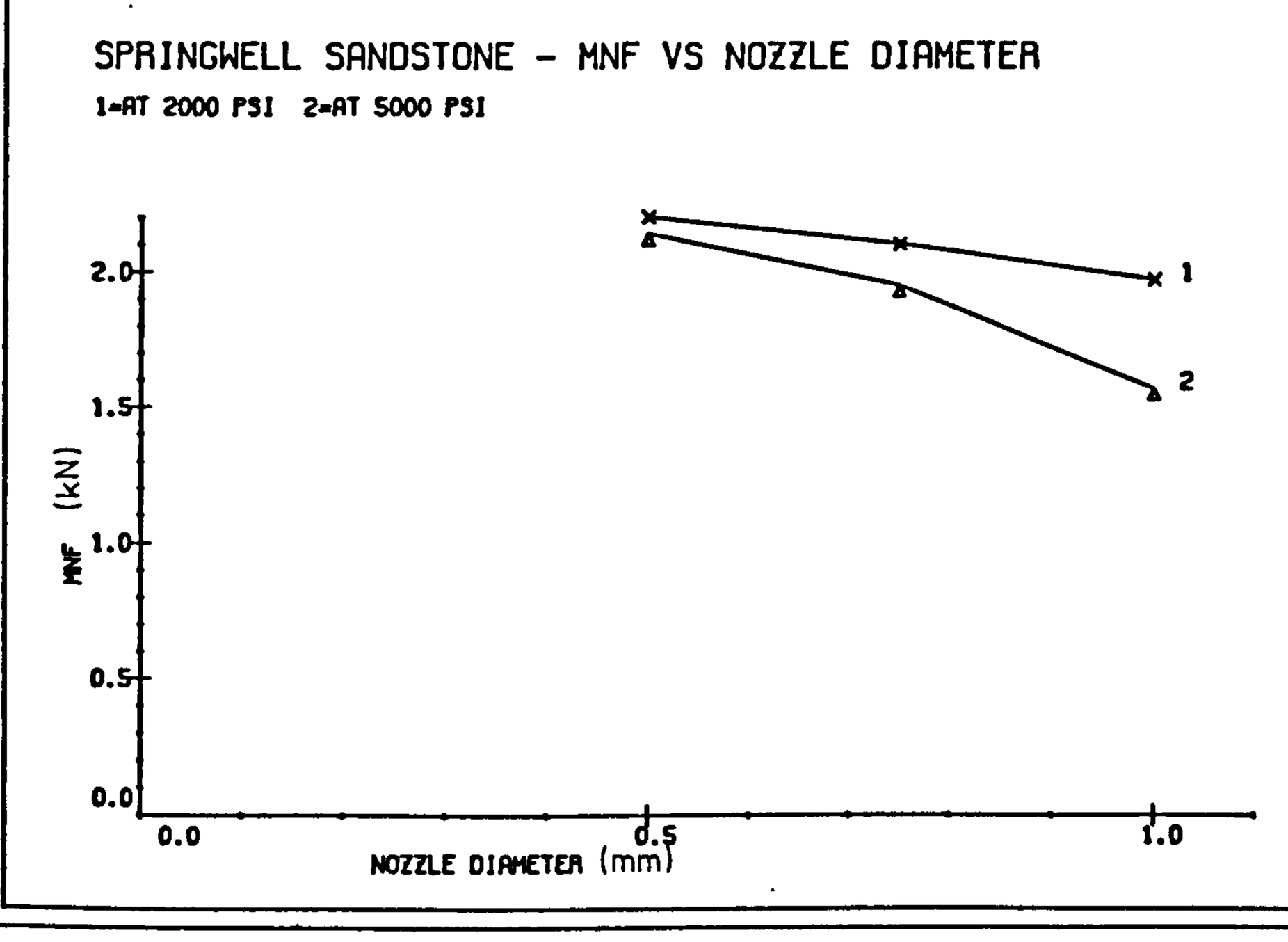
SPRINGWELL SANDSTONE - MNF VS NOZZLE DIAMETER
1=AT 2000 PSI 2=AT 5000 PSI
2.0
1.5
1.0
0.5
0.0
MNF (kN)
0.0
0.5
1.0
NOZZLE DIAMETER (mm)
1
2

FIG. 7.20

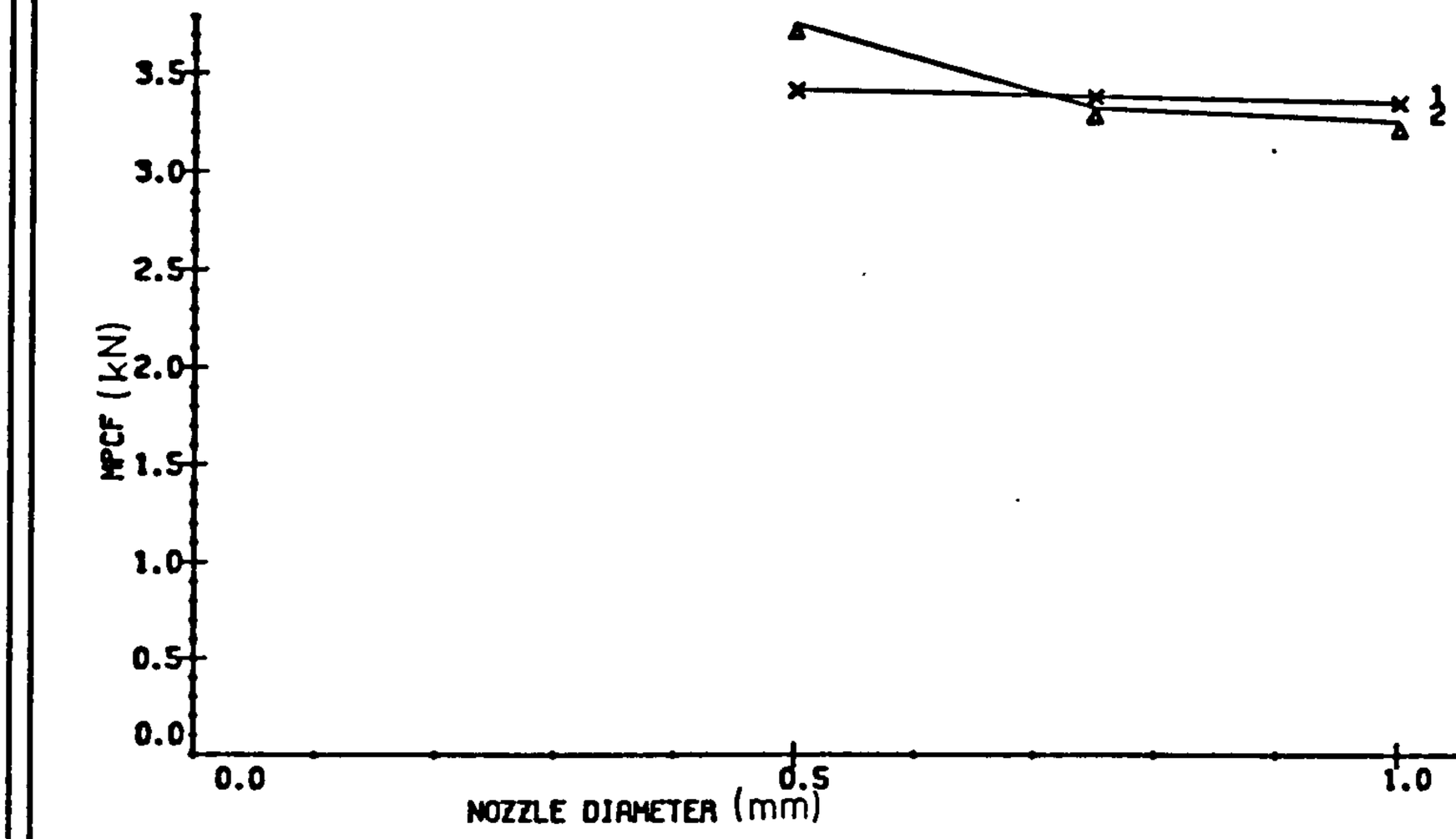
SPRINGWELL SANDSTONE - MPCF VS NOZZLE DIAMETER
1=AT 2000 PSI 2=AT 5000 PSI
MPCF (kN)
3.5
3.0
2.5
2.0
1.5
1.0
0.5
0.0
0.0
0.5
1.0
NOZZLE DIAMETER (mm)
1
2

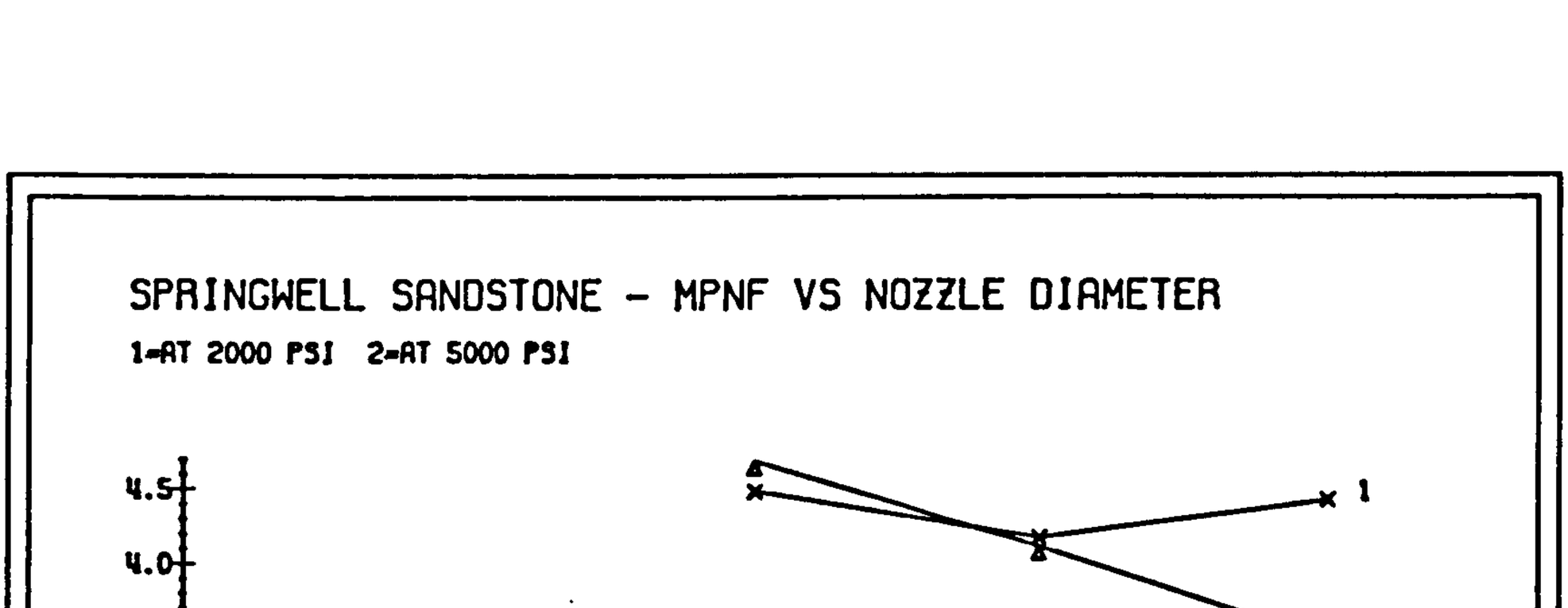
SPRINGWELL SANDSTONE - MPNF VS NOZZLE DIAMETER
1=AT 2000 PSI 2=AT 5000 PSI
MPNF (kN)
4.5
4.0
3.5
3.0
2.5
2.0
1.5
1.0
0.5
0.0
0.0
0.5
1.0
NOZZLE DIAMETER (mm)
1
2

FIG. 7.21

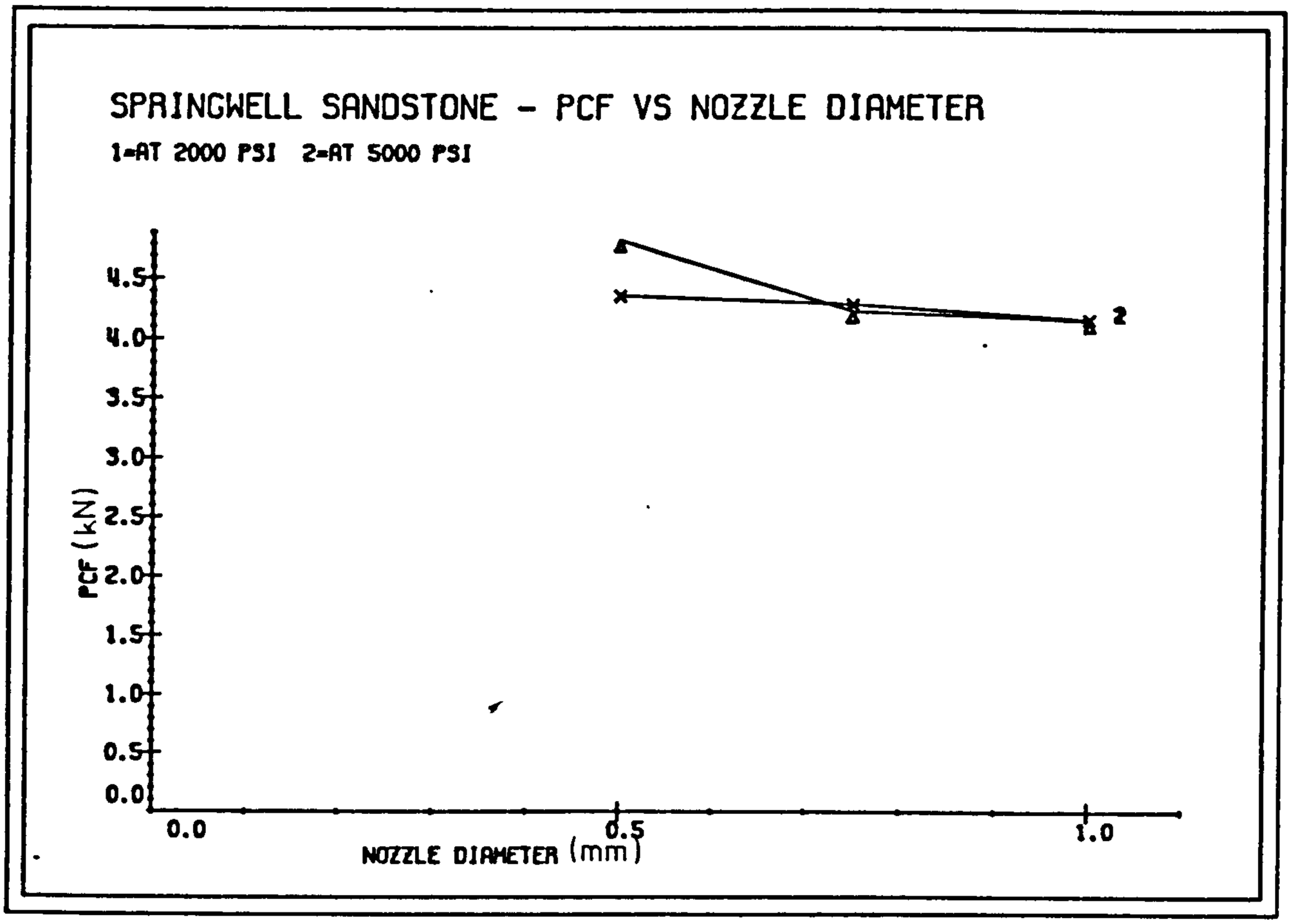
SPRINGWELL SANDSTONE - PCF VS NOZZLE DIAMETER
1=AT 2000 PSI 2=AT 5000 PSI
4.5
4.0
3.5
3.0
2.5
2.0
1.5
1.0
0.5
0.0
PCF (kN)
2
0.0
0.5
1.0
NOZZLE DIAMETER (mm)

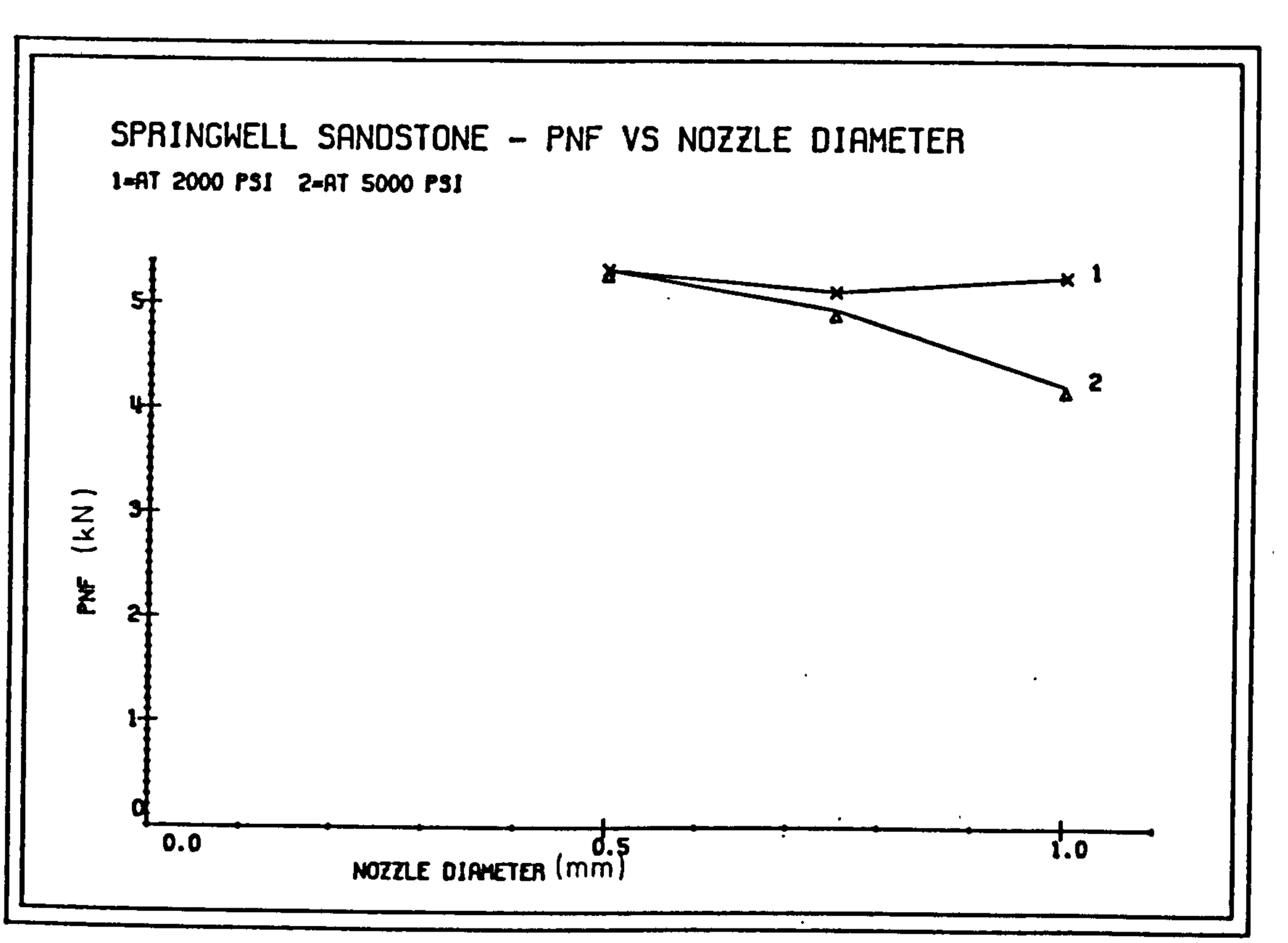
SPRINGWELL SANDSTONE - PNF VS NOZZLE DIAMETER
1=AT 2000 PSI 2=AT 5000 PSI
5
4
3
2
1
0
PNF (kN)
1
2
0.0
0.5
1.0
NOZZLE DIAMETER (mm)

FIG. 7.22

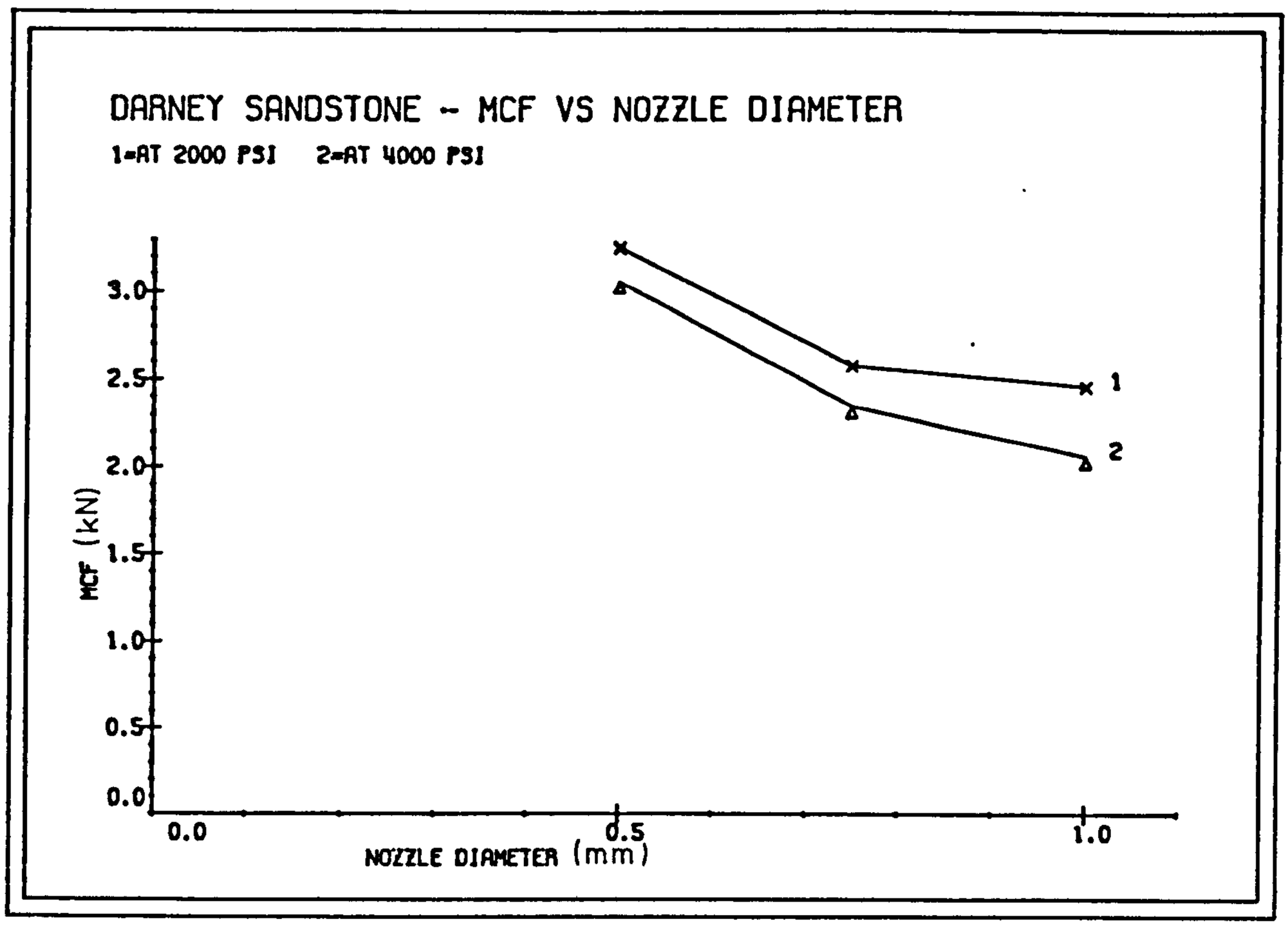
DARNEY SANDSTONE - MCF VS NOZZLE DIAMETER
1=AT 2000 PSI 2=AT 4000 PSI
MCF (kN)
3.0
2.5
2.0
1.5
1.0
0.5
0.0
0.0
0.5
1.0
NOZZLE DIAMETER (mm)
1
2

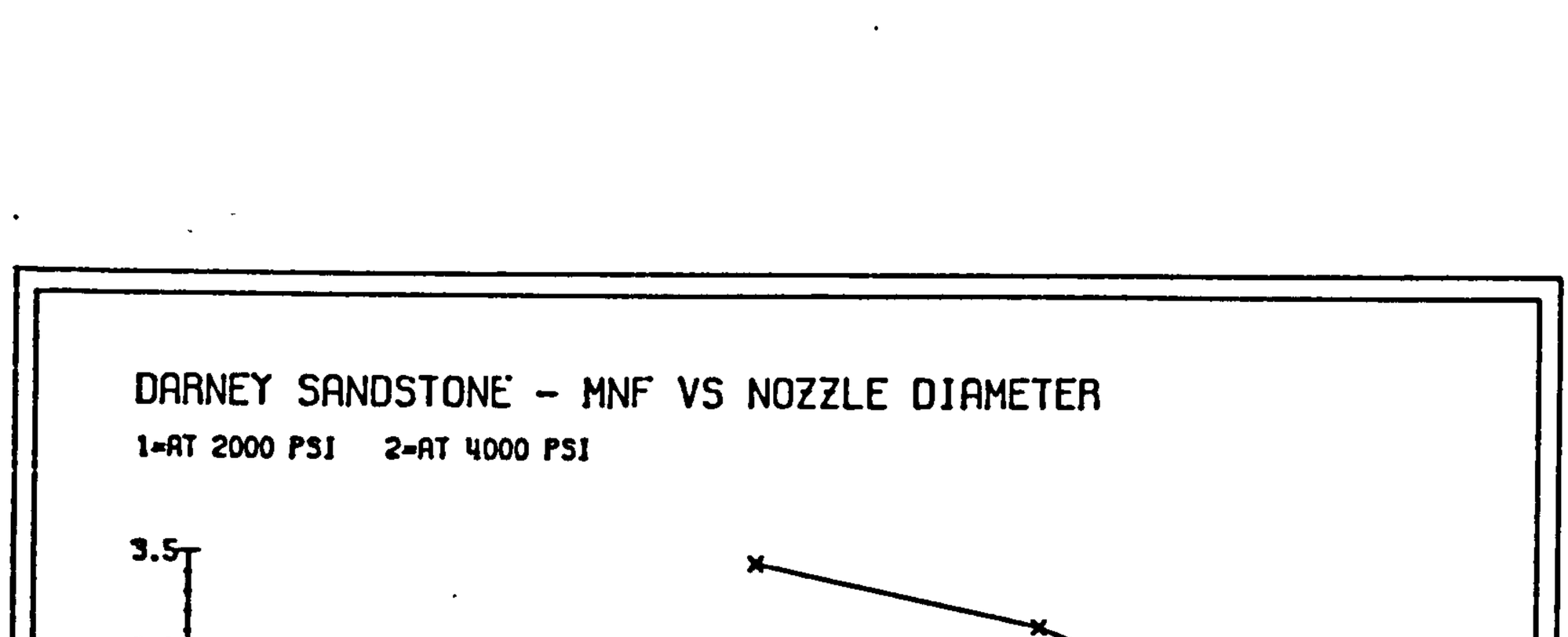
DARNEY SANDSTONE - MNF VS NOZZLE DIAMETER
1=AT 2000 PSI 2=AT 4000 PSI
MNF (kN)
3.5
3.0
2.5
2.0
1.5
1.0
0.5
0.0
0.0
0.5
1.0
NOZZLE DIAMETER (mm)
1
2

FIG. 7.23

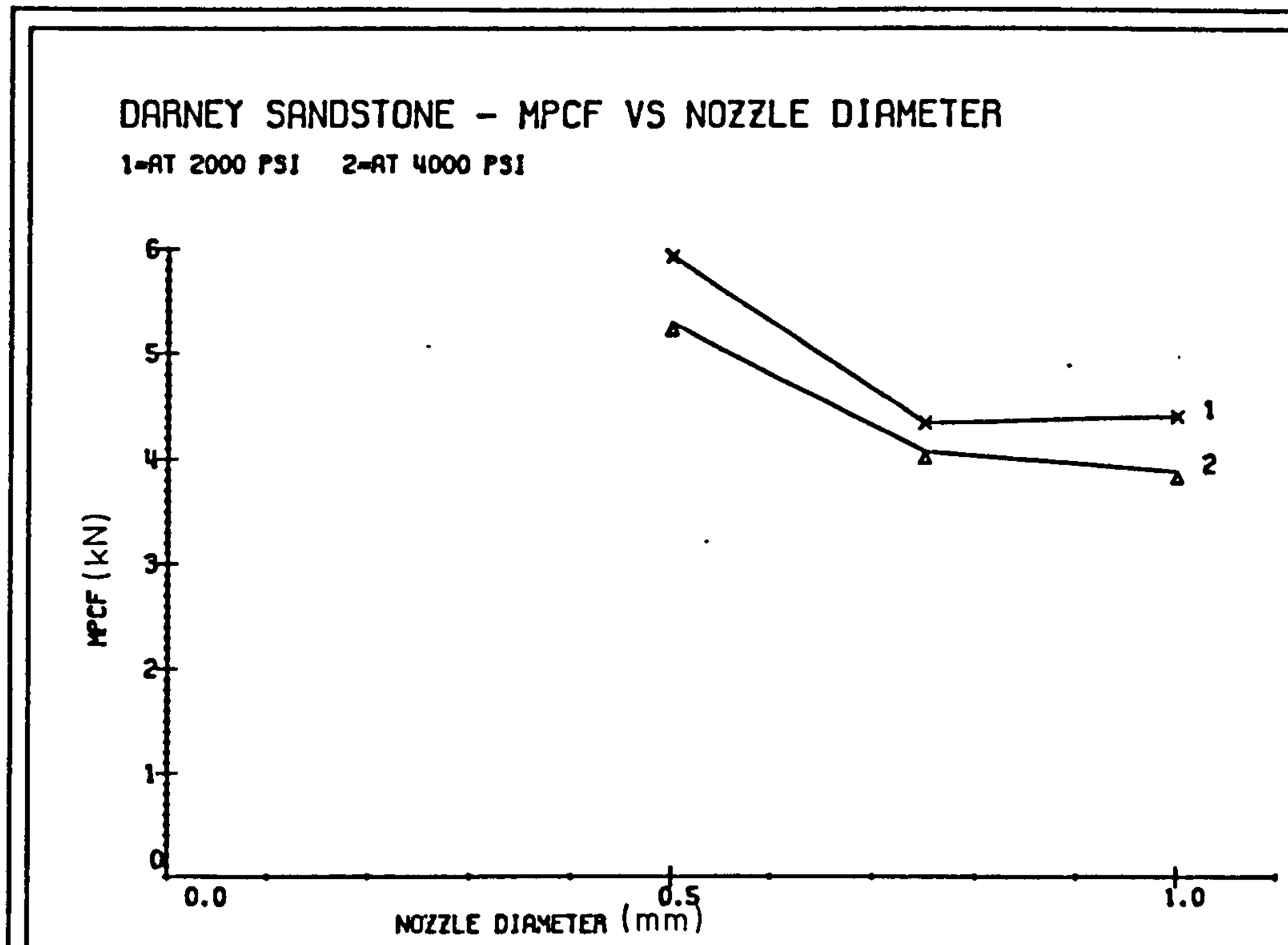
DARNEY SANDSTONE - MPCF VS NOZZLE DIAMETER
1=AT 2000 PSI 2=AT 4000 PSI
MPCF (kN)
0
1
2
3
4
5
6
0.0
0.5
1.0
NOZZLE DIAMETER (mm)
1
2

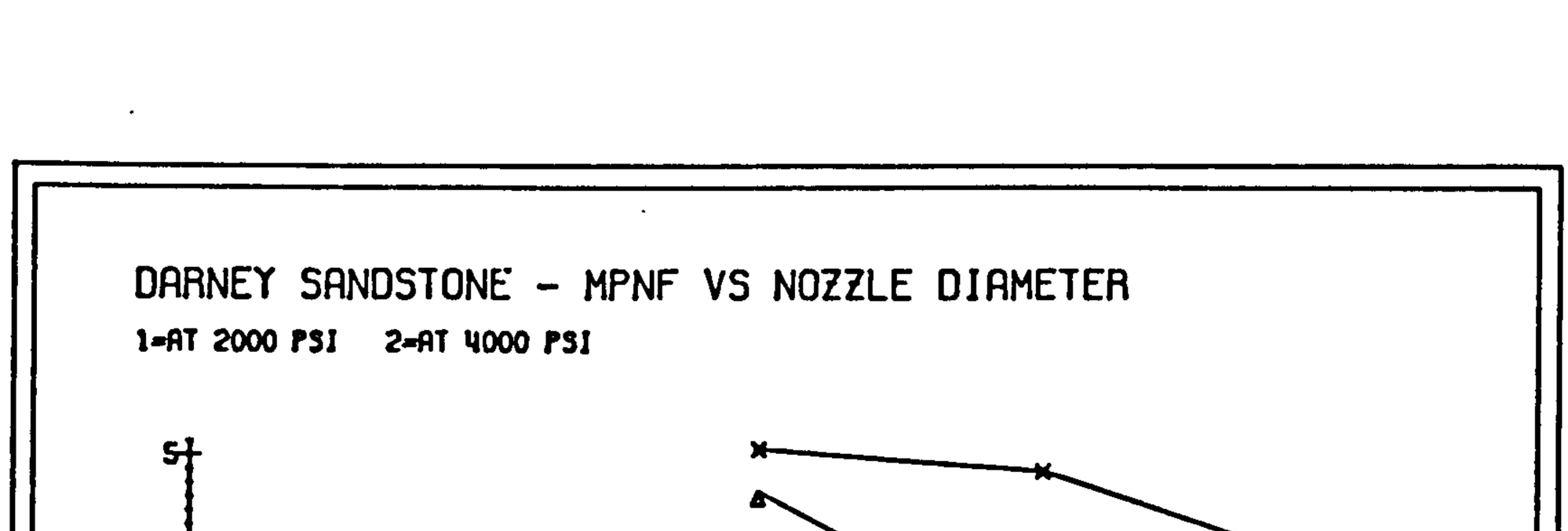
DARNEY SANDSTONE - MPNF VS NOZZLE DIAMETER
1=AT 2000 PSI 2=AT 4000 PSI
MPNF (kN)
0
1
2
3
4
5
0.0
0.5
1.0
NOZZLE DIAMETER (mm)
1
2

FIG. 7.24

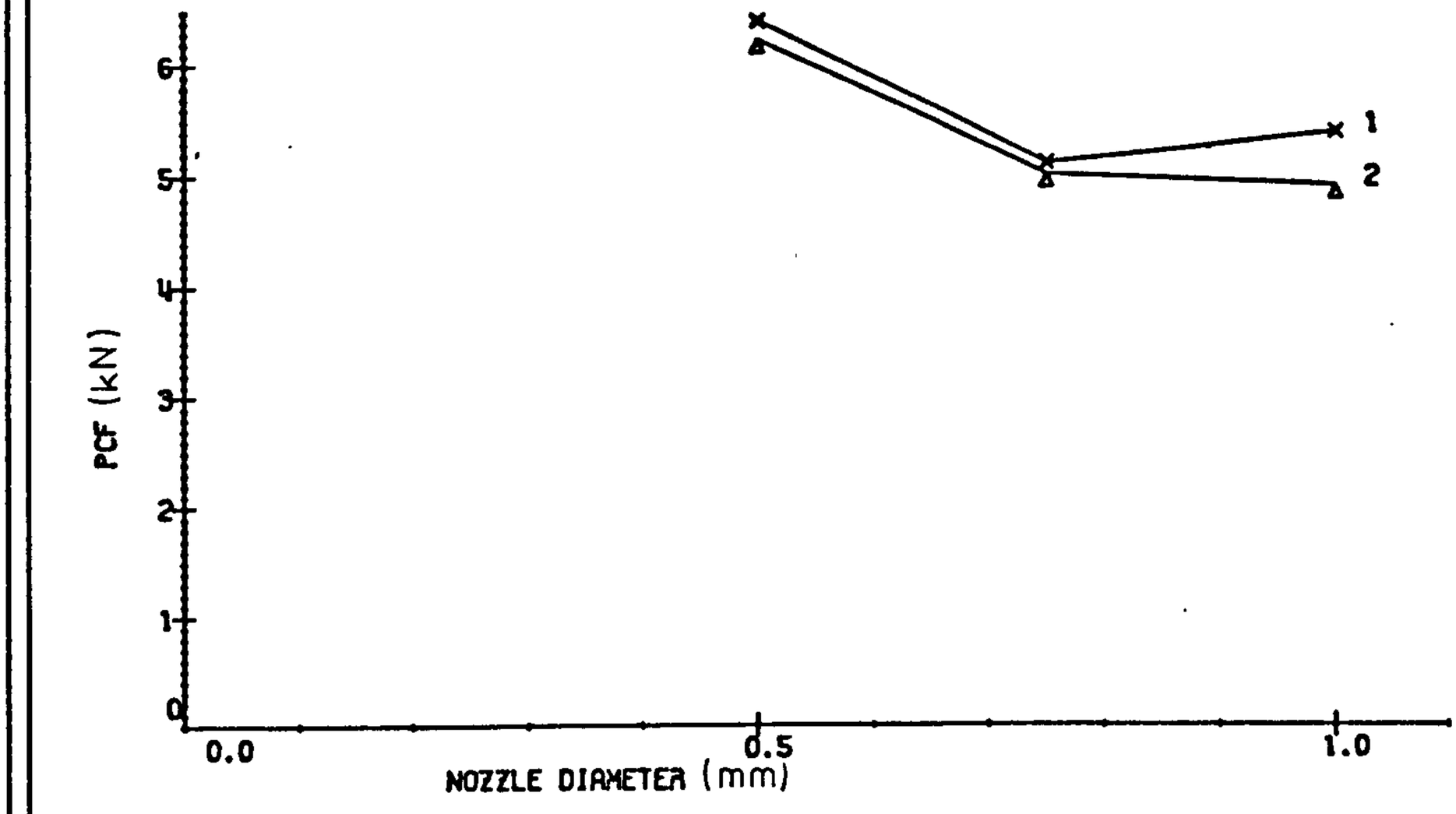
DARNEY SANDSTONE - PCF VS NOZZLE DIAMETER
1=AT 2000 PSI 2=AT 4000 PSI
PCF (kN)
0
1
2
3
4
5
6
0.0
0.5
1.0
NOZZLE DIAMETER (mm)
1
2

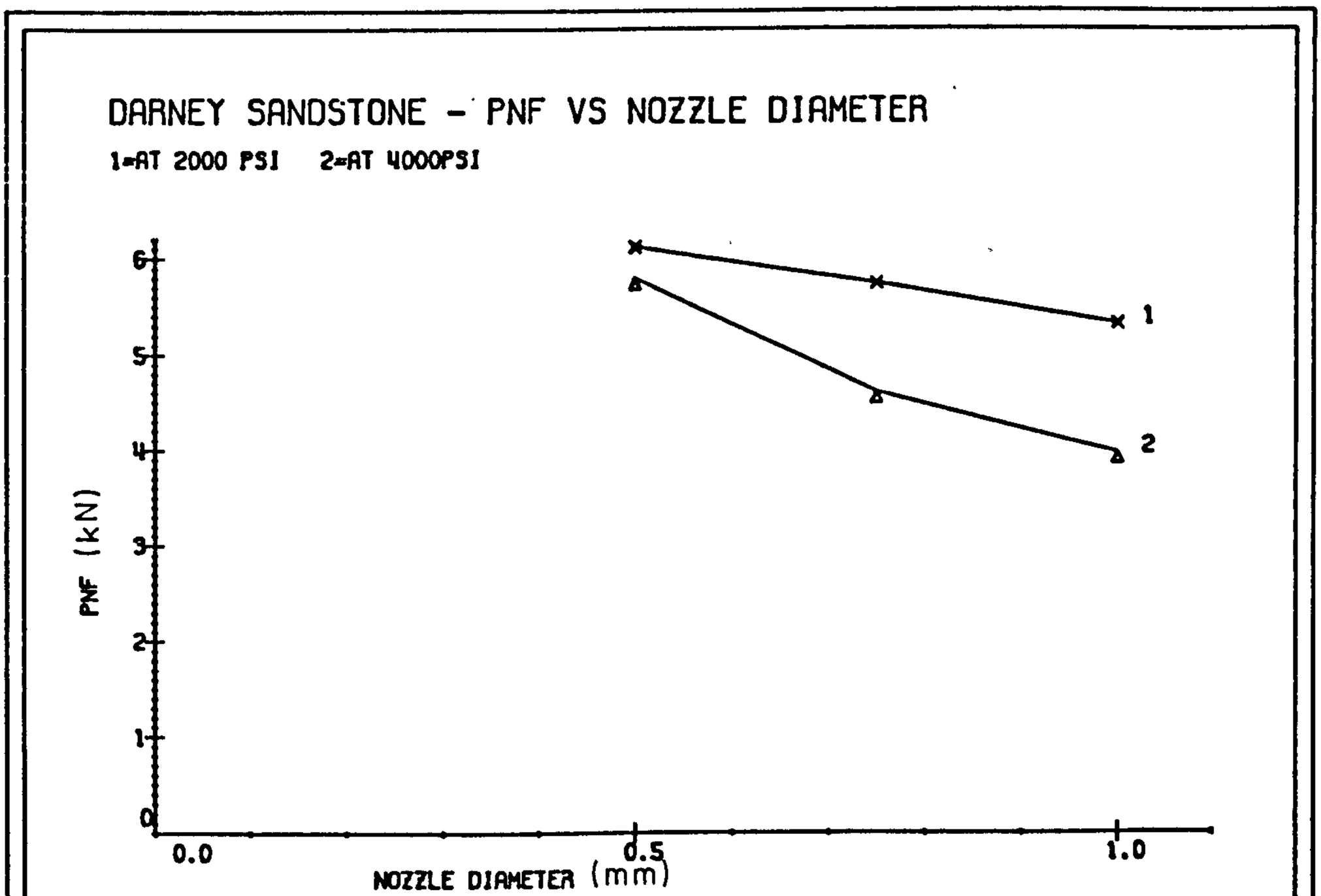
DARNEY SANDSTONE - PNF VS NOZZLE DIAMETER
1=AT 2000 PSI 2=AT 4000PSI
PNF (kN)
0
1
2
3
4
5
6
0.0
0.5
1.0
NOZZLE DIAMETER (mm)
1
2

FIG. 7.25

On Yield

With the 13.79 MPa pressure jet, cutting results imply that with increasing nozzle diameter rock yield increases too, but in a small scale. However, when the pressure was increased to 27.58 MPa for Darney sandstone and to 34.48 MPa for Springwell sandstone, the yield results showed no significant change with increased nozzle diameter, (Figures 7.26,7.27).

One important observation that can be made from both yield versus nozzle diameter graphs is that, there is a noticeable reduction of rock yield with increased water jet pressure and this reduction was more apparent on Springwell sandstone cutting.

On Mechanical Specific Energy

Mechanical Specific Energy decreased with increase in nozzle diameter, more so at higher water jet pressure, (Figure 7.27). At 13.79 MPa pressure, mechanical specific energy decreased till 0.85mm, then approached to a constant value.

For Springwell sandstone, at 13.79 MPa jet pressure, Mechanical Specific Energy increased with nozzle diameter then decreased and at higher pressure it decreased then started to increase, (Figure 7.26).

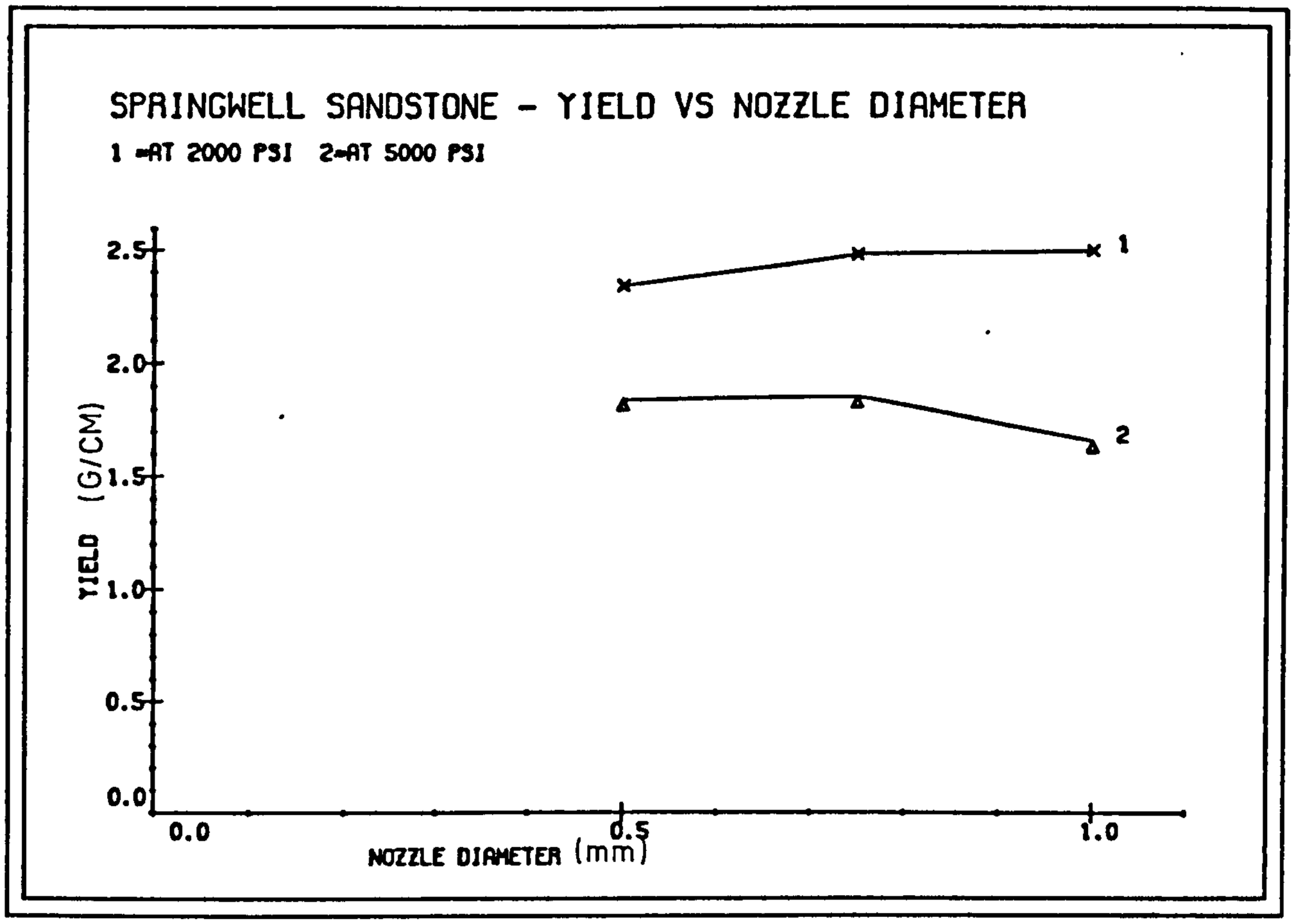

PLOT NUMBER= 2

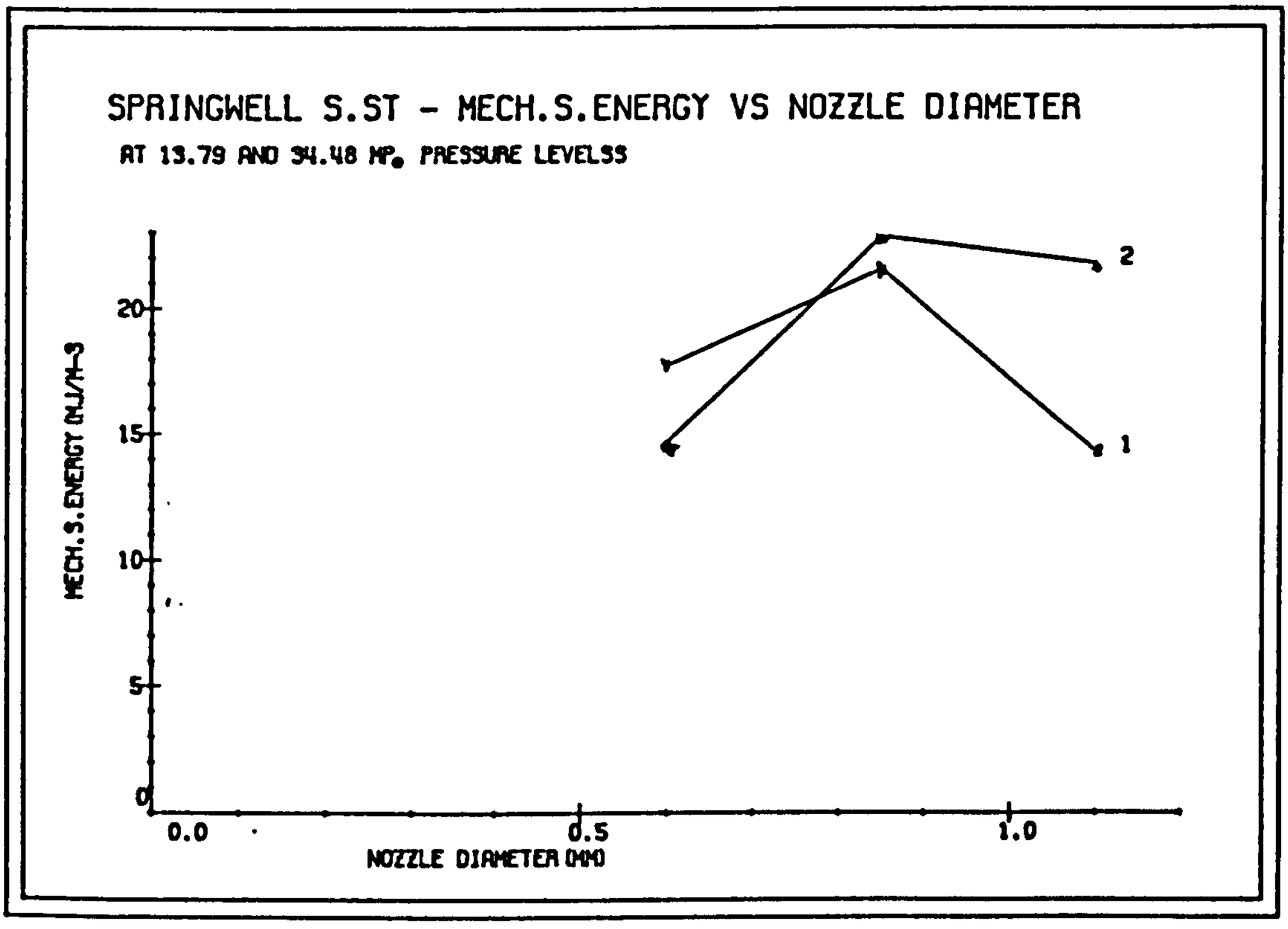

FIG. 7.26

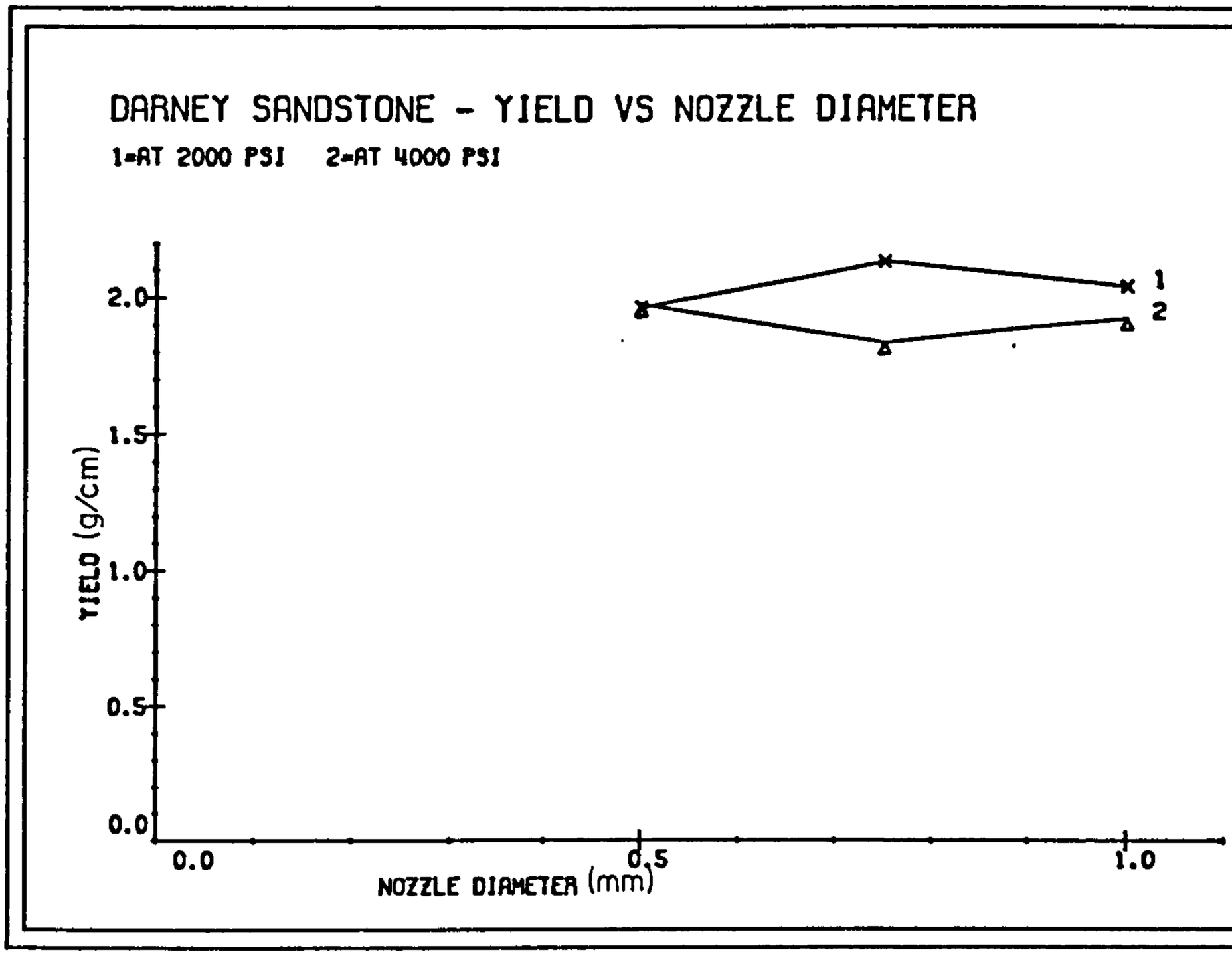
DARNEY SANDSTONE - YIELD VS NOZZLE DIAMETER
1=AT 2000 PSI 2=AT 4000 PSI
YIELD (g/cm)
2.0
1.5
1.0
0.5
0.0
0.0
0.5
1.0
NOZZLE DIAMETER (mm)
1
2

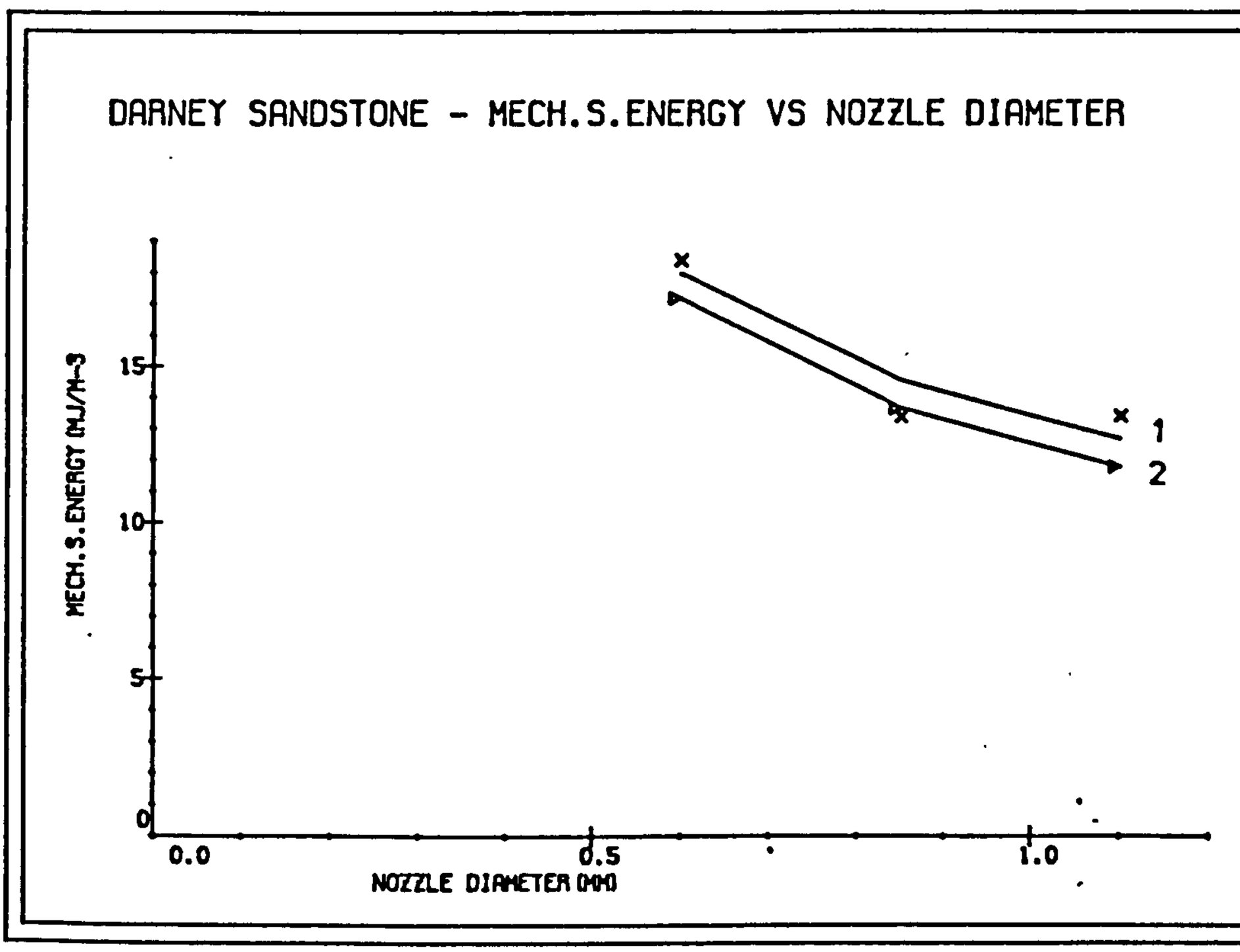
DARNEY SANDSTONE - MECH.S.ENERGY VS NOZZLE DIAMETER
MECH.S.ENERGY (MJ/M-3)
15
10
5
0
0.0
0.5
1.0
NOZZLE DIAMETER (MM)
1
2

FIG. 7.27

7.3.2 Discussion

Power requirements for water jet cutting increase as the first power of pressure and the second power of volume. Because of this the nozzle diameter should be such that it will cost less to penetrate a required depth. It must be, however borne in mind that although it is cheaper to use smaller diameter nozzles, at higher pressures, they dissipate in shorter distances than larger jets if no additives were used.

At a constant stand-off distance, generally an increase in nozzle diameter leads to a corresponding increase in jet penetration depth because of the increased power output at the nozzle.

The optimum nozzle diameter is dependent on the type of mechanical tool with which it will be used together and on the location of the nozzle with respect to the mechanical tool as well as on the power available and the pressure range desired.

The width of the cut is dependent on the nozzle diameter and is approximately three times the nozzle diameter. Therefore, if a larger diameter ,i.e. 1.1mm, nozzle is used -with a point attack tool and penetrates the rock to a depth equal to the mechanical tools- it will make a slot width of approximately 3mm, which is bigger than the point attack tool tip diameter and only the upper edges of the carbide tip will come into contact with the walls of the kerf and hence the cutting will be less efficient.

The larger diameter nozzles have performed better in terms of reductions in the tool forces and mechanical specific energy, when they were compared at a constant stand-off distance.

7.3.3 Conclusions

The jet penetration depth has increased directly with the increase in the nozzle diameter, at a constant water jet pressure and constant stand-off distance. The rate of increase was greater at high water jet pressures.

Because, increasing nozzle diameter caused an increase in jet penetration depth, all the tool forces were decreased as a result. The decrease was more pronounced between 0.6 - 0.85mm diameters. Three nozzles have performed equally well on Springwell sandstone at a constant stand-off/nozzle diameter and 13.79 MPa pressure.

Mechanical Specific Energy decreased with increasing nozzle diameter, more so at high pressures. The optimum nozzle diameter is dependent on the mechanical tool type as well as on the available power and desired pressure range. Whenever possible, smaller diameter nozzles should be used to keep the energy costs down.

7.4 SIDE-OFF DISTANCE

High pressure water jets have to operate at an optimum location with respect to mechanical tool to be most effective i.e. minimize specific energy and maximise yield and debris size. The optimum location may be found if the influences of positional variables, e.g. lead-on distance, stand-off distance and side-off distance, operating in isolation and interacting together are known.

In this section, side-off distance and its effect on the combined system parameters is investigated and discussed.

Springwell sandstone experimental results were given in the previous chapter. However, they will briefly be repeated here to give the overall picture of the influence of nozzle spacing between mechanical cutting tools.

Experimental plan for Springwell sandstone was given in (Chapter 6) and the results tabulated in (Appendix C). The variables and their levels were as follows:

Variable		Level
Depth of cut	(mm)	6
Pressure	(MPa)	34.48
Lead-on dist.	(mm)	5
Stand-off dist.	(mm)	45
Nozzle diameter	(mm)	0.85
Traverse speed	(mm/sec)	165
Side-off dist.	(mm)	0, 10, 20, 30, 40
Side-off/depth of cut		0, 1.66, 3.32, 4.98, 6.64

Darney sandstone experimental plan was designed to find the effect of jet penetration depth in addition to that of side-off distance. The water jet pressures were chosen such that at one level it penetrated the rock less then, and at the other pressure level it penetrated to a depth equal to that of mechanical tools. Experimental variables and their levels were as follows:

Variable		Level
Depth of cut	(mm)	7
Nozzle diameter	(mm)	0.85
Stand-off dist.	(mm)	45
Traverse speed	(mm/sec)	165
Water jet pressure	(MPa)	13.79, 34.48
Side/depth of cut ratio		1, 2, 3, 4, 5

The rock was precut with the water jet. Parallel cuts at predetermined spacings were made on the rock surface by the traversing jet. The mechanical tool then cut, exactly at the mid-point of the rib left behind by the jets.

Tests at each experimental level was repeated four times and randomized to counteract the influence of variations in the rock properties and operating conditions. Overall 2 x 5 x 4 = 40 tests were conducted on Darney sandstone.

7.4.1 Effect of Side-off Distance On Tool Forces

It can be deduced from Springwell sandstone cutting results that all the tool forces increase with increasing side-off distance, reaching a constant value after s/d>6 when two systems were cutting in isolation i.e. no interaction taking place between the hydraulic and mechanical parts of the hybrid cutting system. The increase was more steep up to an s/d ratio of 3.32. After this point, further increase was very gradual and small. Mean Peak Sideways Force increased linearly within the range considered, however it may be expected to reach a constant value like cutting and normal forces.

Increasing side-off distance caused a small decrease in tool forces when Darney sandstone was cut with a 13.79 Mpa pressure water jet. However, with a 34.48 MPa pressure jet, (when the jet penetration depth was equal with the mechanical tools), the effect of side-off distance was more pronounced. Cutting and normal forces increased at a decreasing rate with side-off distance reaching a constant value after s/d > 5, (Figures 7.28-7.30).

On Yield

The yield was increased with side-off distance up to s/d = 3.32 for Springwell and s/d = 3 for Darney sandstones, (Fig 7.31). When the s/d ratio was increased further, yield decreased by a small amount before assuming a constant value at which point the water jet and the mechanical tool were both cutting in isolation.

On Mechanical Specific Energy

Mechanical Specific Energy varied inversely with the increase in side-off/depth of cut ratio, reaching a minimum value at s/d = 3.33 for Springwell and s/d = 3 for Darney Sandstones respectively. The cutting was at its most efficient at the minimum. Any further increase in s/d ratio caused an increase in Mechanical Specific Energy before it reached to an constant value, (Figure 7.31).

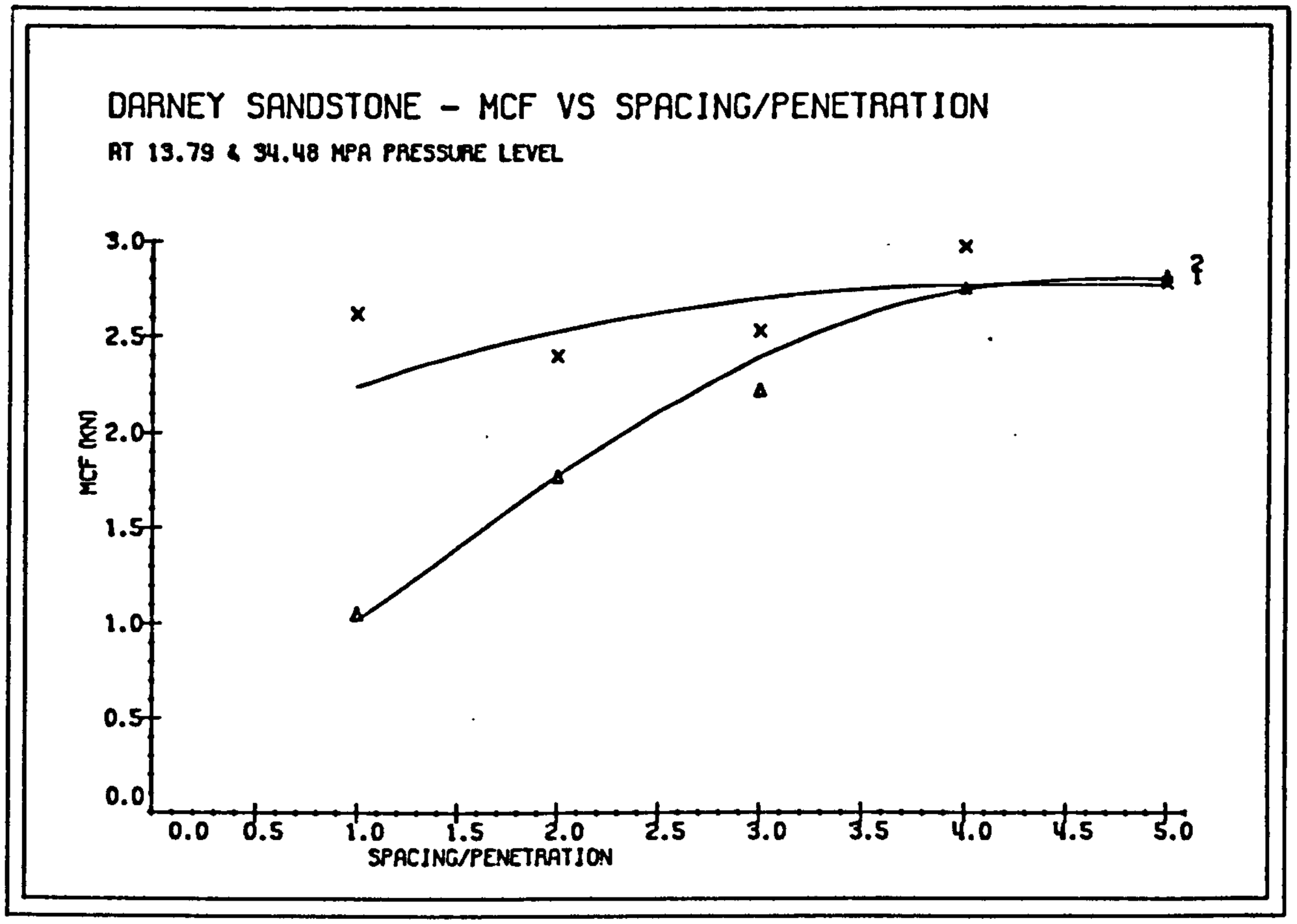
DARNEY SANDSTONE - MCF VS SPACING/PENETRATION
AT 13.79 & 34.48 MPA PRESSURE LEVEL
MCF (KN)
3.0
2.5
2.0
1.5
1.0
0.5
0.0
0.0 0.5 1.0 1.5 2.0 2.5 3.0 3.5 4.0 4.5 5.0
SPACING/PENETRATION
1
2

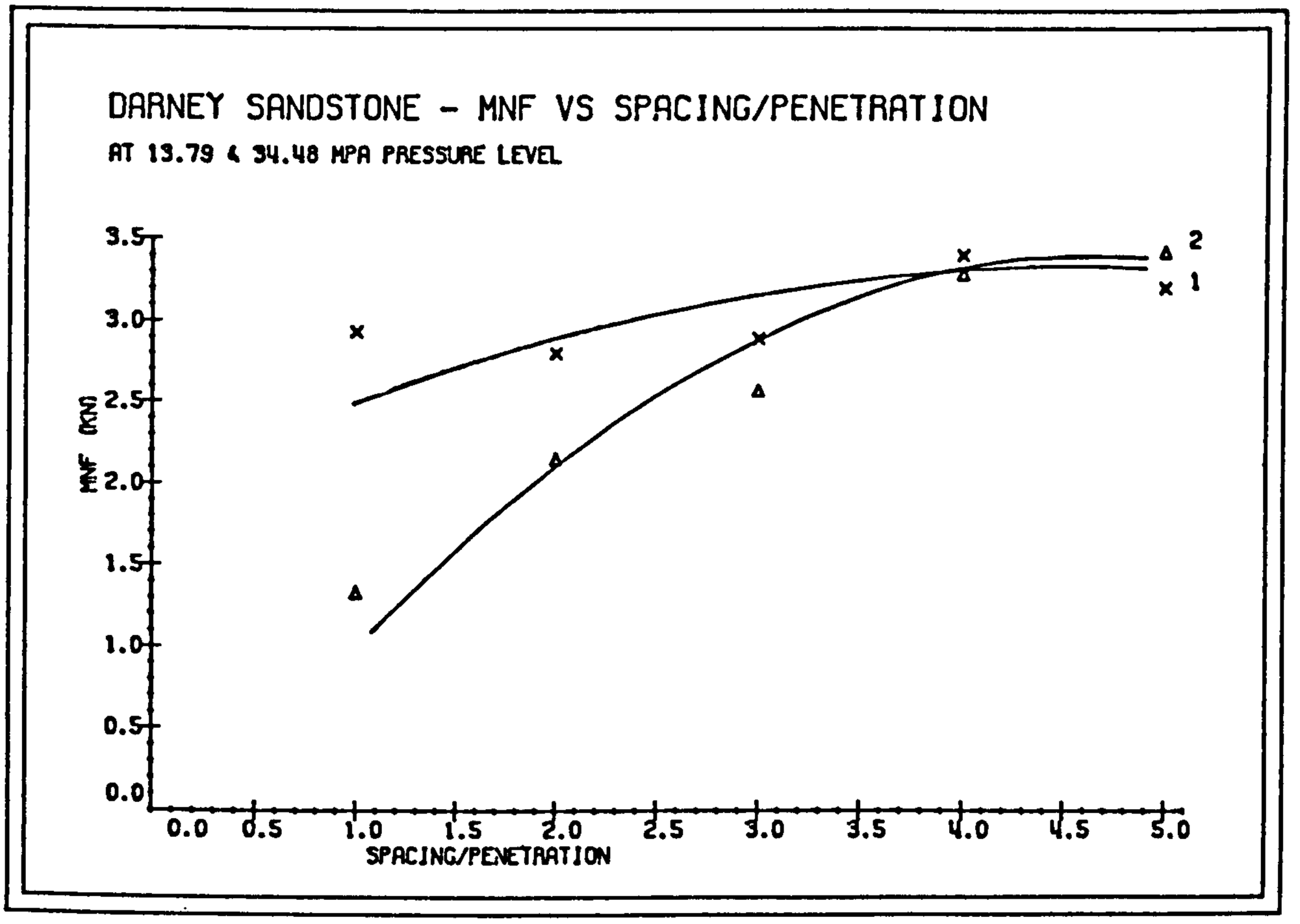
DARNEY SANDSTONE - MNF VS SPACING/PENETRATION
AT 13.79 & 34.48 MPA PRESSURE LEVEL
MNF (KN)
3.5
3.0
2.5
2.0
1.5
1.0
0.5
0.0
0.0 0.5 1.0 1.5 2.0 2.5 3.0 3.5 4.0 4.5 5.0
SPACING/PENETRATION
1
2

FIG. 7.28

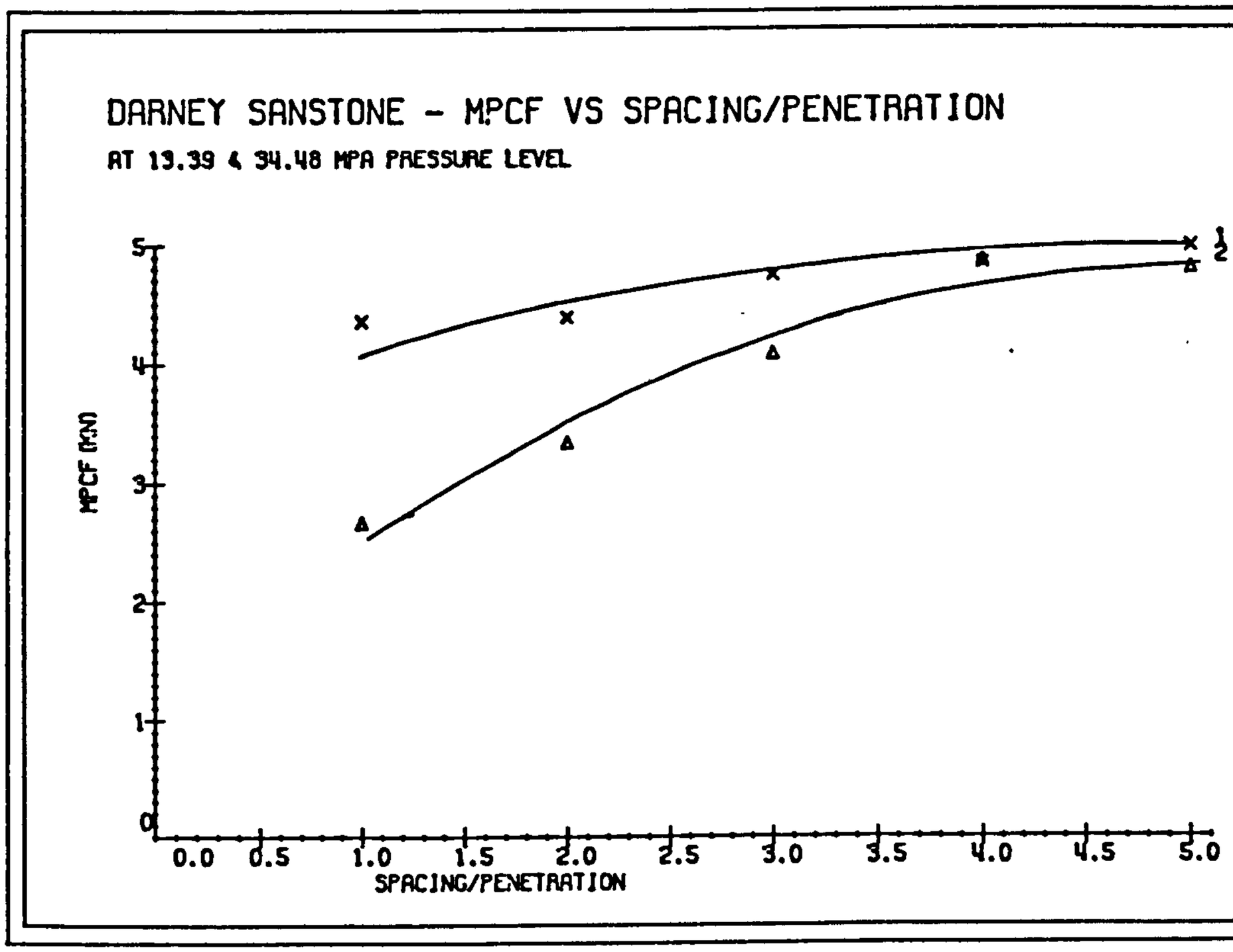
DARNEY SANSTONE - MPCF VS SPACING/PENETRATION
AT 13.39 & 34.48 MPA PRESSURE LEVEL
MPCF (KN)
0
1
2
3
4
5
0.0
0.5
1.0
1.5
2.0
2.5
3.0
3.5
4.0
4.5
5.0
SPACING/PENETRATION
1
2

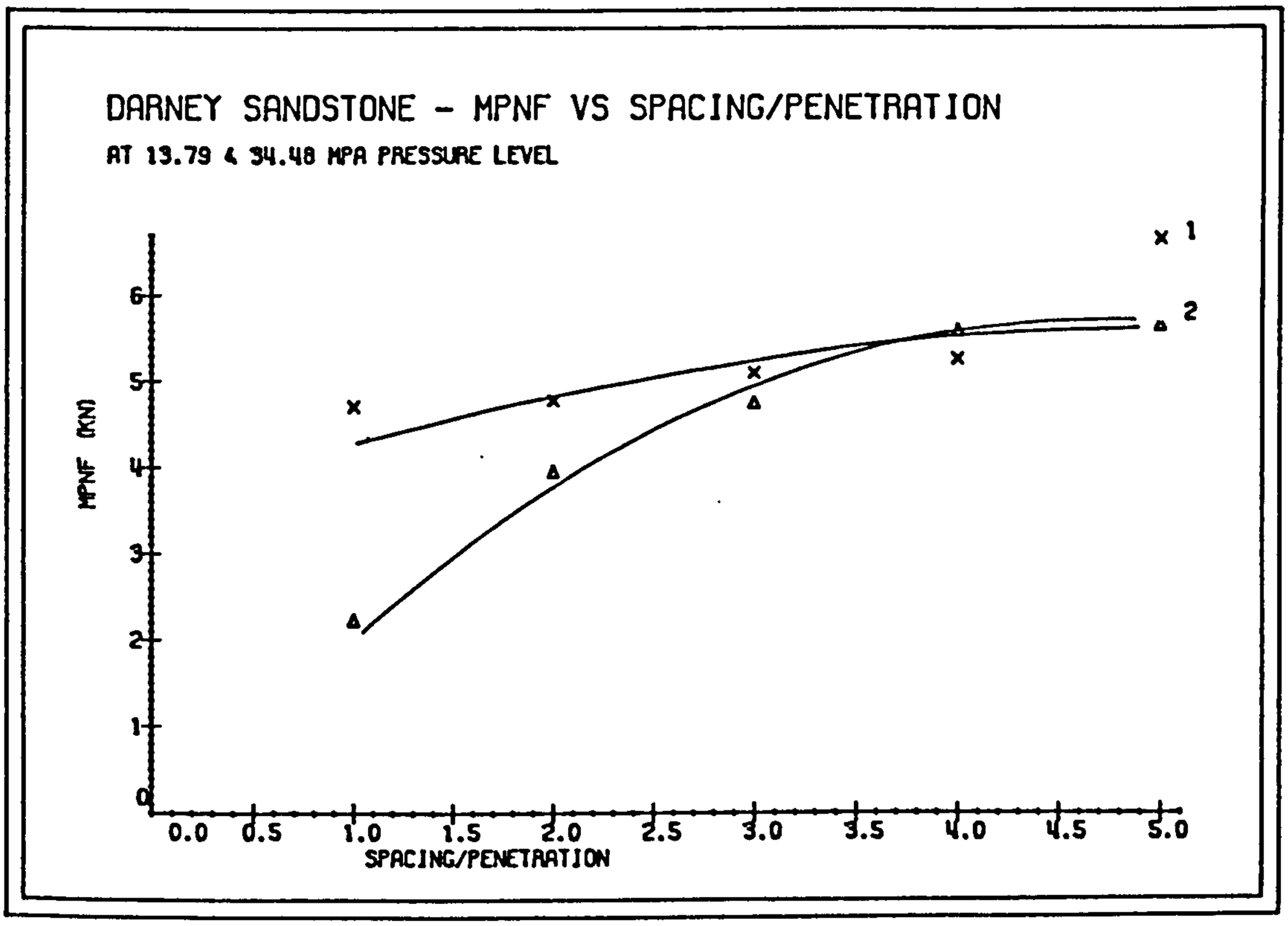
DARNEY SANDSTONE - MPNF VS SPACING/PENETRATION
AT 13.79 & 34.48 MPA PRESSURE LEVEL
MPNF (KN)
0
1
2
3
4
5
6
0.0
0.5
1.0
1.5
2.0
2.5
3.0
3.5
4.0
4.5
5.0
SPACING/PENETRATION
1
2

FIG. 7.29

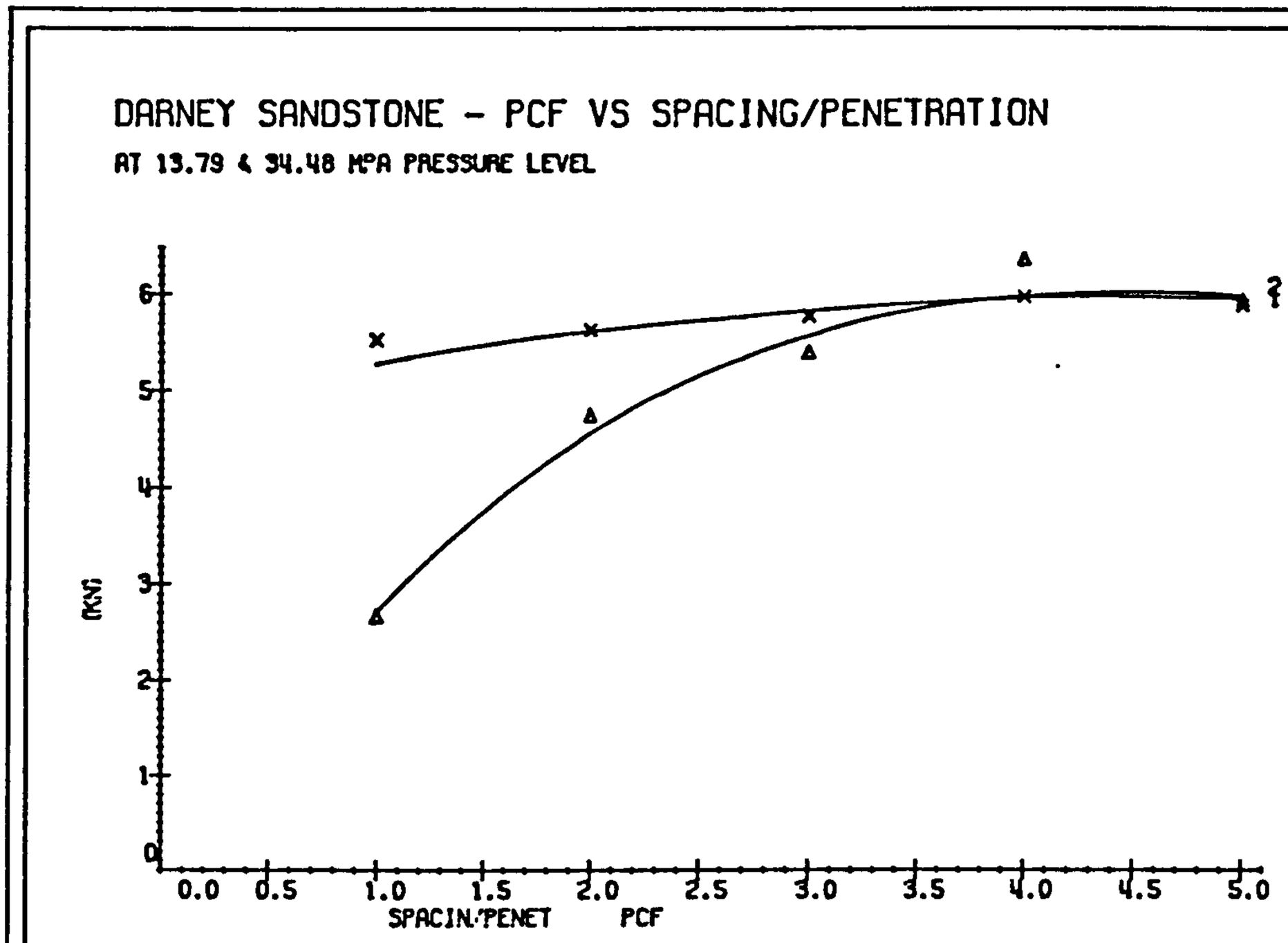
DARNEY SANDSTONE - PCF VS SPACING/PENETRATION
AT 13.79 & 34.48 MPA PRESSURE LEVEL
PCF (KN)
0
1
2
3
4
5
6
0.0
0.5
1.0
1.5
2.0
2.5
3.0
3.5
4.0
4.5
5.0
SPACIN./PENET

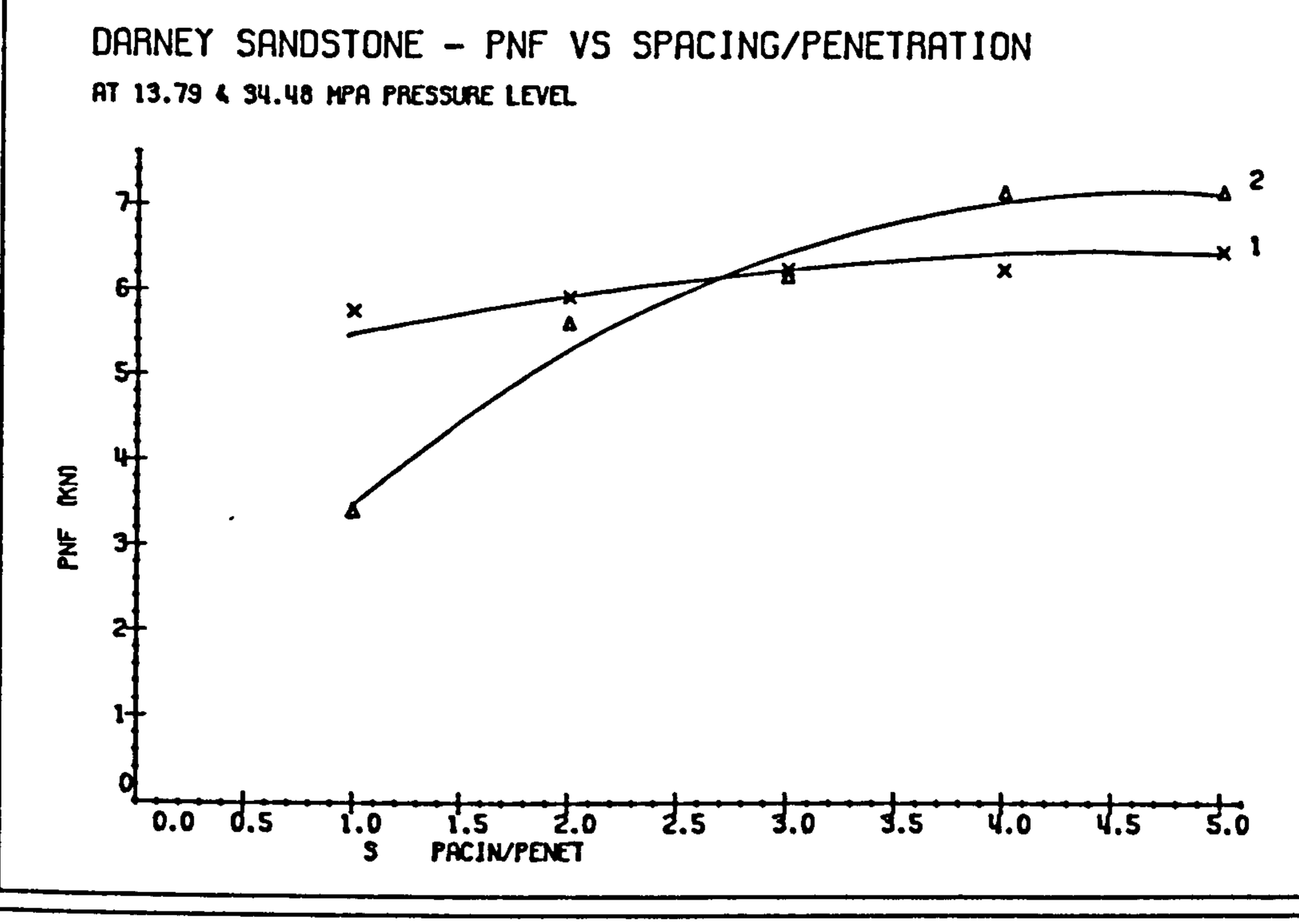
DARNEY SANDSTONE - PNF VS SPACING/PENETRATION
AT 13.79 & 34.48 MPA PRESSURE LEVEL
PNF (KN)
0
1
2
3
4
5
6
7
1
2
0.0
0.5
1.0
1.5
2.0
2.5
3.0
3.5
4.0
4.5
5.0
S
PACIN/PENET

FIG. 7.30

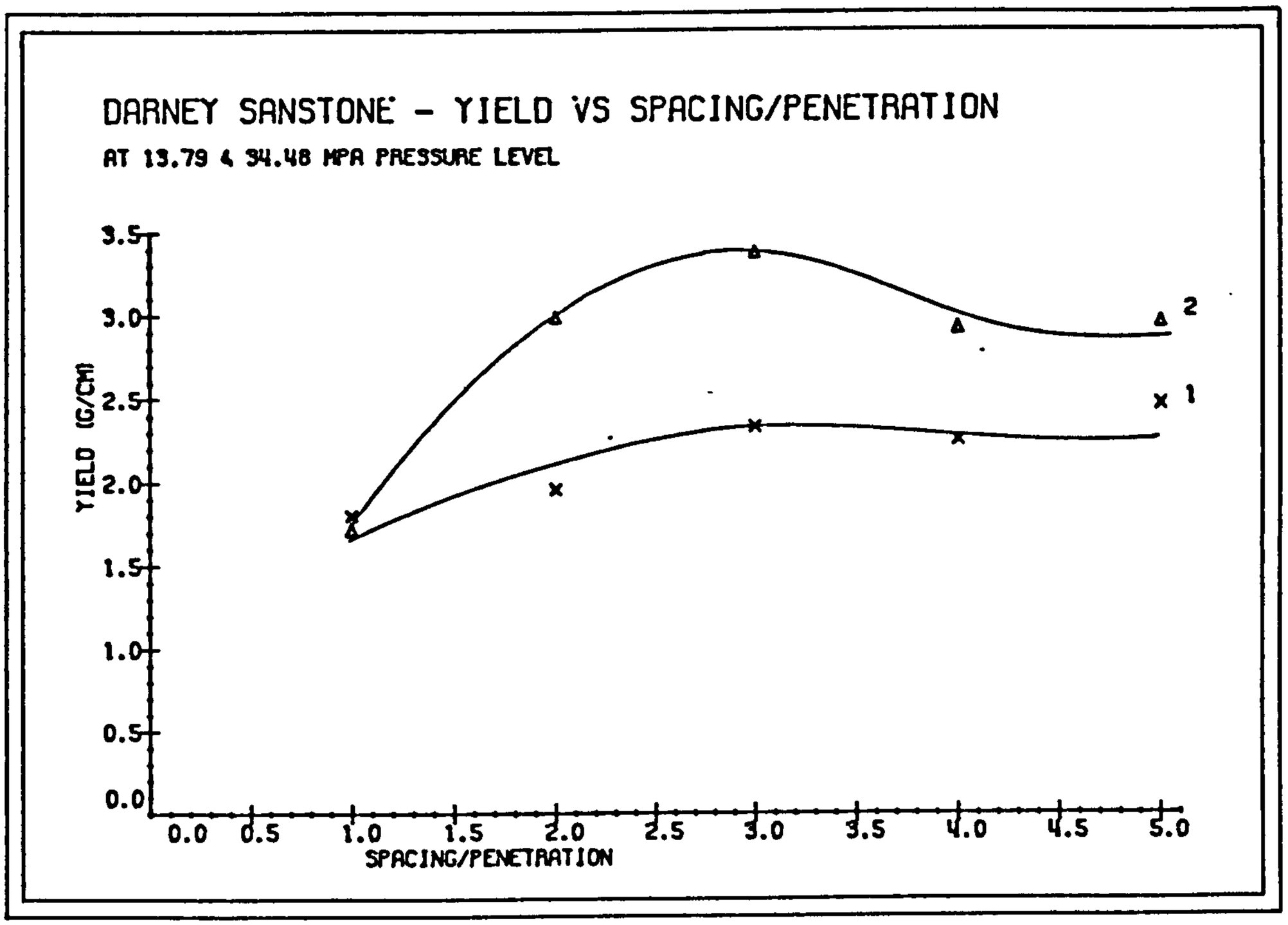
DARNEY SANSTONE - YIELD VS SPACING/PENETRATION
AT 13.79 & 34.48 MPA PRESSURE LEVEL
YIELD (G/CM)
3.5
3.0
2.5
2.0
1.5
1.0
0.5
0.0
0.0 0.5 1.0 1.5 2.0 2.5 3.0 3.5 4.0 4.5 5.0
SPACING/PENETRATION
1
2

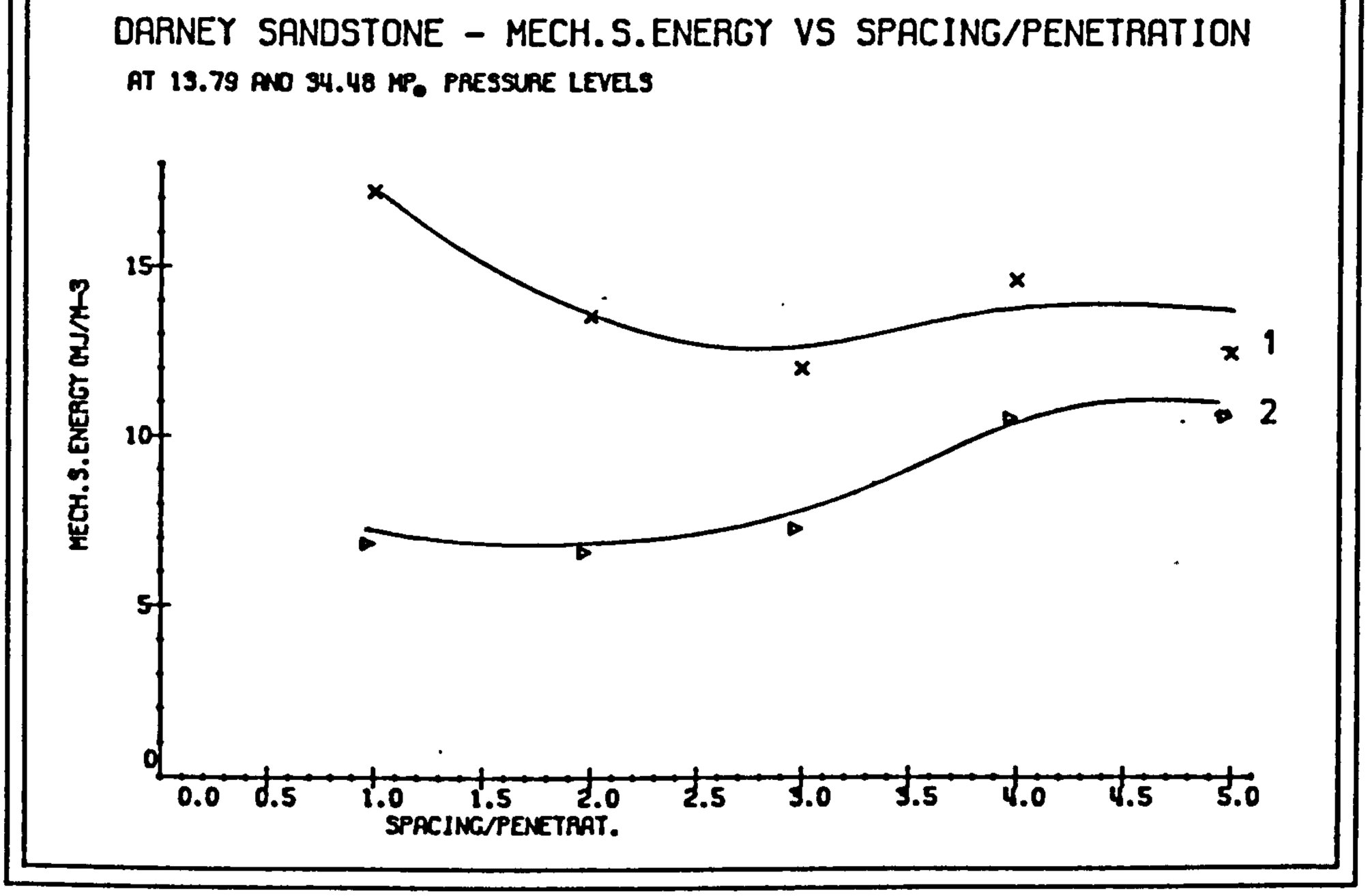
DARNEY SANDSTONE - MECH.S.ENERGY VS SPACING/PENETRATION
AT 13.79 AND 34.48 MP. PRESSURE LEVELS
MECH.S.ENERGY (MJ/M-3
15
10
5
0
0.0 0.5 1.0 1.5 2.0 2.5 3.0 3.5 4.0 4.5 5.0
SPACING/PENETRAT.
1
2

FIG. 7.31

7.4.2 Discussion

Cutting tools in practice do not operate in isolation but are required to work together. Hence, the optimal positioning of tools must be derived for an array to minimize specific energy and maximize yield and debris size.

The first tool in an array operates as a single tool in isolation and succeeding tools should be able to exploit the new free faces created in the surface of the rock by breaking into grooves produced by the initial tools. The optimal spacing is a function of tool shape, rock break-out angle and varies with depth of cut, (Plate 12).

When close spacing is employed, each tool may partially operate in the groove cut by the previous tool and the specific energy of the whole tool array may be high, approaching a maximum when the swept cutting area of following tool approaches zero. When wide spacing is employed between tools, there is no interaction and each tool may be considered to be cutting in isolation. The specific energy of the array will be equal to the sum of the individual tool specific energies. Somewhere between these two extreme cases there is likely to be an optimum position for the spacing where the specific energy is minimized.

A mechanical tool excavates a volume of rock greater than its shape. The angle of break-out(side splay) is approximately 70 degrees. However, high pressure water jet cuts a rectangular slot with no sidesplay. The

Water Jet Leading in Front

PLATE 12 - At The Side of Tool

width of the groove is dependent on the nozzle diameter and the stand-off distance and the depth is dependent on the energy of the jet.

The water jet pressure was found to be the controlling factor on the effect of side-off distance on the parameters under investigation. Essentially changing the jet pressure have resulted in different depths of jet penetration and the effect of side-off distance was more pronounced at deeper depths.

Small increases in the cutting and normal forces were obtained with increasing side-off distance, when the jet penetration depth was small in comparison to the mechanical tool depth of cut. However, when the jet penetration depth was equal with the mechanical tools, forces acting on the tool increased rapidly at a decreasing rate and reached a constant value after s/d>4 when both components were operating in isolation.

Because the groove left behind by a high pressure water jet has no side splay the optimum spacing between the jet and the mechanical tool is less than the optimum spacing between two mechanical tools, (Fig 7.32,7.33).

The optimum spacing, where the mechanical specific energy had its lowest value and yield had its maximum, was at a s/d ratio of 3 for Darney and 3.32 for Springwell Sandstones. Mechanical tool spacing experiments were conducted on Dumfries Sandstone in the past and these revealed that the minimum specific energy occurred at spacing/depth of cut ratios between 4.5 to 5. If this magnitude is taken to be the same with other

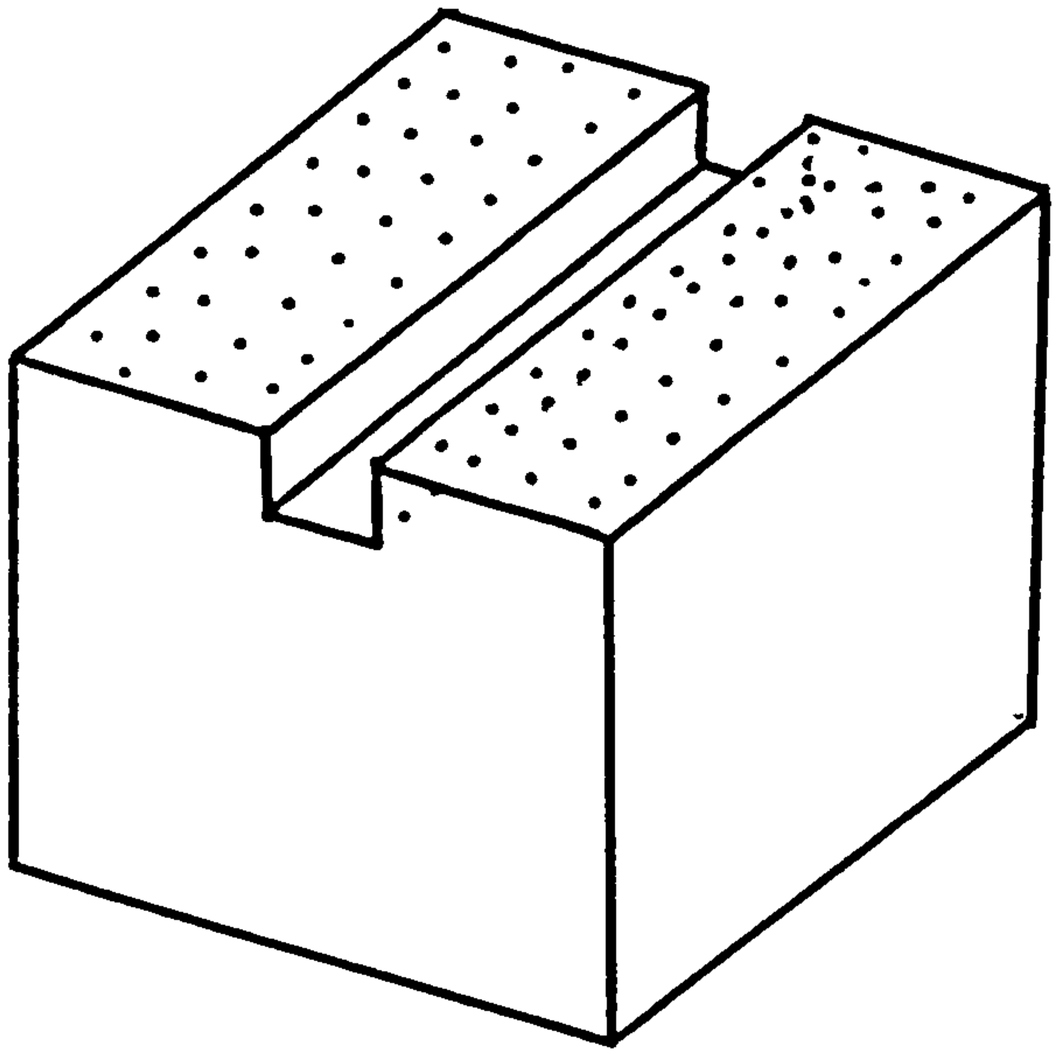

CLOSE SPACING (complete removal of the debris)

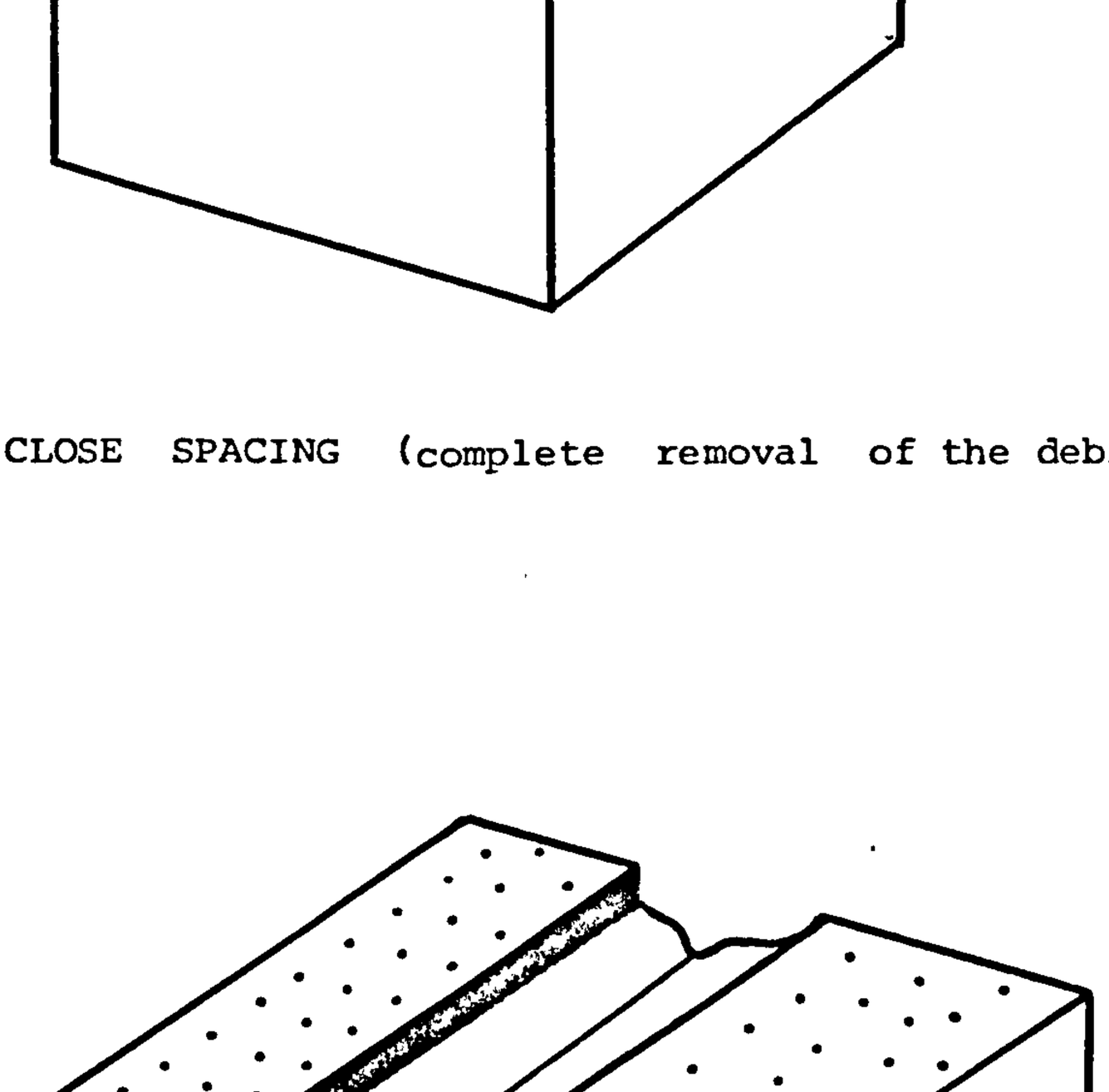

FIG. 7.32 - OPTIMAL SPACING (maximum interaction between jet and tool)

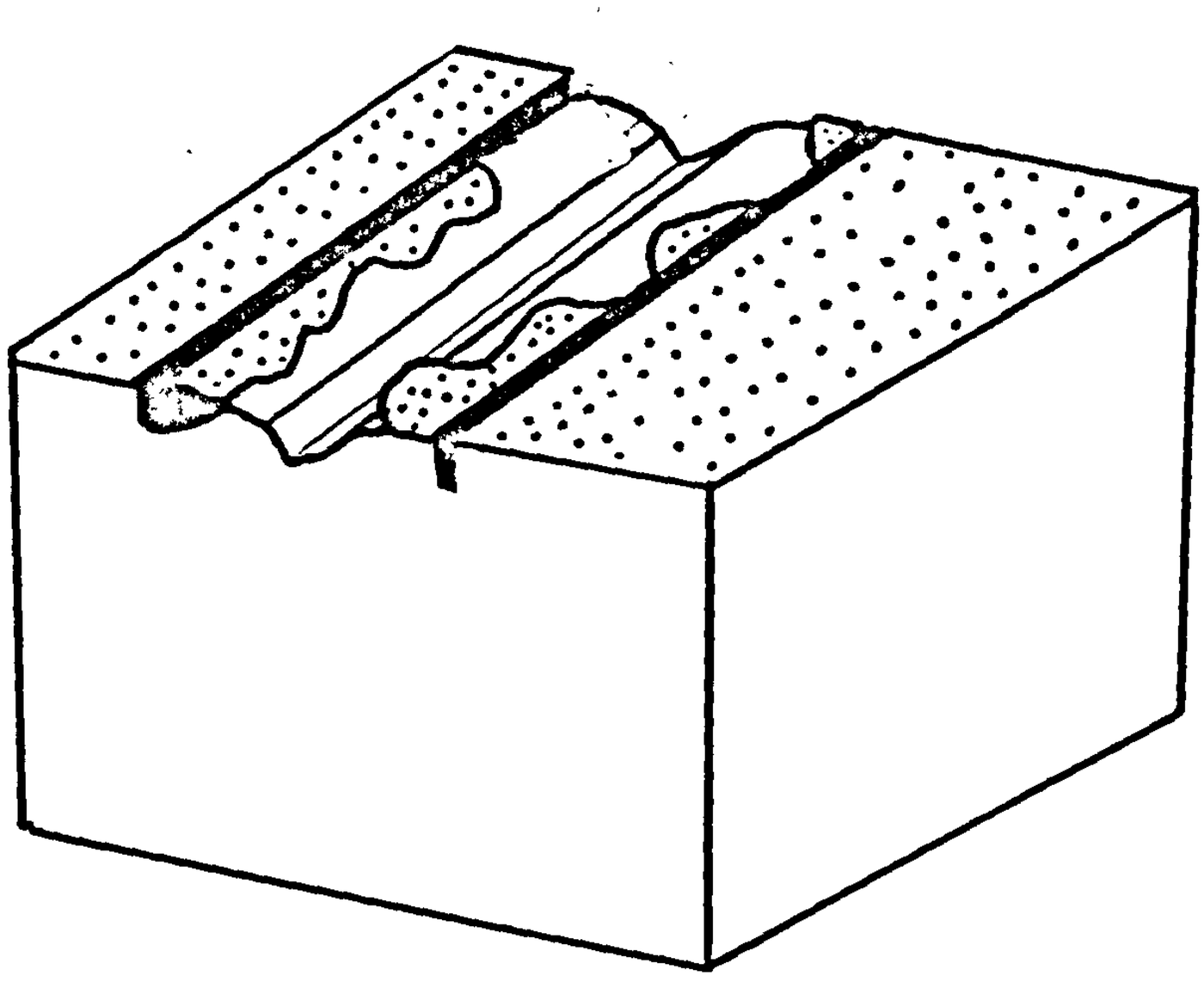

WIDE SPACING (Little interaction taking place)

FIG. 7.33

sandstones, having water jets between tools as opposed to two mechanical tools, reduces the effective s/d ratio by a factor of 1.45. The experimental results had shown that for a similar s/d ratio higher tool forces were experienced at shallow depths of jet penetration.

A finite element stress analysis was carried out to map out the area of influence of a mechanical tool tip as shown in (Figure 7.34). The direction of cutting was perpendicular and into the paper and the stresses in the area either side of the point attack tool were investigated.

The stress vector plots have revealed that cutting depth of mechanical tool has a strong influence on the area. At deeper depths more force is needed to initiate and propagate the fracture of the rock and hence the stressed area increases with increasing tool depth. Assuming the rock is homogenous and there is no bedding, when the water jet is placed somewhere over this stressed region at an optimum position, it would cause a change in the distribution of stress in the rock, (Fig 7.35-7.40). Therefore, the effect of the water jet when it is placed between mechanical cutters is to create free surfaces to which the mechanical tools will break the rock into. The width of slot has little or no significance. Therefore, narrower jets at high pressures may be used at this location to conserve energy.

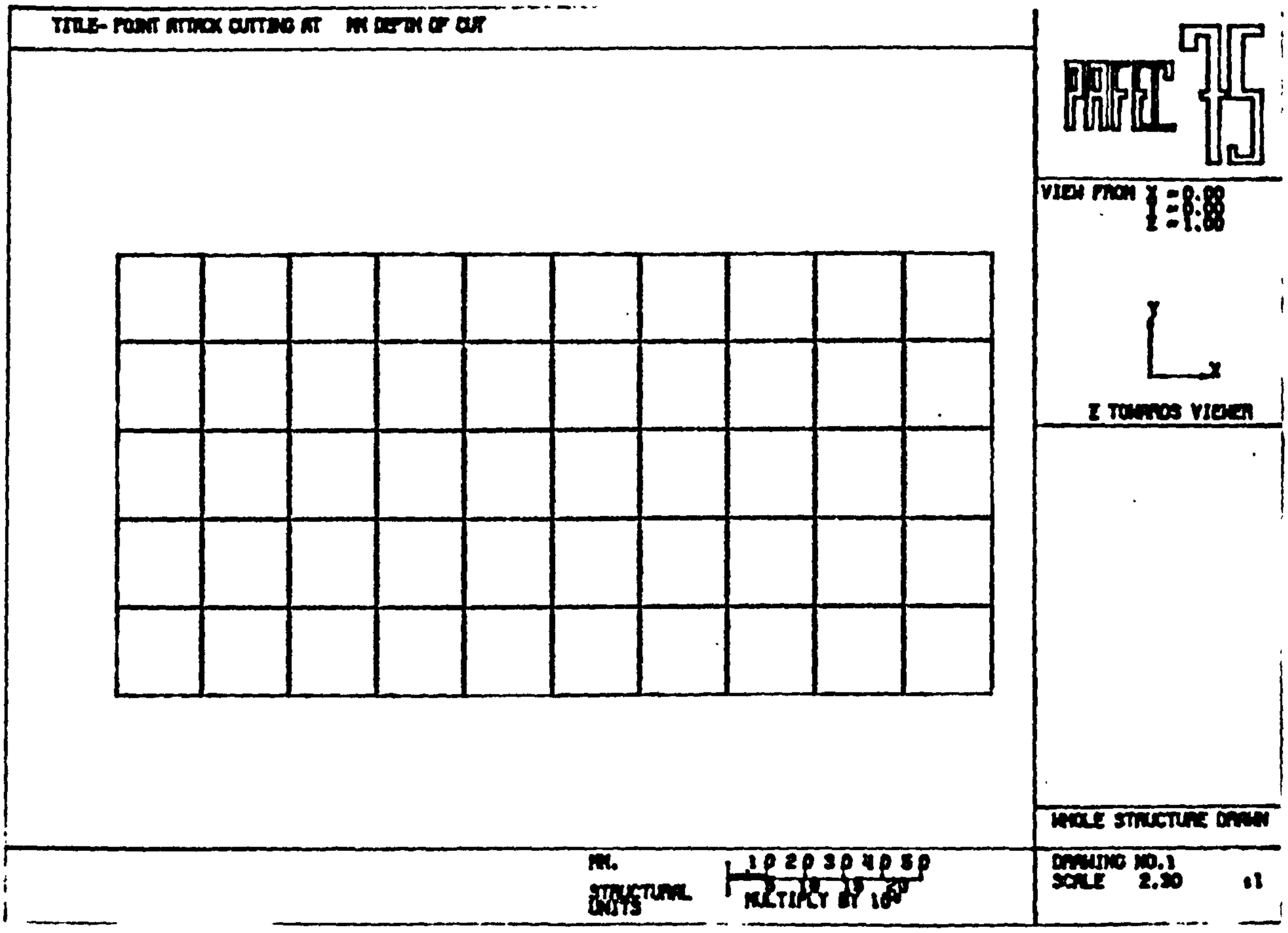
TITLE- POINT ATTACK CUTTING AT MM DEPTH OF CUT
PARTEC 75
VIEW FROM
Y
X
Z TOWARDS VIEWER
WHOLE STRUCTURE DRAWN
DRAWING NO.1
SCALE 2.30
MM.
STRUCTURAL UNITS
1.0 2.0 3.0 4.0 5.0
MULTIPLY BY 10
TITLE- POINT ATTACK CUTTING AT 10MM DEPTH OF CUT
PARTEC 75
VIEW FROM
Y
X
Z TOWARDS VIEWER
WHOLE STRUCTURE DRAWN
DRAWING NO.1
SCALE 2.30
MM.
STRUCTURAL UNITS
1.0 2.0 3.0 4.0 5.0
MULTIPLY BY 10

FIG. 7.34

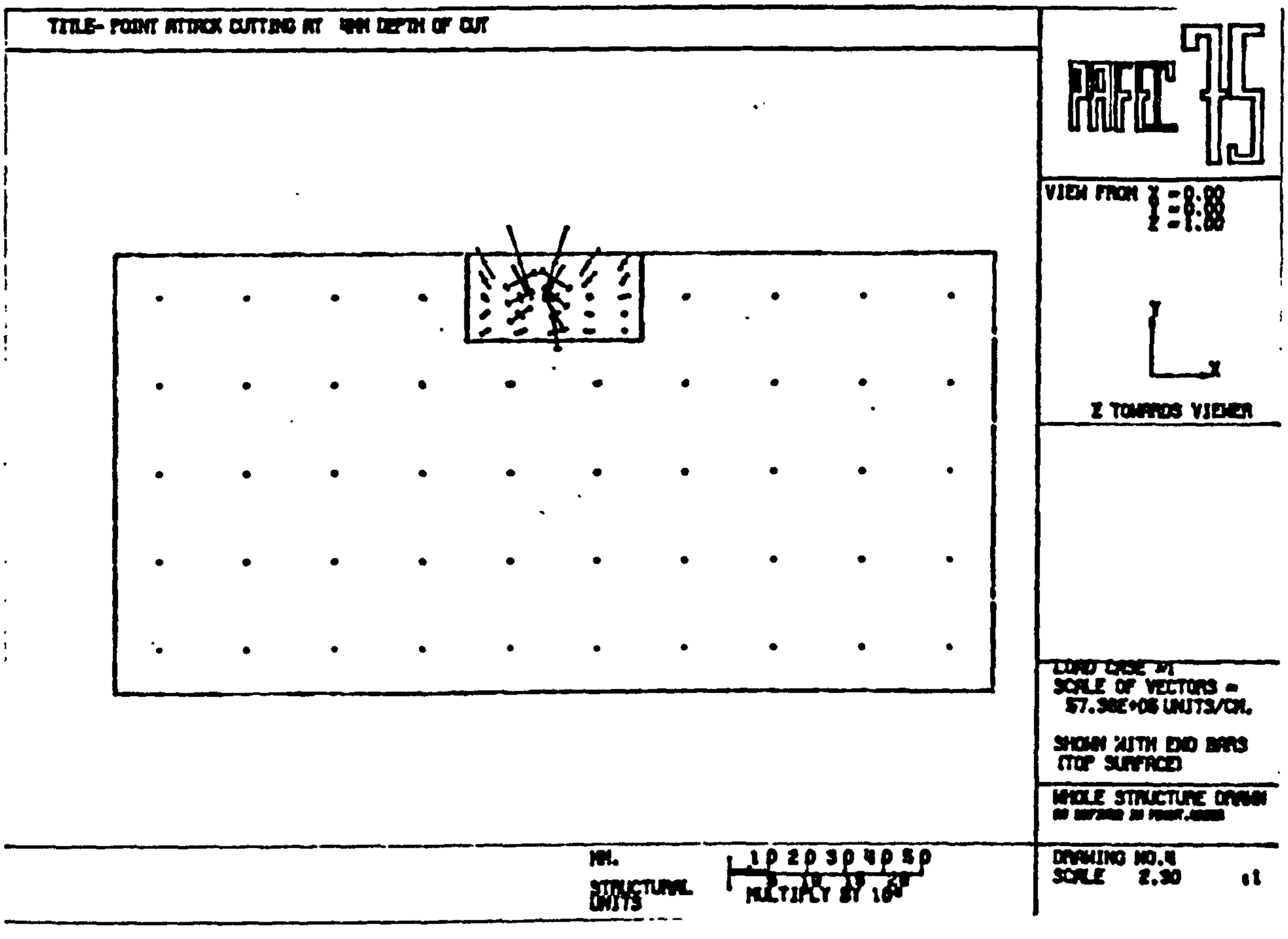
TITLE- POINT ATTACK CUTTING AT MM DEPTH OF CUT
PREFEC 75
VIEW FROM X = 0.00
Z = 1.00
Y
X
Z TOWARDS VIEWER
LOAD CASE #1
SCALE OF VECTORS =
57.38E+06 UNITS/CM.
SHOWN WITH END BARS
(TOP SURFACE)
WHOLE STRUCTURE DRAWN
MM.
STRUCTURAL UNITS
1.0 2.0 3.0 4.0 5.0
MULTIPLY BY 10
DRAWING NO.4
SCALE 2.30

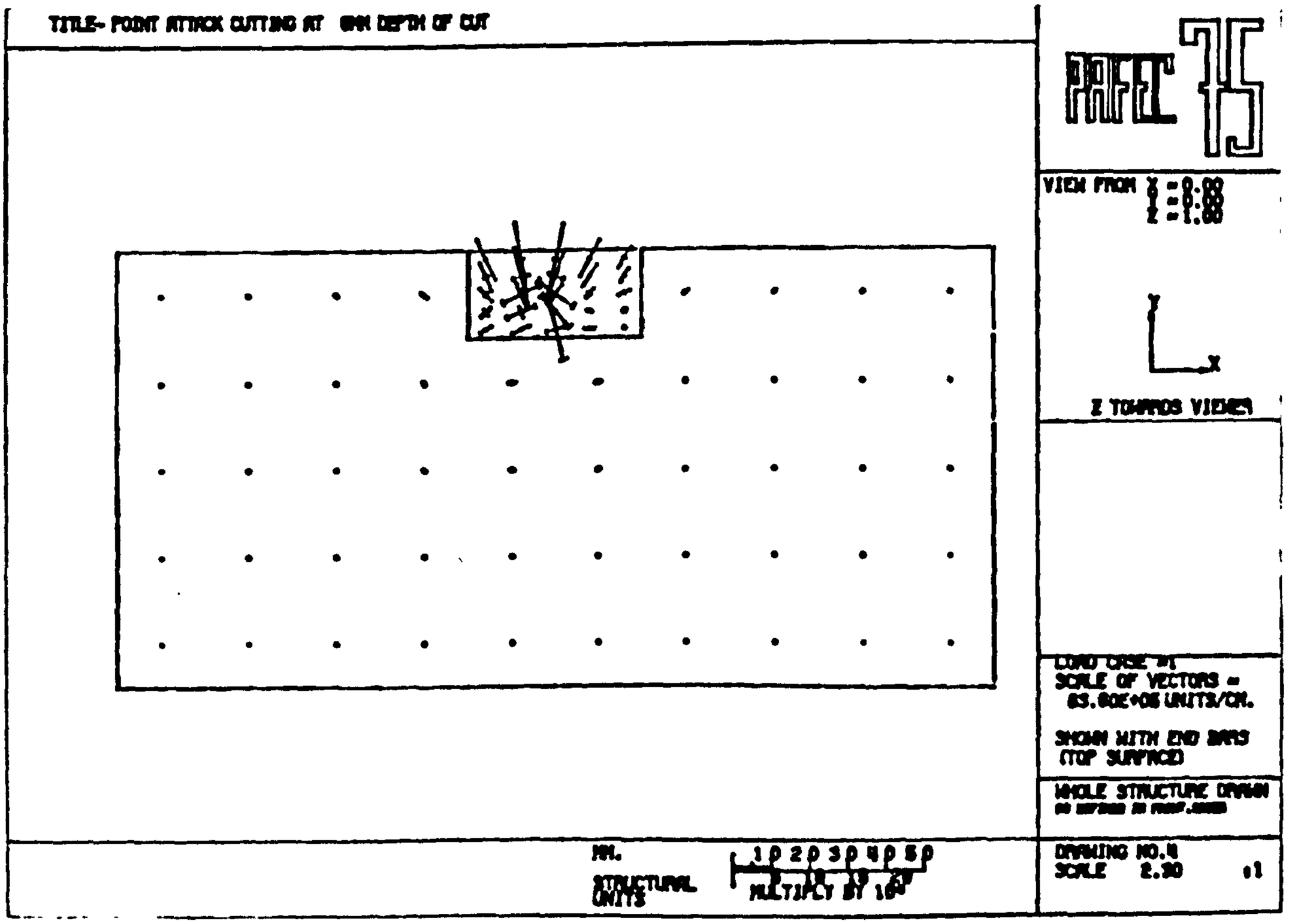
TITLE- POINT ATTACK CUTTING AT MM DEPTH OF CUT
PREFEC 75
VIEW FROM X = 0.00
Z = 1.00
Y
X
Z TOWARDS VIEWER
LOAD CASE #1
SCALE OF VECTORS =
83.80E+06 UNITS/CM.
SHOWN WITH END BARS
(TOP SURFACE)
WHOLE STRUCTURE DRAWN
MM.
STRUCTURAL UNITS
1.0 2.0 3.0 4.0 5.0
MULTIPLY BY 10
DRAWING NO.4
SCALE 2.30

FIG. 7.35

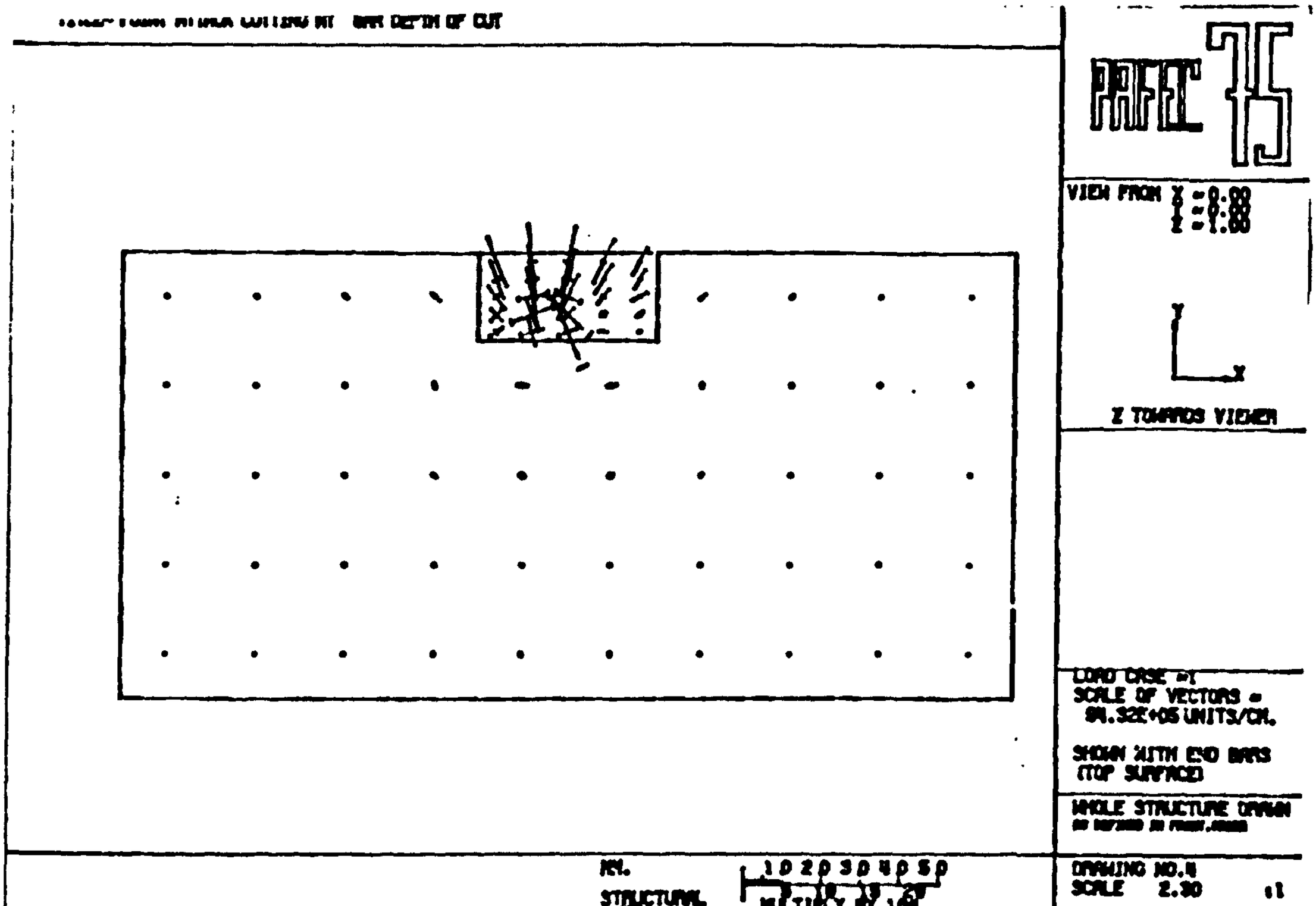
PAFEC 75
VIEW FROM
Y
X
Z TOWARDS VIEWER
LOAD CASE #1
SCALE OF VECTORS =
SHOWN WITH END BARS
(TOP SURFACE)
WHOLE STRUCTURE DRAWN
DRAWING NO.4
SCALE 2.30
STRUCTURAL UNITS
MULTIPLY BY

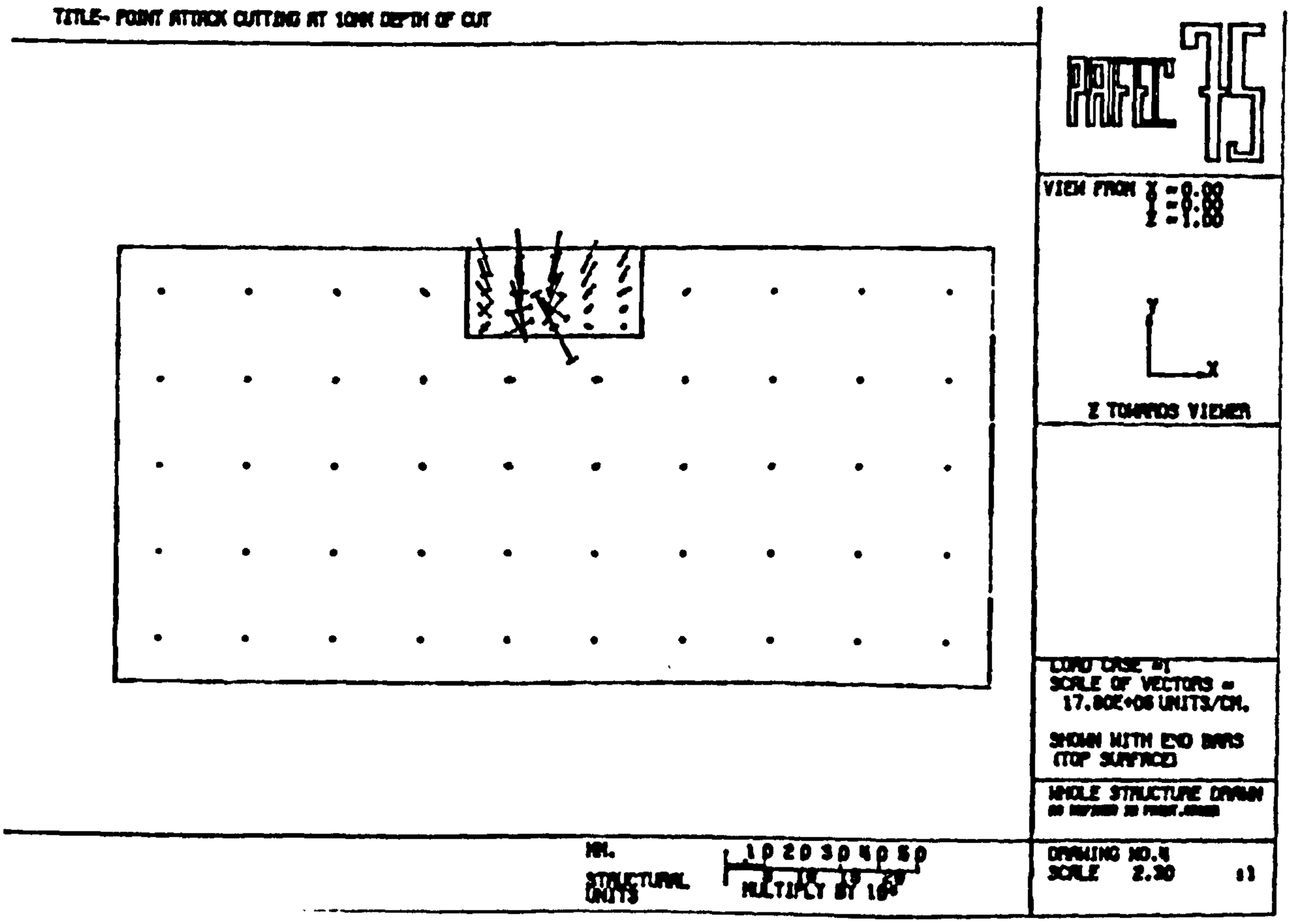
TITLE- POINT ATTACK CUTTING AT 10MM DEPTH OF CUT
PAFEC 75
VIEW FROM
Y
X
Z TOWARDS VIEWER
LOAD CASE #1
SCALE OF VECTORS =
SHOWN WITH END BARS
(TOP SURFACE)
WHOLE STRUCTURE DRAWN
DRAWING NO.4
SCALE 2.30
STRUCTURAL UNITS
MULTIPLY BY

FIG. 7.36

TITLE- POINT ATTACK CUTTING AT [illegible] DEPTH OF CUT

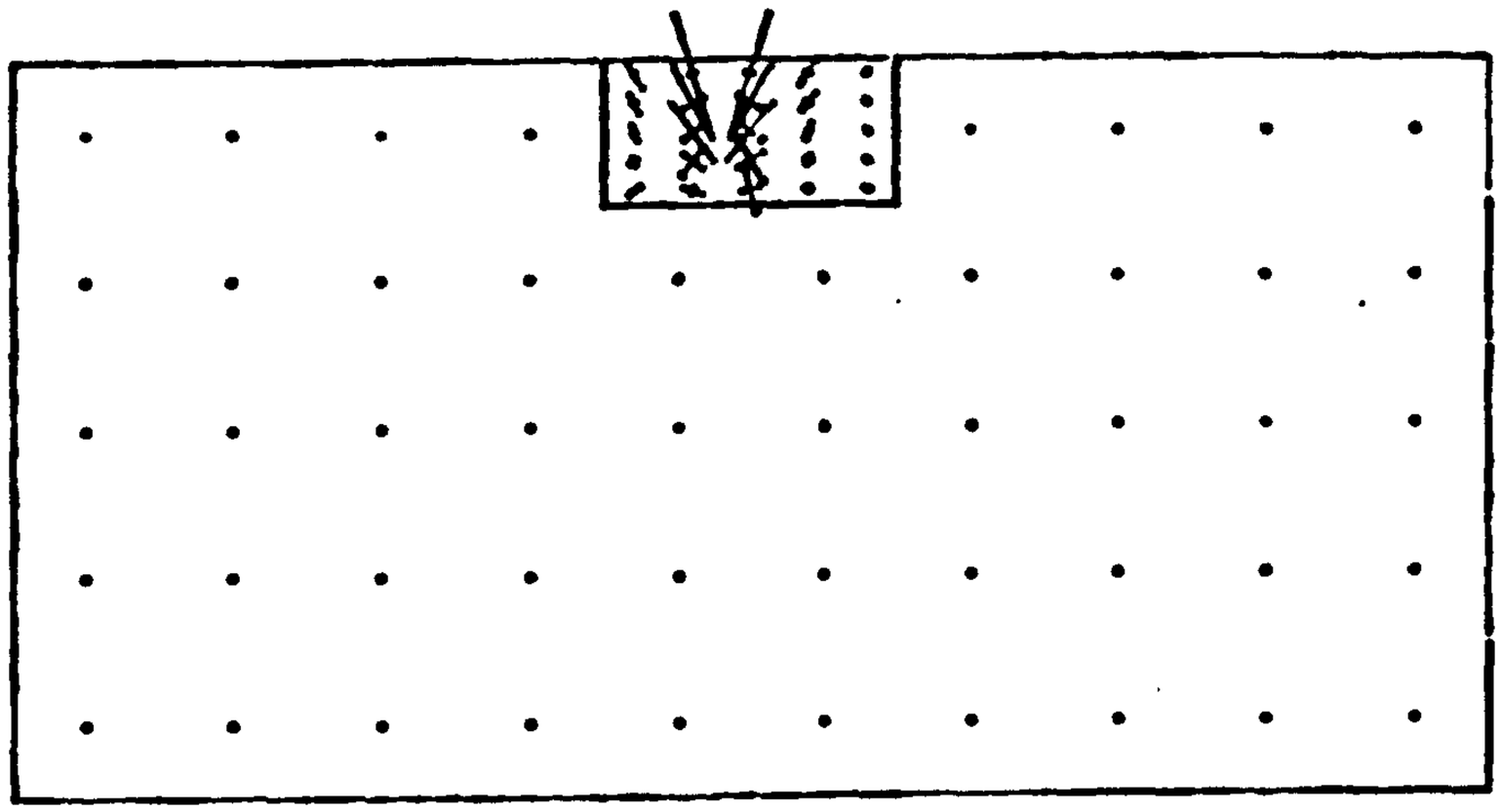

PREFEC 75

VIEW FROM X = 0.00
Z = 1.00

Y
X

Z TOWARDS VIEWER

LOAD CASE #1
SCALE OF VECTORS = 41.78E+05 UNITS/CM.

SHOWN WITH END BARS @MIDDLE SURFACE

WHOLE STRUCTURE DRAWN

MM.
STRUCTURAL UNITS

1 0 2 0 3 0 4 0 5 0
MULTIPLY BY 10^3

DRAWING NO.3
SCALE 2.30 E1

TITLE- POINT ATTACK CUTTING AT [illegible] DEPTH OF CUT

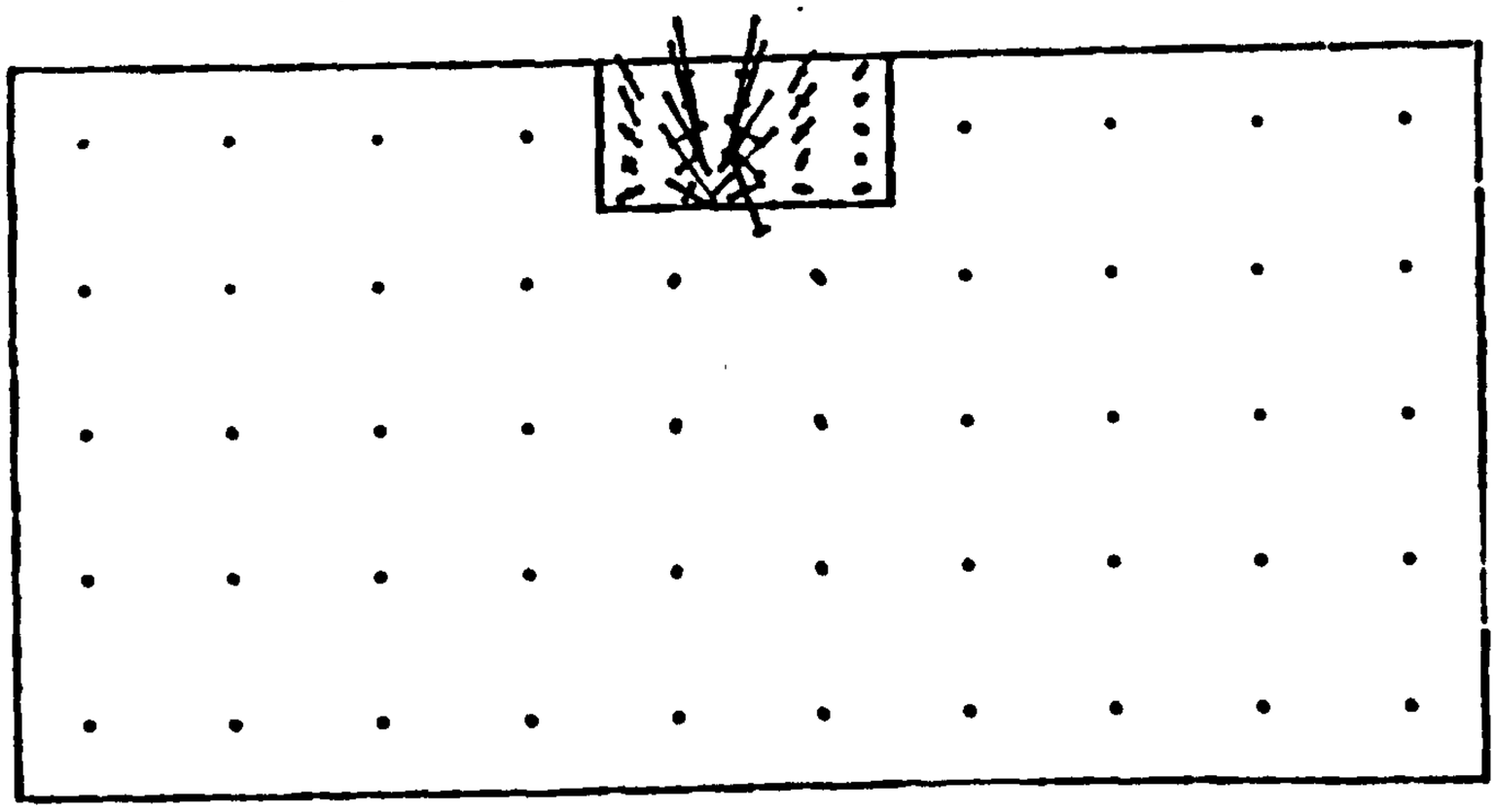

PREFEC 75

VIEW FROM X = 0.00
Z = 1.00

Y
X

Z TOWARDS VIEWER

LOAD CASE #1
SCALE OF VECTORS = 83.74E+05 UNITS/CM.

SHOWN WITH END BARS @MIDDLE SURFACE

WHOLE STRUCTURE DRAWN

MM.
STRUCTURAL UNITS

1 0 2 0 3 0 4 0 5 0
MULTIPLY BY 10^3

DRAWING NO.3
SCALE 2.30 E1

FIG. 7.37

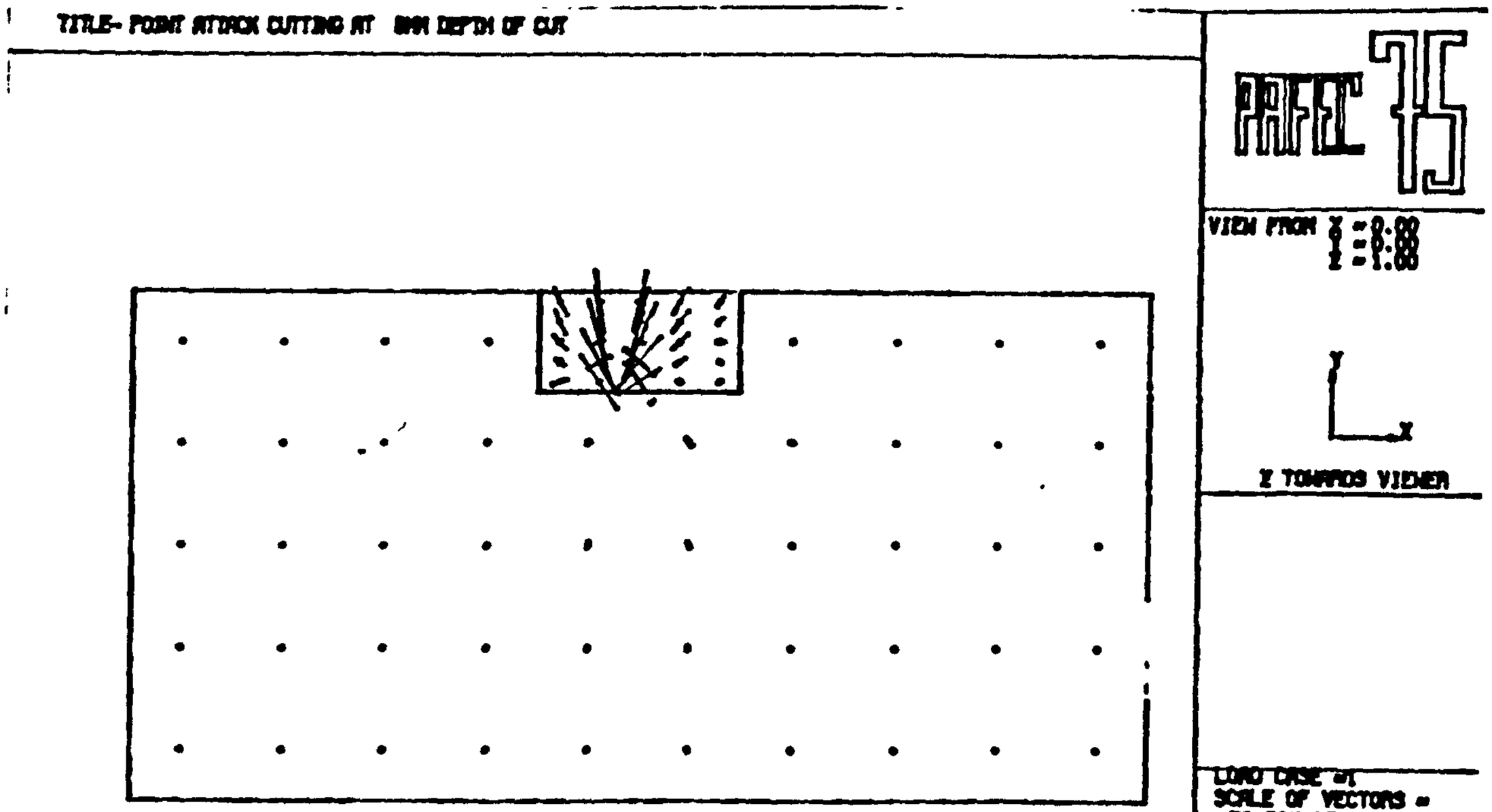
TITLE- POINT ATTACK CUTTING AT 8MM DEPTH OF CUT
PARFEC 7.5
VIEW FROM X = 0.00
Y = 0.00
Z = 1.00
Y
X
Z TOWARDS VIEWER
LOAD CASE #1
SCALE OF VECTORS =
58.58E+06 UNITS/CM.
SHOWN WITH END BARS
(MIDDLE SURFACE)
WHOLE STRUCTURE DRAWN
MM.
STRUCTURAL
UNITS
1.0 2.0 3.0 4.0 5.0
MULTIPLY BY 10
DRAWING NO.3
SCALE 2.30 E1

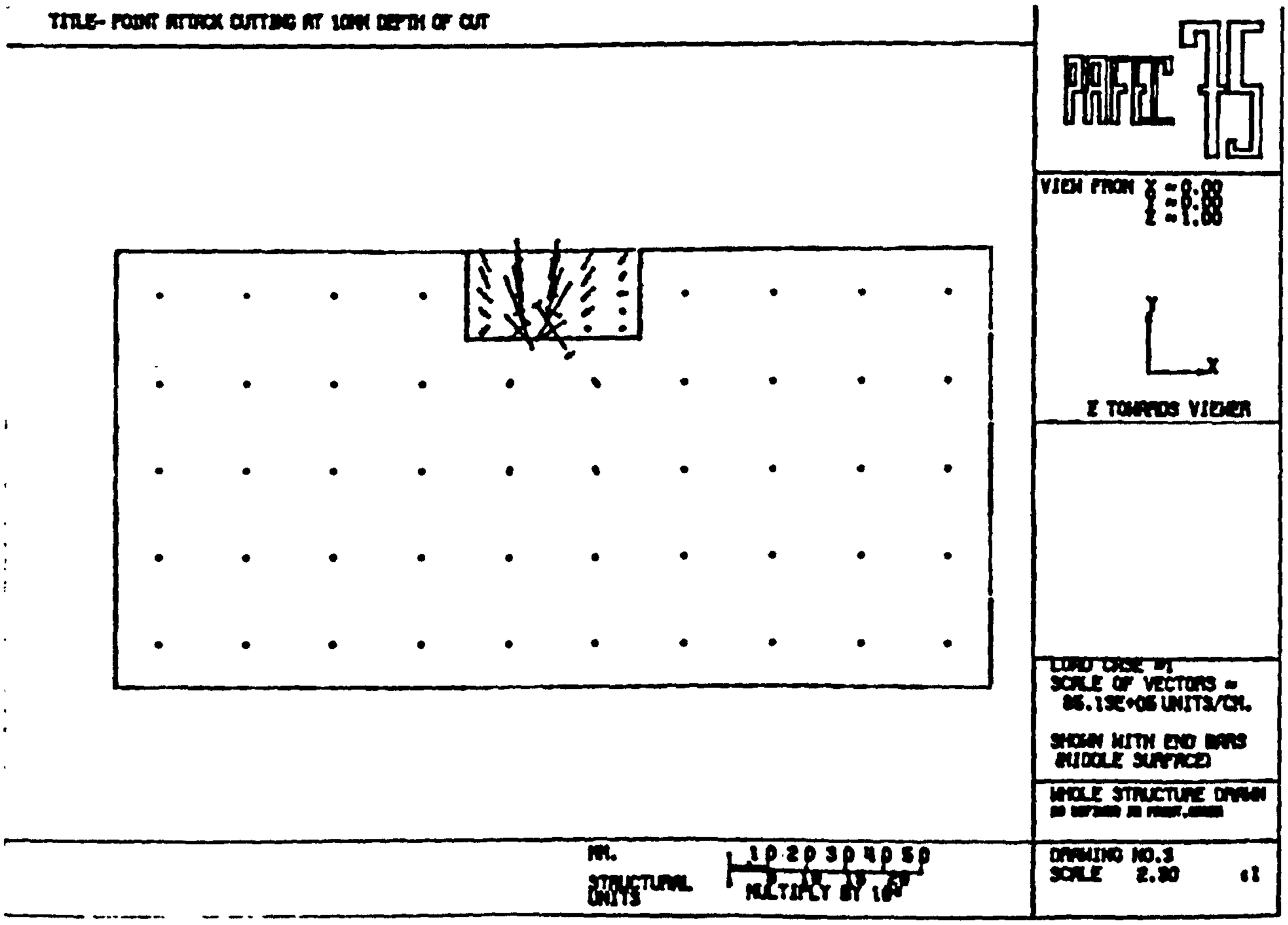
TITLE- POINT ATTACK CUTTING AT 10MM DEPTH OF CUT
PARFEC 7.5
VIEW FROM X = 0.00
Y = 0.00
Z = 1.00
Y
X
Z TOWARDS VIEWER
LOAD CASE #1
SCALE OF VECTORS =
86.19E+06 UNITS/CM.
SHOWN WITH END BARS
(MIDDLE SURFACE)
WHOLE STRUCTURE DRAWN
MM.
STRUCTURAL
UNITS
1.0 2.0 3.0 4.0 5.0
MULTIPLY BY 10
DRAWING NO.3
SCALE 2.30 E1

FIG. 7.38

TITLE- POINT ATTACK CUTTING AT [illegible] DEPTH OF CUT

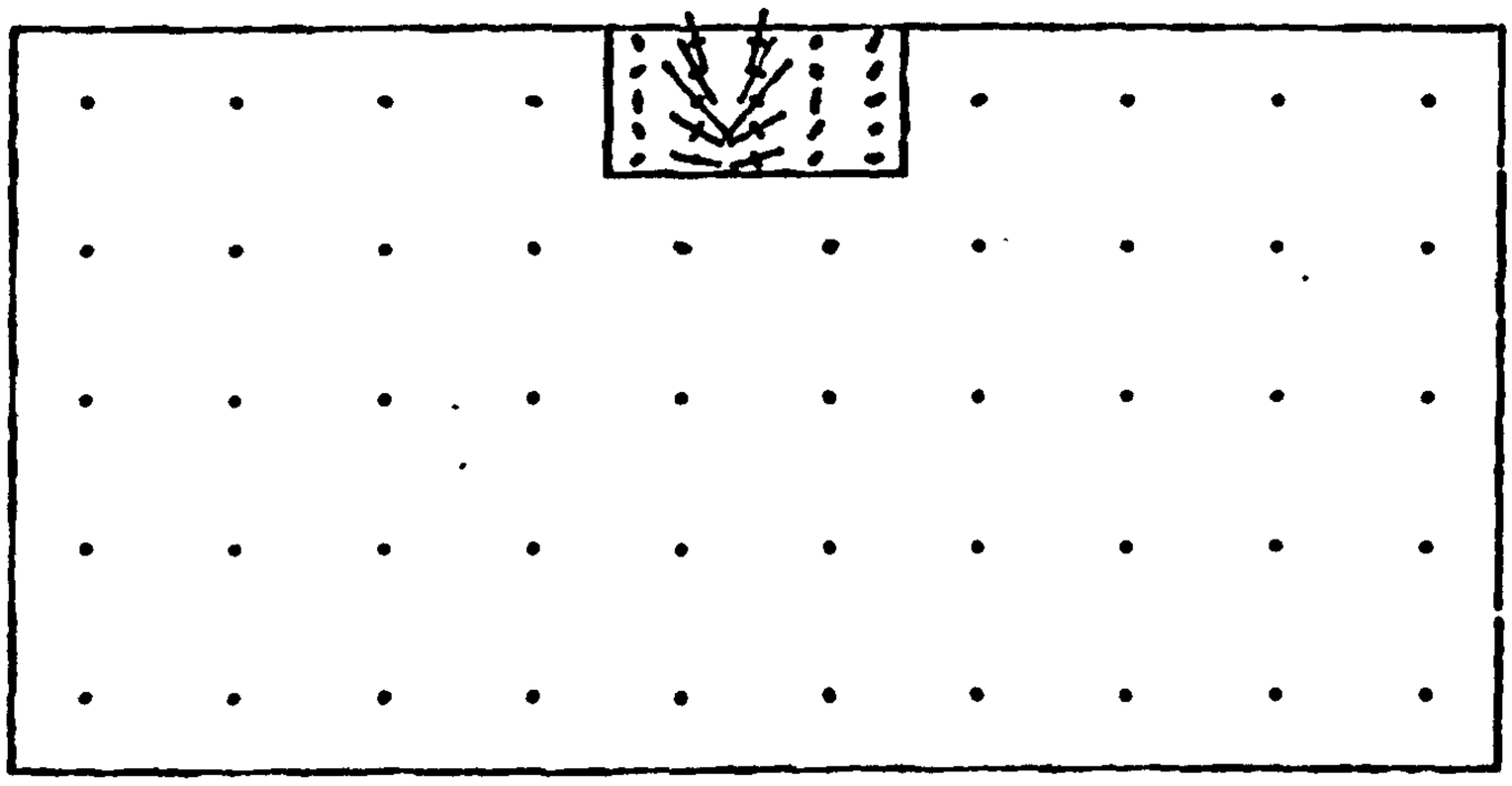

PAFEC 75

VIEW FROM X = 0.00
Z = 1.00

Y
X

Z TOWARDS VIEWER

LOAD CASE #1
SCALE OF VECTORS =
57.36E+05 UNITS/CM.

SHOWN WITH END BARS
(BOTTOM SURFACE)

WHOLE STRUCTURE DRAWN
[illegible]

MM.
STRUCTURAL UNITS

1.0 2.0 3.0 4.0 5.0
MULTIPLY BY 10^[illegible]

DRAWING NO.5
SCALE 2.30 #1

TITLE- POINT ATTACK CUTTING AT [illegible] DEPTH OF CUT

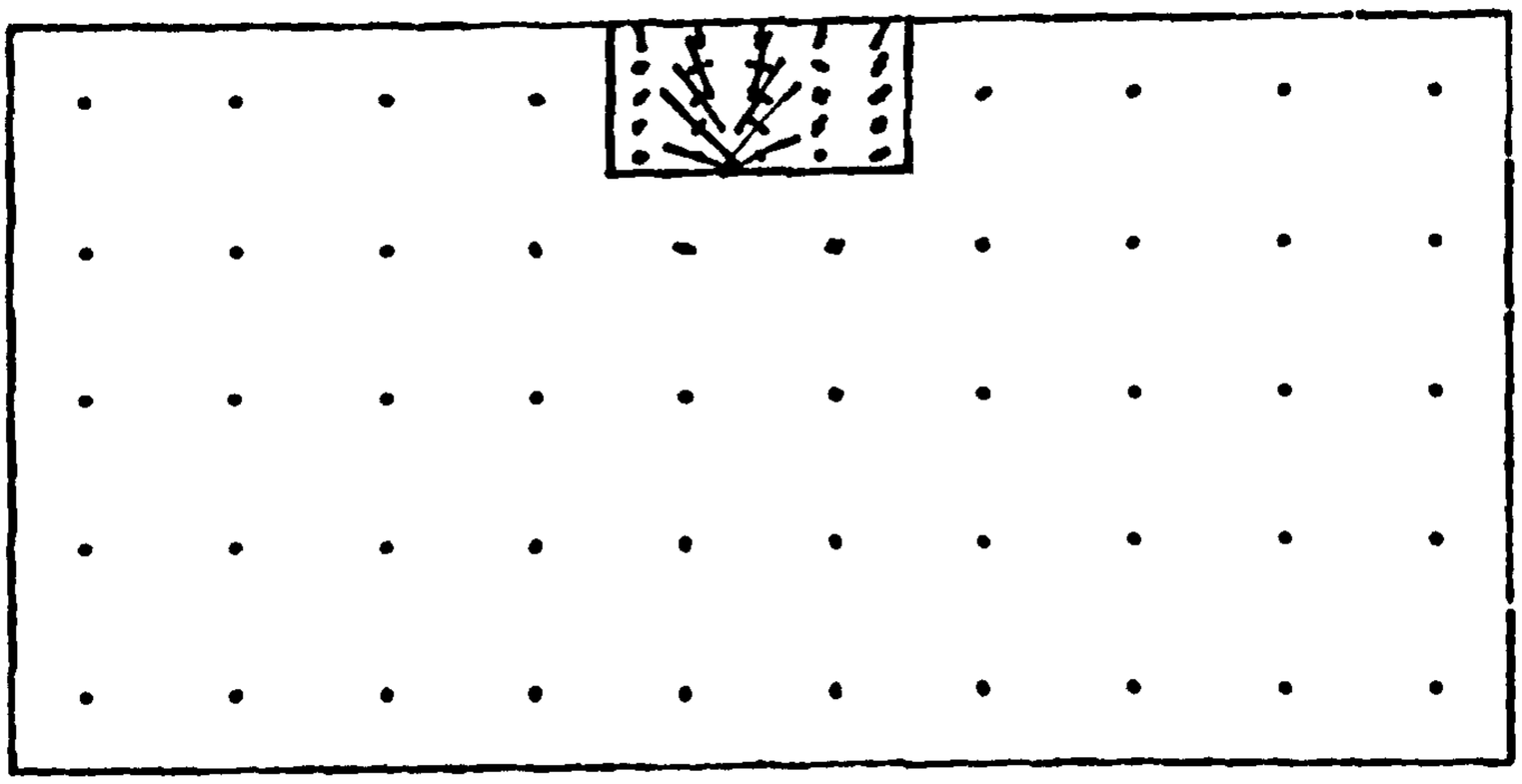

PAFEC 75

VIEW FROM X = 0.00
Z = 1.00

Y
X

Z TOWARDS VIEWER

LOAD CASE #1
SCALE OF VECTORS =
83.80E+05 UNITS/CM.

SHOWN WITH END BARS
(BOTTOM SURFACE)

WHOLE STRUCTURE DRAWN
[illegible]

MM.
STRUCTURAL UNITS

1.0 2.0 3.0 4.0 5.0
MULTIPLY BY 10^[illegible]

DRAWING NO.5
SCALE 2.30 #1

FIG. 7.39

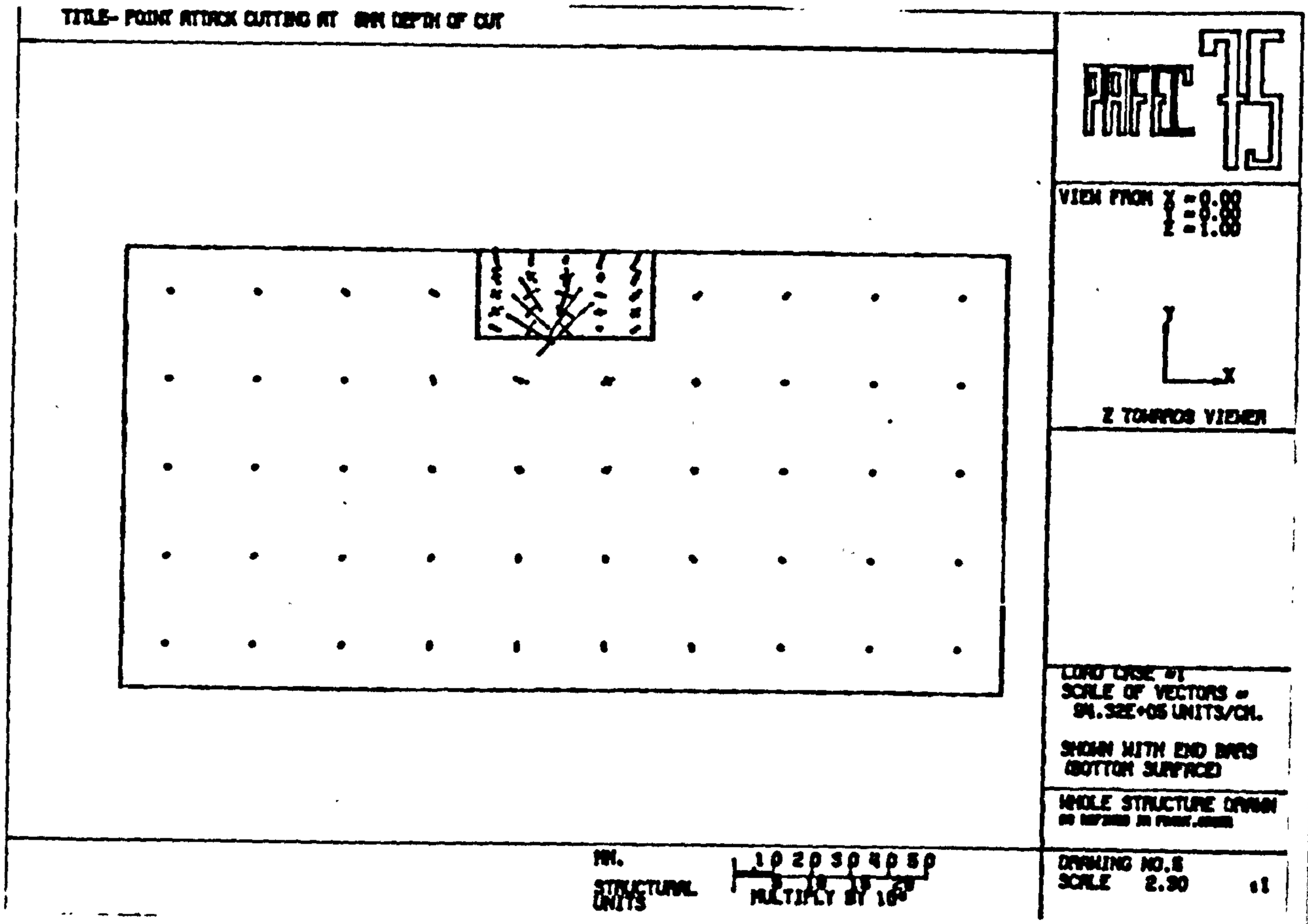
TITLE- POINT ATTACK CUTTING AT 60% DEPTH OF CUT
PAFEC 75
VIEW FROM X = 0.00
Y = 0.00
Z = 1.00
Y
X
Z TOWARDS VIEWER
LOAD CASE #1
SCALE OF VECTORS = 94.32E+05 UNITS/CM.
SHOWN WITH END BARS (BOTTOM SURFACE)
WHOLE STRUCTURE DRAWN
MM.
STRUCTURAL UNITS
1 0 2 0 3 0 4 0 5 0
MULTIPLY BY 10
DRAWING NO.5
SCALE 2.30 :1

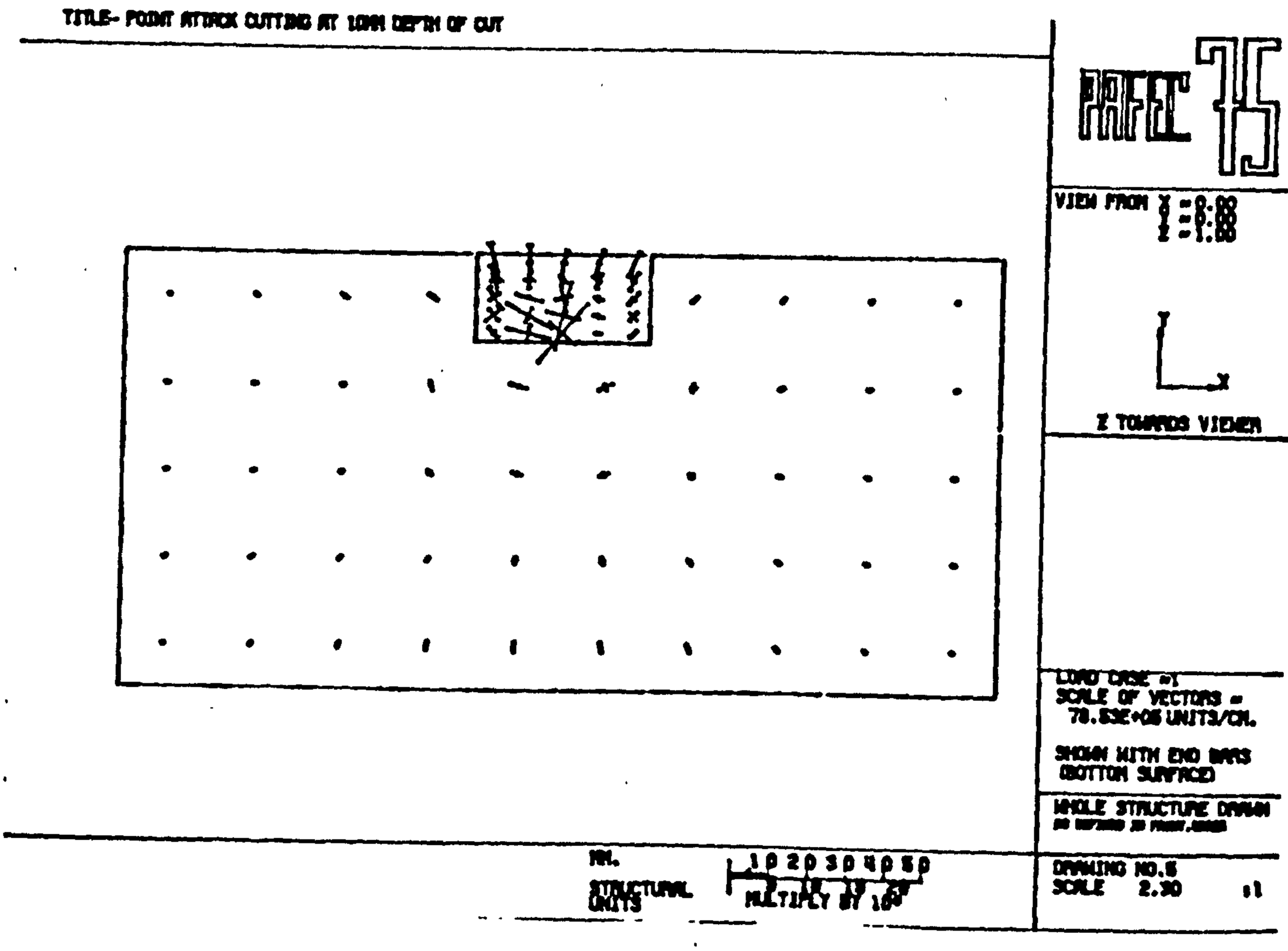
TITLE- POINT ATTACK CUTTING AT 100% DEPTH OF CUT
PAFEC 75
VIEW FROM X = 0.00
Y = 0.00
Z = 1.00
Y
X
Z TOWARDS VIEWER
LOAD CASE #1
SCALE OF VECTORS = 78.83E+05 UNITS/CM.
SHOWN WITH END BARS (BOTTOM SURFACE)
WHOLE STRUCTURE DRAWN
MM.
STRUCTURAL UNITS
1 0 2 0 3 0 4 0 5 0
MULTIPLY BY 10
DRAWING NO.5
SCALE 2.30 :1

FIG. 7.40

7.4.3 Conclusions

The jet penetration consequently the jet pressure has a major influence on operating efficiency of the hybrid cutting system. Experiments conducted on Darney Sandstone, at two pressures indicate that the water jet should penetrate the rock to a depth equal with mechanical tools, if jets are placed between the mechanical cutters.

Cutting and Normal Forces have increased at a decreasing rate with increase in side-off distance/depth of cut ratio. Yield increased to a maxima then dropped off to a constant value and Mechanical Specific Energy decreased -indicating an increase in efficiency- down to a minima, at an s/d ratio of 3 for Darney Sandstone and 3.32 for Springwell Sandstone, then started to increase again up to a constant value at which it ran parallel to the horizontal axis.

The effect of jets placed between mechanical tools is to create free surfaces for mechanical tools to break the rock into. The effective s/d ratio was reduced by a factor of 1.44 when the jet was placed between cutters as opposed to mechanical tools cutting without jets.

7.5 LEAD-ON DISTANCE

The influence of the location of the water jet nozzle placed between mechanical cutters, in which the mechanical cutters removed the rib of rock left behind by traversing water jets, was dealt with previously. Alternatively, water jets may be located so as to lead the mechanical tool, impacting the rock surface right in front of the cutter. The mode of rock breakage was thought to be different from the nozzle located between the cutters and experiments were designed to show if this was so, (Plate 12).

Springwell sandstone experiments were planned to yield the minimum distance by which the water jets should lead the tool to reduce forces when the nozzles are placed between the mechanical cutters. Experimental variables and their levels are tabulated below:

Variable		Level
Depth of cut	(mm)	6
Side-off distance	(mm)	20
Stand-off distance	(mm)	45
Nozzle diameter	(mm)	0.85
Traverse speed	(mm/sec)	94
Water jet pressure	(MPa)	34.48
Lead-on distance	(mm)	2, 5, 8, 11, 14

Darney sandstone experiments were designed primarily to find the effect of the alternative nozzle position at which water jets and mechanical tools cut along the same path, the distance at which nozzles lead the mechanical tools subject to change. It was thought before the experiments were carried out that the penetration depth of water jets might have an influence on the optimum lead-on distance. Therefore, the water jet pressure levels were chosen such that, at one level it penetrated the rock less than, and at the other level it penetrated to a depth equal with the mechanical tools. Experimental variables and their levels were as follows:

Variable	Level
Depth of cut (mm)	7
Stand-off distance (mm)	45
Side-off distance (mm)	0
Nozzle diameter (mm)	0.85
Traverse speed (mm/sec)	165
Water jet pressure (MPa)	27.58, 41.37
Lead-on distance (mm)	1, 3, 5, 7, 9

Each experiment was repeated four times and carried out in random order. Overall, 2 x 5 x 4 = 40 tests were conducted on Darney sandstone.

7.5.1 Effect of Lead-on Distance

Springwell Sandstone :

On Tool Forces

Cutting normal and sideways forces all decreased with increasing lead-on distance (Figures 6.15,6.16). Forces slowly approached to a constant value after which no more reduction have occurred.

On Yield

Increasing lead-on distance has caused a small increase in yield, (Figure 6.17). However, the magnitude of this increase was very small. Therefore, it may be assumed that, within limits, yield remained constant.

On Mechanical Specific Energy

Mechanical Specific Energy decreased at a decreasing rate, reaching to a constant value after the last level, with increase in lead-on distance. The relationship between parameters was of exponential type.

Darney Sandstone

On Tool Forces

Mechanical tool forces have exhibited differring relationships at varied depths of jet penetration. The tool forces(cutting and normal) remained approximately constant and curves ran parallel to the axis when the water jet pressure has penetrated to a depth equal to or more than the mechanical tools, (Figure 7.41). But, when the water jet penetrated the rock less than the mechanical tool depth of cut, rather an interesting relationship was observed. (Figure 7.42) All the tool forces increased rapidly with increasing lead-on distance. Much of the increase took place between the first three experimental levels and curves have shown tendency to run parallel to the horizontal axis after the last level.

The tool forces were reduced by half when the water jet was leading the tool by 1mm in comparison to the jet leading by 9mm, proving the critical influence of the lead-on distance.

On Yield

Increase in lead-on distance caused a very small decrease in rock yield when the water jet pressure was 41.37 MPa. At the lower pressure level (27.58 MPa), yield decreased then assumed a constant value after 3mm lead-on distance. (Figure 7.43)

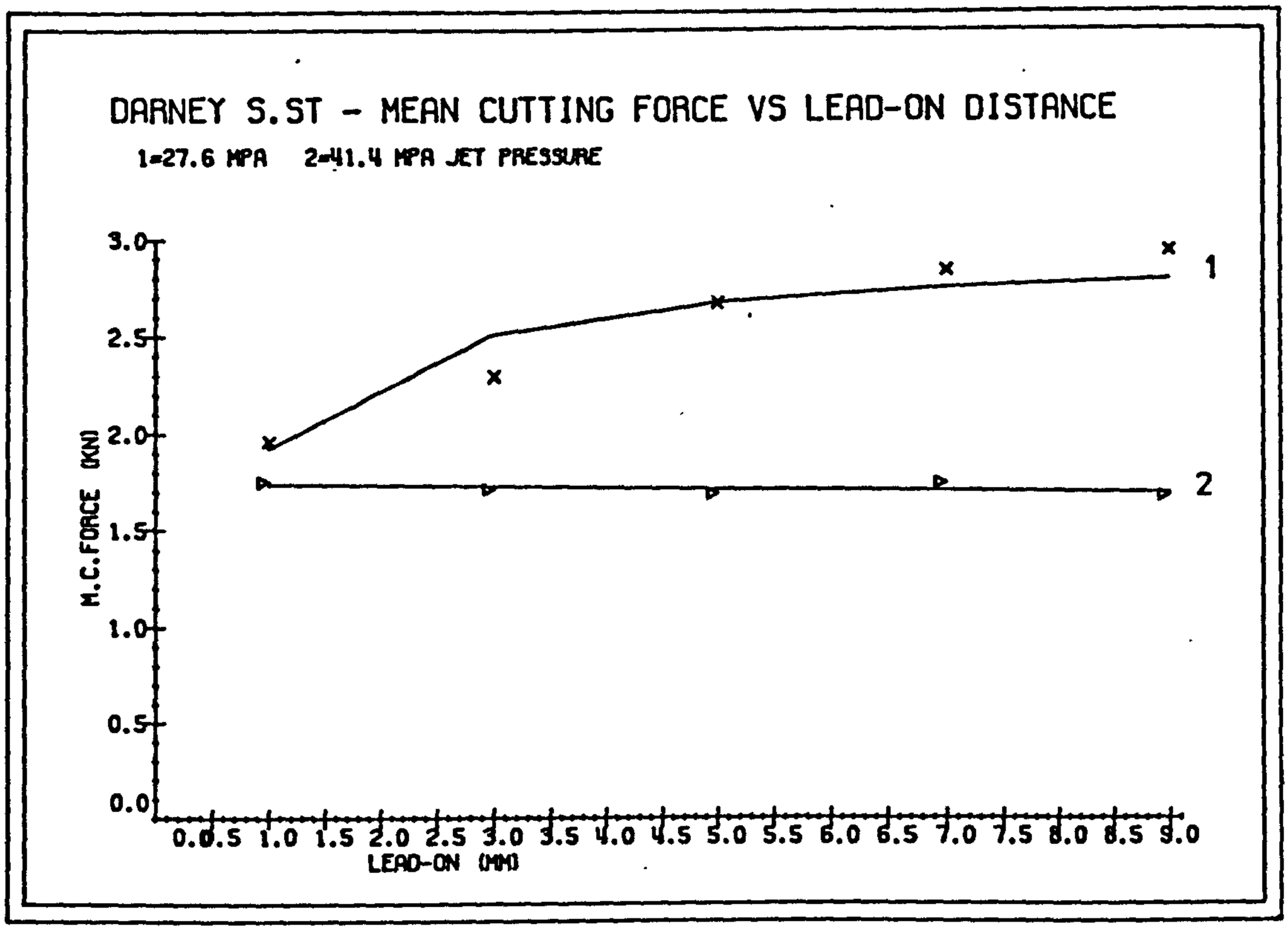
DARNEY S.ST - MEAN CUTTING FORCE VS LEAD-ON DISTANCE
1=27.6 MPA 2=41.4 MPA JET PRESSURE
M.C.FORCE (KN)
3.0
2.5
2.0
1.5
1.0
0.5
0.0
1
2
0.0 0.5 1.0 1.5 2.0 2.5 3.0 3.5 4.0 4.5 5.0 5.5 6.0 6.5 7.0 7.5 8.0 8.5 9.0
LEAD-ON (MM)

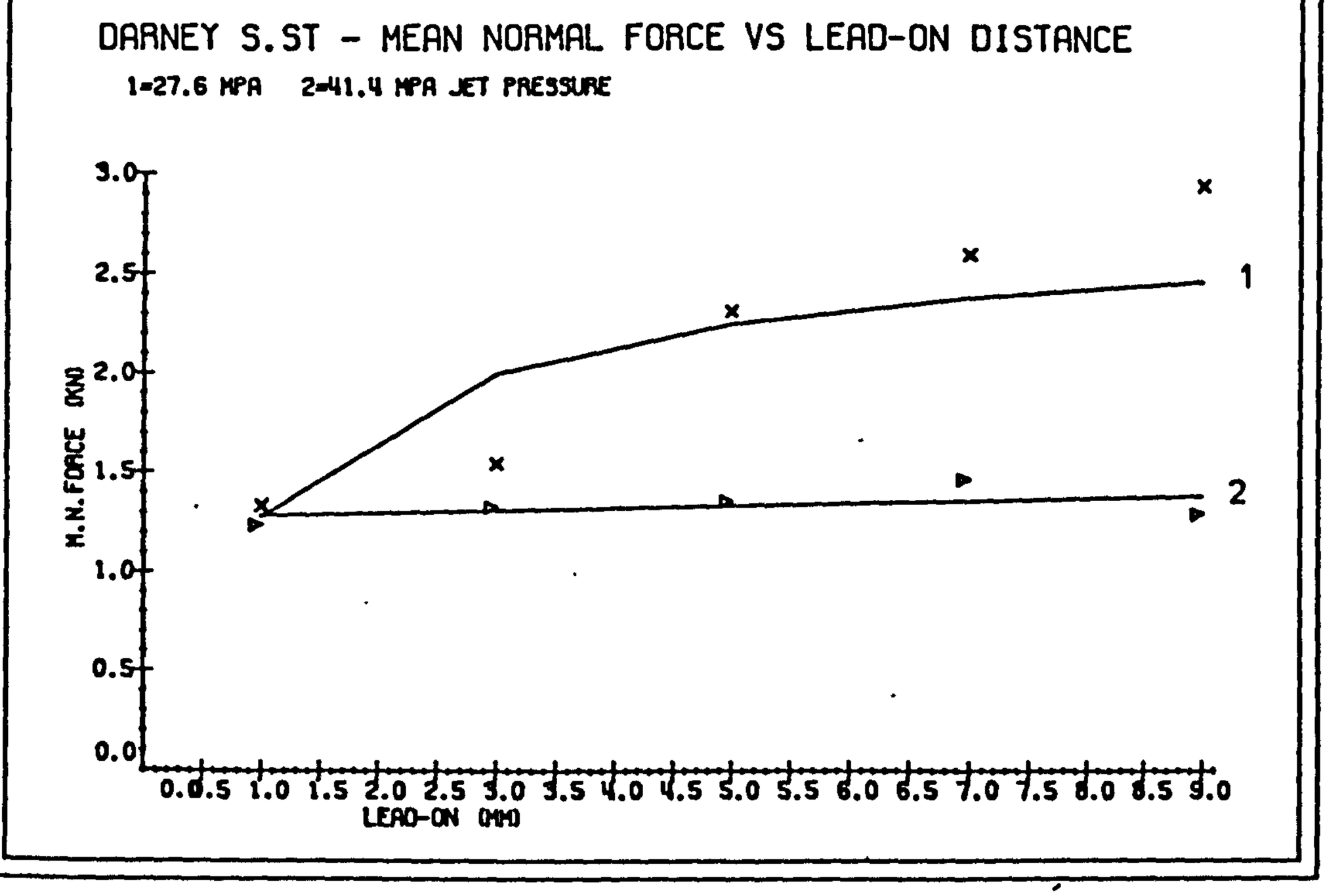
DARNEY S.ST - MEAN NORMAL FORCE VS LEAD-ON DISTANCE
1=27.6 MPA 2=41.4 MPA JET PRESSURE
M.N.FORCE (KN)
3.0
2.5
2.0
1.5
1.0
0.5
0.0
1
2
0.0 0.5 1.0 1.5 2.0 2.5 3.0 3.5 4.0 4.5 5.0 5.5 6.0 6.5 7.0 7.5 8.0 8.5 9.0
LEAD-ON (MM)

FIG. 7.41

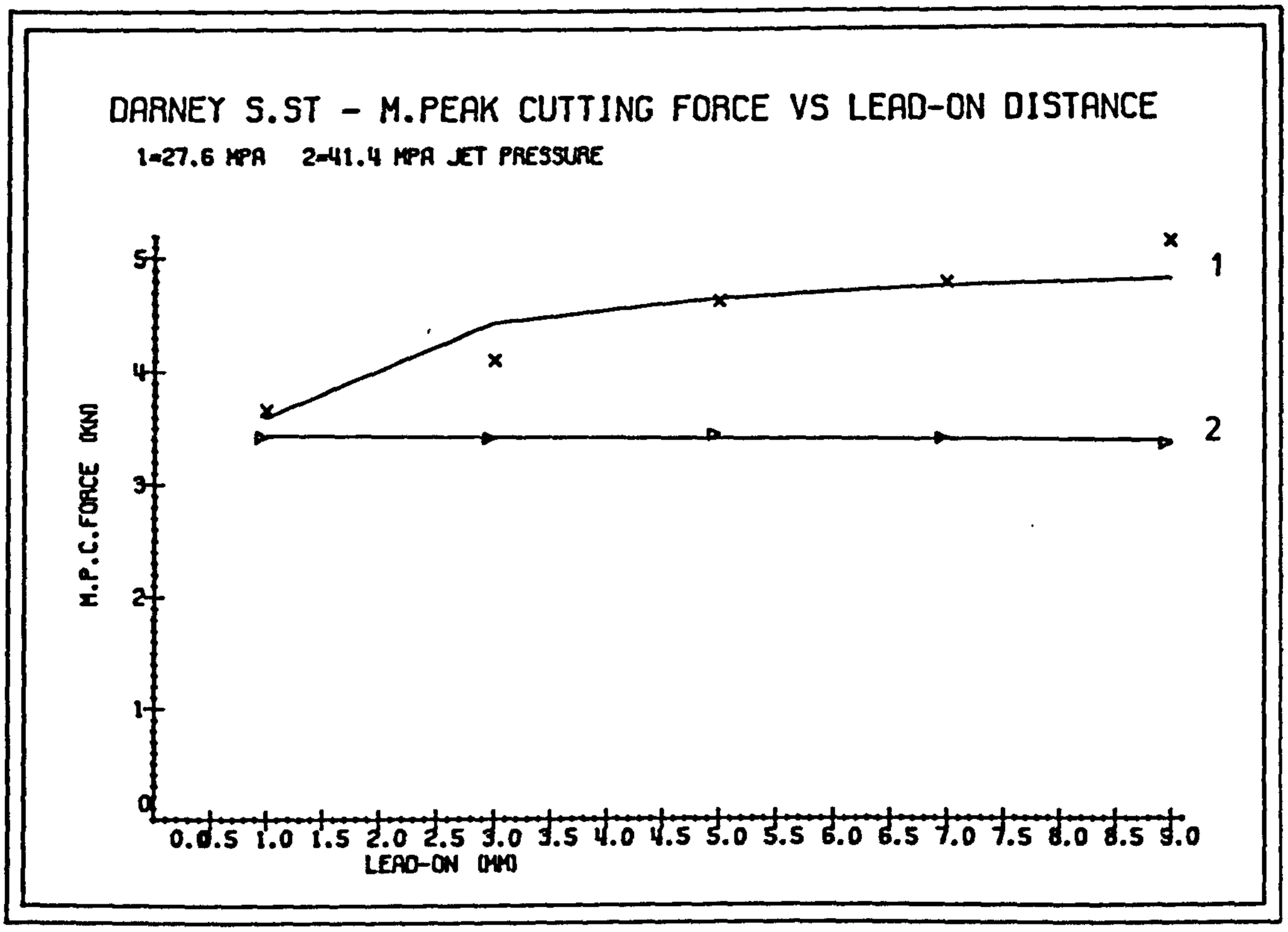
DARNEY S.ST - M.PEAK CUTTING FORCE VS LEAD-ON DISTANCE
1=27.6 MPA 2=41.4 MPA JET PRESSURE
M.P.C.FORCE (KN)
0
1
2
3
4
5
0.0 0.5 1.0 1.5 2.0 2.5 3.0 3.5 4.0 4.5 5.0 5.5 6.0 6.5 7.0 7.5 8.0 8.5 9.0
LEAD-ON (MM)
1
2

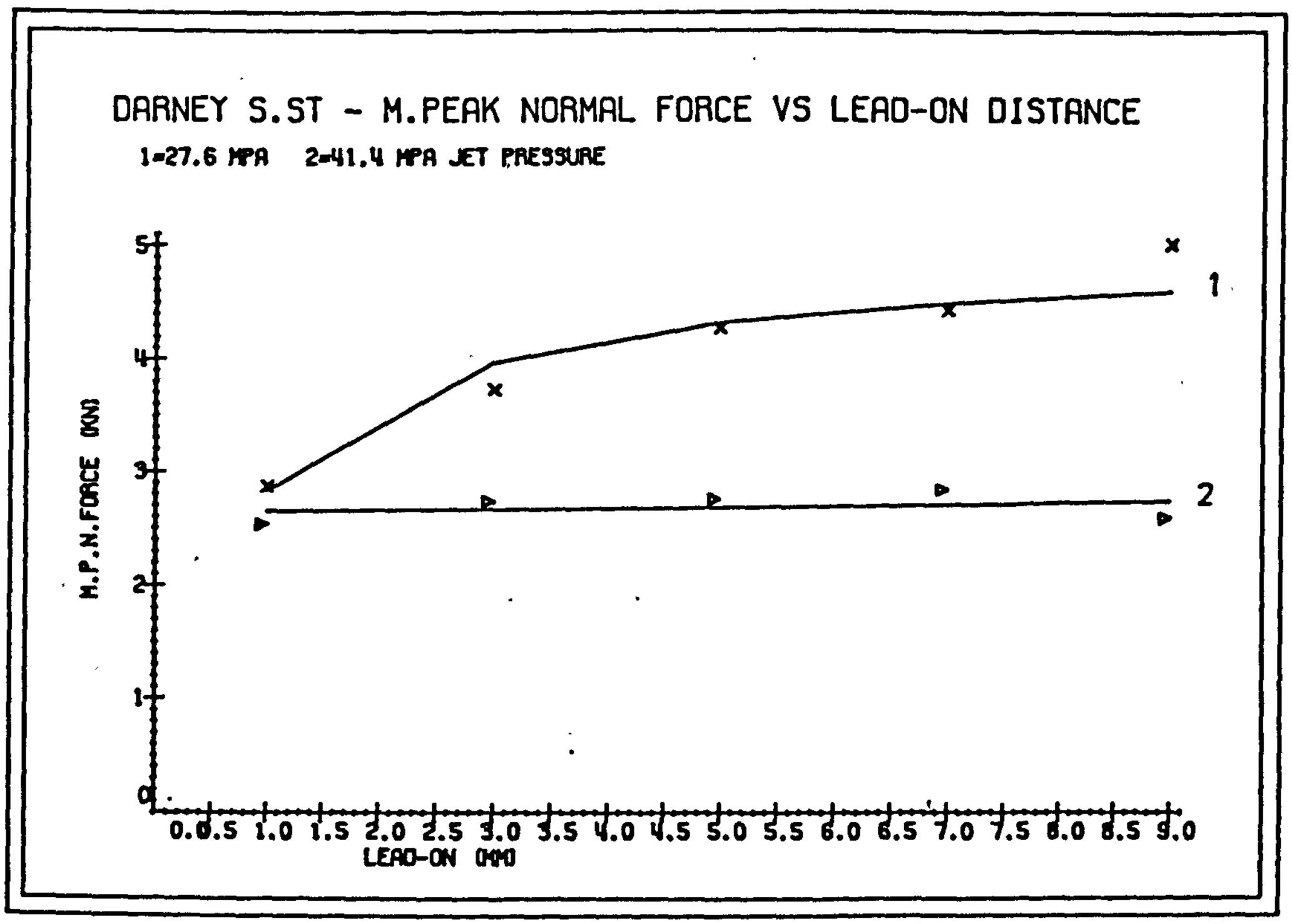
DARNEY S.ST - M.PEAK NORMAL FORCE VS LEAD-ON DISTANCE
1=27.6 MPA 2=41.4 MPA JET PRESSURE
M.P.N.FORCE (KN)
0
1
2
3
4
5
0.0 0.5 1.0 1.5 2.0 2.5 3.0 3.5 4.0 4.5 5.0 5.5 6.0 6.5 7.0 7.5 8.0 8.5 9.0
LEAD-ON (MM)
1
2

FIG. 7.42

On Mechanical Specific Energy

The increasing lead-on distance caused an increase(at a decreasing rate) in mechanical specific energy, when the jet penetration depth was less than the the mechanical tools. Hydraulic specific energies remained constant (Figure 7.43). The curve levelled off after 7mm lead-on distance. With the higher pressure water jet (41.37 MPa), there was no noticeable change in mechanical specific energy with increase in lead-on distance.

7.5.2 Discussion

The lead-on distance has a critical influence on the tool forces, yield, and mechanical specific energy when it is placed either between or, in front of mechanical cutters.

Small scale qualitative finite element stress analysis of a mechanical tool, cutting on Springwell Sandstone was mentioned in (Chapter 5). Plots of stress vectors and stress contours had shown that the rock is stressed at the point of contact between the tool and the rock. This stress field, both compressive and tensile in nature, spread to an area, the dimension of which was governed by the depth of cut. At a 10mm depth of cut example the area extended to approximately 11.5mm from the tool tip. The stresses were compressive under the tip, and with increasing distance they dissipated.

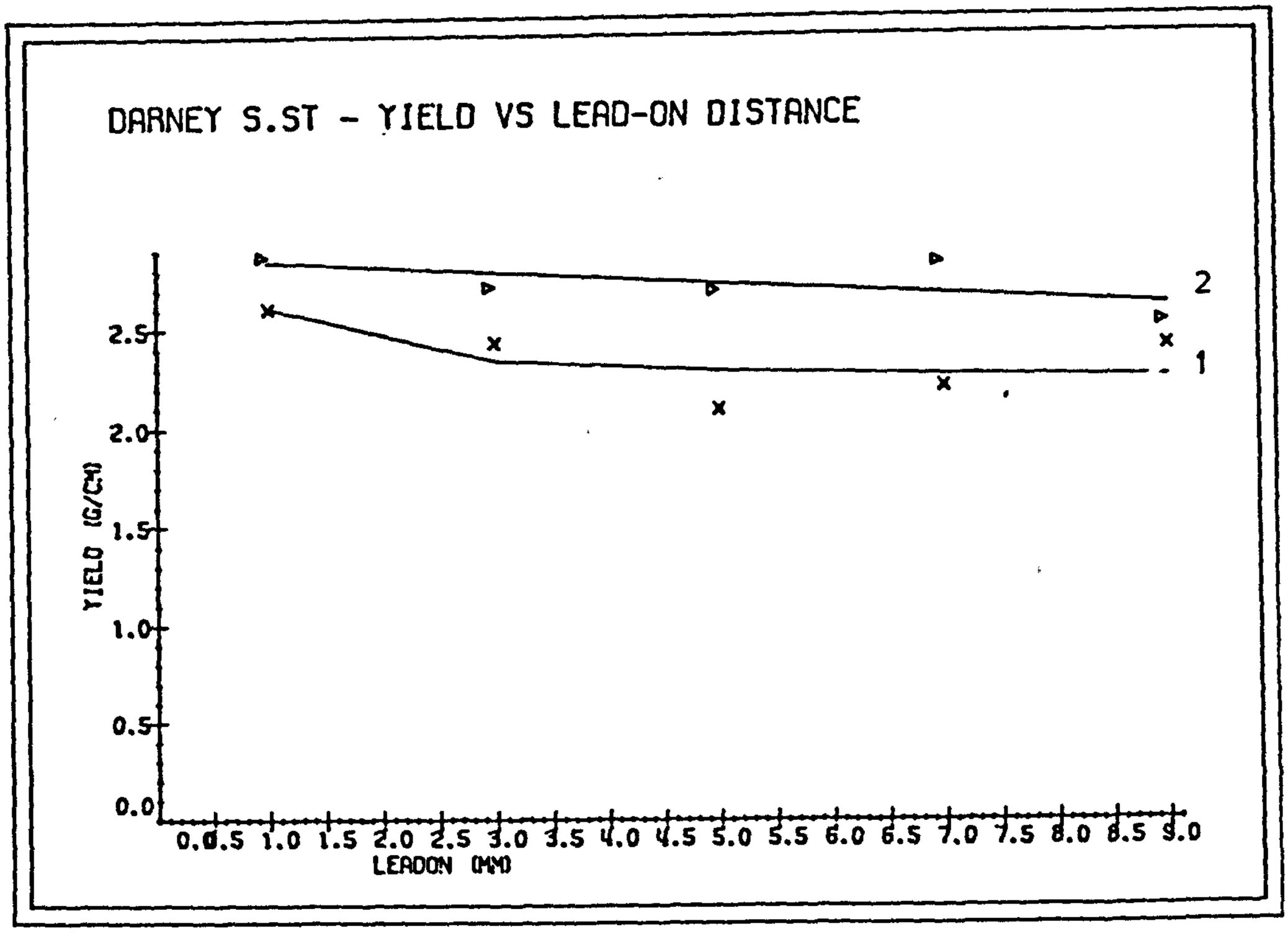
DARNEY S.ST - YIELD VS LEAD-ON DISTANCE
YIELD (G/CM)
2.5
2.0
1.5
1.0
0.5
0.0
0.0 0.5 1.0 1.5 2.0 2.5 3.0 3.5 4.0 4.5 5.0 5.5 6.0 6.5 7.0 7.5 8.0 8.5 9.0
LEADON (MM)
1
2

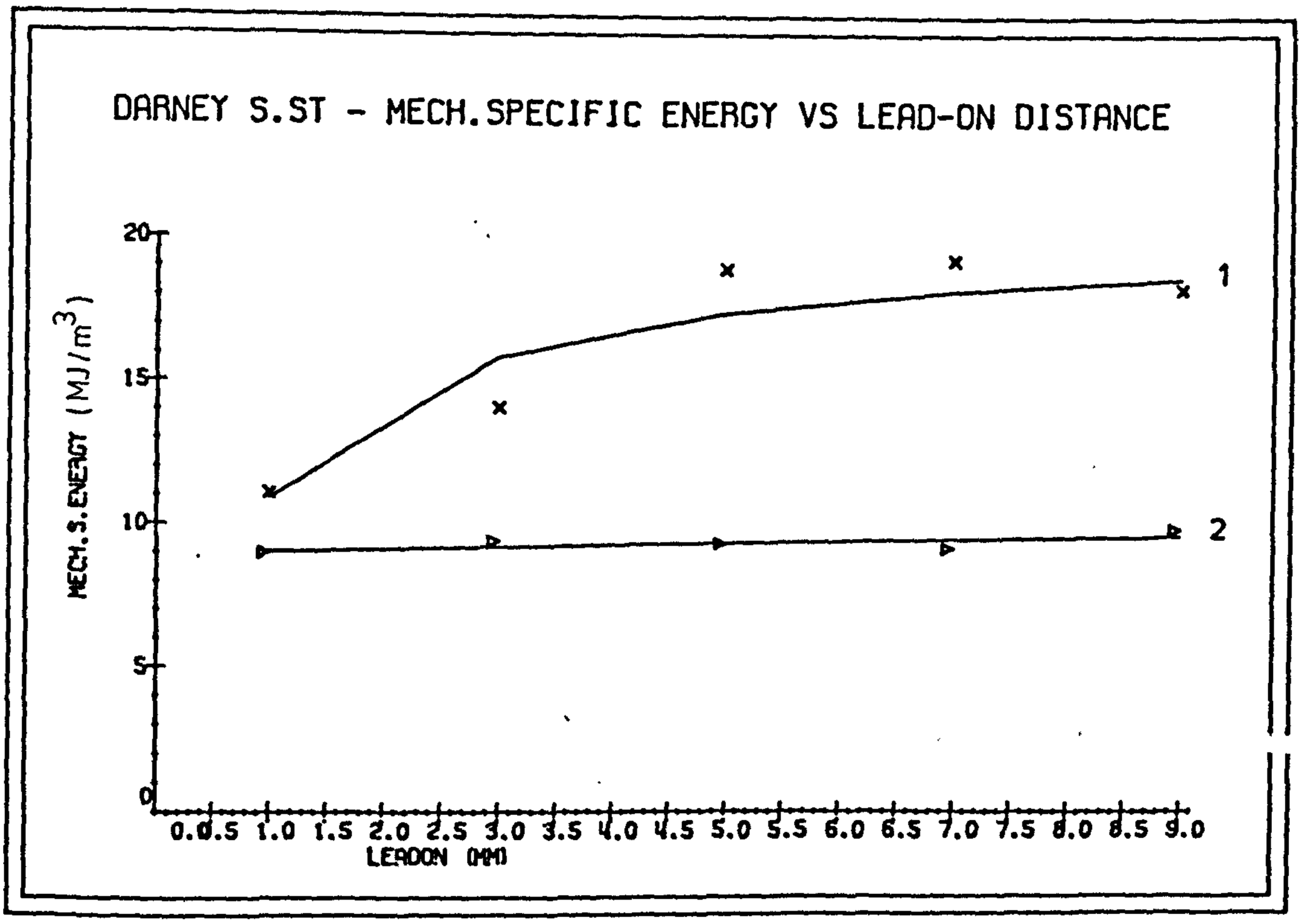
DARNEY S.ST - MECH.SPECIFIC ENERGY VS LEAD-ON DISTANCE
MECH.S.ENERGY (MJ/m3)
20
15
10
5
0
0.0 0.5 1.0 1.5 2.0 2.5 3.0 3.5 4.0 4.5 5.0 5.5 6.0 6.5 7.0 7.5 8.0 8.5 9.0
LEADON (MM)
1
2

FIG. 7.43

The influence of high pressure water jet is to penetrate the rock and create a free face which subsequently causes stress redistribution around the tool. If the penetration depth is less than the mechanical tools, experimental evidence has shown that the water jet should be located between a distance range of 0-11.5mm. And for most efficient cutting, the jet must impact the rock at the minimum lead-on distance. As can be seen from curves, tool forces had lower values in magnitude at the 1mm lead-on distance than at 5mm distance.

There was no change in the force values with increasing lead-on distance when the jet pressure was high enough to cause a penetration depth equal with or greater than the mechanical tools. When the two pressure curves were compared, it was found that a low pressure jet, which impacted the rock surface at 1mm lead-on distance, gave approximately the same results as did the higher pressure jet.

The rock surface was examined after the 27.58 MPa pressure jet had traversed the rock at the minimum lead-on distance, together with the mechanical tool. Although the jet -without the mechanical tool- at this pressure caused a penetration less than the mechanical tools; upon examination it was observed that with mechanical tool assisted cutting, it penetrated the rock to the same depth as the mechanical tools. This may be due to the mechanical tool initiating cracks and fractures in the rock and the high pressure water jet getting into these cracks, exerting pressure on the walls of the crack and hydraulically fracturing it.

The resultant action of the water jet impacting the rock surface at the minimum lead-on distance is threefold. These are

1. actually cutting the rock,

2. getting into the cracks - caused by mechanical tool impact- and assist in propagation of these cracks,

3. assist in clearing the debris.

High temperatures exist at the tool rock interface when cutting rock with mechanical tools, (Plate 14). If the rock is abrasive (contains quartz), the high temperatures cause hairline cracks at the tool tip because tungsten carbide has poor hardness characteristics at elevated temperatures. Applying water jets at minimum lead-on distance may provide cooling at source and reduce frictional heating. This might prove to be useful, especially in coal mines where firedamp is a hazard, and increase the tool life.

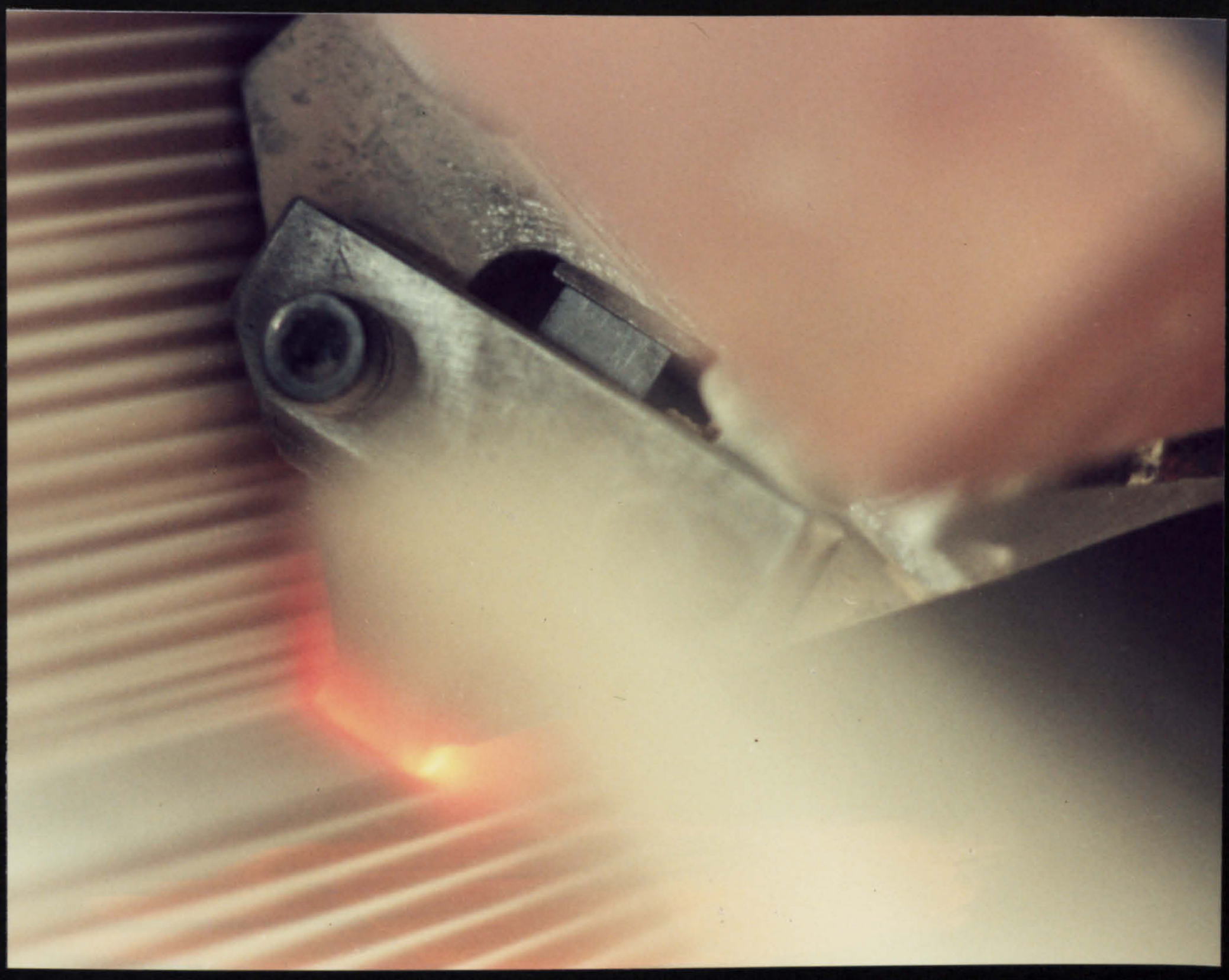

PLATE I4 - Temperature built up at the tool tip during continuous cutting.

7.5.3 Conclusions

Assuming that it is possible for a mechanical tool to cut along the same groove which is created by a water jet,(i.e. no vibrations, that might cause the mechanical tool to deviate from the track) then the lead-on distance has an important effect on tool forces (cutting, normal and, sideways), yield and mechanical specific energy.

The penetration depth of water jet, consequently its pressure, has a significant influence on the tool forces. The tool forces increased hyperbolically at a decreasing rate with the increase in lead-on distance, when the high pressure water jet penetrated the rock less than the mechanical tool depth of cut. A large percentage of the increase took place between 1-3mm. After the 5mm Further increase was small after the 5 mm lead-on distance and the curve ran parallel to the horizontal axis after 9 mm. The yield decreased by a small amount and then assumed a constant value and the Mechanical Specific Energy increased with lead-on distance, indicating that the cutting operation became less efficient.

However, when the jet penetrated the rock to a depth equal with, or greater than the mechanical tools no significant change in tool forces, yield and Mechanical Specific Energy was noticed.

The graphs of parameters drawn against lead-on distance at two pressure levels have shown that same amount of reduction in forces can be achieved by the lower pressure jet impacting the rock at the minimum lead-on

distance and by the higher pressure jet. Therefore, it may be suggested that for sandstones, it is not necessary for the water jet to attain high pressures so as to cause penetration depth equal to that of the mechanical tools. Instead at a minimum lead-on distance the lower pressure jet can achieve the same amount of reductions in forces. This in turn means that less hydraulic power will be required by the hybrid cutting system.

The action of the water jet on the rock surface, when it is leading the mechanical tool may classified to be threefold. Firstly, as a result of its energy it cuts the rock to a depth which is governed by the rock properties, e.g. compressive strength, porosity, grain size, etc. Secondly, it gets into the already existing microcracks and cracks initiated by the following mechanical tool and exerts pressure at the walls of these cracks, thus causing crack propagation and hydraulic fracturing. Finally, it aids in removal of the debris.

Locating water jets as close to the tool tip as possible provides cooling at source and thus, reduces frictional heating. This would, in turn, increase the mechanical tool life by reducing the tool wear caused by high temperatures etc. and eliminate frictional sparks, which are an explosion hazard in coal mines.

7.6 STAND-OFF DISTANCE

Nozzles for a water jet assisted mechanical cutting system have to operate at some distance from the rock surface to prevent damage from rock chippings and plugging of dirt. Experiments were planned and conducted on Springwell and Darney Sandstones, to investigate the influence of the increasing stand-off distance on the measured and calculated parameters of performance.

The nozzle diameter, traversing speed, lead-on and side-off distances were kept constant to isolate the main effect of the stand-off distance. The experimental variables and their levels were as follows:

Variable	Level	
	Springwell Sandstone	Darney Sandstone
Depth of cut (mm)	6	7
Lead-on dist. (mm)	8	8
Side-off dist. (mm)	20	0
Nozzle diameter (mm)	0.85	0.85
Traverse speed (mm/sec)	94	165
Water jet pressure (MPa)	13.79, 24.14, 34.48 44.83, 55.17	27.58
Stand-off distance (mm)	15, 30, 45, 60, 75 90, 105, 120	15,30,45,60,75

The pressure of the jet was changed in increments up to 55.17 MPa to examine the influence of jet pressure on the optimum stand-off distance when cutting Springwell sandstone. The stand-off distance range was taken well above the stand-off/nozzle diameter >100 up to 120mm for the same sandstone.

Each cutting experiment was repeated four times and the cutting order was randomised. Computer curve fitting analysis was performed on the experimental results and best-fitting curves through the data points were computer drawn and functions are listed in (Appendix C).

7.6.1 The Effect of Stand-off Distance

On Jet Penetration Depth

Springwell sandstone experimental results have shown that the water jet pressure had an influence on the effective stand-off distance. Increase in pressure lead to a decrease in the stand-off distance, (Figure 7.44). The penetration depth increased up to an optimum and then started to decrease with increase in stand-off distance. The depth dropped sharply after stand-off/nozzle diameter(st/dn) greater than 100.

SPRINGWELL SANDSTONE - PENETRATION VS STAND-OFF DISTANCE

AT DIFFERENT WATER JET PRESSURE LEVELS

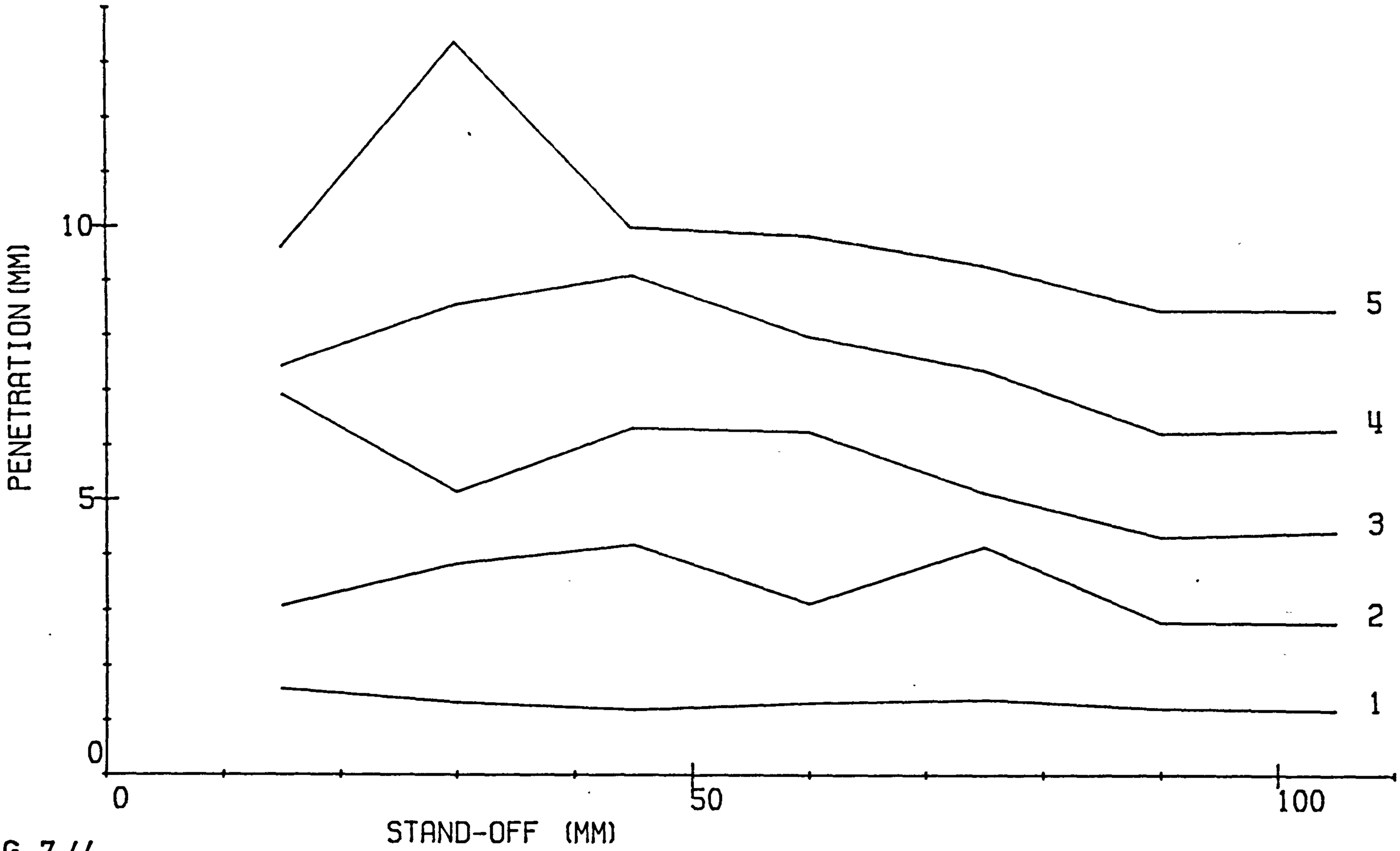

FIG. 7.44

No such optimum stand-off distance was noted when Darney Sandstone was cut with a 27.58 MPa pressure water jet. The penetration depth decreased linearly with a gentle dip with increasing stand-off distance within the $20<st/dn<100$ range. The Hydraulic Specific Energy has increased -indicating that the jet was becoming inefficient- with the increase in stand-off distance, (Figure 7.45).

On Tool Forces

The cutting and normal forces all decreased with increase in stand-off distance for both types of sandstones. The relationship between the forces and the stand-off distance,(within the experimental distance range) was of linear type. (Figures 7.46-7.48).

On Yield and Mechanical Specific Energy

The yield has remained approximately constant and Mechanical Specific Energy has increased with increase in stand-off distance, (Figure 7.49).

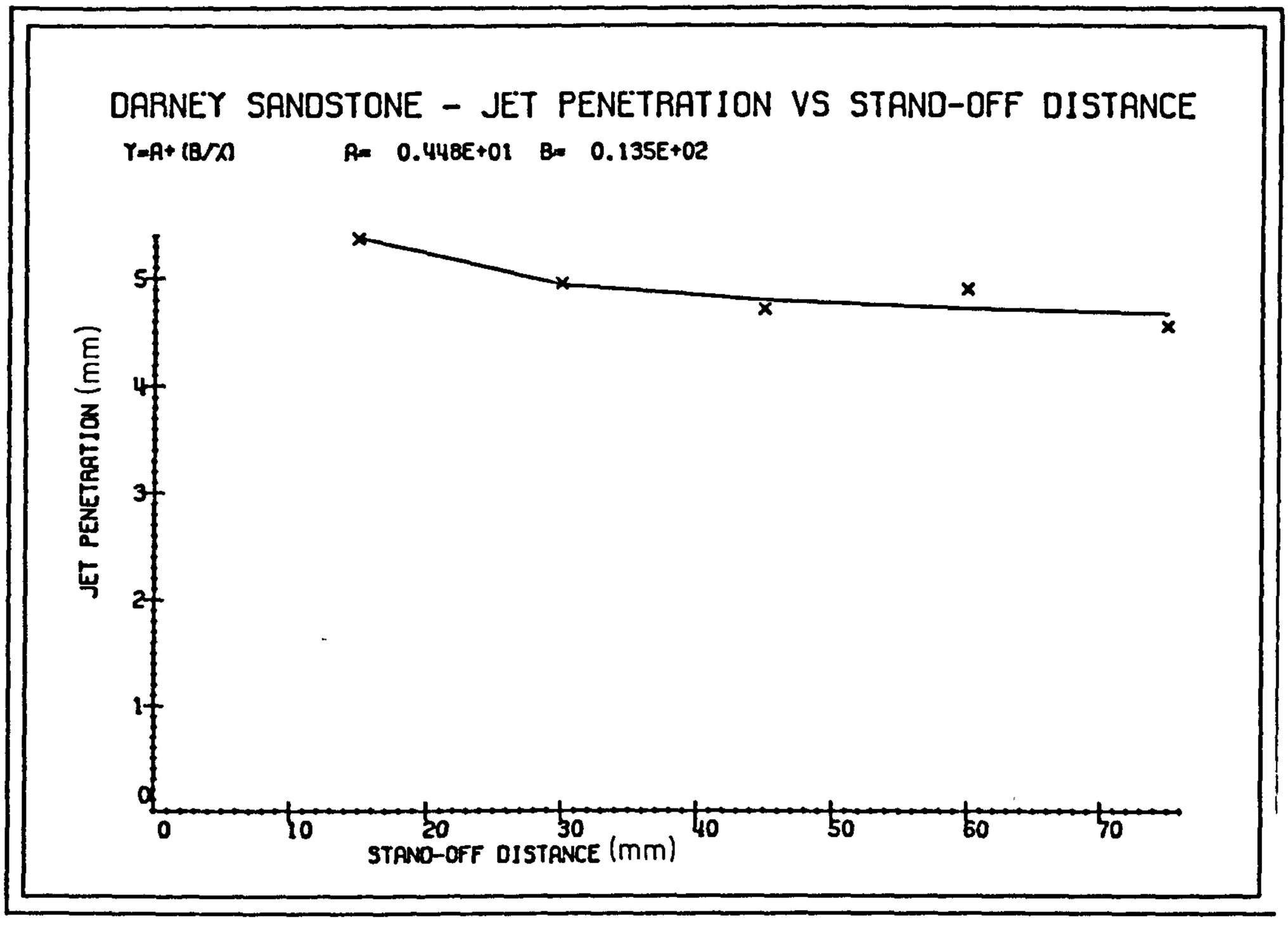
DARNEY SANDSTONE - JET PENETRATION VS STAND-OFF DISTANCE
Y=A+(B/X)
A= 0.448E+01
B= 0.135E+02
JET PENETRATION (mm)
0
1
2
3
4
5
0
10
20
30
40
50
60
70
STAND-OFF DISTANCE (mm)

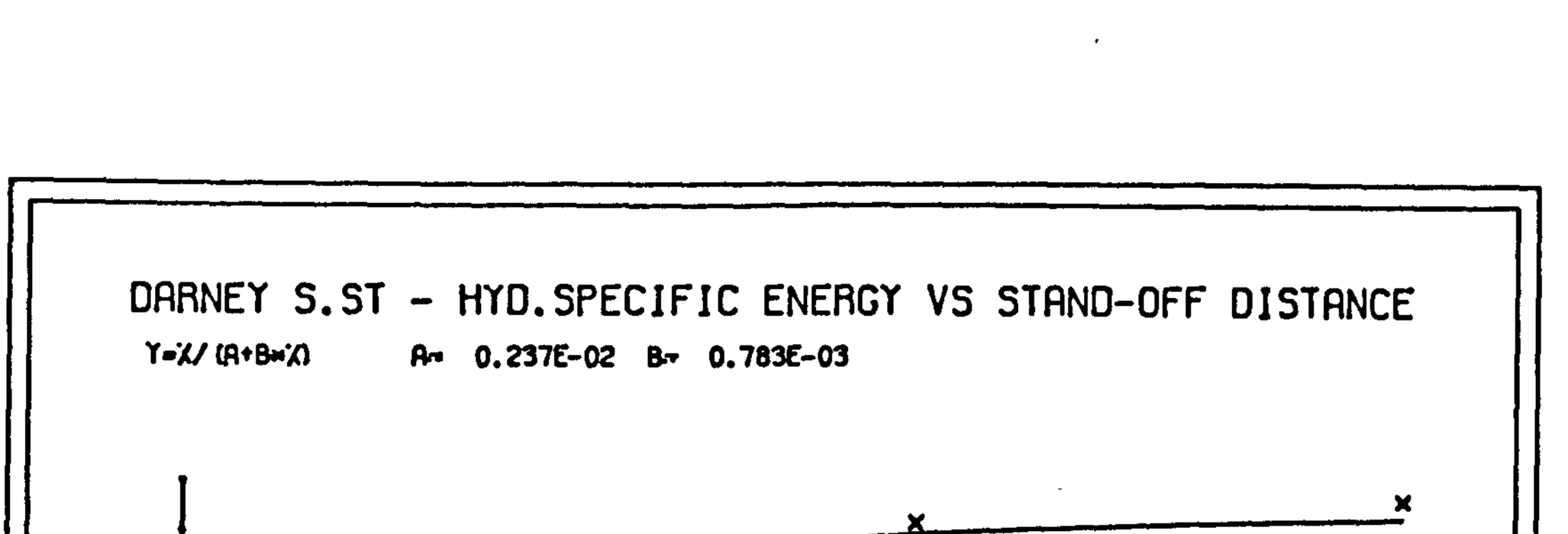
DARNEY S.ST - HYD.SPECIFIC ENERGY VS STAND-OFF DISTANCE
Y=X/(A+B*X)
A= 0.237E-02
B= 0.783E-03
HYD.S.ENERGY (MJ/M-3)
0
500
1000
0
10
20
30
40
50
60
70
STAND-OFF DIST. (MM)

FIG. 7.45

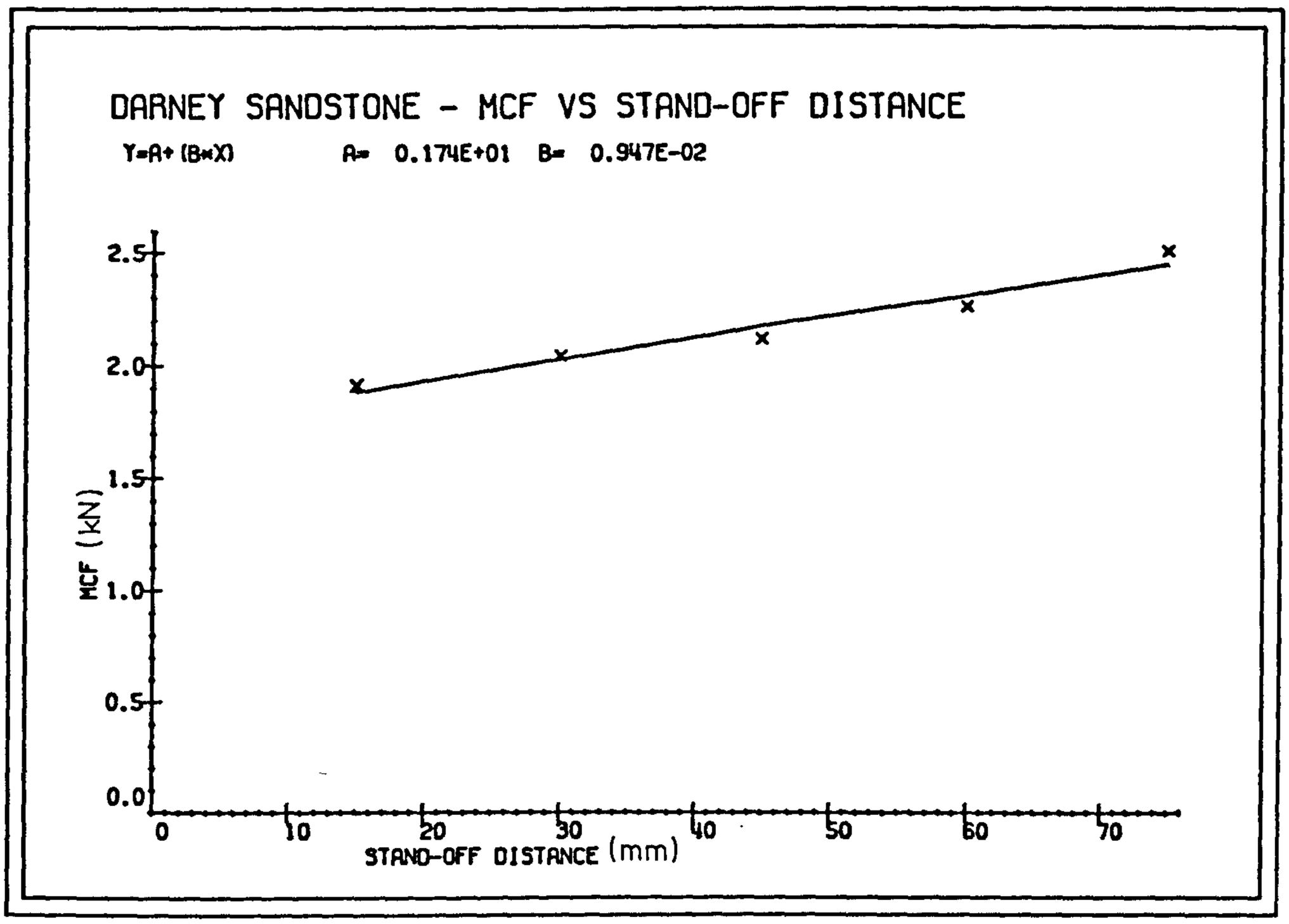
DARNEY SANDSTONE - MCF VS STAND-OFF DISTANCE
Y=A+(B*X)
A= 0.174E+01
B= 0.947E-02
MCF (kN)
2.5
2.0
1.5
1.0
0.5
0.0
0
10
20
30
40
50
60
70
STAND-OFF DISTANCE (mm)

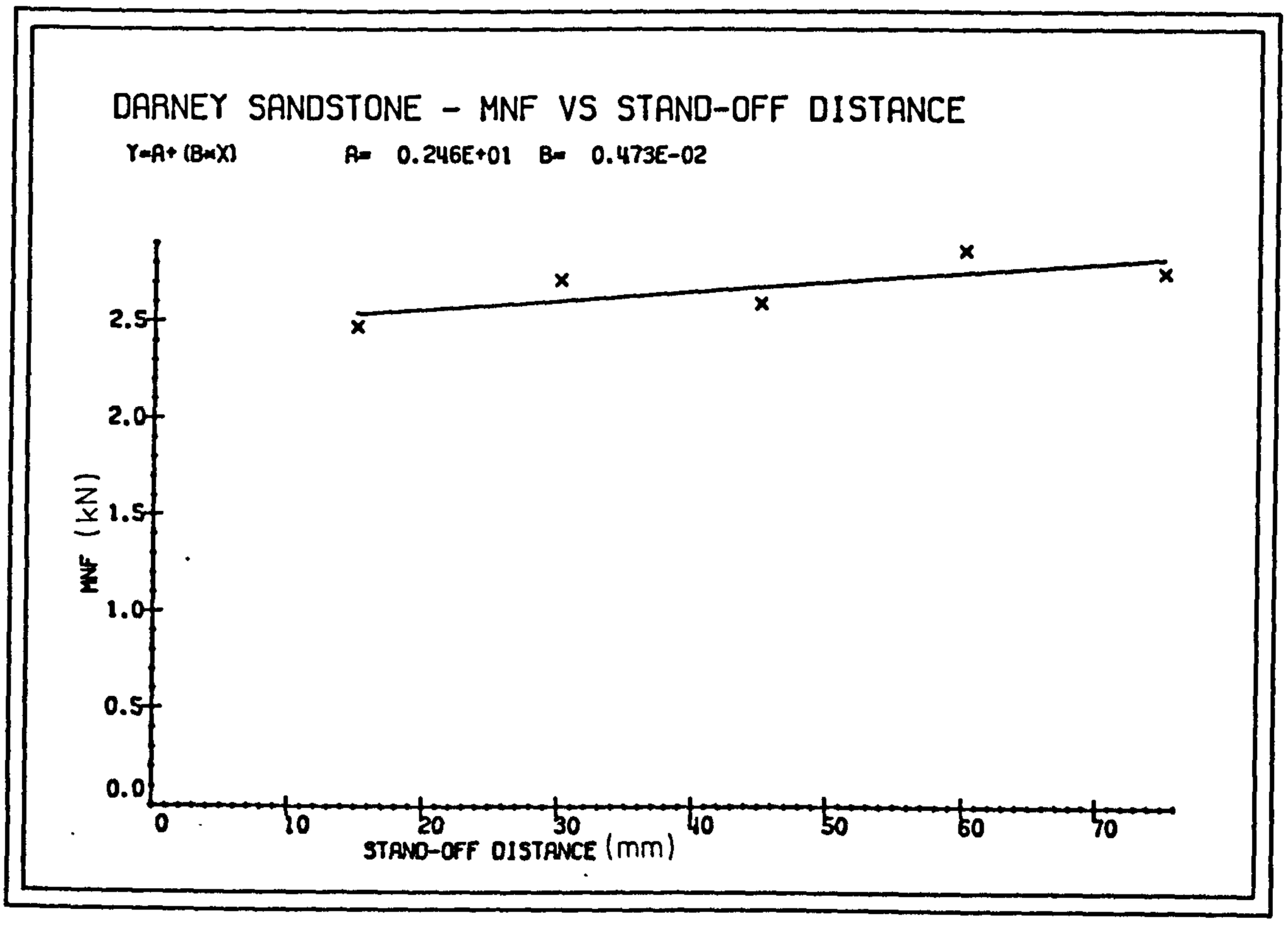
DARNEY SANDSTONE - MNF VS STAND-OFF DISTANCE
Y=A+(B*X)
A= 0.246E+01
B= 0.473E-02
MNF (kN)
2.5
2.0
1.5
1.0
0.5
0.0
0
10
20
30
40
50
60
70
STAND-OFF DISTANCE (mm)

FIG. 7.46

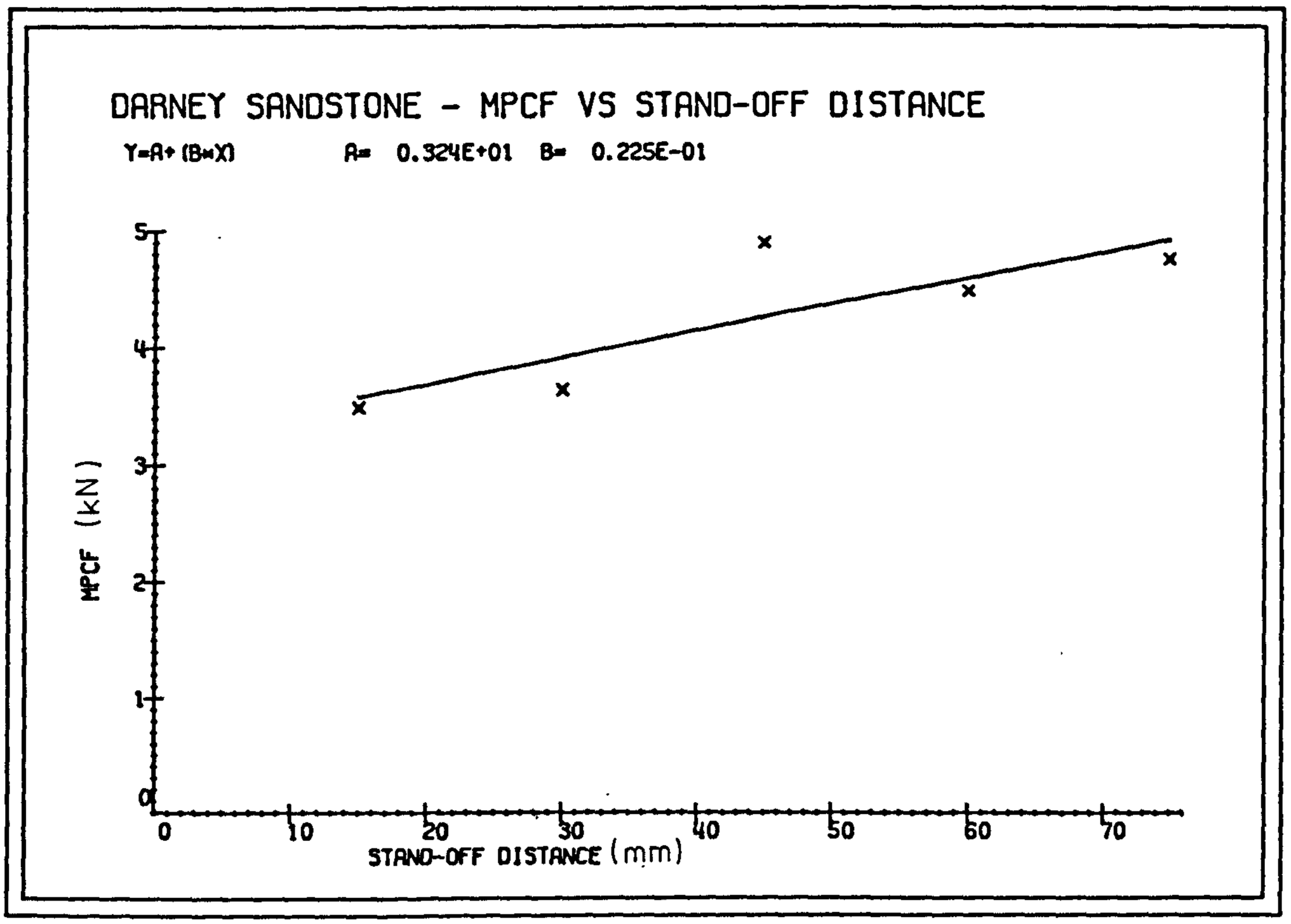
DARNEY SANDSTONE - MPCF VS STAND-OFF DISTANCE
Y=A+(B*X)
A= 0.324E+01
B= 0.225E-01
MPCF (kN)
0
1
2
3
4
5
0
10
20
30
40
50
60
70
STAND-OFF DISTANCE (mm)

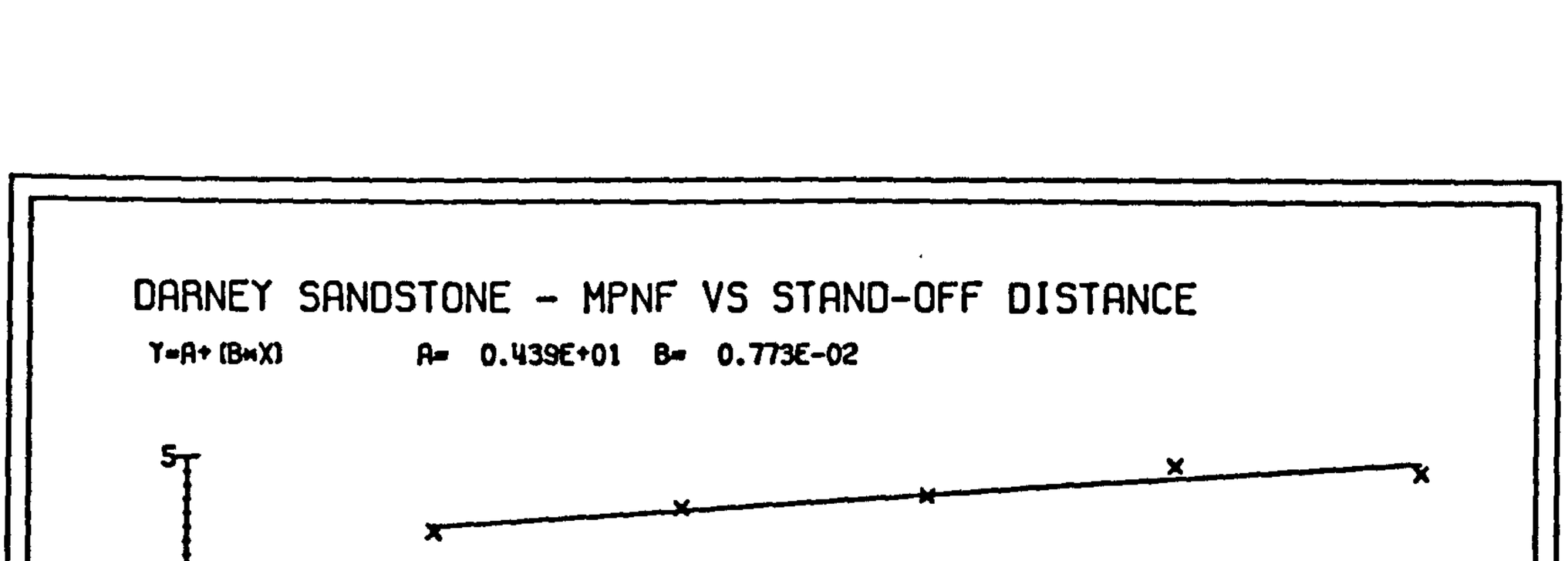
DARNEY SANDSTONE - MPNF VS STAND-OFF DISTANCE
Y=A+(B*X)
A= 0.439E+01
B= 0.773E-02
MPNF (kN)
0
1
2
3
4
5
0
10
20
30
40
50
60
70
STAND-OFF DISTANCE (mm)

FIG. 7.47

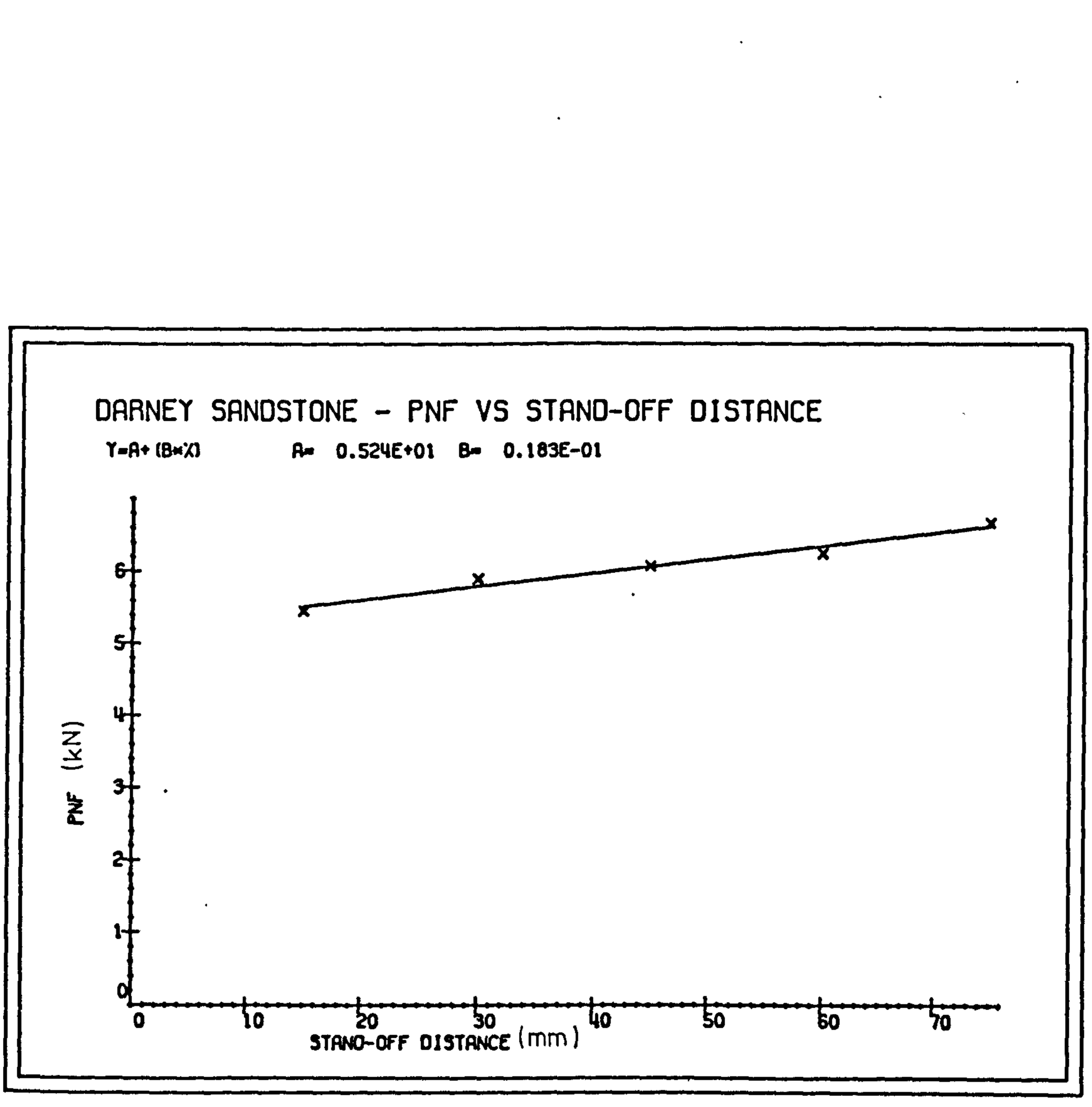
DARNEY SANDSTONE - PNF VS STAND-OFF DISTANCE
Y=A+(B*X)
A= 0.524E+01 B= 0.183E-01
PNF (kN)
0
1
2
3
4
5
6
0
10
20
30
40
50
60
70
STAND-OFF DISTANCE (mm)

FIG. 7.48

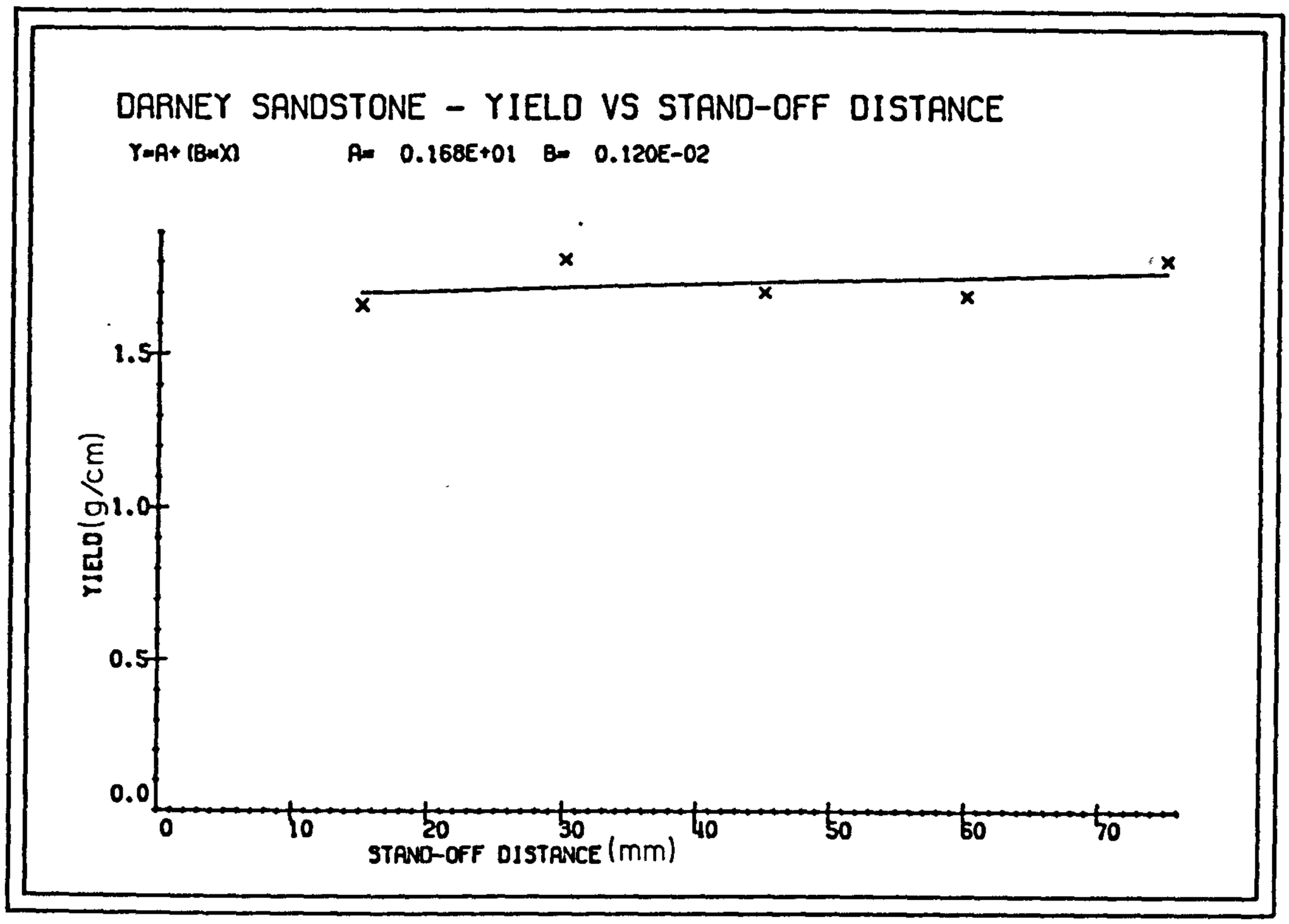
DARNEY SANDSTONE - YIELD VS STAND-OFF DISTANCE
Y=A+(B*X)
A= 0.168E+01
B= 0.120E-02
YIELD(g/cm)
1.5
1.0
0.5
0.0
0
10
20
30
40
50
60
70
STAND-OFF DISTANCE (mm)

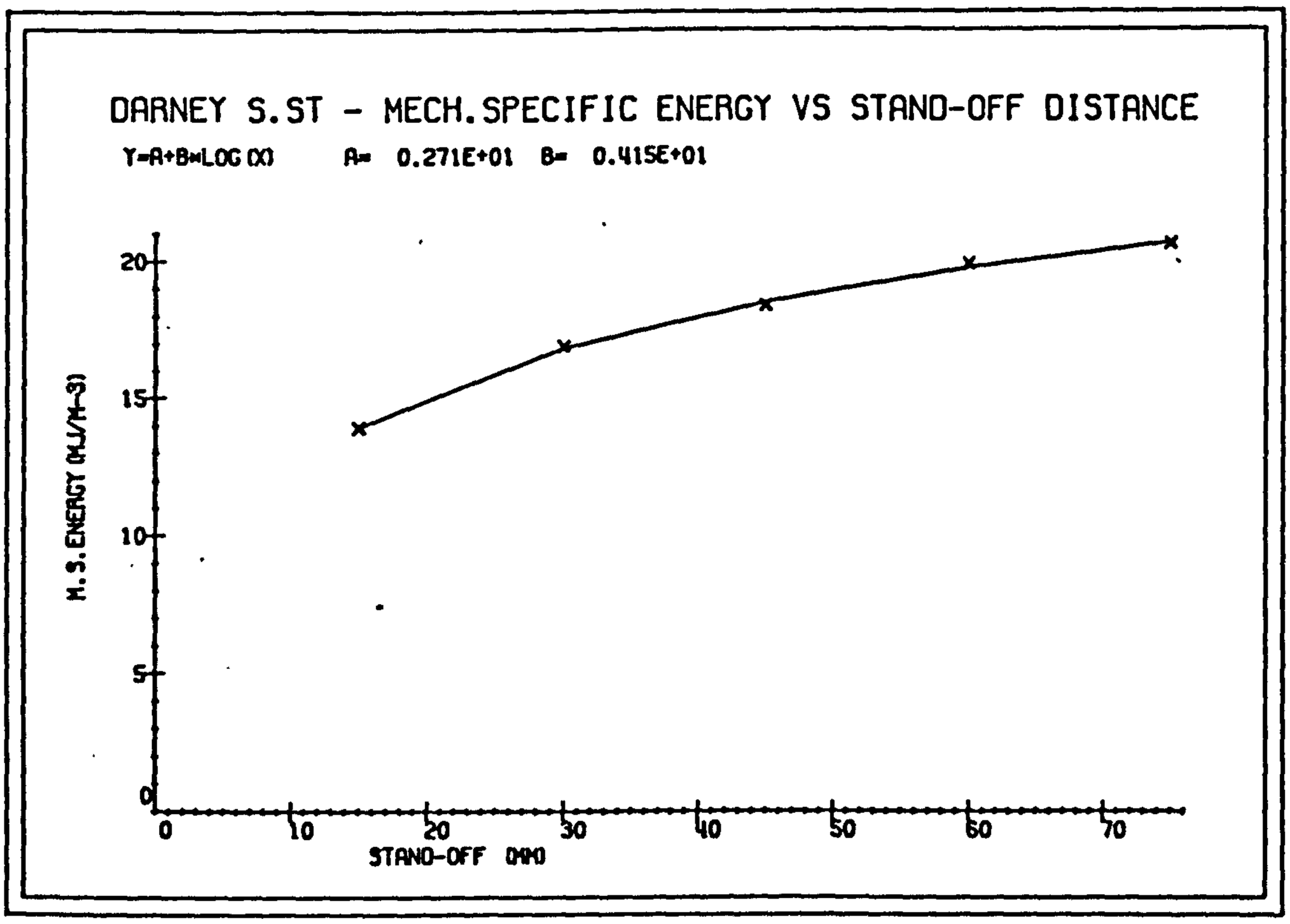
DARNEY S.ST - MECH.SPECIFIC ENERGY VS STAND-OFF DISTANCE
Y=A+B*LOG(X)
A= 0.271E+01
B= 0.415E+01
M.S.ENERGY (MJ/M-3)
20
15
10
5
0
0
10
20
30
40
50
60
70
STAND-OFF DMD

FIG. 7.49

7.6.2 Discussion

The performance of a water jet at various stand-off distances is related to the properties of the jet. A high pressure (high velocity) liquid jet does not retain its original shape, but breaks up as the stand-off distance increases. The jet may be divided into three parts which differ from each other by the nature of the change taking place in the axial (steady state) pressure and in structural properties. The stand-off distance shows its effect differently in each of the sections of the jet.

The steady state pressure of the water jet is given by:

$P = 1/2\rho v^2$ where P = water-jet pressure

ρ = the density of the water

v = the velocity of the jet

and, impact pressure of the jet is given by:

$P = \rho c v$ where c = velocity of wave propagation.

When a continuous high pressure water jet impacts the surface of a target, the resultant loading is due to the combined effect of the steady-state pressure and impact pressure. The magnitude of impact pressure, which acts in an extremely short time on the target surface may be several times higher than the steady-state pressure as indicated by

above equations. The steady-state pressure acts on the surface while the issued jet is continuous (corresponds to the initial section of the jet). With increasing stand-off distance, the portion of the jet that impacts the target surface is the transition section in which the impact pressure component is increased and the axial pressure is reduced due to air friction and expansion. Finally, at the greatest distance from the nozzle (in the dispersed region) the loading is due to discrete elements of water. The area of the rock surface which is loaded by the water jet increases and the energy per unit area decreases with an increase in stand-off distance due to increased spreading of the jet. By varying the impact and steady state pressures, e.g. changing the stand-off distance, an optimal pump pressure may be achieved for each type of target material.

Farmer et.al reported that the greatest jet penetration took place at zero stand-off distance. The results of Springwell sandstone experiments contradict his conclusion, as the greatest penetration had not taken place at zero stand-off but at some distance away from the target surface. Increasing jet pressure has caused the maximum penetration point to shift to a smaller stand-off distance, which correspond to the lesser impact pressure rate and increased steady-state pressure, as suggested by Erdmann-Jesnitzer et al(38).

The influence of stand-off distance was measured by the variation in the penetration depth and this is what caused similar changes in tool forces and mechanical specific energy.

7.6.3 Conclusions

The effect of stand-off distance is dependent on the energetic properties of the jet which vary with increased stand-off distance. In general, the jet penetration depth decreased when the distance between the nozzle and the target surface was increased. As a result of this, hydraulic specific energy increased and the jet became less efficient. The nature of the relationship was of linear type, within the experimental distance ranges 17<st/dn<90 for Darney sandstone, and exponential for Springwell sandstone 17<st/dn<120. Cutting and normal forces increased linearly with stand-off distance and yield remained approximately constant, while mechanical specific energy was increased.

The optimum stand-off distance depends on the diameter of the nozzle as well as on the rock type. For efficient cutting it should be less than s/d <90, which for a nozzle diameter of 0.85mm is equal to 77.5mm.

7.7 NUMBER OF PASSES

In previous sections the influences of hydraulic variables on the penetration depth were examined in detail. Another method of increasing penetration depth is to use several jets in tandem, that is more than one jet cutting progressively along the same track. The effect of more than one jet cutting along the same path created by the first jet was investigated on Springwell sandstone. The pressure of the water jet was chosen such that, after the last experimental level, the jet penetrated the rock to a distance equal with, or more than, the mechanical tool depth of cut. Experimental variables and their levels were as follows:

Variable		Level
Depth of cut	(mm)	8
Nozzle diameter	(mm)	0.85
Water jet pressure	(MPa)	24.14
Traverse speed	(mm/sec)	124
Stand-off distance	(mm)	45
Lead-on distance	(mm)	5
Side-off distance	(mm)	0
Number of jet passes		1, 2, 3, 4, 5

Each test was repeated four times and the cutting order was randomised. Overall, 5 x 4 = 20 tests were conducted on the Springwell sandstone. The rock was pre-conditioned with water jets according to pass number and at

the last pass number the mechanical tool cut the rock together with the water jet. Computer curve-fitting analysis was performed on the experimental results. Best-fit curves, together with correlation coefficients are listed in (Appendix 3).

7.7.1 The Effect of Number of Passes of the Water jet

On the Penetration Depth

The water jet penetration depth increased with increasing pass number, showing a hyperbolic relationship (Figure 7.50). The equation was of the form

$$h = Np/(A+BxNp)$$

where h = penetration depth

A,B = constants

Np= number of jet passes

As can be seen from the graph, most of the penetration had taken place after the first jet pass. Any further increase in jet passes did not result in equal increases in the penetration. The curve has shown tendency to level off to an asymptote with increasing passes of the jet. This was confirmed by the hydraulic specific energy graph, which indicated that it became increasingly inefficient to cut with more than one jet in tandem, and

after five passes the hydraulic specific energy curve levelled off, (Figure 7.50).

On Tool forces

Cutting and Normal forces decreased with increasing jet number. The relationship was of exponential type (Figure 7.51-7.53). The slope of normal force curves showed that they were more sensitive to change than cutting forces.

On Yield

Yield was reduced with increase in the number of passes,(Figure 7.54). After the second pass, the incremental changes in yield were relatively insignificant.

On Mechanical Specific Energy

An improvement in the Cutting efficiency was seen with increasing pass number, (Figure 7.54). However, the improvement was very gradual and small.

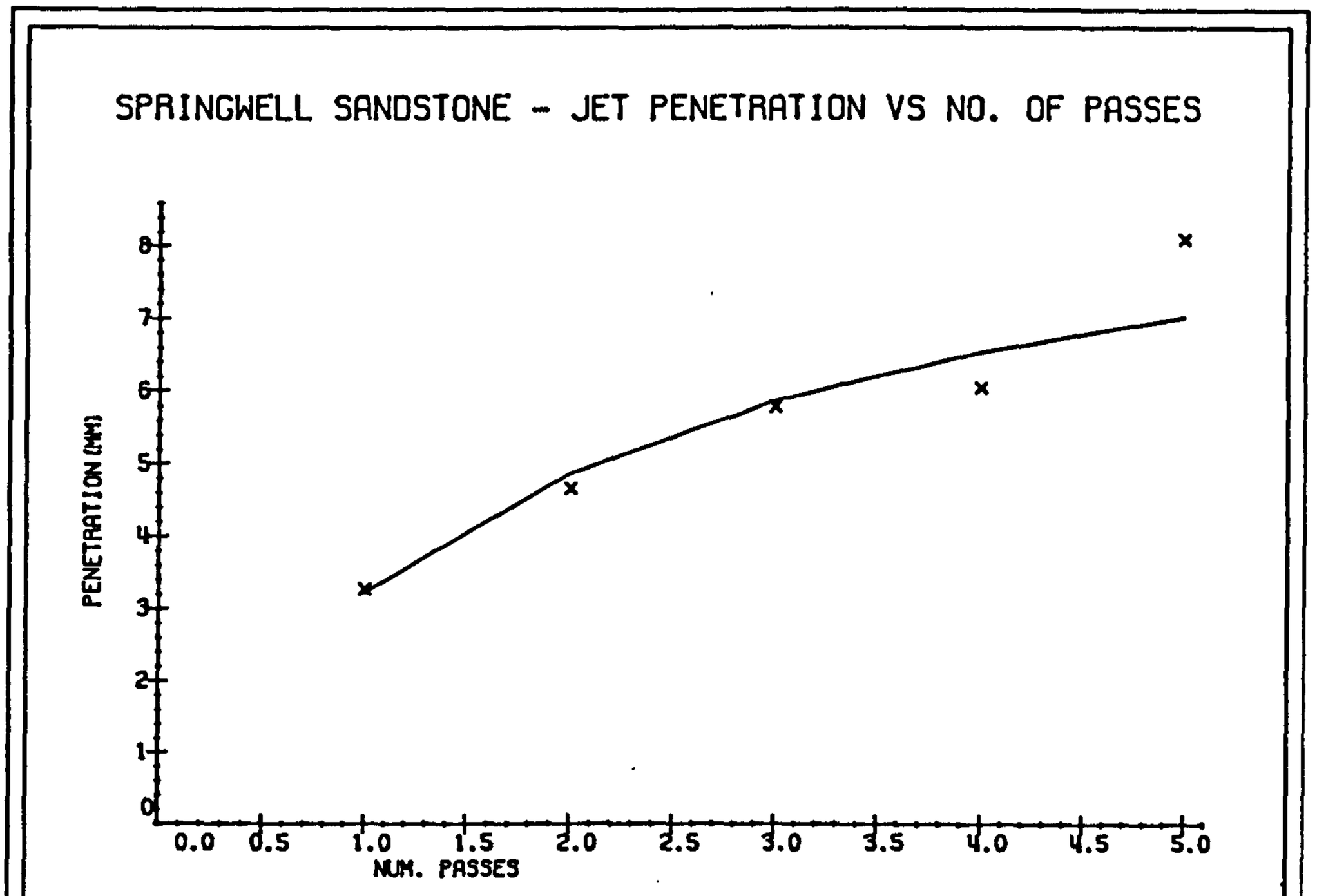
SPRINGWELL SANDSTONE - JET PENETRATION VS NO. OF PASSES
PENETRATION (MM)
0
1
2
3
4
5
6
7
8
0.0
0.5
1.0
1.5
2.0
2.5
3.0
3.5
4.0
4.5
5.0
NUM. PASSES

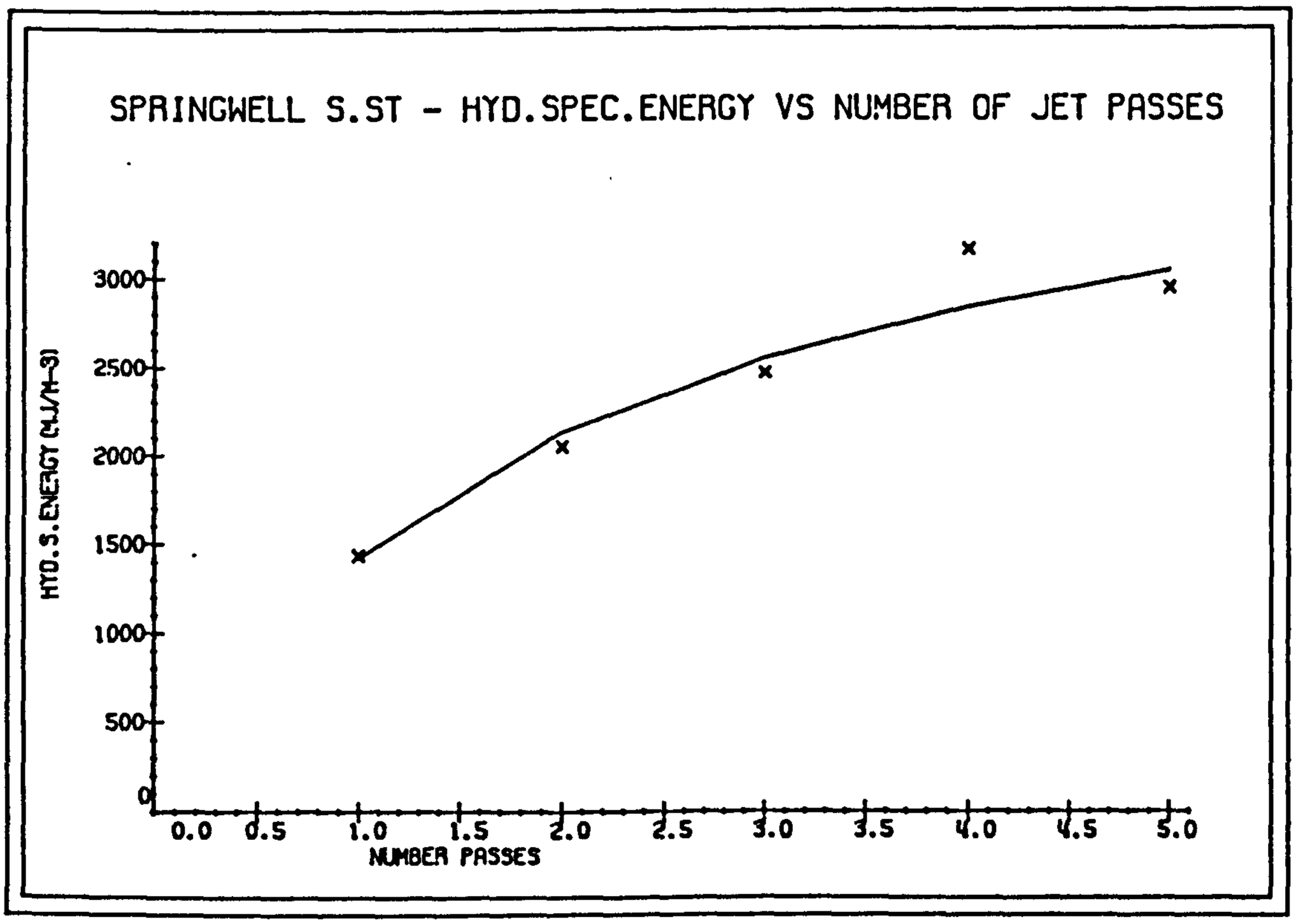
SPRINGWELL S.ST - HYD.SPEC.ENERGY VS NUMBER OF JET PASSES
HYD.S.ENERGY (MJ/M-3)
0
500
1000
1500
2000
2500
3000
0.0
0.5
1.0
1.5
2.0
2.5
3.0
3.5
4.0
4.5
5.0
NUMBER PASSES

FIG. 7.50

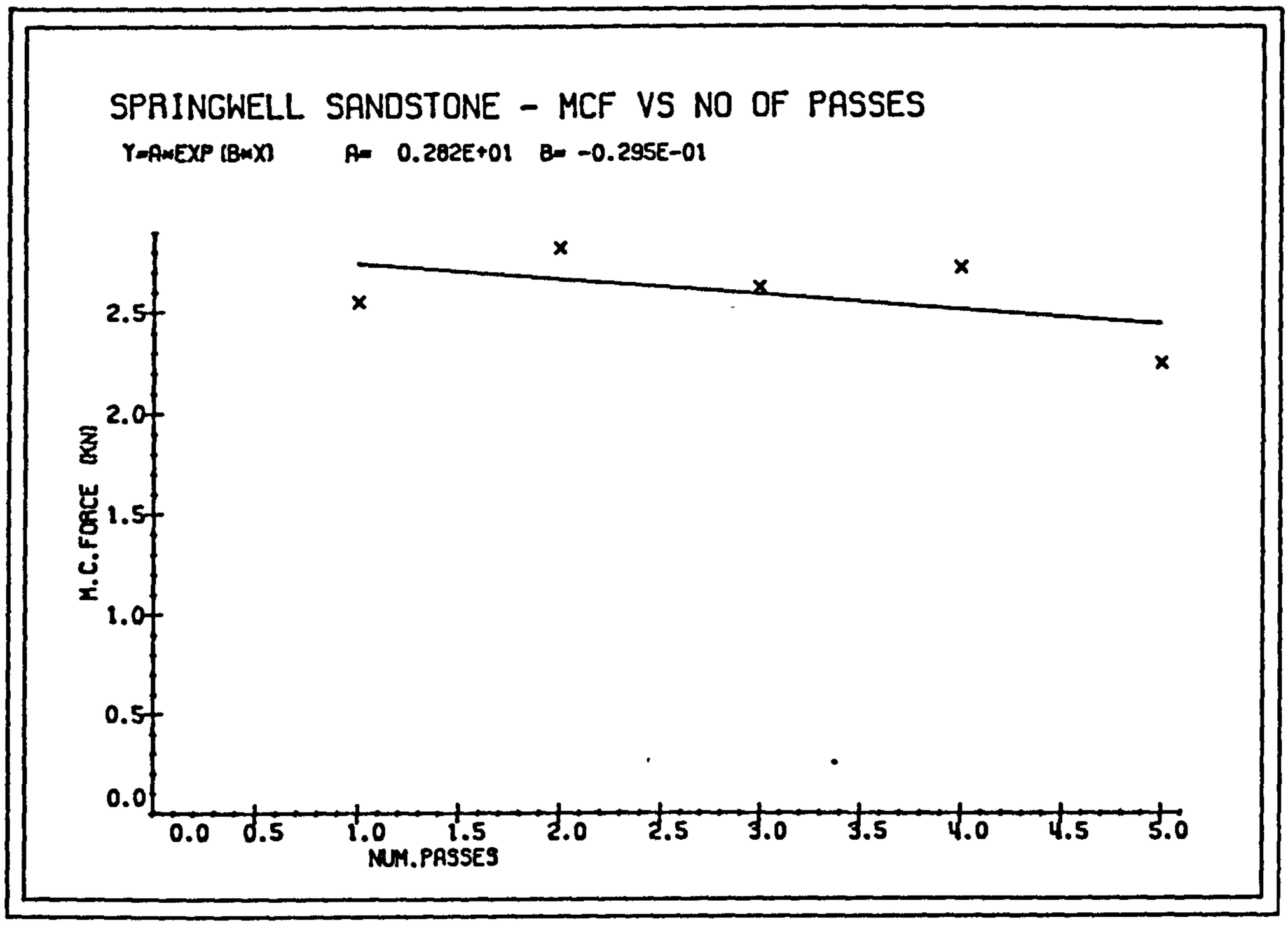
SPRINGWELL SANDSTONE - MCF VS NO OF PASSES
Y=A*EXP(B*X) A= 0.282E+01 B= -0.295E-01
M.C.FORCE (KN)
2.5
2.0
1.5
1.0
0.5
0.0
0.0 0.5 1.0 1.5 2.0 2.5 3.0 3.5 4.0 4.5 5.0
NUM.PASSES

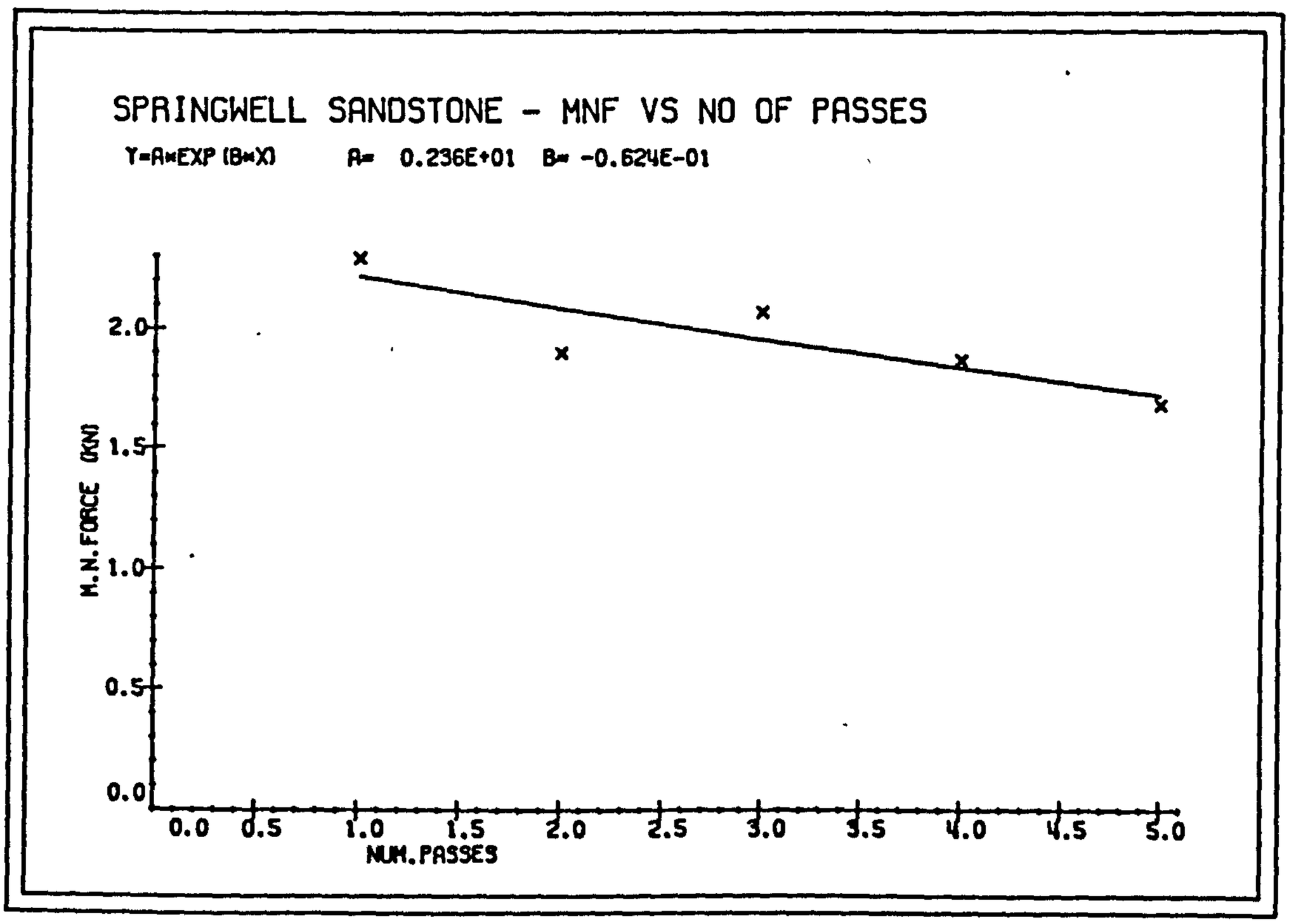
SPRINGWELL SANDSTONE - MNF VS NO OF PASSES
Y=A*EXP(B*X) A= 0.236E+01 B= -0.624E-01
M.N.FORCE (KN)
2.0
1.5
1.0
0.5
0.0
0.0 0.5 1.0 1.5 2.0 2.5 3.0 3.5 4.0 4.5 5.0
NUM.PASSES

FIG. 7.51

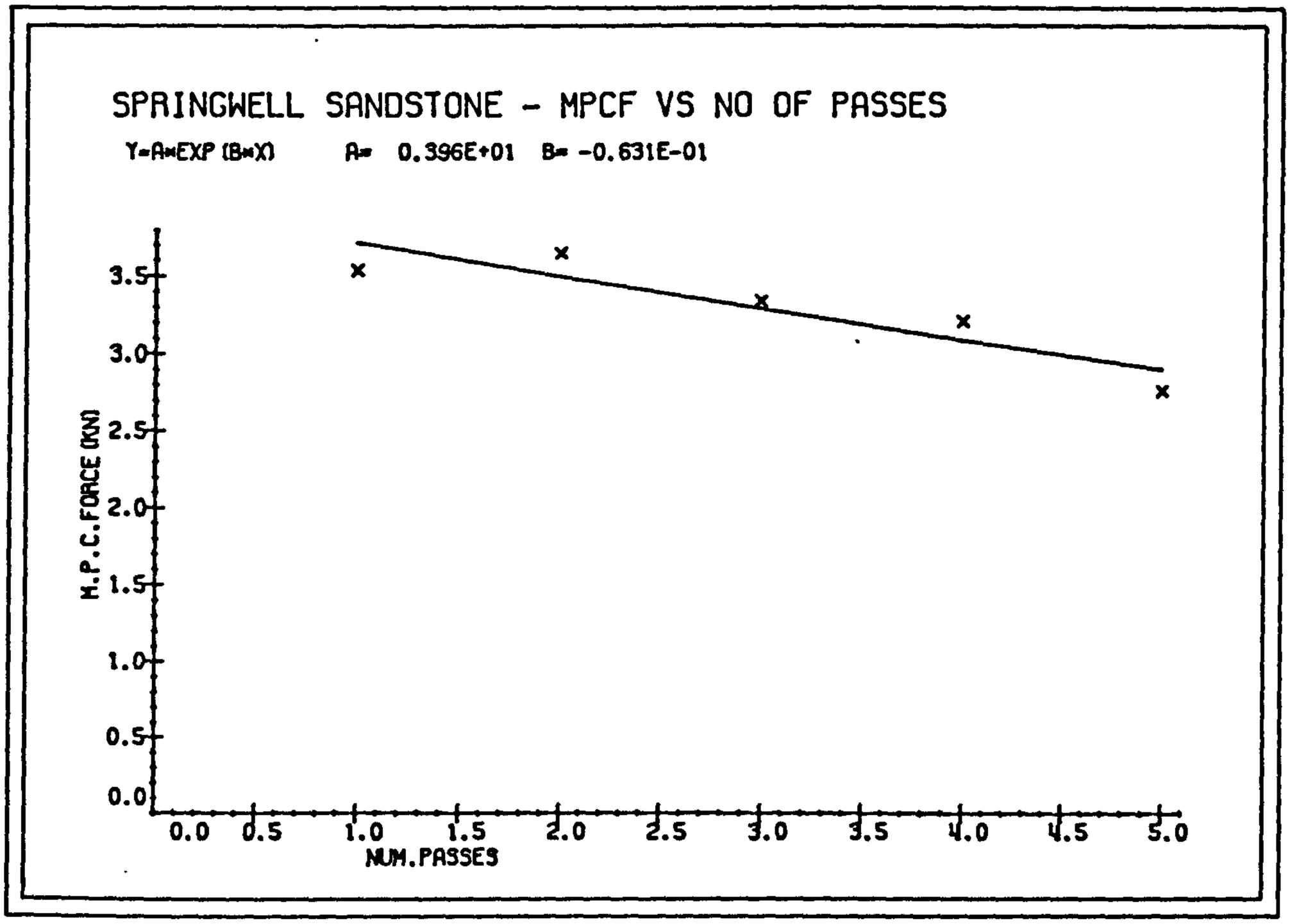
SPRINGWELL SANDSTONE - MPCF VS NO OF PASSES
Y=A*EXP(B*X) A= 0.396E+01 B= -0.631E-01
M.P.C.FORCE (KN)
3.5
3.0
2.5
2.0
1.5
1.0
0.5
0.0
0.0 0.5 1.0 1.5 2.0 2.5 3.0 3.5 4.0 4.5 5.0
NUM.PASSES

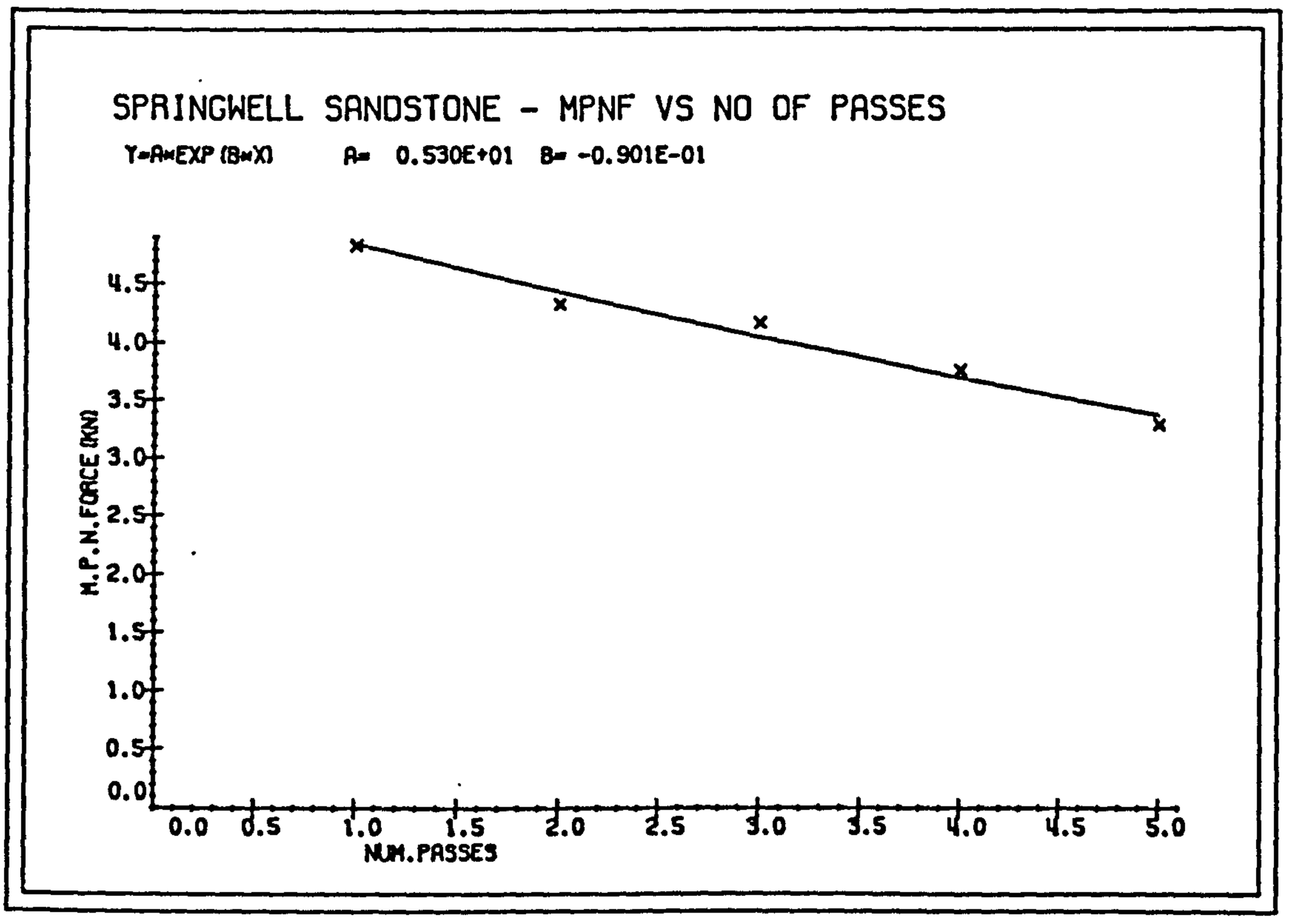
SPRINGWELL SANDSTONE - MPNF VS NO OF PASSES
Y=A*EXP(B*X) A= 0.530E+01 B= -0.901E-01
M.P.N.FORCE (KN)
4.5
4.0
3.5
3.0
2.5
2.0
1.5
1.0
0.5
0.0
0.0 0.5 1.0 1.5 2.0 2.5 3.0 3.5 4.0 4.5 5.0
NUM.PASSES

FIG. 7.52

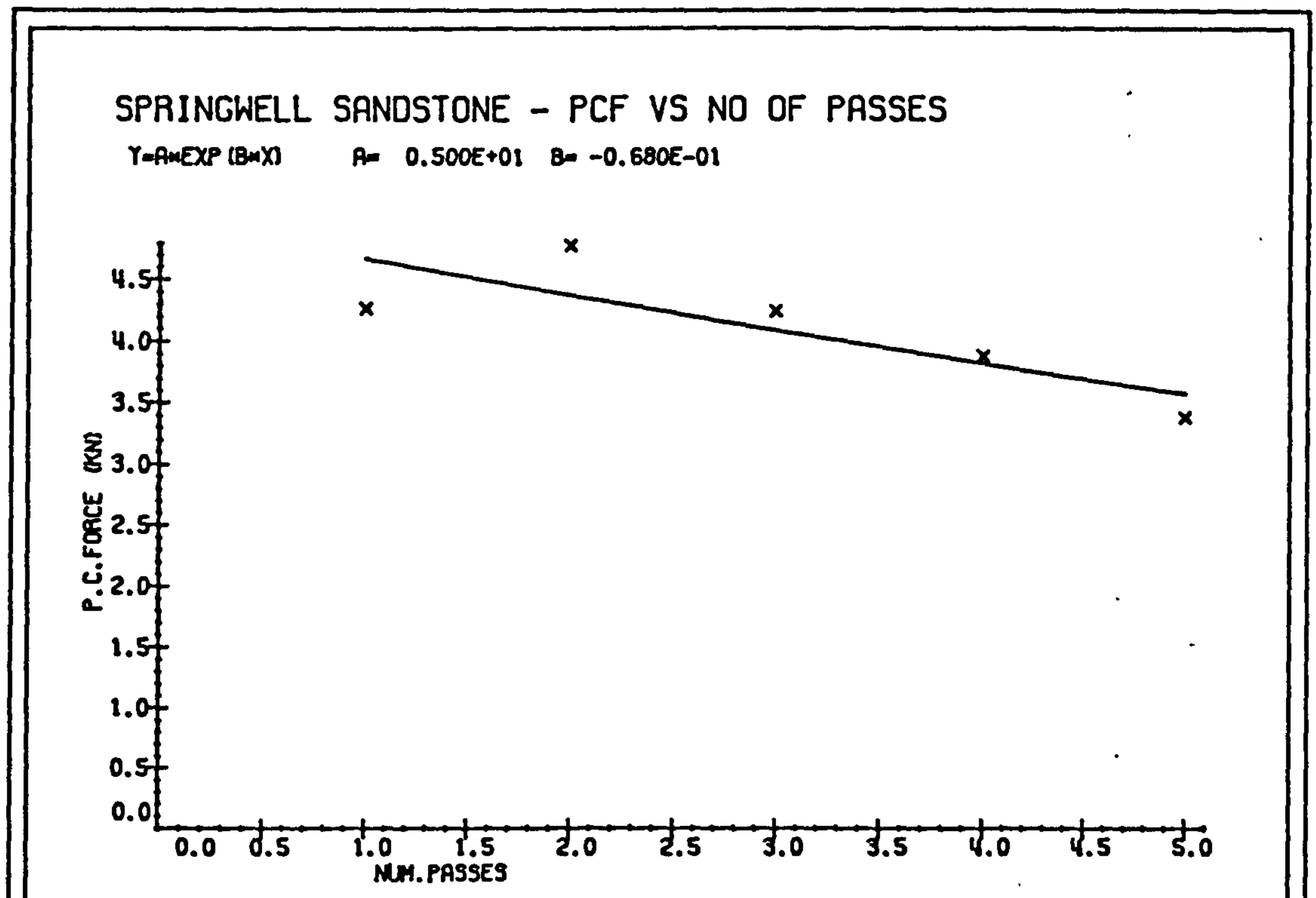
SPRINGWELL SANDSTONE - PCF VS NO OF PASSES
Y=A*EXP(B*X)
A= 0.500E+01
B= -0.680E-01
P.C.FORCE (KN)
4.5
4.0
3.5
3.0
2.5
2.0
1.5
1.0
0.5
0.0
0.0
0.5
1.0
1.5
2.0
2.5
3.0
3.5
4.0
4.5
5.0
NUM.PASSES

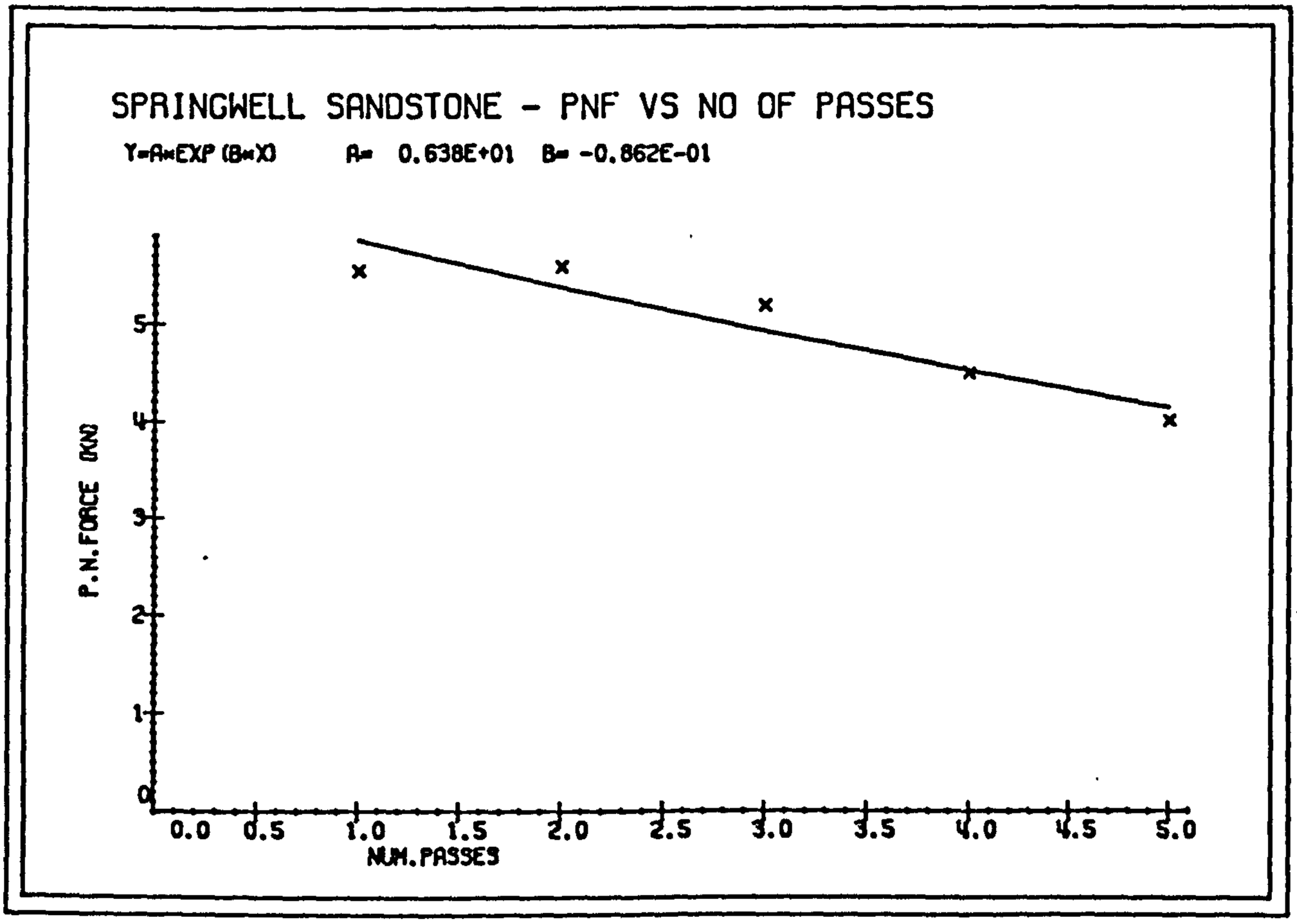
SPRINGWELL SANDSTONE - PNF VS NO OF PASSES
Y=A*EXP(B*X)
A= 0.638E+01
B= -0.862E-01
P.N.FORCE (KN)
5
4
3
2
1
0
0.0
0.5
1.0
1.5
2.0
2.5
3.0
3.5
4.0
4.5
5.0
NUM.PASSES

FIG. 7.53

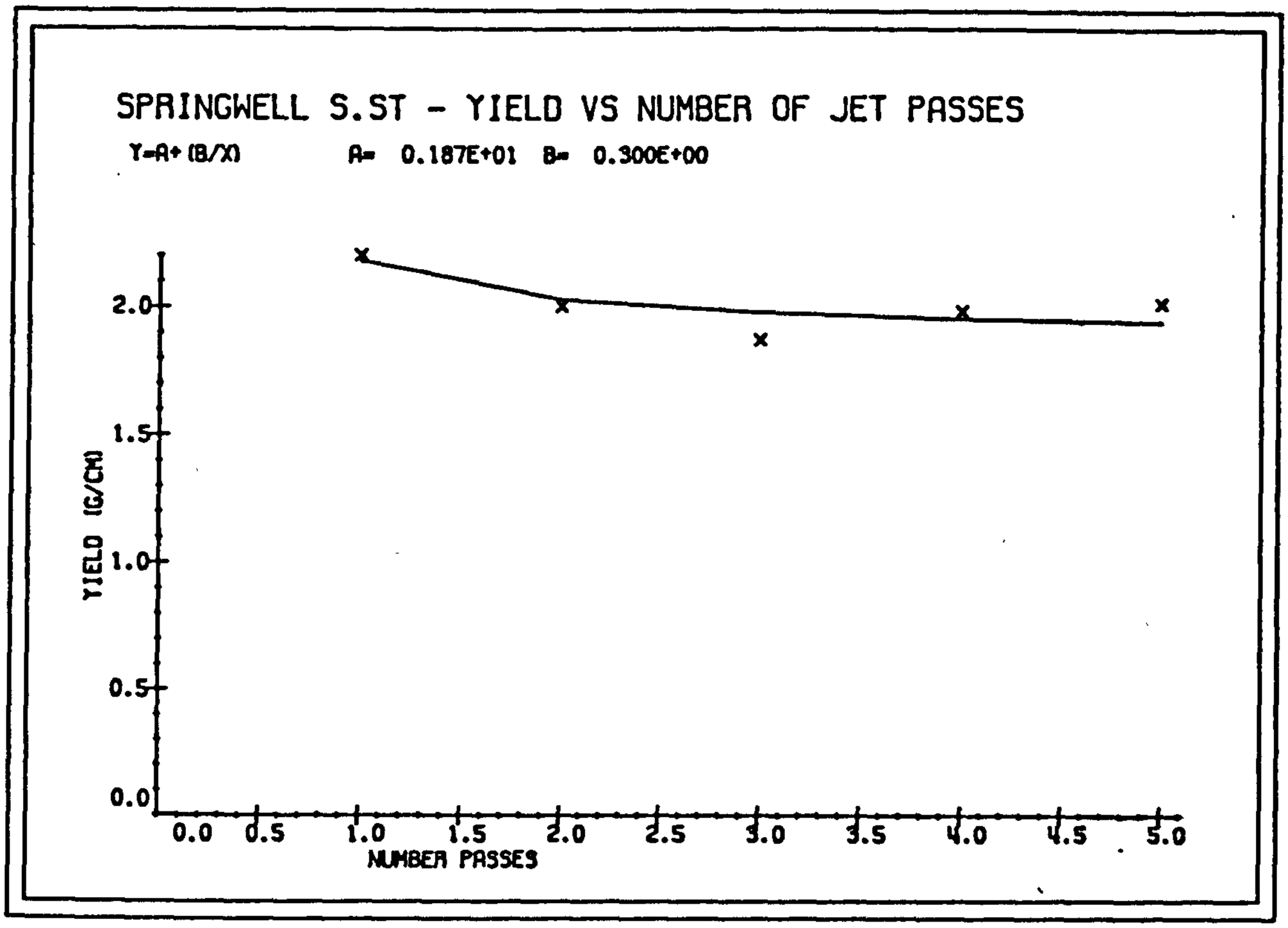
SPRINGWELL S.ST - YIELD VS NUMBER OF JET PASSES
Y=A+(B/X)
A= 0.187E+01 B= 0.300E+00
YIELD (G/CM)
2.0
1.5
1.0
0.5
0.0
0.0 0.5 1.0 1.5 2.0 2.5 3.0 3.5 4.0 4.5 5.0
NUMBER PASSES

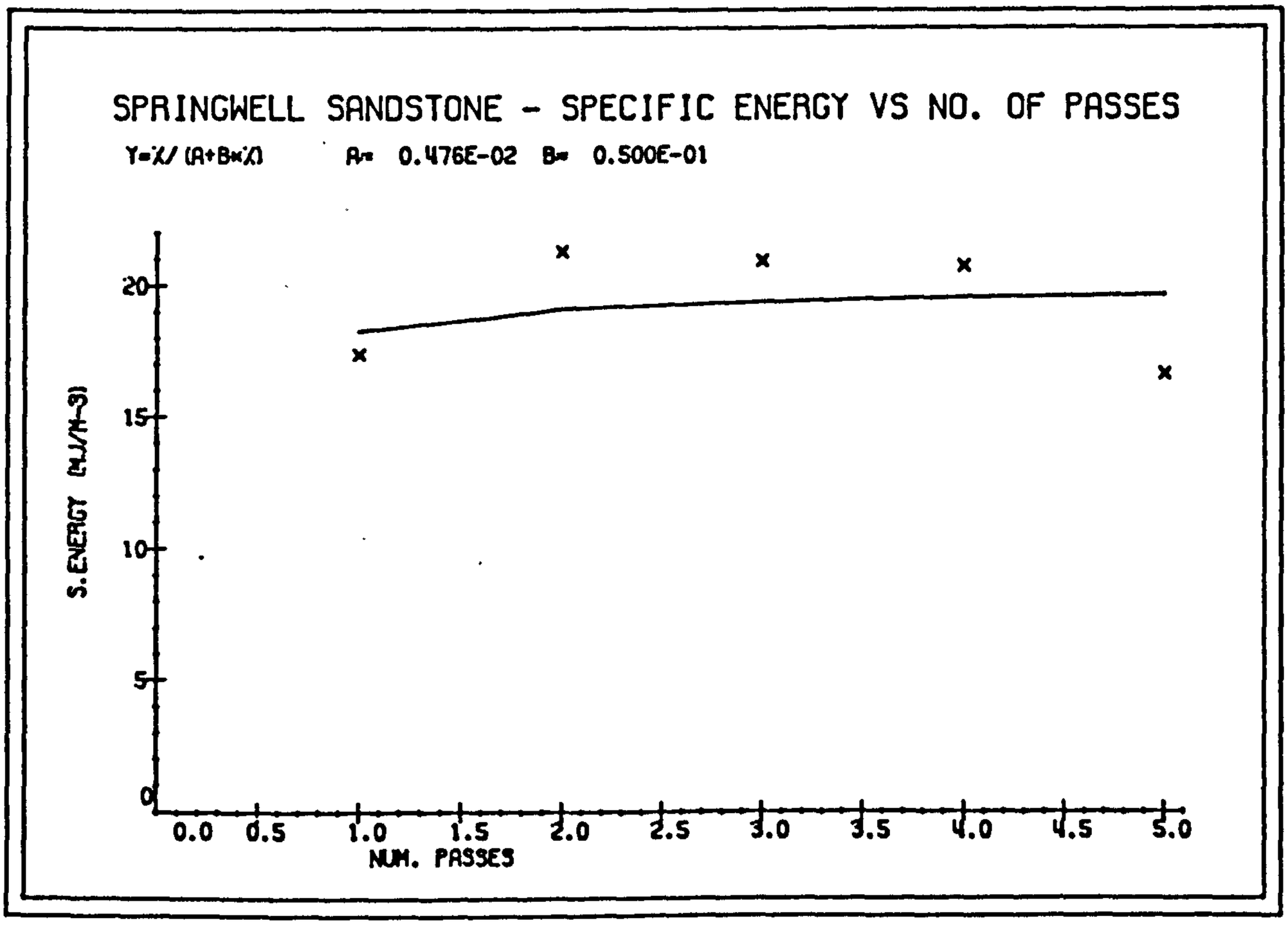
SPRINGWELL SANDSTONE - SPECIFIC ENERGY VS NO. OF PASSES
Y=X/(A+B*X)
A= 0.476E-02 B= 0.500E-01
S.ENERGY (MJ/M-3)
20
15
10
5
0
0.0 0.5 1.0 1.5 2.0 2.5 3.0 3.5 4.0 4.5 5.0
NUM. PASSES

FIG. 7.54

7.7.2 Discussion

The essential principle of water jet cutting is to make deeper cut while minimizing the energy expended per unit area of cut.

Assuming the cutting action of each jet is not hindered by the following jets, it may be advantageous to multiply the jets rather than to increase the diameter. Because, increasing the nozzle diameter by a factor of two causes volumetric flow to increase by a factor of four and the power by a similar amount.

Springwell sandstone experimental results had revealed that penetration depth increased at a decreasing rate -indicating that the jet cutting was becoming less efficient- with increase in the number of jets. Cutting and Normal forces, and Mechanical Specific Energy have decreased.

Although it may be possible to locate jets in order on the cutting head of an excavation machine, while in operation it may not be possible for each jet to cut along the same groove because of the vibrations. The diameter of the jets are small and a minimal vibration would throw the cutting direction off its course.

7.7.3 Conclusions

One of the ways of achieving deeper jet penetration depth is to increase the number of jet, each of which cut along the same groove.

Penetration depths have varied directly with the jet number, showing a hyperbolic relationship. The Hydraulic Specific Energy graph indicated that jet cutting was becoming less efficient with increase in the number of jets.

Cutting and Normal forces decreased exponentially and Mechanical Specific Energy decreased slowly with the number of jets. Yield has decreased, but after two jet passes relatively small change was seen. The reduction in forces were not commensurate with the increase in jet penetration depth.

The maximum number of jets used in tandem should not exceed five. Because cutting becomes less efficient with each increasing pass.

8 COMPARISION EXPERIMENTS

The range of applicability of hybrid cutting system can be assessed if the operating performances of point attack tool cutting systems, both with and without high-pressure water jet assistance, are investigated in a variety of rock materials, e.g. strong, weak, porous, non-permeable, sedimentary, crystaline, etc.

The cutting experiments described in this thesis have all been conducted on sedimentary rocks. Care was taken in the selection of experimental rocks which included four sandstones namely Springwell, Darney, Darley Dale, Sandstone D, and three limestones - so that they exhibited differring rock properties when compared and covered the cutting range described above.

Experiments were planned such that, the water jet operated at its maximum available pressure and at optimum nozzle position in relation to the mechanical tool(chosen from the previous experiments), when cutting with hybrid system.

The depth of cut of the mechanical tool was chosen to be the operating variable that would enable the comparison to be made between the two cutting systems in terms of tool forces (cutting and normal), yield and mechanical specific energy.

8.1 EXPERIMENTAL DESIGN

Experimental variables and their levels for each rock type were as follows:

	Mechanical Cutting System	Hybrid Cutting System
Nozzle diameter (mm)	---	0.85
Waterjet pressure (MPa)	---	55.17
Stand-off distance (mm)	---	15
Lead-on distance (mm)	---	1
Side-off distance (mm)	---	0
Cutting speed (mm/sec)	165	165
Mech. depth of cut (mm)	2, 4, 6, 8, 10	2, 4, 6, 8, 10
Point Attack Tool :		
Tip angle (degrees)	87	87
Off-set angle (degrees)	6.5	6.5
Angle of attack (degrees)	45	45

2 x 5 x 4 = 40 cutting tests were conducted on each rock with a new pristene condition point attack tool. Experiments were carried out in random order to minimise the effects of changes that might occur in experimental conditions.

The diameter of the tool tip was measured under the microscope, after each experiment, to note the wear flat. Within the experimental cutting distance range this remained approximately constant. In addition to microscopic examination, a standard cutting test was carried out after each experimental cut. These were compared with each other and found to remain approximately constant too.

Computer curve-fitting analysis was carried out on the experimental output and results are presented graphically. The index of determinations of equations selected, together with regression formulae's are given in (Appendix D).

Further laboratory testing was undertaken to classify each rock according to their physical and mechanical properties.

8.2 ROCK PROPERTIES

Rock Type	Bulk Density Dry (g/cm^3)	Bulk Density Wet (g/cm^3)	Porosity Apparent (%)	Porosity True (%)
Darley Dale	2.18	2.35	7.93	21.2
L.st B	2.20	2.41	10.00	17.4
Portland	2.33	2.46	6.10	14
S.st D	2.38	2.462	3.40	N.M

Rock Type	Sclr Rebound Hardness	Plasticity (%)	Schmidt Hammer Hardness
Darley Dale	58.38	27.3	44.8
L.st B	53.6	31.9	35.2
Portland	42.5	30.1	36.1
S.st D	47.3	15.6	N.M

Rock Type	Dynamic Mod (GPa)	NCB Cone Indr Hardness	Grain Density (g/cm^3)
Darley Dale	9.80	2.48	2.67
L.st B	28.00	2.65	2.85
Portland	18.80	3.14	2.71
S.st D	55.40	3.83	2.65

Rock Type	Comprsv Strh (MPa)	Tensile Strh (MPa)	Comp/ Tensile
Darley Dale	57.5	3.7	15.6
L.st B	71.3	4.4	11.8
Portland	71.7	6.1	11.9
S.st D	149.1	12.3	12.1

8.2.1 Thin Section Analysis

Darley Dale Sandstone

This is a highly porous sandstone. It is medium to fine grained with a sparse siliceous cement and some inclusion of clay(mica) material. The quartz grains are subangular.

	%	Grain size
Quartz	62	0.2 mm
Clay and mica	1	
Pores	37	

Sandstone D

This is a very fine grained sandstone. There are very few quartz grains visible and these are set in a siliceous cement. As second infill cement of calcite is also present, hence porosity is very low.

	%	Grain size
Quartz	70	0.05mm
Siliceous cement	20	
Calcareous cement	10	
Pores	<1	

Portland Limestone

This is a oolitic limestone. It contains some large shell fragments and a small amount of detrial material as very fine angular grains of quartz.

	%	Grain size
Calcite	85	0.03 mm
Quartz	5	0.25 mm
Pores	10	

Limestone B

This is a highly porous dolomitised limestone. It is composed almost exclusively of dolomite crystalls forming near perfect rhombs. There is virtually no detriatal material present.

	%
Dolomite	70
Quartz	<1
Pores	29

Average grain size : 0.3mm

8.3 EFFECT OF DEPTH OF CUT

8.3.1 On Tool Forces

Cutting and Normal forces have increased linearly with increase in depth of cut for all rock types, (Fig. 8.1-8.10). Hybrid cutting gave lower forces than mechanical cutting at corresponding depth of cuts. Slopes of curve-fitted lines were steeper for mechanical cutting than hybrid cutting.

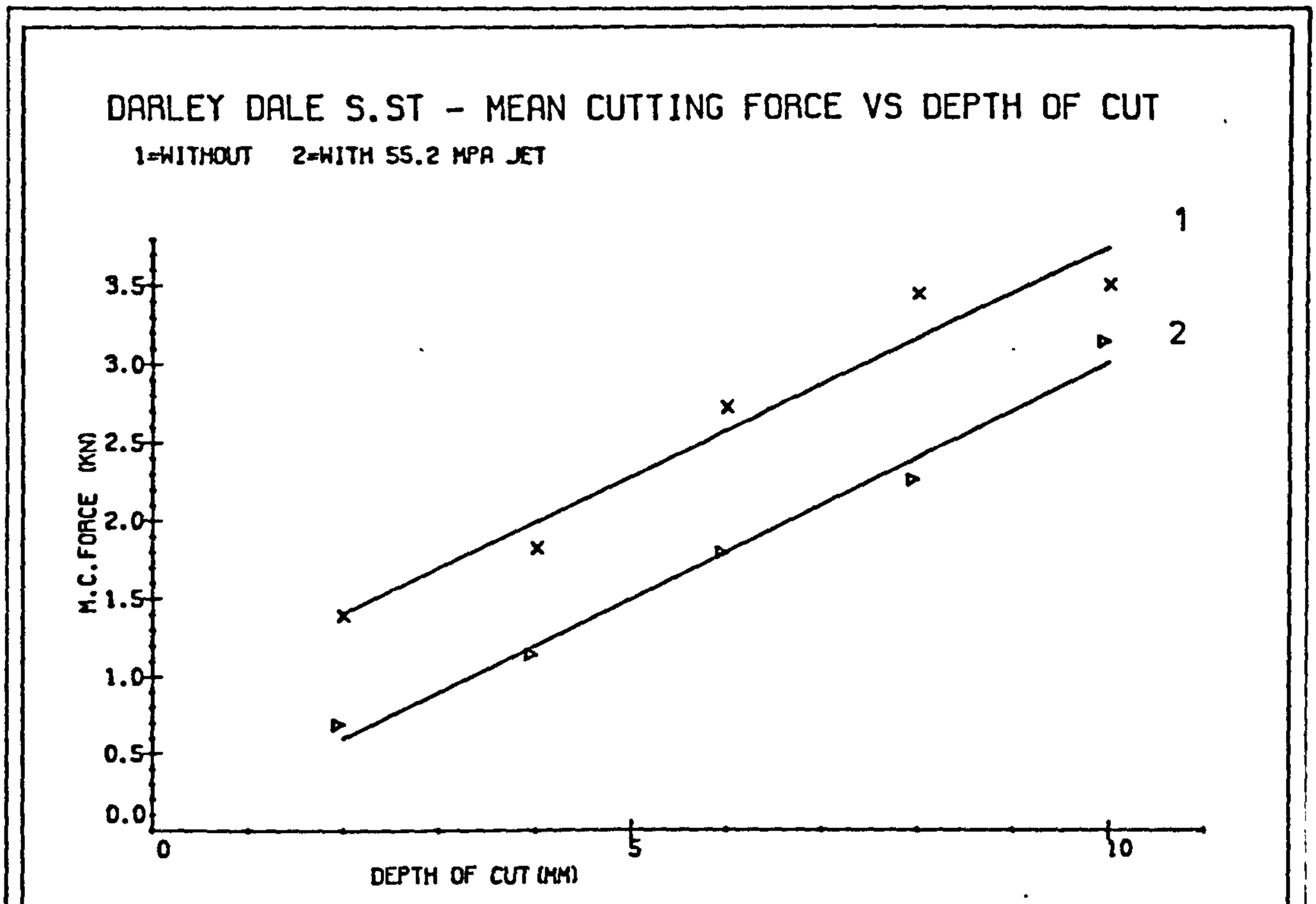
DARLEY DALE S.ST - MEAN CUTTING FORCE VS DEPTH OF CUT
1=WITHOUT 2=WITH 55.2 MPA JET
M.C.FORCE (KN)
3.5
3.0
2.5
2.0
1.5
1.0
0.5
0.0
0
5
10
DEPTH OF CUT (MM)
1
2

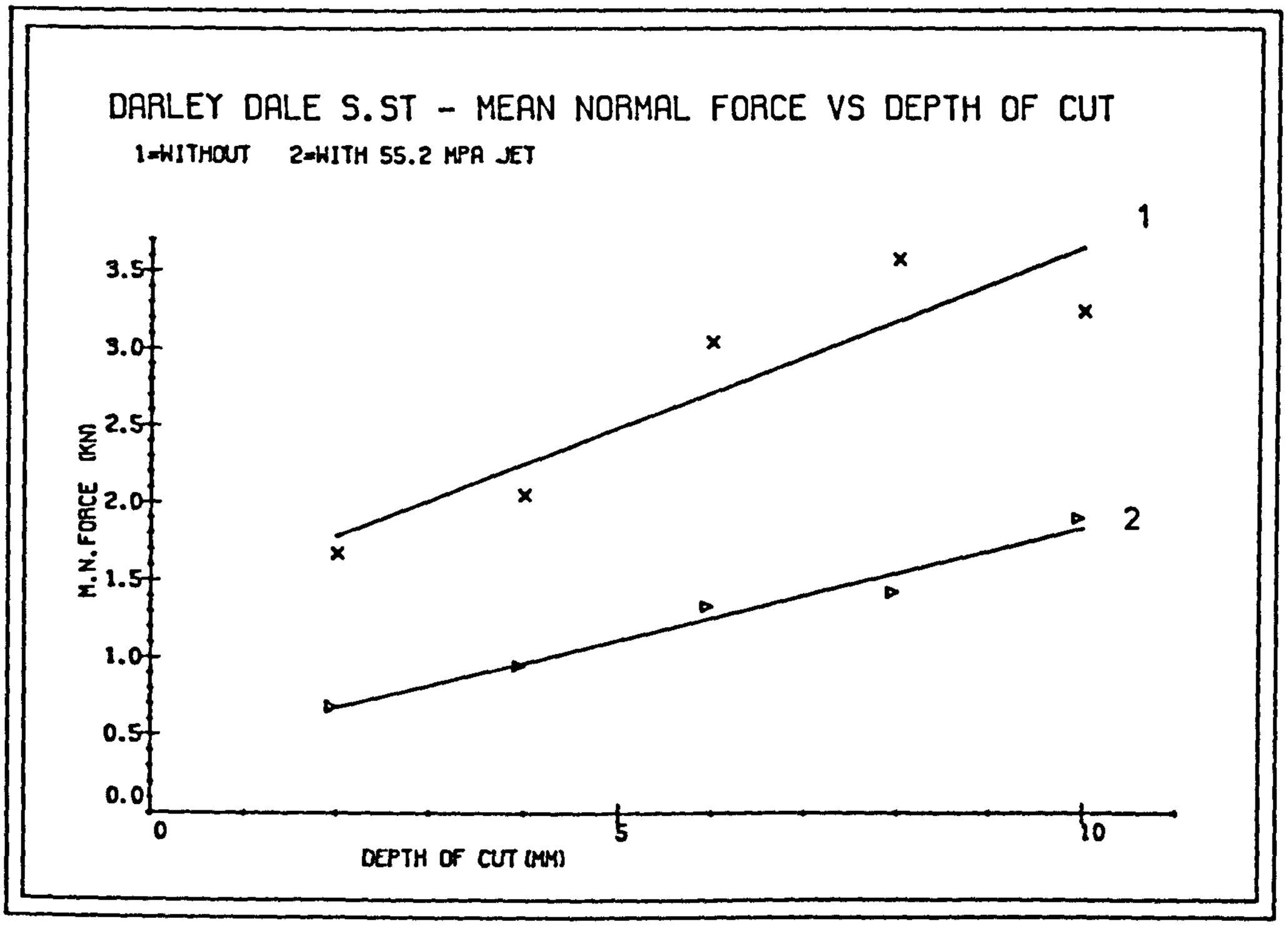
DARLEY DALE S.ST - MEAN NORMAL FORCE VS DEPTH OF CUT
1=WITHOUT 2=WITH 55.2 MPA JET
M.N.FORCE (KN)
3.5
3.0
2.5
2.0
1.5
1.0
0.5
0.0
0
5
10
DEPTH OF CUT (MM)
1
2

FIG. 8.1

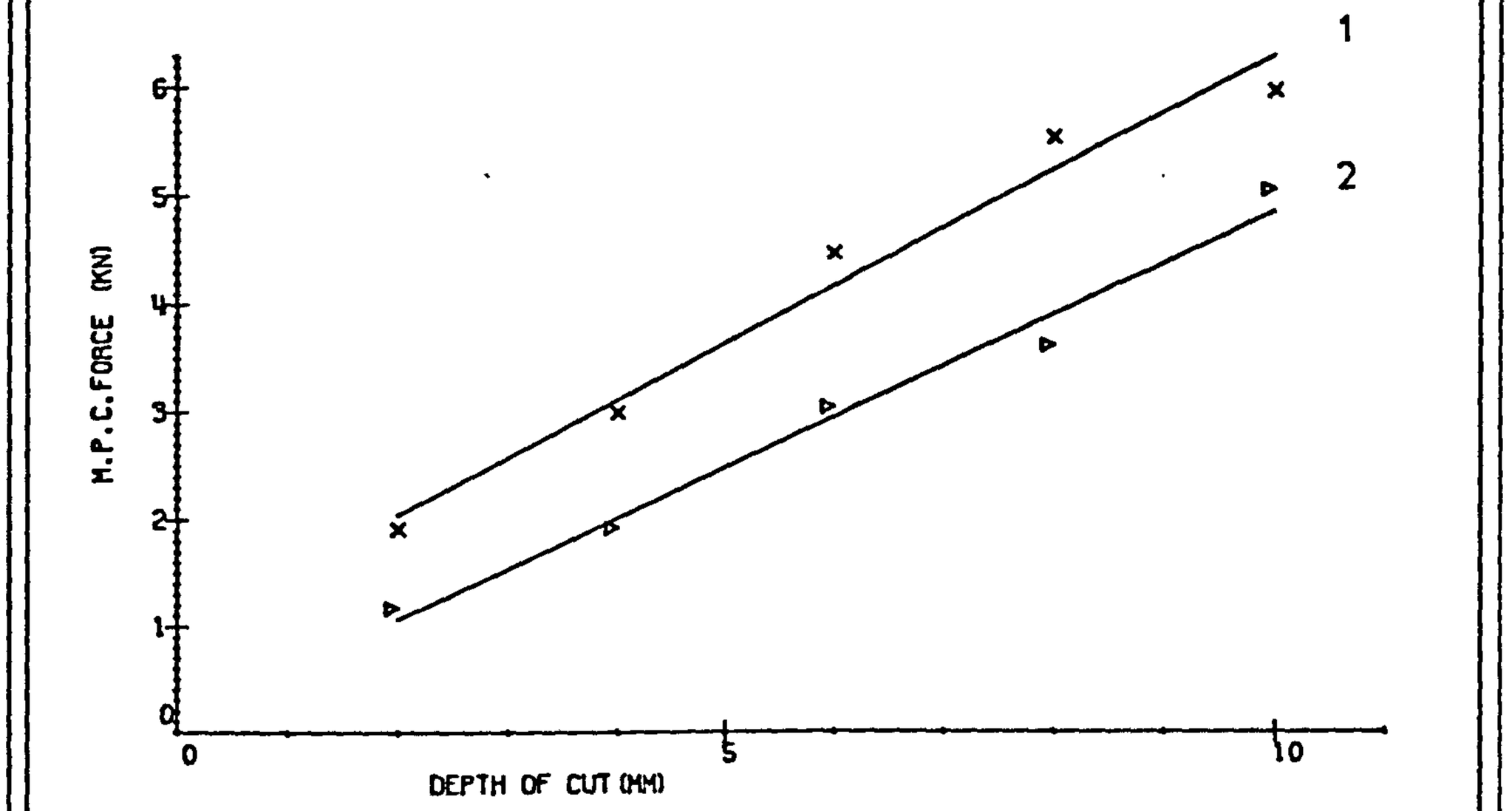
DARLEY DALE S.ST - M.PEAK CUTTING FORCE VS DEPTH OF CUT
1=WITHOUT 2=WITH 55.2 MPA JET
M.P.C.FORCE (KN)
0
1
2
3
4
5
6
0
5
10
DEPTH OF CUT (MM)
1
2

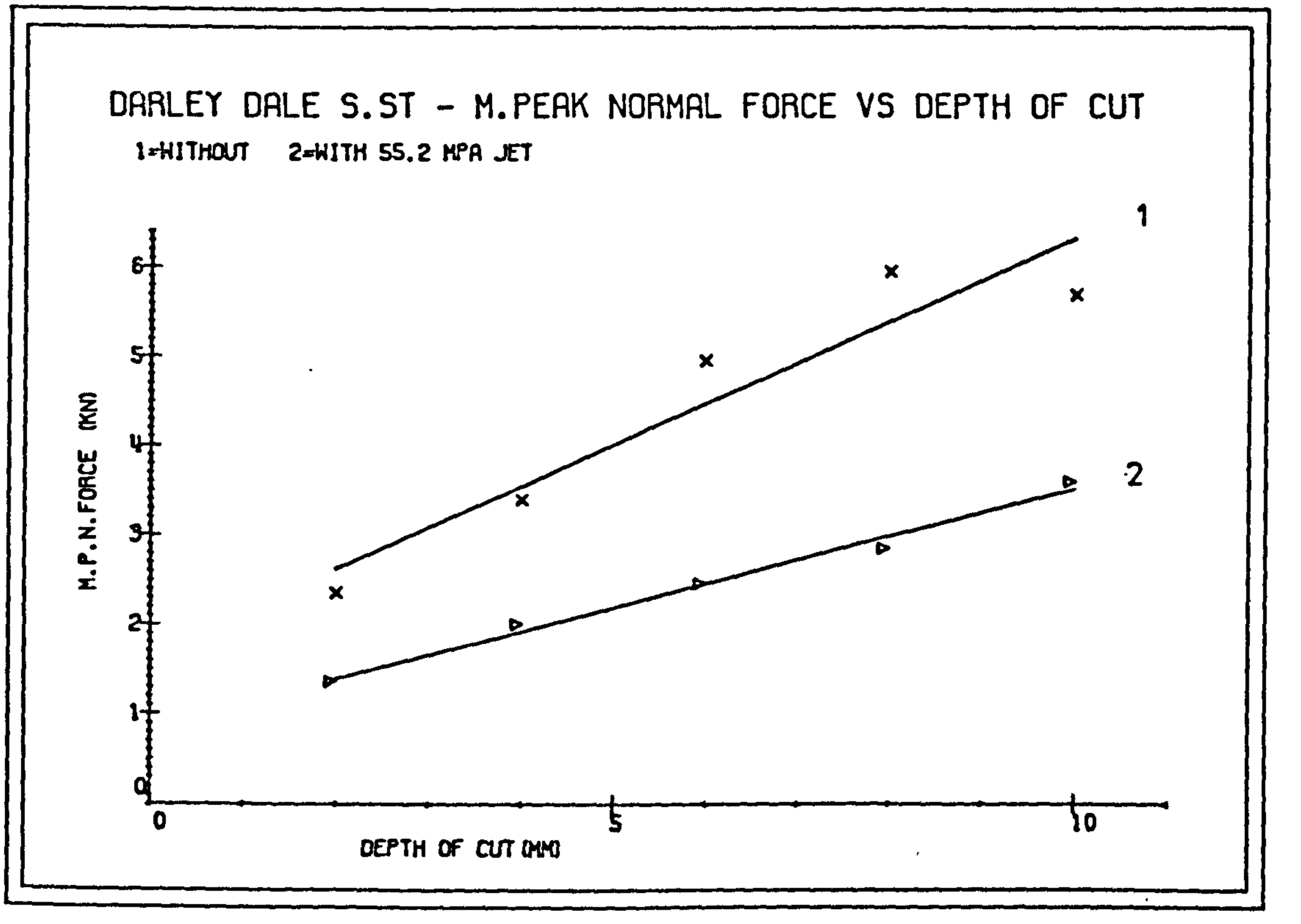
DARLEY DALE S.ST - M.PEAK NORMAL FORCE VS DEPTH OF CUT
1=WITHOUT 2=WITH 55.2 MPA JET
M.P.N.FORCE (KN)
0
1
2
3
4
5
6
0
5
10
DEPTH OF CUT (MM)
1
2

FIG. 8.2

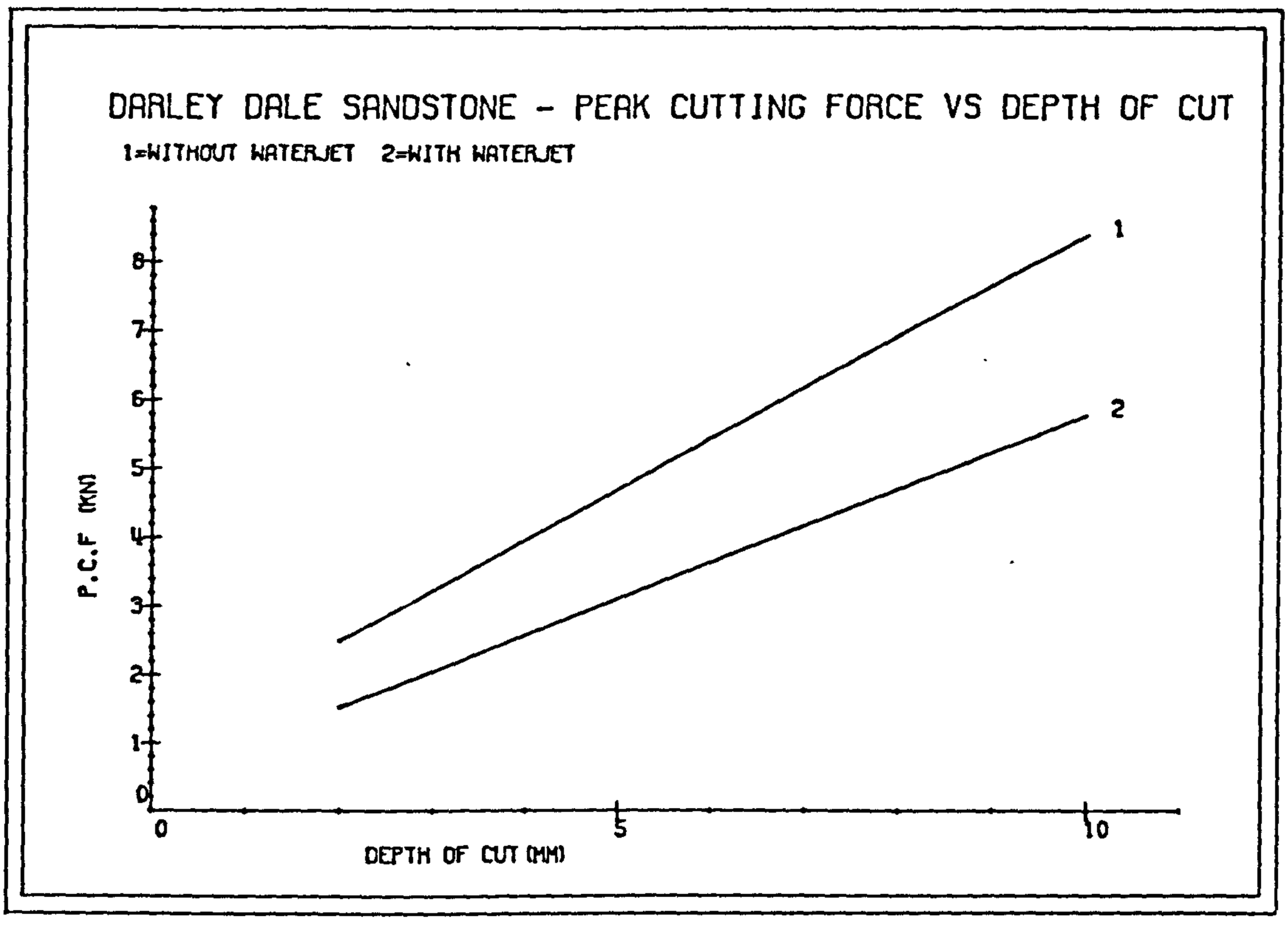
DARLEY DALE SANDSTONE - PEAK CUTTING FORCE VS DEPTH OF CUT
1=WITHOUT WATERJET 2=WITH WATERJET
P.C.F (KN)
0
1
2
3
4
5
6
7
8
1
2
0
5
10
DEPTH OF CUT (MM)

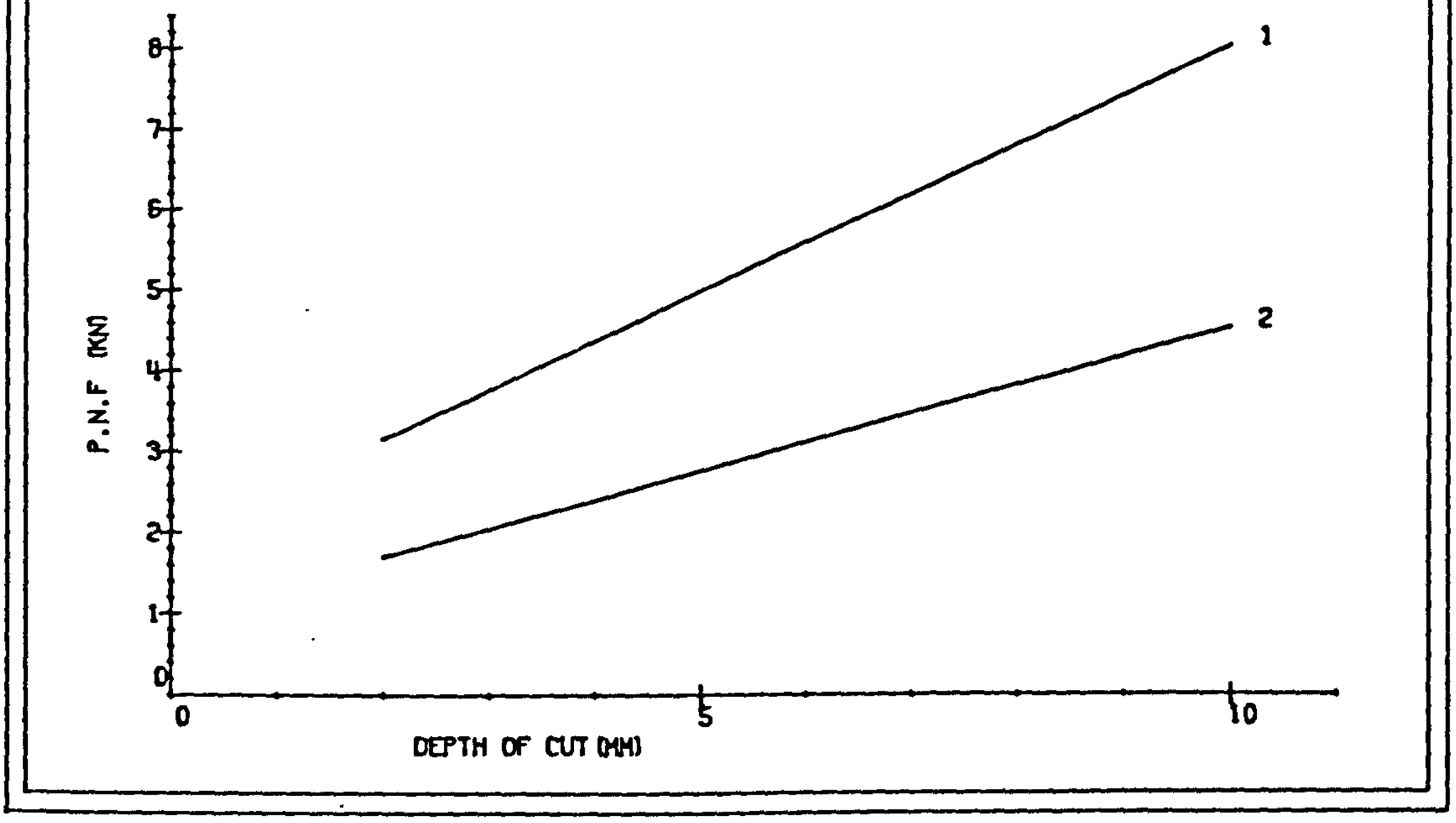
DARLEY DALE SANDSTONE - PEAK NORMAL FORCE VS DEPTH OF CUT
1=WITHOUT WATERJET 2=WITH WATERJET
P.N.F (KN)
0
1
2
3
4
5
6
7
8
1
2
0
5
10
DEPTH OF CUT (MM)

FIG. 8.3

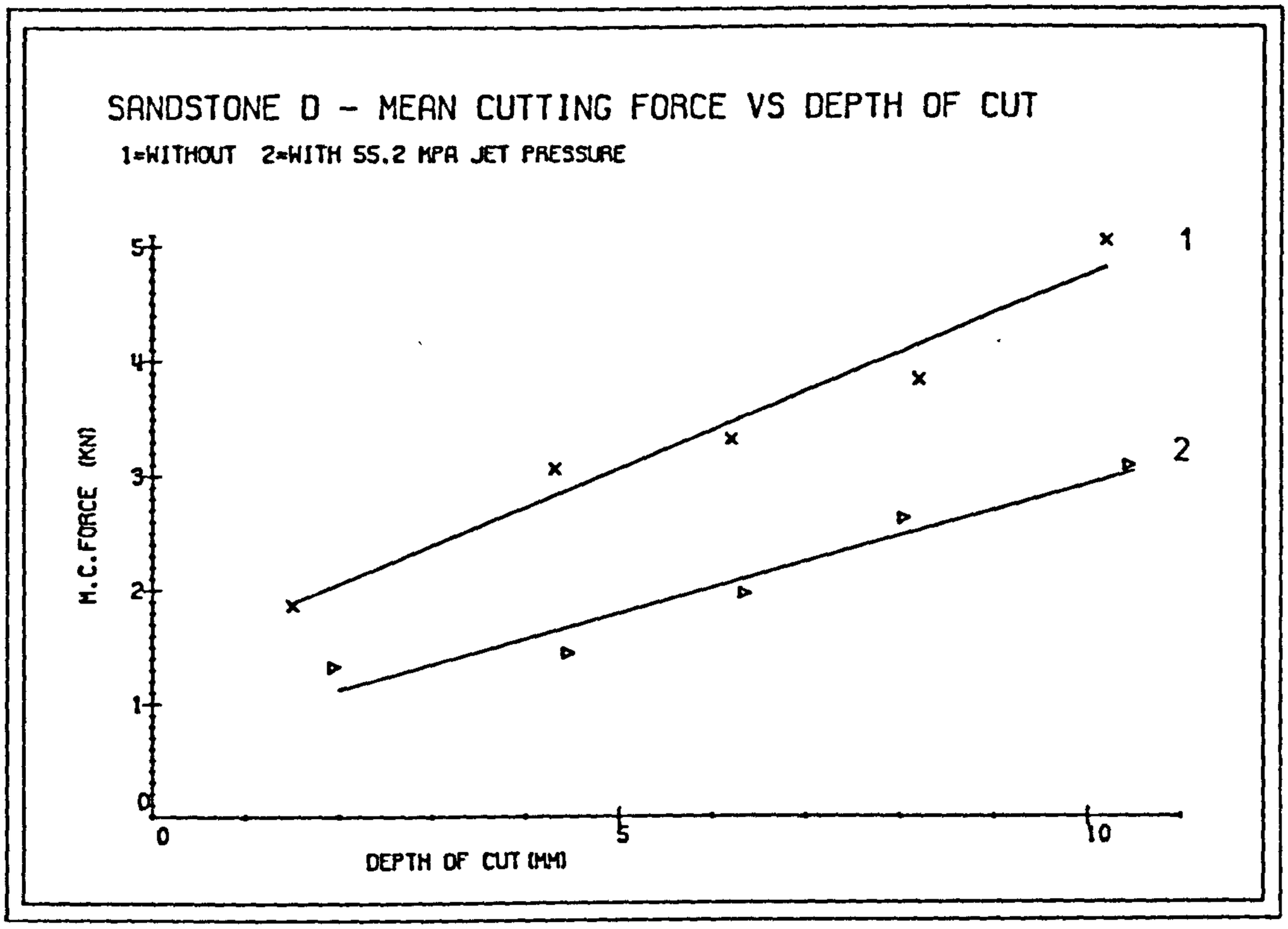
SANDSTONE D - MEAN CUTTING FORCE VS DEPTH OF CUT
1=WITHOUT 2=WITH 55.2 MPA JET PRESSURE
M.C.FORCE (KN)
0
1
2
3
4
5
0
5
10
DEPTH OF CUT (MM)
1
2

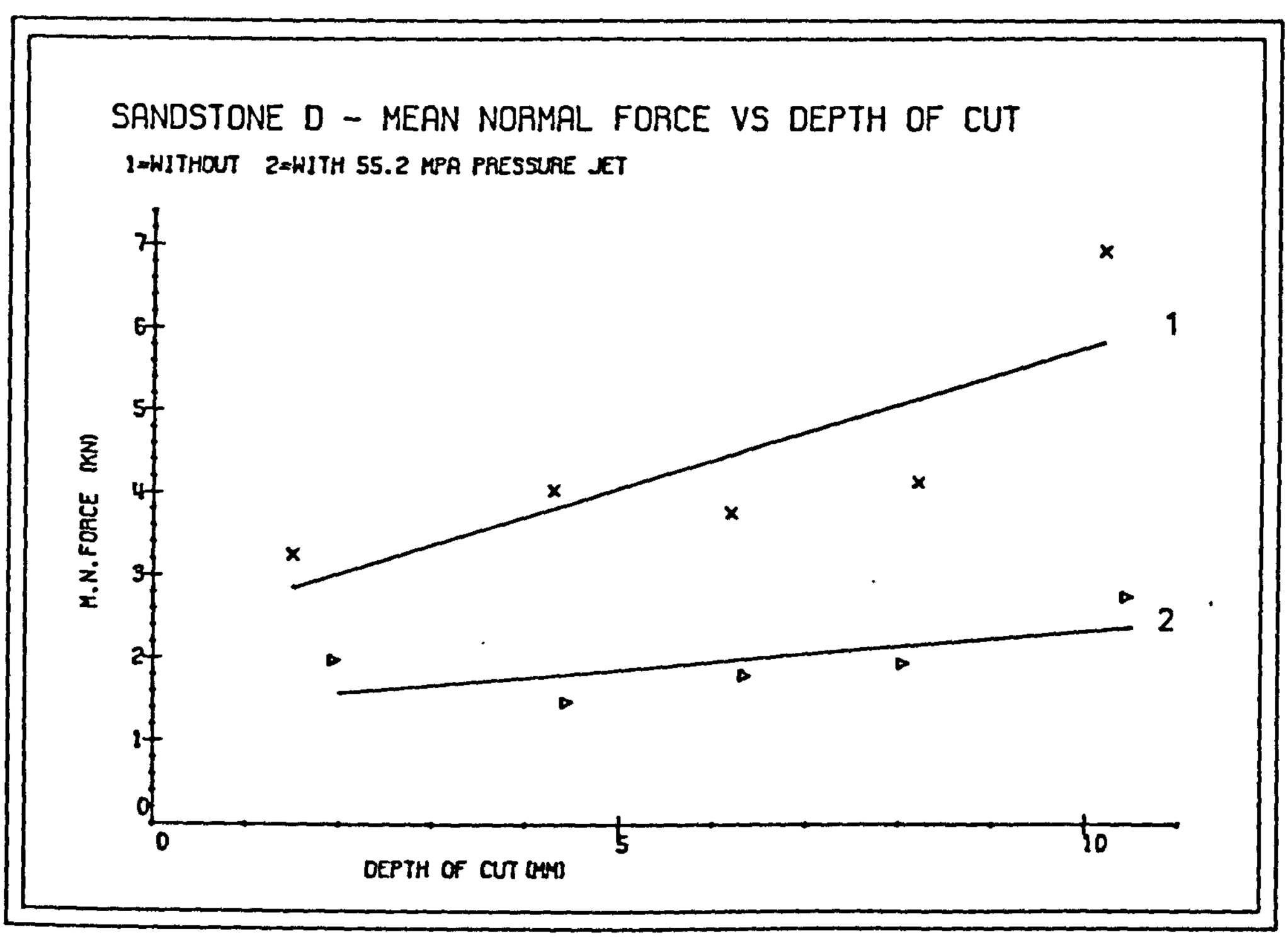
SANDSTONE D - MEAN NORMAL FORCE VS DEPTH OF CUT
1=WITHOUT 2=WITH 55.2 MPA PRESSURE JET
M.N.FORCE (KN)
0
1
2
3
4
5
6
7
0
5
10
DEPTH OF CUT (MM)
1
2

FIG. 8.4

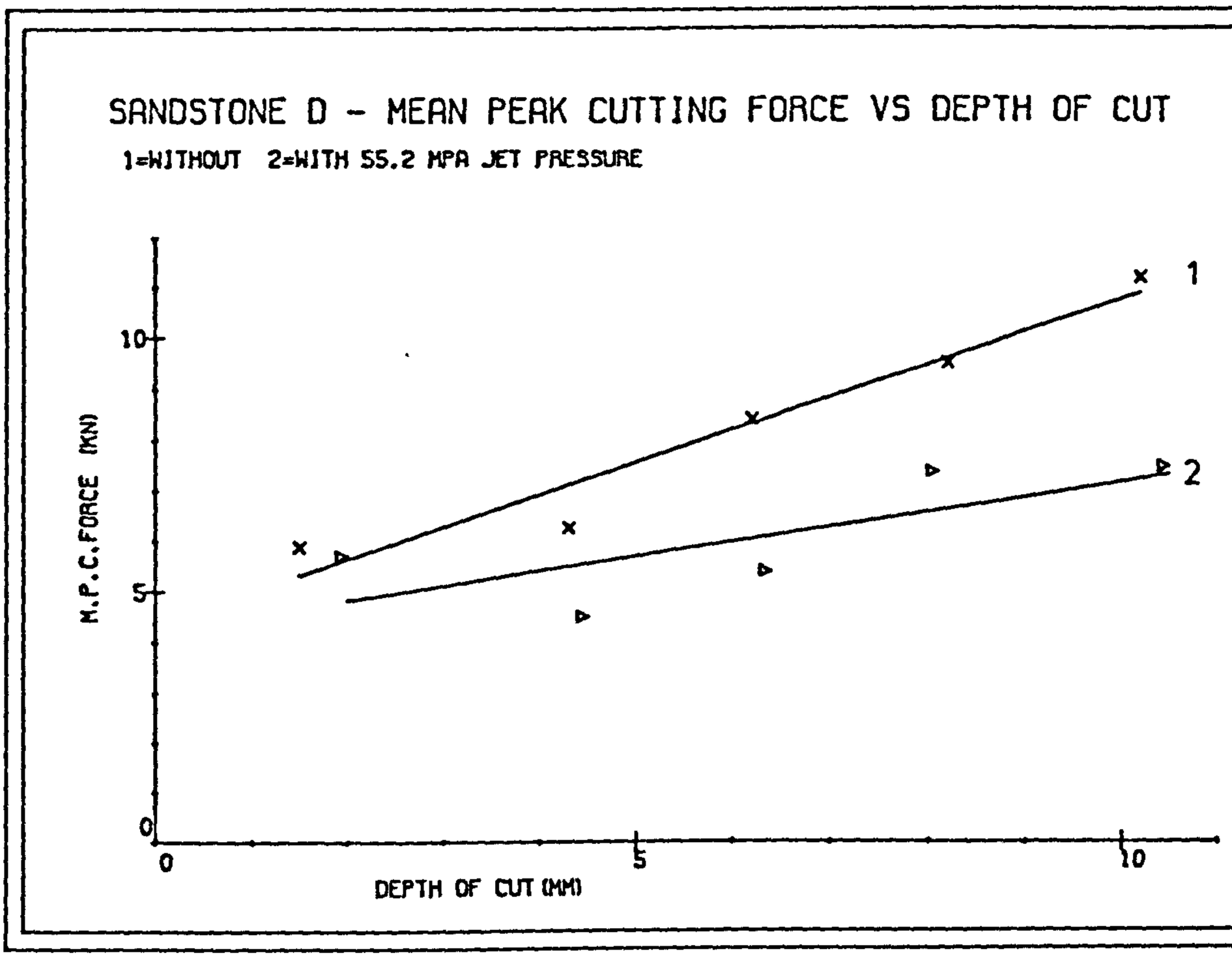
SANDSTONE D - MEAN PEAK CUTTING FORCE VS DEPTH OF CUT
1=WITHOUT 2=WITH 55.2 MPA JET PRESSURE
M.P.C.FORCE (KN)
10
5
0
0
5
10
DEPTH OF CUT (MM)
1
2

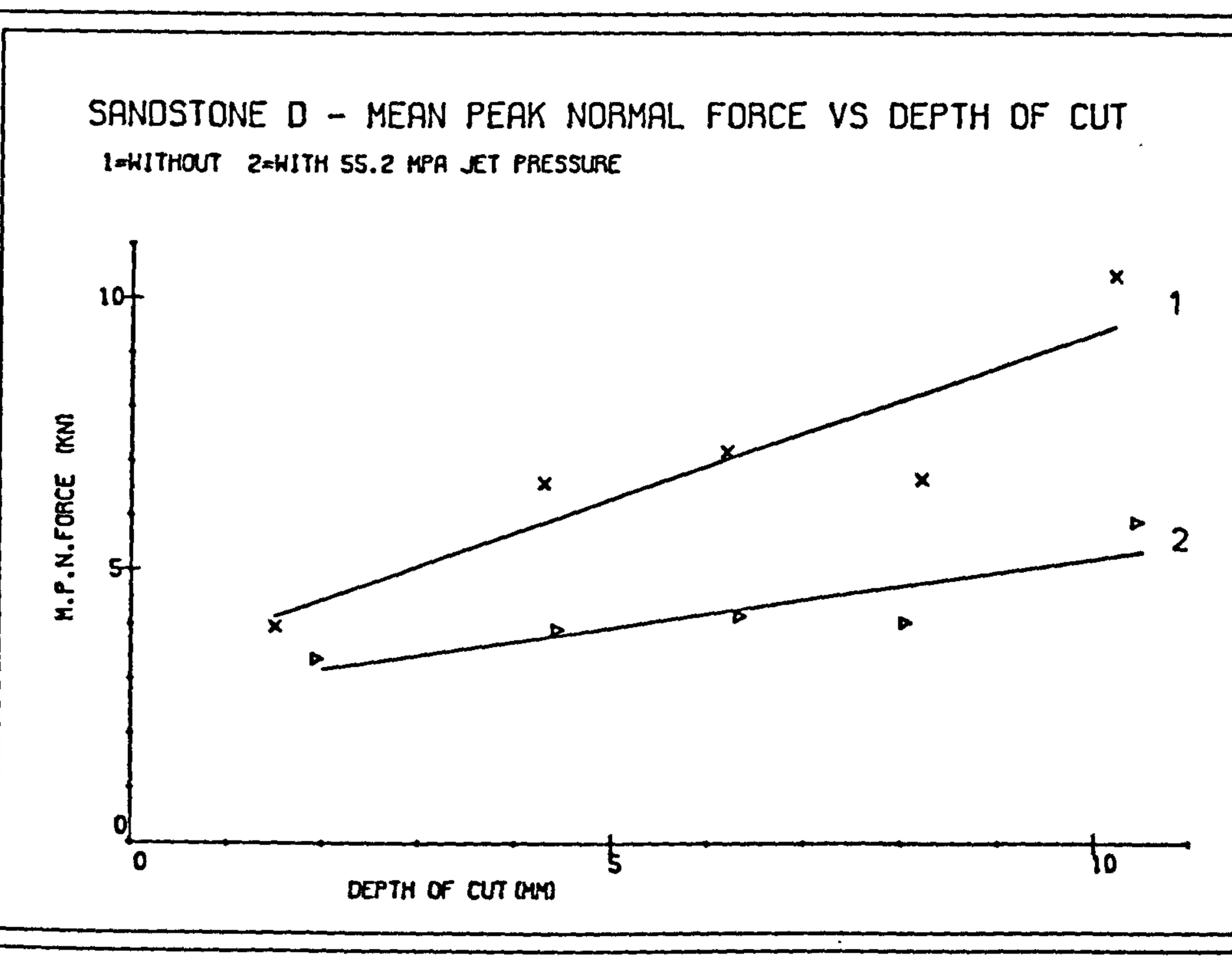
SANDSTONE D - MEAN PEAK NORMAL FORCE VS DEPTH OF CUT
1=WITHOUT 2=WITH 55.2 MPA JET PRESSURE
M.P.N.FORCE (KN)
10
5
0
0
5
10
DEPTH OF CUT (MM)
1
2

FIG. 8.5

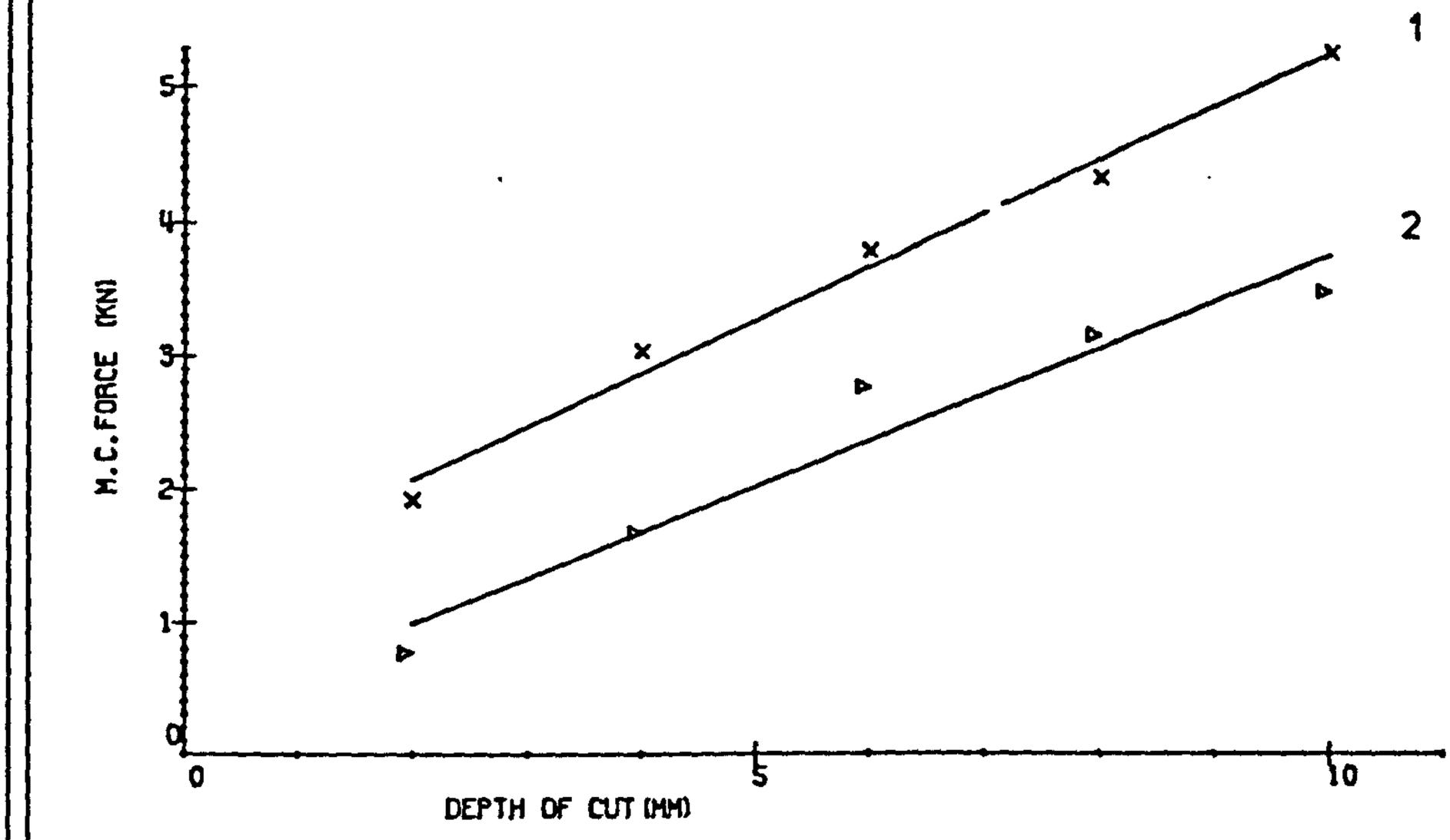
PORTLAND L.ST - MEAN CUTTING FORCE VS DEPTH OF CUT
1=WITHOUT 2=WITH 55.2 MPA JET
M.C.FORCE (KN)
0
1
2
3
4
5
0
5
10
DEPTH OF CUT (MM)
1
2

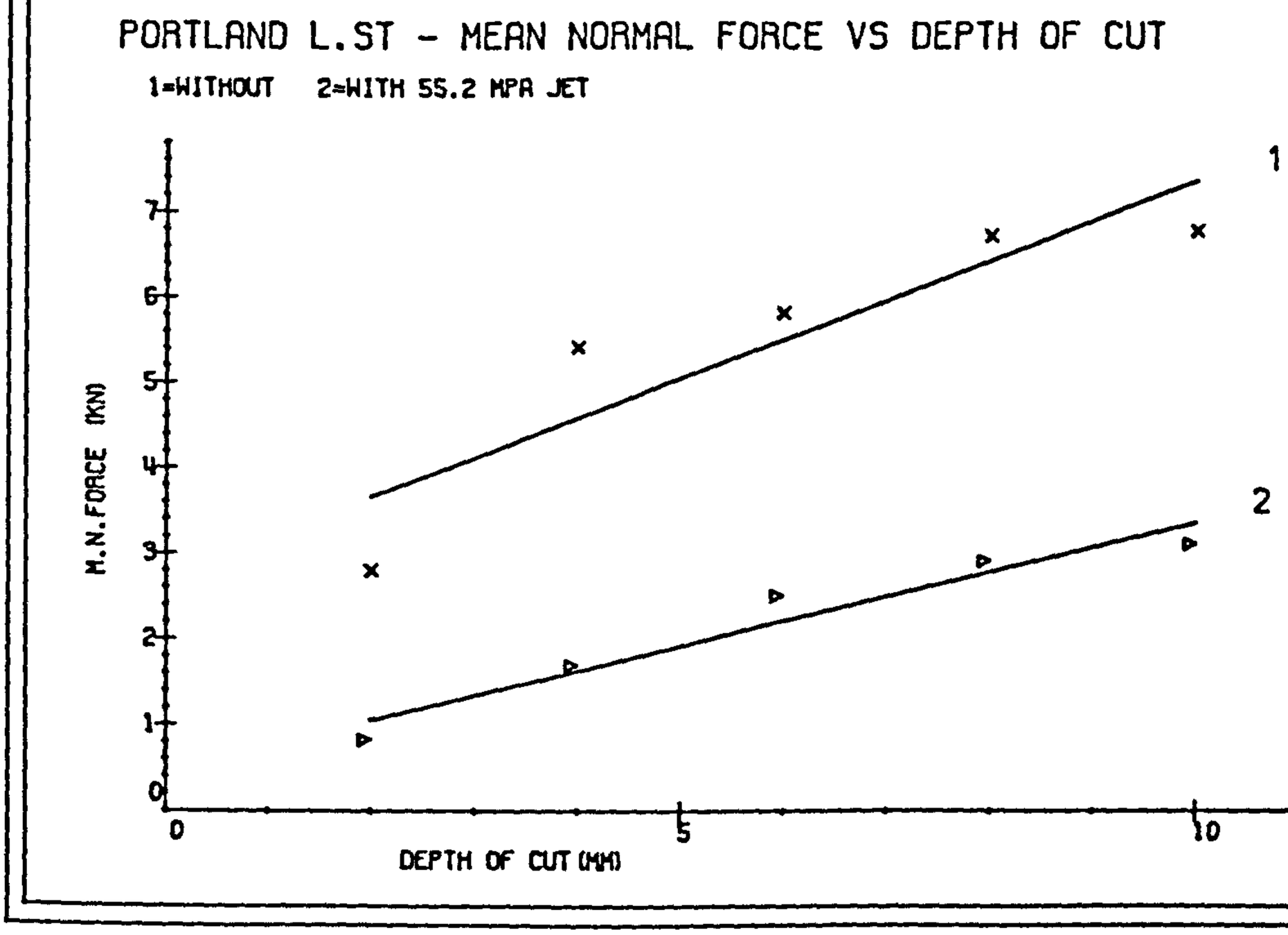
PORTLAND L.ST - MEAN NORMAL FORCE VS DEPTH OF CUT
1=WITHOUT 2=WITH 55.2 MPA JET
M.N.FORCE (KN)
0
1
2
3
4
5
6
7
0
5
10
DEPTH OF CUT (MM)
1
2

FIG. 8.6

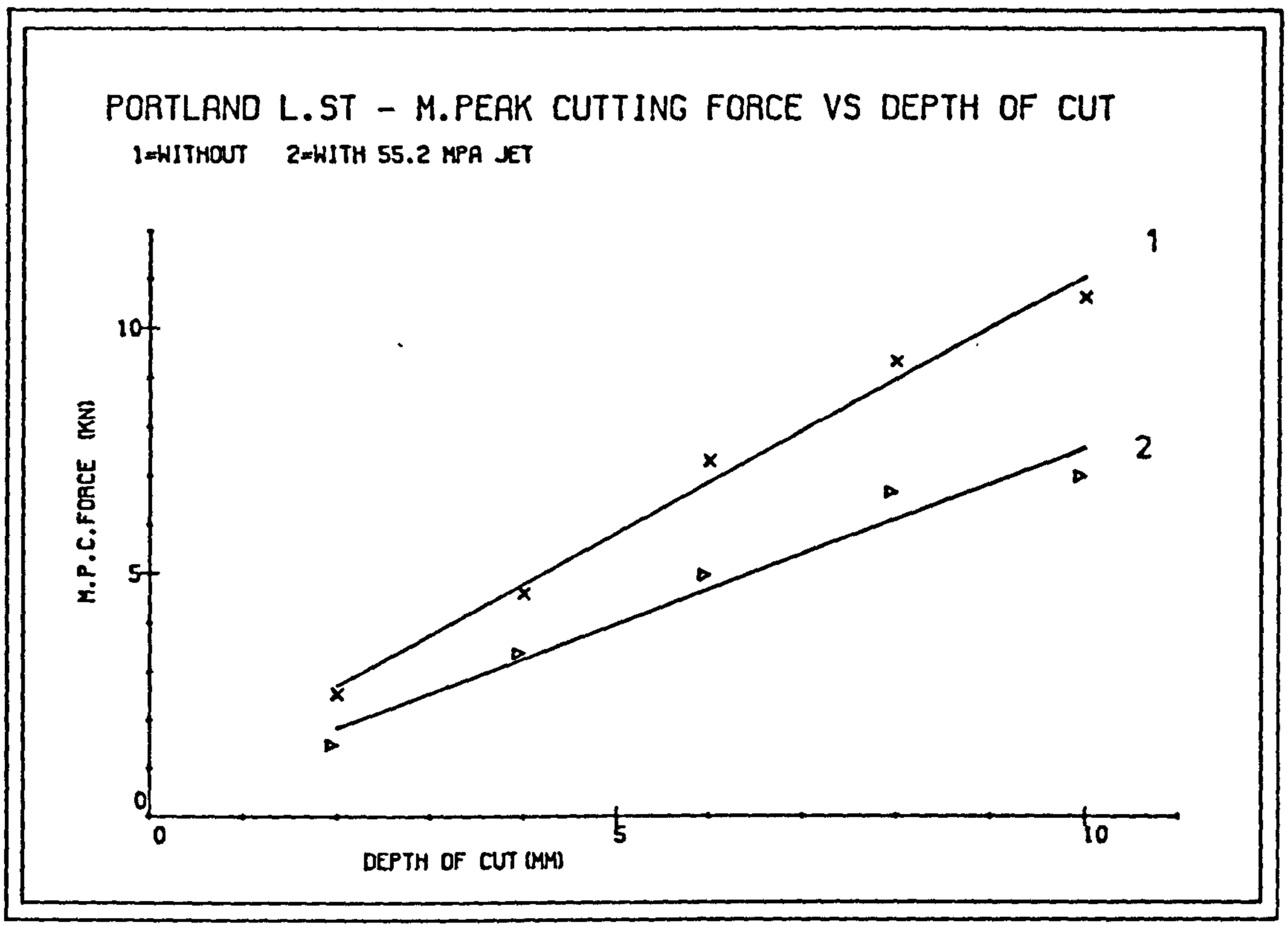
PORTLAND L.ST - M.PEAK CUTTING FORCE VS DEPTH OF CUT
1=WITHOUT 2=WITH 55.2 MPA JET
M.P.C.FORCE (KN)
10
5
0
0
5
10
DEPTH OF CUT (MM)
1
2

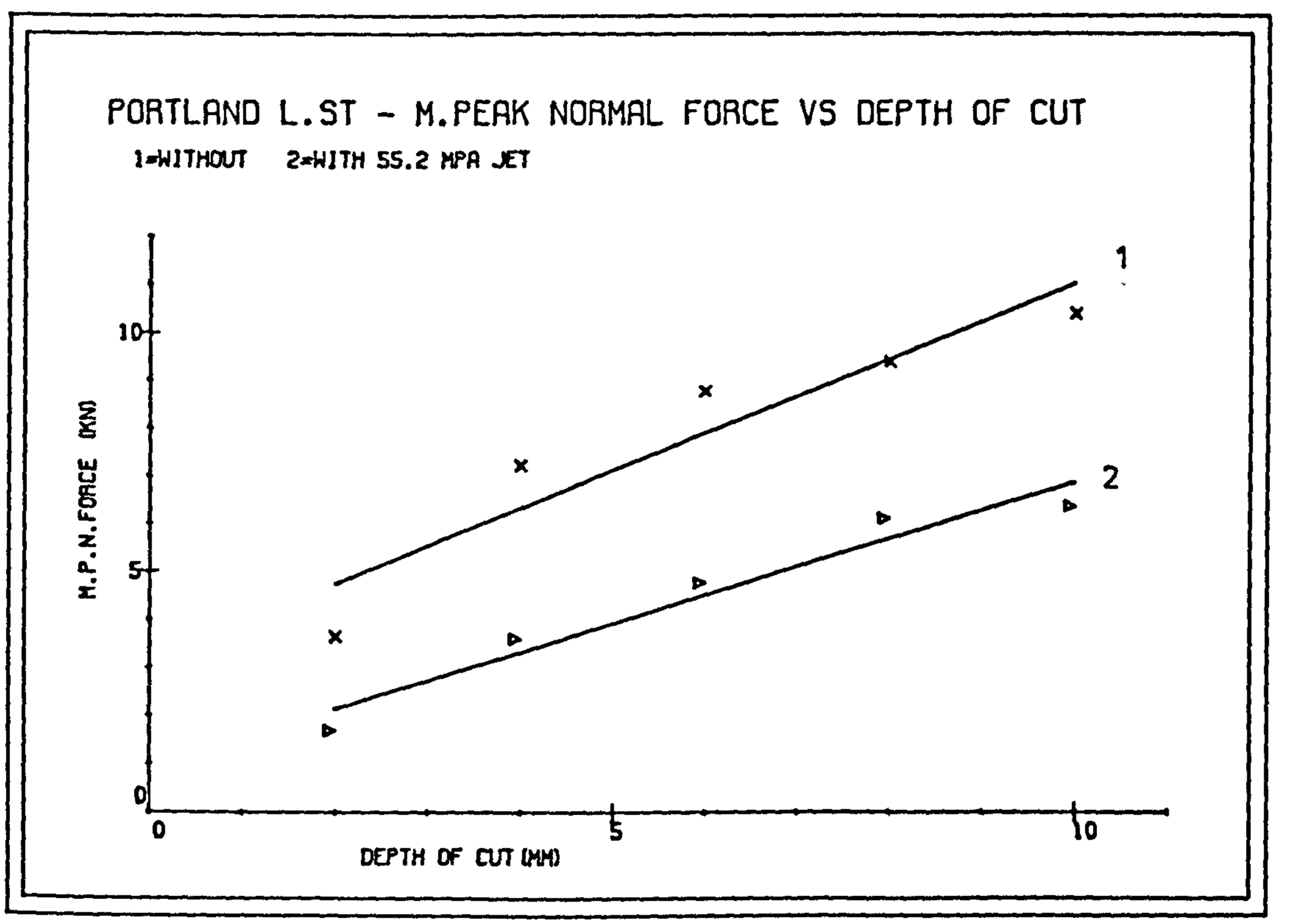
PORTLAND L.ST - M.PEAK NORMAL FORCE VS DEPTH OF CUT
1=WITHOUT 2=WITH 55.2 MPA JET
M.P.N.FORCE (KN)
10
5
0
0
5
10
DEPTH OF CUT (MM)
1
2

FIG. 8.7

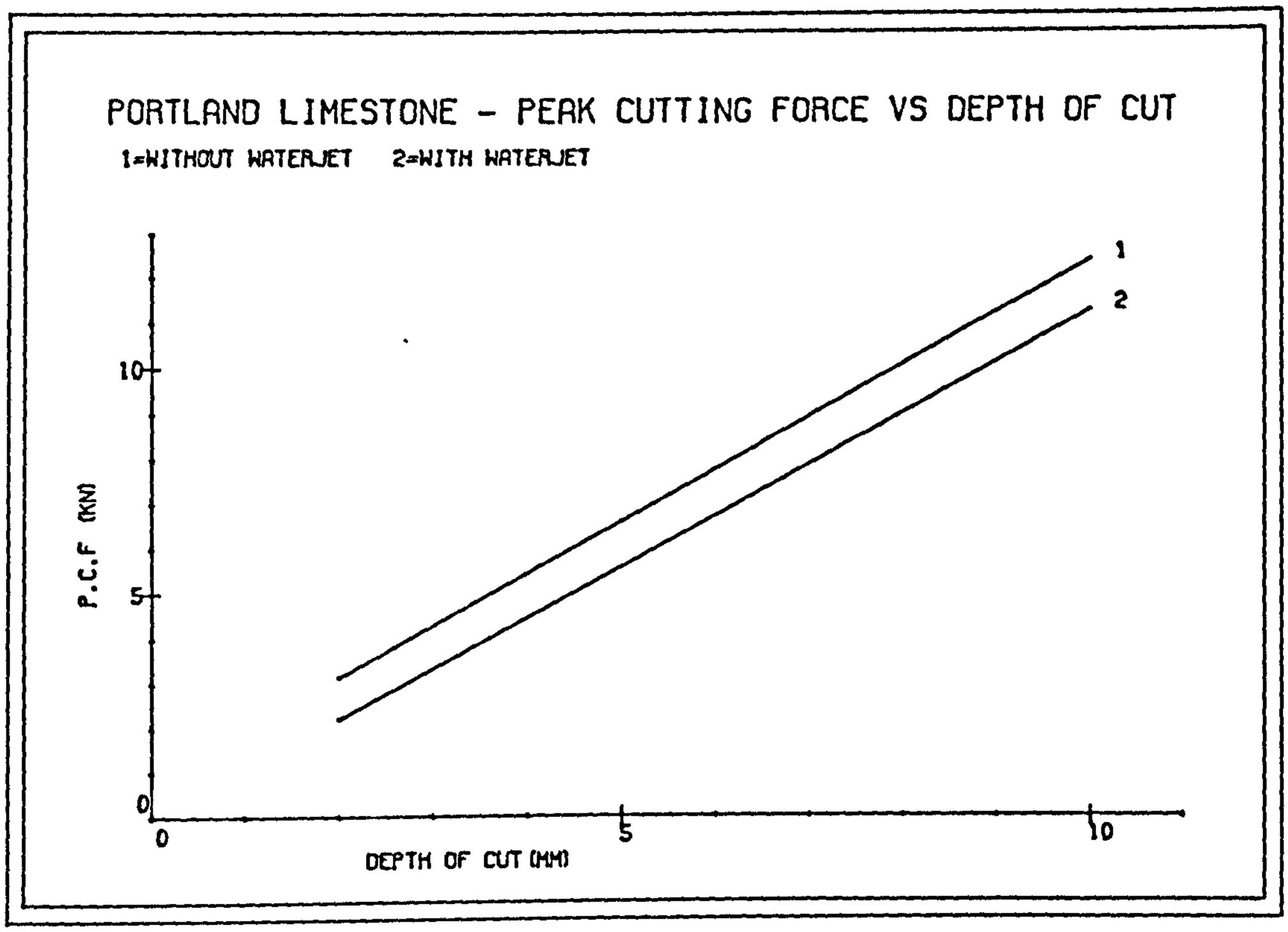
PORTLAND LIMESTONE - PEAK CUTTING FORCE VS DEPTH OF CUT
1=WITHOUT WATERJET 2=WITH WATERJET
P.C.F (KN)
10
5
0
0
5
10
DEPTH OF CUT (MM)
1
2

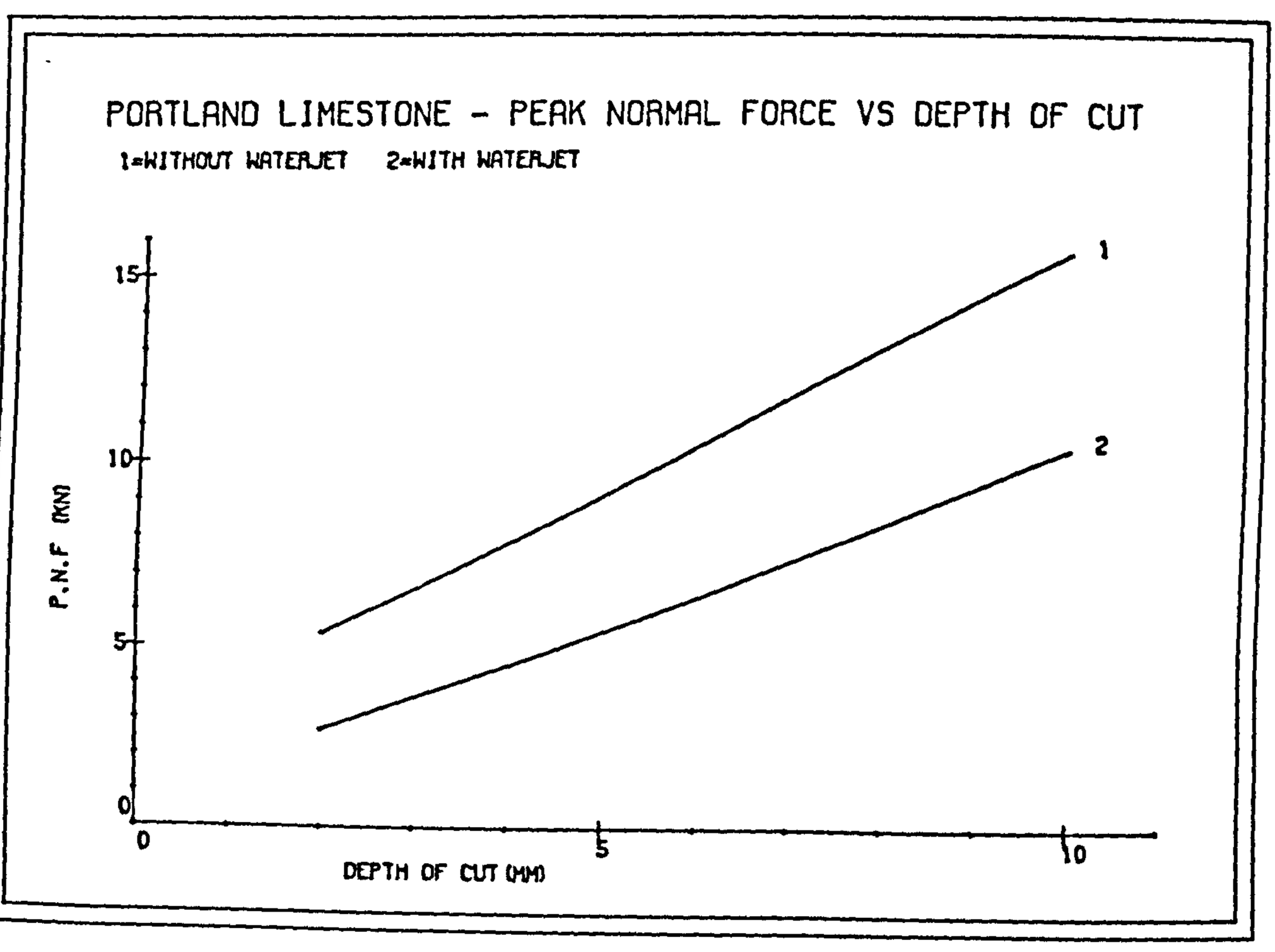
PORTLAND LIMESTONE - PEAK NORMAL FORCE VS DEPTH OF CUT
1=WITHOUT WATERJET 2=WITH WATERJET
P.N.F (KN)
15
10
5
0
0
5
10
DEPTH OF CUT (MM)
1
2

FIG. 8.8

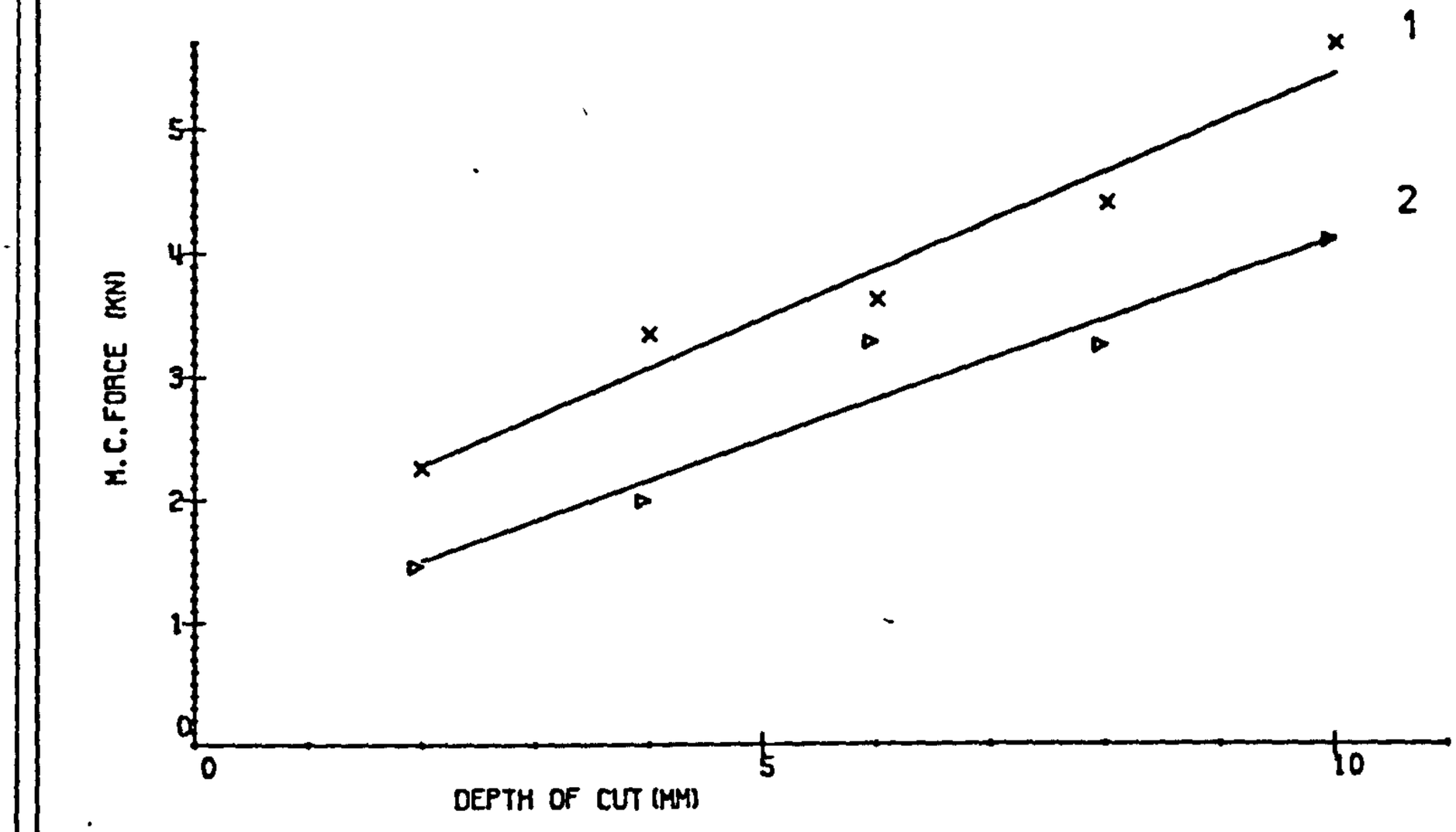
LIMESTONE B - MEAN CUTTING FORCE VS DEPTH OF CUT
1=WITHOUT 2=WITH 55.2 MPA JET PRESSURE
M.C.FORCE (KN)
0
1
2
3
4
5
0
5
10
DEPTH OF CUT (MM)
1
2

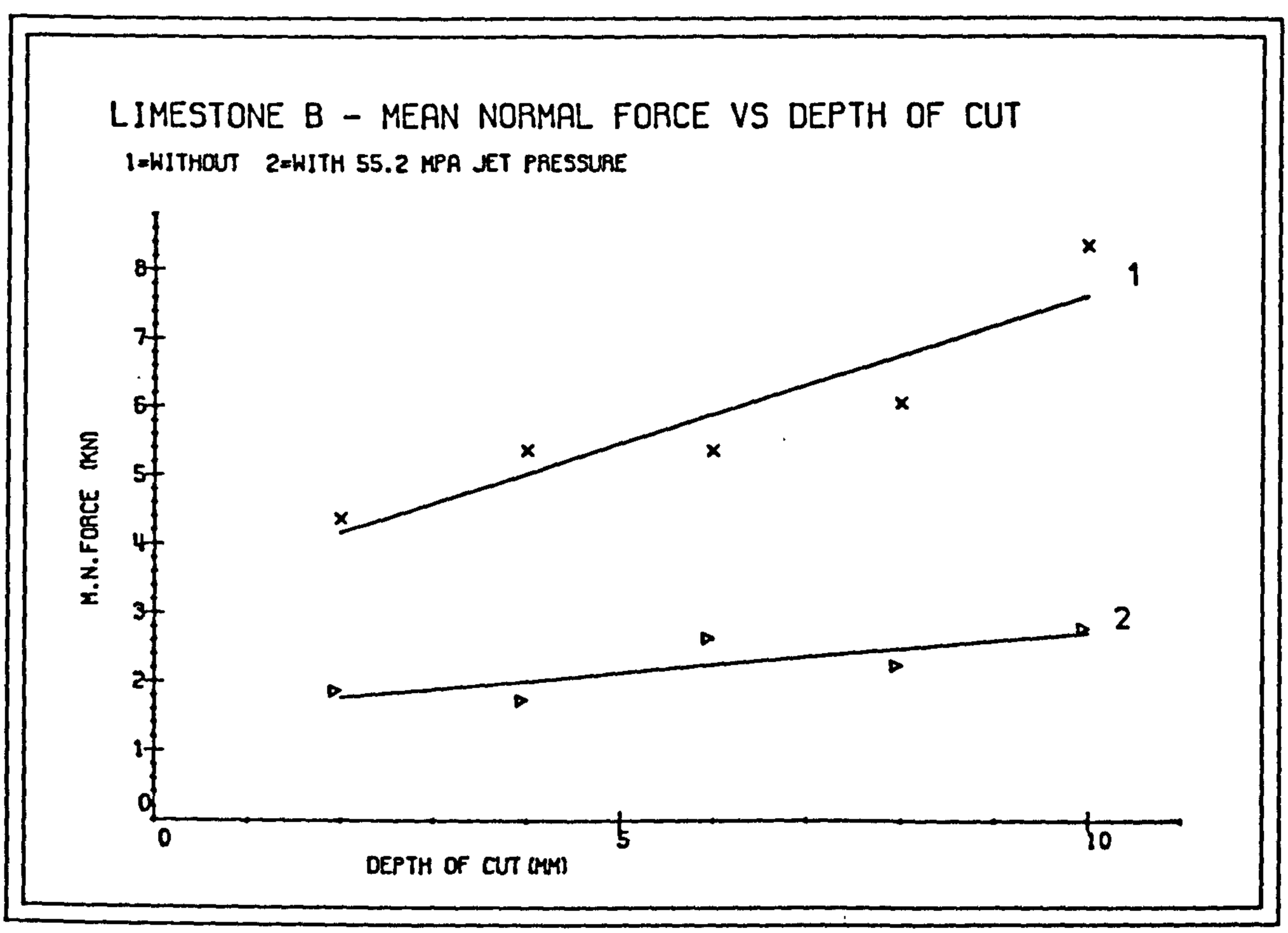
LIMESTONE B - MEAN NORMAL FORCE VS DEPTH OF CUT
1=WITHOUT 2=WITH 55.2 MPA JET PRESSURE
M.N.FORCE (KN)
0
1
2
3
4
5
6
7
8
0
5
10
DEPTH OF CUT (MM)
1
2

FIG. 8.9

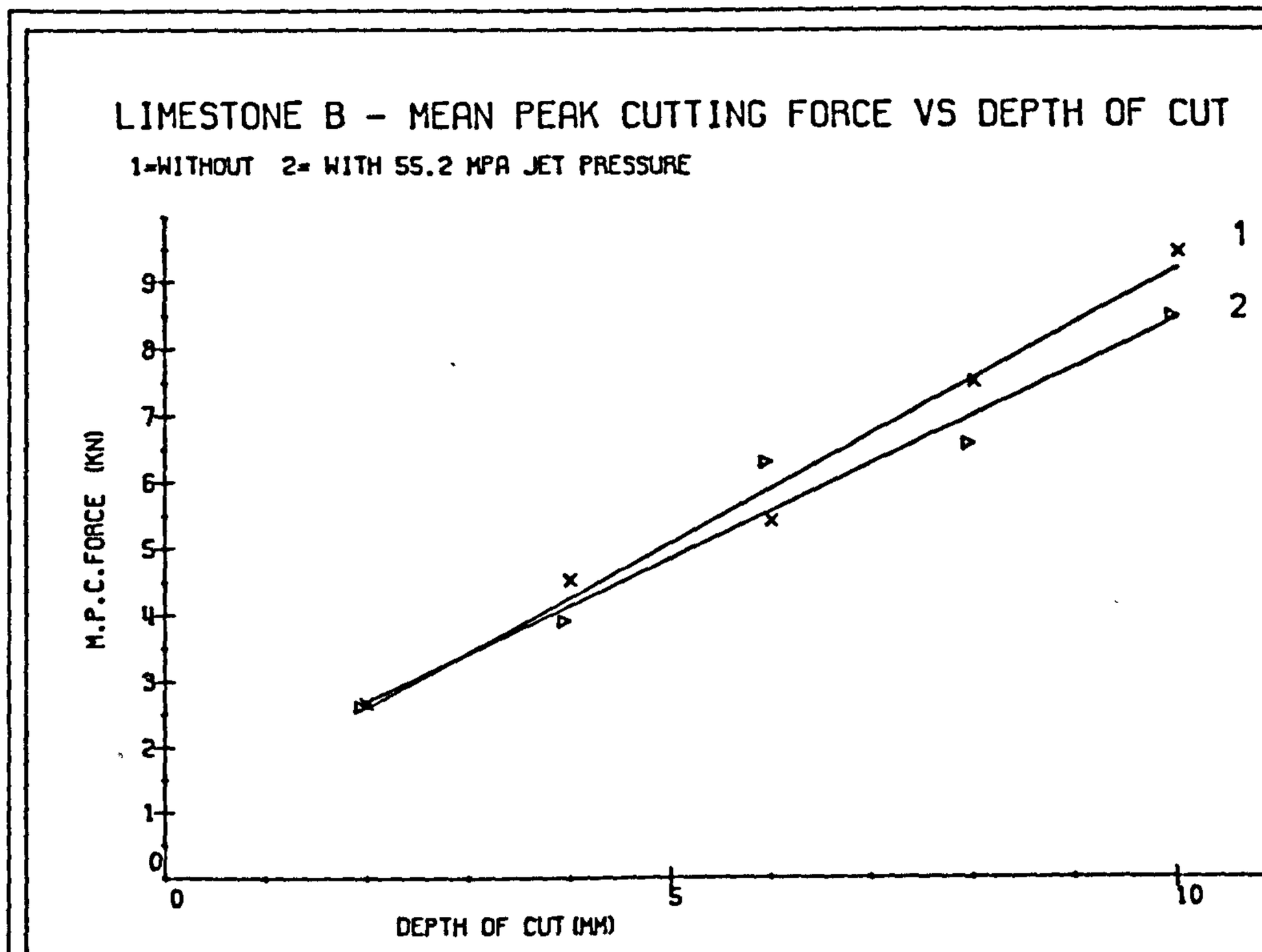
LIMESTONE B - MEAN PEAK CUTTING FORCE VS DEPTH OF CUT
1=WITHOUT 2= WITH 55.2 MPA JET PRESSURE
M.P.C.FORCE (KN)
0
1
2
3
4
5
6
7
8
9
0
5
10
DEPTH OF CUT (MM)
1
2

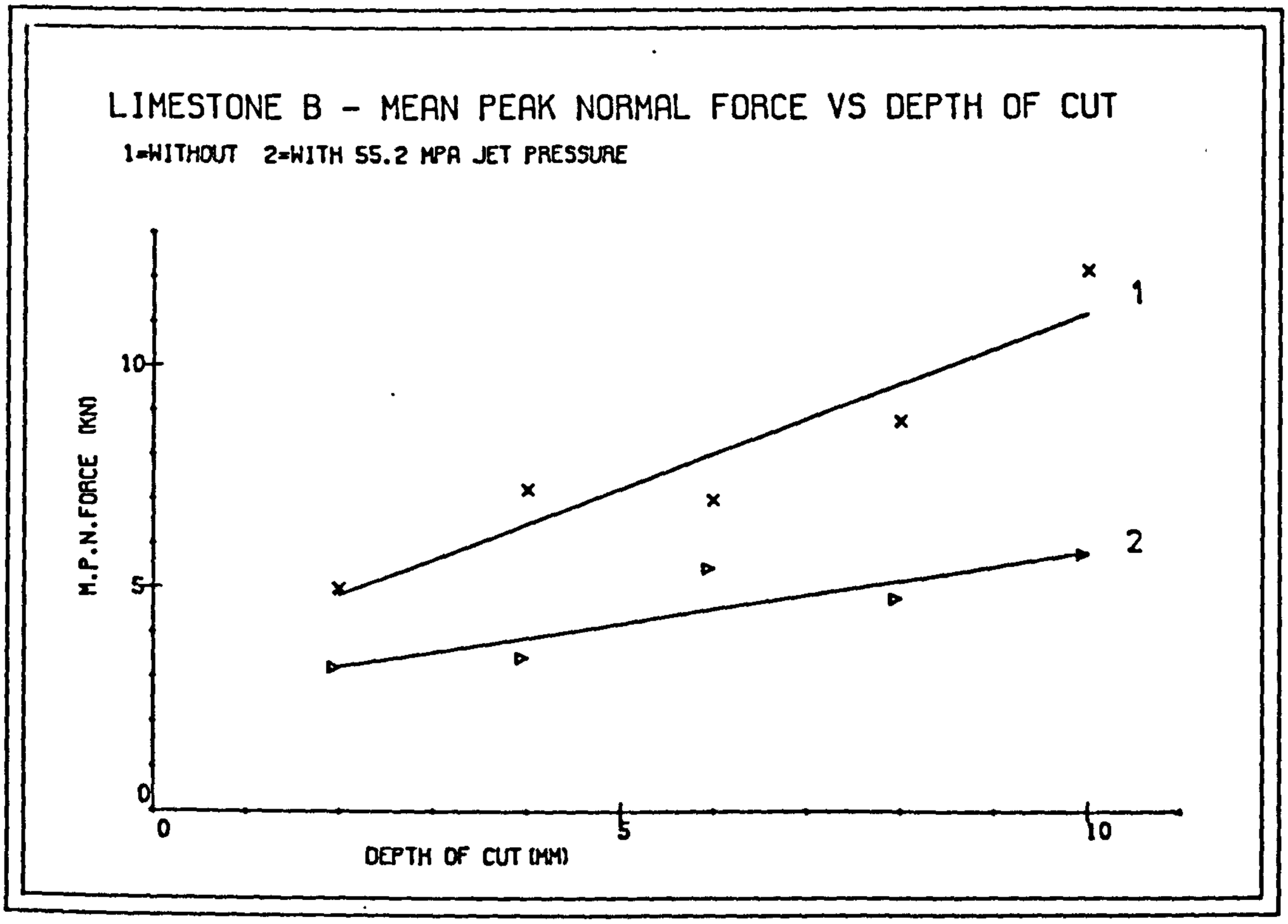
LIMESTONE B - MEAN PEAK NORMAL FORCE VS DEPTH OF CUT
1=WITHOUT 2=WITH 55.2 MPA JET PRESSURE
M.P.N.FORCE (KN)
0
5
10
0
5
10
DEPTH OF CUT (MM)
1
2

FIG. 8.10

Normal forces have displayed higher sensitivity to change with waterjet assistance than cutting forces.

8.3.2 On Yield

Yield has increased at an accelerating rate with increase in depth of cut, (Figures 8.11-8.14). The relationship between the variables were of power type.

On some rocks, hybrid cutting gave higher yield than mechanical cutting.

8.3.3 On Mechanical Specific Energy

Mechanical Specific Energy has decreased at a decreasing rate with increase in depth of cut. (Figures 8.11-8.14). The curves showed tendency to run parallel to x-axis at deeper cuts.

Hybrid cutting gave lower specific energy values than mechanical cutting at corresponding depths.

DARLEY DALE S.ST - YIELD VS DEPTH OF CUT

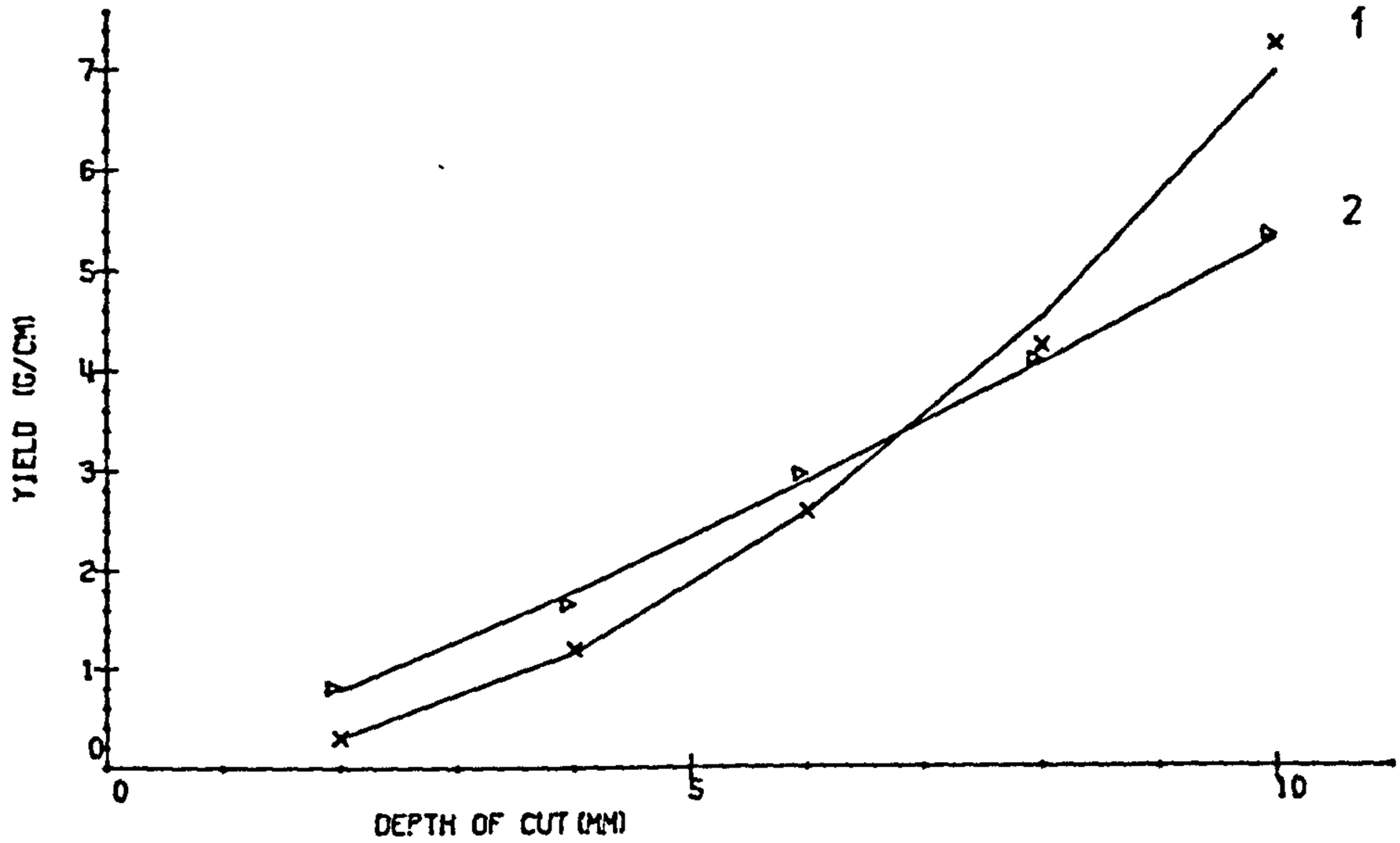

DARLEY DALE S.ST - MECH.SPECIFIC ENERGY VS DEPTH OF CUT

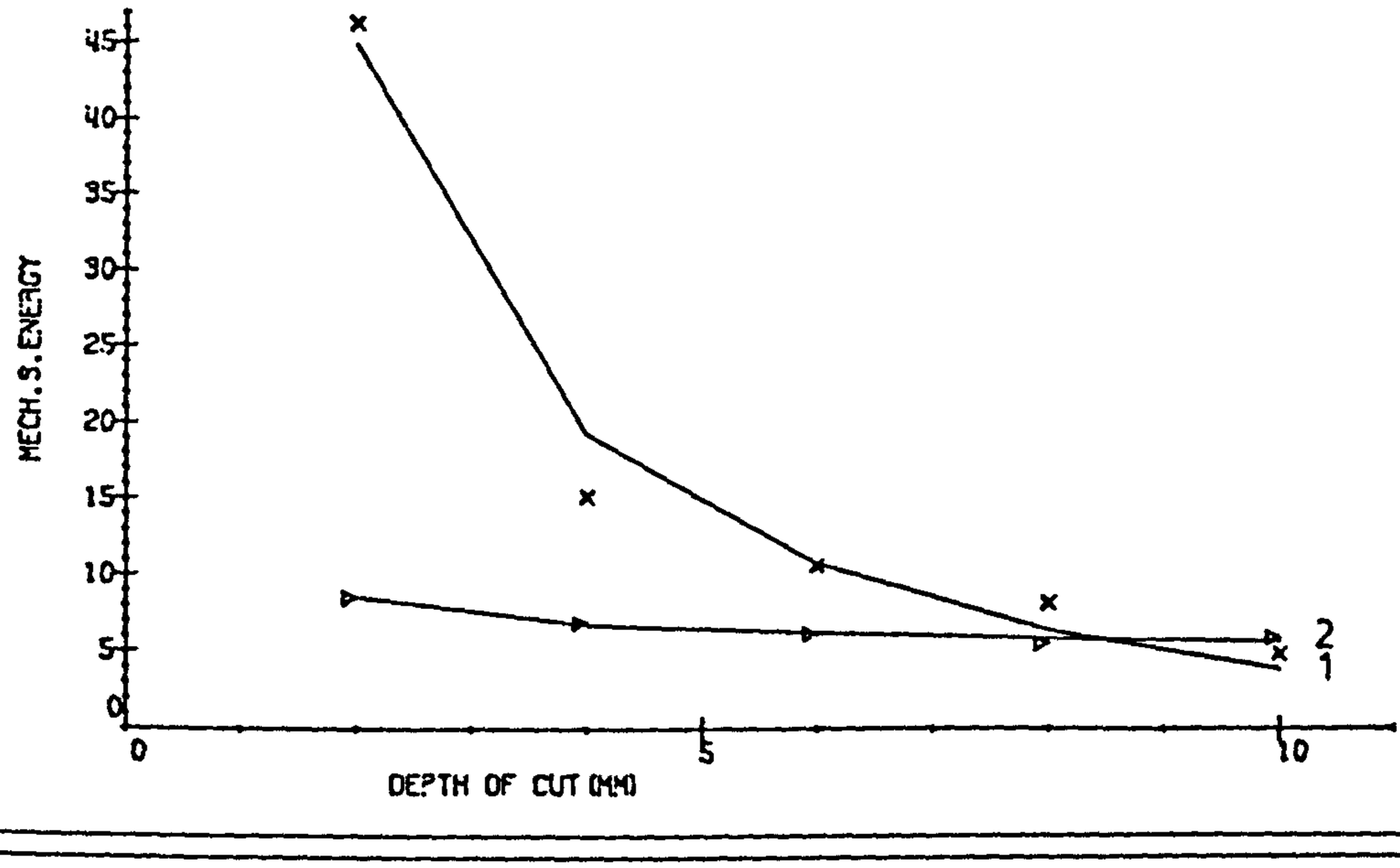

FIG. 8.11

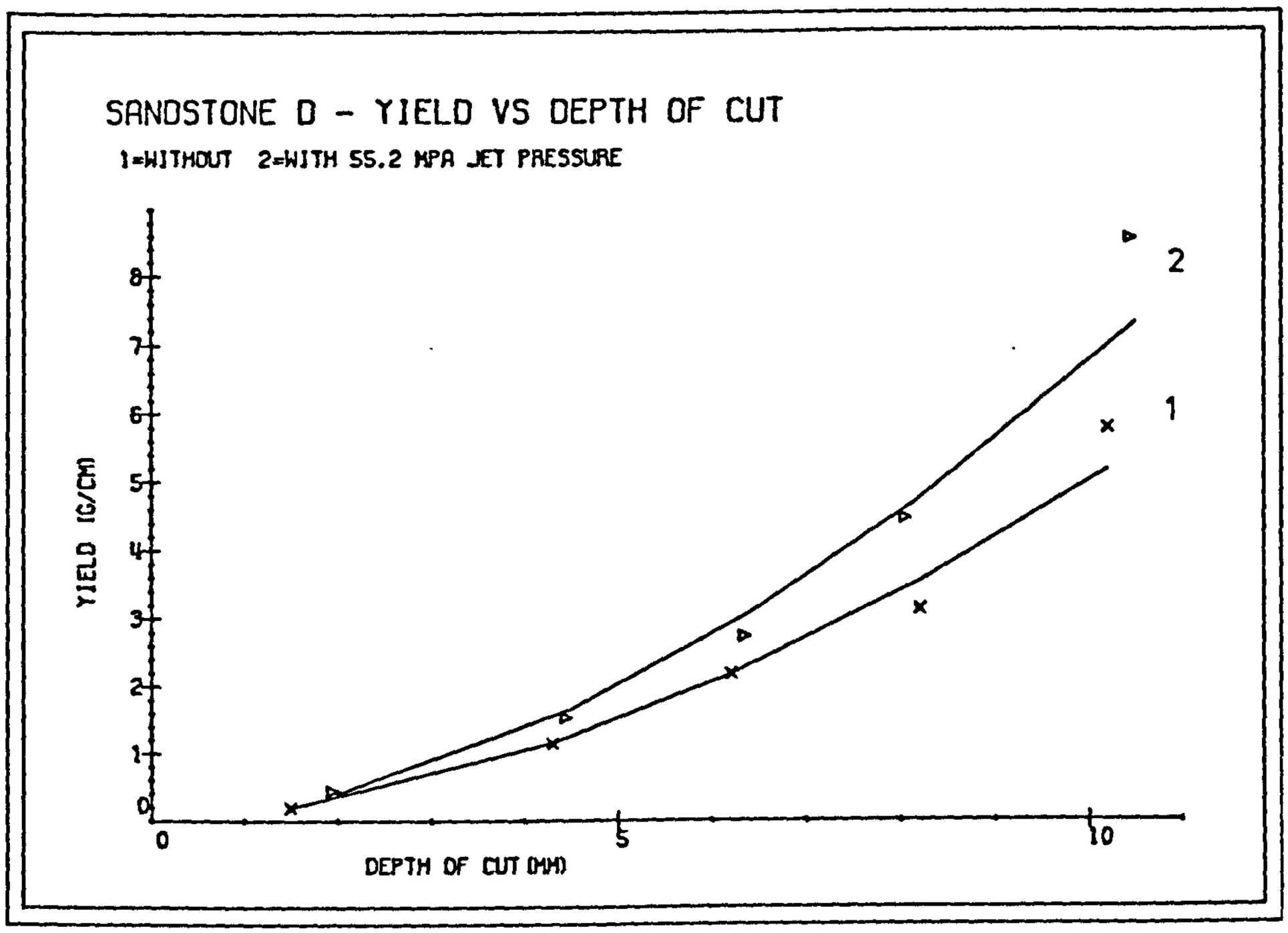
SANDSTONE D - YIELD VS DEPTH OF CUT
1=WITHOUT 2=WITH 55.2 MPA JET PRESSURE
YIELD (G/CM)
0
1
2
3
4
5
6
7
8
0
5
10
DEPTH OF CUT (MM)
1
2

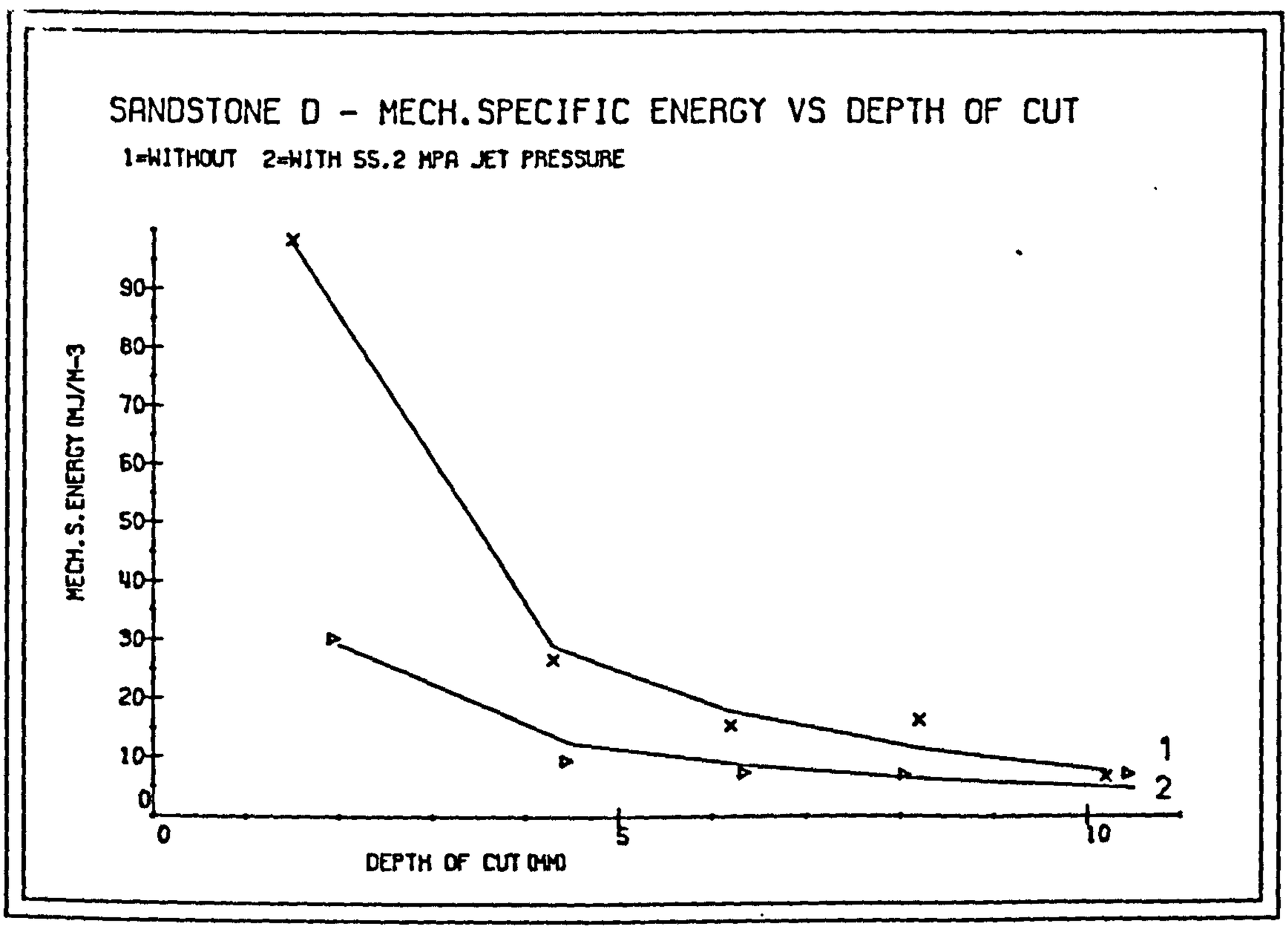
SANDSTONE D - MECH.SPECIFIC ENERGY VS DEPTH OF CUT
1=WITHOUT 2=WITH 55.2 MPA JET PRESSURE
MECH.S.ENERGY (MJ/M-3)
0
10
20
30
40
50
60
70
80
90
0
5
10
DEPTH OF CUT (MM)
1
2

FIG. 8.12

PORTLAND L.ST - YIELD VS DEPTH OF CUT

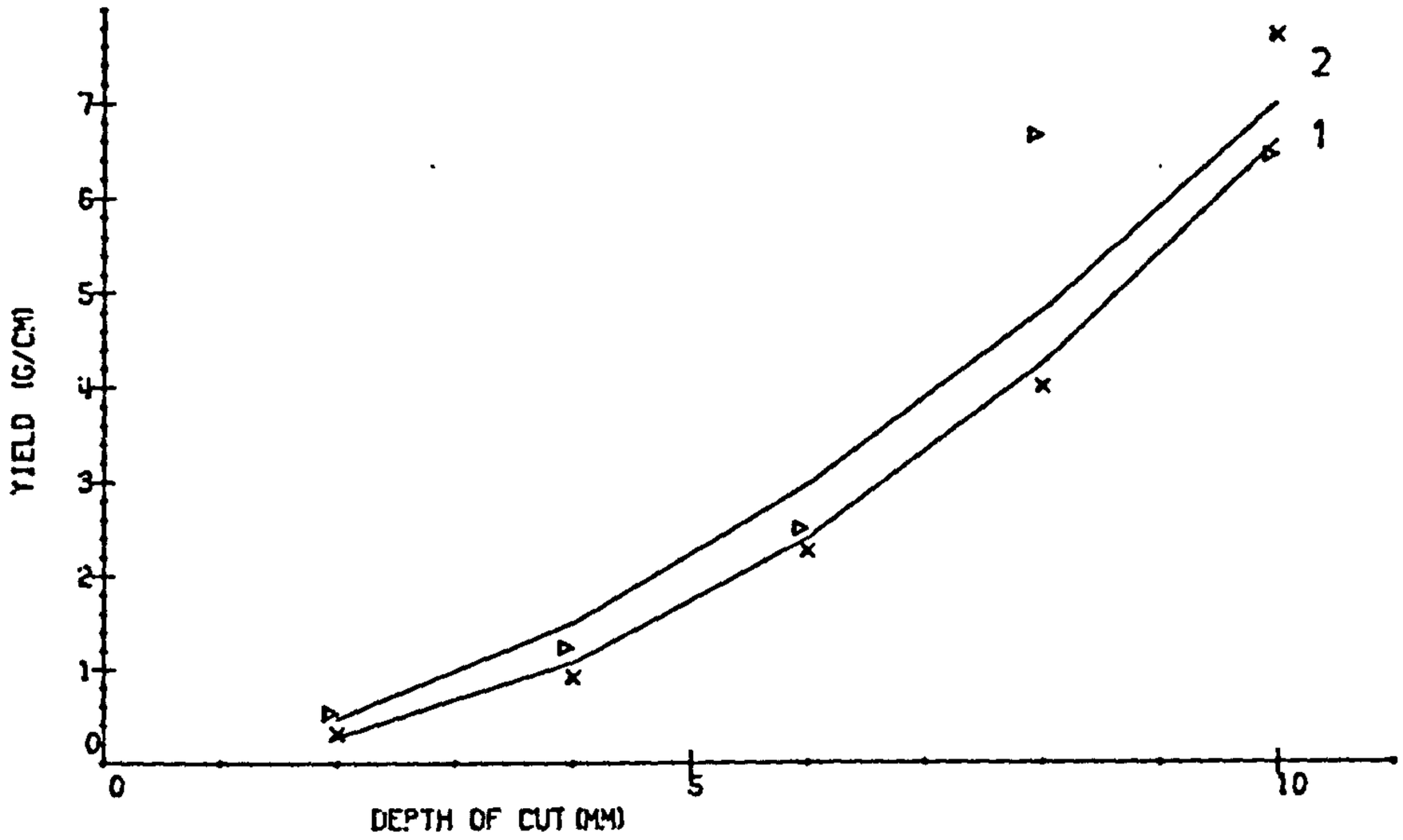

PORTLAND L.ST - MECH.SPECIFIC ENERGY VS DEPTH OF CUT

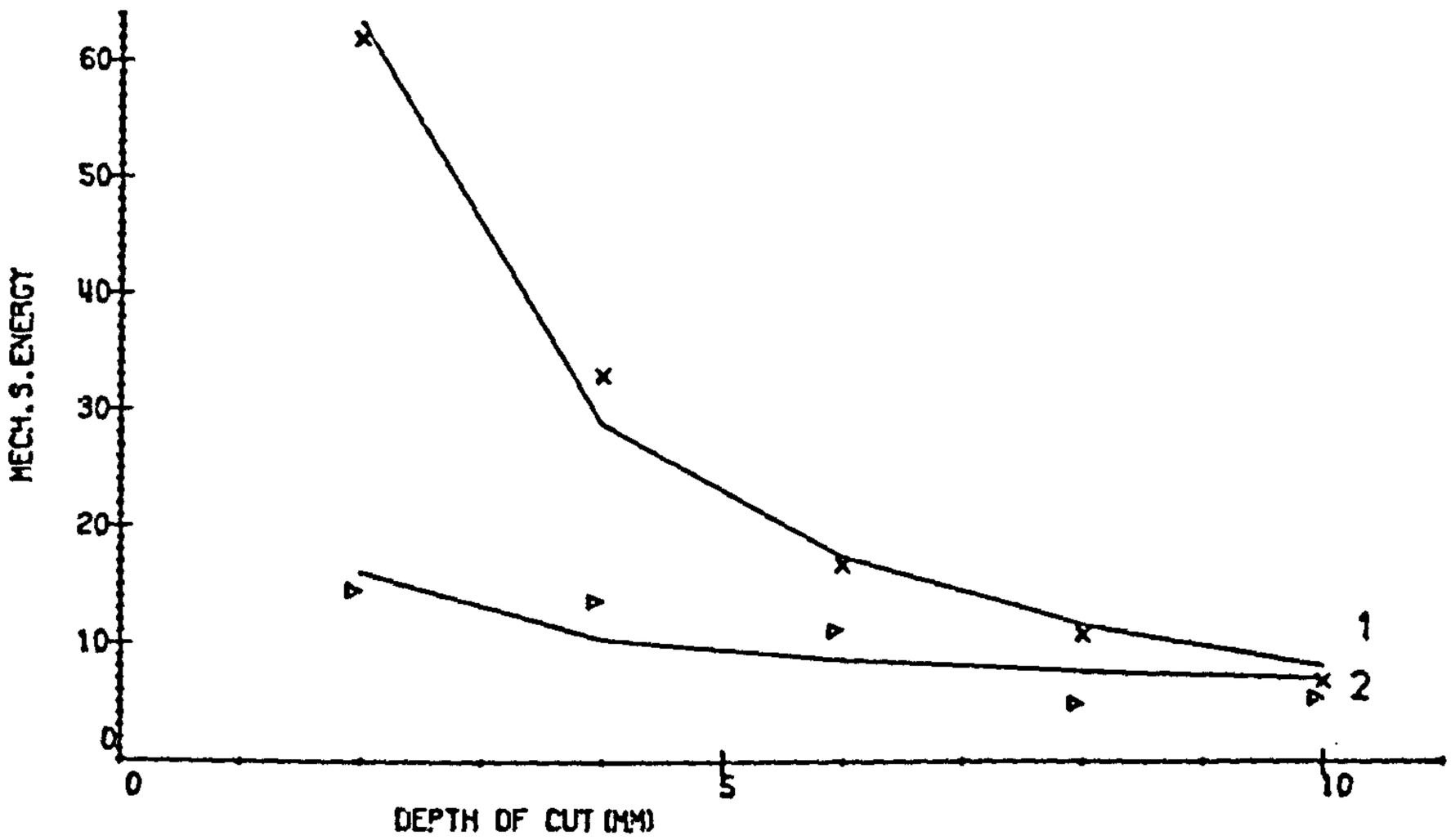

FIG. 8.13

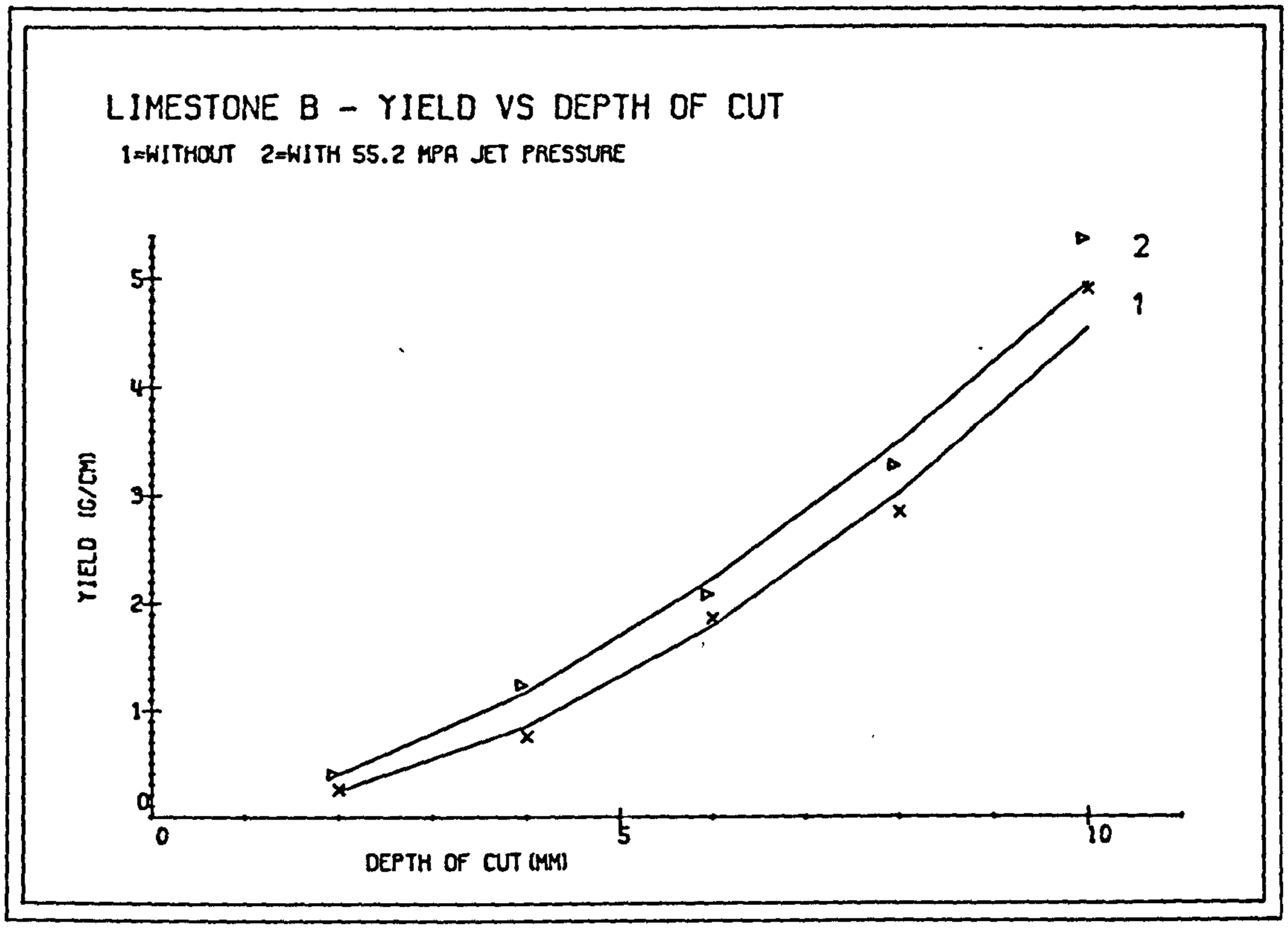
LIMESTONE B - YIELD VS DEPTH OF CUT
1=WITHOUT 2=WITH 55.2 MPA JET PRESSURE
YIELD (G/CM)
0
1
2
3
4
5
0
5
10
DEPTH OF CUT (MM)
1
2

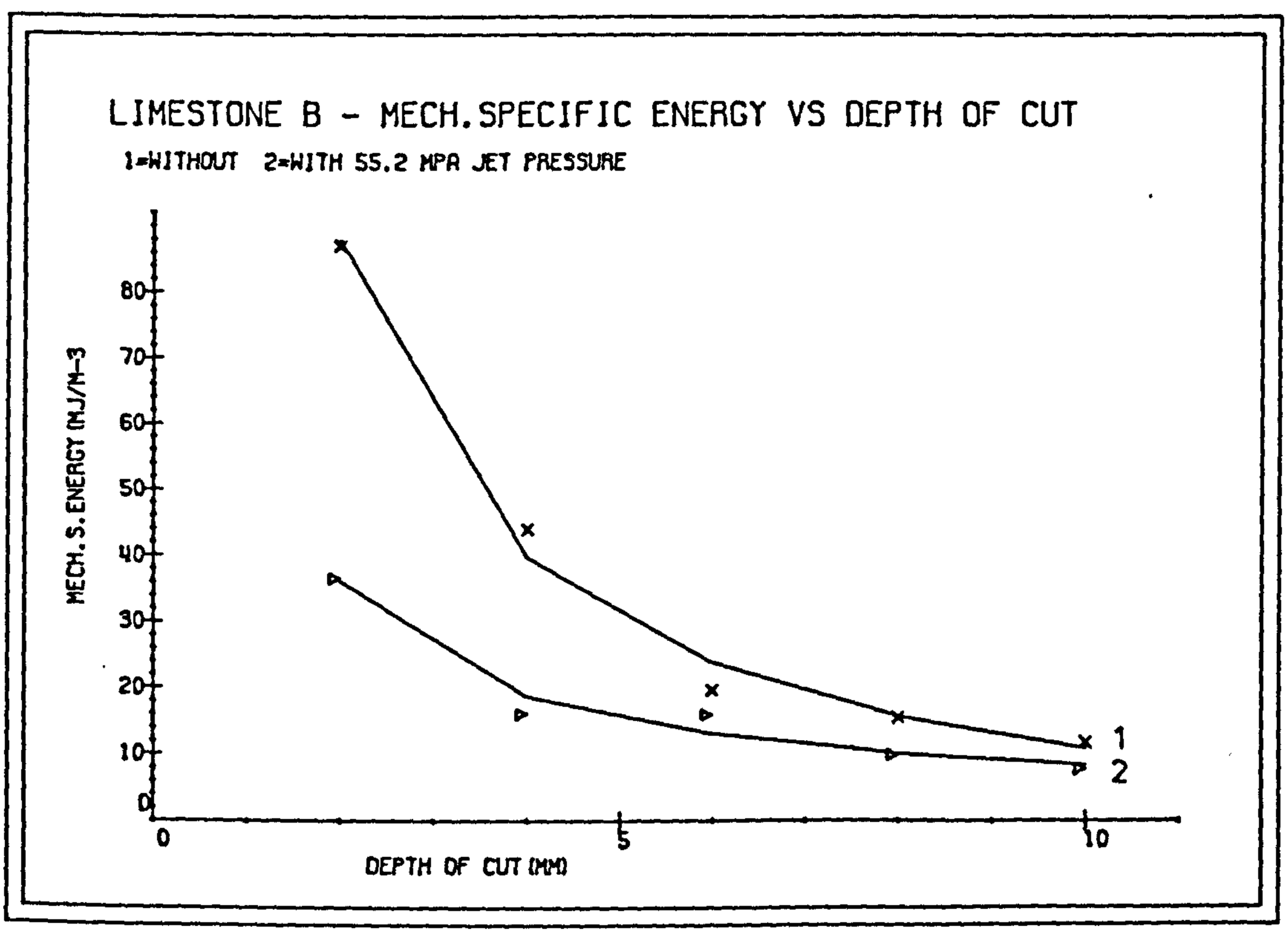
LIMESTONE B - MECH.SPECIFIC ENERGY VS DEPTH OF CUT
1=WITHOUT 2=WITH 55.2 MPA JET PRESSURE
MECH.S.ENERGY (MJ/M-3)
0
10
20
30
40
50
60
70
80
0
5
10
DEPTH OF CUT (MM)
1
2

FIG. 8.14

8.4 DISCUSSION

The graphs of performance parameters e.g. tool forces, yield and mechanical specific energy have shown that under identical cutting conditions water jet assisted system consistently have produced lower tool forces and mechanical specific energies.

The main action of the waterjet on sandstones can be said to be its erosive action. The jet gets into the already existing microcracks and pores and exerts pressure. If the cement matrix that is holding the sand grains is not too strong, the waterjet pressure may be high enough to scour away individual sand grains.

The mechanics of rock breakage due to the effect of high pressure waterjet assistance may be examined in two stages.

1. before mechanical cutter impacts the rock.

2. during mechanical cutter is in contact with the rock

It must be born in mind that the waterjet was leading the mechanical tool by 1mm and impinging the rock surface in perpendicular direction and mechanical tool was cutting along the same path immediately afterwards.

Initially, high pressure waterjet impinges the rock surface. Depending on the ratio of Jet Pressure/Threshold Pressure, it penetrates the rock to

a certain depth. The damage to rock surface is, however, localised and is in commensurate with the jet diameter. Factors influencing the jet penetration depth have been examined and discussed in detail at (Chapters 6,7).

The cutting action of the following mechanical tool varies with water jet pressure(when it is increased from threshold pressure to the rock's compressive strength).

The width of the groove left behind by the waterjet approximately equals to three times the nozzle diameter i.e. 2.5mm in our case. The tip diameter of the mechanical tool is less than this width. Therefore, if the jet penetration is deeper than the mechanical tools, because of its shape, it is the angled sides of the tungsten carbide tip which do the actual cutting when the mechanical tool comes into contact with the rock. The tip of the tool does not initiate any cracking ahead of the tool since it is not in contact with the rock. The material in the immediate vicinity of the tool is crushed which lead to tensile fracturing of the surrounding material with a bursting action. This explains the reason why normal forces show higher sensitivity to waterjet assisted cutting than the cutting forces. Since the tip of the tool does not come into contact with the rock, less thrust is required to keep the tool at its selected depth of cut and jet groove acts as a guiding track for the following mechanical tool.

When the mechanical tool penetrates the rock, and the penetration force approaches some critical force cracks are initiated at the tool rock interface. These cracks will propagate to the unstressed surface of the rock, if the force is increased further and the conditions are favourable. Thus with waterjet assisted system, if the jet penetration is less than mechanical tool depth of cut, the mechanical tool initiates the cracks and waterjet gets into these cracks, exerts pressure at the walls of the crack and propagate them by hydraulic fracturing.

As a routine the rock surface was examined after cutting experiments. This showed that, although water jet when cutting by itself only penetrated the rock by 1-2 millimetres (on limestones), with waterjet assisted system at some parts on the rock surface it penetrated more than mechanical tool depth of cut. This supports the view that waterjet causes hydraulic fracturing of cracks initiated by the mechanical tools thereby relieving the mechanical tool of the stress concentrations, resulting in lower tool forces.

The water jet assisted cutting has required more energy than the mechanical cutting system, when the total energy expended to cut a unit volume of rock was considered. However energy costs form only a small percentage of the total excavation cost. The reduction in cutting and normal forces would enable the machine manufacturers to build excavation machines which will be lighter and more mobile and more versatile and applicable to many cutting situations. The efficiency of an excavation method can be improved if the particle size produced is increased and

percentage of fine particles are minimised. This can be achieved by taking deeper cuts and increasing the cutting tool size. However, as the cutting experiments have shown, deeper cuts necessitates the use of higher tool forces, and on strong rocks, it may not be possible to take deeper cuts because of limitations of the machine and the tool. If a high pressure waterjet is used to augment this machine, the tool penetration and cutting rates can be increased considerably. Further, a study of drag bits cutting through quartzite showed that more energy is dissipated as heat and in producing fines than went into creating new surfaces (63). This resulted in heating of the cutting tool and surrounding rock, (Plate 14) which caused increase in tool wear and costs. Having waterjets near the tool tip would enable higher transfer of power to the rock by the waterjet and mechanical tool, thus stressing the rock mass and cause breakage at lower tool forces and provide cooling of the tool at source, thus increase the tool life.

PLATE 15 - Drag Tool Cutters

8.5 LIMESTONE C

A drag tool of shape as shown in (Plate 15) was used instead of point attack tool to compare the performances of mechanical and hybrid cutting systems on strong limestone.

8.5.1 Properties of Limestone

Bulk Density (g/cm^3).....	Dry :	2.68
.....	Wet :	2.682
Apparent Porosity (%)	:	0.1
Dynamic Modulus (GPa)	:	97.3
Sclerescope Rebound Hardness	:	59.5
Plasticity (%)	:	16.4
Schmidt Rebound Hardness	:	55.2
NCB Cone Indentor Hardness	:	4.9
Compressive Strength (MPa)	:	117.3
Tensile Strength (MPa)	:	9.5
Compressive/Tensile	:	12.35

8.5.2 Thin Section Analysis: Biosparite (Shelly Limestone)

The petrographic thin section showed a tightly packed medium grained assemblage of forams, crinoid columns and occasional broken brijozoens, bivalve fragments and fibrous algal debris set in a comparatively clear recrystallized calcite matrix.

8.5.3 Experimental Plan

Depth of cut was selected to be the main operational variable to compare the performances of the cutting systems as described previously.

Experimental variables and their levels were as follows :

		Mechanical	Hybrid
Depth of cut	(mm)	2.5,5,7.5,10	2.5,5,7.5,10
Water jet pressure	(MPa)	---	55.17
Stand-off distance	(mm)	---	13
Lead-on distance	(mm)	---	3
Side-off distance	(mm)	---	0
Nozzle diameter	(mm)	---	0.85
Cutting speed	(mm/s)	165	165

Mechanical tool had a cutting tip of V-face with a round nose and had a negative rake and backclearance angles.

The waterjet at 55.17 Mpa pressure did not penetrate the limestone.

8.5.4 Effect of Depth of Cut

On Tool Forces

Mean Cutting and Mean Normal forces have shown no appreciable difference with waterjet assistance, (Figure 8.15).

Mean Peak and Peak Cutting and Normal forces showed some improvement, (Figure 8.16).

On Yield

Yield for hybrid cutting system was slightly higher than that produced by mechanical tool, (Figure 8.17).

On Mechanical Specific Energy

Specific Energy has shown small improvement at shallow depth of cuts, but this has diminished at deeper cuts, (Figure 8.17).

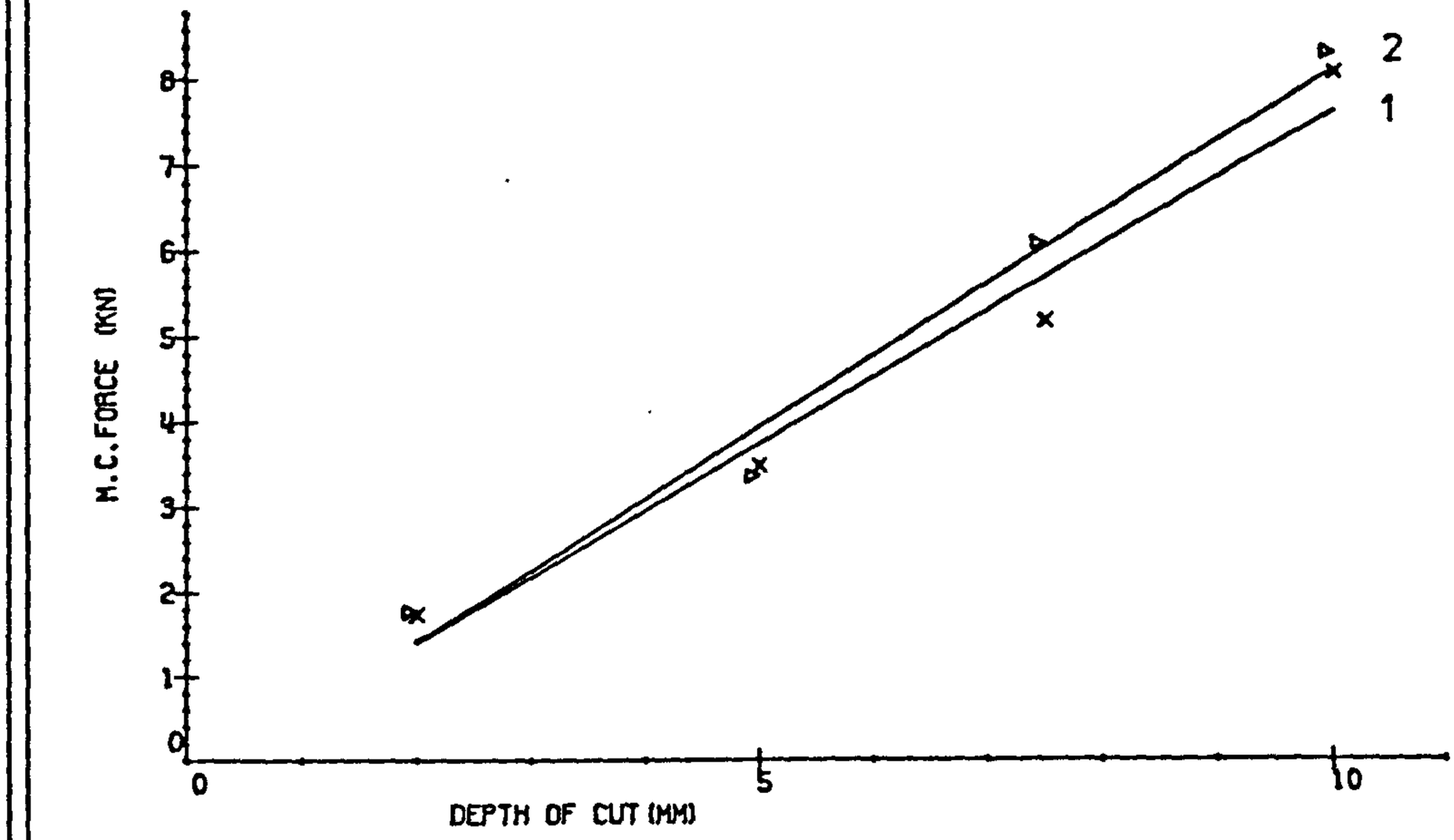
LIMESTONE C - MEAN CUTTING FORCE VS DEPTH OF CUT
1=WITHOUT 2=WITH 55.2 MPA JET
M.C.FORCE (KN)
0
1
2
3
4
5
6
7
8
0
5
10
DEPTH OF CUT (MM)
1
2

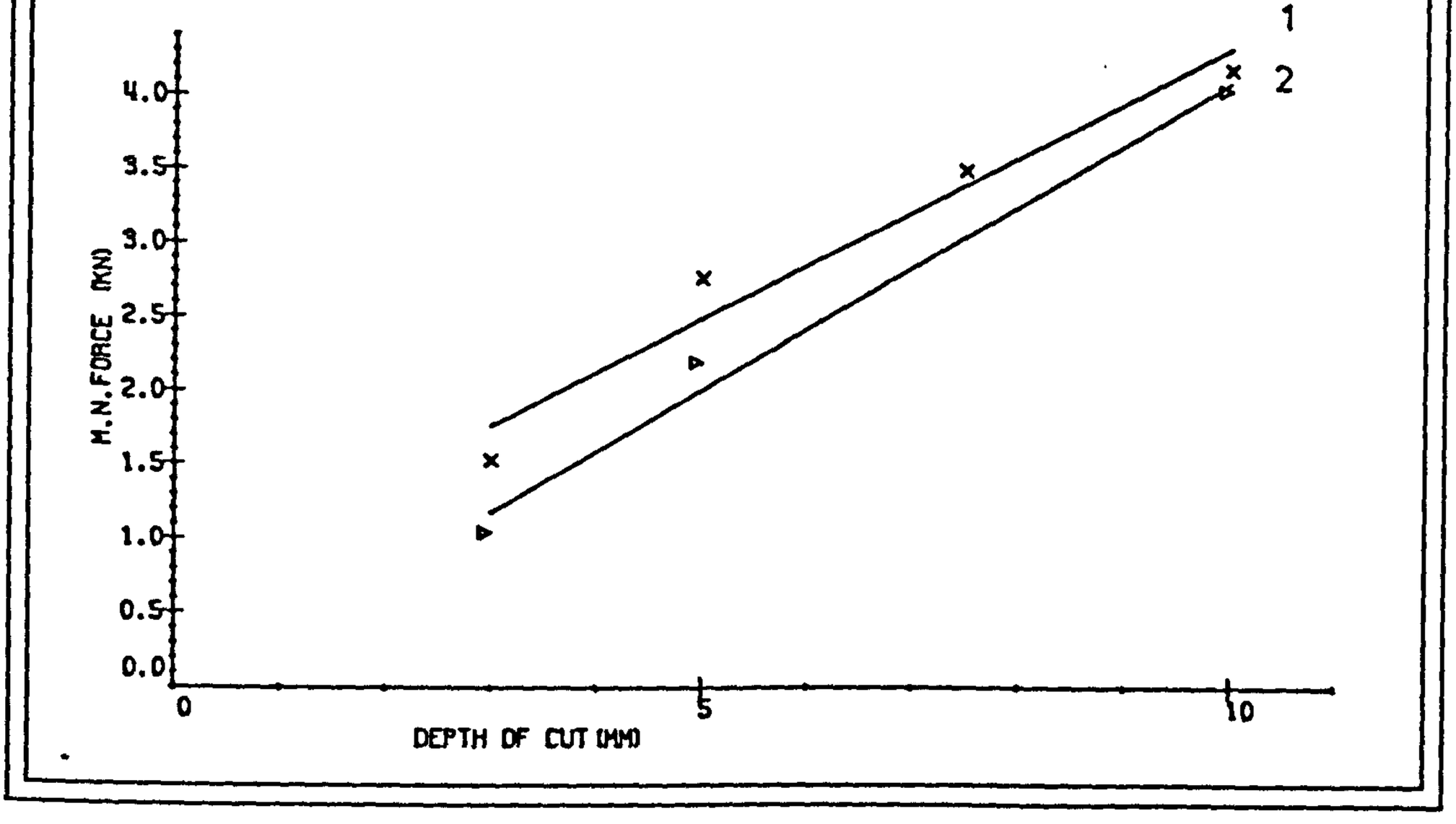
LIMESTONE C - MEAN NORMAL FORCE VS DEPTH OF CUT
1=WITHOUT 2=WITH 55.2 MPA JET PRESSURE
M.N.FORCE (KN)
0.0
0.5
1.0
1.5
2.0
2.5
3.0
3.5
4.0
0
5
10
DEPTH OF CUT (MM)
1
2

FIG. 8.15

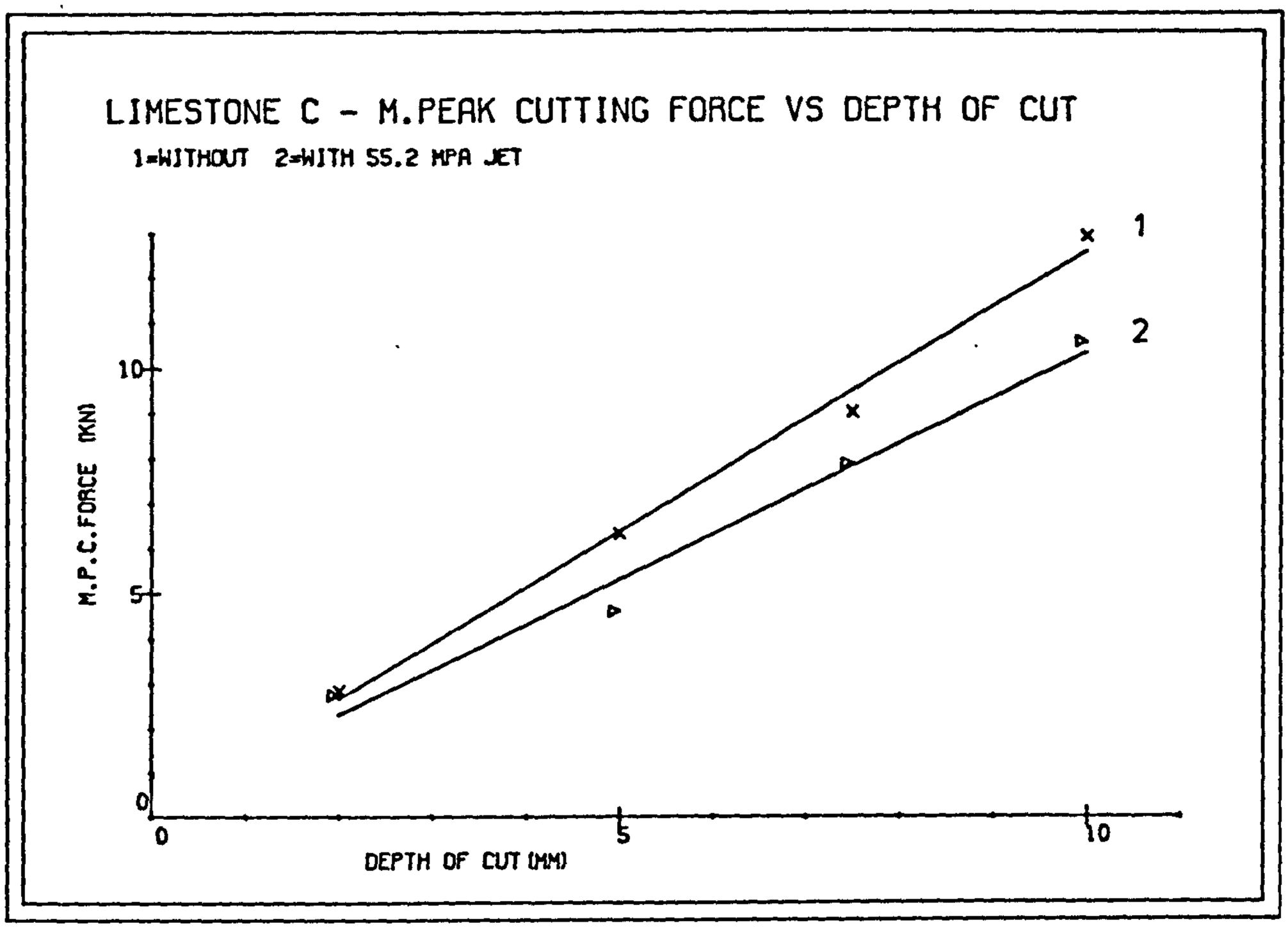
LIMESTONE C - M.PEAK CUTTING FORCE VS DEPTH OF CUT
1=WITHOUT 2=WITH 55.2 MPA JET
M.P.C.FORCE (KN)
10
5
0
0
5
10
DEPTH OF CUT (MM)
1
2

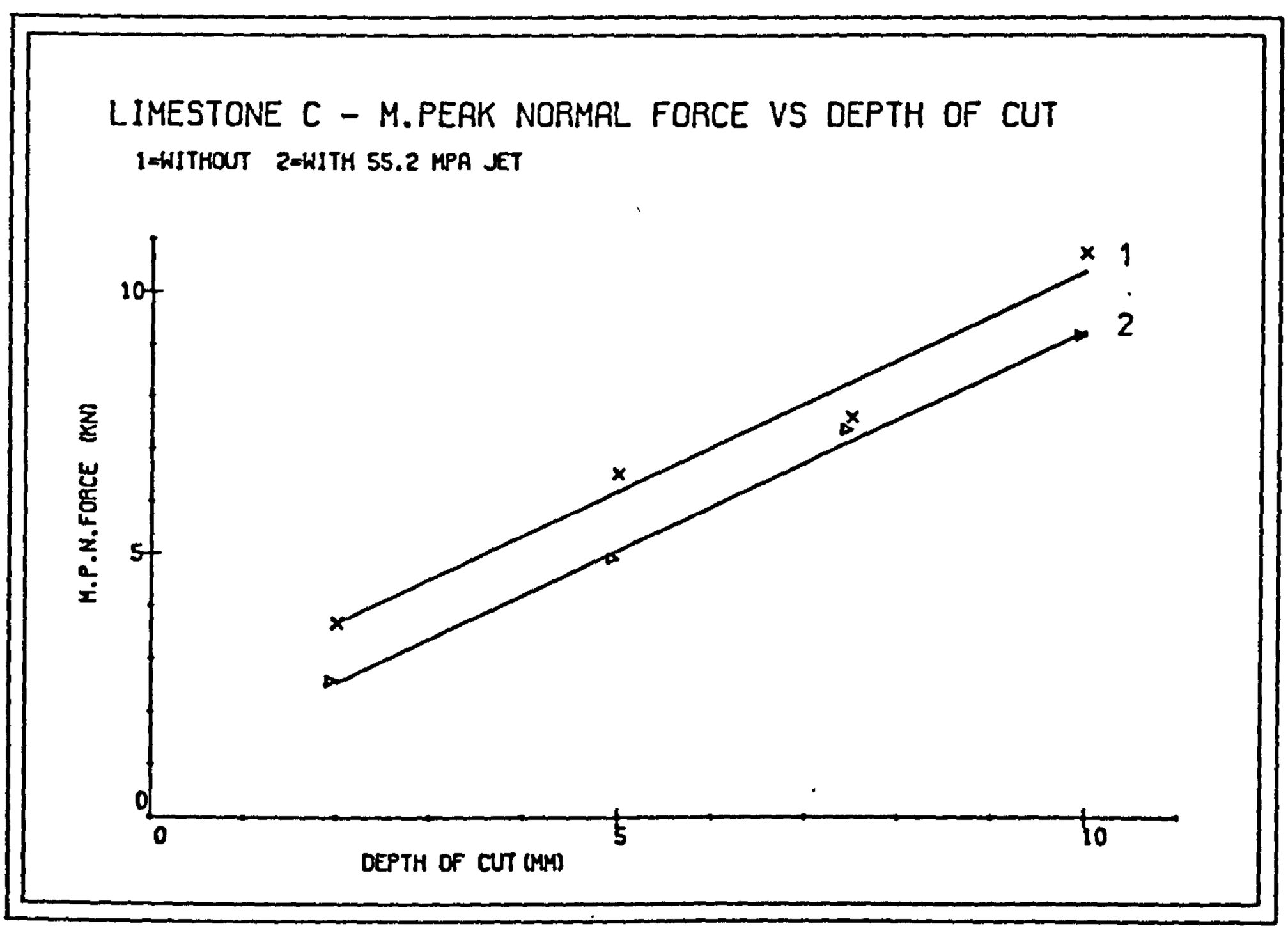
LIMESTONE C - M.PEAK NORMAL FORCE VS DEPTH OF CUT
1=WITHOUT 2=WITH 55.2 MPA JET
M.P.N.FORCE (KN)
10
5
0
0
5
10
DEPTH OF CUT (MM)
1
2

FIG. 8.16

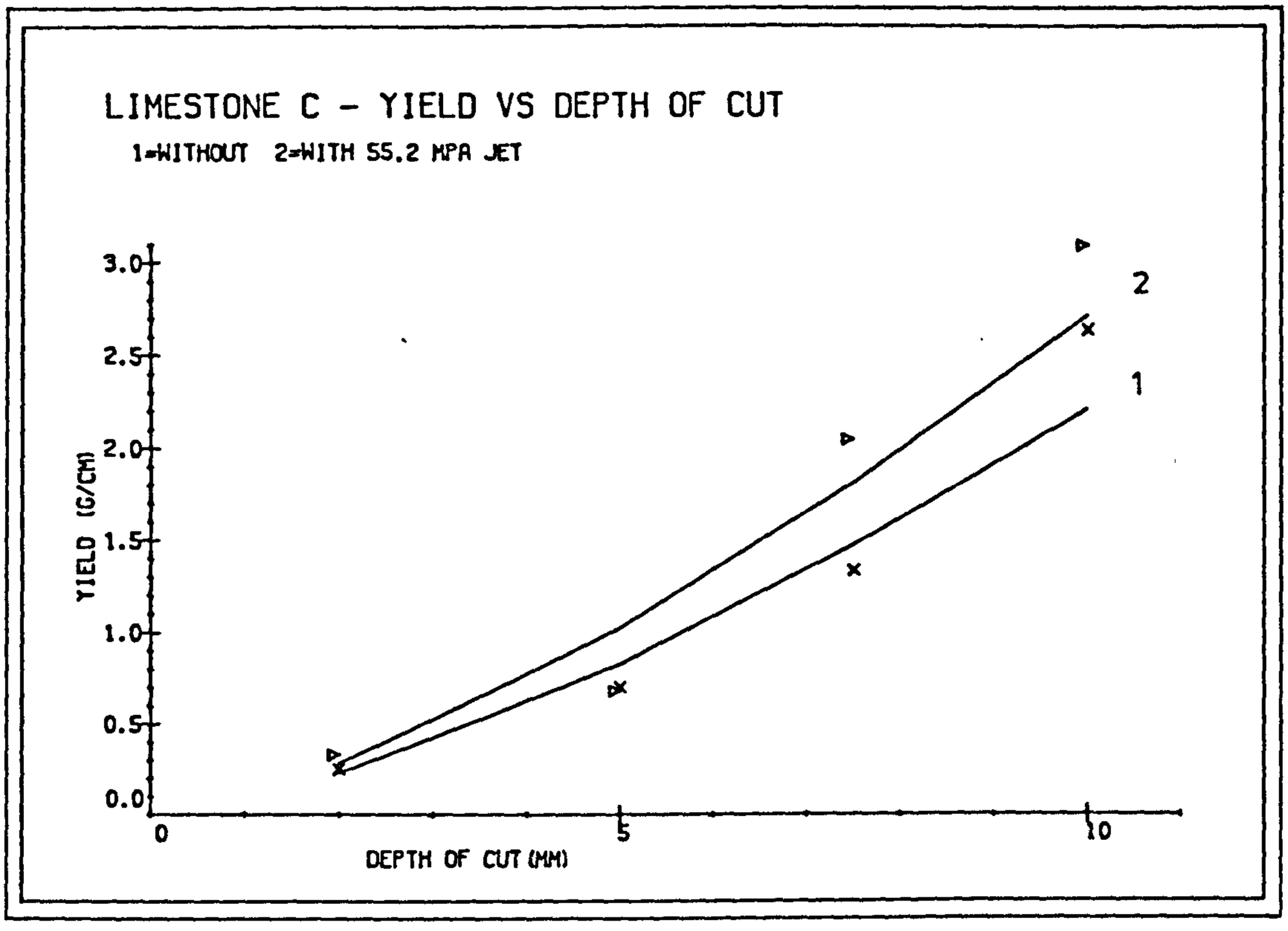
LIMESTONE C - YIELD VS DEPTH OF CUT
1=WITHOUT 2=WITH 55.2 MPA JET
YIELD (G/CM)
3.0
2.5
2.0
1.5
1.0
0.5
0.0
0
5
10
DEPTH OF CUT (MM)
2
1

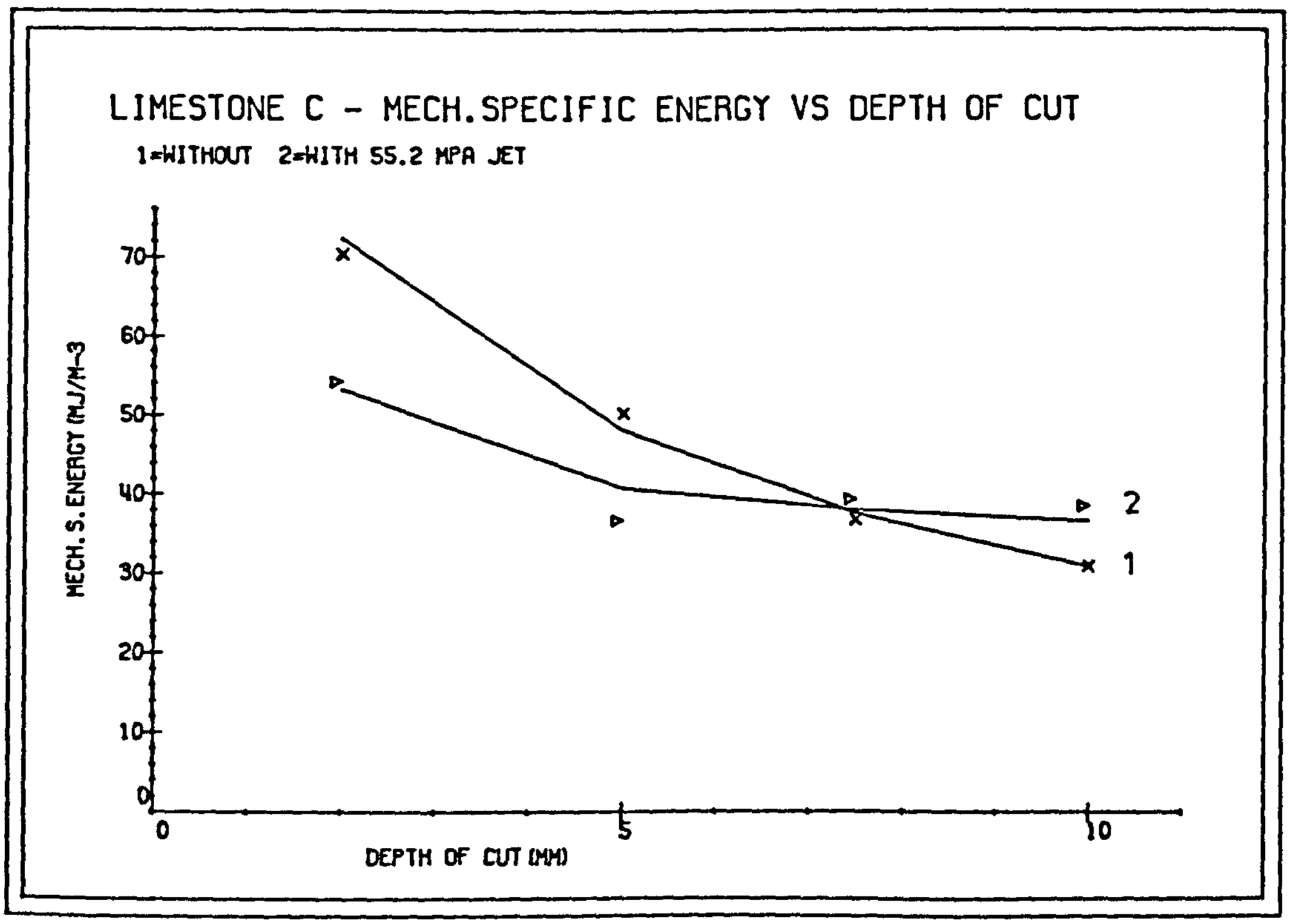
LIMESTONE C - MECH.SPECIFIC ENERGY VS DEPTH OF CUT
1=WITHOUT 2=WITH 55.2 MPA JET
MECH.S.ENERGY (MJ/M-3
70
60
50
40
30
20
10
0
0
5
10
DEPTH OF CUT (MM)
2
1

FIG. 8.17

8.5.5 Discussion

Considering the shape of the mechanical tool which had negative rake and back clearance angles, addition of high pressure waterjet did not have significant effect on cutting parameters measured and calculated. In addition the limestone had negligible porosity.

Waterjet did not penetrate the rock and examination of the debris and rock surface had suggested that, since the limestone was very brittle, the crack initiation and propogation by the mechanical tool must have been almost done instantaneously. Waterjet did not have time to act over the cracks.

If the jet pressure was high enough to exceed the threshold pressure of the limestone more reduction in forces and mechanical specific energy may have been expected.

8.6 CONCLUSIONS

Increase in depth of cut caused linear increase in cutting and normal tool forces for both cutting systems. Yield increased at an increasing rate showing a power relationship and Mechanical Specific Energy decreased showing a tendency to level off at deeper depth of cuts.

The waterjet assisted cutting system gave lower force results and Mechanical Specific Energy than the mechanical cutting system under identical cutting situations. The slopes of regressed lines were steeper with mechanical cutting.

Since the efficiencies of cutting systems increase with increase in depth of cut,when the operating performances of the two cutting system were compared at 10mm depth of cut, the tool forces were reduced by following percentages with high pressure waterjet assistance. The figures are rounded.

Darley Dale Sandstone

Mean Cutting Force : 22 %

Peak Cutting Force : 33 %

Mean Normal Force : 51 %

Mean Peak Normal Force : 46 %

Darney Sandstone

Mean Cutting Force : 41 %

Mean Peak Cutting Force : 23 %

Mean Normal Force : 55 %

Mean Peak Normal Force : 46 %

Springwell Sandstone

Mean Cutting Force : 44 %

Mean Peak Cutting Force : 44 %

Mean Normal Force : 61 %

Mean Peak Normal Force : 60 %

Limestone B

Mean Cutting Force : 26 %

Mean Normal Force : 63 %

Mean Peak Normal Force : 51 %

Peak Normal Force : 49 %

Portland Limestone

Mean Cutting Force : 28 %

Mean Peak Cutting Force : 32 %

Mean Normal Force : 54 %

Sandstone D

Mean Cutting Force : 36 %

Mean Peak Cutting Force : 32 %

Mean Normal Force : 59 %

Mean Peak Normal Force : 44 %

Overall 33 % reduction in the cutting forces and 51 % reduction in normal forces were realised. These had shown that high pressure waterjet assisted cutting was more efficient than mechanical tool cutting in terms of reduction in mechanical tool forces.

9 THE INFLUENCE OF ROCK PROPERTIES

Cutting experiments were carried out on sedimentary rocks (sandstones and limestones) as described and investigated in previous chapters. The rocks were:

SANDSTONES	LIMESTONES
Springwell	Portland
Darney	Lst B.
Darley Dale	Lst C.
S.st D	

Although care was taken in the selection of experimental rocks so that they covered a wide range of rock properties, the results of subsequent analysis must be treated with caution as only seven rocks were investigated.

The influence of high-pressure waterjet was measured in terms of its penetration depth and this depth varied with jet pressure, nozzle diameter, stand-off distance number of jet passes and the jet residence time. It was observed that at the jet pressure used for the experiments, 55-17 MPa, the jet on some rocks, penetrated to a depth equal to or more than the mechanical tool depth of cut and on some rocks it did not penetrate at all. Therefore, the effect of waterjet when used in conjunction with the mechanical tool in the latter case may be to propagate the cracks initiated by the mechanical tool. Because of the

differences in the phenomenon of rock breakage, the cutting results might exhibit varying trends with rock properties.

The rocks are classified in order of ascendancy according to each property measured, and tabulated as follows:

COMP ST (MN/m^2)	TENS ST (MN/m^2)	COMP/TENS	DENSITY (g/cm^3)	GRAIN DENSITY (g/cm^3)
Springwell	Springwell	Portland	D.Dale	Springwell
D.Dale	D.Dale	S.st D	Darney	Darney
Darney	Darney	Lst. C	S'well	D.Dale
L.st B	L.st B	Springwell	L.st B	Portland
Portland	Portland	Darney	Portland	L.st B
Lst. C	Lst. C	D.Dale	S.st D	S.st D
S.st D	S.st D	L.st B	Lst. C	L.st C

APP POR (%)	NCB CONE INDENTER	SCH HAMMER HARDNESS	SCLERO. HARDNESS	PLASTICITY (%)	D.MODUL (GPa)
Lst. C	S'well	L.st B	Darney	S.st D	D.Dale
S.st D	D.Dale	Portland	S'well	Lst. C	Darney
Portland	Darney	Darney	Ptland	D.Dale	S'well
D.Dale	L.st B	D.Dale	S.st D	Ptland	Ptland
Darney	Portland	Springwell	L.st B	Darney	L.st B
L.st B	S.st D	Lst. C	D.Dale	L.st B	S.st D
S'well	Lst. C	S.st D	Lst. C	S'well	Lst. C

As can be seen from the above table the order of rocks vary with each property.

The results are analysed seperately for mechanical cutting and hybrid cutting at 10mm depth of cut.

9.1 THE EFFECT OF ROCK PROPERTIES

9.1.1 On Mechanical Cutting

On Mean Cutting Force

When the rocks were classified according to increasing force required for cutting at 10mm depth of cut, this gave:

	kN
D.Dale.....	3.50
Darney.....	3.80
Springwell...	3.84
Portland.....	5.25
L.st B	5.69
S.st D.....	7.87

When this ordering was compared with the rock properties Dynamic Elastic Modulus gave the best correlation. When a computer curve-fitting analysis was performed on the data, the best-fit curve equations together with correlation coefficients were as follows:

Compressive Strength	= 20.7 MCF - 27.23	IOD = 0.85
Tensile Strength	= 1.82 MCF - 3.38	IOD = 0.83
Comp./Tensile	= 1/(0.06 + 0.0025 MCF)	IOD = 0.17
Bulk Density	= 2.03 + 0.043 MCF	IOD = 0.69
NCB Cone Indenter	= 0.34 MCF + 1.07	IOD = 0.78
Apparent Porosity	= 1/(0.04 MCF - 0.06)	IOD = 0.682

Scleroscope Hardness = $1/(0.03 - 7.7x10^{-4} MCF)$ IOD = 0.08

Plasticity = $1/(2.9x10^{-3} + 6.82x10^{-3} MCF)$ IOD = 0.66

Dynamic Modulus = 0.99MCF - 2.61 IOD = 0.93

(C/T)(B.D/G.D)(NCB/DM) = $1/(2.7x10^{-2} MCF - 0.07)$ IOD = 0.97

On Mean Peak Cutting Force

If the rocks are classified in increasing force required for cutting

	kN
Springwell....	5.44
D.Dale.....	5.96
Darney.....	6.01
L.st B	9.44
Portland.....	10.61
S.st D	17.8

The best fit curve functions together with correlation coefficients were:

Compressive St. = 7.62MPCF+ 5.95 IOD = 0.92

Tensile St.	= 0.68MPCF- 0.56	IOD = 0.93
Comp./Tensile	= $1/(6.4\text{x}10^{-2} + 1.03\text{x}10^{-3}$ MPCF)	IOD = 0.23
Bulk Density	= 0.043MPCF+ 2.03	IOD = 0.69
NCB Cone Indenter	= 0.129MPCF + 1.58	IOD = 0.90
Apparent Porosity	= $1/(1.6\text{x}10^{-2}$ MPCF $- 1.97\text{x}10^{-4})$	IOD = 0.85
Scleroscope Hardness	= $1/(2.65\text{x}10^{-2} - 7.7\text{x}10^{-4}$ MPCF.)	IOD = 0.08
Plasticity	= $1/(1.27\text{x}10^{-2} + 2.63\text{x}10^{-3}$ MPCF)	IOD = 0.79
Dynamic Mod.	= 0.34MPCF- 0.804	IOD = 0.88
(C/T)(BD/GD)(NCB/DM)	= $1/(9.25\text{x}10^{-3}$ MPCF $- 0.024$)	IOD = 0.93

Mean Normal Force

	kN
Springwell...	2.79
D.Dale.....	3.24
Darney.....	3.90
Portland.....	6.77
L.st B	8.32
S.st D.....	14.8

Compressive St.	= 7.85 MNF+ 23.98	IOD = 0.91
Tensile St.	= 0.68 MNF+ 1.21	IOD = 0.86
Comp/Tensile	= $1/(0.068 + 7.6\times10^{-4}$ MNF)	IOD = 0.115
Bulk Density	= 0.015MNF+ 2.15	IOD = 0.64
NCB Cone Indenter	= 0.128MNF. + 1.922	IOD = 0.824
Apparent Porosity	= $1/(4.26\times10^{-2} + 0.015$ MNF)	IOD = 0.75
Scleroscope Hardness	= 1/(0.025 - 0.00032 MNF)	IOD = 0.1
Plasticity	= $1/(1.92\times10^{-2} + 2.67\times10^{-3}$ MNF)	IOD = 0.75
Dynamic Mod.	= 0.36 MNF- 0.06	IOD = 0.92
(C/T)(BD/GD)(NCB/DM)	= $1/(9.9\times10^{-3}$ MNF $- 4.39\times10^{-3})$	IOD = 0.99

Mean Peak Normal Force

	kN
Springwell....	5.05
D.Dale.....	5.70
Darney.....	6.55
Portland.....	10.4
L.st B	12.1
S.st D.....	19.8

Compressive St.	= 6.37MPNF+ 12.83	IOD = 0.904
Tensile St.	= 0.55MPNF+ 0.24	IOD = 0.85
Comp/Tensile	= $1/(6.7\times10^{-2} + 6.21\times10^{-4}$ MPNF)	IOD = 0.117
Bulk Density	= 0.0125MPNF+ 2.12	IOD = 0.65
NCB Cone Indenter	= 0.105 MPNF+ 1.73	IOD = 0.84
Apparent Porosity	= $1/(2.03\times10^{-2} + 1.25\times10^{-2}$ MPNF)	IOD = 0.75
Scleroscope Hardness	= $1/2.53\times10^{-2} - 2.63\times10^{-4}$ MPNF)	IOD = 0.104
Plasticity	= $1/(1.55\times10^{-2} + 2.16\times10^{-3}$ MPNF)	IOD = 0.74
Dynamic Modulus	= 0.292MPNF- 0.565	IOD = 0.91
(C/T)(BD/GD)(NCB/DM)	= $1/(8.06\times10^{-3}$ MPNF - 0.019)	IOD = 0.99

9.1.2 On Hybrid Cutting

Mean Cutting Force

	kN
Springwell	2.14
Darney	2.73
D.Dale	3.13
Portland Lst	3.46
L.st B	4.09
S.st D.....	5.98

Compressive Strength	= 26.71MCF- 19.91	IOD = 0.92
Tensile Strength	= 2.25 MCF- 2.36	IOD = 0.82
Comp/Tensile	= $1/(6.78\times10^{-2} + 1.54\times10^{-3}$ MCF.)	IOD = 0.04
Bulk Density	= 4.72×10^{-2}MCF+ 2.08	IOD = 0.54
Apparent Porosity	= $1/(5.35\times10^{-2}$ MCF - 0.048)	IOD = 0.79
NCB Cone Indenter	= 0.435 MCF + 1.204	IOD = 0.83
Scleroscope Hardness	= MCF /$(2.69\times10^{-2} + 1.44\times10^{-2}$ MCF)	IOD = 0.37
Plasticity	= $1/(9.53\times10^{-3}$MCF+ 2.67×10^{-3})	IOD = 0.83
Dynamic Modulus	= 1.167 MCF- 1.863	IOD = 0.84
(C/T)(BD/GD)(NCB/DM)	= $1/(3.32\times10^{-2}$ MCF - 5.8×10^{-2})	IOD=0.97

Mean Peak Cutting Force

	kN
Springwell	3.07
Darney	4.62
D.Dale	5.04
Portland	6.96
L.st B	8.5
S.st D.....	9.8

Compressive St.	= 12.16MPCF- 0.89	IOD = 0.69
Tensile St.	= 0.99MPCF- 0.54	IOD = 0.57
Comp/Tensile	= 14.28 + (-2.35 MPCF)	IOD = 0.01
Bulk Density	= 0.0227MPCF+ 2.103	IOD = 0.45
Apparent Porosity	= 0.49 + (44.4/ MPCF)	IOD = 0.70
NCB Cone Indenter	=MPCF/0.91 + 0.21MPCF)	IOD = 0.82
Scleroscope Hardness	=MPCF /(0.03 + 0.0167 MPCF)	IOD = 0.35
Plasticity	= 14.7 + (81.11/ MPCF)	IOD = 0.61
Dynamic Modulus	= 0.55MPCF- 1.12	IOD = 0.66
(C/T)(BD/GD) (NCB/DM)	= 118.73 exp (-0.28 MPCF)	IOD = 0.99

Mean Normal Force

	kN
Springwell	1.09
Darney	1.77
D.Dale	1.90
L.st B	2.79
Portland Lst	2.84
S.st D	7.33

Compressive St.	= 16.84MNF + 26.64	IOD = 0.99
Tensile St.	= 1.48MNF + 1.38	IOD = 0.96
Comp/Tensile	= 1/(0.16 + 0.068 MNF)	IOD = 0.155
Bulk Density	= 0.032 MNF + 2.15	IOD = 0.68
Apparent Porosity	= 1/(0.043 + 0.035 MNF)	IOD = 0.90
NCB Cone Indenter	= 1.90 + 0.97 log MNF	IOD = 0.94
Scleroscope Hardness	= MNF /(8.9×10^{-3} + 1.84×10^{-2} MNF)	IOD = 0.27
Plasticity	= 1/(1.91×10^{-2} + 6.07×10^{-3} MNF)	IOD = 0.92
Dynamic Modulus	= 0.73MNF + 0.193	IOD = 0.88
(C/T)(BD/GD)(NCB/DM)	= (56.45/ MNF) - 2.35	IOD = 0.944

Mean Peak Normal Force

	kN
Darney	3.53
D.Dale	3.6
L.st B	5.7
Portland Lst	5.87
S.st D	11.6

Compressive St.	= 11.13 MPN + 15.37	IOD = 0.954
Tensile St.	= 1.05MPNF - 0.189	IOD = 0.95
Comp/Tensile	= (MPNF)/(-0.085 + 0.089 MPNF)	IOD = 0.44
Bulk Density	= 1.96 + 0.17 log MPNF	IOD = 0.78
Apparent Porosity	= 1/(0.03 + 0.0217 MPNF)	IOD = 0.85
NCB Cone Indenter	= 0.165MPNF + 1.92	IOD = 0.92
Scleroscope Hardness	= MPNF./(0.01 + 0.02 MPNF)	IOD = 0.036
Plasticity	= 1/(0.0166 + 3.8×10^{-3} MPNF)	IOD = 0.82
Dynamic Modulus	= 0.563MPNF - 0.992	IOD = 0.963
(C/T)(BD/GD)(NCB/DM)	= 1/(1.33×10^{-2} MPNF - 1.15×10^{-2})	IOD = 0.94

9.2 DISCUSSION

The mechanics of rock failure due to the action of point attack tool or of high pressure water jet or a combination of the two is very complicated and poorly understood. Because the rock is subjected to several separate processes each of which can cause failure and further the rock itself may not be homogenous and isotropic.

Most rocks are granular and contain pores and microfracturing. Some theories of fracture have tried to relate the condition and properties of the rock to the imposed stresses by external devices(79). The Coulomb-Navier and Mohr's theories of failure are concerned with the fracture mechanism and yield occurring on a macroscopic scale. Failure on an internal or microscopic basis was examined by Griffith. He hypothesized that tensile stress concentrations develop at the end of cracks causing the crack to propagate and contribute to microscopic failure. The Griffith theory of fracture was originally developed for glass and it has been modified for rocks. The criterion postulates that although the exerted stress is compressive, fracture is initiated in a brittle metal by tensile failure along the microfractures, i.e. grain boundaries and the length of Griffith cracks in rock are approximately equal to the maximum grain diameter. But, this is valid for competent rocks and is of little use in incompetent rocks.

Failure due to action of mechanical tools has been examined by Merchant, Nishimatsu and Evans. Merchant assumed that a shear failure

takes place over a line rising from the tip of the tool to the surface of the metal. The strength of the metal is characterised by a shear strength and friction between tool and metal by a coefficient of friction associated with an angle of friction.

Evans developed a cutting theory for rock (especially for coal) by considering the normal penetration of sharp symmetrical wedge into a buttock of the rock material. The wedge penetrates the rock and drives a tensile crack along a circular arc from the wedge tip to the free surface, encountering some frictional resistance during penetration. As a rock property he used the tensile strength of the rock in his formulae. As can be noted shear strength was used for metals and tensile strength for coals. The cutting experiments performed with point attack tool alone and together with a 55.17 MPa pressure water jet have yielded interesting results.

Uniaxial compressive strength and indirect tensile strength of rocks exhibited a good correlation with all the tool forces. That is higher the strength more difficult it is to break the rock, for both cutting situations e.g. with and without waterjet assistance, (Figures 9.1-9.6).

However, rocks of similar strength but differing composition and structure show variations in forces. NCB cone indenter, which is essentially used to test the hardness of the cement material in the rock also have shown direct relationship with the forces, (Figures 9.1-9.6). Increasing cone indenter hardness resulted in higher tool forces, meaning

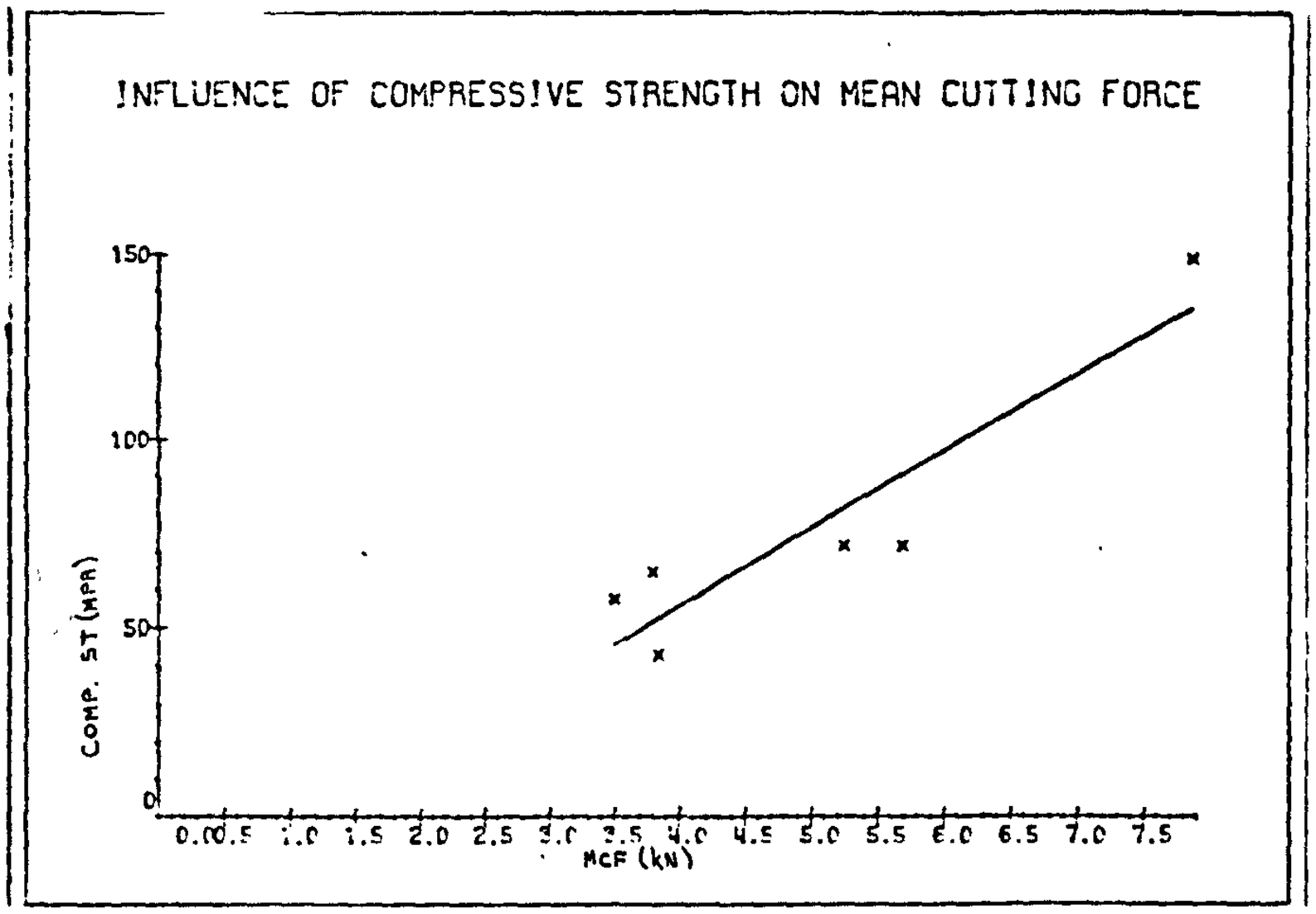
INFLUENCE OF COMPRESSIVE STRENGTH ON MEAN CUTTING FORCE
COMP. ST (MPA)
150
100
50
0
0.0 0.5 1.0 1.5 2.0 2.5 3.0 3.5 4.0 4.5 5.0 5.5 6.0 6.5 7.0 7.5
MCF (kN)

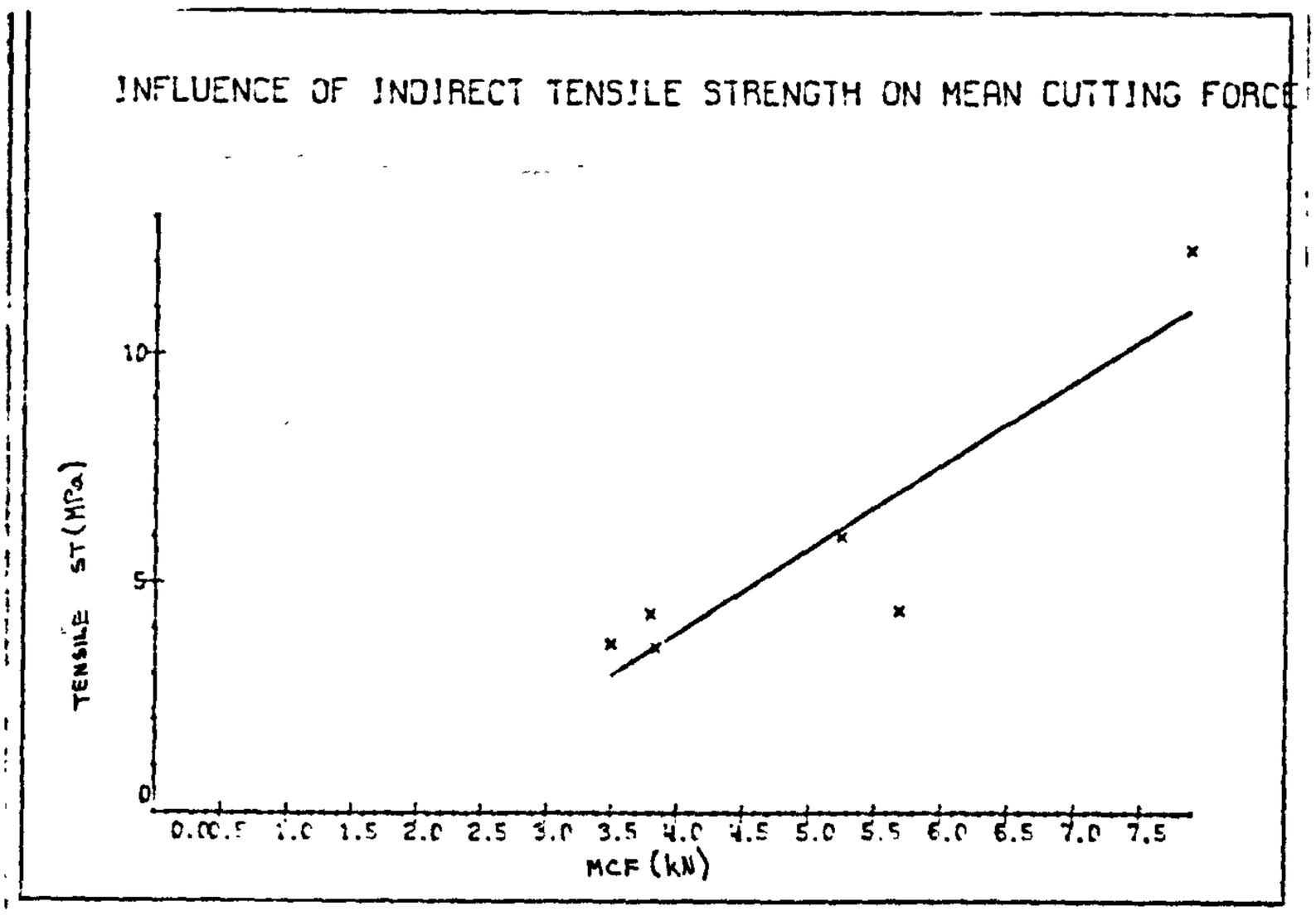
INFLUENCE OF INDIRECT TENSILE STRENGTH ON MEAN CUTTING FORCE
TENSILE ST (MPa)
10
5
0
0.0 0.5 1.0 1.5 2.0 2.5 3.0 3.5 4.0 4.5 5.0 5.5 6.0 6.5 7.0 7.5
MCF (kN)

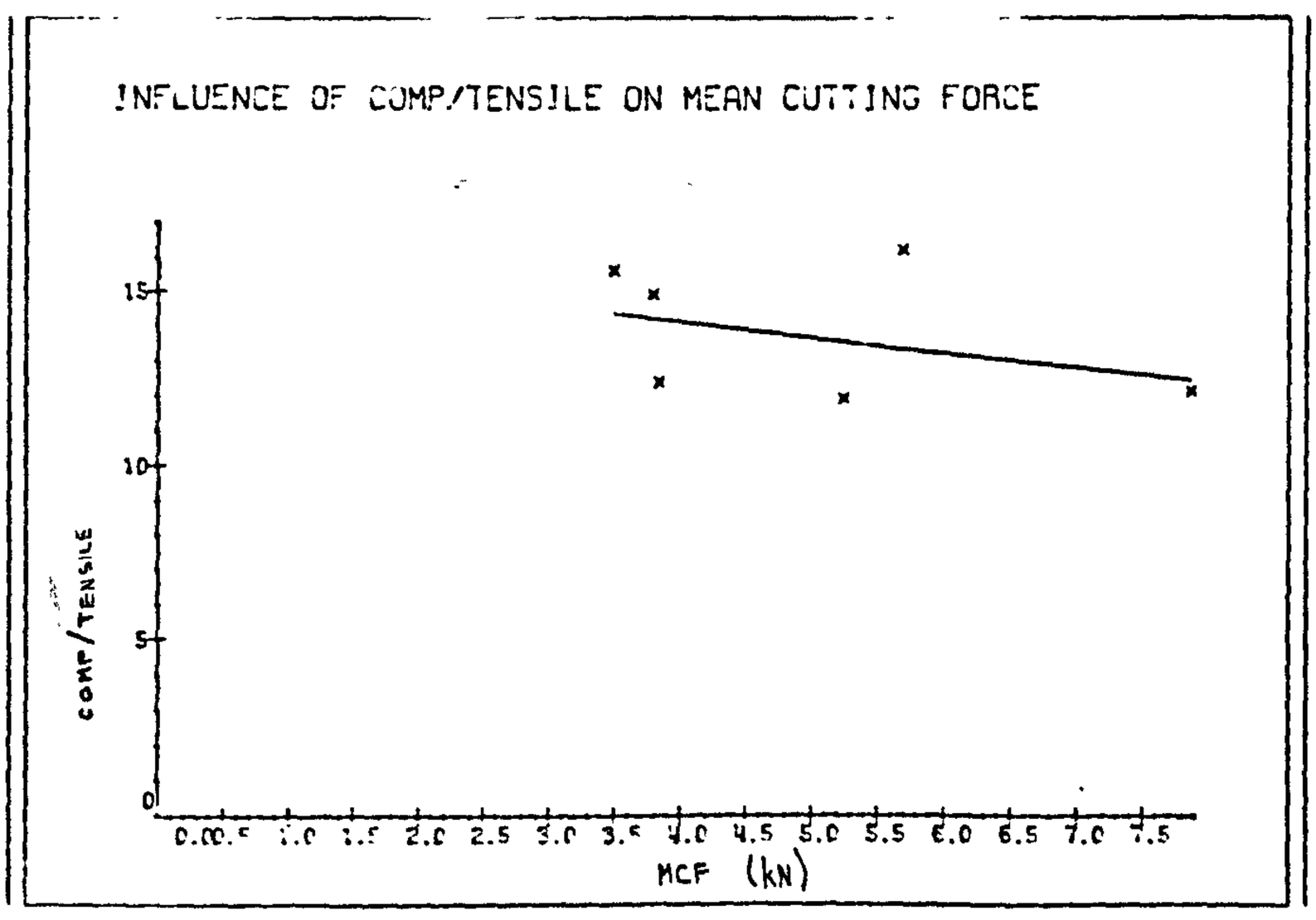
INFLUENCE OF COMP./TENSILE ON MEAN CUTTING FORCE
COMP/TENSILE
15
10
5
0
0.0 0.5 1.0 1.5 2.0 2.5 3.0 3.5 4.0 4.5 5.0 5.5 6.0 6.5 7.0 7.5
MCF (kN)

FIG. 9.1

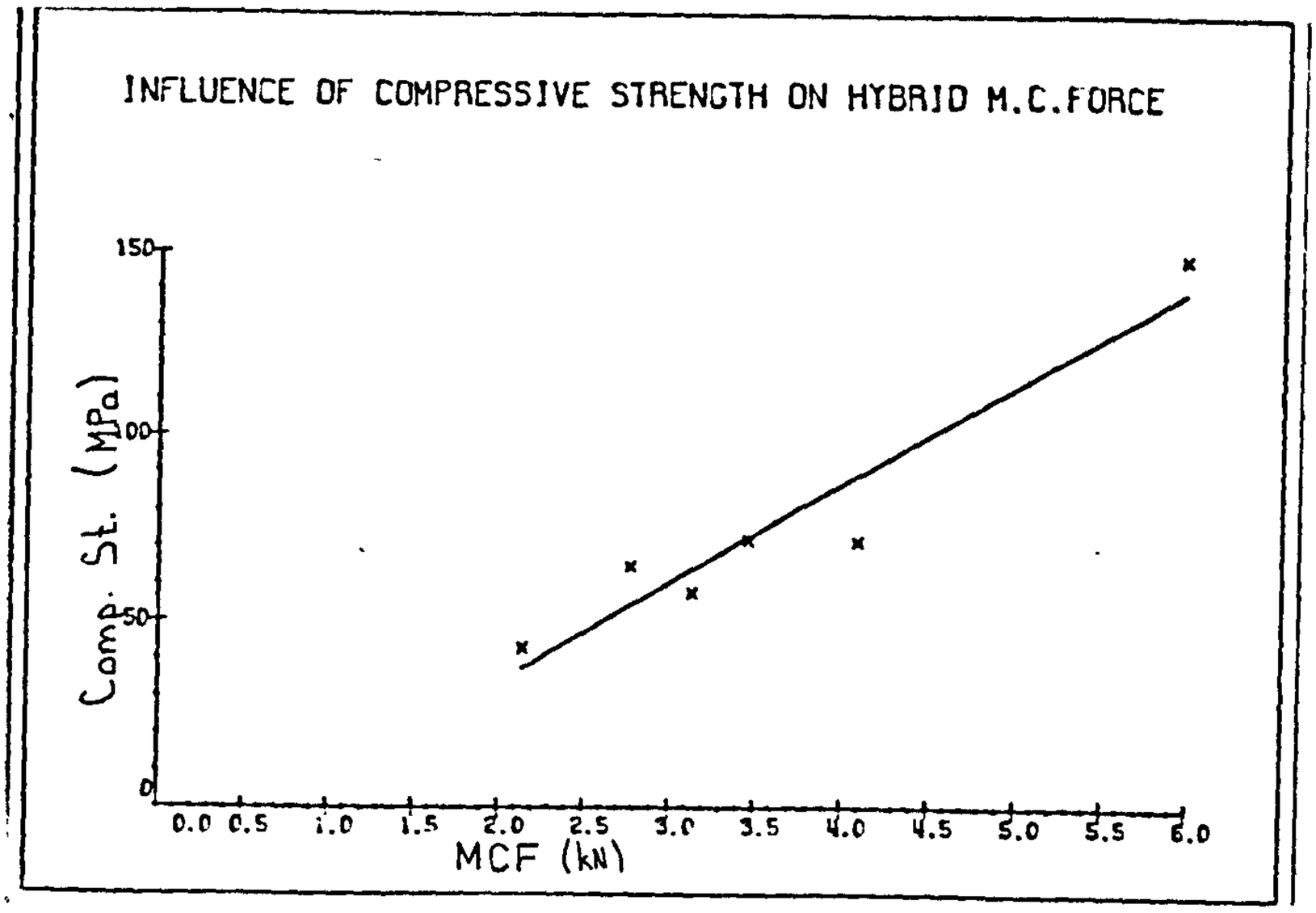
INFLUENCE OF COMPRESSIVE STRENGTH ON HYBRID M.C.FORCE
Comp. St. (MPa)
150
100
50
0
0.0 0.5 1.0 1.5 2.0 2.5 3.0 3.5 4.0 4.5 5.0 5.5 6.0
MCF (kN)

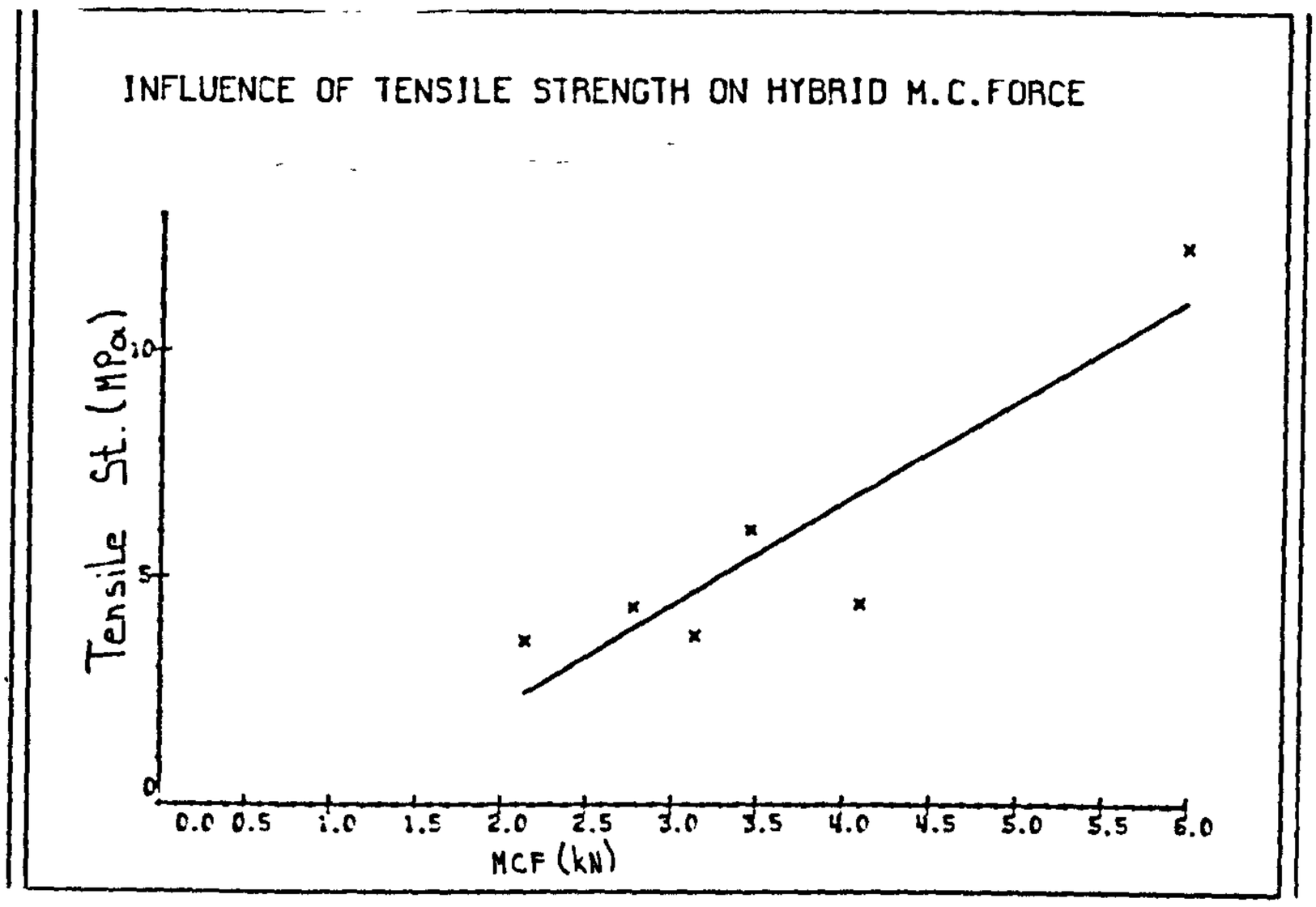
INFLUENCE OF TENSILE STRENGTH ON HYBRID M.C.FORCE
Tensile St. (MPa)
10
5
0
0.0 0.5 1.0 1.5 2.0 2.5 3.0 3.5 4.0 4.5 5.0 5.5 6.0
MCF (kN)

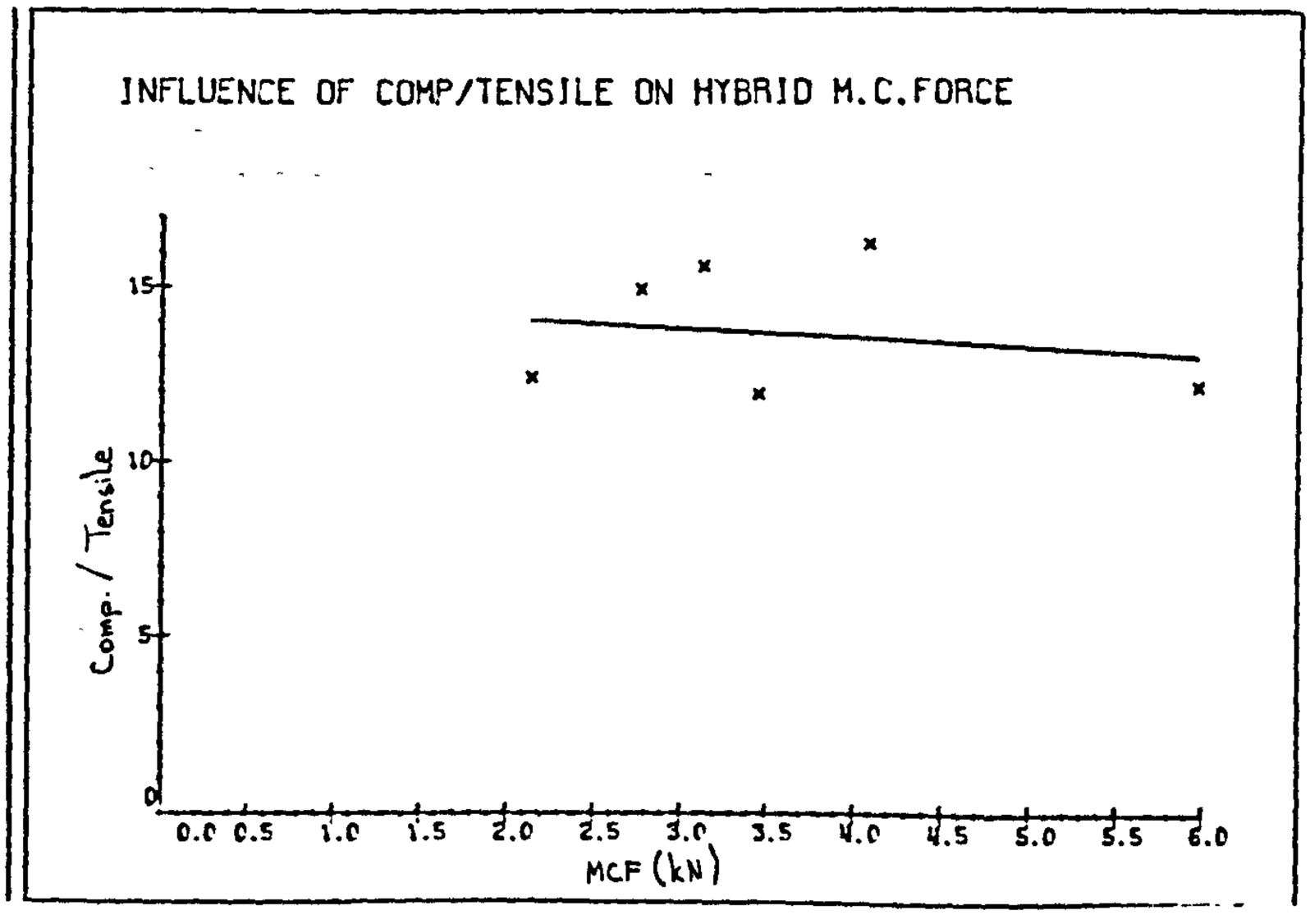
INFLUENCE OF COMP/TENSILE ON HYBRID M.C.FORCE
Comp. / Tensile
15
10
5
0
0.0 0.5 1.0 1.5 2.0 2.5 3.0 3.5 4.0 4.5 5.0 5.5 6.0
MCF (kN)

FIG. 9.2

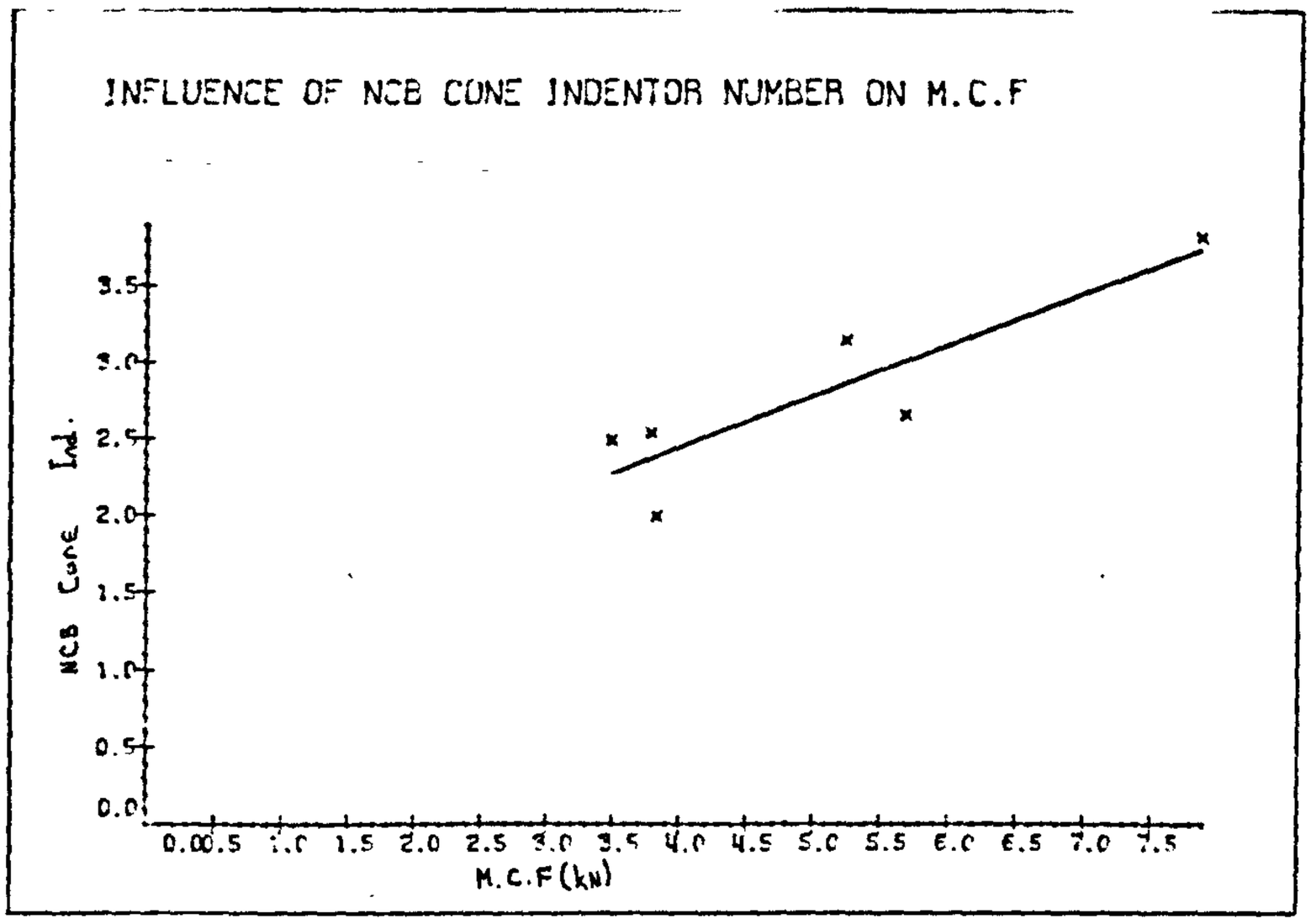
INFLUENCE OF NCB CONE INDENTOR NUMBER ON M.C.F
NCB Cone Ind.
0.0
0.5
1.0
1.5
2.0
2.5
3.0
3.5
0.0 0.5 1.0 1.5 2.0 2.5 3.0 3.5 4.0 4.5 5.0 5.5 6.0 6.5 7.0 7.5
M.C.F(kN)

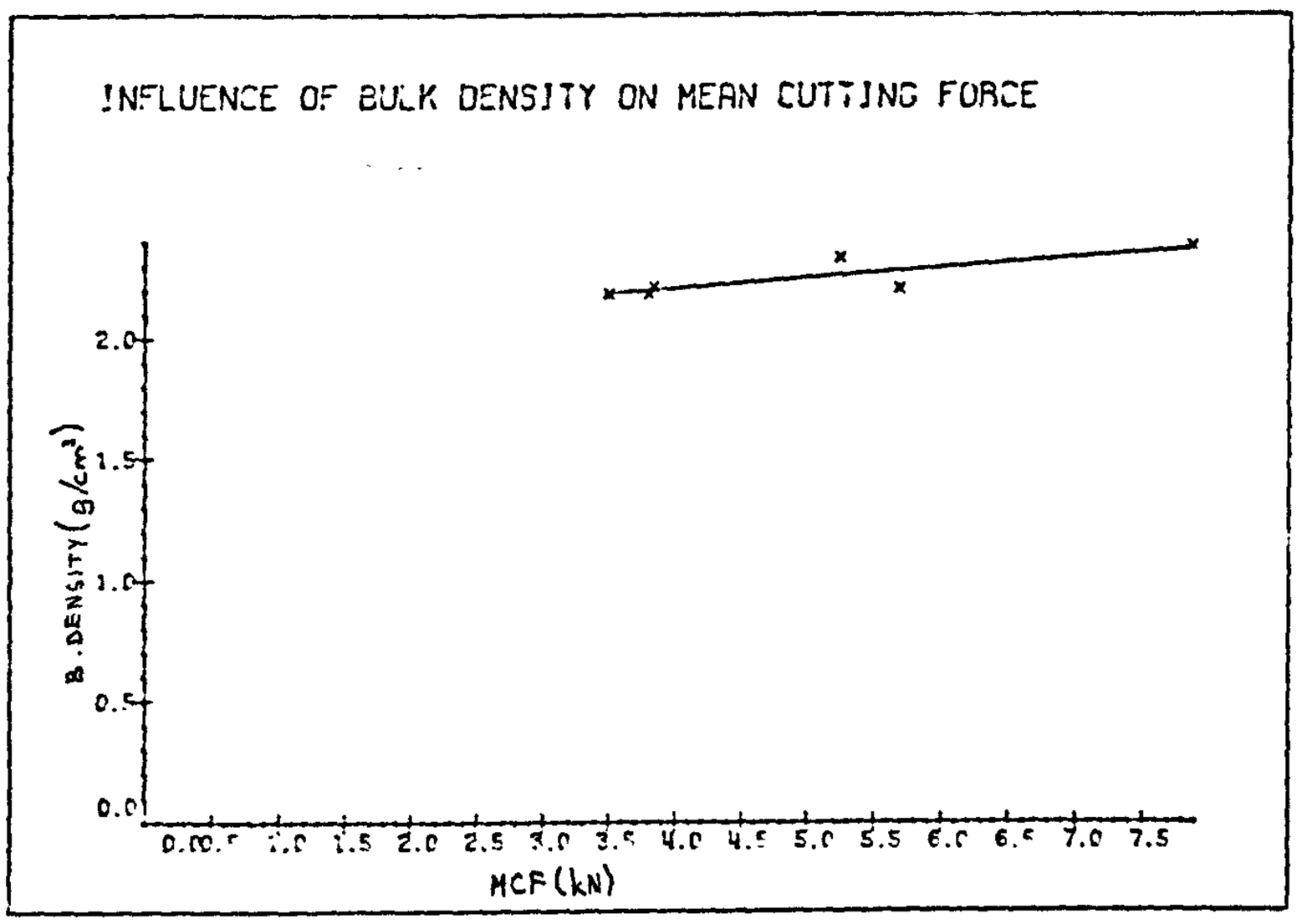
INFLUENCE OF BULK DENSITY ON MEAN CUTTING FORCE
B.DENSITY(g/cm³)
0.0
0.5
1.0
1.5
2.0
0.0 0.5 1.0 1.5 2.0 2.5 3.0 3.5 4.0 4.5 5.0 5.5 6.0 6.5 7.0 7.5
MCF(kN)

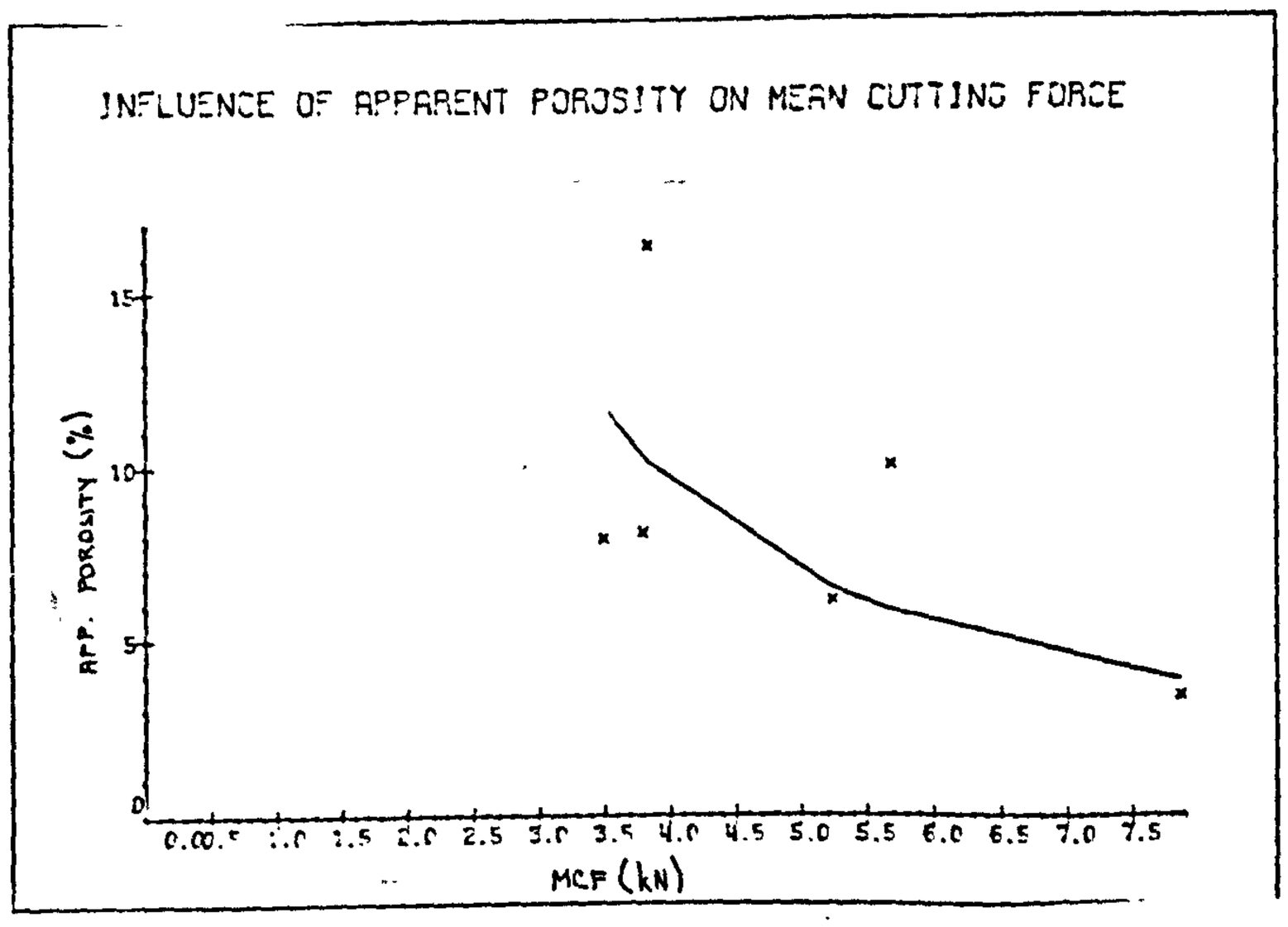
INFLUENCE OF APPARENT POROSITY ON MEAN CUTTING FORCE
APP. POROSITY (%)
0
5
10
15
0.0 0.5 1.0 1.5 2.0 2.5 3.0 3.5 4.0 4.5 5.0 5.5 6.0 6.5 7.0 7.5
MCF (kN)

FIG. 9.3

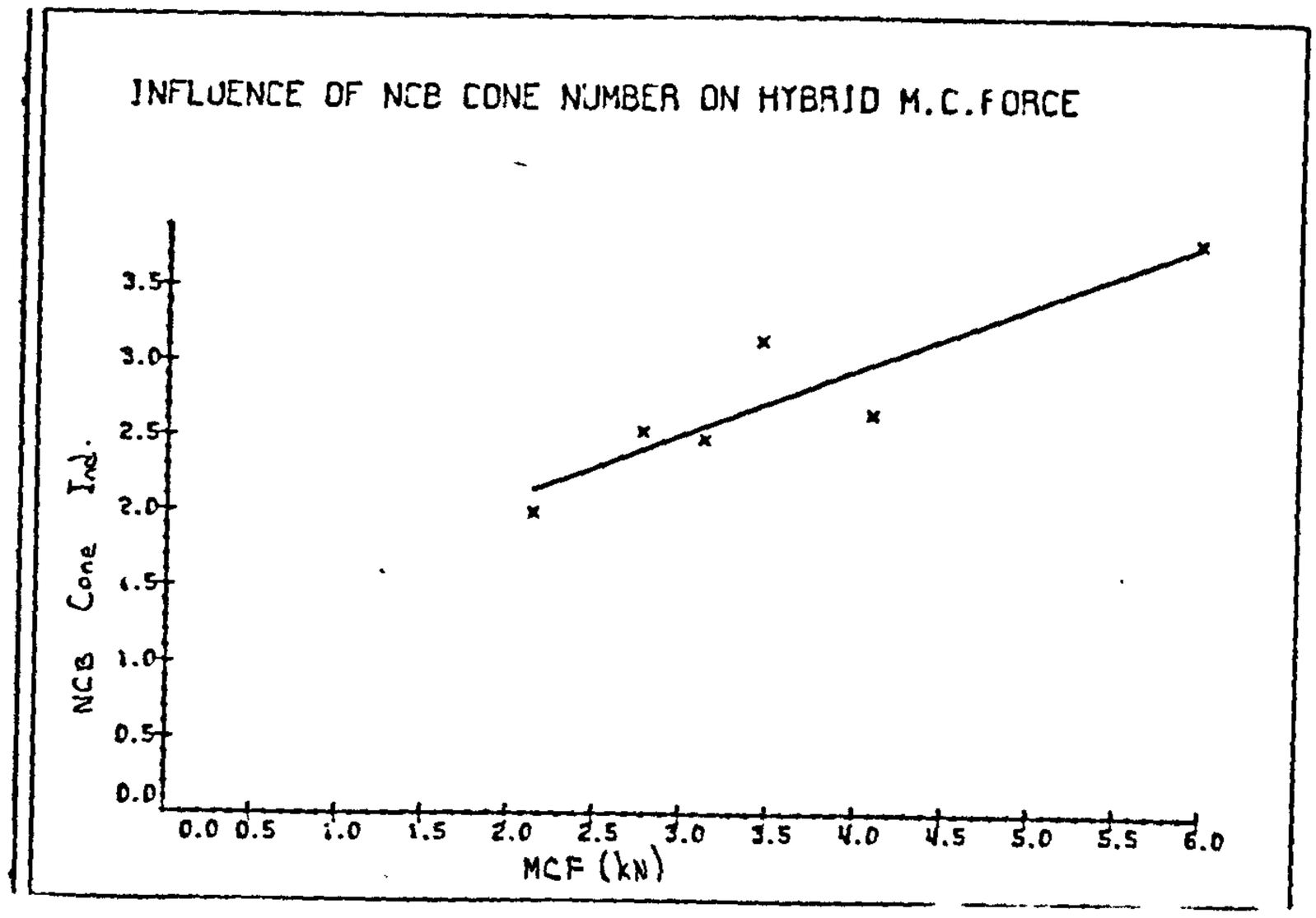
INFLUENCE OF NCB CONE NUMBER ON HYBRID M.C.FORCE
NCB Cone Ind.
3.5
3.0
2.5
2.0
1.5
1.0
0.5
0.0
0.0 0.5 1.0 1.5 2.0 2.5 3.0 3.5 4.0 4.5 5.0 5.5 6.0
MCF (kN)

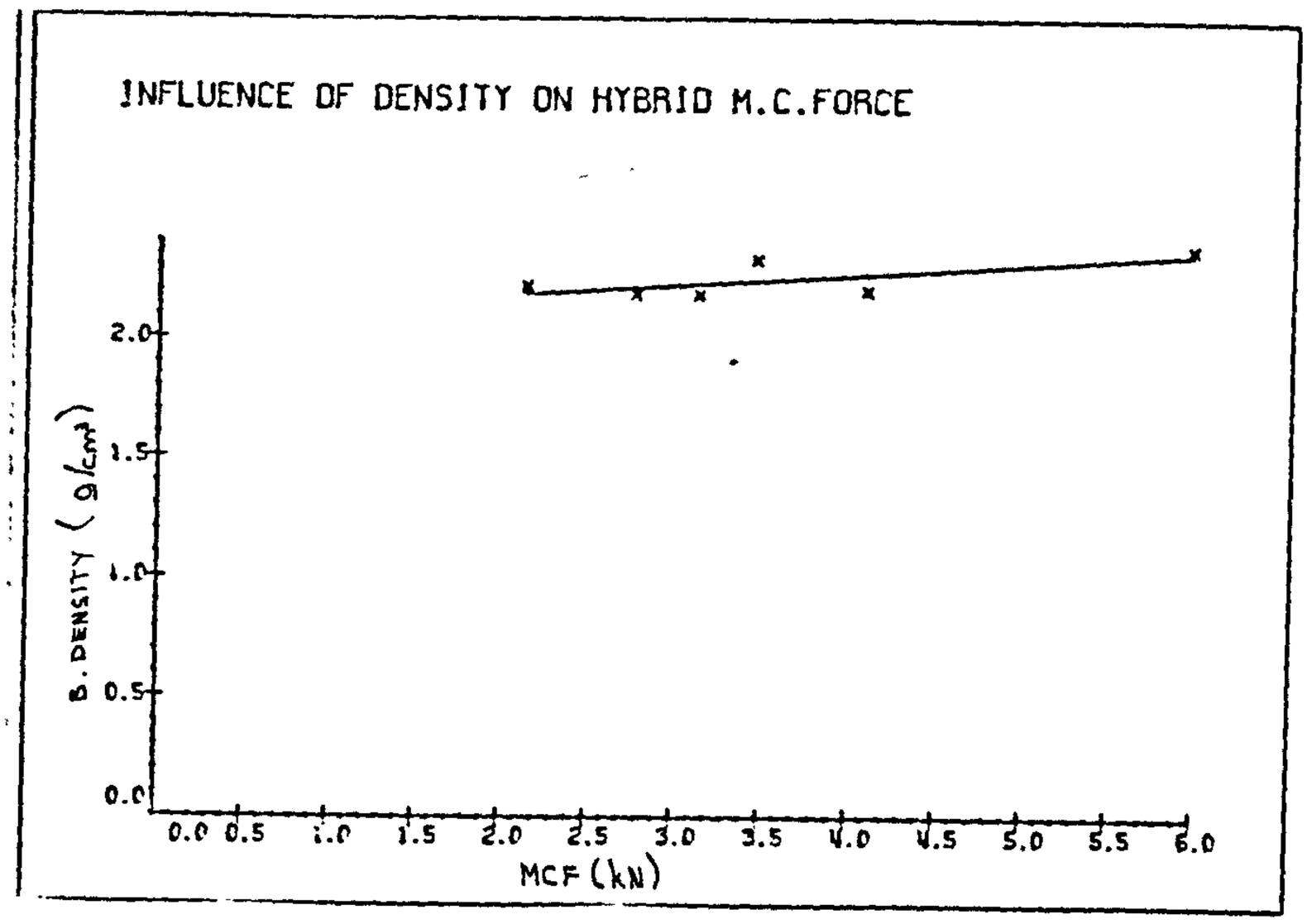
INFLUENCE OF DENSITY ON HYBRID M.C.FORCE
B. DENSITY (g/cm³)
2.0
1.5
1.0
0.5
0.0
0.0 0.5 1.0 1.5 2.0 2.5 3.0 3.5 4.0 4.5 5.0 5.5 6.0
MCF (kN)

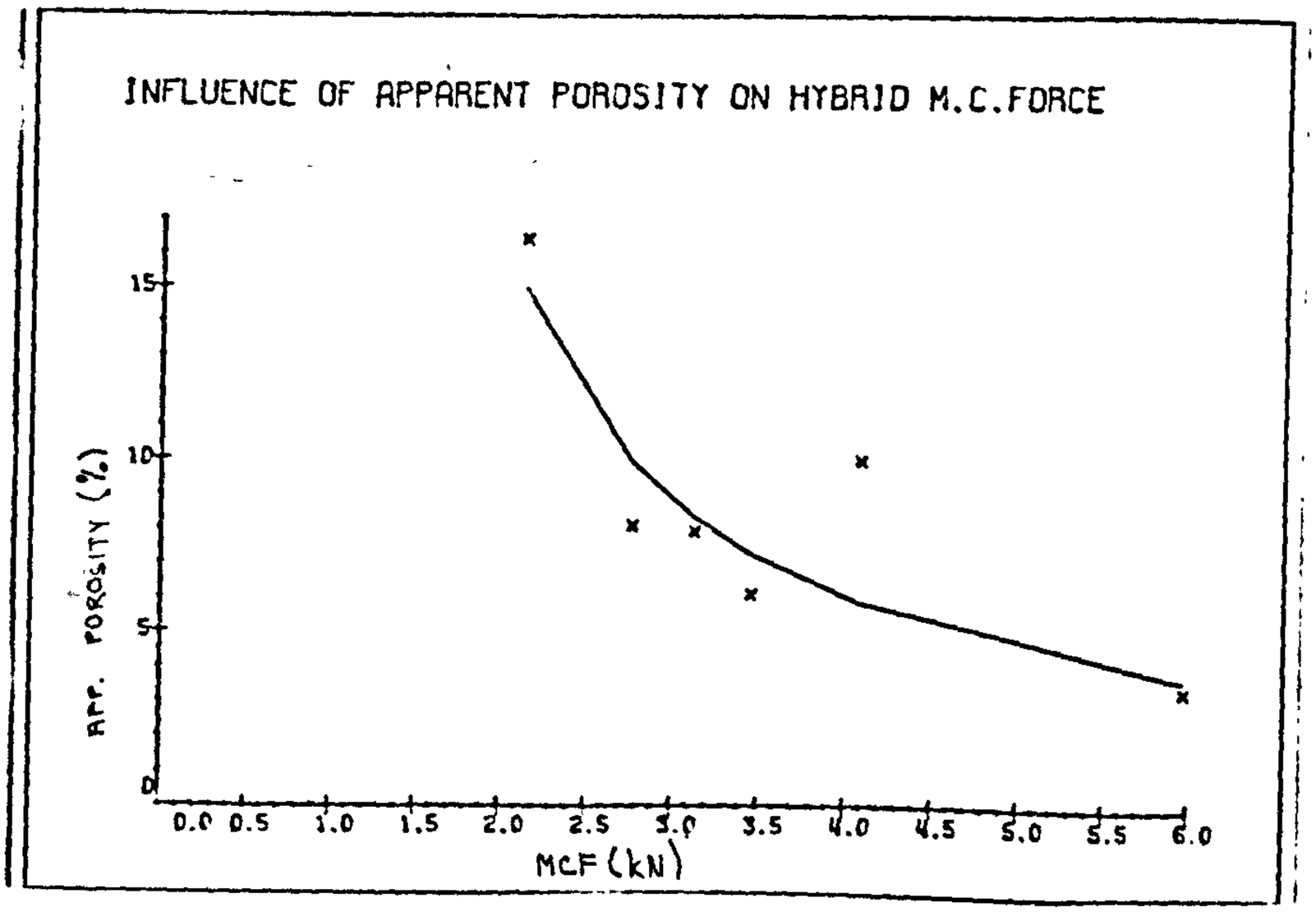
INFLUENCE OF APPARENT POROSITY ON HYBRID M.C.FORCE
APP. POROSITY (%)
15
10
5
0
0.0 0.5 1.0 1.5 2.0 2.5 3.0 3.5 4.0 4.5 5.0 5.5 6.0
MCF (kN)

FIG. 9.4

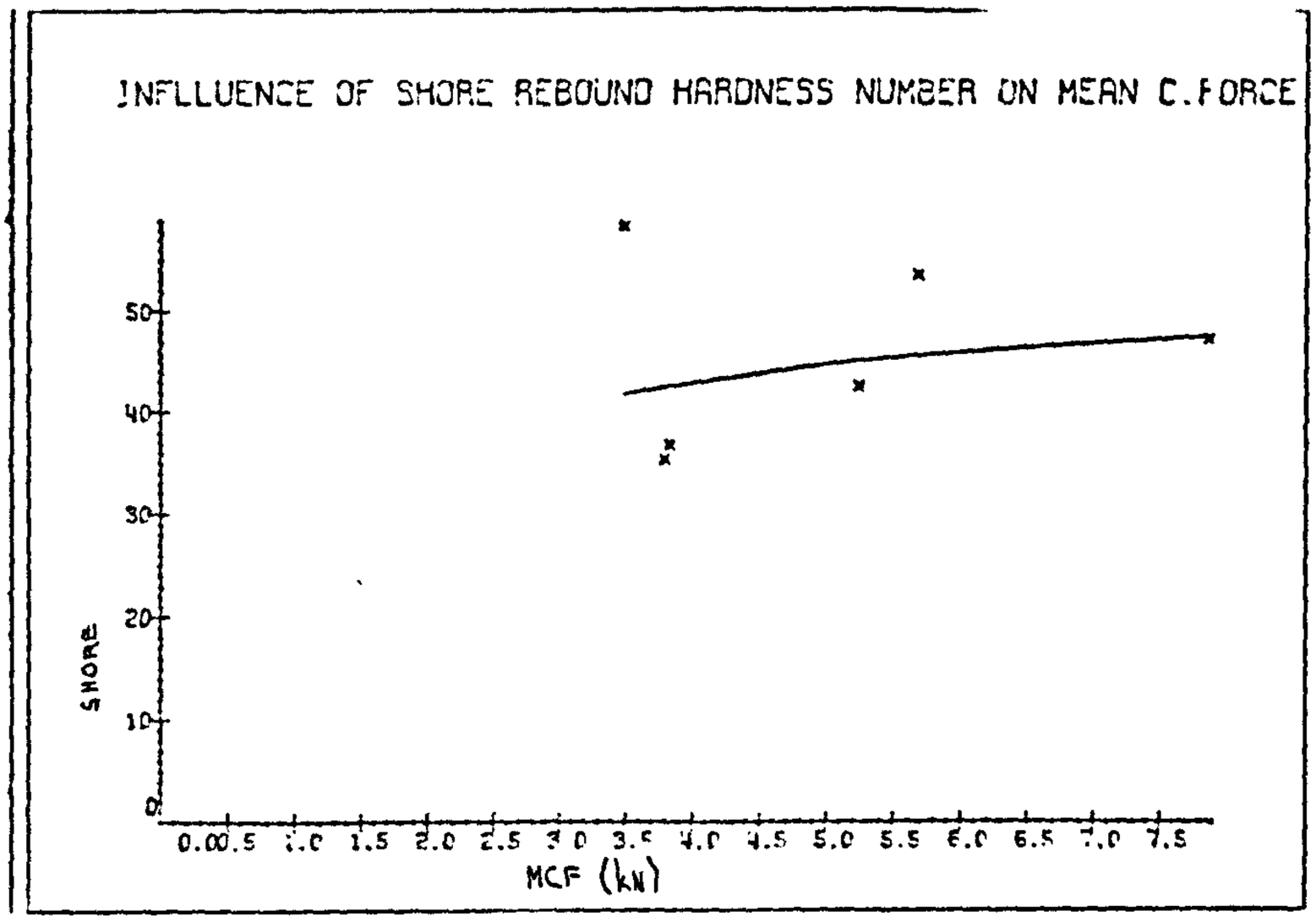
INFLUENCE OF SHORE REBOUND HARDNESS NUMBER ON MEAN C.FORCE
SHORE
0
10
20
30
40
50
0.0 0.5 1.0 1.5 2.0 2.5 3.0 3.5 4.0 4.5 5.0 5.5 6.0 6.5 7.0 7.5
MCF (kN)

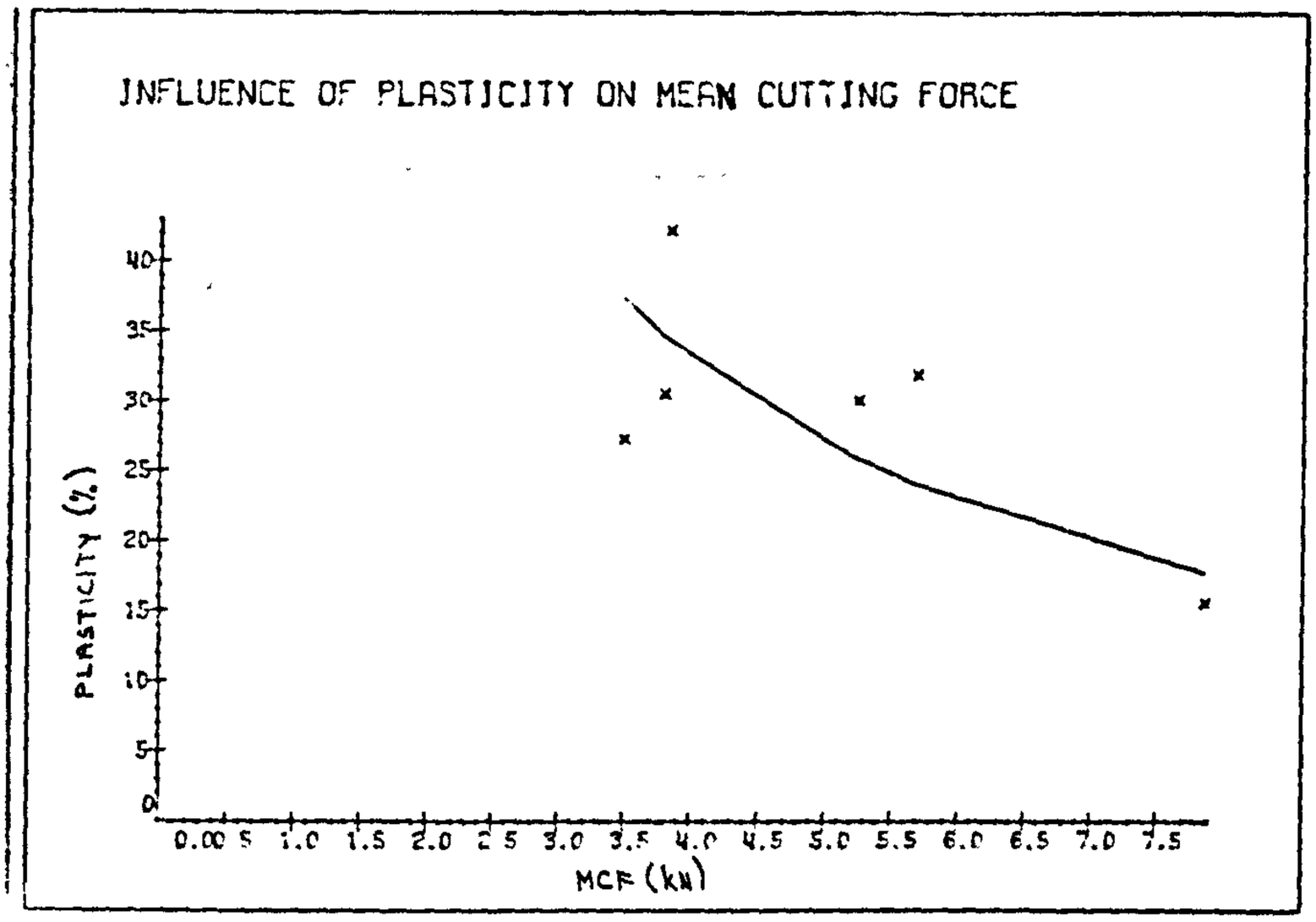
INFLUENCE OF PLASTICITY ON MEAN CUTTING FORCE
PLASTICITY (%)
0
5
10
15
20
25
30
35
40
0.0 0.5 1.0 1.5 2.0 2.5 3.0 3.5 4.0 4.5 5.0 5.5 6.0 6.5 7.0 7.5
MCF (kN)

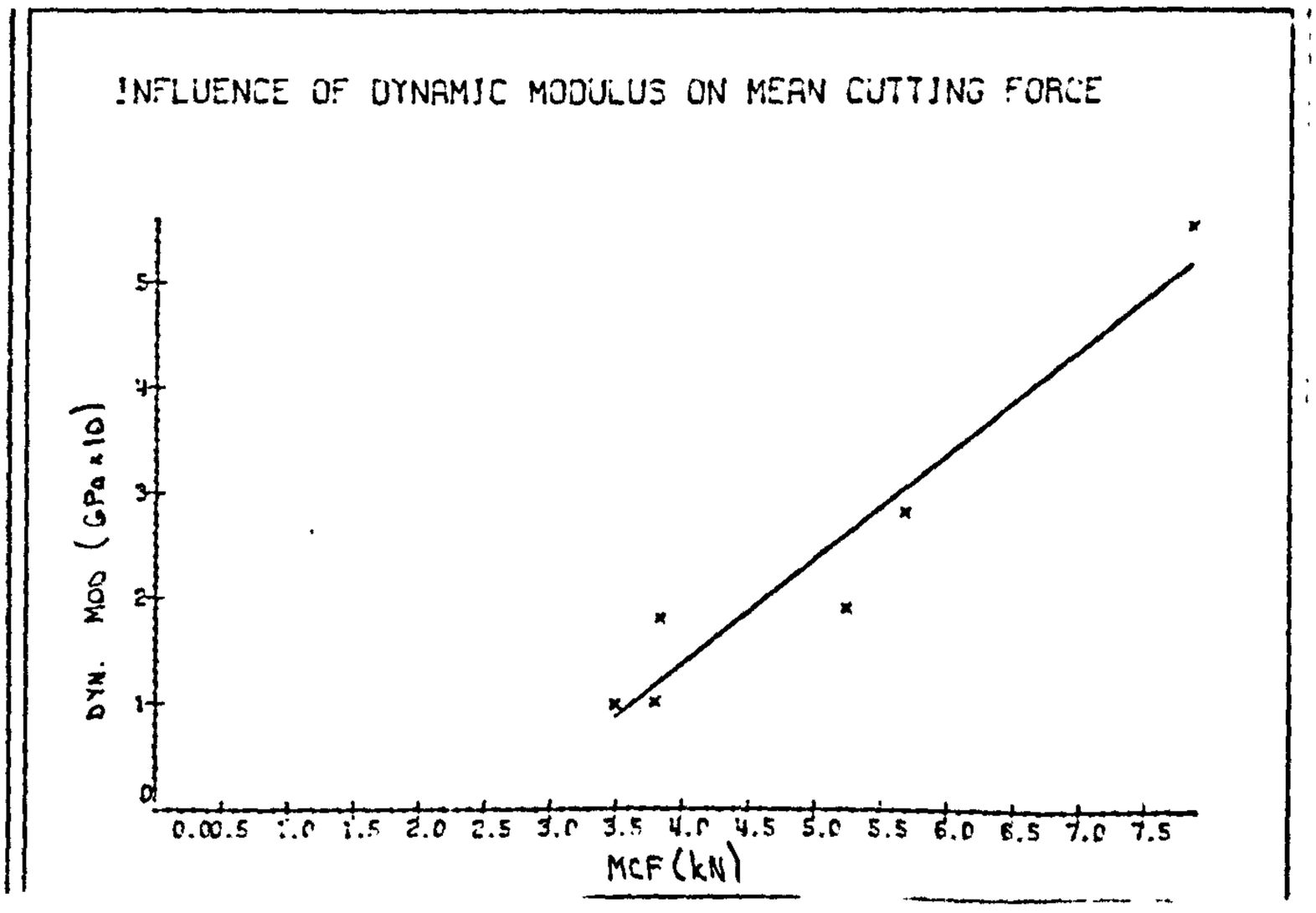
INFLUENCE OF DYNAMIC MODULUS ON MEAN CUTTING FORCE
DYN. MOD (GPa x 10)
0
1
2
3
4
5
0.0 0.5 1.0 1.5 2.0 2.5 3.0 3.5 4.0 4.5 5.0 5.5 6.0 6.5 7.0 7.5
MCF (kN)

FIG. 9.5

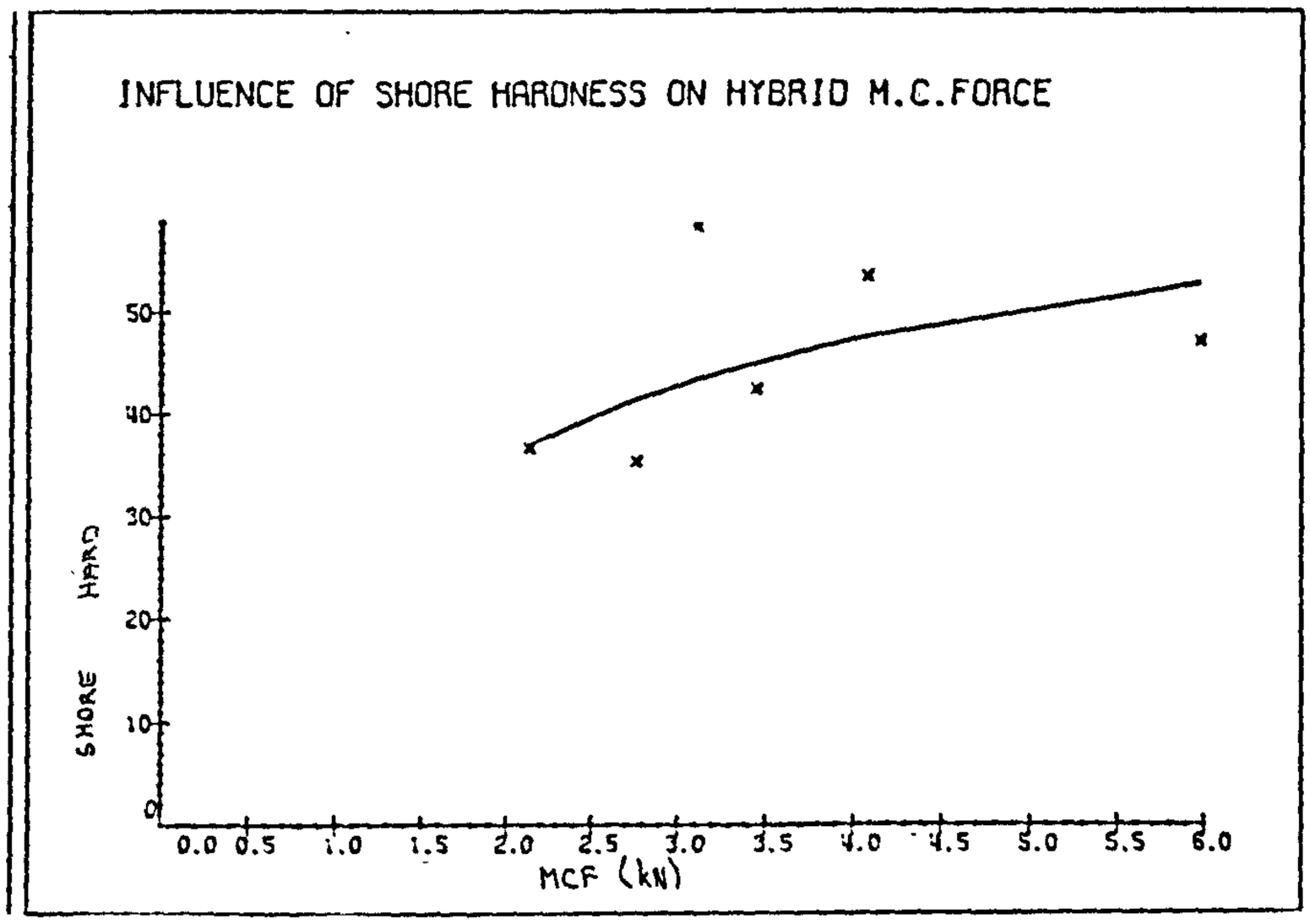
INFLUENCE OF SHORE HARDNESS ON HYBRID M.C.FORCE
SHORE HARD
0
10
20
30
40
50
0.0 0.5 1.0 1.5 2.0 2.5 3.0 3.5 4.0 4.5 5.0 5.5 6.0
MCF (kN)

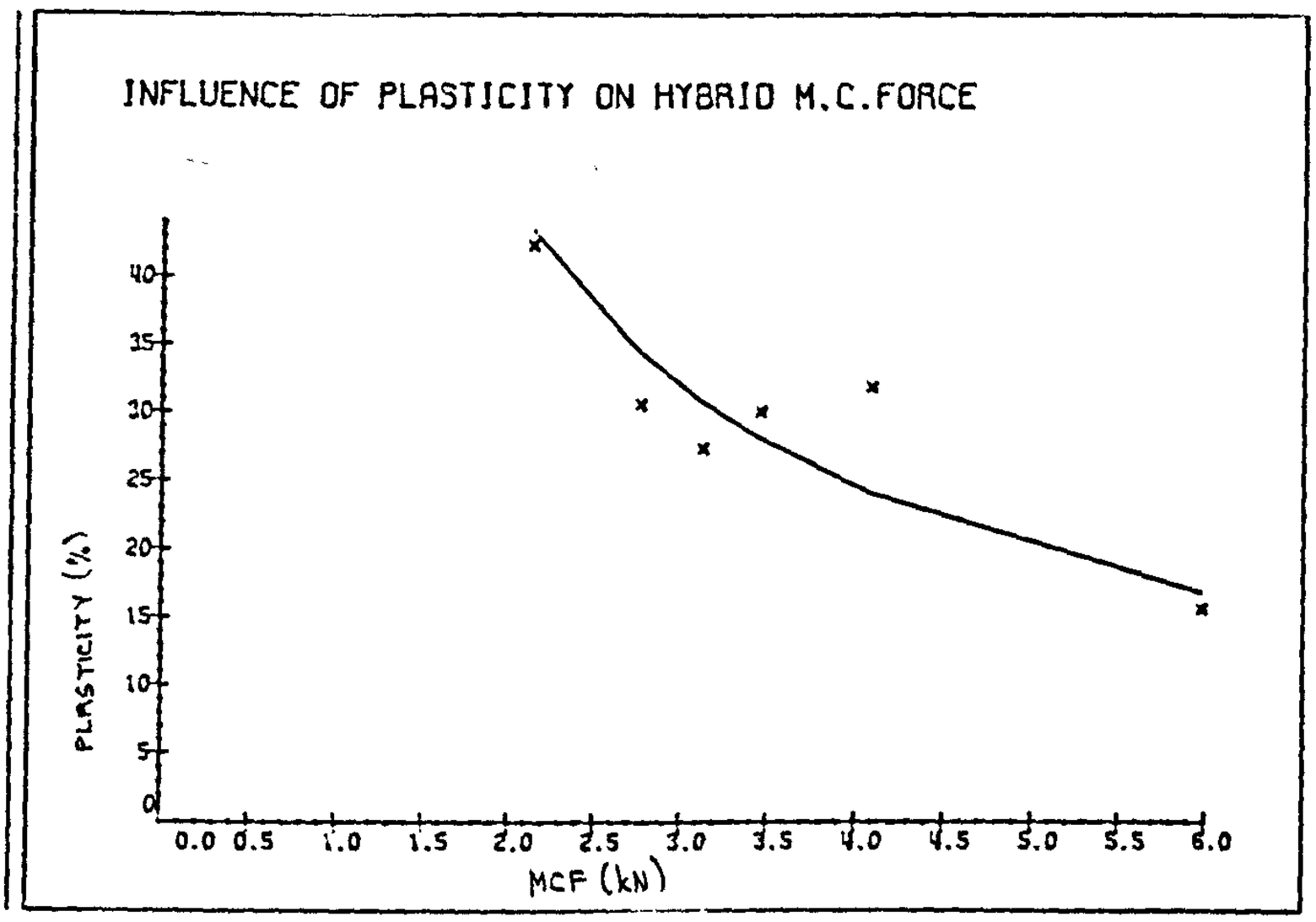
INFLUENCE OF PLASTICITY ON HYBRID M.C.FORCE
PLASTICITY (%)
0
5
10
15
20
25
30
35
40
0.0 0.5 1.0 1.5 2.0 2.5 3.0 3.5 4.0 4.5 5.0 5.5 6.0
MCF (kN)

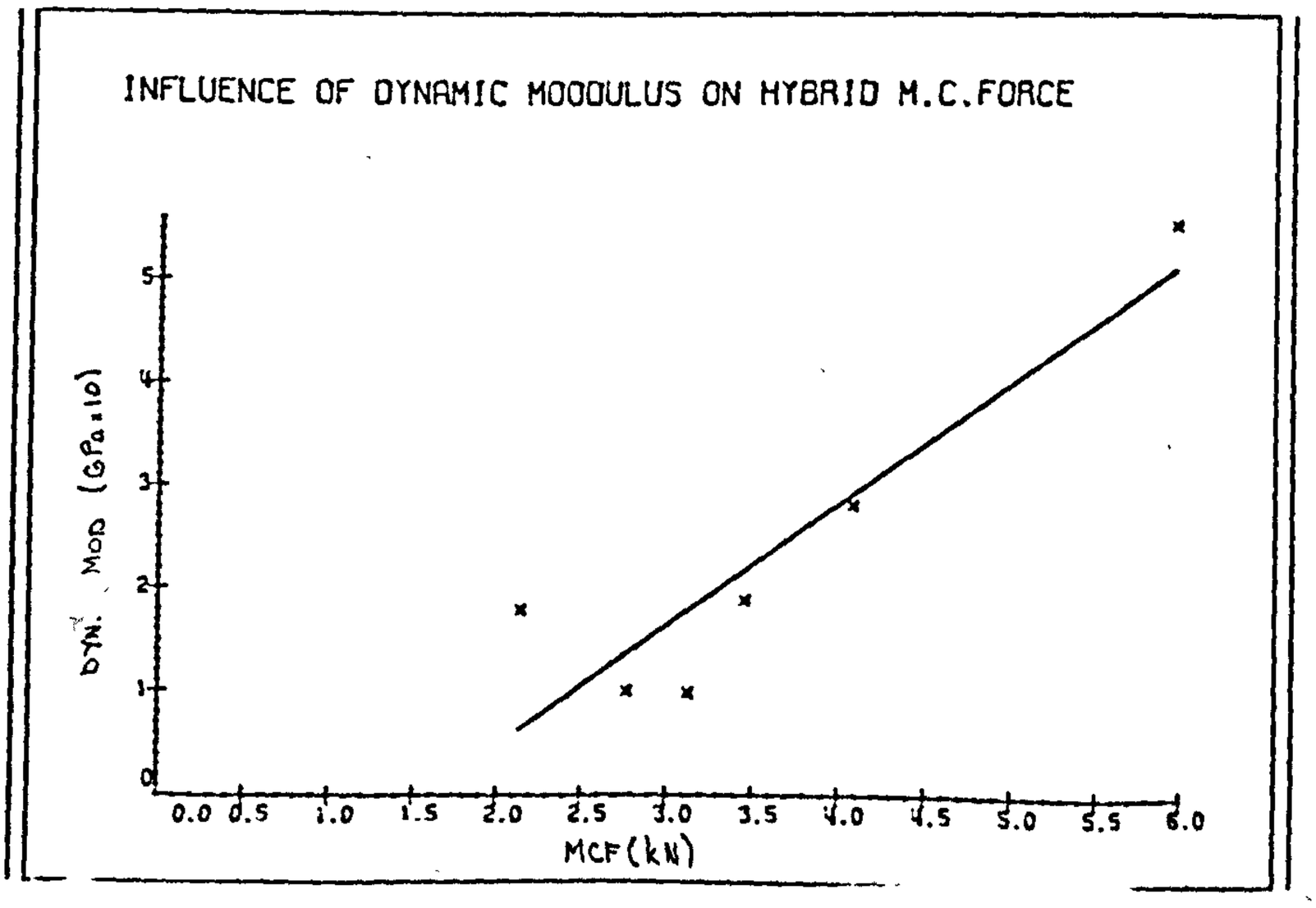
INFLUENCE OF DYNAMIC MOOOULUS ON HYBRID M.C.FORCE
DYN. MOD (GPa.10)
0
1
2
3
4
5
0.0 0.5 1.0 1.5 2.0 2.5 3.0 3.5 4.0 4.5 5.0 5.5 6.0
MCF(kN)

FIG. 9.6

rocks with a closely intergrown fabric are more difficult to break than those in which the mineral grains are seperated by a weak matrix. Dynamic Elastic Modulus, which is related to the microfracturing in rock gave good correlation with the tool forces. Higher the modulus more forces are required for cutting at constant depth of cut. Apparent porosity had shown a trend in which it is easier to cut porous material all other properties being equal.

The individual influences of some rock properties were combined to give overall effect. The highest correlation between tool forces and properties was given by:

$$\frac{\text{Compressive Strength x Bulk Density x NCB Cone Indenter Hardness}}{\text{Tensile Strength x Grain Density x Dynamic Elastic Modulus}}$$

For all tool forces, increasing the value of the above expression caused a significant decrease in the cutting and normal forces, (Figures 9.7,9.8).

But if a percentage reduction in tool forces as a result of high pressure waterjet assistance are considered, no rock property have shown any significant influence. The apparent porosity, dynamic modulus, Scleroscope rebound hardness and combined rock properties have shown a trend. But the occurence of coincidence cannot be ruled out, (Figure 9.9).

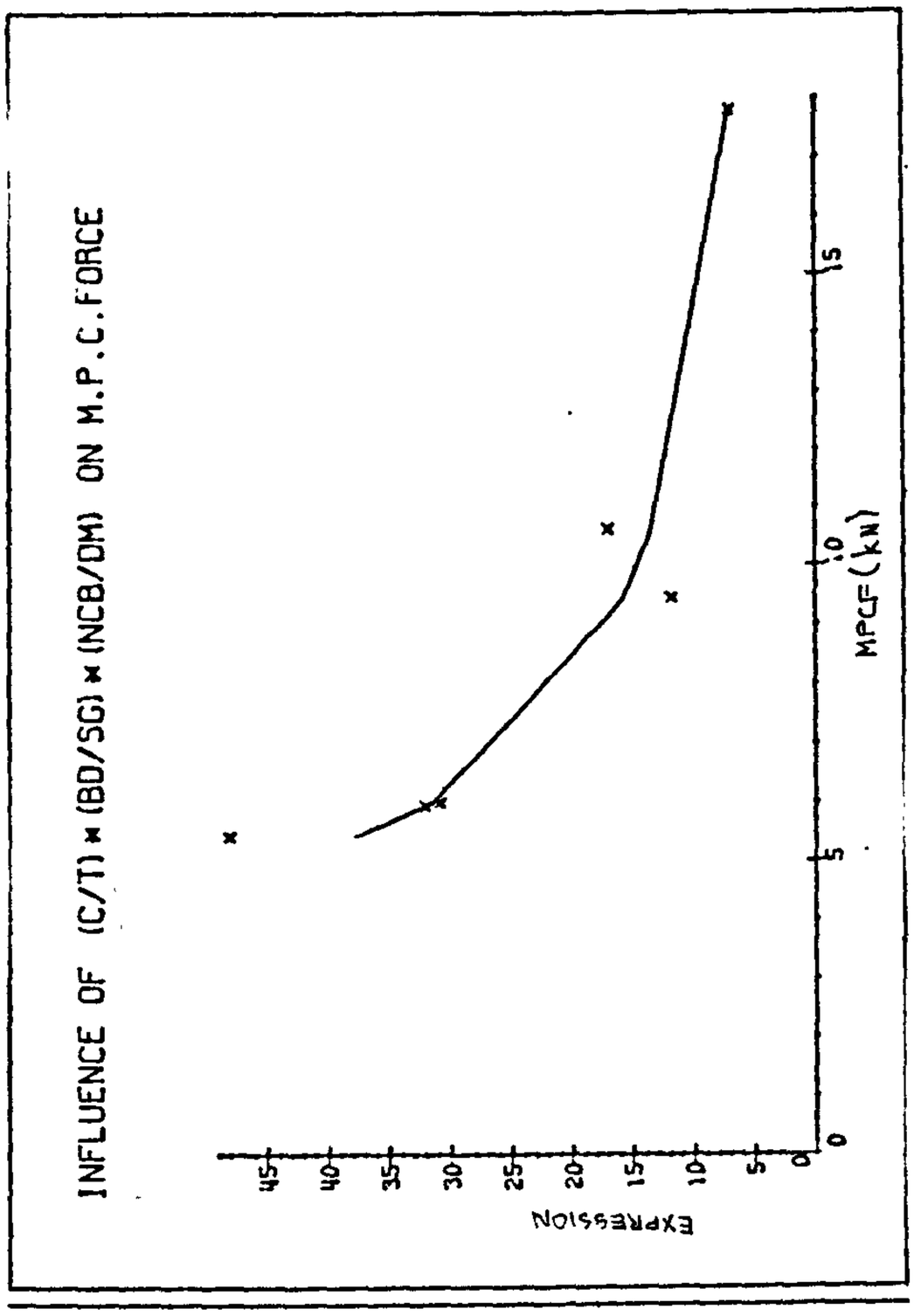
INFLUENCE OF (C/T) * (BD/SG) * (NCB/DM) ON M.P.C.FORCE
EXPRESSION
0
5
10
15
MPCF(kN)

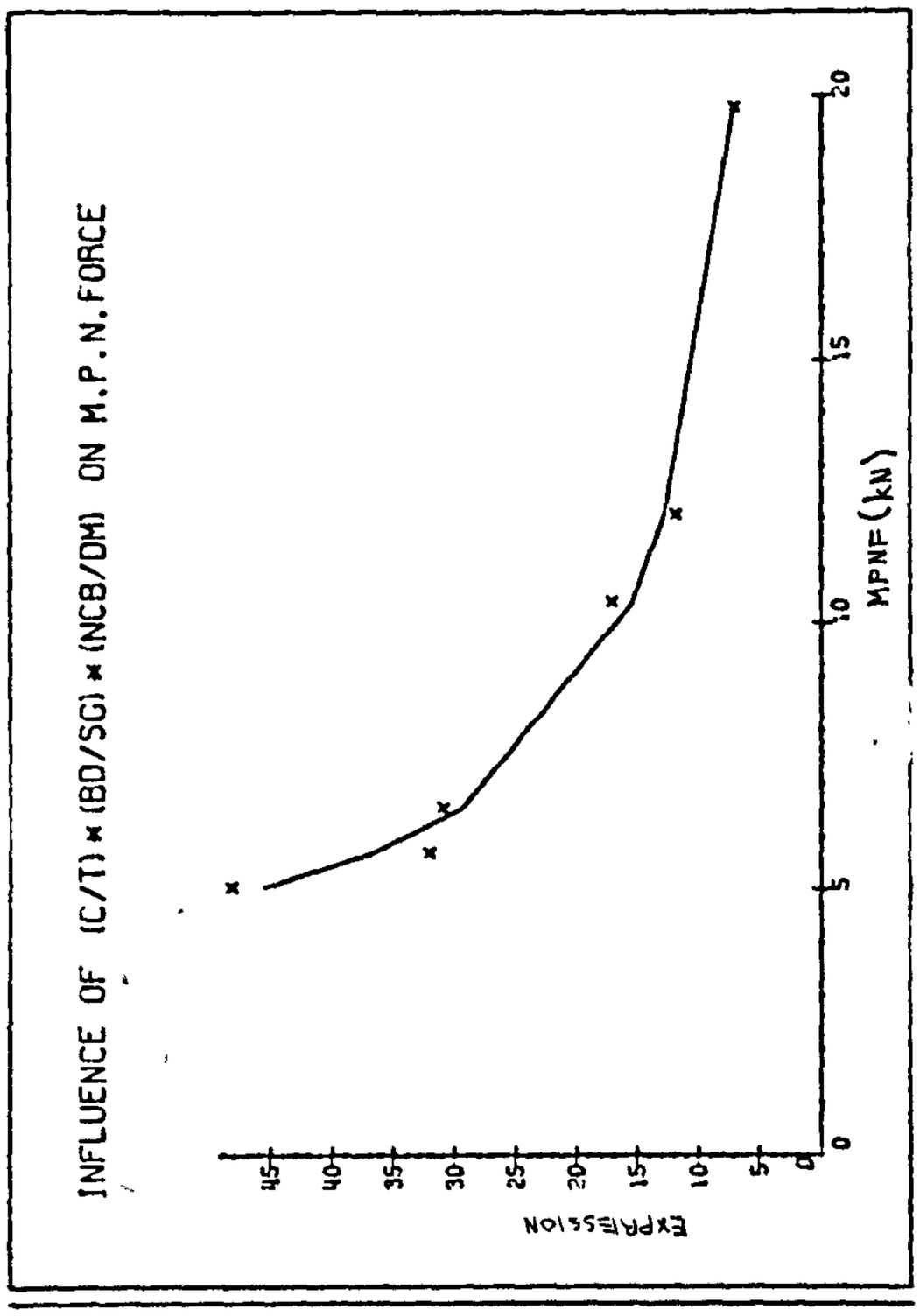
INFLUENCE OF (C/T) * (BD/SG) * (NCB/DM) ON M.P.N.FORCE
EXPRESSION
0
5
10
15
20
MPNF(kN)

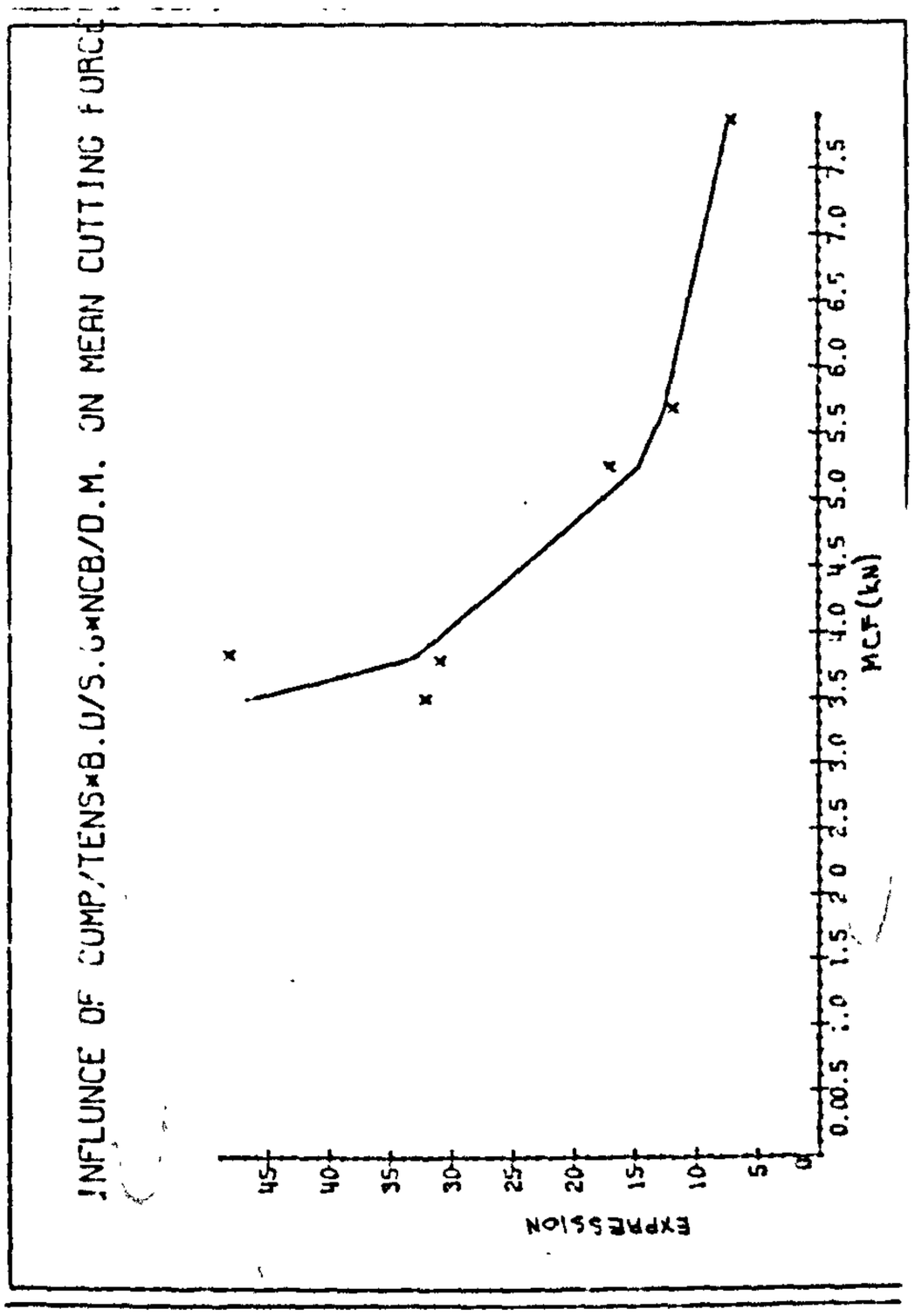
INFLUENCE OF COMP/TENS*B.D/S.G*NCB/D.M. ON MEAN CUTTING FORCE
EXPRESSION
0
5
10
15
20
25
30
35
40
45
0.0 0.5 1.0 1.5 2.0 2.5 3.0 3.5 4.0 4.5 5.0 5.5 6.0 6.5 7.0 7.5
MCF(kN)

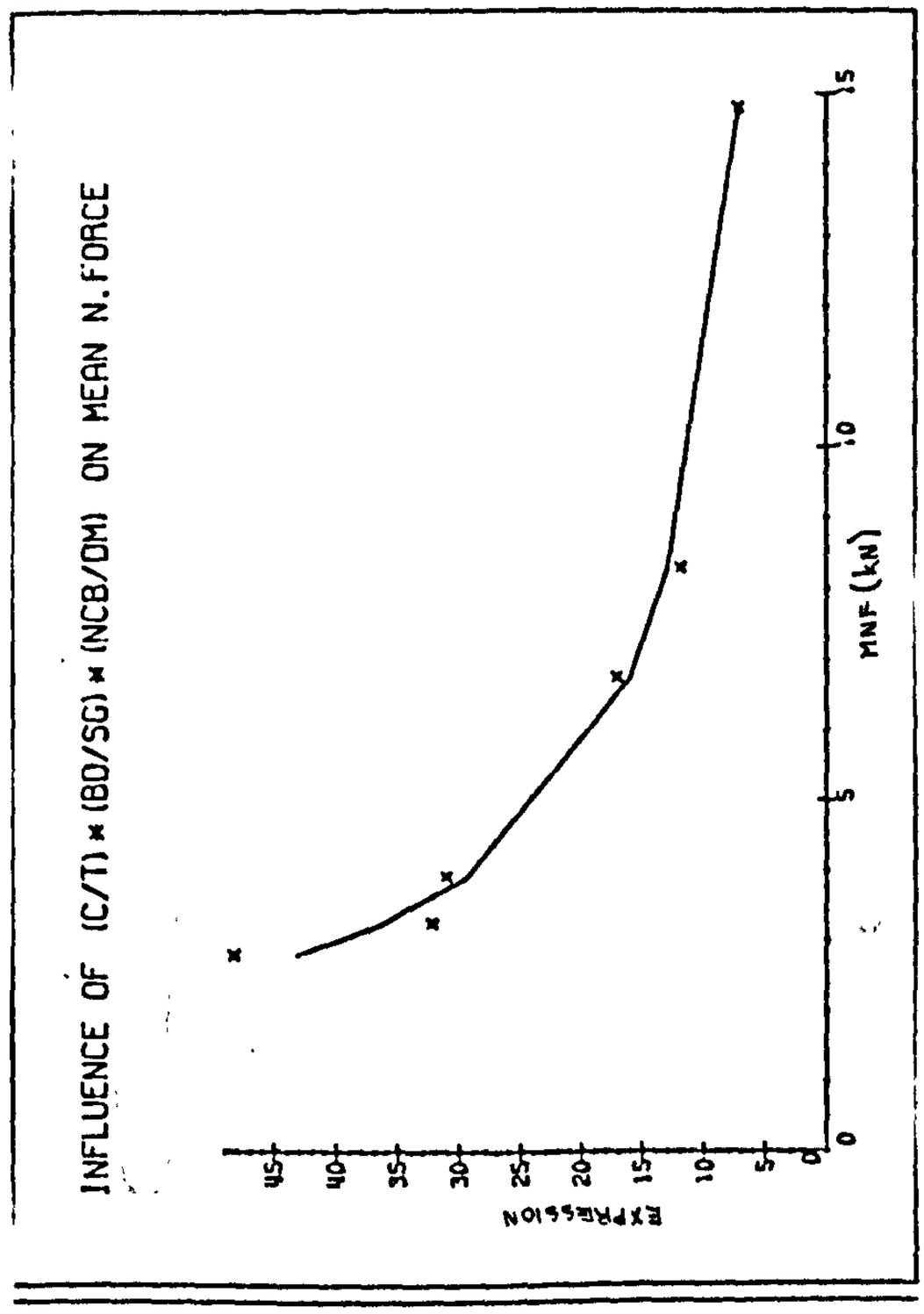
INFLUENCE OF (C/T) * (BD/SG) * (NCB/DM) ON MEAN N.FORCE
EXPRESSION
0
5
10
15
20
25
30
35
40
45
5
10
15
MNF(kN)

FIG. 9.7

FIG.9.8

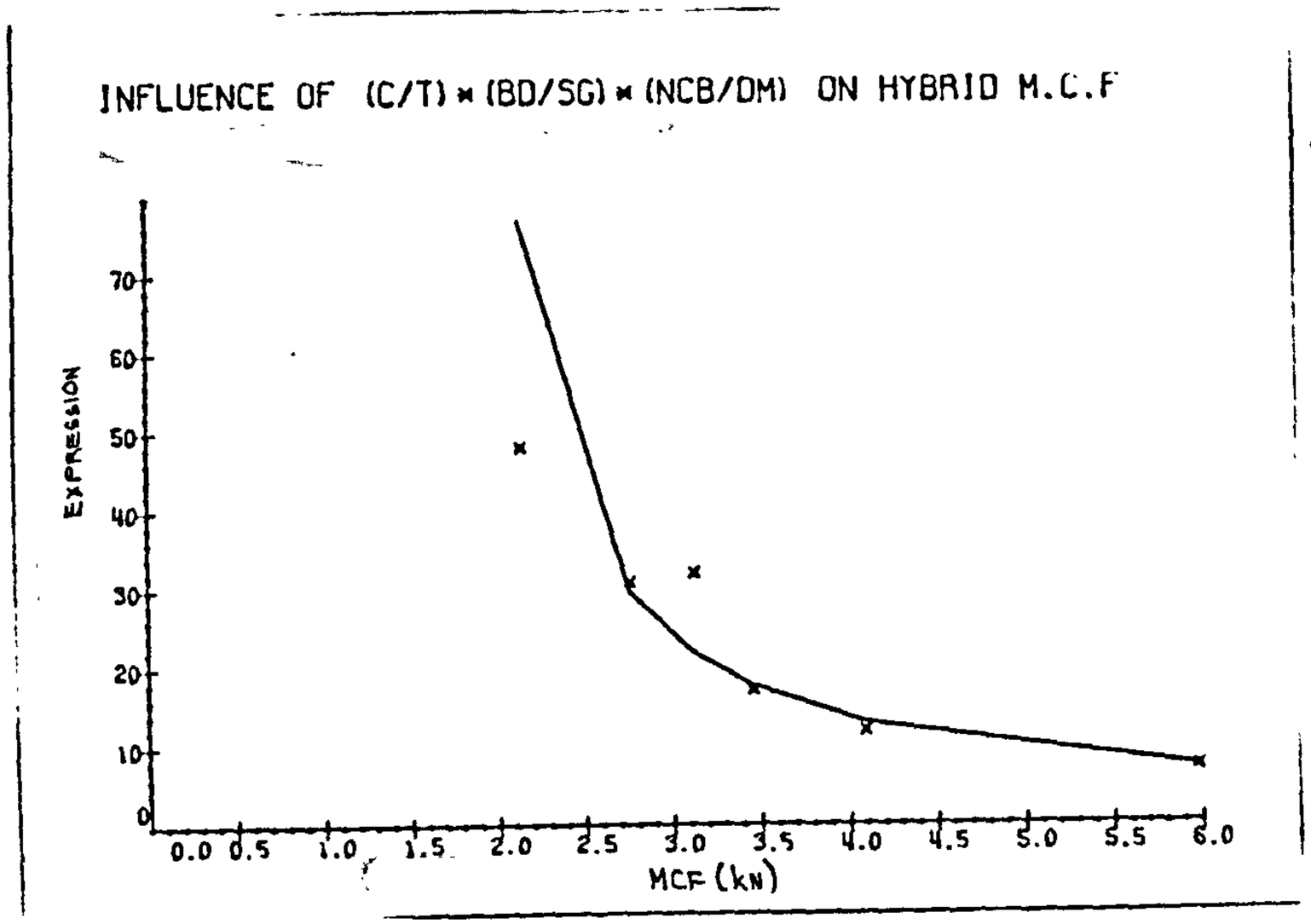
INFLUENCE OF (C/T) * (BD/SG) * (NCB/DM) ON HYBRID M.C.F
EXPRESSION
0
10
20
30
40
50
60
70
0.0 0.5 1.0 1.5 2.0 2.5 3.0 3.5 4.0 4.5 5.0 5.5 6.0
MCF (kN)

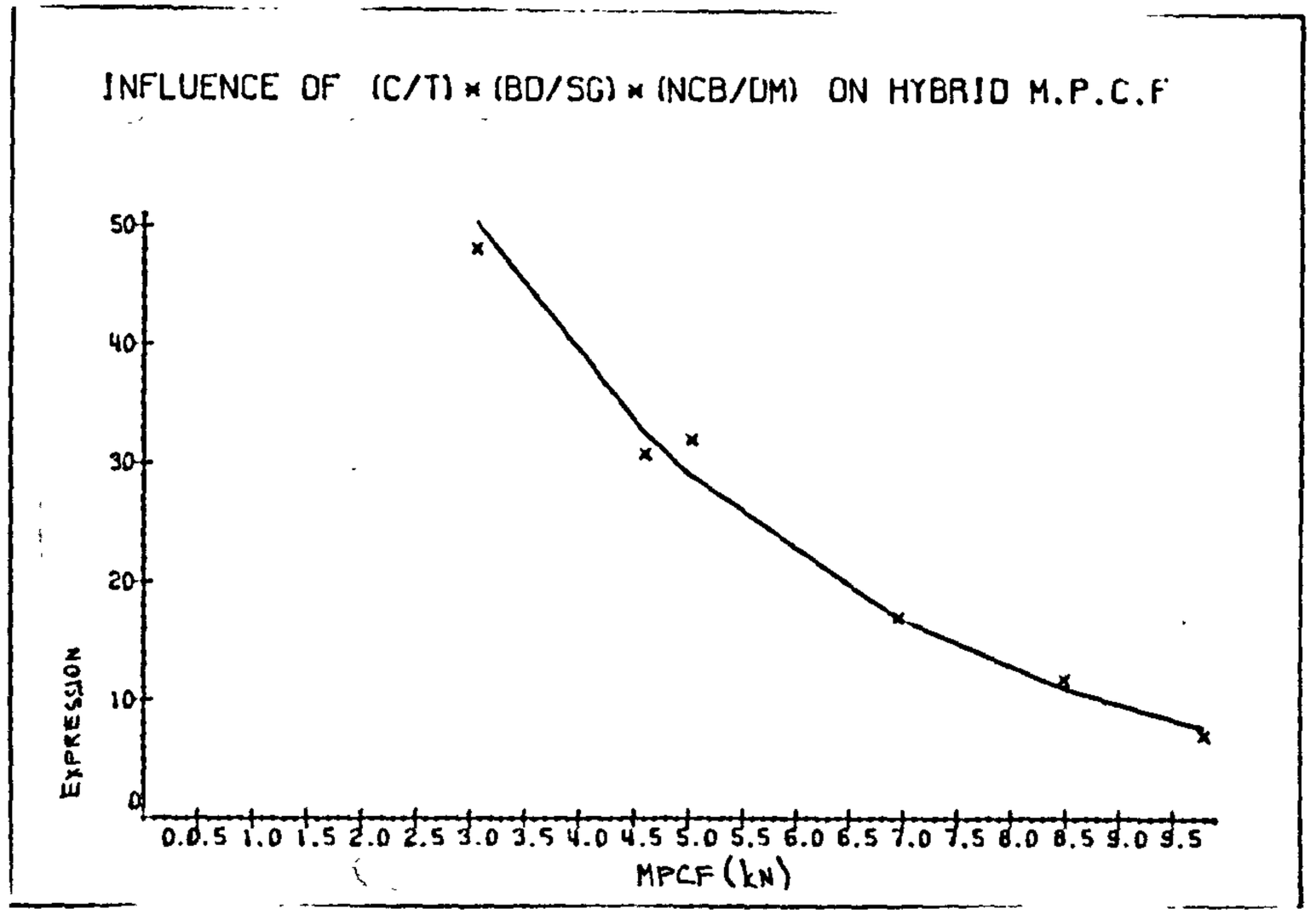
INFLUENCE OF (C/T) * (BD/SG) * (NCB/DM) ON HYBRID M.P.C.F
EXPRESSION
0
10
20
30
40
50
0.0 0.5 1.0 1.5 2.0 2.5 3.0 3.5 4.0 4.5 5.0 5.5 6.0 6.5 7.0 7.5 8.0 8.5 9.0 9.5
MPCF (kN)

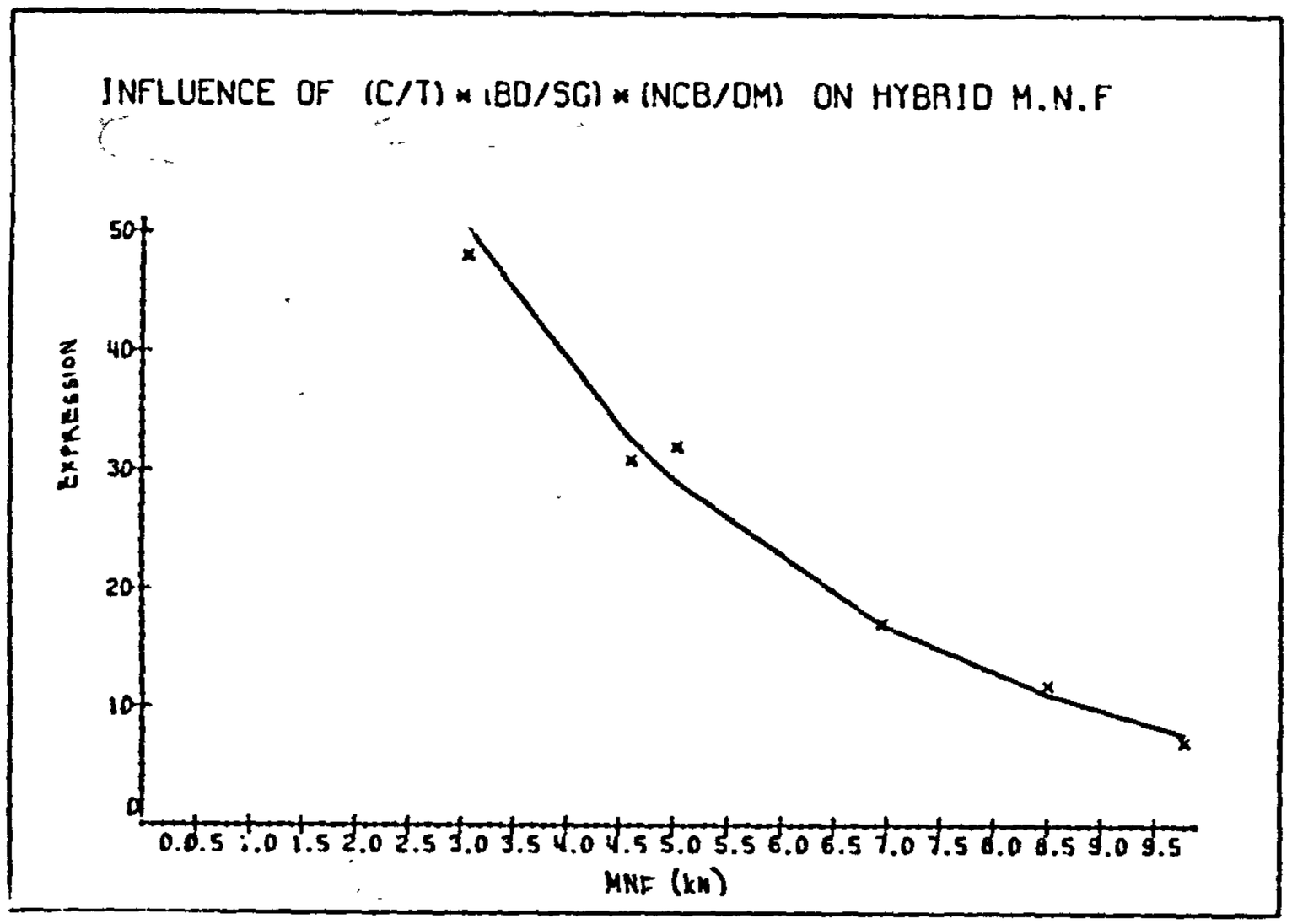
INFLUENCE OF (C/T) * (BD/SG) * (NCB/DM) ON HYBRID M.N.F
EXPRESSION
0
10
20
30
40
50
0.0 0.5 1.0 1.5 2.0 2.5 3.0 3.5 4.0 4.5 5.0 5.5 6.0 6.5 7.0 7.5 8.0 8.5 9.0 9.5
MNF (kN)

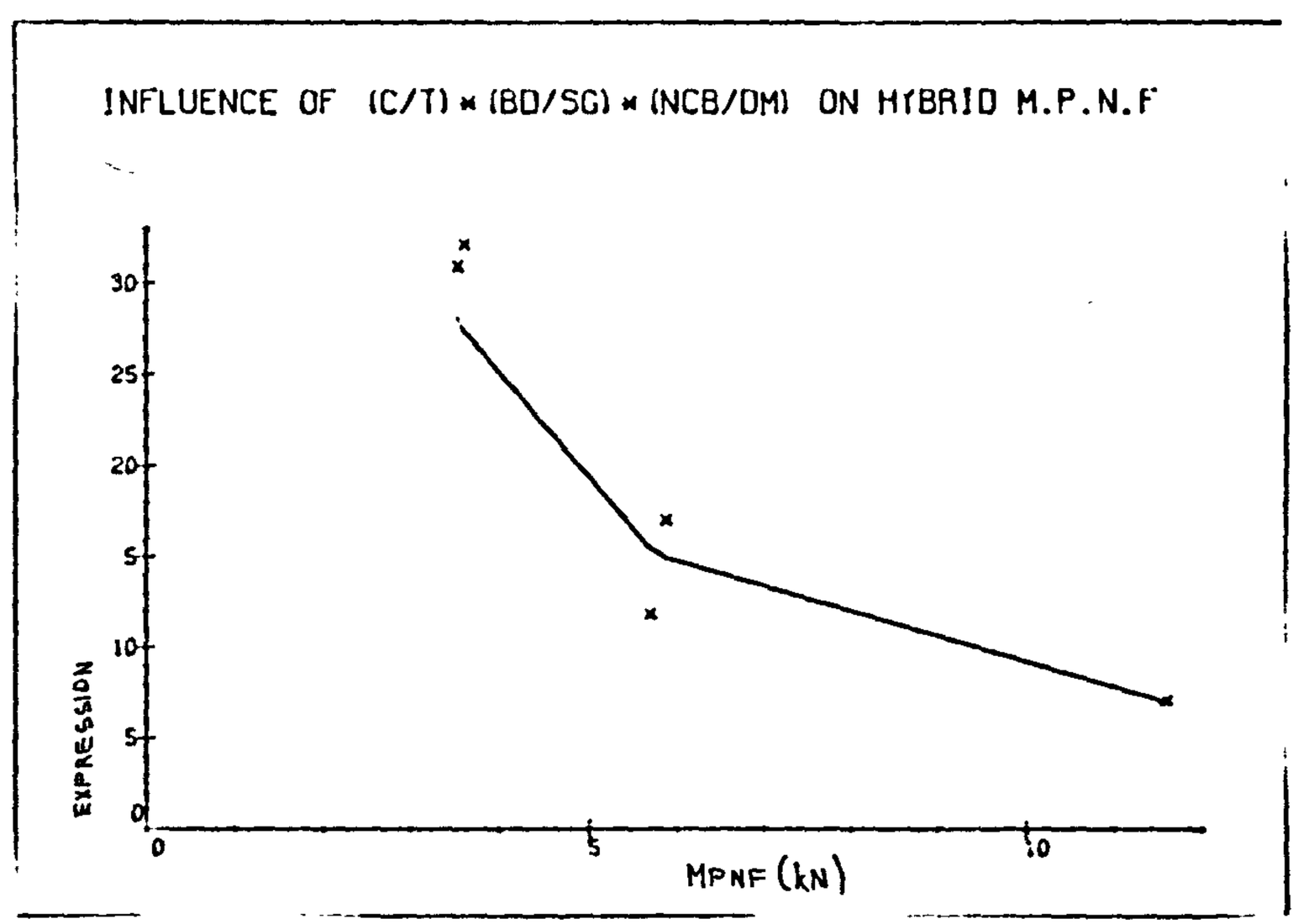
INFLUENCE OF (C/T) * (BD/SG) * (NCB/DM) ON HYBRID M.P.N.F
EXPRESSION
0
5
10
15
20
25
30
0
5
10
MPNF (kN)

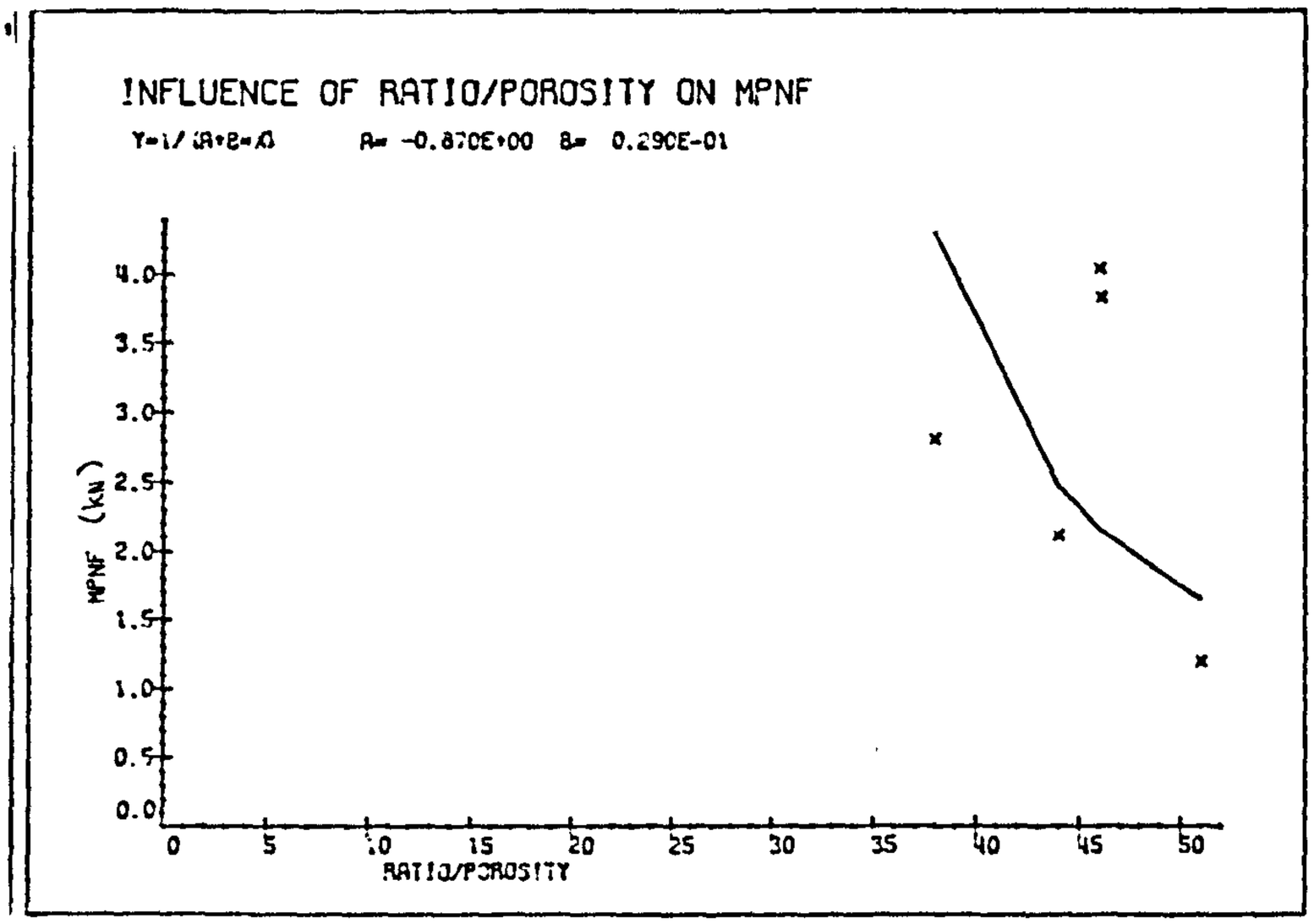
INFLUENCE OF RATIO/POROSITY ON MPNF
Y=1/(A+B*X) A= -0.870E+00 B= 0.290E-01
MPNF (kN)
4.0
3.5
3.0
2.5
2.0
1.5
1.0
0.5
0.0
0
5
10
15
20
25
30
35
40
45
50
RATIO/POROSITY

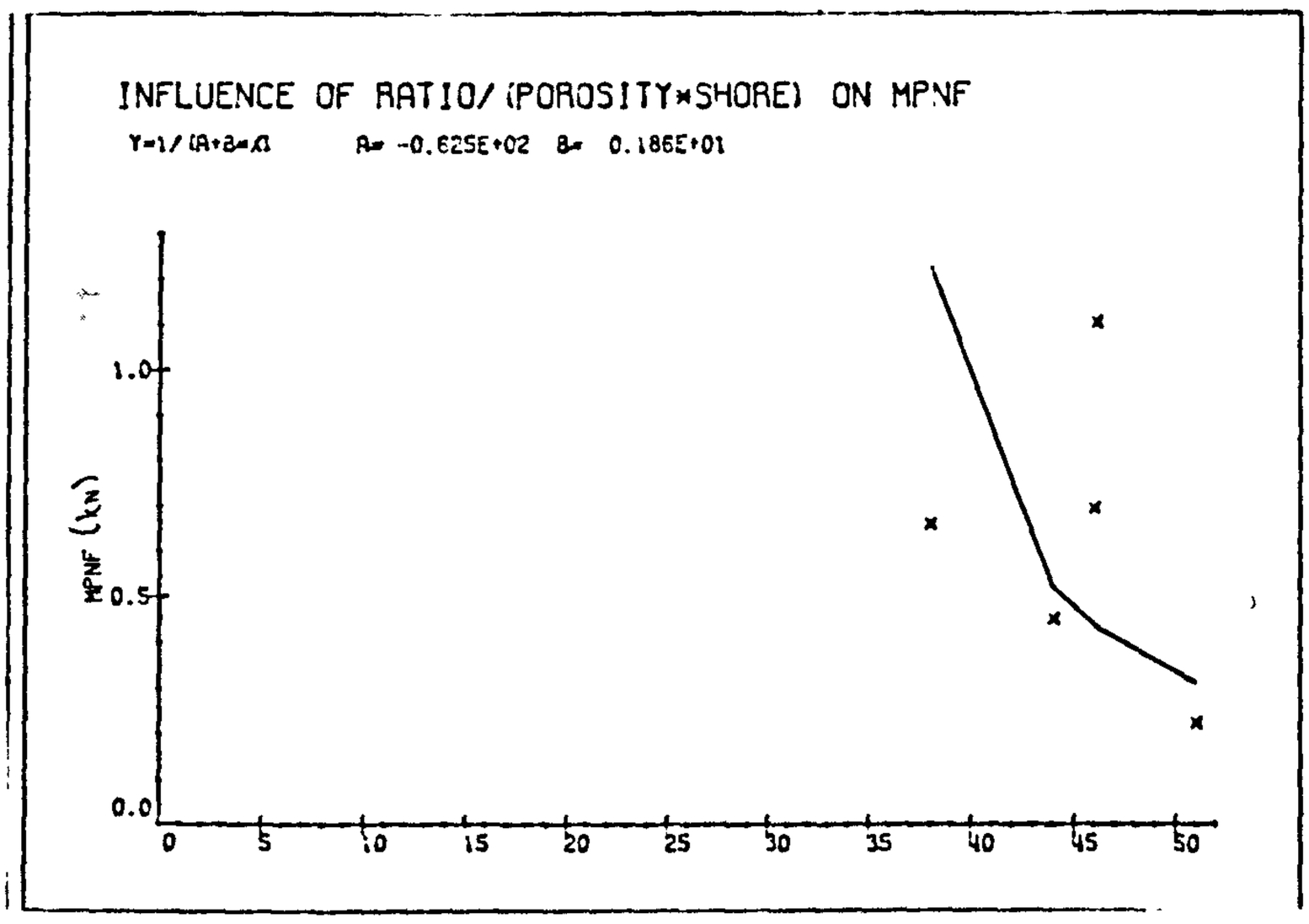
INFLUENCE OF RATIO/(POROSITY*SHORE) ON MPNF
Y=1/(A+B*X) A= -0.625E+02 B= 0.186E+01
MPNF (kN)
1.0
0.5
0.0
0
5
10
15
20
25
30
35
40
45
50

FIG. 9.9

The hybrid cutting experiments were performed with waterjet operating at a constant 55.17 MPa pressure. At this pressure, waterjet, in some rocks, have penetrated to a depth equal to mechanical tool, in some rocks it has penetrated less than mechanical tool and in some cases it did not penetrate at all. Therefore, whereas it is possible to see the influences of rock properties when cutting with a point attack tool, with a hybrid tool, it is difficult to state the influences on percentage reduction in tool forces because of the differences in rock breakage phenomenon.

More experiments should be carried out on different rock types at higher jet pressures to extend the range of influence of rock properties on tool forces. Another factor that should be taken into consideration when transferring data from the laboratory to field conditions is that, rock underground is not only subjected to stresses imposed by the cutting tools be it either mechanical or hybrid, but also those imposed by the overbearing strata. It has been reported in the literature that high reduction in tool forces are achieved underground than the laboratory cutting, because of the increased stresses which cause increased fracturing of the rock and also due to presence of joints, faults, bedding, partings. Furthermore, presence of water in underground workings affect the uniaxial compressive strength and the elastic properties of the rock. In general, the strength decreases with increase in moisture content.

9.3 CONCLUSIONS

The breakage of rock due to the action of point attack tool is very complicated. In this chapter, the influences of rock properties on the tool forces are examined for

1. a point attack tool cutting,

2. water jet assisted point attack tool cutting

3. and percentage reduction caused on the tool forces as a result of waterjet assistance

The uniaxial compressive strength and indirect tensile strength of rocks provide a basis for estimating the rock cuttability by point attack tools. The force required to cause penetration of the mechanical tool is essentially related to the compressive strength of rock and the resultant 'initial failure' is tensile in character as suggested by the Modified Griffiths and Evans' theories, and the 'secondary failure' is in shear. Increasing rock strength causes a corresponding increase in tool forces required for cutting. However, rocks of similar strength but differing structure and composition show significant variations in tool forces.

NCB cone indenter which is used to measure the hardness of the cementing matrix which hold the grains together and Dynamic Elastic

Modulus which is a measure of micro-fracturing in rock show direct relationship with the tool forces. Increase in both properties result in increase in the cutting and normal forces. The Bulk density and apparent porosity also show a trend. Increase in density yields increase in tool forces and increase in porosity causes a decrease in forces.

Similar type of relationships are observed when the rocks are cut with the water jet assisted point attack tool cutting.

The individual rock properties were combined to give the overall effect of properties. The parameter which gave the best predictor of the forces experienced by the pencil point tool was found to be a function of rock toughness, as measured by the ratio of compressive to tensile strengths; porosity, as measured by the ratio of bulk to grain densities, cementing material hardness and degree of micro-fracturing in rock.

$$\text{Forces} = \text{Function}\left(\frac{\text{Comp Strength} \times \text{Bulk Dens.} \times \text{NCB Cone Inden Hard}}{\text{Tensile Stren} \times \text{Grain Dens} \times \text{Dynamic Modulus}}\right)$$

gave a very good correlation with all the tool forces.

If the percentage reduction in tool forces as a result of water jet assistance is considered it was seen that no rock property has displayed any significant correlation.

It must be realized that, experiments were carried out at a constant waterjet pressure, and at this pressure waterjet caused differing penetration depths in relation to the mechanical tool on the rock samples.

More experiments should be carried out on different rocks at higher waterjet pressures to examine the very complex influence of rock properties when cutting with waterjet assisted point attack tool cutting.

10 CONCLUSIONS

Experimental results and conclusions are discussed at the end of each chapter. Summary of these conclusions appears below.

Most of the machine driven roadways in British Coal Mines are excavated by boom type partial face tunnelling machines which increasingly use point attack tools as the cutting elements. The influence of point attack tool variables, e.g .angle of attack, off-set angle, tool tip angle and spacing were examined previously(152,65,66). For the purpose of this research, the effect of point attack tool depth of cut was examined.

10.1 INFLUENCE OF POINT ATTACK TOOL DEPTH OF CUT

The depth of cut of the mechanical tool has a strong influence on the cutting efficiency. All the tool forces increase linearly, volume of rock cut increases following a power law relationship and mechanical specific energy decreases hyperbolically hence, cutting becomes more efficient with the increase in depth of cut. The minimum depth of cut taken by the tool should be greater than 4 mm.\ Below this depth the cutting tool is only a rubbing contact with the rock, causing high abrasive tool wear.

The results have shown that the efficiency of an excavation method can be improved by minimizing the production of fines and increasing the particle size. This can be achieved by taking deeper cuts and increasing

the tool size. However, deeper cuts requires the use of higher tool forces. In some ground -with hard and abrasive cutting conditions- it may not be possible to take deeper cuts because of the limitations of the cutting picks and the machine. High impact loads lead to increase in shattered bits and to high tool consumption. The application of boom type partial face tunnelling machines is restricted therefore by the limitations of cutting picks. It seems that the performances of these machines can be increased considerably by hybridizing cutting tools with high pressure water jets.

10.2 INFLUENCE OF HYDRAULIC VARIABLES

Partial factorial experimental design as proposed by Protodyakonov Jr and Teder was used for the initial water jet assisted cutting experiments. Although satisfactory conclusions were derived from these tests, this method of design was not used for later studies due to interaction taking place between the variables.

10.2.1 Water Jet Pressure

The influence of the water jet pressure may be examined in two stages. Initially, when cutting by jet only, increase in pressure leads to an increase in the energy input available for rock cutting, which causes deeper depths of jet penetration. Hydraulic specific energy decreases

hence, cutting efficiency increases with increase in pressure. When the influence of jet pressure on the operating efficiency of an hybrid cutting system is considered, it is seen that at a constant mechanical tool depth of cut, increasing pressure lead to a decrease in the forces acting on the tool. The magnitude of reduction is dependent on the penetration depth of the water jet. Increasing both the mechanical tool depth of cut and pressure of the water jet have caused reductions in mechanical specific energy, however when both the hydraulic and mechanical specific energies were taken into account, the total specific energy for water jet assisted cutting was much higher than cutting with mechanical tool at the same depth of cut.

The two main conclusions are that the optimum pressure for jet assisted cutting is not necessarily the highest pressure that can be attained. This is dependent on the rock type and on the other hydraulic variables such as the nozzle diameter, cutting speed and nozzle positioning. Also the pressure of the water jet should be such that the jet will not penetrate the rock surface more than the mechanical tool depth of cut. This keeps power requirements to a minimum.

10.2.2 Cutting Speed

The cutting speed has different effects on the mechanical and hydraulic components of the hybrid cutting system.

Mechanical Component: Effect of speed becomes more apparent with increase

in length of cut . As the distance increases, tool wear progresses due to heat build up at tool/rock interface and poor hardness characteristics of tungsten carbide at elevated temperatures. This leads to increase in tool forces and specific energy. It may be assumed that in the absence of wear, cutting speed effects neither the forces acting on the tool nor the specific energy.

Hydraulic Component: The longer the material surface is exposed to a high pressure water jet, the deeper will be its penetration depth, assuming the water jet pressure exceeds the threshold pressure of the rock. At a constant water jet pressure, the penetration depth varies inversely with the cutting speed, however the actual area of cut increases. Hence, the hydraulic specific energy decreases and jet cutting becomes more efficient.

Combined System: Tool forces increase with the increase in cutting speed due to decreasing depths of jet penetration. Curves show tendency to reach a constant value and run parallel to the horizontal at high speeds(indicating that at high speeds, tool forces are independent of speed). Although an increase in cutting speed causes a decrease in hydraulic specific energy, it results in increase in the mechanical specific energy, hence a compromise has to be found for each cutting condition. For most efficient cutting, at a selected speed the jet should not penetrate the rock surface deeper than the mechanical tools.

10.2.3 Nozzle Diameter

At a constant water jet pressure and constant stand-off distance, the jet penetration depth increases directly with increase in nozzle diameter, more so at higher pressures. Because increasing nozzle diameter causes an increase in jet penetration depth, the tool forces are reduced as a result. Three nozzles have performed equally well on Springwell sandstone at a constant Stand-off/Nozzle diameter ratio.

The optimum nozzle diameter is dependent both on the type of mechanical tool it is to be used with and on the location of the nozzle with respect to tool tip. Also on the power available and desired pressure range. Power requirements for water jet cutting increase with the first power of pressure and second power of nozzle radius, hence the nozzle diameter should be selected to minimize the cost to penetrate to a required depth. This necessitates the use of smaller diameter nozzles whenever possible.

10.2.4 Number of Jet Passes

The main principle of water jet cutting is to make deeper cuts while minimizing the energy expended per unit area of cut. One way of achieving this is to increase the number of jets which progressively cut along the same groove.

Penetration of the water jet increases at a decreasing rate with the jet number, displaying hyperbolic relationship. The hydraulic specific energy graph showed that the jet becomes les efficient with increase in number of jets. Because of this loss of efficiency, the maximum number of jets in tandem should not exceed five. Cutting and normal forces decrease exponentially and mechanical specific energy decreases with increasing number of jet passes.

10.2.5 Side-off Distance

The water jet pressure is found to be the controlling factor on the effect of side-off distance on the tool forces and specific energy. Essentially, changing the jet pressure results in different depths of jet penetration and the effect of side-off distance becomes more pronounced at deeper depths.

The optimum spacing, where the cutting speed was at its most efficient was at a side-off/depth of cut(s/d) ratio of 3-3.33 for the two main experimental sandstones. Cutting and normal forces increase at a decreasing rate with increase in s/d ratio and become constant when the jet and mechanical tool are operating in isolation. The groove left behind by a high pressure water jet has no break out, hence the optimum spacing between the jet and mechanical tool is less than the optimum spacing between two mechanical tools(reduced by a factor of 1.45). The effect of jets placed between mechanical tools is to create free surfaces

for mechanical tools to break the rock into. The width of slot has no significance, therefore narrower jets at high pressures may be used at these locations to conserve energy.

10.2.6 Lead-on Distance

The lead-on distance has an important effect on tool forces, yield and mechanical specific energy when the jet is located in front of mechanical cutters.

When the jet penetration depth is less than mechanical tools, all the forces acting on the tool increase hyperbolically at a decreasing rate with increase lead-on distance and cutting becomes less efficient. No significant change takes place in the tool forces, yield or specific energy, when the jet penetrates the rock to a depth equal with or greater than the mechanical tool. A low pressure jet operating at the optimum lead-on distance and a higher pressure jet both effected reductions of similar magnitude in tool forces. Therefore, it appears that it is not necessary for jets to attain high pressures so as to cause penetration depth equal to or greater than that of mechanical tools. At a optimum lead-on distance the lower pressure jet can achieve the same results and this in turn means less hydraulic power will be needed by the hybrid cutting system. In addition, locating water jets as close to the tool tip as possible will provide cooling at source and reduce frictional heating, this in turn would increase the mechanical tool life by reducing the tool

wear caused by high temperatures, eliminate frictional sparks which are an explosion hazard in coal mines.

10.2.7 Stand-off Distance

The effect of stand-off distance is dependent on the energetic properties of the water jet which vary with increasing stand-off distance. In general, the penetration depth decreases when the distance between the nozzle and the rock surface is increased. As a result, hydraulic specific energy increases and jet cutting becomes less efficient. Forces acting on the tool increased linearly with increase in stand-off distance, yield remains approximately constant and mechanical specific energy increased.

The optimum stand-off distance depends on the diameter of the nozzle and on the rock type. This distance should be such that potential damage to nozzles from rock chippings and dirt is minimized and cutting is at its most efficient. Stand-off/nozzle diameter ratio shoull not be more than 90.

10.3 INFLUENCE OF ROCK PROPERTIES

A unique parameter was found to give the best prediction of forces experienced by the cutting tools. It was a function of rock toughness as measured by the ratio of compressive to tensile strengths; porosity as

measured by the ratio of bulk density to grain density, cementing material hardness and degree of microfractures. For both cutting systems an increase in the value of this parameter has resulted in significant reductions in force components.

$$\text{Forces} = \text{Function}\left(\frac{\text{Comp.stx} \times \text{Bulk den.}}{\text{Tensilex} \times \text{Grain den.}} \quad \frac{\text{NCB cone Ind Hardness}}{\text{Dynamic Elastic Modul.}}\right)$$

However, when percentage reduction in tool forces as a consequence of water jet assistance was considered, it was found that no single rock property exhibited any significant correlation.

The action of high pressure water jet impacting the rock surface at the optimum lead-on distance is threefold. These are

1. actually cutting the rock,

2. getting into cracks -caused by mechanical tool impact- and assist in propagation of these cracks,

3. assist in debris clearance.

Performances of Mechanical and Hybrid cutting systems were compared on six rocks. Overall, 33% reduction in cutting forces and 51% reduction in normal forces were attained with water jet assistance. When the total specific energy expended for cutting unit volume of rock is considered, it

is seen that the water jet assisted cutting requires more energy than mechanical cutting system. However, energy costs form only a small percentage of the total excavation cost. The reduction in cutting and normal forces would enable the machine manufacturers to build excavation machines which will be lighter, more versatile, more mobile and which will be applicable to many cutting conditions. When cutting weak and or medium strength rock , the high pressure water jet may be switched off, and when a strong rock is encountered it may be put back into operation.

10.4 RECOMMENDATIONS FOR FUTURE WORK

Due to limitations of the present experimental set-up, it was not possible to generate pressures higher than 55 MPa., although it seems that it is not necessary to use pressures above this if the water jet is leading the mechanical tool. If the jets are placed between the tools jet pressure must be high enough to penetrate the rock surface to a depth similar to the mechanical tool to be most effective.

Maximum speed that the shaping machine cutting head could attain was 220 mm/second. This is slow in comparison to speeds attained by tunnelling machines cutting heads. It will be beneficial to carry out high cutting speed experiments to simulate actual cutting speeds. The penetration depth of high pressure water jet plays the most significant part on the performance of a hybrid cutting system along with mechanical tool depth of cut. At high speeds, jet pressure must increase to cause a

sizeable penetration.

It will prove useful to examine the influence of lead-on distance when other types of mechanical tools, e.g. chisel picks or disks are used and more experiments should be carried out on rocks of differing strength and composition to widen the cutting range of hybrid cutting tools. This will lead to a deeper understanding of the influences of rock properties on the percentage reduction achieved with water jet assistance.

Although minimizing energy favours the use of smaller diameter nozzles, the resulting jets dissipate at shorter distances. Therefore, water soluble additives might be used to improve jet coherence at high stand-off distances. Nikonov type nozzles were used. It might prove beneficial to investigate the influence of nozzle shape on jet cutting. Continuous hybrid cutting experiments should be carried out to yield data with regards to the effectiveness of water jets in terms of providing cooling at source and reduction in tool wear.

REFERENCES and Bibliography

1. Proc. 1 st.International Symposium on Jet Cutting Technology
Coventry, ENGLAND 5-7th April 1972

2. Proc. 2 nd.International Symposium on Jet Cutting Technology
Cambridge, ENGLAND 1974

3. Proc. 3 rd.International Symposium on Jet Cutting Technology
Chicago, U.S.A 1976

4. Proc. 4 th.International Symposium on Jet Cutting Technology
Canterbury, ENGLAND 12-14th April 1978

5. Proc. 5 th.International Symposium on Jet Cutting Technology
Hanover, FGR 2-4th June 1980

6. Proc. 6 th.International Symposium on jet Cutting Technology
Surrey, ENGLAND April 1982
BHRA Fluid Engineering, Cranfield, Bedford, U.K

7. Ahmed El-Saie "Rock slotting by high pressure waterjet for use in tunnelling"
Proc 21st. Rock Mech. Conf., 1980 U.S.A

8. Altinoluk, S. "Ph.D. Thesis"
1981, University of Newcastle upon Tyne

9. Baumann, L.
Heneke, J. "Attempt of technical-economical optimization of high pressure jet assistance for tunnelling machines"
Paper C4, 5th.Int. Symp. on JCT, 1980

10. Baumeister, T. "Marks Standard Handbook for Mechanical Engineers"
7 th.Edition

11. Beckwith, T.G.
Buck, N.L. "Mechanical Measurements"
2 nd.Edition Addison-Wesley, 1973

12. Beutin, E.F.
Erdmann-Jesnitzer F.
Louis, H. "Material behaviour in the case of high speed liquid jet attack"
Paper C1, 2nd.Int.Symp.on JCT, 1974

13. Bieniawski, Z. "Exploration for rock engineering"
Vol.2, Johannesburg, 1976

14. Bilgin, N. "Ph.D. Thesis' June 1977
University of Newcastle upon Tyne

15. Bowden, F.F.
Brunton, J.H
"The deformation of solids by liquid impact at supersonic speeds"
Proc.Roy.Soc. A263, pp.433-450, Oct 1961

16. Bowles, A.G.
"Circuit design to permit high pressure systems"
1972 Design Eng. Conf. Chicago, USA Paper B Session 20, May 8-11 1972

17. Bresee, J.C
Christy, G.A
McLain, W.C
"Research results show interesting potential of hydraulic tunnelling"
Eng. Min. J. pp 75-80, 1970

18. Brook, N.
"The use of irregular specimens for rock strength tests"
Int.J.Rock Mech. Min.Sci.& Geomech. Abstr. Vol. 14, pp.193-202

19. Brownlee, K.H.
"Industrial Experimentation"
HMSO

20. Cerni,R.H.
Foster, L.E.
"Instrumentation for Engineering Measurements"
Wiley, 1962

21. Castleman, "The mechanism of the atomization of liquids"
J.Res.Bureau of Standards, RP281, Vol.6
pp.359-67, 1931

22. Clark, G.B, Haas,C.J "Hypervelocity impact on rock"
Brown, J.W, 11th.Symp. on Rock Mech. pp.645-685
Summers, D.A. June 1969

23. Cochran, W.G. "Experimental Designs"
Cox,G.M. Wiley, Chapman & Hall

24. Cooley, W.C. "Survey of water jet coal mining technology"
Paper D1, 3rd.Int.Symp. on JCT,Chicago 1976

25. Cooley, W.C. "Correlation of data on jet cutting by water jet using dimensionless parameters"
Paper H4,2nd.Int.Symp.on JCT,Cambridge 1974

26. Cooley, W.C. "Correlation of data on erosion&breakage of rock by high pressure water jet"
Proc. 12th.Symp.on Rock Mech. 1970

27. Crossland, B. "Development of equipment for jet cutting"
Paper C1,1st.Int.Symp.on JCT, 1972

28. Crow, S.C. "The effect of porosity on hydraulic rock cutting" Univ. California at L.A. School of Eng&Apld Sci. Report No. UCLA-ENG-7349 July 1973

29. Crow, S.C.
Lade, P.V.
Hurlburt, G.H. "The mechanics of hydraulic rock cutting" Paper B1,2nd.Int.Symp.on JCT,Cambridge 1974

30. Crow, S.C. "A theory of hydraulic rock cutting" Int. J. Rock Mech. Min. Sci. Vol.10 pp. 567-584, 1973

31. Crow, S.C.
Hurlburt, G.H.
Lade, P.V. "Experiments in hydraulic rock cutting" Int. J. Rock Mech. Min. Sci. & Geomech. Abstr. Vol.12, pp.203-212, 1975

32. Crow, S.C. "The effect of porosity on hydraulic rock cutting" Int.J.Rock Mech. Min. Sci & Geomech Abstr. Vol.11, pp.103-105, 1974

33. Dalziel, J.A
Jordan, D.W
Whittaker, D "Force dynamometers for coal and rock cutting research" J.Strain Analysis Vol.3, No.2, 1968

34. Davies, D.A "Some experiments on water jet cutting and consideration of its use as a drilling tool in rocks" Aust.Inst.Min.Met. No.232,pp.73-80, 1969

35. Davies, W.L "Roadheading equipment" Colliery Guardian, March 1980,pp.99-105

36. Dixon, W.J. Massey, F.J "Introduction to Statistical Analysis" 2nd.Edition, 1957 McGraw - Hill

37. Dunne, B Cassen, B "Some phenomena associated with supersonic liquid jets" J.App.Physics Vol.25,pp.569-582, May 1954

38. Erdmann-Jesnitzer, F Louis, H Wiedemeier, J "Material behaviour, material stressing, principle aspects in the application of high speed water jets" Paper E3, 4th.Int.Symp. on Jet Cutting Technology, 1978

39. Erdmann-Jesnitzer, F Louis, H Wiedemeier, J "Rock excavation with high speed waterjets. A view on drilling & cutting results of rock materials in relation to their fracture mechanical behaviour" Paper C3, 5th.Int. Symp. on JCT,1980

40. Erdmann-Jesnitzer, F
Hassan, A.M
Louis, H
"A study of the effect of nozzle configuration on the performance of submerged water jets"
Paper A2, 4th. Int.Symp.on JCT, 1978

41. Evans, I
Pomeroy, C.D
"The strength, fracture and workability of coal"
Pergamon Press, 1966

42. Farmer, I.W
Attewell, P.B
"Rock penetration by high velocity waterjet"
Int.J.Rock Mech.Min.Sci.Vol.2,pp.135-153,1964

43. Farmer, I.W
Attewell, P.B
"Experiments with water as a dynamic pressure medium"
Min.and Quarry Eng. pp.524-530, 1963

44. Faenstra, R
Pols, A.C
Steveninck, J.V
"Rock cutting by jets"
Mining Engineering, no.26 pp.41-47
June 1974

45. Field, J.E
"Stress waves, deformation & fracture caused by liquid impact"
Proc.R.Soc.London A260, pp.86-93,1966

46. Field, J.E
Lesser, M.B
"On the mechanics of high speed liquid jets"
Proc.R.Soc.London A357, pp.143-162,1977

47. Forman, S.E
Secor, G.A
"The mechanics of rock failure due to waterjet impingement"
6th Conf.on Drilling & Rock Mech.Soc.of Pet.Eng.of AIME, Paper No.SPE 4247

48. Frank, N
Lohn, P.D
"Fragmentation of native copper ores with hydraulic jets"
Paper H3,2nd Int.Symp.on JCT, 1974

49. Frank, J.N
"Hydraulic fragmentation research in the USA"
34th Ann.Symp.Duluth, Minnesota
pp.129-142, Jan 1973

50. Franz, N.C
"The influence of stand-off distance on cutting with high velocity fluid jets"
Paper B3,2nd Int.Symp.on JCT,Cambridge 1974

51. Glenn, L.A
"On the dynamics of hypervelocity liquid jet impact on a flat rigid plate"
Report No.13 Institut CERAC, S.A.
Ecublens Switzerland, Aug 1973

52. Grimson, J — "Mechanics and thermodynamics of fluids" McGraw-Hill, 1970

53. Hahs, C.A. — "Design parameters for waterjet tunnelling machines" Rock Mechanics 1972, pp.555-567

54. Harle, M.R — "Ph.D. Thesis" Aug 1977, Univ of Newcastle upon Tyne

55. Harris, H.D; Mellor, M — "Cutting rock with water jets" Int.J.Rock Mech.Min.Sci&Geomech Abstr. Vol.11, pp.343-358, 1974

56. Harris, H.D; Brierley, W.H — "Application of water jet cutting" Paper G1, 1st Int.Symp.on JCT, 1972

57. Harris, H.D; Brierley, W.H — "A rotating waterjet device and data on its use for slotting Berea S.st" Int.J.Rock Mech.Min.Sci&Geomech Abstr. Vol.11, pp.359-366, 1974

58. Hashish, M.; Du Plesis, M.P — "The application of a generalized jet cutting equation" Paper F1, 4th Int.Symp.on JCT, 1978

59. Hoshino, K
Nagono, T
Tsuchishima, H
"Rock cutting & breaking using high speed water jets together with TBM cutters"
Paper B6,1st Int.Symp.on JCT,Cambridge 1972

60. Hoshino, K
Nagono, T
Takagi, K
Narita, Y Sato, M
"The development & the experiment of the water jet drill for tunnel construction"
Paper E4, 3rd Int.Symp.on JCT, 1976

61. Hewitt, K.S
"Ph.D. Thesis"
Dec. 1975, Univ of Newcastle upon Tyne

62. Heymann, F.J
"High speed impact between a liquid drop and a solid surface"
J.Applied Physics 40, 1969

63. Hood, M
"Cutting strong rock with a drag bit assisted by a high pressure waterjets"
J.of the SA Inst. of Min&Metal. Nov.1976

64. Hood, M
"High pressure waterjet assisted drag bit cutting of strong rock"
Research Report No. 72/76, S.Africa

65. Hurt, K.G
Evans, I
"A laboratory study of rock cutting using point attack tools"
MRDE Laboratory Note, Sept., I979

66. Hurt, K.G
Jones, J.P
"The effect of presentation angles on the performance of a point attack rock cutting tool"
MRDE Report No. 86

67. Hustrulid, W
"A technical and economic evaluation of waterjet assisted tunnel boring"
PB-264 625,NSF/RA-760174, 15 July,1976
Utah Univ., Salt Lake City

68. Imanaka, O
Fujino, S
Shihohara, K
Kawate, Y
"Experimental study of machining characteristics by liquid jets of high power density up to 10E8 W/CM 2"
Paper G3,1st Int.Symp.on JCT, 1972

69. Jansson, B
"Underground forecast"
Tunnels and Tunnelling Vol.6,No.1, 1974

70. Jeffreys, H
"On the formation of water waves by wind"
Proc.Roy.Soc.,A107,pp.189-205, 1925

71. Johnson, S.N
Kenny, P
"The performance and wear characteristics of a selection of coal and rock cutting tools"
NCB, MRDE Report No.74/26, July 1974

72. Khomyak, I
"Note on the mechanism of decay of a jet into large drops"
Inzhenerno-Fizicheskii Zhurnal, Vol.10
No.5, pp.681-682, 1966

73. Kinoshita, T
"An investigation of the mechanics of a high speed liquid jet and its practical application"
Paper B4,2nd Int.Symp.on JCT,Cambridge 1974

74. Kondo, M
Fujii, K
Syoji, H
"On the destruction of mortar specimens by submerged water jets"
Paper B5,2nd Int.Symp.on JCT, 1974

75. Kurko, M.C
"High pressure intensifier can supply 1 gpm water at 70000 psi"
Product Eng. 43,11 p.29,Nov 1972

76. Kee, W.R
Kurko, M.C
"Development of jet cutting machine system"
Paper G5,1st Int.Symp.on JCT, 1972

77. Kuzmich, I.A
Ruthberg, M.A
"Investigation into the interaction between high speed water jet and cutter during breakage of a rock mass"
Paper J4,4th Int.Symp.on JCT, 1978

78. Labus, T.J
"High pressure water jet applications in drilling operations"
Proc.6th AIRAPT Int.High.Pres.Conf.
Paper No. C-2-D, July 25-29,1977

79. Lama-Vutukuri
"Mechanical properties of rocks II"
Series on Rock and Soil Mechanics
Trans-Tech Publications, I978

80. Larsen-Basse, J
"Wear of hard metals in rock drilling
A survey of the literature"
J.Powder Metall. 16 No.31,pp.1-32,1973

81. Lawrence, R.J
"Elastic-plastic target deformation due to a high speed pulsed water jet impact
Paper X21,2nd Int.Symp.on JCT, 1974

82. Leach, S.J
Walker, G.L
"The application of high speed liquid jets to cutting"
Phil.Trans.Roy.Soc.London, Vol.260A,
pp.295-308, 1966

83. Lichtarowicz, A
Sakkejha, M.F
"Cutting with cavitating jets"
Paper G6,1st Int.Symp.on JCT, 1972

84. Lohn, P.D
Brent, D.A
"Improved mineral excavation nozzle design study"
Interim report USBM Contract.J0255024

85. Lohn, P.D
Brent, D.A
"Nozzle design for improved water jet cutting"
Paper A3,3rd Int.Symp.on JCT, 1976

86. Lysehevskii, A.S
"Some laws governing the cutting of rock with a liquid jet of ultra-high pressure
Ugol, Ukrainy, 6,9, pp.28-9,Sept 1962

87.
"Materials for metal cutting"

88. Matsumoto, K
Hamada, H
Fukuda, T Shizyo, A
"High pressure jet cutting"
Paper B4,1st Int.Symp.on JCT, 1972

89. Mazurkiewicz, M
Sebastian, Z
Galecki, G
"Analysis of the mechanism of interaction between high pressure water jet and the material being cut"
Paper F3,4th Int.Symp.on JCT, 1978

90. Maurer, W.C "Novel drilling techniques"
Pergamon Press, 1968

91. Maurer, W.C
Heilhecker, J.K
Love, W.W "High pressure drilling"
Paper X80,2nd Int.Symp.on JCT, 1974

92. McCarthy, M.J
Molloy, N.A "Review of the stability of liquid jets and the influence of nozzle design"
The Chem. Eng. J 7,pp.1-20, 1974

93. McClain, W.C
Cristy, G.A "Examination of high pressure water jet for use in rock tunnel excavation"
Oak Ridge National Lab. Tenn,Jan 1970

94. Bresee, J.C
Cristy, G.A
McClain, W.C "Some comparisons of continuous and pulsed jets for excavation"
Paper B9,1st.Int.Symp.on JCT, 1972

95. McNary, O
Blair, J.R
Novak, D.D
Johnson, D.I "Augmentation of a mining machine with a high pressure jet"
Paper D2,3rd.Int.Symp.on JCT, 1976

96. McFeat-Smith, I "PH.D Thesis" University of Newcastle upon Tyne, October 1975.

97. Merchant, M.E "Basic mechanics of the metal cutting process" J.Applied Mechanics, 11, 1945, p.A168

98. Misawa, S
Sakurai, T
Takahashi, A "Some methods of test and survey for estimating the machineability of rocks in excavation by rock tunnelling machines" Q.Rep.Ry.Tech.Res.Inst.13,4 Dec.1972,pp.187-91

99. Moodie, K
Taylor, G "A review of current work on the cutting and fracturing of rocks by high pressur water jets" Proc. Fluid Power Equip. in Mining, Quarrying, tunnelling I.Mech E UK Paper C22/74, 1974

100. Moodie, K
Artingstall, G "Some experiments on the application of high pressure water jets for mineral excavation" Paper E3,1st.Int.Symp.on JCT, 1972

101. Moodie, K "Coal ploughing assisted with a high pressure water jet" Paper D6,3rd.Int.Symp.on JCT, 1976

102. Muirhead, I.R
Glossop, L.G
"Hard rock tunnelling machines"
Trans.Inst.of Min.& Metall.Vol.77
Section A, pp.A1-A48, 1968

103. Murakami, M
Katayama, K
"Discharge coefficients of fire nozzle"
Trans.ASME(J.Basic Eng),pp.706-16,1966

104. Nath, B
"Fundamentals of finite elements for Engineers"
Published by The Athlone Press, 1974

105. Anon
"NCB Cone Indenter"
MRDE Handbook No.5, 1977

106. Nikonov, G.P
"Research into the cutting of coal by small dia. high pres. water jets"
Proc. 12th.Symp.on Rock Mech. held at the UMRM, 1970

107. Nikonov, G.P
Goldin, A
"Coal and rock penetration by fine , continuous high pressure jets"
Paper E2,1st.Int.Symp.on JCT, 1972

108. O'Dogherty, M.J
Whittaker,
"An exanination of the characteristics of a solid plate dynamometer designed for triaxial force measurements"
NCB, MRDE Tecnical Memo No.197, 1965

109. O'Reilly, M.P
Roxborough, F.F
Hignett, H.J
"Programme of laboratory, pilot and full-scale experiments in tunnel boring"
Tunnelling '76, The Inst.Min.& Metal,1976

110. Ostrovski, A.P
"Deep hole drilling with explosives"
Gostoptikhizat, Moscow, 1960

111. Anon
"Easy Data"
"Data preparation"
"Theory and Results" PAFEC 75
User's Manuals Pafec Ltd.,Nottingham

112. Page, C
"Penetration of rocks with high pressure water jets"
Ph.D. Thesis, Univ. of Leeds, 1971

113. Pai, Shih I
"Fluid dynamics of jets"
D.Van Nostrand Co.Inc.New York, 1954

114. Phillips, H.R "Ph.D Thesis"
Univ.of Newcastle upon Tyne, 1975

115. Pols, A.C "Hard rock cutting"
The Oil and Gas J. Part 1,pp.134-144
Jan 31,1977, Part2,pp.71-75,Feb 1977

116. Ponomorev, P.V "Dynamic method of calculating processes occurring when rock ruptures by impact"
Gorgi Zhurnal, Vol.139,pp.52-57, 1964

117. Porkat, J
Zukal, F "Effect of increase of velocity of discharge on disrupting capacity of water jet"
Chech.Heavy Ind.Vol.5,pp.11-16, 1968

118. Powell, J.H
Simpson, S.P "Theoretical study of the mechanical effects of waterjets impinging on a semi-infinite elastic solid"
Int.J.Rock Mech.& Mining Sci.6,
pp.353-364, July 1969

119. Pritchett, J.W
Riney, T.D
"Analysis of dynamic stresses imposed on rocks by water jet impact"
Paper B2,2nd.Int.Symp.on JCT, 1974

120. Pritchard, R.S
"Effects of water jet slotting on roller cutter forces" Proc., 2I st. Symp on Rock Mech.Conf. May 28-30 I980, p. 86-94

121. Protodyakonov, M.M
"Mechanical properties and drillabilty of rocks"
Proc.of the 5th.Symp.Rock Mech, Minnesota
pp.103-108, 1963

122. Rayleigh, Lord
"The theory of sound"
Dover Publications, Vol.2, 1949

123. Rehbinder, G
"Slot cutting in rock with a high speed water jet"
Int.J.Rock Mech.Min.Sci.Vol.14,
pp.229-234, 1977

124. Reichman, J.H
Cheung, J.B
"Water jet cutting of deep-kerfs"
Paper E2,4th.Int.Symp.on JCT, 1978

125. Robbins, R.J "Mechanical tunnelling-Progress and Expectations"
12th.Sir Julius Werner Memorial Lecture
Tunnelling '76, The Inst.Min.& Metal,1976

126. Rockey, K.C
Evans, H.R
Griffiths, D.W
Nethercot, D.A
"The Finite Element Method"
Wiley, 1975

127. Rodford, I.G "Appraisal of the application of high pressure waterjets to the excavation of coal and rock"
MRDE Report No.58, 1975

128. Rowe, M "Measurements and computations of flow in pipe bends"
J.Fluid Mech. 43,4 pp.771-783, 1970

129. Sandstrom, G.E "The History of Tunnelling"
Barrie and Rockliff (Barrie books Ltd)
London, 1963

130. Sauer, R "Introduction to theoretical gas dynamics"
Edwards, 1947

131. Schimazek, J — "Working group of rock borability, cuttability and drillability" From the contribution by Gehring, K Int.Soc.Rock Mech.Newsletter, April 1980

132. Schimazek, J; Knatz, H — "Assessing the effectiveness of cutting and rolling bit drilling tools working on rock" Ertzmetall, 29, pp.113-119, 1976

133. Schweitzer, P.H — "Mechanism of disintegration of liquid jets" J.App.Phys.Vol.8,pp.513-521, Aug 1937

134. Semerchan, A.A; Vereschagin, L.F; Filler, F.M; Kuzin, N.N — "Distribution of momentum in a continuous liquid jet of supersonic velocity" Soviet Physics Tech.1958,pp.1894-1903

135. Sheshtawy, A.A; Mitchell, B.J — "Applicability of high pressure fluid jet to oil well drilling" 18th.Symp.on Rock Mech.1977,pp.4A1-9

136. Shpitbaum, I.M — "Determination of the minimum pressure head of a hydromonitor jet" Skopaemykh, Vol.5, pp.63-69, 1971

137. Vereschagin, L.F
Semerchan, A.A
Sekoyan, S.S
"On the problem of the breakup of high speed jets of water"
Soviet Physics-Tech.,1959, pp.38-42

138. Shavlovsky, D.S
"Hydrodynamics of high pressure fine continuous jets"
Paper A6,1st.Int.Symp.on JCT, 1972

139. Sheshtawy, A.A
Mitchell, B.J
"Applicability of high pressure fluid jet to oil well drilling"
18th.Symp.on Rock Mech., 1977

140. Sims, J.S et al
"Jet delivery optimization"
For US Dept.of Trans.Contract No.7-35381

141. Singh, M.M
Huck, P.J
"Correlation of rock properties to damage effected by water jet"
Proc.12th.Symp.Rock Mech., 1970

142. Summers, D.A
Lehnhoff, T.F
"Water jet drilling in sandstone and granite"
Proc.18th.Symp.on Rock Mech., 1977

143. Summers, D.A
"Water jet cutting related to jet and rock properties"
Rock Mech., 1972, pp.569-588

144. Brook, N
Summers, D.A
"The penetration of rock by high speed water jets"
Int.J.Rock Mech.Min.Sci.Vol.8,pp.249-58,1969

145. Summers, D.A
"Disintegration of rocks by high pressure jets"
Ph.D Thesis Univ.of Leeds, 1968

146. Summers, D.A
Henry, R.L
"Water jet cutting with and without mechanical assistance"
AIME Soc.of Petro.Eng.SPE 3533, Oct.1971

147. Summers, D.A
Barker, C.R
Selberg, B.P
"Can nozzle design be effectively improved for drilling purposes"
The American Soc.of Mech.Eng., 1978

148. Mazurkiewicz, M
Summers, D.A
"The effect of jet traverse velocity on the cutting of coal and jet structure"
Paper D5, 3rd.Symp.on JCT, 1976

149. Summers, D.A
Barker, C.R
Keith, H.D
"Water jet drilling horizontal holes in coal" pp 698-701
Mining Engineering, June 1980

150. Swain, M.V
Lawn, B.R
"Indentation fracture in brittle rocks and glasses"
Int.J.Rock Mech.Min.Sci.& Geomech.Abstr.
Vol.13, pp.311-319, Pergamon, 1976

151. Szlavin, J
"Relationship between some physical properties of rock determined by laboratory tests"
Int.J.Rock Mech.Min.Sci.& Geomech.Abstr.
Vol.10, pp.57-66, 1974

152. Tecen, O
"M.Sc Thesis"
Sept. 1978, Univ. of Newcastle upon Tyne

153. Tecen, O
"High pressure water jet assisted mechanical cutting of Springwell sandstone"
Progress Report,Sept.1980, Newcastle Univ.

154. Tecen, O
"High pressure water jet assisted mechanical cutting"
Symp.for Young Research workers in Geotechnical Engineering held at City Univ. London
30-31 March, 1981

155. Thorne, P.F
Theobold, C.R
"The effect of nozzle geometry on the turbulent structure of waterjets"
Paper A4, 4th.Int.Symp.on JCT, 1978

156. Tregelles, P.G
Woodley, J.N.L
"High speed tunnelling"
Symp.on Mining Methods Harrogate, p.11
Oct.1975

157. Tunneling 76
Proc.Int.Symp.1976
Inst.of Mining and Metallurgy

158. Veenhuizen, S.D
Cheung, J.B
Hill, J.R.M
"Water jet drilling of small diameter holes"
Paper C3, 4th.Int.Symp.on JCT, 1978

159. Vereschagin, L.F
Semerchan, A.A
Mashlennikov, M.V
Sekoian, S.S
"On the problem of friction of a stream of water against the walls of a nozzle at ultrasonic speeds"
Soviet Physics - Tech.1957, pp.1472-73

160. Vijay, M.M
Brierley, W.H
"Drilling of rocks by high pressure liquid jets. A Review"
The American Soc.of Mech.Eng., 1980

161. Walstad, D.M
Noecker, P.W
"Development of high pressure pumps and associated equipment for fluid jet cutting"
Paper C3, 1st.Int.Symp.on JCT, 1972

162. Wang, F.D
Robbins, R
Olsen, J
"Water jet assisted tunnel boring"
Paper E6, 3rd.Int.Symp.on JCT, 1976

163. Wang, F.D
Wolgamott, J
"Application of water jet assisted pick cutter for rock fragmentation"
Paper C1, 4th.Int.Symp.on JCT, 1978

164. Wang, F.D
Robbins, R
Olsen, J
"Temporary underground excavation through the application of hydraulic water jet assisted mechanical tunnel boring"
Prepared for the Excn.Technology Prog. of the Research Applied to National needs prog.National Science Foundation
Feb.1976

165. Wang, F.D
Wolgamott, J
"Study of hydraulic jet kerfing to improve the efficiency of mechanical disc cutting"
Washington, D.C., USA, Dept Of Transport
Jan., I976, 79 p (DOT-OS-40I02)
(Report DOT/tst/-76/54)

166. Wang, F.D
Robbins, R
Olsen, J
"Feasability study of hydraulic jet kerfing to improve the efficiency of disc cutting"
DOT-TST-75-76, Sept.1974

167. Wang, J.K
Lehnhoff, T.F
"Bit penetration into rock - A finite element study"
Int.J.Rock Mech.Min.Sci&Geomech.Abstr., Vol. 13, pp.11-16, Pergamon, 1976

168. Winer, B.J
"Statistical principles in experimental design"
2nd.Edition McGraw-Hill, 1962

169. Yanaida, K
"Flow characteristics of water jets"
Paper A2, 2nd.Int.Symp.on JCT, 1974

170. Zelenin, A.N
Vesselov, G.M
Koniashin, Y.G
"Rock breaking with jet stream under pressure up to 2000 atm"
Problems of Mining, Turpigorev
Vol.112-122, Moscow 1958

171. Zienkiewicz, O.C
Holister, G.S
"Stress analysis"
Wiley, 1965

172. Aufmuth, R.E.
"Engineering criteria for Rock"
Military Engineer, Vol. 66, No.432
July. 1974

Appendix A

MECHANICAL CUTTING RESULTS

A-1 POINT ATTACK MECHANICAL CUTTING

SPRINGWELL SANDSTONE :

DEPTH OF CUT (mm)	MCF (kN)	MPCF (kN)	MNF (kN)	MPNF (kN)	MPSF (kN)	YIELD (g/cm)	S.E (MJ/m^3)
2.0	1.41	1.60	1.15	1.97	0.48	0.30	103.63
4.0	2.22	2.76	1.69	3.07	0.54	0.92	53.57
6.0	3.15	4.15	2.32	4.29	0.67	2.13	32.76
8.0	3.47	4.61	2.41	4.52	0.67	3.40	22.63
10.0	3.84	5.44	2.79	5.05	0.88	5.04	17.01

DARNEY SANDSTONE :

2.0	1.57	2.43	2.05	3.00	---	0.59	58.11
5.0	2.30	3.63	2.82	4.20	---	1.47	34.36
7.0	2.87	4.41	3.48	5.39	---	3.14	17.91
9.0	3.20	5.23	3.46	5.86	---	4.98	14.51
11.0	3.83	6.01	3.90	6.55	---	8.20	10.08

A-2 COMPUTER CURVE FITTING ANALYSIS OF EXPERIMENTAL DATA

VARIABLE NAME	ROCK TYPE	CURVE TYPE	INDEX OF DETERMIN.	VALUE OF'A'	VALUE OF'B'
MCF	S'well	A+(BxD)	0.95	0.985	0.306
	Darney	"	0.98	0.957	0.25
MPCF	S'well	A+(BxD)	0.97	0.853	0.48
	Darney	"	0.96	1.374	0.44
MNF	S'well	A+(BxD)	0.95	0.872	0.20
	Darney	"	0.90	1.623	0.22
MPNF	S'well	A+(BxD)	0.934	1.500	0.38
	Darney	"	0.967	1.934	0.44
S.E	S'well	1/(A+BxD)	0.995	-0.005	0.006
	Darney	"	0.977	-0.02	0.010

Appendix B

INITIAL WATER JET ASSISTED CUTTING RESULTS

S'WELL S.ST WATERJET ASSISTED PROTO DESIGN CUTTING RESULTS

ACTUAL MCF	F'	F'' ($x10^{-4}$)	F'''	PREDICTED MCF
0.73	0.23	8.91	1.11	0.73
1.19	0.23	8.29	1.03	1.09
1.73	0.24	8.12	1.01	1.80
1.69	0.18	6.91	0.86	1.76
2.31	0.21	7.21	0.90	2.57
1.07	0.21	7.74	1.01	1.12
1.51	0.21	7.34	0.95	1.42
2.13	0.23	9.05	1.18	1.81
2.59	0.23	8.38	1.09	2.63
0.77	0.24	8.13	1.06	0.69
1.71	0.24	8.61	1.17	1.46
1.73	0.19	6.35	0.86	2.22
2.11	0.19	7.08	0.96	2.08
0.77	0.24	8.42	1.14	0.71
0.73	0.14	5.49	0.75	0.88
1.81	0.20	6.88	0.98	1.75
2.37	0.21	8.27	1.17	2.12

0.38	0.12	4.30	0.61	0.56
1.11	0.21	7.21	1.03	1.08
1.33	0.19	6.95	0.99	1.49
2.25	0.20	6.79	1.01	2.00
0.66	0.21	7.76	1.15	0.57
1.21	0.23	8.14	1.21	1.11
1.05	0.15	5.70	0.85	1.18
1.63	0.18	6.42	0.95	1.80

Computed Regression Line Formulae for Mean Cutting Force

Actual MCF = 0.97xPredicted MCF + 0.0478

Correlation Coefficient = 0.963

Group Mean Values for Mean Cutting Force

Level Variable	1	2	3	4	5
SIDE-OFF	1.156	1.350	1.486	1.556	1.594
DEPTH CUT	0.626	1.024	1.432	1.810	2.250
PRESSURE	1.534	1.432	1.472	1.372	1.332
LEAD-ON	1.586	1.454	1.490	1.238	1.374

ACTUAL MPCF	F′	F″ ($x10^{-3}$)	F‴	PRDICTED MPCF
0.91	0.36	1.81	1.15	0.87
1.60	0.36	1.61	1.03	1.48
2.31	0.36	1.48	0.94	2.58
2.65	0.31	1.48	0.94	2.52
3.36	0.32	1.39	0.88	3.80
1.51	0.34	1.60	1.06	1.50
2.11	0.32	1.41	0.94	2.02
2.74	0.32	1.61	1.07	2.56
2.95	0.38	1.71	1.14	3.83
0.94	0.38	1.56	1.04	0.86
2.32	0.36	1.62	1.13	2.05
2.65	0.31	1.30	0.90	3.23
3.03	0.29	1.37	0.96	3.01
0.87	0.35	1.51	1.05	0.87
1.07	0.24	1.19	0.83	1.16
2.47	0.29	1.26	0.92	2.54
3.10	0.30	1.48	1.08	3.02
0.42	0.17	0.76	0.56	0.68
1.69	0.38	1.56	1.14	1.48
1.91	0.29	1.40	1.02	2.06
3.45	0.33	1.37	1.05	2.94

0.74	0.30	1.41	1.08	0.68
1.60	0.36	1.54	1.19	1.49
1.46	0.22	1.12	0.86	1.60
2.52	0.30	1.35	1.04	2.56

Computed Regression Line Formulae for Mean Peak Cutting Force

Actual MPCF = 0.98xPredicted MPCF + 0.0471

Correlation Coefficient = 0.963

Group Mean Values for Mean Peak Cutting Force

Level Variable	1	2	3	4	5
SIDE-OFF	1.536	1.942	2.146	2.118	2.338
DEPTH CUT	0.732	1.442	1.974	2.650	3.282
PRESSURE	2.182	2.014	2.072	1.890	1.922
LEAD-ON	2.314	1.976	2.052	1.700	2.038

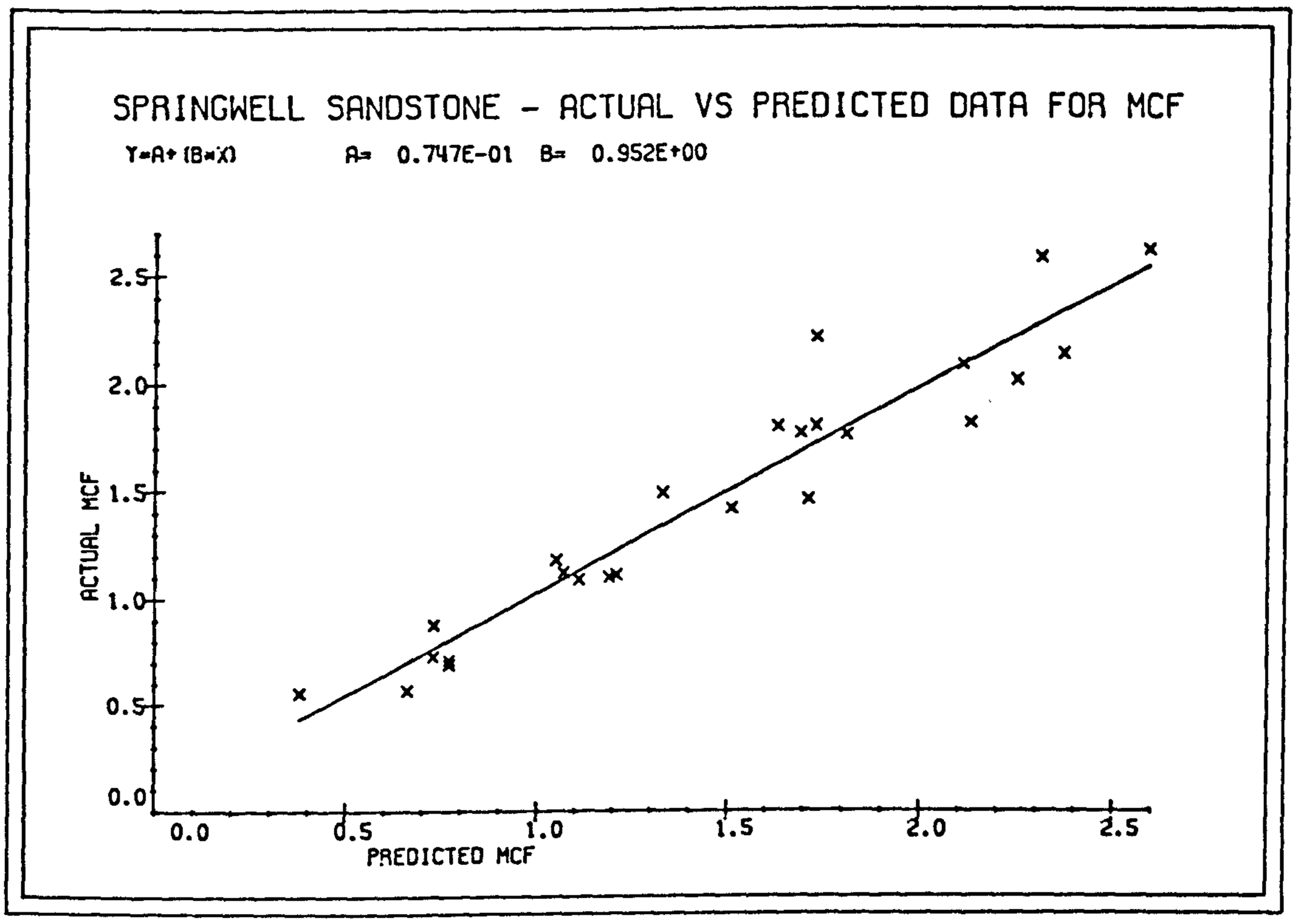
SPRINGWELL SANDSTONE - ACTUAL VS PREDICTED DATA FOR MCF
Y=A+(B*X)
A= 0.747E-01 B= 0.952E+00
ACTUAL MCF
PREDICTED MCF
0.0
0.5
1.0
1.5
2.0
2.5

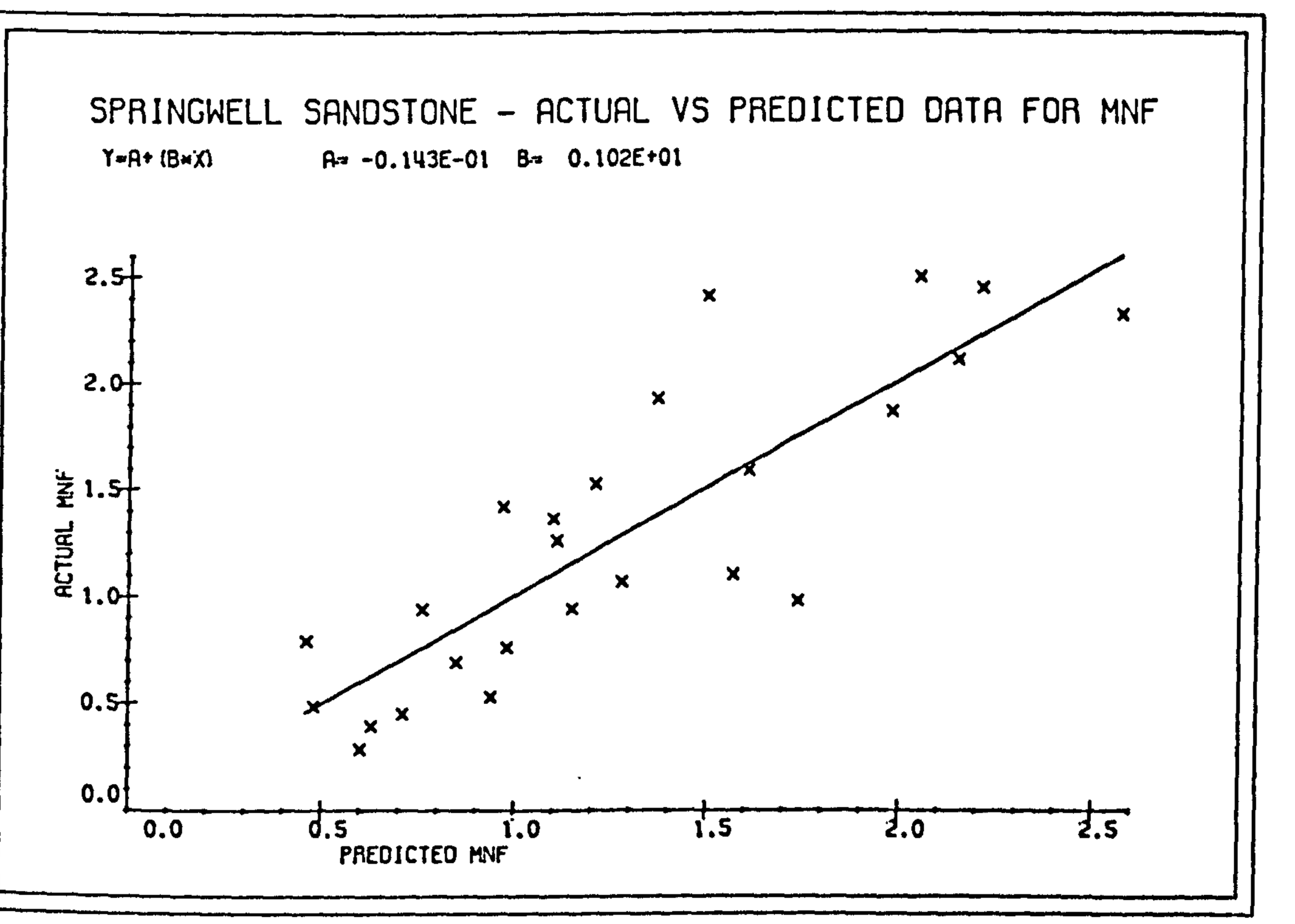
SPRINGWELL SANDSTONE - ACTUAL VS PREDICTED DATA FOR MNF
Y=A+(B*X)
A= -0.143E-01 B= 0.102E+01
ACTUAL MNF
PREDICTED MNF
0.0
0.5
1.0
1.5
2.0
2.5

FIG. 6.17

ACTUAL MNF	F′	F″ ($\times 10^{-3}$)	PREDICTED MNF
0.48	0.12	3.16	0.48
1.36	0.22	3.91	1.10
1.87	0.23	3.00	1.97
2.41	0.24	5.07	1.50
2.33	0.19	2.87	2.57
0.69	0.11	2.41	0.85
1.59	0.20	2.93	1.61
1.26	0.13	3.37	1.11
2.50	0.21	3.62	2.05
0.53	0.13	1.68	0.94
1.07	0.13	2.32	1.28
2.12	0.21	2.73	2.15
1.10	0.09	1.93	0.76
0.39	0.06	1.73	0.63
0.98	0.10	1.45	1.74
0.94	0.08	2.10	1.15
0.28	0.07	1.20	0.60
1.53	0.25	3.26	1.21
0.76	0.09	2.00	0.98
2.45	0.20	2.63	2.21
0.79	0.19	4.10	0.46

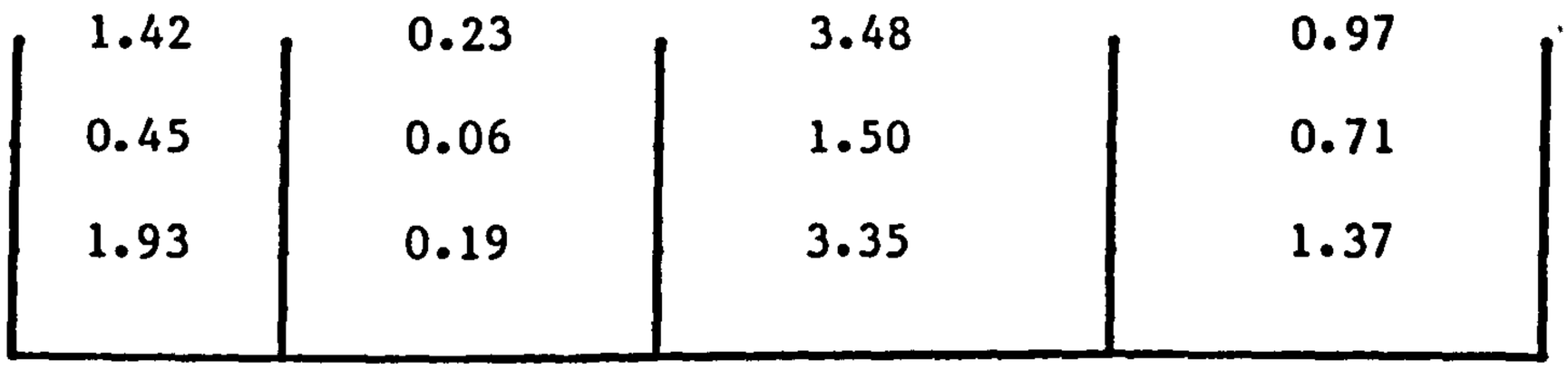

Computed Regression Line Formulae for Mean Normal Force

Actual MNF =1.00xPredicted MNF + 0.0078

Correlation Coefficient = 0.83

Group Mean Values for Mean Normal Force

Level Variable	1	2	3	4	5
SIDE-OFF	0.578	1.168	1.418	1.492	1.816
DEPTH CUT	0.598	1.058	1.140	1.828	1.848
PRESSURE	1.714	1.204	1.230	0.906	1.418
LEAD-ON	1.540	1.272	1.354	0.800	1.506

ACTUAL MPNF	F'	F'' ($\times 10^{-3}$)	PREDICTED MPNF
1.01	0.30	6.80	0.97
2.80	0.52	8.15	2.26
3.75	0.51	6.06	4.00
4.77	0.51	9.47	3.30
5.03	0.44	6.00	5.50
1.64	0.30	5.66	1.78
3.34	0.45	6.13	3.36
2.55	0.27	6.23	2.52
5.56	0.49	7.67	4.46
1.06	0.31	3.72	1.76
2.37	0.32	5.04	2.72
4.40	0.47	5.60	4.54
2.64	0.23	4.32	3.52
1.64	0.48	6.53	1.45
1.02	0.19	4.33	1.36
2.22	0.24	3.21	3.72
2.13	0.19	4.29	2.67
0.55	0.16	2.54	1.17
3.17	0.59	7.01	2.43
1.83	0.25	4.62	2.13
5.33	0.47	5.59	4.76

1.41	0.41	7.72	0.91
2.67	0.49	6.71	1.99
1.20	0.16	3.72	1.61
4.12	0.44	6.89	2.98

Computed Regression Line Formulae for Mean Peak Normal Force

Actual MPNF = 1.02xPredicted MPNF - 0.024

Correlation Coefficient = 0.863

Group Mean Values for Mean Peak Normal Force

Level Variable	1	2	3	4	5
SIDE-OFF	1.306	2.480	3.058	3.050	3.784
DEPTH CUT	1.112	2.210	2.466	3.794	4.096
PRESSURE	3.520	2.594	2.616	1.994	2.954
LEAD-ON	3.274	2.628	2.818	1.790	3.168

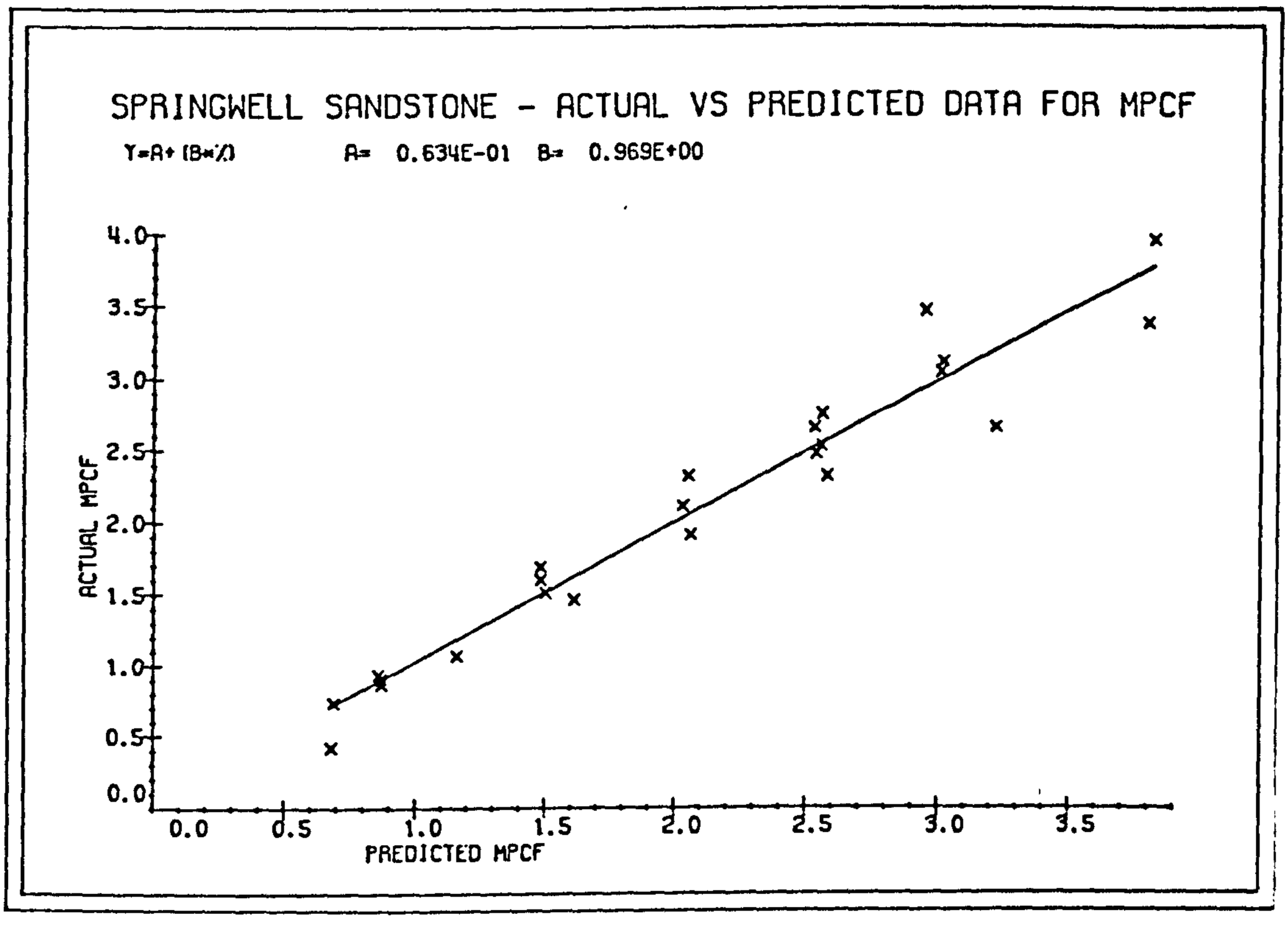
SPRINGWELL SANDSTONE - ACTUAL VS PREDICTED DATA FOR MPCF
Y=A+(B*X)
A= 0.634E-01 B= 0.969E+00
ACTUAL MPCF
PREDICTED MPCF
0.0
0.5
1.0
1.5
2.0
2.5
3.0
3.5
4.0

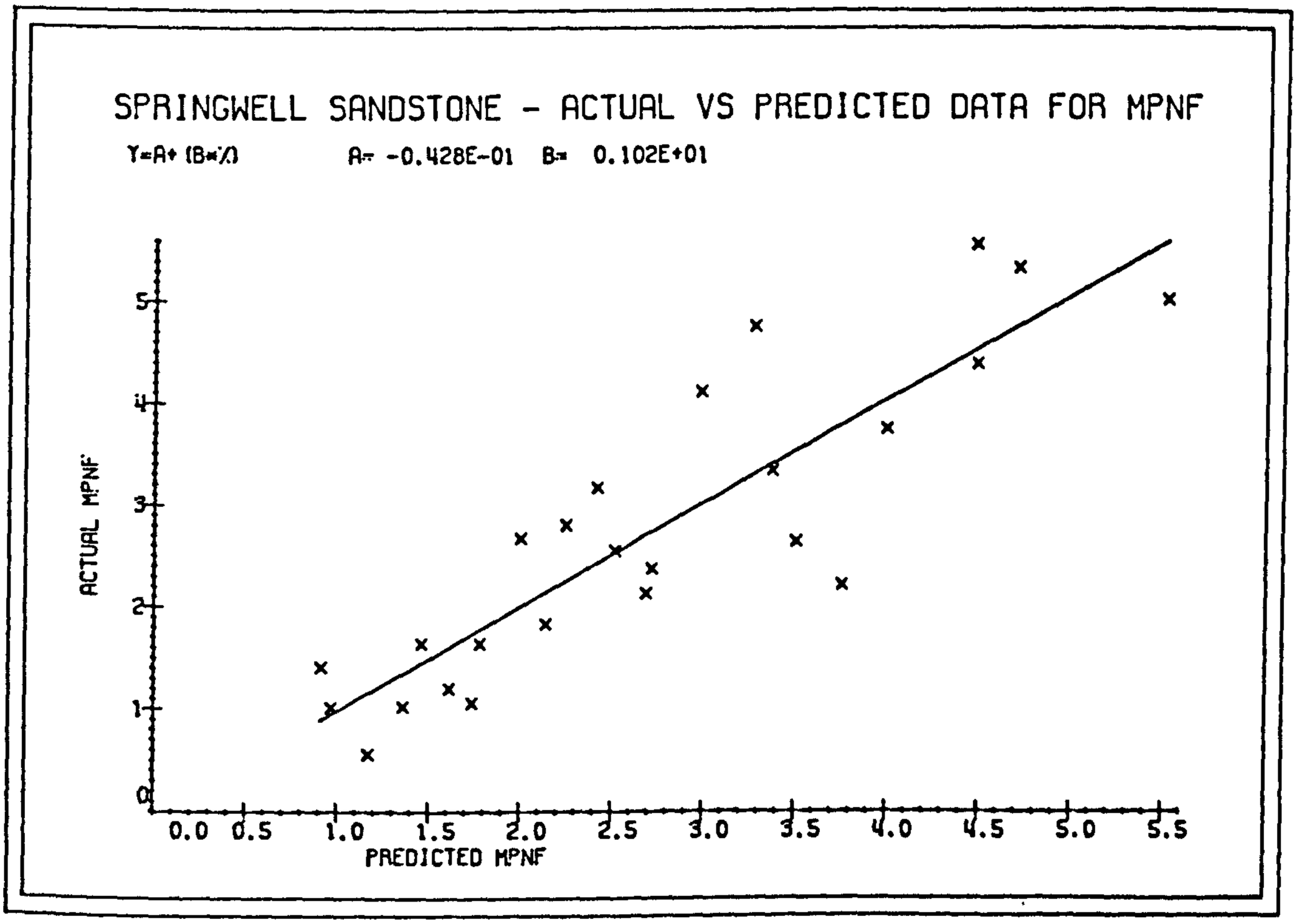
SPRINGWELL SANDSTONE - ACTUAL VS PREDICTED DATA FOR MPNF
Y=A+(B*X)
A= -0.428E-01 B= 0.102E+01
ACTUAL MPNF
PREDICTED MPNF
0
1
2
3
4
5
0.0
0.5
1.0
1.5
2.0
2.5
3.0
3.5
4.0
4.5
5.0
5.5

FIG. 6.18

ACTUAL MPSF	F′	F″	F″′	PREDICTED MPSF
0.26	0.08	1.33	1.21	0.25
0.72	0.13	1.30	1.18	0.57
1.24	0.17	1.13	1.03	1.29
1.36	0.15	1.80	1.64	0.71
1.60	0.14	1.12	1.01	1.58
0.23	0.04	0.53	0.51	0.49
1.04	0.14	1.12	1.07	0.84
0.67	0.07	1.23	1.17	0.57
1.47	0.13	1.25	1.19	1.41
0.29	0.09	0.58	0.55	0.49
0.45	0.06	0.59	0.59	0.76
1.40	0.15	1.01	1.01	1.58
0.33	0.03	0.36	0.36	0.85
0.52	0.15	1.22	1.23	0.45
0.18	0.03	0.58	0.58	0.27
0.48	0.05	0.41	0.43	1.04
0.58	0.05	0.88	0.93	0.67
0.21	0.06	0.60	0.64	0.28
0.87	0.16	1.09	1.16	0.76
0.54	0.07	0.91	0.96	0.64
1.73	0.15	1.03	1.15	1.30

0.45	0.13	1.66	1.85	0.24
0.86	0.16	1.27	1.42	0.69
0.24	0.03	0.56	0.63	0.36
1.29	0.14	1.34	1.49	0.93

Computed Regression Line Formulae for Mean Peak Sideways Force

Actual MPSF = 1.04xPredicted MPSF - 0.025

Correlation Coefficient = 0.84

Group Mean Values for Mean Peak Sideways Force

Level Variable	1	2	3	4	5
SIDE-OFF	0.318	0.614	0.826	0.922	1.184
DEPTH CUT	0.344	0.568	0.702	1.102	1.148
PRESSURE	1.052	0.686	0.658	0.542	0.926
LEAD-ON	0.966	0.778	0.786	0.380	0.954

ACTUAL YIELD	Q'	Q" ($x10^{-2}$)	PREDICTED YIELD
0.24	0.15	2.37	0.30
0.76	2.73	2.78	0.81
1.42	2.97	3.00	1.34
2.42	3.19	3.30	2.16
3.56	3.18	3.22	3.25
0.87	3.13	3.23	0.85
1.57	3.28	3.32	1.44
2.01	2.65	4.14	1.54
3.43	3.07	3.12	3.49
0.45	2.84	2.87	0.50
1.57	3.28	3.34	1.53
2.42	3.19	3.22	2.56
3.22	2.88	2.98	3.68
0.40	2.53	2.56	0.53
0.69	2.48	3.87	0.61
2.69	3.55	3.59	2.71
2.83	2.53	3.95	2.60
0.45	2.84	2.89	0.56
1.01	3.63	3.66	1.00
1.76	3.68	3.80	1.60
4.12	3.68	3.72	4.27

0.55	3.47	3.59	0.59
1.03	3.70	3.75	1.06
1.55	3.24	5.06	1.13
2.67	3.52	3.58	2.87

Computed Regression Line Formulae for YIELD

Actual Yield = 0.98xPredicted Yield + 0.0623

Correlation Coefficient = 0.99

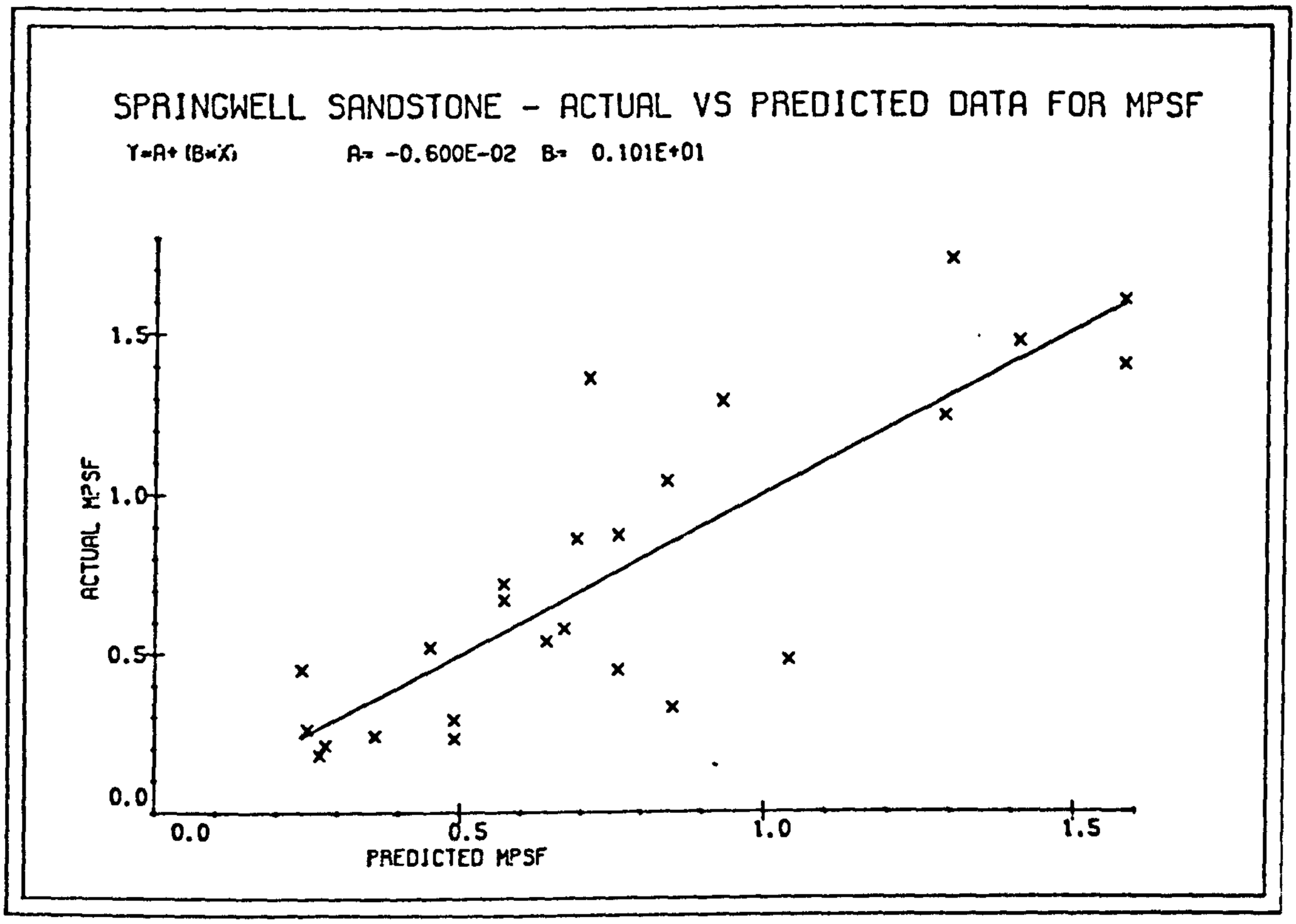
SPRINGWELL SANDSTONE - ACTUAL VS PREDICTED DATA FOR MPSF
Y=A+(B*X)
A= -0.600E-02 B= 0.101E+01
ACTUAL MPSF
PREDICTED MPSF
0.0
0.5
1.0
1.5

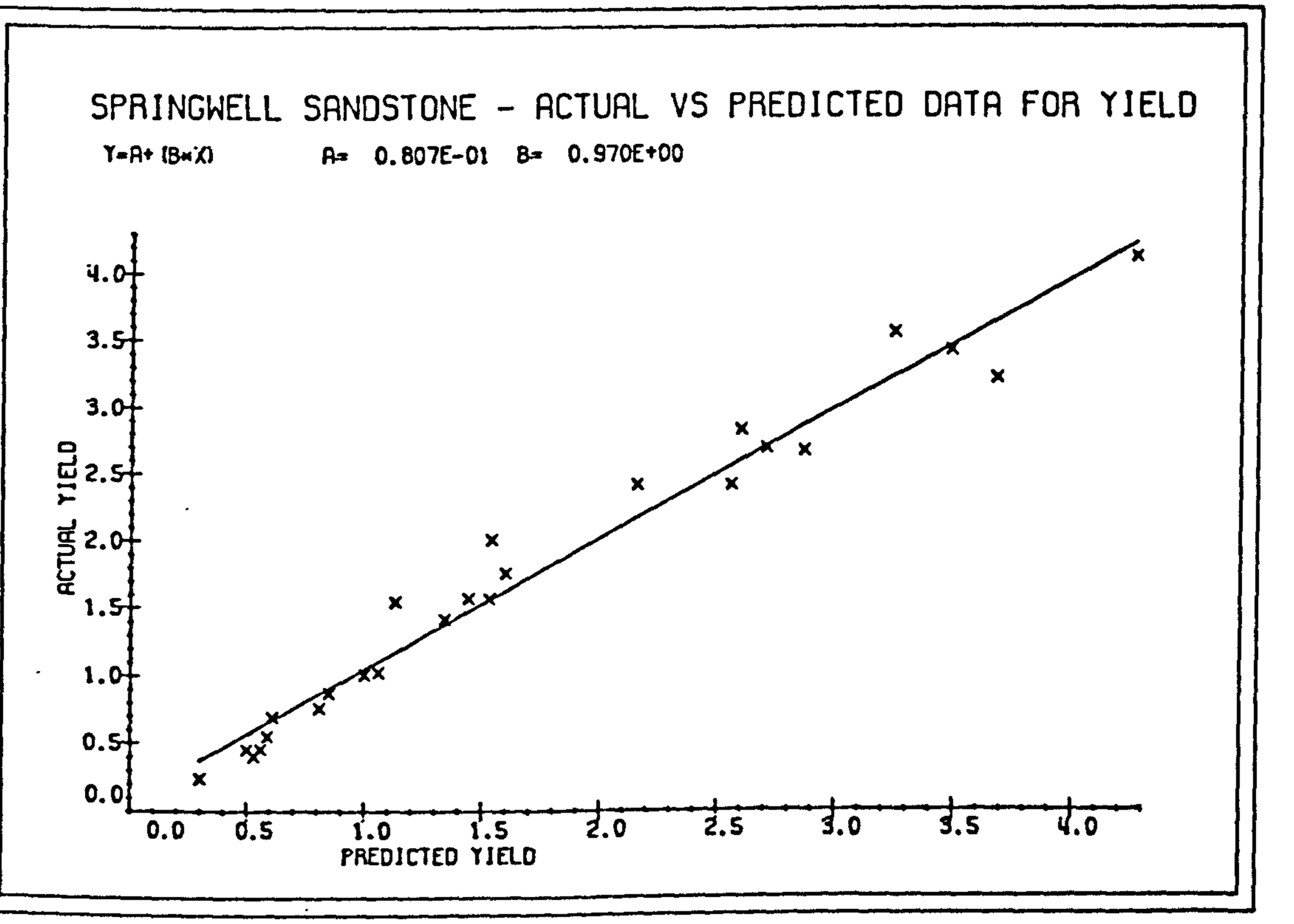
SPRINGWELL SANDSTONE - ACTUAL VS PREDICTED DATA FOR YIELD
Y=A+(B*X)
A= 0.807E-01 B= 0.970E+00
ACTUAL YIELD
PREDICTED YIELD
0.0
0.5
1.0
1.5
2.0
2.5
3.0
3.5
4.0

FIG. 6.19

Appendix C

HYBRID CUTTING RESULTS

C-1 EXPERIMENTS WITH INCREASING WATER JET PRESSURES

C-1.1 Darney Sandstone

DEPTH OF CUT (mm)	JET PRES (MPa)	MCF (kN)	MPCF (kN)	MNF (kN)	MPNF (kN)	Q (g/cm)	MECH.SE ENERGY (MJ/kg)
3.0	13.79	1.51	2.24	1.93	2.78	0.39	57.55
"	24.14	0.88	1.72	0.90	1.86	0.95	14.66
"	34.48	0.91	1.66	0.91	1.76	1.04	13.67
"	44.83	0.90	1.66	0.90	1.76	1.09	12.95
"	55.17	0.91	1.59	0.91	1.65	1.13	12.27
5.0	13.79	2.50	3.99	3.04	5.87	1.26	29.38
"	24.14	1.89	3.35	2.03	3.43	1.25	22.37

"	34.48	1.42	2.60	1.31	2.46	1.65	12.82
"	44.83	1.24	2.39	0.58	1.09	1.82	10.08
"	55.17	1.35	2.35	1.10	2.10	1.96	10.28
7.0	13.79	2.55	4.41	2.80	4.58	2.83	14.96
"	24.14	2.46	4.29	2.41	4.09	2.20	17.67
"	34.48	2.02	3.70	1.75	3.24	2.48	12.01
"	44.83	1.73	3.06	1.33	2.55	2.59	9.95
"	55.17	1.85	3.30	1.44	2.71	2.83	9.67
9.0	13.79	3.04	4.84	3.06	5.48	4.37	10.30
"	24.14	3.20	5.91	2.94	5.62	4.17	11.55
"	34.48	2.54	4.83	2.06	4.62	3.68	10.22
"	44.83	2.24	4.08	1.64	3.37	3.89	8.57
"	55.17	2.24	3.78	1.57	2.99	4.07	8.40
11.0	13.79	3.80	6.01	3.90	6.55	6.89	8.17
"	24.14	3.48	6.08	3.26	6.31	6.06	8.56
"	34.48	3.15	5.62	2.41	5.77	5.22	8.95
"	44.83	2.83	4.81	1.93	3.73	5.36	7.81
"	55.17	2.77	4.62	1.77	3.53	4.92	8.35

C-1.2 Springwell Sandstone

WATER-JET PRESSURE (MPa)	STAND-OFF DISTANCE (mm)	DEPTH OF PENETRAT. (mm)
13.79	15	1.57
"	30	1.32
"	45	1.19
"	60	1.32
"	75	1.38
"	90	1.21
"	105	1.17
24.14	15	3.07
"	30	3.82
"	45	4.17
"	60	3.10
"	75	4.13
"	90	2.76
"	105	2.74
34.48	15	6.91
"	30	5.13
"	45	6.30

"	60	6.22
"	75	5.11
"	90	4.30
"	105	4.39
44.83	15	7.43
"	30	8.54
"	45	9.08
"	60	7.94
"	75	7.32
"	90	6.18
"	105	6.23
55.17	15	9.61
"	30	12.34
"	45	9.96
"	60	9.79
"	75	9.24
"	90	8.40
"	105	8.39
13.79	45	1.19
24.14	"	4.17
34.48	"	6.30
44.83	"	9.08
55.17	"	9.96

C-1.3 Darney Sandstone

WATERJET PRESSURE (MPa)	DEPTH OF PENETRATION (mm)+/- ST.DV
13.79	2.18 +/- 0.39
24.14	4.26 +/- 0.49
34.48	7.00 +/- 0.98
44.83	10.43 +/- 1.74
55.17	14.92 +/- 1.72

COMPUTED REGRESSION LINE FORMULAES

ROCK TYPE	CURVE TYPE	INDEX OF DETERMINAT.	VALUE OF'A'	VALUE OF'B'
Springwell	A+(BxP)	0.98	-1.34	0.22
Darney	A+(BxP)	0.98	-2.79	0.31

DARNEY SANDSTONE : HYDRAULIC SPECIFIC ENERGY CALCULATIONS

PRESSURE (MPa)	POWER ($x10^{-3}$)	$\dot{V}$ ($x10^{-6}$)	HYD.S.ENERGY (MJ/m^3)
13.79	1.05	0.697	1513.07
24.14	2.44	1.360	1793.37
34.48	4.17	2.240	1863.05
44.83	6.18	3.330	1853.74
55.17	8.43	4.770	1769.16

C-1.4 Computed Regression Line Formulaes for Darney Sandstone

At constant water jet pressure and increasing mechanical depth of cut.

VARIABLE NAME	JET PRES (MPa)	CURVE TYPE	INDEX OF DETERMIN	VALUE OF'A'	VALUE OF'B'
MCF	13.79	A+(BxD)	0.94	0.97	0.26
	24.14	"	0.97	0.08	0.33
	34.48	"	0.999	0.05	0.28
	44.83	"	0.99	0.09	0.24
	55.17	"	0.998	0.21	0.23
MPCF	13.79	A+(BxD)	0.93	1.36	0.42
	24.14	"	0.95	0.28	0.56
	34.48	"	0.997	0.13	0.51
	44.83	"	0.995	0.40	0.40
	55.17	"	0.993	0.51	0.38
MNF	13.79	A+(BxD)	0.79	1.56	0.20
	24.14	"	0.94	0.31	0.28
	34.48	"	0.996	0.38	0.19
	44.83	"	0.82	0.184	0.156
	55.17	"	0.98	0.59	0.11

MPNF	13.79	A+(BxD)	0.60	2.55	0.36
	24.14	"	0.97	0.36	0.55
	34.48	"	0.98	0.04	0.50
	44.83	"	0.81	0.32	0.31
	55.17	"	0.99	0.97	0.23
YIELD	13.79	"	0.998	0.04	2.21
	24.14	AxEXP(BxD)	0.99	0.42	0.25
	34.48	"	0.997	0.59	0.20
	44.83	"	0.994	0.64	0.20
	55.17	$Ax(D^B)$	0.998	0.32	1.15
S.ENER.	---	A+(B/D)	0.996	-7.60	199.40
	13.79	"	0.995	-12.76	209.71
	24.14	1/(A+BxD)	0.61	0.03	0.01
	34.48	AxEXP(BxD)	0.95	16.38	-0.05
	44.83	A+(B/D)	0.951	6.41	19.7
	55.17	"	0.96	6.81	16.7

At constant mechanical depth of cut and increasing water jet pressures.

VARIABLE NAME	DEPTH OF CUT	CURVE TYPE	INDEX OF DETERMIN	VALUE OF'A'	VALUE OF'B'
MCF	3.0	AxEXP(BxP)	0.68	1.49	-0.011
	5.0	"	0.89	2.55	-0.014
	7.0	"	0.90	2.89	-0.009
	9.0	"	0.83	3.38	-0.008
	11.0	"	0.94	3.98	-0.070
MPCF	3.0	AxEXP(BxP)	0.84	2.34	-0.008
	5.0	"	0.94	4.09	-0.011
	7.0	"	0.89	4.962	-0.009
	9.0	"	0.57	5.62	-0.006
	11.0	"	0.91	6.71	-0.006
MNF	11.0	"	0.95	4.51	-0.02
MPNF	3.0	AxEXP(BxP)	0.83	2.90	-0.012
	5.0	"	0.75	5.75	-0.025
	7.0	"	0.94	6.12	-0.02
	9.0	"	0.87	6.53	-0.01
	11.0	"	0.83	7.71	-0.01

YIELD	3.0	A+(BxP)	0.73	0.50	0.01
	5.0	"	0.64	1.24	0.012
	7.0	A+(B/P)	0.48	2.59	0.0001
	9.0	A+BxLOG(P)	0.78	4.30	-0.08
	11.0	1/(A+BxP)	0.94	0.127	0.002
S.E	3.0	1/(A+BxP)	0.80	0.018	0.0013
	5.0	"	0.91	0.021	0.0015
	7.0	"	0.87	0.047	0.001
	9.0	"	0.86	0.073	0.0009
	11.0	A+(B/P)	0.77	8.37	0.0002

C-2 DARNEY SANDSTONE : SPACING/DEPTH OF CUT EXPERIMENTS

JET PRES	S/D RATIO	MCF (kN)	MPCF (kN)	MNF (kN)	MPNF (kN)	Q (g/cm)	MECH.S.E. (MJ/kg)
13.8	1	2.62	4.36	2.93	4.71	2.41	17.21
"	2	2.40	4.39	2.80	4.78	2.63	13.53
"	3	2.53	4.75	2.89	5.10	3.12	11.97
"	4	2.97	4.85	3.39	5.25	3.01	14.57
"	5	2.78	4.98	3.19	6.63	3.30	12.42
34.5	1	1.08	2.71	1.36	2.29	2.34	6.84
"	2	1.80	3.39	2.18	4.01	4.05	6.60
"	3	2.25	4.13	2.60	4.81	4.57	7.27
"	4	2.78	4.92	3.31	5.64	3.95	10.50
"	5	2.84	4.84	3.44	5.70	3.99	10.54

C-3 CUTTING SPEED EXPERIMENTS

SPRINGWELL SANDSTONE

TRAVER. SPEED (cm/s)	PENET DEPTH (mm)	MCF (kN)	MPCF (kN)	MNF (kN)	MPNF (kN)	Q (g/cm)	MECH.S.E (MJ/m^3)
6.12	9.00	1.46	2.04	1.00	2.33	2.09	10.21
9.95	7.67	2.22	2.71	1.54	3.08	1.88	17.63
12.03	7.42	2.36	2.76	1.82	3.48	1.93	18.27
16.73	5.52	2.60	3.35	2.12	4.24	1.93	20.10
21.63	4.94	2.83	4.02	2.39	5.24	1.92	21.90

DARNEY SANDSTONE

T.SPED (cm/s)	P.DEP (mm)	MCF (kN)	MPCF (kN)	MNF (kN)	MPNF (kN)	Q (g/cm)	MECH.S.E (MJ/m^3)
5.4	9.17	1.73	2.91	1.42	2.31	2.53	10.11
12.2	6.47	2.62	4.24	2.56	4.07	2.28	17.12
14.4	6.10	2.44	4.04	2.33	3.84	2.33	15.56
16.5	5.58	2.59	4.32	2.53	4.38	2.29	16.65
18.6	5.42	2.67	4.62	2.31	4.28	2.09	18.89
21.5	4.77	2.84	5.82	3.00	5.02	2.29	18.51

HYDRAULIC SPECIFIC ENERGY

ROCK TYPE	TRAVERSE SPEED	POWER ($x10^{-3}$)	$\dot{V}$ ($x10^{-6}$)	HYD.S.ENER (MJ/m^3)
Springwell	6.12	4.99	1.38	3620.95
	9.95	"	1.91	2613.35
	12.03	"	2.23	2234.33
	16.73	"	2.31	2159.64
	21.63	"	2.67	1866.52
Darney	5.40	2.41	1.26	1907.10
	12.20	"	2.01	1196.40
	14.40	"	2.57	938.26
	16.50	"	2.44	988.5
	18.60	"	2.57	936.75
	21.50	"	2.62	920.80

COMPUTED REGRESSION LINE FORMULAES FOR VARIABLES

VARIABLE NAME	ROCK TYPE	CURVE TYPE	INDEX OF DETERMIN	VALUE OF'A'	VALUE OF'B'
PENET	S'well	$Ax(TS^B)$	0.94	18.03	-0.495
DEPTH	Darney	"	0.988	19.93	-0.45
MCF	S'well	$Ax(TS^B)$	0.92	0.82	0.505
	Darney	"	0.92	1.00	0.350
MPCF	S'well	"	0.983	1.04	0.518
	Darney	"	0.886	1.38	0.43
PCF	S'well	"	0.967	1.50	0.45
	Darney	"	0.945	2.17	0.34
MNF	S'well	"	0.97	0.434	0.69
	Darney	"	0.844	0.667	0.475
MPNF	S'well	"	0.995	1.006	0.633
	Darney	"	0.948	0.968	0.532
PNF	S'well	"	0.988	1.433	0.57
	Darney	"	0.93	1.36	0.494

YIELD	S'well	A+(B/TS)	0.56	1.71	1.17
	Darney	"	0.68	2.12	2.24
SPECIF.	S'well	A+(B/TS)	0.97	27.50	0.72
ENERGY	Darney	TS/(A+BxTS	0.96	0.326	0.038

C-4 INFLUENCE OF LEAD-ON DISTANCE ON PARAMETERS (DARNEY S.ST)

JET-PRES (MPa)	LEAD-ON DIST(mm)	MCF (kN)	MPCF (kN)	MNF (kN)	MPNF (kN)	Q (g/cm)	MECH.S.E (MJ/m^3)
27.58	1.0	1.96	3.66	1.33	2.87	2.61	11.08
"	3.0	2.29	4.10	1.54	3.73	2.43	14.02
"	5.0	2.67	4.62	2.31	4.28	2.09	18.89
"	7.0	2.84	4.77	2.59	4.43	2.20	19.21
"	9.0	2.94	5.14	2.93	5.00	2.40	18.23
41.37	1.0	1.75	3.42	1.23	2.53	2.87	8.99
"	3.0	1.71	3.41	1.32	2.74	2.71	9.38
"	5.0	1.69	3.44	1.35	2.76	2.69	9.29
"	7.0	1.74	3.39	1.46	2.84	2.83	9.13
"	9.0	1.67	3.34	1.28	2.58	2.52	9.83

COMPUTED REGRESSION LINE FORMULAS FOR LEAD-ON DISTANCE

DARNEY SANDSTONE

VARIABLE NAME	JET PRESS	CURVE TYPE	INDEX OF DETERMN.	VALUE OF 'A'	VALUE OF 'B'
MCF	27.58	L/(A+BxL)	0.90	0.18	0.34
	41.37	A+(BxL)	0.38	1.74	-0.006
MPCF	27.58	L/(A+BxL)	0.86	0.08	0.2
	41.37	A+(BxL)	0.56	3.45	-0.009
MNF	27.58	L/(A+BxL)	0.78	0.43	0.36
	41.37	A+(BxL)	0.19	1.27	0.012
MPNF	27.58	L/(A+BxL)	0.95	0.15	0.20
	41.37	A+(BxL)	0.06	2.64	0.01
YIELD	27.58	A+(B/L)	0.56	2.2	0.42
	41.37	A+(BxL)	0.45	2.87	-0.03
S.E	27.58	L/(A+BxL)	0.91	0.04	0.05
	41.37	A+(BxL)	0.50	8.97	0.072

C-5 STAND-OFF DISTANCE EXPERIMENTAL RESULTS

DARNEY SANDSTONE

DEPTH CUT(mm)	STANDOFF DIST(mm)	MCF (kN)	MPCF (kN)	MNF (kN)	MPNF (kN)	Q g/cm	MECH.S.E (MJ/m^3)
7.0	15.0	1.91	3.49	2.47	4.47	1.66	17.07
7.25	30.0	2.04	3.64	2.71	4.64	1.81	16.90
7.0	45.0	2.11	4.89	2.59	4.73	1.70	18.40
7.0	60.0	2.26	4.48	2.86	4.94	1.69	19.86
7.25	75.0	2.51	4.76	2.75	4.90	1.81	20.59

DARNEY SANDSTONE :COMPUTED REGRESSION LINE FORMULAES FOR STAND-OFF DISTANCE

VARIABLE NAME	CURVE TYPE	INDEX OF DETERM.	VALUE OF'A'	VALUE OF'B'
JET PENET.	A+(B/SD)	0.85	4.48	13.54
MCF	A+(B/SD)	0.98	0.56	-0.002
MPCF	1/(A+BxSD)	0.72	0.30	-0.0014
MNF	SD/(A+BxSD)	0.68	0.81	0.35
MPNF	A+(BxSD)	0.91	4.39	0.008
YIELD	SD/(A+BxSD)	0.23	0.52	0.56
S.E	A+BxLOG(SD)	0.998	2.71	4.15
HYDRAULIC POWER	A+(B/SD)	0.86	1.9x10-6	5.6x10E-6
HYDRAULIC S.ENERGY	SD/(A+BxSD)	0.85	0.0024	0.0008

C-6 INFLUENCE OF NOZZLE DIAMETER ON PARAMETERS

SPRINGWELL SANDSTONE:

JET PRESS (MPa)	NOZZLE DIAM. (mm)	JET PENET (mm)	MCF (kN)	MPCF (kN)	MNF (kN)	MPN (kN)	Q g/cm)	MECH. S.E. (MJ/m^3)
13.79	0.60	1.28	2.71	3.41	2.20	4.48	2.28	17.74
	0.85	1.50	2.82	3.37	2.10	4.17	1.96	21.50
	1.10	2.21	2.38	3.34	1.97	4.42	2.50	14.29
34.48	0.60	4.36	2.75	3.76	2.14	4.68	2.51	14.67
	0.85	5.35	2.45	3.31	1.95	4.11	1.80	22.77
	1.10	7.07	2.40	3.24	1.57	3.48	1.65	21.72
DARNEY SANDSTONE								
13.79	0.60	1.49	3.25	5.93	3.45	5.04	2.63	18.37
	0.85	1.59	2.57	4.33	3.14	4.88	2.85	13.40
	1.10	2.21	2.45	4.39	2.53	4.21	2.73	13.45
27.58	0.60	3.71	3.05	5.28	2.85	4.74	2.64	17.17
	0.85	5.79	2.34	4.06	2.19	3.68	2.45	13.65
	1.10	6.85	2.05	3.87	1.83	3.37	2.57	11.79

WATER JET PRESSURE (MPa)	NOZZLE DIAMETER (mm)	POWER ($x10^{-4}$)	$\dot{V}$ (x10E-7)	HYD.S.ENERGY (MJ/m^3)
13.79	0.60	5.90	3.85	1531.43
	0.85	8.51	4.51	1887.24
	1.10	17.20	6.65	2590.37
34.48	0.60	23.3	13.10	1785.62
	0.85	33.7	16.10	2091.90
	1.10	68.1	21.30	3201.19

C-7 INFLUENCE OF NUMBER OF JET PASSES

SPRINGWELL SANDSTONE

NO.OF PASSES	JETPENET (mm)	MCF (kN)	MPCF (kN)	MNF (kN)	MPNF (kN)	Q (g/cm)	MECH.S.E (MJ/m^3)
1	3.27	2.55	3.53	2.29	4.83	2.20	17.37
2	4.66	2.82	3.65	1.90	4.32	2.00	21.27
3	5.78	2.62	3.33	2.07	4.17	1.87	20.90
4	6.04	2.72	3.20	1.87	3.76	1.98	20.69
5	8.10	2.24	2.75	1.69	3.30	2.01	16.64

NUMBER OF PASSES	POWER ($x10^{-3}$)	$\bar{\dot{V}}$ ($x10^{-6}$)	HYD.S.ENERGY (MJ/m^3)
1	1.97	1.35	1439.5
2	3.94	1.92	2052.4
3	5.91	2.38	2473.6
4	6.88	2.49	3156.2
5	9.85	3.34	2941.9

COMPUTED REGRESSION LINE FORMULAS FOR NO OF JET PASSES

VARIABLE NAME	CURVE TYPE	INDEX OF DETERMIN.	VALUE OF 'A'	VALUE OF'B'
PENETRAT DEPTH	NP/(A+BxNP)	0.97	0.21	0.1
MCF	AxEXP(BxNP)	0.28	2.82	-0.03
MPCF	AxEXP(BxNP)	0.82	3.96	-0.06
MNF	"	0.74	2.36	-0.06
MPNF	"	0.97	5.30	-0.09
HYDRAULIC POWER	$Ax(NP^B)$	0.96	1.3x10-6	0.52
HYDRAULIC SPECIFIC ENERGY	NP/(A+BxNP)	0.98	0.00047	0.00024

Appendix D

COMPARISON EXPERIMENTS

D-1 DARLEY DALE SANDSTONE

JET PRESS (MPa)	DEPTH OF-CUT (mm)	MCF (kN)	MPCF (kN)	MNF (kN)	MPNF (kN)	Q (g/cm)	MECH.S.E (MJ/kg)
---	2.0	1.39	1.91	1.67	2.35	0.30	46.33
---	4.0	1.82	2.99	2.05	3.39	1.20	15.17
---	6.0	2.72	4.47	3.04	4.96	2.58	10.54
---	8.0	3.44	5.52	3.57	5.95	4.23	8.13
---	10.0	3.50	5.96	3.24	5.70	7.23	4.13
55.17	2.0	0.69	1.17	0.68	1.36	0.81	8.52
"	4.0	1.14	1.92	0.95	2.00	1.66	6.87
"	6.0	1.79	3.04	1.33	2.46	2.95	6.07
"	8.0	2.25	3.60	1.42	2.85	4.09	5.50
"	10.0	3.13	5.04	1.90	3.61	5.32	5.88

COMPUTED REGRESSION LINE FORMULAS FOR DARLEY DALE S.ST.

VARIAB. NAME	JET PRES. (MPa)	CURVE TYPE	INDEX OF DETERMIN	VALUE OF'A'	VALUE OF'B'
MCF	0	A+(BxD)	0.95	0.82	0.29
	55.17	"	0.99	0.00	0.30
MPCF	0	A+(BxD)	0.95	0.82	0.29
	55.17	"	0.98	0.13	0.47
MNF	0	A+(BxD)	0.82	1.32	0.23
	55.17	"	0.97	0.38	0.15
MPNF	0	A+(BxD)	0.89	1.69	0.46
	55.17	"	0.99	0.85	0.27
PCF	0	A+(BxD)	0.98	1.02	0.74
	55.17	"	0.97	0.47	0.53
YIELD	0	$A+(D^B)$	0.999	0.078	1.95
	55.17	"	0.997	0.345	1.19
S.E	0	A+(B/D)	0.98	-6.44	102.68
	55.17	"	0.97	4.91	7.28

D-2 LIMESTONE B

JET PRESS (MPa)	DEPTH OF CUT (mm)	MCF (kN)	MPCF (kN)	MNF (kN)	MPNF (kN)	Q (g/cm)	MECH.S.E (MJ/m^3)
---	2.0	2.26	2.67	4.36	4.98	0.26	86.92
---	4.0	3.34	4.52	5.36	7.19	0.76	43.95
---	6.0	3.62	5.42	5.35	6.96	1.86	19.46
---	8.0	4.39	7.50	6.05	8.72	2.84	15.46
---	10.0	5.69	9.44	8.32	12.07	4.89	11.64
55.17	2.0	1.46	2.62	1.86	3.21	0.40	36.50
"	4.0	1.99	3.91	1.73	3.42	1.24	16.05
"	6.0	3.28	6.29	2.62	5.41	2.08	15.77
"	8.0	3.24	6.56	2.24	4.74	3.27	9.81
"	10.0	4.09	8.46	2.79	5.74	5.36	7.63

COMPUTED REGRESSION LINE FORMULAS FOR LIMESTONE B

VARIABLE NAME	JET PRESS	CURVE TYPE	INDEX OF DETERMIN	VALUE OF'A'	VALUE OF'B'
MCF	0	A+(BxD)	0.96	1.49	0.40
	55.17	"	0.93	0.86	0.33
MPCF	0	"	0.99	0.95	0.83
	55.17	"	0.96	1.27	0.72
PCF	0	"	0.99	1.15	1.07
	55.17	"	0.97	0.96	1.08
MNF	0	"	0.84	3.31	0.43
	55.17	"	0.66	1.54	0.12
MPNF	0	"	0.88	3.27	0.79
	55.17	"	0.78	2.59	0.32
YIELD	0	$Ax(D^B)$	0.995	0.07	1.82
	55.17	"	0.996	0.135	1.564
S.E	0	A+(B/D)	0.991	-8.51	192.68
	55.17	"	0.97	1.32	69.36

D-3 PORTLAND LIMESTONE

JET PRESS (MPa)	DEPTH OF CUT (mm)	MCF (kN)	MPCF (kN)	MNF (kN)	MPNF (kN)	Q (g/cm)	MECH.S.E (MJ/m^3)
---	2.0	1.92	2.24	2.80	3.65	0.31	61.94
---	4.0	3.03	4.30	5.41	7.20	0.92	32.93
---	6.0	3.78	7.30	5.82	8.77	2.27	16.65
---	8.0	4.31	9.31	6.71	9.40	4.00	10.78
---	10.0	5.25	10.61	6.77	10.40	7.70	6.82
55.17	2.0	0.77	1.48	0.82	1.68	0.53	14.53
"	4.0	1.67	3.37	1.69	3.60	1.24	13.47
"	6.0	2.76	4.96	2.50	4.76	2.50	11.04
"	8.0	3.14	6.65	2.90	6.11	6.64	4.86
"	10.0	3.46	6.96	3.11	6.37	6.42	5.39

COMPUTED REGRESSION LINE FORMULAS FOR PORTLAND LIMESTONE

VARIABLE NAME	JET PRESS	CURVE TYPE	INDEX OF DETERMIN	VALUE OF'A'	VALUE OF'B'
MCF	0	A+(BxD)	0.99	1.28	0.40
	55.17	"	0.94	0.31	0.34
MPCF	0	"	0.98	0.47	1.06
	55.17	"	0.96	0.41	0.71
PCF	0	"	0.997	0.83	1.16
	55.17	"	0.95	-0.06	1.13
MNF	0	"	0.82	2.73	0.46
	55.17	"	0.94	0.47	0.29
MPNF	0	"	0.89	3.17	0.79
	55.17	"	0.95	0.94	0.60
YIELD	0	$Ax(D^B)$	0.99	0.07	1.97
	55.17	"	0.96	0.15	1.67
S.E	0	A+(B/D)	0.99	-5.70	138.04
	55.17	"	0.65	4.76	22.51

D-4 SANDSTONE D

JET PRESS (MPa)	DEPTH OF CUT (mm)	MCF (kN)	MPCF (kN)	MNF (kN)	MPNF (kN)	Q (g/cm)	MECH.S.E (MJ/m^3)
---	1.5	1.87	5.88	3.25	3.96	0.19	98.42
---	4.3	3.06	6.25	4.03	6.59	1.15	26.66
---	6.2	3.32	8.40	3.96	7.17	2.18	15.23
---	8.2	3.83	9.49	4.13	6.68	3.12	16.19
---	10.2	5.05	11.16	6.92	10.42	5.75	6.66
55.17	2.0	1.33	4.49	1.93	3.37	0.44	30.23
"	4.5	1.45	5.39	1.47	3.92	1.53	9.48
"	6.4	1.97	5.70	1.79	4.16	2.73	7.22
"	8.1	2.62	7.35	1.93	4.05	4.45	6.92
"	10.5	3.08	7.41	2.75	5.90	8.53	7.01

COMPUTED REGRESSION LINE FORMULAS FOR SANDSTONE D

VARIABLE NAME	JET PRESS	CURVE TYPE	INDEX OF DETERMIN	VALUE OF'A'	VALUE OF'B'
MCF	0	A+(BxD)	0.96	1.39	0.34
	55.17	"	0.94	0.68	0.22
MPCF	0	"	0.94	4.35	0.64
	55.17	"	0.91	3.72	0.37
MNF	0	A+(BxD)	0.65	2.33	0.34
	55.17	"	0.48	1.34	0.01
MPNF	0	"	0.82	3.23	0.61
	55.17	"	0.77	2.66	0.26
YIELD	0	$Ax(D^B)$	0.996	0.093	1.73
	55.17	"	0.983	0.12	1.77
S.E	0	A+(B/D)	0.999	-10.17	162.454
	55.17	"	0.963	1.302	61.14

D-5 LIMESTONE C

JET PRESS (MPa)	DEPTH OF CUT (mm)	MCF (kN)	MPCF (kN)	MNF (kN)	MPNF (kN)	Q (g/cm)	MECH.S.E (MJ/m^3)
—	3.0	1.73	2.84	1.53	3.68	0.25	70.40
—	5.0	3.47	6.32	2.76	6.52	0.70	50.24
—	7.5	5.16	9.00	3.49	7.61	1.33	36.80
—	10.0	8.07	12.91	4.16	10.73	2.63	30.93
55.17	3.0	1.77	2.74	1.04	2.58	0.33	54.12
"	5.0	3.35	4.60	2.19	4.91	0.68	36.69
"	7.5	6.06	7.86	4.87	7.37	2.04	39.31
"	10.0	8.30	10.54	4.02	9.18	3.09	38.51

COMPUTED REGRESSION LINE FORMULAES FOR LIMESTONE C

VARIABLE NAME	JET PRESS	CURVE TYPE	INDEX OF DETERMIN	VALUE OF'A'	VALUE OF'B'
MCF	0	A+(BxD)	0.99	1.022	0.883
	55.17	"	0.997	1.19	0.951
MPCF	0	"	0.993	1.13	1.40
	55.17	"	0.997	0.81	1.14
MNF	0	A+(BxD)	0.96	0.67	0.36
	55.17	"	0.73	0.09	0.49
MPNF	0	"	0.96	1.13	0.94
	55.17	"	0.99	0.002	0.94
YIELD	0	$Ax(D^B)$	0.996	0.031	1.91
	55.17	"	0.98	0.0364	1.94